# CIPM Key comparison CCPR-K1.a.2017

# Spectral Irradiance 250 nm to 2500 nm

## Final Report

Boris Khlevnoy[1], Maksim Solodilov[1], Svetlana Kolesnikova[1], Denis Otryaskin[1], Alicia Pons[2], Joaquin Campos[2], Dong-Joo Shin[3], Seongchong Park[3], Gaël Obein[4], Mai-Huong Valin[4], Alain Vissière[4], Caihong Dai[5], Zhifeng Wu[5], Yanfei Wang[5], Ling Li[5], Yandong Lin[5], Howard Yoon[6], Charles Gibson[6], Yuanjie Liu[7], Peter Manson[8], Errol Atkinson[8], Tatsuya Zama[9], Hiroshi Shitomi[9], Teresa Goodman[10], William Servantes[10], Angela Gamouras[11], Donald J. Woods[11], Peter Sperfeld[12], Sven Pape[12]

1 All-Russian Research Institute for Optical and Physical Measurements (VNIIOFI), Russia
2 Instituto de Optica (IO-CSIC), Spain
3 Korea Research Institute of Standards and Science (KRISS), Republic of Korea
4 Laboratoire Commun de Métrologie (LNE-CNAM), France
5 National Institute of Metrology (NIM), China
6 National Institute of Standards and Technology (NIST), USA
7 National Metrology Centre, A*STAR (NMC, A*STAR), Singapore
8 National Measurement Institute of Australia (NMIA), Australia
9 National Metrology Institute of Japan, AIST (NMIJ), Japan
10 National Physical Laboratory (NPL), UK
11 National Research Council Canada (NRC), Canada
12 Physikalisch-Technische Bundesanstalt (PTB), Germany

Pilot: All-Russian Research Institute for Optical and Physical Measurement (VNIIOFI). Russia

Moscow, 2023

**ABSTRACT**

This report describes the Key Comparison of the Consultative Committee for Photometry and Radiometry CCPR-K1.a.2017 for Spectral Irradiance in the wavelength range of 250 nm to 2500 nm. Tungsten quartz halogen lamps of the FEL type (1000 W) were used as artefacts. Each participant used its own set of lamps. The *star* scheme of measurements was applied with the sequence *participant – pilot – participant*. Twelve National Metrology Institutes participated in the comparison. Each participant's measurement data were based on a totally independent spectral irradiance scale realisation. VNIIOFI (the Russian Federation) served as a pilot. The measurements were carried out from 2017 – 2020.

The analysis of the comparison was performed following the *step-by-step* approach described in the Appendix B of the Guidelines for CCPR Key Comparison Report Preparation (CCPR-G2 Rev.4). The key comparison reference values (KCRV) were calculated independently at each wavelength as the weighted means with cut-off. The measurement data of all participants were used for the KCRV excluding just a few outliers in the wavelength range of 1700 nm to 2500 nm. The relative uncertainties of the KCRV were minimal, 0.08 %, at the wavelengths of 900 nm to 1500 nm and increasing towards the limits of the spectral range up to 0.28 % at 250 nm and 0.20 % at 2500 nm. Consistency checks were satisfied at 17 of the 28 measured wavelengths, but failed at 11 wavelengths, mostly in the infrared range. For the latter wavelengths the Mandel-Paule method was applied resulting in an additional uncertainty that varied depending on wavelength from 0.11 % to 0.89 %.

In general, the measurement uncertainties submitted by the participants in this comparison were less than those submitted in the previous CCPR-K1.a comparison. This is evidenced by the values of the cut-off, which had decreased at all wavelengths by a factor of 1.2 to 3.0 depending on wavelength. However, only for seven participants the degrees of equivalence do not exceed the expanded uncertainties at almost all wavelengths. About 80 % of all results (all participants at all wavelengths) agree with the KCRV within 1 % over the whole spectral range and within 0.7 % in the visible, which is comparable with the results of the previous CCPR-K1.a comparison.

# Content

# 1. Introduction

This report describes an international Key Comparison CCPR-K1.a.2017 of Spectral Irradiance with a wavelength range from 250 nm to 2500 nm, organised and conducted by the Consultative Committee for Photometry and Radiometry (CCPR) of the International Committee for Weights and Measures (CIPM).

The CIPM Mutual Recognition Arrangement (CIPM MRA) was signed in 1999 with the objectives of establishing the degree of equivalence of national measurement standards and providing for the mutual recognition of calibration and measurement certificates issued by National Metrology Institutes (NMIs) [1]. Under the CIPM MRA the equivalence of national measurement standards maintained by the NMIs is determined by a set of Key Comparisons which are chosen and organised by the Consultative Committees of the CIPM.

CCPR has identified several key comparisons in the field of optical radiation metrology. In particular, CCPR decided that a key comparison of spectral irradiance is to be carried out in two spectral ranges: from 250 nm to 2500 nm (identification code is CCPR-K1.a) and from 200 nm to 350 nm (CCPR-K1.b). The first CCPR-K1.a comparison was piloted by The National Physical Laboratory (NPL), the NMI of the United Kingdom, and was completed in 2006 [2]. In 2013 CCPR announced the second round of the key comparison CCPR-K1.a. The All-Russian Research Institute for Optical and Physical Measurements (VNIIOFI), the NMI of the Russian Federation, was chosen to pilot this comparison. VNIIOFI participated in the first round of CCPR-K1.a and later served as a link laboratory in the bilateral comparison APMP.PR-K1a.1-2008 with the Korea Research Institute of Standards and Science (KRISS) [3].

The technical protocol of this comparison was drawn up by the seven-member Task Group (TG), agreed by all the participants and approved by the CCPR Working Group on Key Comparisons (CCPR WG-KC). The comparison was registered in the key comparison data base (KCDB) in 2017 with the identification code of CCPR-K1.a.2017.

Measurements within CCPR-K1.a.2017 were performed in the period from 2017 to 2020. Data analysis and the report preparation were done in accordance with the CCPR-G2 Guidelines for CCPR Key Comparison Report Preparation [4].

# 2. Organization of comparison

## 2.1. Participants

In May 2013 the CCPR WG-KC appointed VNIIOFI as the pilot laboratory of the second-round CCPR-K1.a comparison.

The invitation to participate in the comparison was prepared by the pilot laboratory and the WG-KC, and was sent to all CCPR members in June 2013. Thirteen NMIs, including the pilot, applied for participation. The selection process for the participants was guided by the criteria described in the document CCPR-G4, Guidelines for preparing CCPR Key Comparisons [5]:

1. The participant must be a member of the CCPR.
2. The participant must be willing to serve as a link laboratory to their RMO.
3. The participant must have an independent realization of the unit or scale of the comparison quantity.
4. The participant's measurement capability of the comparison quantity, over the full range of the comparison (e.g., full spectral range), must be listed in the CMC table published at the time of the call for participants.

Since the number of applications exceeded the maximum of 12, the RMO Groups were requested to select the maximum number of participants in accordance with limits fixed in CCPR-G4 [5] and presented in Table 2.1.

Table 2.1. RMO participant limits.

| RMO group | Group Members | Maximum number of participants |
|---|---|---|
| Group 1 | EURAMET+COOMET | 6 |
| Group 2 | APMP+AFRIMETS | 4 |
| Group 3 | SIM | 2 |

Finally, the participants were selected and approved by CCPR WG-KC. The list of participants and their contact information are presented in Table 2.2.

## 2.2. Task Group

A subset of the participants was discussed and selected by participants to serve as the Task Group. The following seven selected Task Group members were approved by WG-KC:

| | |
|---|---|
| VNIIOFI | All-Russian Research Institute for Optical and Physical Measurements, Russia |
| KRISS | Korea Research Institute of Standards and Science, Republic of Korea |
| NIST | National Institute of Standards and Technology, USA |
| NMIA | National Measurement Institute, Australia |
| NMIJ | National Metrology Institute of Japan |
| NPL | National Physical Laboratory, UK |
| PTB | Physikalisch-Technische Bundesanstalt, Germany |

The Task Group was responsible for the selection of the type of the comparison artefacts and for the development of the Technical Protocol.

Table 2.2. List of participant and contact information

| NMI | | | NMI Contact | |
|---|---|---|---|---|
| **NMI** | **Full name, Address** | **RMO** | **Name** | **Contact Details** |
| VNIIOFI (pilot) | All-Russian Research Institute for Optical and Physical Measurements.<br>46 Ozernaya str., 119361 Moscow, RUSSIA | COOMET | Boris Khlevnoy | TEL: +7 (495) 437-29-88<br>Email: khlevnoy-m4@vniiofi.ru |
| IO-CSIC | Instituto de Optica<br>Serrano, 144, 28006 Madrid, SPAIN | EURAMET | Joaquin Campos Acosta<br>Alicia Pons Aglio, | TEL: +34 915618806<br>Email: joaquin.campos@csic.es |
| KRISS | Korea Research Institute of Standards and Science<br>267 Gajeong-Ro, Yuseong-Gu, Daejeon 305-340, REPUBLIC OF KOREA | APMP | Dong-Joo Shin<br>Seongchong Park | TEL: +82-42-868-5209<br>Email: djshin@kriss.re.kr<br>spark@kriss.re.kr |
| LNE-CNAM | Laboratoire Commun de Métrologie<br>61, rue du Landy<br>93210 La Plaine Saint Denis, FRANCE | EURAMET | Gaël Obein,<br>Mai-Huong Valin | TEL: +33 6 29 55 34 04<br>Email: gael.obein@lecnam.net<br>TEL: +33 1 30 69 14 53<br>mai-huong-christine.valin@lecnam.net |
| NIM | National Institute of Metrology<br>No. 18, Bei San Huan Dong Lu, Beijing, 100013, Building 13, Room 109,<br>P.R.CHINA | APMP | Lin Yandong<br>Dai Caihong | TEL: 86-10-64524805<br>Email: linyd@nim.ac.cn<br>TEL: 86-10-64524813<br>Email: daicaihong@nim.ac.cn |
| NIST | National Institute of Standards and Technology<br>100 Bureau Drive, MS 8442<br>Room A313, Bldg. 220,<br>Gaithersburg, MD 20899, USA | SIM | Howard Yoon<br>Charles Gibson | TEL: +1 301-975-2482<br>Email: howard.yoon@nist.gov<br>TEL: +1 301-975-2329<br>Email: charles.gibson@nist.gov |
| NMC, A*STAR | National Metrology Centre, A*STAR<br>1 Science Park Drive<br>118221, SINGAPORE | APMP | LIU Yuanjie | TEL: +65 62791940<br>Email:<br>liu_yuanjie@nmc.a-star.edu.sg |
| NMIA | National Measurement Institute, Australia<br>Bradfield Rd,<br>West Lindfield, NSW 2070,<br>AUSTRALIA | APMP | Peter Manson<br>Errol Atkinson | TEL: +61 2 8467 3858<br>Email:peter.manson@measurement.gov.au,<br>errol.atkinson@measurement.gov.au |
| NMIJ | Optical Radiation Section<br>Photometry and Radiometry Division<br>National Metrology Institute of Japan<br>National Institute of Advanced Industrial Science and Technology (AIST)<br>Tsukuba Central 3-1, 1-1-1 Umezono,<br>Tsukuba, Ibaraki, 305-8563, JAPAN | APMP | Tatsuya Zama<br>Hiroshi Shitomi | TEL: +81 29 861 5649<br>Email: zama-t@aist.go.jp<br>h-shitomi@aist.go.jp |
| NPL | Optical Radiometric Metrology Group<br>Thermal and Radiometric Metrology Division<br>National Physical Laboratory<br>Teddington, Middlesex<br>TW11 0LW United Kingdom | EURAMET | Teresa Goodman<br>William Servantes | TEL: +44 (0)20 8943 6863<br>Email:<br>teresa.goodman@npl.co.uk<br>william.servantes@npl.co.uk |
| NRC | National Research Council of Canada<br>Measurement Science and Standards<br>1200 Montreal Road, Building M36<br>Ottawa, Ontario, K1A 0R6, CANADA | SIM | Angela Gamouras | TEL: +1 613-993-2489<br>Email: angela.gamouras@nrc-cnrc.gc.ca |
| PTB | Physikalisch-Technische Bundesanstalt<br>Bundesallee 100<br>38116 Braunschweig, GERMANY | EURAMET | Peter Sperfeld<br>Sven Pape | TEL: +49 531 592 4144<br>Email: Peter.Sperfeld@ptb.de<br>TEL: +49 531 592 4112<br>Email: Sven.Pape@ptb.de |

## 2.3. Form of comparison

The comparison had the form of a star comparison. The sequence of measurements was the following:

Participant – Pilot – Participant.

The artifacts were initially calibrated by the participants. Then they were transported to the pilot for pilot calibration. They were finally returned to the participants and calibrations were repeated to monitor possible drift.

## 2.4. Comparison artifacts

The comparison was carried out through calibration of groups of traveling standard lamps (traveling standards). These lamps had been shown to have reasonable stability and robustness, suitable for the transfer of a spectral irradiance scale maintained in a participating laboratory to that of the pilot laboratory.

Each participant used a separate set of lamps to minimise the effects of ageing. This also allows the participants to maintain a record of the compared quantity.

Each participant provided its own set of three traveling standard lamps.

Traveling standard lamps were FEL type tungsten halogen lamps with nominal voltage and electrical power of 120 V and 1000 W, respectively. The lamps were operated at constant DC current. Each lamp set was equipped with an alignment jig that allowed for precise lamp alignment. According to a CCPR WG-KC decision, participants were not able to use lamps that were used for any previous spectral irradiance international comparison; all lamps were new lamps of the same type selected by the Task Group. A full description of the traveling standard lamps is given in section 4.

The Technical Protocol requested that “Preferably, the traveling standards should be carried by hand between each participating laboratory and the pilot laboratory”, but “the shipping of carefully-packaged lamps via a postal service” was also accepted. Five participants, KRISS, LNE, NIST, NRC and PTB, transported the lamps by hand, and the other six, CSIC, NIM, NMC, NMIA and NMIJ, used a postal service. All traveling standards were transported by plane. Each set of traveling standards was accompanied by an ATA CARNET document when transported to the pilot and back.

Each traveling standard lamp was inspected for possible damage after delivery to the pilot laboratory and after the return to the participants. At the pilot laboratory no damage was detected for any of the lamps except one: the CSIC lamp number BN-9101-610 had a broken filament although the transportation box had no signs of damage. No damages were reported by the participants after transportation of the lamps from the pilot.

The Technical Protocol requested that “the traveling standard lamps should only be handled by authorized persons and stored in such a way as to prevent damage. No cleaning of any lamp envelopes should normally be attempted. If a traveling standard lamp appears to have been mishandled and either the pilot laboratory or the participant laboratory consider that cleaning appears to be required, this information should be communicated between the two laboratories”. No lamp cleaning was reported during the comparison.

Some lamps demonstrated white-spot deposits on the bulb inner surface. But only one lamp, LNE-CNAM lamp number BN-9101-656, was considered unstable by the participant due to these deposits.

## 2.5. Timetable

The Technical Protocol was developed by the Task Group in April 2017 and approved by CCPR-WGKC in May 2017. The comparison was registered in the KCDB on 31 May 2017.

According to the original timetable published in the Protocol the participant first-round measurements of the traveling standards should be completed by October 2017, and all the lamps should be transported to the pilot by November 2017. The pilot measurements should be completed in February 2018. The participant second-round measurements should be completed in May 2018, and the measurement data should be reported to the pilot by June 2018. The actual dates were significantly different from the original plan. The actual measurement timetable is presented in Table 2.3.

Table 2.3. Measurement timetable of CCPR-K1.a.2017

| NMI | 1st round measurement | Lamps delivered to pilot | Pilot measurements | 2st round measurement | Measurement data submitted to Pilot |
|---|---|---|---|---|---|
| VNIIOFI (pilot) | Feb-Mar 2018 | March 2018 | April-June 2018 | Feb 2019, Feb 2020 | February 2020 |
| IO-CSIC | September 2017 | October 2017 | April-June 2018 | by July 2019 | July 2019 |
| KRISS | Sep-Oct 2017 | November 2017 | April-July 2018 | Aug-Sep 2019 | January 2020 |
| LNE-CNAM | June 2018 | July 2018 | July-Aug 2018 | March 2019 | August 2019 |
| NIM | Nov 2017 – Jan 2018 | March 2018 | April-July 2018 | Nov 2018 – Jan 2019 | September 2019 |
| NIST | June 2018 | August 2018 | Aug-Oct 2018 | Aug 2019 | August 2019 |
| NMC, A*STAR | Nov 2017 | June 2018 | July-Aug 2018 | May 2019 | January 2020 |
| NMIA | Jan-Apr 2018 | August 2018 | October 2018 | Feb-Nov 2019 | August 2020 |
| NMIJ | July-Sep 2018 | November 2018 | January 2019 | Oct 2019 | August 2020 |
| NPL | February 2018 | March 2018 | April-June 2018 | - | November 2020 |
| NRC | Nov-Dec 2017 | December 2017 | April-June 2018 | May-June 2019 | December 2019 |
| PTB | June 2017 | October 2017 | April-June 2018 | Nov-Dec 2018 | September 2019 |

# 3. Measurand

The measurand of the comparison is the **spectral irradiance** (unit $W \cdot m^{-2} \cdot nm^{-1}$) of a lamp in a plane at 500 mm from the reference plane defined by the front plane of the lamp base (see section 4.4.9) aligned to the optical axis of the lamp system (see alignment procedures in section 4.4), at the wavelengths (in nm):

250, 260, 270, 280, 290, 300, 320, 340, 360, 380, 400, 450, 500, 555, 600, 700, 800, 900, 1000, 1100, 1300, 1500, 1700, 2000, 2200, 2300, 2400 and 2500.

The spectral irradiance of each lamp had to be measured for the defined operating current of 8.100 A. The measurements should be performed in suitable laboratory conditions maintained at a temperature of 20 °C to 25 °C.

The spectral irradiances of each lamp should be measured independently at least three times. Each independent measurement should consist of the lamp being realigned in the measurement facility. But only the mean or final spectral irradiance values for each lamp should be reported by the participants as a combination of the results of these independent measurements.

# 4. Description of the traveling standards and measurement instructions

## 4.1. Type of the Traveling Standards

The traveling standards (artifacts) were tungsten halogen lamps of the FEL type with nominal power of 1000 W and nominal voltage of 120 V produced by OSRAM-Sylvania. This lamp consists of a double-coiled tungsten filament, supported at the top and bottom of the filament and operated in a bromine-filled quartz envelope. Each lamp had to be mounted in a special mount and equipped with an alignment jig.

Each participant had to use three aged and calibrated traveling standards.

The Task Group decided that all participants had to use commercially available lamps of the type described above, which had been mounted and pre-aged by the company Gigahertz-Optik GmbH (Germany). The Gigahertz-Optik product number is BN-9101-02. The same type of lamps were used as the traveling standards for the previous CCPR-K1a comparison [2]. All participants used the lamps BN-9101-02.

The lamp BN-9101-02 and the alignment jig are shown in Figure 4.1.

## 4.2. Electrical Parameters

The traveling standards were operated with DC electrical power, with the positive (+) and negative (-) polarity terminals clearly marked for each lamp.

All lamps were operated at the same fixed electrical current of 8.100 A. The value of the related voltage at this current varied from lamp to lamp in the range from 103 V to 110 V.


Figure 4.1. Measurement artifact – tungsten halogen lamp of FEL 120V-1000W type mounted by Gigahertz-Optik with alignment jig (right).

## 4.3. Seasoning and selection of lamps

Gigahertz-Optic performed seasoning and selection of the CCPR-K1a.2017 lamps to ensure suitable stability and provided appropriate certificates. The following seasoning and selection procedure developed and approved by the Task Group was used:

1. Visual inspection.

   Quartz envelope must not display striations (variations in thickness), must be clear and free of bubbles and white markings. Lamp must be mounted straight without visible tilts in any direction.

2. Initial seasoning.

   Season a lamp at the defined working current of 8.1A for 24-48 hours. If, during the initial or further seasoning, obvious dark and white depositions appear on the lamp envelope in front of the filament, the lamp is not selected.

3. Monitoring stability.

   Then burn the lamp at the working current and continuously measure lamp voltage and the photosignal of a monitor-detector (any visible or UV photo-detector). Turn the lamp off after every 2 h of burning time and allow it to cool down for at least 30 minutes. Then turn the lamp back on and continue measuring. Perform this cycle three times for a total of six hours of burn time. So, the working sequence for each time this step 3 is performed should be the following: ON 2h – OFF 0.5h – ON 2h – OFF 0.5h – ON 2h.

4. Analysis of stability.

   Then analyze the voltage and monitor signal when the lamp was ON (excluding the time for lamp heating (ca. 15 min.) of each ON period). If for the total ON time (6 hours) of the last time step 3 was performed no significant voltage jumps (> 0.05 V) are observed, the relative change of the voltage is less than $1.5 \cdot 10^{-4} \cdot h^{-1}$ and the relative change of the signal is less than $2 \cdot 10^{-4} \cdot h^{-1} \cdot (550\ nm/\lambda)$, respectively ($\lambda$ is the effective wavelength of the detector in nm), then the lamp is selected. If not, repeat the steps 3 and 4.

5. If the test is still failed after 72 h of seasoning, the lamp is not selected.

## 4.4. Aligning the lamps, instruction

Before measuring spectral irradiance, each lamp had to be aligned using the following instruction:

4.4.1 Position an alignment laser to define the optical axis of the spectral irradiance facility. It is assumed that the laser points towards the facility entrance optics, and the lamp is placed between the laser and the facility.

4.4.2 Carefully remove the protective cover while lying on a table (Fig. 4.2). Make sure that the fixing screw is untightened and the cover is not tilted while being removed.

4.4.3 The lamp envelope should never be touched. It is recommended that gloves are worn when handling the lamp, since any finger marks would be burnt into the lamp envelope when it is run and would result in changes in output or possibly even lamp failure.

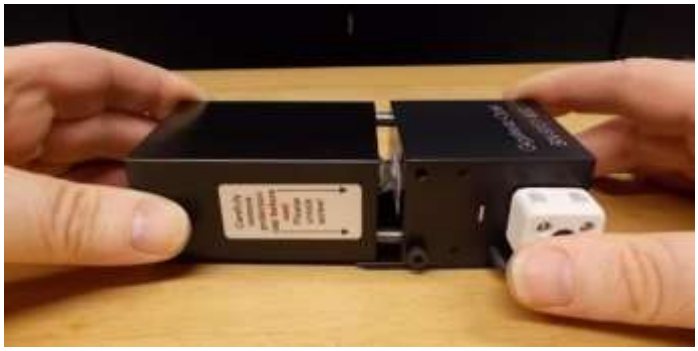

Figure 4.2. Removing the lamp cover

4.4.4 Place the lamp in a mount that provides 6 degrees of freedom (3 rotational and 3 positional)

4.4.5 Connect the four electrical terminals, observing the proper polarity, to a power supply and to the measuring devices for lamp current and lamp voltage (Fig.4.3). Do not switch on.

4.4.6 Position the alignment jig in the rear holes of the lamp holder. The side with the engraved crosslines on the alignment jig should face towards the laser (away from the measurement facility). The position of the warning sticker at the bottom of the alignment jig is thereby not taken into account (it may vary between different jigs).

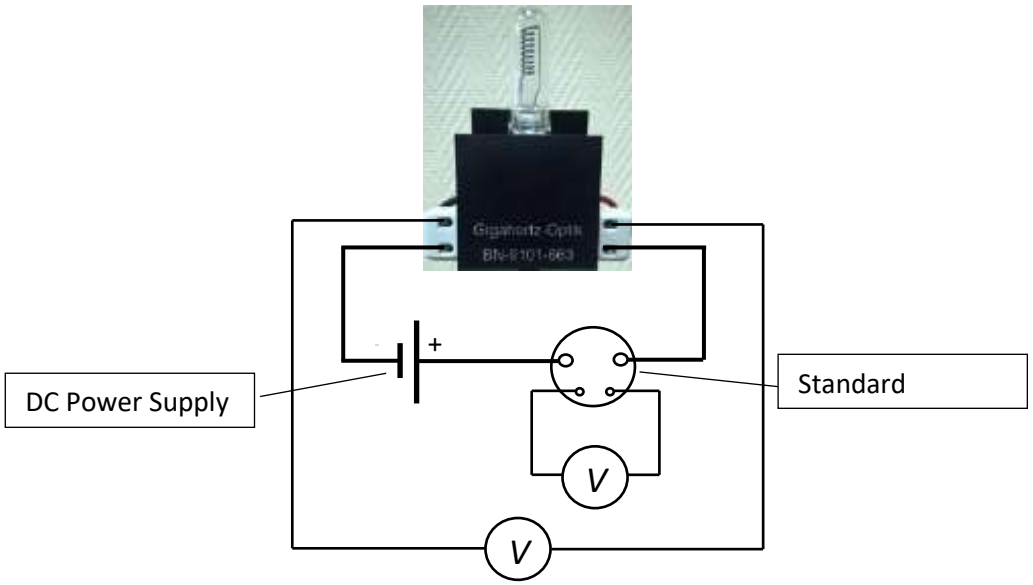


Figure 4.3. Electrical connections

4.4.7 Rest a spirit level on the top of the alignment jig (taking care not to touch the lamp envelope) and rotate the lamp such that the top of the jig is leveled (Fig.4.4).

4.4.8 Turn on the laser and move/rotate the lamp such that the laser hits the centre of the target and the laser beam is back-reflected back to the laser (Fig.4.5).

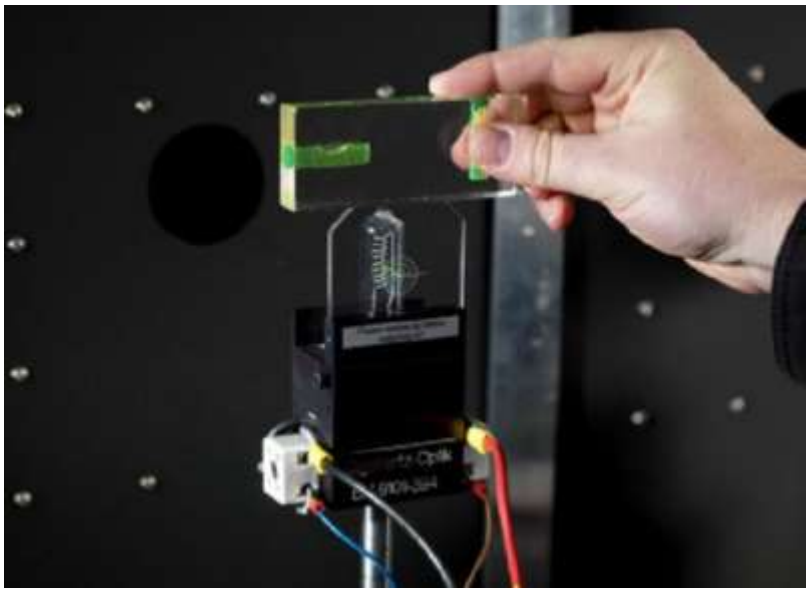

Figure 4.4. Aligning the lamp: using a level

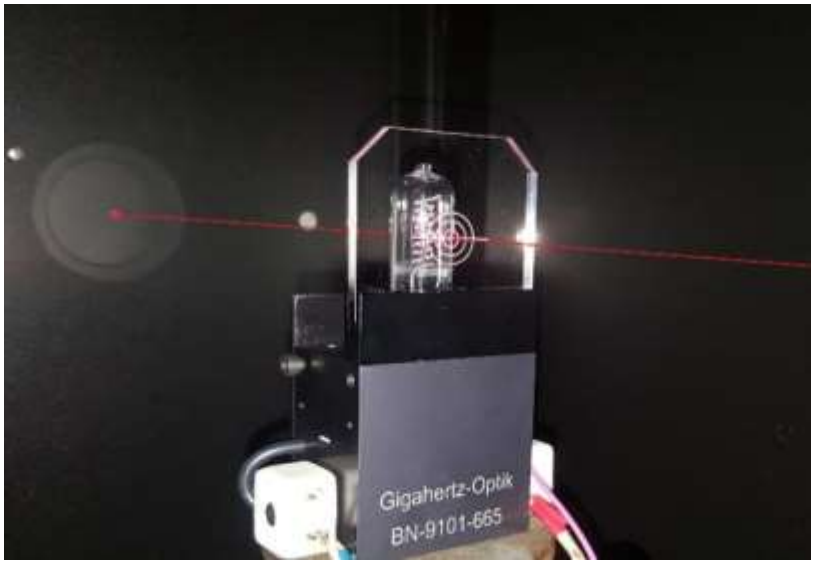


Figure 4.5. Aligning the lamp: using the laser

4.4.9 Move the lamp towards to the facility until the front plate of the lamp is 500 mm from the entrance reference plane of the spectral irradiance measurement facility. The area of the front plate to measure the distance from is above the upper central screw, as shown in Figure 4.6.

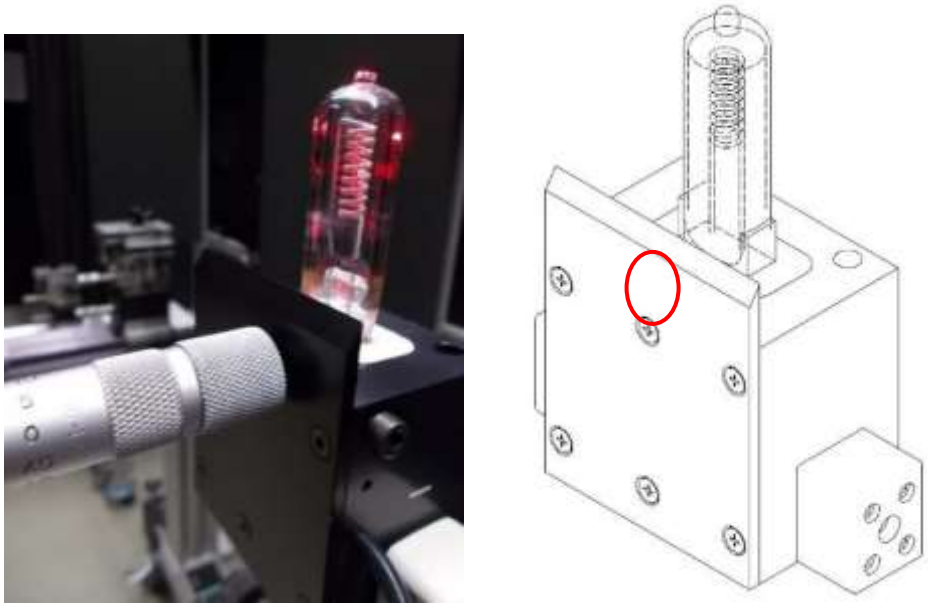

Figure 4.6. Measuring distance: The area of the front plate of the lamp to measure the distance from is marked by a red a circle.

4.4.10 Repeat step 4.4.8 to check the alignment

4.4.11 Carefully remove the alignment jig with a smooth upward lift. It should be easy to remove. If it is not easy to remove, then the alignment process should be repeated.

4.4.12 Repeat step 4.4.9 to check the distance.

4.4.13 Double check that the alignment jig has been removed before turning on a power supply.

## 4.5. Instruction of lamp warming-up and cooling-down

All participants had to use the following instructions for warming-up and cooling-down the lamps:

4.5.1 Check again that the alignment jig has been removed and that the power supply and the measurement devices for lamp current and voltage are connected with proper polarity before turning on.

4.5.2 The lamps should be turned on slowly by increasing the electrical current (voltage) over a 2 minute period to prevent sudden thermal shock.

4.5.3 Each lamp must be warmed up at the operational current (8.100 A) for at least 20 minutes prior to the measurements being taken. Check lamp current setting again after the warm-up time and write down the lamp voltage at that time.

4.5.4 After operation the lamp should be cooled down slowly by decreasing the electrical current (voltage) over a 2 minute period to prevent sudden thermal shock. The lamp should not be moved after switching off until the lamp base is cool enough to be touched (for approximately 20 to 30 minutes).

## 4.6. Measurement instruction

Spectral irradiance of each lamp had to be measured at the distance of 500 mm from the lamp reference plane (see section 4.4.9) for the defined operating current of 8.100 A in suitable ambient temperature of 20 to 25 °C. The ambient temperature of the laboratory during the time of the measurements should be reported. The spectral irradiance of each lamp had to be measured independently at least 3 times, each time after realignment of the lamp in the measurement facility. But only the mean or final spectral irradiance value for each lamp should be reported by the participant as a combination of the results of these independent measurements.

The other measurement instructions were the following:

4.6.1 Before use, the lamps should be inspected for any damage or contamination to the lamp envelope, lamp filament or lamp mount. Any damage should be documented with photos or a drawing and the pilot and participant should immediately exchange this information using the form in Appendix A.1 of the Technical Protocol.

4.6.2 The operating time for each lamp should be recorded each time the lamp is used during this comparison and a summary form, such as given in Appendix A.2 of the Technical Protocol, returned to the pilot laboratory with the lamps, as well as a part of the measurement report.

4.6.3 The power supply should be connected observing proper polarity with the positive (+) and negative (-) terminals clearly marked on the base of the lamp.

4.6.4 Before switching on the current to any lamp, the lamp should be aligned (see the section 4.4) and then all alignment jigs removed.

4.6.5 After connecting the electrical power to the lamps the prescribed warm-up procedure (see section 4.5) for each lamp should be followed. At the end of the warm-up time the lamp current should be adjusted to the exact value of 8.100 A, and the lamp voltage should be measured and recorded and compared with those supplied with the lamp. If the voltage is outside expected values for the lamp, the lamp should be turned off and this information exchanged between the participant and the pilot laboratory. The lamp voltage should be also measured and recorded after the spectral irradiance measurements before ramping down the lamp voltage.

4.6.6 The spectral irradiance of the traveling standards should then be measured at the specified wavelengths. If the participating laboratory cannot cover the complete spectral range, it should declare this before the start of the comparison.

4.6.7 The bandwidth used to measure the spectral irradiance should be less than 10 nm (Full Width at Half Maximum) and ideally less than 5 nm in the visible and UV spectral regions. The exact bandwidth used for each spectral point should be reported, together with the wavelength uncertainty. If the data is corrected for bandwidth, then the correction should be as though for negligible bandwidth.

4.6.8 No other measurements are to be attempted by the participants, nor any modification to the operating conditions during the course of this comparison. Any test measurements or modifications on the traveling standards should be carried out prior to the beginning of the comparison.

4.6.9 Any information obtained relating to the use or any results obtained by a participant during the course of the comparison shall be sent only to the pilot laboratory, who will be responsible for coordinating how the information should be disseminated to other participants.

## 4.7. Instruction for reporting results

On completion of the first round of measurements by the participating laboratory the provisional results of these measurements should be sent to the pilot laboratory together with the standard lamps.

As soon as possible after the completion of the second round of measurements the participant should provide a full measurement report. This should include the measurement results of both rounds, description of the scale realization, description of the measurement facility and procedure, a schematic diagram of the facility and full uncertainty analysis.

The uncertainty budget of each of the traveling standard lamps should include the following components:

***Type B***:

- Uncertainty of the s***cale***. This is the uncertainty of the scale realization if the traveling standard lamps are calibrated directly against the primary standard (a blackbody); Or the uncertainty of the working standard lamp if that is used to calibrate the traveling standard.
- Uncertainty associated with the ***distance*** from the working standard lamp (or blackbody), and from the traveling standard lamp.
- Uncertainty associated with the operating ***current of the working standard lamp***.
- Uncertainty associated with the operating ***current of the traveling standard lamp***.
- Uncertainty associated with ***wavelength*** setting.
- Other components such as non-linearity, stability, stray light etc. might be included in the budget if necessary.

***Type A:***

- ***Reproducibility*** – Standard deviation of the mean calculated from the results of independent measurements, where each independent measurement is carried out after realignment of the traveling standard lamp and (if necessary) the working standard.
- ***Repeatability*** of traveling / working standard lamp – Standard deviation of the mean calculated from a set of readings when measuring the traveling / working standard lamp.

Reproducibility already partly includes repeatability. Therefore, when combining all components, the repeatability components should be divided by a factor of $1/\sqrt{n}$ part where $n$ is the number of independent measurements.

All values should be given as standard uncertainties, in other words, for a coverage factor of $k$=1.

Each wavelength is considered entirely independently for this comparison.

# 5. Measurement facilities and uncertainty budgets

Measurement facilities and procedures as well as uncertainty budgets of all participants are described below as submitted by the participants.

## 5.1. VNIIOFI (Pilot), Russia

### 5.1.1. VNIIOFI Measurement facility

The VNIIOFI spectral irradiance facility is shown schematically in Figure 5.1.1. The facility consists of the following elements:

1. High-temperature blackbody of BB3500M type
2. Precision aperture
3. Lamps to be measured
4. Alignment lasers
5. Radiation thermometer
6. Integrating sphere
7. Monochromator
8. Detectors
9. Focusing mirror
10. Flat mirrors
11. Alignment laser
12. Set of light shields
13. Shutters

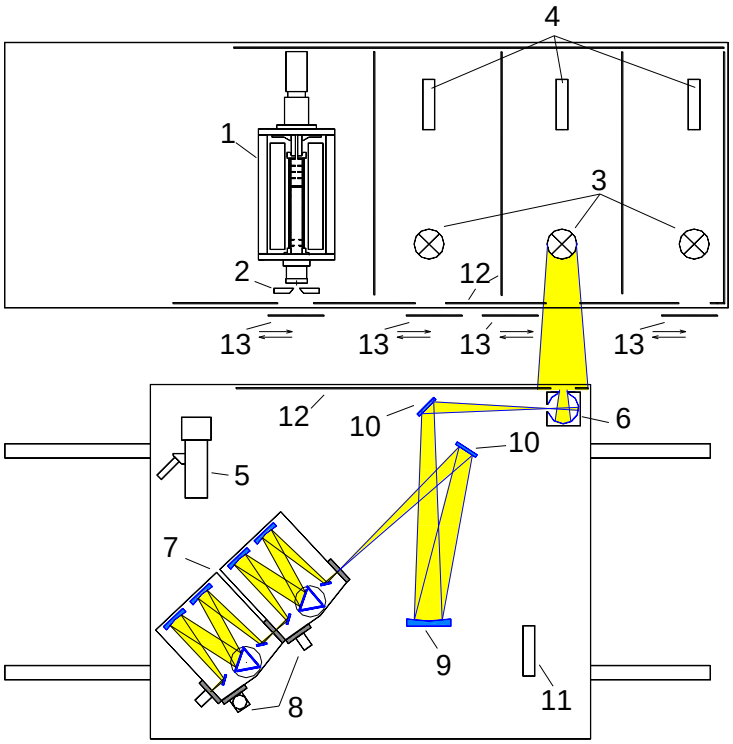


Figure 5.1.1. Spectral Irradiance facility of VNIIOFI

The blackbody and lamps were installed on an optical table and covered with a light tight box with holes in front of the sources equipped with shutters (13).

In front of the sources there was a spectral comparator that consisted of the integrating sphere (6), monochromator (7), focusing optics (9, 10) and detectors (8). The comparator was assembled on a translation stage, moving along the sources. The radiation thermometer (5) and the alignment laser (11) were installed on the same translation stage. The optical table top of the translation stage was covered with a light tight box with holes in front of the sphere and thermometer.

Spectral irradiance of the sources was measured in the plane of the entrance aperture of the integrating sphere. The distance from the lamps to the sphere was 500 mm, and the distance from the blackbody aperture to the sphere was approximately 470 mm. The exit aperture of the sphere was imaged to the monochromator entrance slit by the focusing mirror through the flat mirrors.

Each lamp measured at VNIIOFI (in both cases, when VNIIOFI as a participant measured its own lamps, and when it as a pilot measures all participant lamps) was measured by comparing with the blackbody.

There were two lamp posts in the facility. Two lamps simultaneously were aligned and prepared for measurement. However, the lamps were measured one by one. Only one lamp was ON and measured each time.

#### *5.1.1.1. Blackbody*

Blackbody used was the high-temperature blackbody of BB3500M type developed at VNIIOFI with a pyrolytic graphite radiator and the temperature range from 1200 K to 3500 K [6]. During the present comparison the blackbody was used at the temperature of 2750 K.

The emissivity was estimated to be 0.9995 using the STEEP321 modeling software [7,8] based on the Monte Carlo ray tracing method for axially symmetric non-isothermal cavities.

An optical feedback system was used for stabilizing the blackbody radiation. The typical noise and drift of the blackbody temperature was ± 0.02 K and 0.1K/h, respectively, at the level of 2750 K.

The temperature of the blackbody was measured with a radiation thermometer of the TSP type [9] with central wavelength of 650 nm, bandwidth of 20 nm and target size of approximately 1.0 x 1.5 mm. The thermometer was originally calibrated against three high-temperature fixed points (HTFP): Co-C (1567.39 K), Re-C (2747.84 K) and WC-C (3020.6 K) [10-13]. Then during whole the comparison measurement time TSP calibration was periodically checked against the Re-C point and corrected.

In front of the blackbody there was an aperture with diameter of 12 mm in a water-cooled jacket. The precise average diameter of the aperture was measured at the facility traceable to the national standard of metre. The temperature of the aperture holder was stabilised at the level of 20 ºC using a water circulating thermostat.

#### *5.1.1.2. Integrating sphere*

The integrating sphere had an internal diameter of 40 mm and was covered inside with PTFE. The sphere had two apertures located on orthogonal sides: a circular entrance aperture with diameter of 11 mm and an exit slit with the dimensions of 4×15 mm.

#### *5.1.1.3. Monochromator*

The monochromator used was an additive-mode double grating monochromator of the DTMc300 type (producer is Bentham Instruments Limited) with focal length of 300 mm. Three pairs of gratings were used: presented in Table 1.1. In the range from 1700 nm to 2500 nm the

monochromator was used as a single one, i.e. a detector was attached to the exit slit of the first monochromator.

Wavelength accuracy and wavelength repeatability of the monochromator were 0.15 nm and 0.05 nm, respectively.

Table 5.1.1. Monochromator gratings used at the VNIIOFI facility.

| Spectral range, nm | Line density, g/mm | Blaze wavelength, nm | Linear dispersion, nm/mm |
|---|---|---|---|
| 250-400 | 1200 | 250 | 1.35 (additive) |
| 400-1000 | 1200 | 500 | 1.35 (additive) |
| 1000-2500 | 600 | 1600 | 2.7 (additive)<br>5.4 (single) |

The slit width used was 2.2 mm for both entrance and exit slits in whole spectral range. Therefore, the bandwidth was:

3 nm for the range from 250 nm to 1100 nm
6 nm for the range from 1100 nm to 1700 nm
12 nm for the range from 1700 nm to 2500 nm

#### *5.1.1.4. Bandwidth correction*

Bandwidth correction was applied following analysis presented in the section 5.4.2.1 of the CCPR-K1b final report [14]. The correction factor was calculated as

$$k_{BW}(\lambda_i) = \frac{\left(S_{Lamp}(\lambda_i) + \Delta S_{Lamp}(\lambda_i)\right)/\left(S_{BB}(\lambda_i) + \Delta S_{BB}(\lambda_i)\right)}{R(\lambda_i)} \tag{5.1.1}$$

Where $S_{Lamp}(\lambda_i)$ and $S_{BB}(\lambda_i)$ are signals of the lamp and blackbody, respectively, at the wavelength $\lambda_i$. $R(\lambda_i)$ is the measured ratio of lamp-to-blackbody signals. $\Delta S_{Lamp}(\lambda_i)$ and $\Delta S_{BB}(\lambda_i)$ are corrections to the signals of the lamp and blackbody, respectively, calculated as

$$\Delta S(\lambda_i) = -\frac{b^2}{12}\left[\frac{S(\lambda_{i-1}) - 2S(\lambda_i) + S(\lambda_{i+1})}{(\Delta\lambda)^2}\right] \tag{5.1.2}$$

where $b$ is the bandwidth (4.05 nm, 8.1 nm, or 16.2 nm depending on wavelength), and $\Delta\lambda$ is the spectral step. Typical correction factors are presented in Table 5.1.2.

Table 5.1.2. Typical Bandwidth correction factor for the VNIIOFI facility.

| $\lambda$, nm | $k_{BW}(\lambda)$ | $\lambda$, nm | $k_{BW}(\lambda)$ | $\lambda$, nm | $k_{BW}(\lambda)$ | $\lambda$, nm | $k_{BW}(\lambda)$ |
|---|---|---|---|---|---|---|---|
| 250 | 1.0005 | 340 | 1.0001 | 600 | 1.0000 | 1500 | 1.0000 |
| 260 | 1.0005 | 360 | 1.0001 | 700 | 1.0000 | 1700 | 1.0000 |
| 270 | 1.0005 | 380 | 1.0001 | 800 | 1.0000 | 2000 | 1.0000 |
| 280 | 1.0005 | 400 | 1.0001 | 900 | 1.0000 | 2200 | 1.0000 |
| 290 | 1.0005 | 450 | 1.0001 | 1000 | 1.0000 | 2300 | 1.0000 |
| 300 | 1.0004 | 500 | 1.0000 | 1100 | 1.0000 | 2400 | 1.0000 |
| 320 | 1.0003 | 555 | 1.0000 | 1300 | 1.0000 | 2500 | 1.0000 |

#### *5.1.1.5. Detectors*

Four detectors were used:

- In the range 250 nm to 450 nm: PMT of the type Hamamatsu R7446P with voltage of 540 V for 250-300 nm and 330 V for 320-450 nm;
- In the range 450 nm to 1000 nm: Silicon photodiode S1337;
- In the range 1000 nm to 1700 nm: InGaAs photodiode, type Hamamatsu G8370-85;
- In the range 1700 nm to 2500 nm: PbS photoresistor, type Hamamatsu P9217-04.

All detectors were used at room temperature.

PbS was connected directly to the exit slit of the first monochromator. PMT and the photodiodes were connected to exit slit of the second monochromator and were changed manually.

The PMT, Si and InGaAs photodiodes were used with a current-voltage converter amplifier. The PbS photoresistor was used together with an optical chopper (EG&G model 197) at the frequency of 121 Hz. The signal of PbS was detected by a lock-in amplifier, model SR810. The output voltage of the amplifiers was measured by a 6½ digital voltmeter.

#### *5.1.1.6. Alignment*

There were three alignment lasers in the facility: two behind the lamps (number 4 in the Fig. 1.1) and the third on the translation stage (number 11). The lasers were preliminary aligned against each other, so when the laser 11 stood opposite any of the lasers 4, their beams coincided. Then the laser 11 was used for aligning the blackbody and its aperture. One of the lasers 4 was used for aligning the integrating sphere. Both lasers 4 were then used for aligning each measured lamp. Typical accuracy of positioning the blackbody aperture, integrating sphere and lamps was approximately 0.5 mm.

#### *5.1.1.7. Distance measurement*

Distance between the lamp and the sphere, as well as between the blackbody aperture and the sphere, was measured using an extension rod-type micrometer (produced by Mitutoyo). The accuracy of the micrometer is 10 μm. However, the actual uncertainty of the distance measurement was higher due to backlash of the mounts of the sphere, aperture and lamps. The distance from the sphere to the aperture was approximately 488 mm and was measured with standard uncertainty of 0.07 mm. A lamp was set at the distance of 500.00 mm within the standard uncertainty of 0.05 mm.

#### *5.1.1.8. Lamp current measurement*

Each lamp post was equipped with a DC power supply. To measure the lamp current, a precision resistor of 0.1 Ω was connected to the electrical circuit of each post in series with the lamp. The voltage across the resistors was measure by 6½ digital voltmeters. Two other voltmeters were used for measuring lamp voltage.

#### *5.1.1.9. Changing lamp posts*

Each lamp was measured at least three times. The lamp post changed every time. No systematic difference between posts was detected.

#### *5.1.1.10. Laboratory conditions*

Room temperature in the laboratory was maintained within (20 ± 1) °C for the whole period of the comparison measurements.

### 5.1.2. Primary scale realisation

The spectral irradiance scale was realised using a high-temperature blackbody of the BB3500M type where the blackbody spectral irradiance $E_{\lambda,\mathrm{BB}}(\lambda,T)$ was calculated from the Planck equation:

$$E_{\lambda,\mathrm{BB}}(\lambda,T) = \frac{A}{l^2}\cdot g\cdot \varepsilon_{\mathrm{eff}}\cdot\frac{c_1}{\pi\lambda^5 n^2}\cdot\frac{1}{\exp\left(\frac{c_2}{\lambda T n}\right)-1} \qquad (5.1.3)$$

where $c_1 = 2\pi hc^2$ = 3,741771852·10$^{-16}$ W m$^2$ – the first radiation constant,
$c_2 = hc/k$ = 1,438776877·10$^{-2}$ m K – the second radiation constant,
$h$ = 6.626 070 15 × 10$^{-34}$ J s – the Planck constant,
$c$ = 299 792 458 m/s – the speed of light in vacuum,
$k$ = 1.380 649 × 10$^{-23}$ J/K – the Boltzmann constant,
$\lambda$ – wavelength,
$T$ – thermodynamic temperature of blackbody cavity,
$n$ – refractive index of air,
$\varepsilon_{\mathrm{eff}}$ – effective emissivity of the blackbody,
$A$ – area of the blackbody aperture,
$l$ – distance between the aperture and the entrance of the integrating sphere,
$g$ – geometric correction factor that takes into account non-point sizes of the blackbody aperture and the sphere entrance diaphragm.

The values of air refractive index applied at VNIIOFI are shown in Table 5.1.3

Table 5.1.3. Values of refractive index of air applied at VNIIOFI.

| $\lambda$ , nm | $k_{BW}(\lambda)$ | $\lambda$ , nm | $k_{BW}(\lambda)$ | $\lambda$ , nm | $k_{BW}(\lambda)$ | $\lambda$ , nm | $k_{BW}(\lambda)$ |
|---|---|---|---|---|---|---|---|
| 250 | 1.000295 | 340 | 1.000282 | 600 | 1.000272 | 1500 | 1.000269 |
| 260 | 1.000293 | 360 | 1.000281 | 700 | 1.000271 | 1700 | 1.000268 |
| 270 | 1.000291 | 380 | 1.000279 | 800 | 1.000270 | 2000 | 1.000268 |
| 280 | 1.000290 | 400 | 1.000278 | 900 | 1.000270 | 2200 | 1.000268 |
| 290 | 1.000288 | 450 | 1.000276 | 1000 | 1.000269 | 2300 | 1.000268 |
| 300 | 1.000287 | 500 | 1.000274 | 1100 | 1.000269 | 2400 | 1.000268 |
| 320 | 1.000284 | 555 | 1.000273 | 1300 | 1.000269 | 2500 | 1.000268 |

The geometric correction was calculated as:

$$g = 2l^2/\left[r_{\mathrm{A}}^2 + r_{\mathrm{S}}^2 + l^2 + ((r_{\mathrm{A}}^2 + r_{\mathrm{S}}^2 + l^2)^2 - 4r_{\mathrm{A}}^2 r_{\mathrm{S}}^2)^{1/2}\right] \qquad (5.1.4)$$

where $r_{\mathrm{A}}$ and $r_{\mathrm{S}}$ are radii of the blackbody aperture and the sphere entrance diaphragm, respectively.

### 5.1.3. Uncertainty budget

#### *5.1.3.1. Uncertainty components associated with the blackbody (scale realisation)*

5.1.3.1.1. The first and second **radiation constants** $c_1$ and $c_2$ of the Planck law are derived from the defining constants of the SI and, therefore, have zero uncertainties.

5.1.3.1.2. Air **refractive index** (**n**) estimation depends on a model and air conditions such as temperature, pressure and humidity. Humidity has low influence on change of **n**. The temperature in the lab was maintained within ± 1 °C and, therefore, also has low influence. Atmospheric pressure varied during the pilot measurement campaign (April 2018 to February 2019) from 987 kPa to 1047 kPa and, therefore, had the main influence. The standard uncertainty of **n** was estimated as $0.5 \cdot 10^{-5}$ in the spectral range from 300 nm to 1700 nm, where the models work well, and as $1 \cdot 10^{-5}$ outside this range. The blackbody spectral irradiance uncertainty associated with **n** was calculated using the Planck law. *Random effect*.

5.1.3.1.3. Estimation of the blackbody **emissivity** and its uncertainty was based on modeling using the STEEP321 software [7,8]. The emissivity was estimated to be approximately equal to 0.9995 with the standard uncertainty of 0.03 % in visible and IR and 0.06 % in UV. *Systematic effect*.

5.1.3.1.4. Blackbody temperature measurement uncertainty included four components associated with the following sources: uncertainty of realisation of the Re-C fixed point; the blackbody uniformity; the radiation thermometer stability; and the blackbody stability. The temperature uncertainty components are described below. The associated blackbody spectral irradiance uncertainties were calculated using the Planck law.

5.1.3.1.4.1. The standard uncertainty of **realisation of the Re-C** fixed point was estimated to be 0.31 K following the CCT recommendations [15]. *Systematic effect*.

5.1.3.1.4.2. The **blackbody non-uniformity** was estimated on the base of preliminary blackbody mapping. It corresponds to the temperature non-uniformity standard uncertainty of approximately 0.15 K. *Systematic effect*.

5.1.3.1.4.3. The standard uncertainty associated **with instability of the radiation thermometer** was estimated as 0.09 K from the data of periodical thermometer calibration against the Re-C fixed point. *Random effect*.

5.1.3.1.4.4. **Blackbody instability** was measured directly during the lamp calibration. The typical temperature instability standard uncertainty was 0.04 K which was combined from a typical drift (0.1K/h divided by 2 and by $3^{1/2}$) and the typical noise (0.02 K). *Random effect*.

5.1.3.1.5. It is known [16] that radiation of a graphite blackbody suffers from **absorption** of carbon-based molecules ($C_2$, $C_3$, CN) at high temperatures. All lamps within this comparison were measured against the blackbody at the temperature of 2748 K. But VNIIOFI lamps were additionally measured against the blackbody at 3020 K. The measurement results had systematic differences in UV. The Fig. 5.1.2 shows the average difference $\Delta_{abs}$ between calibration at 3020 K and calibration at 2748 K. We think the absorption is the reason of the difference. Although we assume that at 2748 K the absorption is negligible, we introduce an uncertainty component $u_c(\text{abs})$ associated with possible absorption effect: $u_c(\text{abs}) = \Delta_{abs}/2/3^{1/2}$. *Systematic effect*.

5.1.3.1.6. Diameter of the blackbody **aperture** was 12.135 mm. Its area was known with standard uncertainty of 0.05 %. *Systematic effect*.

5.1.3.1.7. Standard uncertainty of the **distance from the blackbody** to the sphere (488 mm) consisted of two components: *Systematic*, 0.06 mm, and *Random*, 0.04 mm. Corresponding spectral irradiance standard uncertainty components are 0.03 % and 0.02 %.

Summary of the uncertainty budget of spectral irradiance scale realization with the high-temperature blackbody is presented in Table 5.1.4.

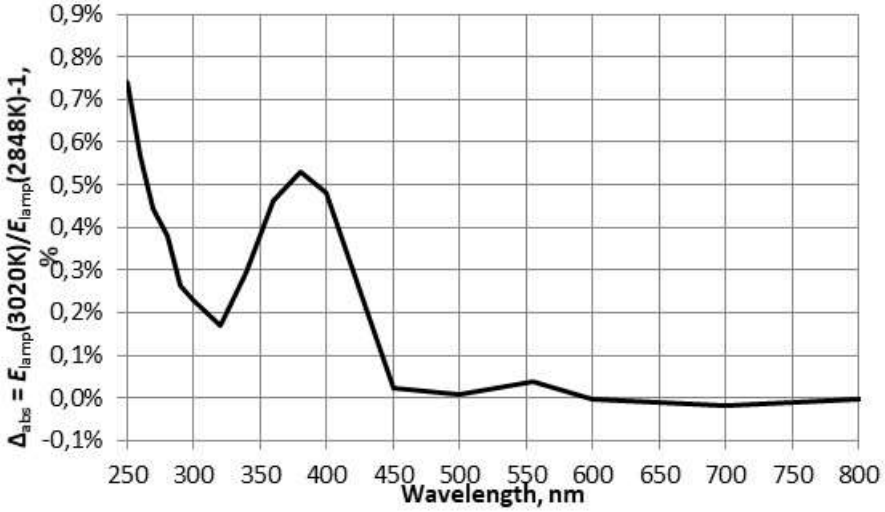


Figure 5.1.2. Average difference $\Delta_{abs}$ between spectral irradiances of lamps measured at VNIIOFI against the blackbody at the temperatures of 3020 K and 2748 K.

### *5.1.3.2. Uncertainty components associated with traveling lamp measurement*

5.1.3.2.1. Standard uncertainty of a **lamp current measurement** was 0.5 mA. The lamp current was 8.1000 A. *Systematic effect*.

5.1.3.2.2. Standard uncertainty of a **lamp current stability** was 0.3 mA. *Random effect*.

5.1.3.2.3. Standard uncertainty of the **distance from a lamp** to the sphere (500.00 mm) consisted of two components: *Systematic*, 0.03 mm, and *Random*, 0.04 mm. Corresponding spectral irradiance standard uncertainty components are 0.01 % and 0.02 %.

5.1.3.2.4. **Wavelength accuracy** of the monochromator $\Delta\lambda$ is better than 0.15 nm. Corresponding lamp spectral irradiance standard uncertainty was calculated as

$$u_{wa} = \frac{dR(\lambda)}{R(\lambda)d\lambda} \cdot \Delta\lambda/\sqrt{3} \qquad (5.1.5)$$

where $R(\lambda)$ is the lamp-to-blackbody ratio measured using the spectral comparator. *Systematic effect*.

5.1.3.2.5. **Wavelength repeatability** is 0.05 nm. Corresponding uncertainty was evaluated using the Eq. 5.1.5 for the wavelength ranges from 250 nm to 300 nm and from 1700 nm to 2500 nm where the ration *R* (*lamp signal / BB signal)* was measured at each wavelength without changing the wavelength. In the range from 320 nm to 1500 nm first the lamp signals were measured by scanning wavelength and then the BB signals were measured. In this range the standard uncertainty was calculated as:

$$u_{wr} = \left( \left( \frac{dS_{\mathrm{BB}}(\lambda)}{S_{\mathrm{BB}}(\lambda)d\lambda} \right)^2 + \left( \frac{dS_{\mathrm{lamp}}(\lambda)}{S_{\mathrm{lamp}}(\lambda)d\lambda} \right)^2 \right)^{1/2} \cdot \Delta\lambda/\sqrt{3} \qquad (5.1.6)$$

where $S_{\mathrm{BB}}(\lambda)$ and $S_{\mathrm{lamp}}(\lambda)$ are signals of the blackbody and lamp, respectively. *Random effect*.

5.1.3.2.6. **Repeatability of lamp measurement** uncertainty component was estimated as the Type A uncertainty, namely as an average (over 36 individual lamps) of standard deviations calculated from independent measurements for each lamp. Independent measurements were done with total realignment of a lamp and the blackbody aperture.

Summary of the uncertainty budget of a lamp spectral irradiance measurement at VNIIOFI as a participant presented in Table 5.1.5.

Table 5.1.4. Standard uncertainty components of the blackbody spectral irradiance in % (Uncertainty budget of scale realisation at VNIIOFI)

| λ, nm | Air refractive index | Blackbody Emissivity | Blackbody Temperature measurement | | | | Self-absorption of BB radiation | Aperture D=12.135 mm *u*=0.003 mm | Blackbody-to-sphere Distance Systematic *u*=0.06 mm | Blackbody-to-sphere Distance Random *u*=0.04 mm | $u_{BB,s}$ Total systematic | $u_{BB,r}$ Total random | $u_{BB,c}$ combined |
|---|---|---|---|---|---|---|---|---|---|---|---|---|---|
| | | | Realisation of Re-C *u*=0.31K | Blackbody Uniformity *u*=0.15K | TSP Stability *u*=0.09K | Blackbody Stability *u*=0.04K | | | | | | | |
| | Uncorrelated | Correlated | Correlated | Correlated | Corr. | Uncorrelated | Correlated | Correlated | Correlated | Uncorrelated | Correlated | Uncorrelated | |
| 250 | 0.02 | 0.06 | 0.24 | 0.11 | 0.07 | 0.03 | 0.20 | 0.05 | 0.03 | 0.02 | 0.34 | 0.08 | 0.35 |
| 260 | 0.02 | 0.06 | 0.23 | 0.11 | 0.07 | 0.03 | 0.16 | 0.05 | 0.03 | 0.02 | 0.31 | 0.08 | 0.32 |
| 270 | 0.02 | 0.06 | 0.22 | 0.11 | 0.06 | 0.03 | 0.13 | 0.05 | 0.03 | 0.02 | 0.29 | 0.07 | 0.30 |
| 280 | 0.02 | 0.06 | 0.21 | 0.10 | 0.06 | 0.03 | 0.11 | 0.05 | 0.03 | 0.02 | 0.27 | 0.07 | 0.28 |
| 290 | 0.02 | 0.06 | 0.20 | 0.10 | 0.06 | 0.03 | 0.08 | 0.05 | 0.03 | 0.02 | 0.25 | 0.07 | 0.26 |
| 300 | 0.02 | 0.06 | 0.18 | 0.10 | 0.06 | 0.03 | 0.07 | 0.05 | 0.03 | 0.02 | 0.25 | 0.07 | 0.26 |
| 320 | 0.01 | 0.06 | 0.17 | 0.09 | 0.05 | 0.02 | 0.05 | 0.05 | 0.03 | 0.02 | 0.22 | 0.06 | 0.23 |
| 340 | 0.01 | 0.06 | 0.16 | 0.08 | 0.05 | 0.02 | 0.10 | 0.05 | 0.03 | 0.02 | 0.23 | 0.06 | 0.24 |
| 360 | 0.01 | 0.06 | 0.16 | 0.08 | 0.05 | 0.02 | 0.13 | 0.05 | 0.03 | 0.02 | 0.24 | 0.06 | 0.24 |
| 380 | 0.01 | 0.06 | 0.15 | 0.08 | 0.05 | 0.02 | 0.15 | 0.05 | 0.03 | 0.02 | 0.25 | 0.06 | 0.25 |
| 400 | 0.01 | 0.03 | 0.13 | 0.08 | 0.04 | 0.02 | 0.14 | 0.05 | 0.03 | 0.02 | 0.23 | 0.05 | 0.23 |
| 450 | 0.00 | 0.03 | 0.12 | 0.07 | 0.04 | 0.02 | 0.00 | 0.05 | 0.03 | 0.02 | 0.16 | 0.05 | 0.17 |
| 500 | 0.00 | 0.03 | 0.11 | 0.06 | 0.03 | 0.02 | 0.00 | 0.05 | 0.03 | 0.02 | 0.15 | 0.04 | 0.15 |
| 555 | 0.00 | 0.03 | 0.10 | 0.06 | 0.03 | 0.01 | 0.00 | 0.05 | 0.03 | 0.02 | 0.14 | 0.04 | 0.14 |
| 600 | 0.00 | 0.03 | 0.08 | 0.05 | 0.03 | 0.01 | 0.00 | 0.05 | 0.03 | 0.02 | 0.13 | 0.04 | 0.13 |
| 700 | 0.00 | 0.03 | 0.07 | 0.05 | 0.02 | 0.01 | 0.00 | 0.05 | 0.03 | 0.02 | 0.11 | 0.03 | 0.11 |
| 800 | 0.00 | 0.03 | 0.07 | 0.04 | 0.02 | 0.01 | 0.00 | 0.05 | 0.03 | 0.02 | 0.10 | 0.03 | 0.11 |
| 900 | 0.00 | 0.03 | 0.06 | 0.04 | 0.02 | 0.01 | 0.00 | 0.05 | 0.03 | 0.02 | 0.10 | 0.03 | 0.10 |
| 1000 | 0.00 | 0.03 | 0.05 | 0.03 | 0.02 | 0.01 | 0.00 | 0.05 | 0.03 | 0.02 | 0.09 | 0.03 | 0.10 |
| 1100 | 0.00 | 0.03 | 0.05 | 0.03 | 0.02 | 0.01 | 0.00 | 0.05 | 0.03 | 0.02 | 0.09 | 0.03 | 0.09 |
| 1300 | 0.00 | 0.03 | 0.04 | 0.03 | 0.01 | 0.01 | 0.00 | 0.05 | 0.03 | 0.02 | 0.08 | 0.02 | 0.09 |
| 1500 | 0.00 | 0.03 | 0.04 | 0.02 | 0.01 | 0.01 | 0.00 | 0.05 | 0.03 | 0.02 | 0.08 | 0.02 | 0.08 |
| 1700 | 0.00 | 0.03 | 0.03 | 0.02 | 0.01 | 0.01 | 0.00 | 0.05 | 0.03 | 0.02 | 0.08 | 0.02 | 0.08 |
| 2000 | 0.00 | 0.03 | 0.03 | 0.02 | 0.01 | 0.00 | 0.00 | 0.05 | 0.03 | 0.02 | 0.07 | 0.02 | 0.08 |
| 2200 | 0.00 | 0.03 | 0.03 | 0.02 | 0.01 | 0.00 | 0.00 | 0.05 | 0.03 | 0.02 | 0.07 | 0.02 | 0.08 |
| 2300 | 0.00 | 0.03 | 0.03 | 0.01 | 0.01 | 0.00 | 0.00 | 0.05 | 0.03 | 0.02 | 0.07 | 0.02 | 0.08 |
| 2400 | 0.00 | 0.03 | 0.03 | 0.01 | 0.01 | 0.00 | 0.00 | 0.05 | 0.03 | 0.02 | 0.07 | 0.02 | 0.08 |
| 2500 | 0.00 | 0.03 | 0.03 | 0.01 | 0.01 | 0.00 | 0.00 | 0.05 | 0.03 | 0.02 | 0.07 | 0.02 | 0.08 |

Table 5.1.5. Standard uncertainty budget of lamp spectral irradiance measurement at VNIIOFI **as participant**, in %

| λ, nm | $u_{BB,s}$ systematic | $u_{BB,r}$ Total random | Lamp current measurement uc=0.5 mA | Lamp current stability uc=0.3 mA | Wavelength accuracy 0.15 nm | Wavelength repeatability 0.05 nm | Distance from lamp Systematic, u(l)=0.03 mm 500 mm | Distance from lamp Random, u(l)=0.04 mm 500 mm | Repeatability of lamp meas-t Type A $u_{repeat}$ | $u_{VNIIOFI,s}$ systematic | $u_{VNIIOFI,r}$ random | **$u_{VNIIOFI,c}$ combined standard** |
|---|---|---|---|---|---|---|---|---|---|---|---|---|
| | Correlated | Uncorrelated | Correlated | Uncorrelated | Correlated | Uncorrelated | Correlated | Uncorrelated | Uncorrelated | Correlated | Uncorrelated | |
| 250 | 0.34 | 0.08 | 0.07 | 0.04 | 0.03 | 0.01 | 0.01 | 0.02 | 0.30 | 0.30 | 0.31 | **0.43** |
| 260 | 0.31 | 0.08 | 0.07 | 0.04 | 0.03 | 0.01 | 0.01 | 0.02 | 0.22 | 0.29 | 0.24 | **0.38** |
| 270 | 0.29 | 0.07 | 0.07 | 0.04 | 0.03 | 0.01 | 0.01 | 0.02 | 0.20 | 0.28 | 0.22 | **0.36** |
| 280 | 0.27 | 0.07 | 0.07 | 0.04 | 0.04 | 0.01 | 0.01 | 0.02 | 0.20 | 0.26 | 0.22 | **0.34** |
| 290 | 0.25 | 0.07 | 0.06 | 0.04 | 0.04 | 0.01 | 0.01 | 0.02 | 0.18 | 0.25 | 0.20 | **0.32** |
| 300 | 0.25 | 0.07 | 0.06 | 0.04 | 0.04 | 0.01 | 0.01 | 0.02 | 0.17 | 0.25 | 0.19 | **0.31** |
| 320 | 0.22 | 0.06 | 0.06 | 0.03 | 0.04 | 0.10 | 0.01 | 0.02 | 0.15 | 0.25 | 0.16 | **0.30** |
| 340 | 0.23 | 0.06 | 0.05 | 0.03 | 0.04 | 0.10 | 0.01 | 0.02 | 0.14 | 0.24 | 0.16 | **0.29** |
| 360 | 0.24 | 0.06 | 0.05 | 0.03 | 0.03 | 0.10 | 0.01 | 0.02 | 0.13 | 0.23 | 0.15 | **0.27** |
| 380 | 0.25 | 0.06 | 0.05 | 0.03 | 0.03 | 0.10 | 0.01 | 0.02 | 0.12 | 0.24 | 0.14 | **0.28** |
| 400 | 0.23 | 0.05 | 0.04 | 0.02 | 0.03 | 0.10 | 0.01 | 0.02 | 0.11 | 0.22 | 0.12 | **0.25** |
| 450 | 0.16 | 0.05 | 0.04 | 0.02 | 0.02 | 0.10 | 0.01 | 0.02 | 0.10 | 0.19 | 0.12 | **0.22** |
| 500 | 0.15 | 0.04 | 0.03 | 0.02 | 0.02 | 0.10 | 0.01 | 0.02 | 0.10 | 0.18 | 0.11 | **0.21** |
| 555 | 0.14 | 0.04 | 0.03 | 0.02 | 0.02 | 0.05 | 0.01 | 0.02 | 0.10 | 0.15 | 0.11 | **0.19** |
| 600 | 0.13 | 0.04 | 0.02 | 0.01 | 0.01 | 0.02 | 0.01 | 0.02 | 0.09 | 0.13 | 0.10 | **0.16** |
| 700 | 0.11 | 0.03 | 0.02 | 0.01 | 0.01 | 0.02 | 0.01 | 0.02 | 0.09 | 0.12 | 0.10 | **0.16** |
| 800 | 0.10 | 0.03 | 0.02 | 0.01 | 0.01 | 0.02 | 0.01 | 0.02 | 0.09 | 0.11 | 0.10 | **0.15** |
| 900 | 0.10 | 0.03 | 0.02 | 0.01 | 0.01 | 0.02 | 0.01 | 0.02 | 0.08 | 0.11 | 0.09 | **0.14** |
| 1000 | 0.09 | 0.03 | 0.01 | 0.01 | 0.01 | 0.02 | 0.01 | 0.02 | 0.08 | 0.10 | 0.09 | **0.13** |
| 1100 | 0.09 | 0.03 | 0.01 | 0.01 | 0.01 | 0.02 | 0.01 | 0.02 | 0.08 | 0.09 | 0.09 | **0.13** |
| 1300 | 0.08 | 0.02 | 0.01 | 0.01 | 0.01 | 0.02 | 0.01 | 0.02 | 0.08 | 0.09 | 0.09 | **0.13** |
| 1500 | 0.08 | 0.02 | 0.01 | 0.00 | 0.01 | 0.02 | 0.01 | 0.02 | 0.08 | 0.08 | 0.09 | **0.12** |
| 1700 | 0.08 | 0.02 | 0.01 | 0.00 | 0.01 | 0.02 | 0.01 | 0.02 | 0.09 | 0.08 | 0.10 | **0.13** |
| 2000 | 0.07 | 0.02 | 0.01 | 0.00 | 0.01 | 0.00 | 0.01 | 0.02 | 0.16 | 0.08 | 0.16 | **0.18** |
| 2200 | 0.07 | 0.02 | 0.01 | 0.00 | 0.01 | 0.00 | 0.01 | 0.02 | 0.18 | 0.07 | 0.18 | **0.19** |
| 2300 | 0.07 | 0.02 | 0.01 | 0.00 | 0.01 | 0.00 | 0.01 | 0.02 | 0.22 | 0.07 | 0.22 | **0.23** |
| 2400 | 0.07 | 0.02 | 0.01 | 0.00 | 0.01 | 0.00 | 0.01 | 0.02 | 0.27 | 0.07 | 0.27 | **0.28** |
| 2500 | 0.07 | 0.02 | 0.01 | 0.00 | 0.01 | 0.00 | 0.01 | 0.02 | 0.33 | 0.07 | 0.33 | **0.34** |

Table 5.1.6. present the final uncertainty values (the uncorrelated components, correlated components and combined standard uncertainties) of the VNIIOFI lamps, as they used for the comparison analysis.

Table 5.1.6. Spectral Irradiance standard uncertainties (k=1) of the VNIIOFI lamps

| **Wavelength, nm** | **Round 1 & 2** | | |
|---|---|---|---|
| | **Uncertainties associated with, %** | | **Combined uncertainty, %** |
| | **Uncorrelated effects** | **Correlated effects** | |
| 250 | 0.31 | 0.30 | 0.43 |
| 260 | 0.24 | 0.29 | 0.38 |
| 270 | 0.22 | 0.28 | 0.36 |
| 280 | 0.22 | 0.26 | 0.34 |
| 290 | 0.20 | 0.25 | 0.32 |
| 300 | 0.19 | 0.25 | 0.31 |
| 320 | 0.16 | 0.25 | 0.30 |
| 340 | 0.16 | 0.24 | 0.29 |
| 360 | 0.15 | 0.23 | 0.27 |
| 380 | 0.14 | 0.24 | 0.28 |
| 400 | 0.12 | 0.22 | 0.25 |
| 450 | 0.12 | 0.19 | 0.22 |
| 500 | 0.11 | 0.18 | 0.21 |
| 555 | 0.11 | 0.15 | 0.19 |
| 600 | 0.10 | 0.13 | 0.16 |
| 700 | 0.10 | 0.12 | 0.16 |
| 800 | 0.10 | 0.11 | 0.15 |
| 900 | 0.09 | 0.11 | 0.14 |
| 1000 | 0.09 | 0.10 | 0.13 |
| 1100 | 0.09 | 0.09 | 0.13 |
| 1300 | 0.09 | 0.09 | 0.13 |
| 1500 | 0.09 | 0.08 | 0.12 |
| 1700 | 0.10 | 0.08 | 0.13 |
| 2000 | 0.16 | 0.08 | 0.18 |
| 2200 | 0.18 | 0.07 | 0.19 |
| 2300 | 0.22 | 0.07 | 0.23 |
| 2400 | 0.27 | 0.07 | 0.28 |
| 2500 | 0.33 | 0.07 | 0.34 |

### 5.1.4. Uncertainty budget of measurements at VNIIOFI as a pilot

The uncertainty budget of the pilot spectral irradiance measurement of a participant lamp is presented in Table 5.1.6.

5.1.4.1. **Systematic components** of measurement of VNIIOFI as a pilot are the same than that of measurement of VNIIOFI as a participant. Therefore, the first component in Table 5.1.6 is the combined systematic uncertainty $u_{\mathrm{VNIIOFI,s}}$ from the Table 5.1.5.

5.1.4.2. The second component $u_{\mathrm{r}}$ in Table 5.1.6 is a combined uncertainty of **random** effects. It is equal to the combined random uncertainty of measurement at VNIIOFI as a participant ($u_{\mathrm{VNIIOFI,r}}$ in Table 1.5), divided by $\sqrt{3}$, because the pilot result of spectral irradiance measurement of each participant lamp was an average of three independent measurement:

$$u_{\mathrm{r}} = u_{\mathrm{VNIIOFI,r}}/\sqrt{3} \tag{5.1.7}$$

5.1.4.3. **Stability of pilot measurement** was evaluated from the data of the four VNIIOFI lamps, which were measured three times:

1st time in March-April 2018 – the participant Round 1 (R1), prior the pilot measurements;

2nd time in May-June 2018 – the Pilot measurement, (round Rp);

3d time in February 2020 – the participant Round 2 (R2), after the pilot measurements.

The differences between the R1, Rp and R2 round measurements are shown in Figure 5.1.3 separately for each lamp. The blue curves are the 2nd to 1st measurements differences (round Rp to round R1). The red curves are the 3d to 1st measurements differences (round R2 to round R1). The green curves are the 3d to 2nd measurements differences (round R2 to round Rp). The bold brown curves are the maximal differences (absolute) between all three measurements for each specific wavelength. The bold black curves present the doubled ***random*** uncertainty component: $\pm\, 2 \cdot u_{\mathrm{r}}$ , where $u_{\mathrm{r}}$ is defined by the equation (5.1.7) and presented in Table 5.1.6.

Fig.5.1.4 shows the maximal differences of all four lamps and the average of these maximal differences for each wavelength (yellow curve). One can see than the average differences are higher than the random uncertainty $2u_{\mathrm{r}}$ in the most part of the wavelength range. Therefore, we introduced a new uncertainty component $u_{\mathrm{pilot,stab}}$, associated with stability of pilot measurements. The value of $u_{\mathrm{pilot,stab}}$ was selected in such a way that its combination with the random uncertainty $u_{\mathrm{r}}$ would be not less than the average of the maximal differences:

$$2 \cdot \left(u_{\mathrm{pilot,stab}}^2 + u_{\mathrm{r}}^2\right)^{\frac{1}{2}} \geq \text{Average of Max. Diff.} \tag{5.1.8}$$

In Fig. 5.1.5 the blue curve presents the doubled pilot stability uncertainty $2u_{\mathrm{pilot,stab}}$, and the red curve presents the doubled pilot random uncertainty $2u_{\mathrm{pilot,r}}$,

where $$u_{\mathrm{pilot,r}} = \left(u_{\mathrm{pilot,stab}}^2 + u_{\mathrm{r}}^2\right)^{\frac{1}{2}} \tag{5.1.9}$$

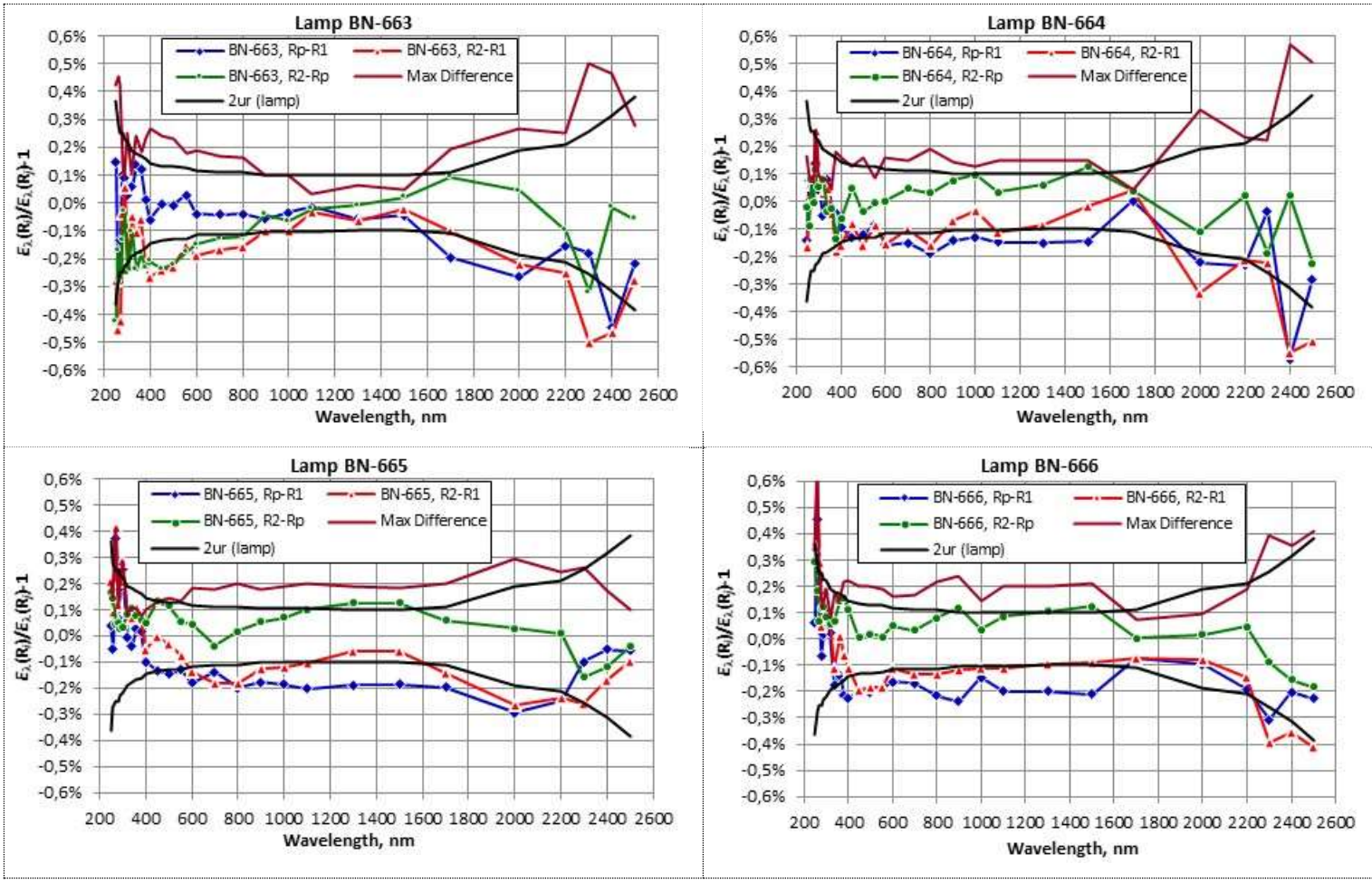


Figure 5.1.3. Differences between three rounds (R1, Rp, R2) of measurement results for VNIIOFI lamps.

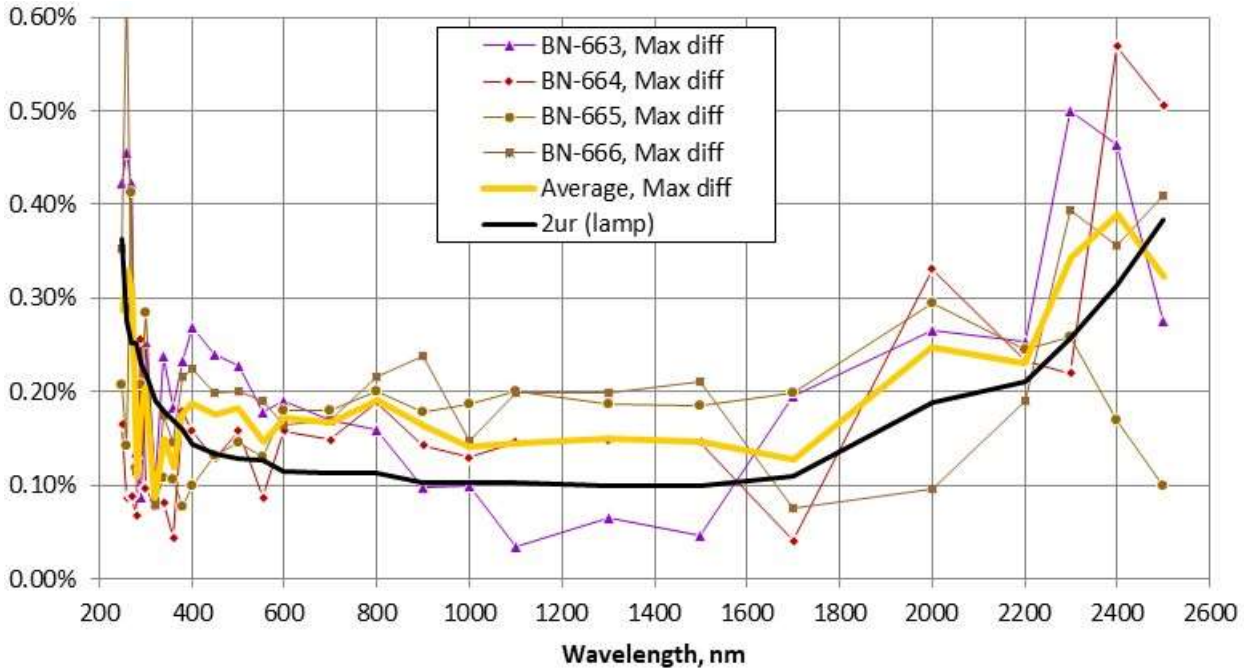


Figure 5.1.4. Evaluation of pilot stability uncertainty: Yellow line – average of maximal differences between pilot measurement results; Black line – random uncertainty $2u_{\mathrm{r}}$ of VNIIOFI measurement (the second column of Table 5.1.6).

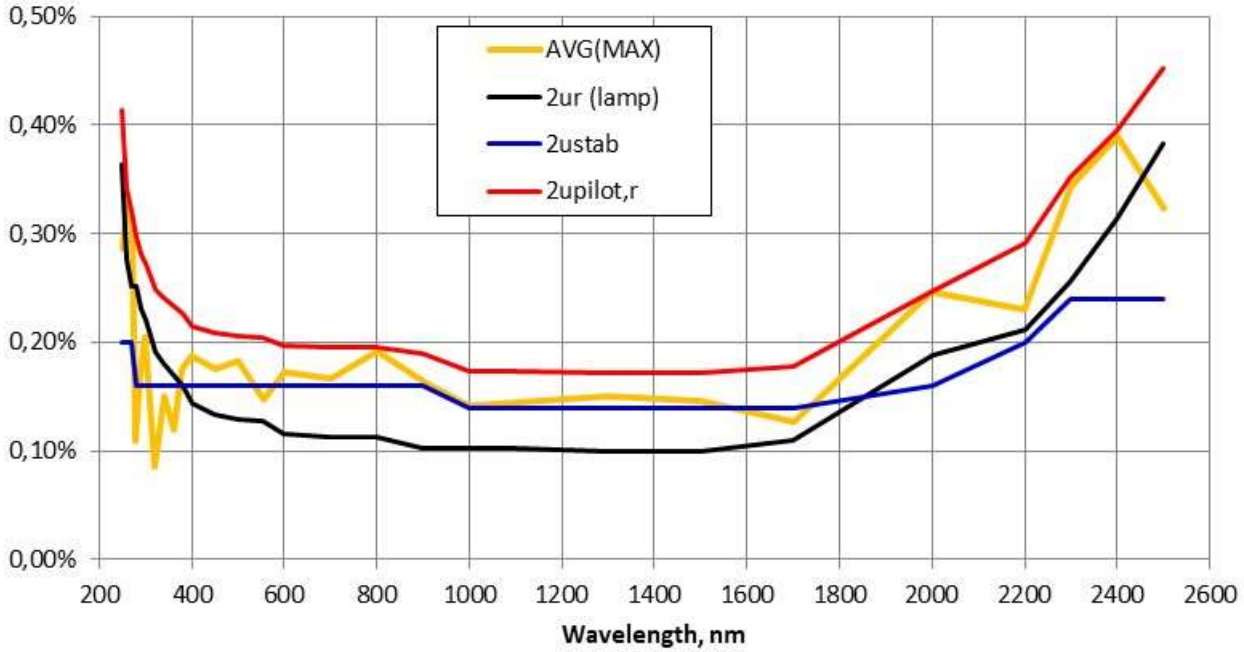


Figure 5.1.5. Evaluation of pilot stability uncertainty: Blue line – pilot stability uncertainty $2u_{\mathrm{pilot,stab}}$; Red line – total random uncertainty of pilot measurement $2u_{\mathrm{pilot,r}}$ (the second column of Table 5.1.6).

The uncertainty component $u_{\mathrm{pilot,stab}}$, associated with stability of pilot measurements is presented in column 3 of Table 5.1.7.

Table 5.1.7. Standard uncertainty of lamp spectral irradiance measurement at VNIIOFI **as pilot**, in %

| λ, nm | $u_{\mathrm{VNIIOFI,s}}$ systematic | $u_{\mathrm{r}} = u_{\mathrm{VNIIOFI,r}}/\sqrt{3}$ random | Stability of pilot measurement $u_{\mathrm{pilot,stab}}$ random | $u_{\mathrm{pilot,s}}$ systematic | $u_{\mathrm{pilot,r}}$ random | **$u_{\mathrm{c,pilot}}$ combined standard** | **$U_{\mathrm{p,pilot}}$ expanded ($k$=2)** |
|---|---|---|---|---|---|---|---|
| | Correlated | Uncorrelated | Uncorrelated | Correlated | Uncorrelated | | |
| 250 | 0.30 | 0.18 | 0.10 | 0.30 | 0.21 | **0.37** | **0.74** |
| 260 | 0.29 | 0.14 | 0.10 | 0.29 | 0.17 | **0.34** | **0.68** |
| 270 | 0.28 | 0.13 | 0.10 | 0.28 | 0.16 | **0.32** | **0.64** |
| 280 | 0.26 | 0.13 | 0.08 | 0.26 | 0.15 | **0.30** | **0.60** |
| 290 | 0.25 | 0.12 | 0.08 | 0.25 | 0.14 | **0.29** | **0.58** |
| 300 | 0.25 | 0.11 | 0.08 | 0.25 | 0.14 | **0.29** | **0.58** |
| 320 | 0.25 | 0.09 | 0.08 | 0.25 | 0.12 | **0.28** | **0.56** |
| 340 | 0.24 | 0.09 | 0.08 | 0.24 | 0.12 | **0.27** | **0.54** |
| 360 | 0.23 | 0.09 | 0.08 | 0.23 | 0.12 | **0.26** | **0.52** |
| 380 | 0.24 | 0.08 | 0.08 | 0.24 | 0.11 | **0.26** | **0.52** |
| 400 | 0.22 | 0.07 | 0.08 | 0.22 | 0.11 | **0.25** | **0.50** |
| 450 | 0.19 | 0.07 | 0.08 | 0.19 | 0.11 | **0.22** | **0.44** |
| 500 | 0.18 | 0.06 | 0.08 | 0.18 | 0.10 | **0.21** | **0.42** |
| 555 | 0.15 | 0.06 | 0.08 | 0.15 | 0.10 | **0.18** | **0.36** |
| 600 | 0.13 | 0.06 | 0.08 | 0.13 | 0.10 | **0.16** | **0.32** |
| 700 | 0.12 | 0.06 | 0.08 | 0.12 | 0.10 | **0.16** | **0.32** |
| 800 | 0.11 | 0.06 | 0.08 | 0.11 | 0.10 | **0.15** | **0.30** |
| 900 | 0.11 | 0.05 | 0.08 | 0.11 | 0.09 | **0.14** | **0.28** |
| 1000 | 0.10 | 0.05 | 0.07 | 0.10 | 0.09 | **0.13** | **0.26** |
| 1100 | 0.09 | 0.05 | 0.07 | 0.09 | 0.09 | **0.13** | **0.26** |
| 1300 | 0.09 | 0.05 | 0.07 | 0.09 | 0.09 | **0.13** | **0.26** |
| 1500 | 0.08 | 0.05 | 0.07 | 0.08 | 0.09 | **0.12** | **0.24** |
| 1700 | 0.08 | 0.06 | 0.07 | 0.08 | 0.09 | **0.12** | **0.24** |
| 2000 | 0.08 | 0.09 | 0.08 | 0.08 | 0.12 | **0.14** | **0.28** |
| 2200 | 0.07 | 0.10 | 0.10 | 0.07 | 0.14 | **0.16** | **0.32** |
| 2300 | 0.07 | 0.13 | 0.12 | 0.07 | 0.18 | **0.19** | **0.38** |
| 2400 | 0.07 | 0.16 | 0.12 | 0.07 | 0.20 | **0.21** | **0.42** |
| 2500 | 0.07 | 0.19 | 0.12 | 0.07 | 0.22 | **0.23** | **0.46** |

### 5.1.5. References to section 5.1

[6] Sapritsky V. I., Khlevnoy B. B., Khromchenko V. B., Lisiansky B. E., Mekhontsev S. N., Melenevsky U. A., Morozova S. P., Prokhorov A. V., Samoilov L. N., Shapoval V. I., Sudarev K. A., Zelener M. F., *Appl. Opt.*, 1997, 36, 5403-5408.

[7] http://www.virial.com/steep321.html

[8] Prokhorov A., Effective emissivities of isothermal blackbody cavities calculated by the Monte Carlo method using the three-component BRDF Model, *Appl. Opt.,* 2012, V. 51, No.13, 2322-2332.

[9] Samoylov M. L., Ogarev S. A., Khlevnoy B. B., Khromchenko V. B., Mekhontsev S. N., Sapritsky V. I., High Accuracy Radiation TSP-type Thermometers for Radiometric Scale Realization in Temperature Range from 600 to 3200 °C, *Temperature: It´s Measurement and Control in Science and Industry: Proc. 8th Symposium on Temperature*, 2003, V. 7, 583–588.

[10] Woolliams E. R., Anhalt K., Ballico M., Bloembergen P., Bourson F., Briaudeau S., Campos J., Cox M. G., Campo D., Dong W., Dury M. R., Gavrilov V., Grigoryeva I., Hernanz M. L., Jahan F., Khlevnoy B., Khromchenko V., Lowe D. H., Lu X., Machin G., Mantilla J. M., Martin M. J., McEvoy H. C., Rougié B., Sadli M., Salim S. G. R., Sasajima N., Taubert D. R., Todd A. D. W., Van den Bossche R., Van der Ham E., Wang T., Whittam A., Wilthan B., Woods D. J., Woodward J. T., Yamada Y., Yamaguchi Y., Yoon H. W. and Yuan Z., Thermodynamic temperature assignment to the point of inflection of the melting curve of high-temperature fixed points, *Phil.Trans.R.Soc.A* **374**: 20150044

[11] B.B. Khlevnoy, I.A. Grigoryeva, D.A. Otryaskin, Development and investigation of WC–C fixed-point cells, *Metrologia* **49**, S59 (2012).

[12] B. B. Khlevnoy and I. A. Grigoryeva, Long-Term Stability of WC-C Peritectic Fixed Point, *Int J Thermophys* (2015) **36**:367–373

[13] I. A. Grigoryeva, B. B. Khlevnoy and M. V. Solodilov, Reproducibility of WC–C High-Temperature Fixed Point, *Int J Thermophys* (2017) **38**:69, DOI 10.1007/s10765-017-2203-0

[14] P. Sperfeld, Final report on the CIPM key comparison CCPR-K1.b: Spectral irradiance 200 nm to 350 nm, *Metrologia*, 2008, **45**, *Tech. Suppl*., 02002, doi:10.1088/0026-1394/45/1A/02002. (http://iopscience.iop.org/article/10.1088/0026-1394/45/1A/02002/meta)

[15] A.D.W. Todd, K. Anhalt, P. Bloembergen, B.B. Khlevnoy, D.H. Lowe, G. Machin, M. Sadli, N. Sasajima and P. Saunders, On the uncertainties in the realization of the kelvin based on thermodynamic temperatures of high-temperature fixed-point cells, *Metrologia* **58,** 035007

[16] P. Sperfeld, S. Pape, B. Khlevnoy and A. Burdakin, Performance limitations of carbon-cavity blackbodies due to absorption bands at the highest temperatures, *Metrologia*, **46** (2009) S170–S173.

## 5.2. IO-CSIC, Spain

This section describes the IO-CSIC measurements of spectral irradiance of the CCPR-K1.a.2017 comparison traveling lamps calibrated by IO-CSIC in the wavelength range from 250 nm to 1700 nm.

### 5.2.1. Description of the measurement facility

A drawing of the measurement facility is shown below.

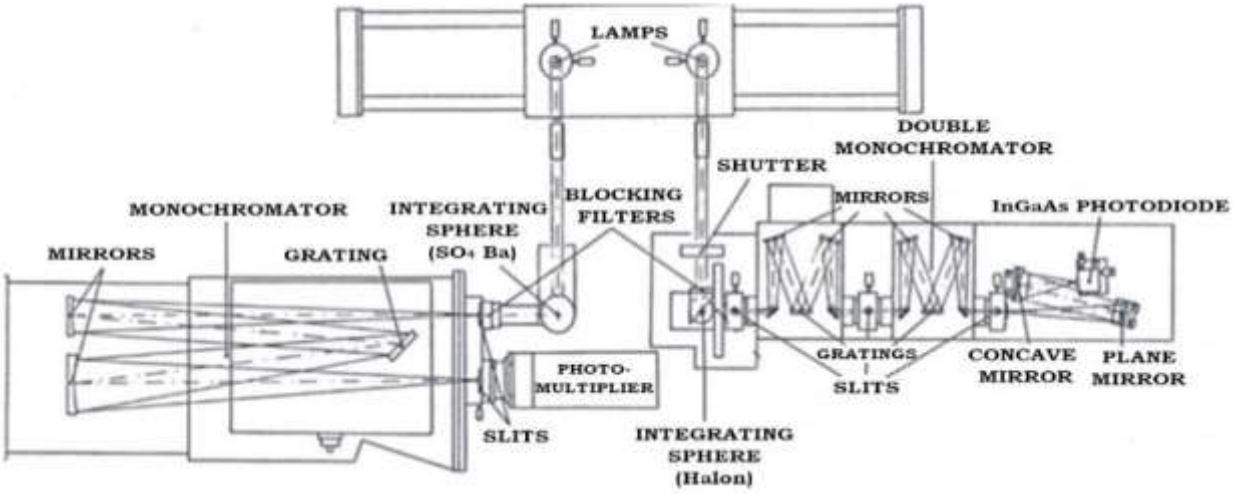


Figure 5.2.1. Measurement facility of IO-CSIC

#### *5.2.1.1. Make and type of spectroradiometer*

The measurements have been done in a purpose built spectroradiometer. In fact, it consists of two different spectroradiometers: one for the UV/Visible spectral range (250 nm-800 nm) and a second one for the NIR spectral range (800 nm-1700 nm). Following are the characteristics of each monochromator as well as detector systems.

##### *5.2.1.1.1. Monochromator*

The monochromator technical parameters are presented in the Table 5.2.1 below.

Table 5.2.1. Monochromator technical parameters

| **Monochromator values** | **VISIBLE-ULTRAVIOLET** | **NIR** |
|---|---|---|
| Manufacturer | Jarrell-Ash | Jobin-Yvon |
| Model | 78-490 | H-225 |
| Type | Grating (single) | Grating (double) |
| Groves/mm | 1180 | 600 (800 nm – 1700nm) |
| Focal length | 0.75 m | 0.25 m |
| f number | f/6.5 | f/3.5 |
| Slit width used | 2 mm | 4 mm |

#### *5.2.1.1.2. Detector*

Table 5.2.2. Detector parameters

| | **VISIBLE-ULTRAVIOLET** | **NIR** | |
|---|---|---|---|
| | | **800-1100 nm** | **1100-1700 nm** |
| Type | Photomultiplier (S-20) | Si photodiode | InGaAs photodiode |
| Manufacturer | EMI | EG&G | Hamamatsu |
| Model | 9558 QB | UV444B | G5852-01 |

### *5.2.1.2. Spectroradiometer characterization*

**Spectral bandpass.** Effective spectral bandpass has been determined by indirect method using fixed wavelength monochromatic beams (first and higher orders of CW Kr+ laser lines). Mean values of 2 nm and 7.5 nm have been obtained for the UV-VIS and NIR respectively.

**Wavelength.** The wavelength setting accuracy has been checked with several pencil style spectral calibration lamps and CW Kr+ laser lines. Uncertainties of 0.058 nm and 0.2 nm have been obtained for the UV-VIS and NIR gratings pair respectively.

**Linearity.** Linear response of the detectors used has been checked by using a stimuli addition method.

**Scattered light**. Scattered light has been checked by measuring the spectral transmittance of blocking filters. The results agreed well with the specifications of the instrument. As a result, no contribution of this effect to uncertainty has been considered.

Long wave pass filters have been used to eliminate second order wavelength radiation.

#### *5.2.1.2.1. Laboratory conditions*

The room temperature and humidity were monitored and recorded. Measurements were performed during July and October 2017 (first round) and during March, June and July 2019 (second round). The room temperature was in the range 22 ºC to 23 ºC and the relative humidity was always under 45%.

The source positioning system consists of a mobile platform which slides on two rigid rails and can be fixed at two predetermined positions. At these positions, two kinematic lamp mounts allow for a precise and reproducible positioning of both sources. They are provided with micrometric displacements along the three axes and two rotations, one around the vertical axis and another around the horizontal axis parallel to the entrance aperture plane of the spectroradiometer. Optical axes are defined by means of a He-Ne laser beam.

### *5.2.1.3. IO-CSIC working standards*

Type FEL (1000 W) quartz-halogen tungsten coiled coil filament lamps of the same type of test lamps have been used as reference. These lamps were used in the previous BIPM comparison of spectral irradiance (CCPR-K1.a).

The electrical supply to the lamps (reference and test) was derived from high-stability DC power supplies operating in current control. The current supplied to the lamps was measured using calibrated standard resistors (0,01 Ω) in the standard 4-terminal measuring configuration. The voltage at the lamps was measured using the terminals supplied at the lamp assembly.

### 5.2.2. Establishment of primary scale

The realization of the scale for spectral irradiance at the Instituto de Óptica (IO-CSIC) was made by measuring the spectral irradiance of a series of tungsten halogen lamps with an electrically calibrated pyroelectric radiometer and a set of interference filters. Full description of the method used is reported in [17,18].

### 5.2.3. Measurement procedure

The basic procedure used is a direct comparison method. Every lamp was measured completely throughout a given wavelength range, before placing another lamp onto the optical axis to repeat the process.

Alignment procedures specified in section 3.4 of the protocol have been used for the lamps.

The spectral range measured at IO-CSIC (250 nm to 1700 nm) was split into three regions, corresponding to the monochromator's gratings and the three detectors. Every wavelength region overlapped with the upper one by at least two measuring points. All the lamps were measured in all spectral regions on three occasions. The lamps were realigned between measurements. In each occasion only one scan was made with a number of repeated measurements for each wavelength.

The spectral irradiance has been calculated according to the expression:

$$E(\lambda) = E_S(\lambda)\frac{R(\lambda)}{R_S(\lambda)} \tag{5.2.1}$$

where $E(\lambda)$ is the spectral irradiance of the test source; $R(\lambda)/R_S(\lambda)$ is the ratio of the test source signal to the standard lamp one obtained in the spectroradiometer, and $E_S(\lambda)$ is the spectral irradiance of the standard lamp.

### 5.2.4. Uncertainty

Actual model of evaluation used is as expressed in equation (5.2.1) but corrected with a series of factors. See equation (5.2.2), where the spectral dependence is omitted for ease of use,

$$E = E_s.\alpha\Delta t.F\,\frac{(R+\delta'_{res}+\delta R_\lambda)\left(\frac{c'_j V'_j}{J'_R R'_j}\right)^m \cos^h(\varphi')\cos^f(\upsilon')\,d_1^2}{(R_s+\delta_{res}+\delta R_{s\lambda})\left(\frac{c_j V_j}{J_R R_j}\right)^m \cos^h(\varphi)\cos^f(\upsilon)d_2^2} \tag{5.2.2}$$

Quantities:

$E$ output quantity, actual spectral irradiance of the test source

$E_s$ spectral irradiance of the standard lamp. Certified value

$\alpha\Delta t$ relative correction for aging of standard lamp.

$F$ factor that takes into account the different amplifier scales used for the measurement of test and standard lamp signals. Certified value. Same scale has been used for test and standard lamp.

$R$ mean value, averaged from the number of readings, of the test source signal.

$R_S$ mean value of the standard lamp signal.

$c'_j$ and $c_j$ calibration factors of the multimeters used to measure the voltage across the standard resistors for test and standard lamp respectively. Certified values.

$V'_j$ and $V_j$ mean values of voltages measured across the series standard resistor.

$J'_R$ and $J_R$ established values of current for test and standard lamp respectively. No uncertainty.

$R'_j$ and $R_j$ values of standard resistors used for the measurement of lamps' current. Certified values.

$m$ exponent for changes of lamp current affecting the spectral irradiance. Dependence on wavelength has been considered.

$\cos^h\varphi$; $\cos^f\nu$ correction factors for angular misalignment of the lamp around the vertical angle ($\varphi$) and horizontal angle ($\nu$) axis.

$d_1$ and $d_2$ distances of measurement for test and standard lamp respectively. A distance of 500 mm has been used for both lamps.

$\delta'_{res}$ and $\delta_{res}$ corrections factors for resolution of measurement system.

$\delta R_\lambda$ and $\delta R_{S\lambda}$ corrections factors for uncertainty in wavelength. The uncertainty is calculated as:

$$u(\delta R_\lambda) = \frac{\partial R}{\partial \lambda} u(\lambda) \qquad u(\delta R_{S\lambda}) = \frac{\partial R_S}{\partial \lambda} u(\lambda)$$

with $u(\lambda)$ uncertainty in the monochromator's wavelength calibration (in nm).

The calculation of uncertainty values has been done by applying the partial derivative rule to equation (5.2.2) as recommended in ISO Guide.

A detailed uncertainty budget of the spectral irradiance measurements is enclosed in Table 5.2.3. Type B contributions have been split into those components that are entirely uncorrelated from lamp to lamp and round to round (distance, orientation and current), and those components that are correlated between lamps, but not between rounds (wavelength accuracy, that has been recalibrated from first round to the second round).

Values reported for uncertainty in orientation are the combined uncertainty of both terms of angular misalignment mentioned. Similarly, values reported for uncertainty in electrical current are the combined uncertainties of contributions: $c_j$; $R_j$; and $V_j$ explained above.

The final uncertainty values submitted by IO-CSIC to the pilot with the spectral irradiance data are presented in Tables 5.5.4. The uncertainties are the same for all lamps and both rounds.

### 5.2.5. References to section 5.2

[17] C. Carreras and A. Corróns, Absolute spectroradiometric and photometric scales based on an electrically calibrated pyroelectric radiometer, *Appl. Opt.*, 1981, 20.

[18] P. Corredera, A. Corróns, A. Pons and J. Campos, Absolute spectral irradiance scale in the 700-2400 nm spectral range, Appl. Opt., 1990, 29.

Table 5.2.3. Uncertainty components (%) of the spectral irradiance measurements at IO-CSIC. All uncertainties are standard uncertainties (k = 1)

| **Wavelength, nm** | **Type A uncertainty, %** | **Type B uncertainty, %** | | | | | **Combined standard uncertainty** |
|---|---|---|---|---|---|---|---|
| | | **Uncertainty of standard lamp** | entirely uncorrelated from lamp to lamp and round to round | | | correlated between lamps, but not between rounds | |
| | | | **Distance** 2 contributions | **Current** 2 contributions | **Orientation** 2 contributions | **Wavelength** 2 contributions | $u_c$ , % |
| 250 | 1.04 | 2.33 | 0.06 | 0.05 | 0.02 | 0.44 | 2.6 |
| 260 | 0.68 | 2.33 | 0.06 | 0.05 | 0.02 | 0.38 | 2.5 |
| 270 | 0.62 | 2.33 | 0.06 | 0.05 | 0.02 | 0.34 | 2.5 |
| 280 | 0.60 | 2.13 | 0.06 | 0.05 | 0.02 | 0.31 | 2.3 |
| 290 | 0.58 | 2.13 | 0.06 | 0.05 | 0.02 | 0.30 | 2.3 |
| 300 | 1.27 | 2.3 | 0.06 | 0.04 | 0.02 | 0.23 | 2.6 |
| 320 | 0.45 | 1.9 | 0.06 | 0.04 | 0.02 | 0.18 | 2.0 |
| 340 | 0.29 | 1.8 | 0.06 | 0.04 | 0.02 | 0.15 | 1.8 |
| 360 | 0.13 | 1.7 | 0.06 | 0.04 | 0.02 | 0.13 | 1.7 |
| 380 | 0.08 | 1.6 | 0.06 | 0.04 | 0.02 | 0.12 | 1.6 |
| 400 | 0.07 | 1.6 | 0.06 | 0.03 | 0.02 | 0.11 | 1.6 |
| 450 | 0.03 | 1.6 | 0.06 | 0.03 | 0.02 | 0.07 | 1.6 |
| 500 | 0.02 | 1.7 | 0.06 | 0.03 | 0.02 | 0.05 | 1.7 |
| 555 | 0.02 | 1.8 | 0.06 | 0.03 | 0.02 | 0.04 | 1.8 |
| 600 | 0.02 | 1.7 | 0.06 | 0.02 | 0.02 | 0.03 | 1.7 |
| 700 | 0.03 | 1.6 | 0.06 | 0.02 | 0.02 | 0.01 | 1.6 |
| 800 | 0.10 | 1.6 | 0.06 | 0.02 | 0.02 | 0.01 | 1.6 |
| 900 | 0.01 | 1.9 | 0.06 | 0.02 | 0.02 | 0.00 | 1.9 |
| 1000 | 0.09 | 1.9 | 0.06 | 0.02 | 0.02 | 0.01 | 1.9 |
| 1100 | 0.12 | 2.3 | 0.06 | 0.02 | 0.02 | 0.01 | 2.3 |
| 1300 | 0.34 | 2.0 | 0.06 | 0.02 | 0.02 | 0.02 | 2.0 |
| 1500 | 0.41 | 2.1 | 0.06 | 0.02 | 0.02 | 0.03 | 2.1 |
| 1700 | 0.42 | 2.1 | 0.06 | 0.02 | 0.02 | 0.07 | 2.1 |

Table 5.2.4. Spectral Irradiance standard uncertainties ($k$=1) of the IO-CSIC lamps

| **Wavelength, nm** | **Round 1 & 2** | | |
|---|---|---|---|
| | **Uncertainties associated with, %** | | **Combined uncertainty, %** |
| | **Uncorrelated effects** | **Correlated effects** | |
| 250 | 1.05 | 2.41 | 2.6 |
| 260 | 0.69 | 2.39 | 2.5 |
| 270 | 0.63 | 2.38 | 2.5 |
| 280 | 0.61 | 2.18 | 2.3 |
| 290 | 0.59 | 2.17 | 2.3 |
| 300 | 1.27 | 2.32 | 2.6 |
| 320 | 0.47 | 1.92 | 2.0 |
| 340 | 0.31 | 1.81 | 1.8 |
| 360 | 0.17 | 1.71 | 1.7 |
| 380 | 0.13 | 1.61 | 1.6 |
| 400 | 0.12 | 1.61 | 1.6 |
| 450 | 0.10 | 1.60 | 1.6 |
| 500 | 0.10 | 1.70 | 1.7 |
| 555 | 0.10 | 1.80 | 1.8 |
| 600 | 0.09 | 1.70 | 1.7 |
| 700 | 0.09 | 1.60 | 1.6 |
| 800 | 0.13 | 1.60 | 1.6 |
| 900 | 0.09 | 1.90 | 1.9 |
| 1000 | 0.12 | 1.90 | 1.9 |
| 1100 | 0.15 | 2.30 | 2.3 |
| 1300 | 0.35 | 2.00 | 2.0 |
| 1500 | 0.42 | 2.10 | 2.1 |
| 1700 | 0.43 | 2.10 | 2.1 |
| 2000 | | | |
| 2200 | | | |
| 2300 | | | |
| 2400 | | | |
| 2500 | | | |

## 5.3. KRISS, Republic of Korea

### 5.3.1. Spectral irradiance scale realisation

The spectral irradiance scale of KRISS is realised using a high-temperature blackbody (BB3500MP) made by VNIIOFI. The effective emissivity of the blackbody estimated using a Monte-Carlo method calculation by VNIIOFI is about 0,999. The blackbody is operated at a temperature of approximately 2950 K. The temperature of the blackbody is measured using the radiation thermometers (LP3 at the 1st round measurement and LP5 at the 2nd round measurement) calibrated against the KRISS radiance temperature scale [19] based on ITS-90 [20]. The standard uncertainty of the blackbody temperature measurement is about 0.71 K including the standard uncertainty of the KRISS radiance temperature scale of 0.51 K and the uncertainty components arising at the step of the thermometer calibration (0.3 K) and at the step of using the thermometer for the blackbody temperature measurement (0.4 K).

A water-cooled precision aperture with a diameter of (7.9785 ± 0.0043) mm is placed in front of the blackbody, which defines the source area of the blackbody. The diameter of the precision aperture was measured using the calibrated vision system at the length standard laboratory of KRISS. The distance from this aperture to the entrance reference plane of the integrating sphere aperture is about 430 mm, which was measured with a micrometre calibrated by the length standard laboratory of KRISS.
The spectral irradiance of the blackbody at the entrance aperture of the integrating sphere is calculated using the Planck's radiation law with the measured blackbody temperature by taking the geometric parameters of the precision aperture diameter and the distance between the precision aperture and the entrance reference plane into account.

The spectral irradiance of the blackbody at the entrance reference plane can be written as equation (5.3.1) for coaxial symmetrical circular apertures.

$$E_{BB}(\lambda,T) = \frac{\int_{A_1}\int_{\Omega} L_{BB}(\lambda,T,\Omega,A_1)\cdot d\Omega\cdot(cos\theta\cdot dA_1)}{A_2} \cong \overline{L}_{BB}(\lambda,T)\cdot\frac{A_1}{d^2} \qquad (5.3.1)$$

Here, $A_1$ is the precision aperture area; $A_2$ is the area of the receiving aperture on the entrance reference plane (it is set to be a unit area such as one $m^2$); and $d$ is the distance between the precision aperture and the entrance reference plane. $\overline{L}_{BB}(\lambda,T)$ is the mean spectral `radiance of the blackbody over the precision aperture given by the Planck's law as equation (5.3.2).

$$\overline{L}_{BB}(\lambda,T,\Omega,A_1) = \varepsilon_{\text{eff}}\cdot\frac{c_1}{\pi\cdot n^2\cdot\lambda^5}\cdot\frac{1}{\left(\exp\left(\frac{c_2}{n\cdot\lambda\cdot T}\right)-1\right)} \quad [\text{W}/(\text{m}^3\cdot\text{sr})] \qquad (5.3.2)$$

where

$\varepsilon_{\text{eff}}$ = 0.999 (effective emissivity of the blackbody).
$c_1$ = 3.741 771 18(19) × $10^{-16}$ [W·$m^2$]
$c_2$ = 1.438 775 2(25) × $10^{-2}$ [m·K]
$n$ = 1.000285 (air refractive index)
$T$: blackbody temperature in K.

### 5.3.2. Description of the measurement facility

The KRISS spectral irradiance measurement facility is shown in Figure 5.3.1. The facility consists of a high temperature blackbody as the spectral radiance standard, a spectroradiometer, lamp stages, a radiation thermometer, and a copper fixed-point blackbody.

The spectroradiometer consists of an integrating sphere, mirrors, a monochromator (Mcpherson

Model 2061) with a prism predisperser, and detectors covering the spectral range of 250 nm to 2500 nm. The inside diameter of the integrating sphere coated with about 12 mm thick PTFE is about 30 mm and its entrance and exit aperture diameters are about 10 mm. The angle between the entrance and exit port of the integrating sphere is about 105 degree and the exit port is imaged on the entrance slit of the monochromator by a spherical mirror. The focal length of the monochromator is 1 m and its f/# is 8.6. Three gratings with 600 grooves/mm blazed at 300 nm, 1000 nm, and 1800 nm are used for the wavelength range from 250 nm to 800 nm, from 800 nm to 1700 nm, and from 1700 nm to 2500 nm, respectively. The bandwidths of the spectroradiometer are about 3.3 nm over the wavelength range from 250 nm to 800 nm and about 5.0 nm from 800 nm to 2500 nm. The wavelength of the monochromator was calibrated by using spectral line sources and a HeNe laser. Four detectors are used: a photomultiplier tube for the spectral range from 250 nm to 800 nm, a Si-photodiode from 800 nm to 1100 nm, an InGaAs detector from 1100 nm to 1700 nm, and an extended InGaAs detector combined with a lock-in amplifier and a chopper from 1700 nm to 2500 nm. Four detectors and a HeNe laser are set on a motorized translator in the detector stage. A spherical mirror and a plane mirror are used to focus the output beam from the exit slit of the monochromator onto active areas of detectors with small active areas of about 1 mm in diameter. The HeNe laser in the detector stage is used for the alignment of the imaging mirror between the exit port of the integrating sphere and the entrance slit of the monochromator to optical axis by irradiating the laser beam through the exit slit of the monochromator.

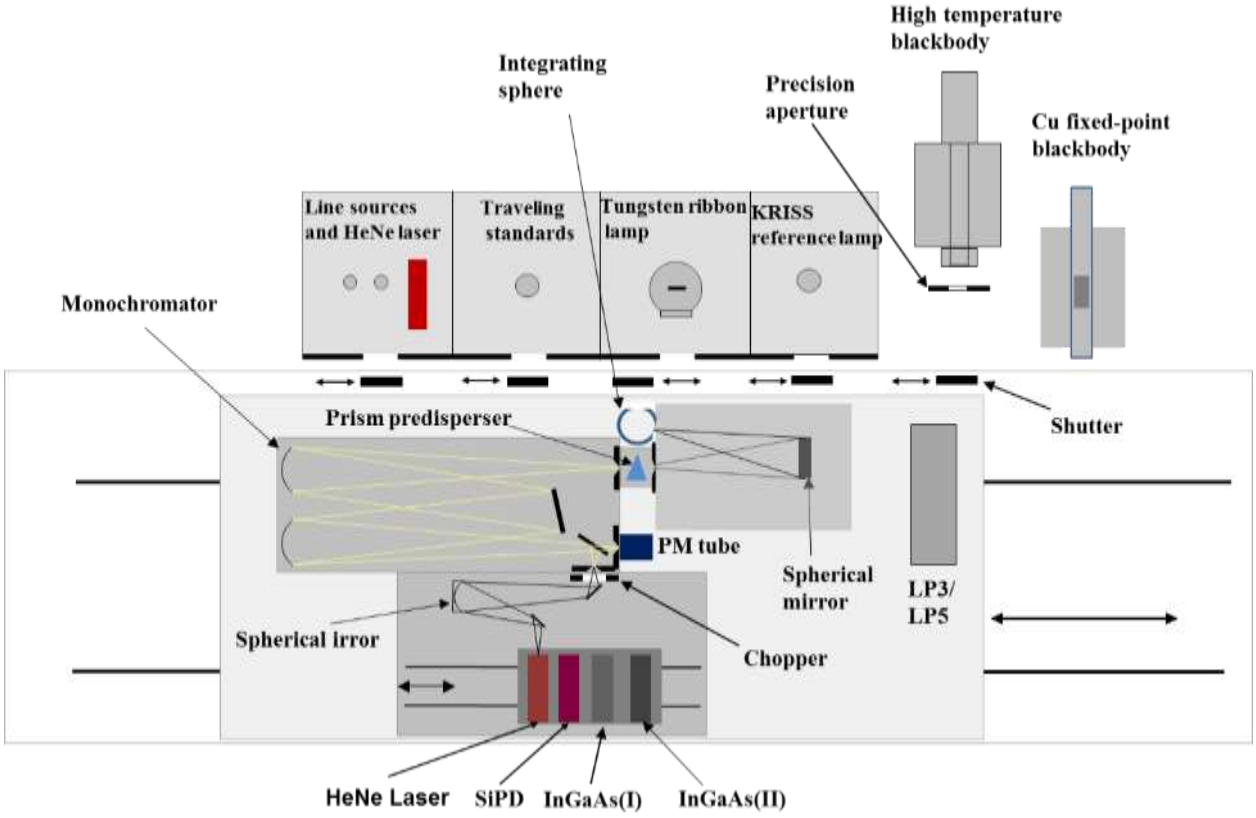


Figure 5.3.1. Schematic diagram of the KRISS spectral irradiance measurement facility.

In the lamp stages, there are four 5-axes mounts including the one for traveling standard lamps used in this comparison. A KRISS reference standard lamp was calibrated against the high temperature blackbody and then used to calibrate traveling standard lamps. Each traveling standard lamp was calibrated three times by comparing with the high temperature blackbody once and with the KRISS reference standard lamp twice. There are also several spectral line sources and a HeNe laser for the wavelength calibration of the monochromator. The HeNe laser is also used for the

alignment of detectors in the detector stage to the optical axis. Each lamp mount is separated by aluminum plates and there is a baffle with an 80 mm hole in diameter in front of each lamp mount. All plates and baffles are painted with black paint of low spectral reflectance from UV to IR. A tungsten ribbon lamp in the lamp stages is used to measure the range adaptation of radiation thermometers between their ranges after the calibration at the copper fixed-point blackbody in the lowest range.

Two radiation thermometers were used to measure the high temperature blackbody in this comparison. LP3 was used in the first round measurement, but it showed a little different values in high temperatures about 2900 K, even just after calibration, from the KRISS reference thermometer. The difference, which was 3.15 K at 2955 K, was taken into account with the standard uncertainty of 0.3 K. Nevertheless, in the second round LP3 was replaced by LP5, which had no such a problem. LP3 and LP5 were preliminary calibrated against the copper fixed-point blackbody at their position in the facility shown in the Figure 5.3.1. The final calibration was performed by comparing with the KRISS reference thermometer (LP4) at the range of 2500 K to 3000 K.

### 5.3.3. Laboratory conditions

Throughout the calibration the laboratory temperature was controlled to be 24±1 ºC.

### 5.3.4. Laboratory standards

The high temperature blackbody was used as the standard for the spectral irradiance scale realization and its temperature was measured by using two radiation thermometers of LP3 and LP5 calibrated against the KRISS temperature scale based on the ITS- 90.

The precision aperture diameter was measured by the length standard laboratory of KRSS using the KRISS reference standard. The distances from the precision aperture and from the traveling standard lamp to the entrance reference plane were measured by using a micrometer calibrated by the length standard laboratory of KRSS using the KRISS reference standard.

All digital voltmeters, electrometers, and shunt resistors were calibrated by the electromagnetic standard laboratory of KRISS using the KRISS reference standard.

### 5.3.5. Measurement procedure

The distance from the water cooled precision aperture placed in front of the blackbody to the entrance reference plane was measured just before the each measurement of traveling standard lamps. Each lamp was aligned following the procedure in the protocol and was turned on about 30 minutes before starting the measurement. The electric current of each lamp was set to be 8.100 A. The wavelength of the spectroradiometer was calibrated using the spectral line sources. The blackbody temperature was measured periodically with an interval of about 30 minutes.

The measurement procedure at a wavelength was as follows:

1) Select a wavelength of the spectroradiometer
2) Move the spectroradiometer to be aligned to the blackbody
3) Open the shutter → read signal for the blackbody → close the shutter → read the dark signal
4) Move the spectroradiometer to be aligned to the lamp
5) Open the shutter → read the signal for the lamp → close the shutter → read the dark signal
6) Repeat once more from 5) to 2) in the reverse order at the same wavelength as selected
7) Save all data

The spectral irradiance of a lamp at a given wavelength was calculated using the geometric mean ratio of two ratios of the lamp to the blackbody signals and the spectral irradiance of the blackbody at the entrance aperture of the integrating sphere.

The spectral irradiance of a traveling standard lamp, $E_{\mathrm{L}}(\lambda)$ is obtained as equation (3.3).

$$E_{\mathrm{L}}(\lambda) = f_{\mathrm{G}} \cdot \frac{S_{\mathrm{L}}(\lambda)}{S_{\mathrm{BB}}(\lambda)} \cdot E_{\mathrm{BB}}(\lambda, T) \tag{3.3}$$

where $S_{\mathrm{L}}(\lambda)$ and $S_{\mathrm{BB}}(\lambda)$ are net output signals of the spectroradiometer at a wavelength $\lambda$ for the lamp and the blackbody, respectively.

$f_{\mathrm{G}}$ is a correction factor (geometric mismatch correction factor, hereafter) to compensate the geometric mismatch between the radiation beams from the blackbody and the lamp. This effect was caused by non-ideal characteristics of the KRISS integrating sphere. The fact that the lamp and the blackbody, having different sizes, illuminate different areas of the sphere inner surface. This is not a problem for the ideal sphere, which provides the same ratio of output radiance to input irradiance regardless of the size of the illuminated inner surface area. For the KRISS sphere there was a dependence of the output radiance to input irradiance ratio on the illuminated area. The $f_{\mathrm{G}}$ factor compensates the difference between the ratio for the lamp and blackbody. If the integrating sphere was an ideal one, $f_{\mathrm{G}}$ should be unity. The geometric mismatch effect was reduced using fused silica diffusers at the entrance and exit apertures of the integrating sphere. But even after reducing, the factor of the KRISS sphere was not a unity. To determine the $f_{\mathrm{G}}$factor, the illuminances of the lamp and blackbody were measured by a photometer with an aperture similar to the aperture of the integrating sphere. The correction factor was obtained by comparing the illuminances measured by the photometer with the illuminances calculated from the measured spectral irradiances of the lamp and blackbody. The value of $f_{\mathrm{G}}$ was 0.9768 with standard uncertainty of 0.20 %.

No other correction was made. Nonlinearities of detectors were not considered because signal ratios of the spectroradiometer for the blackbody and for a lamp were kept within 0.5 to 1.5 by adjusting the blackbody temperature within (2955 ± 20) K.

### 5.3.6. Uncertainties of spectral irradiance calibration at KRISS

#### *5.3.6.1. Uncertainties of spectral irradiance scale realisation*

Since the spectral irradiance scale of KRISS was realized by using a high temperature blackbody, the uncertainty of the spectral irradiance scale includes uncertainties related to the blackbody and uncertainties related to the geometric parameters such as the precision aperture area and the distance from the precision aperture to the entrance reference plane of the spectral irradiance measurement facility. Table 5.3.1 shows the uncertainty components for spectral irradiance scale realization of KRISS.

#### *5.3.6.2. Uncertainties of spectral irradiance lamp calibration at KRISS*

Table 5.3.2 shows the typical uncertainties of spectral irradiance calibration at KRISS. The uncertainty due to the reproducibility was estimated using the standard deviation of several independent measurement results and it includes uncertainties due to alignment, spectroradiometer stability, and repeatability of a lamp measurement. The uncertainty of the geometric mismatch correction means the uncertainty of the geometric mismatch correction factor, $f_{\mathrm{G}}$.

The uncorrelated uncertainty component associated with random effects differed from lamp to lamp and from round to round.

The final uncertainty values submitted by KRISS to the pilot are presented in Tables 5.3.3 – 5.3.5.

Table 5.3.1. Uncertainty components for spectral irradiance scale realisation at KRISS

| Wavelength, nm | Air refractive index, % | BB spectral emissivity, % | BB temperature measurement, % | BB spatial uniformity, % | BB temperature stability, % | Precision aperture area, % | Distance measurement, % | Combined standard uncertainty, % |
|---|---|---|---|---|---|---|---|---|
| 250 | 0.04 | 0.06 | 0.47 | 0.11 | 0.07 | 0.01 | 0.05 | 0.49 |
| 260 | 0.03 | 0.06 | 0.45 | 0.11 | 0.06 | 0.01 | 0.05 | 0.48 |
| 270 | 0.03 | 0.06 | 0.43 | 0.11 | 0.06 | 0.01 | 0.05 | 0.46 |
| 280 | 0.03 | 0.06 | 0.42 | 0.10 | 0.06 | 0.01 | 0.05 | 0.44 |
| 290 | 0.03 | 0.06 | 0.40 | 0.10 | 0.06 | 0.01 | 0.05 | 0.43 |
| 300 | 0.03 | 0.06 | 0.39 | 0.10 | 0.06 | 0.01 | 0.05 | 0.41 |
| 320 | 0.03 | 0.06 | 0.37 | 0.09 | 0.05 | 0.01 | 0.05 | 0.39 |
| 340 | 0.02 | 0.06 | 0.35 | 0.08 | 0.05 | 0.01 | 0.05 | 0.37 |
| 360 | 0.02 | 0.06 | 0.33 | 0.08 | 0.05 | 0.01 | 0.05 | 0.35 |
| 380 | 0.02 | 0.06 | 0.31 | 0.08 | 0.04 | 0.01 | 0.05 | 0.33 |
| 400 | 0.02 | 0.06 | 0.29 | 0.07 | 0.04 | 0.01 | 0.05 | 0.31 |
| 450 | 0.02 | 0.06 | 0.26 | 0.06 | 0.04 | 0.01 | 0.05 | 0.28 |
| 500 | 0.02 | 0.06 | 0.23 | 0.06 | 0.03 | 0.01 | 0.05 | 0.26 |
| 555 | 0.01 | 0.06 | 0.21 | 0.05 | 0.03 | 0.01 | 0.05 | 0.23 |
| 600 | 0.01 | 0.06 | 0.20 | 0.05 | 0.03 | 0.01 | 0.05 | 0.22 |
| 700 | 0.01 | 0.06 | 0.17 | 0.04 | 0.02 | 0.01 | 0.05 | 0.19 |
| 800 | 0.01 | 0.06 | 0.15 | 0.04 | 0.02 | 0.01 | 0.05 | 0.17 |
| 900 | 0.01 | 0.06 | 0.13 | 0.03 | 0.02 | 0.01 | 0.05 | 0.16 |
| 1000 | 0.01 | 0.06 | 0.12 | 0.03 | 0.02 | 0.01 | 0.05 | 0.14 |
| 1100 | 0.00 | 0.06 | 0.11 | 0.03 | 0.02 | 0.01 | 0.05 | 0.13 |
| 1300 | 0.00 | 0.06 | 0.09 | 0.02 | 0.01 | 0.01 | 0.05 | 0.12 |
| 1500 | 0.00 | 0.06 | 0.08 | 0.02 | 0.01 | 0.01 | 0.05 | 0.11 |
| 1700 | 0.00 | 0.06 | 0.07 | 0.02 | 0.01 | 0.01 | 0.05 | 0.11 |
| 2000 | 0.00 | 0.06 | 0.06 | 0.02 | 0.01 | 0.01 | 0.05 | 0.10 |
| 2200 | 0.00 | 0.06 | 0.06 | 0.01 | 0.01 | 0.01 | 0.05 | 0.10 |
| 2300 | 0.00 | 0.06 | 0.06 | 0.01 | 0.01 | 0.01 | 0.05 | 0.10 |
| 2400 | 0.00 | 0.06 | 0.06 | 0.01 | 0.01 | 0.01 | 0.05 | 0.10 |
| 2500 | 0.00 | 0.06 | 0.05 | 0.01 | 0.01 | 0.01 | 0.05 | 0.09 |

Table 5.3.2. Uncertainty components for spectral irradiance lamp calibration at KRISS

| Wavelength, nm | Irradiance scale, % | Distance, % | Lamp current, % | Wavelength, % | Reproducibility, % | Geometric mismatch correction, % | Combined standard uncertainty, % |
|---|---|---|---|---|---|---|---|
| 250 | 0.49 | 0.02 | 0.03 | 0.75 | 0.73 | 0.20 | 1.18 |
| 260 | 0.48 | 0.02 | 0.03 | 0.69 | 0.59 | 0.20 | 1.04 |
| 270 | 0.46 | 0.02 | 0.03 | 0.63 | 0.44 | 0.20 | 0.92 |
| 280 | 0.44 | 0.02 | 0.03 | 0.58 | 0.27 | 0.20 | 0.80 |
| 290 | 0.43 | 0.02 | 0.03 | 0.53 | 0.26 | 0.20 | 0.76 |
| 300 | 0.41 | 0.02 | 0.02 | 0.49 | 0.25 | 0.20 | 0.72 |
| 320 | 0.39 | 0.02 | 0.02 | 0.42 | 0.22 | 0.20 | 0.64 |
| 340 | 0.37 | 0.02 | 0.02 | 0.36 | 0.20 | 0.20 | 0.58 |
| 360 | 0.35 | 0.02 | 0.02 | 0.31 | 0.18 | 0.20 | 0.54 |
| 380 | 0.33 | 0.02 | 0.02 | 0.27 | 0.18 | 0.20 | 0.50 |
| 400 | 0.31 | 0.02 | 0.02 | 0.23 | 0.18 | 0.20 | 0.48 |
| 450 | 0.28 | 0.02 | 0.01 | 0.17 | 0.18 | 0.20 | 0.43 |
| 500 | 0.26 | 0.02 | 0.01 | 0.12 | 0.17 | 0.20 | 0.39 |
| 555 | 0.23 | 0.02 | 0.01 | 0.09 | 0.16 | 0.20 | 0.36 |
| 600 | 0.22 | 0.02 | 0.01 | 0.07 | 0.17 | 0.20 | 0.35 |
| 700 | 0.19 | 0.02 | 0.01 | 0.04 | 0.19 | 0.20 | 0.34 |
| 800 | 0.17 | 0.02 | 0.01 | 0.02 | 0.20 | 0.20 | 0.33 |
| 900 | 0.16 | 0.02 | 0.01 | 0.02 | 0.20 | 0.20 | 0.32 |
| 1000 | 0.14 | 0.02 | 0.01 | 0.00 | 0.20 | 0.20 | 0.32 |
| 1100 | 0.13 | 0.02 | 0.01 | 0.02 | 0.20 | 0.20 | 0.31 |
| 1300 | 0.12 | 0.02 | 0.01 | 0.03 | 0.23 | 0.20 | 0.33 |
| 1500 | 0.11 | 0.02 | 0.01 | 0.04 | 0.26 | 0.20 | 0.35 |
| 1700 | 0.11 | 0.02 | 0.01 | 0.04 | 0.29 | 0.20 | 0.37 |
| 2000 | 0.10 | 0.02 | 0.01 | 0.04 | 0.31 | 0.20 | 0.39 |
| 2200 | 0.10 | 0.02 | 0.01 | 0.04 | 0.40 | 0.20 | 0.46 |
| 2300 | 0.10 | 0.02 | 0.01 | 0.04 | 0.45 | 0.20 | 0.50 |
| 2400 | 0.10 | 0.02 | 0.01 | 0.04 | 0.48 | 0.20 | 0.53 |
| 2500 | 0.09 | 0.02 | 0.01 | 0.04 | 0.78 | 0.20 | 0.81 |

Table 5.3.3. Spectral Irradiance standard uncertainties (k=1) of the lamp **BN-9101-639**

| Wavelength, nm | Round 1 | | | Round 2 | | |
|---|---|---|---|---|---|---|
| | Uncertainties associated with, % | | Combined uncertainty, % | Uncertainties associated with, % | | Combined uncertainty, % |
| | Uncorrelated effects | Correlated effects | | Uncorrelated effects | Correlated effects | |
| 250 | 0.43 | 0.92 | 1.02 | 0.68 | 0.92 | 1.15 |
| 260 | 0.30 | 0.86 | 0.91 | 0.42 | 0.86 | 0.96 |
| 270 | 0.27 | 0.80 | 0.85 | 0.44 | 0.80 | 0.92 |
| 280 | 0.28 | 0.75 | 0.81 | 0.27 | 0.75 | 0.80 |
| 290 | 0.39 | 0.71 | 0.81 | 0.26 | 0.71 | 0.76 |
| 300 | 0.31 | 0.67 | 0.74 | 0.25 | 0.67 | 0.72 |
| 320 | 0.31 | 0.60 | 0.68 | 0.19 | 0.60 | 0.63 |
| 340 | 0.22 | 0.55 | 0.59 | 0.20 | 0.55 | 0.58 |
| 360 | 0.33 | 0.51 | 0.60 | 0.18 | 0.51 | 0.54 |
| 380 | 0.23 | 0.47 | 0.52 | 0.16 | 0.47 | 0.50 |
| 400 | 0.21 | 0.44 | 0.49 | 0.18 | 0.44 | 0.48 |
| 450 | 0.21 | 0.39 | 0.44 | 0.14 | 0.39 | 0.41 |
| 500 | 0.21 | 0.35 | 0.41 | 0.17 | 0.35 | 0.39 |
| 555 | 0.26 | 0.32 | 0.41 | 0.16 | 0.32 | 0.36 |
| 600 | 0.26 | 0.30 | 0.40 | 0.17 | 0.30 | 0.35 |
| 700 | 0.23 | 0.28 | 0.36 | 0.19 | 0.28 | 0.34 |
| 800 | 0.27 | 0.26 | 0.38 | 0.20 | 0.26 | 0.33 |
| 900 | 0.19 | 0.25 | 0.32 | 0.17 | 0.25 | 0.30 |
| 1000 | 0.19 | 0.25 | 0.31 | 0.17 | 0.25 | 0.30 |
| 1100 | 0.17 | 0.24 | 0.30 | 0.20 | 0.24 | 0.31 |
| 1300 | 0.17 | 0.24 | 0.29 | 0.16 | 0.24 | 0.29 |
| 1500 | 0.15 | 0.23 | 0.28 | 0.16 | 0.23 | 0.28 |
| 1700 | 0.29 | 0.23 | 0.37 | 0.29 | 0.23 | 0.37 |
| 2000 | 0.50 | 0.23 | 0.55 | 0.31 | 0.23 | 0.39 |
| 2200 | 0.65 | 0.23 | 0.69 | 0.37 | 0.23 | 0.44 |
| 2300 | 0.71 | 0.23 | 0.74 | 0.44 | 0.23 | 0.49 |
| 2400 | 0.71 | 0.23 | 0.75 | 0.47 | 0.23 | 0.52 |
| 2500 | 0.88 | 0.23 | 0.90 | 0.77 | 0.23 | 0.81 |

Table 5.3.4. Spectral Irradiance standard uncertainties (k=1) of the lamp **BN-9101-640**

| Wavelength, nm | Round 1 | | | Round 2 | | |
|---|---|---|---|---|---|---|
| | Uncertainties associated with, % | | Combined uncertainty, % | Uncertainties associated with, % | | Combined uncertainty, % |
| | Uncorrelated effects | Correlated effects | | Uncorrelated effects | Correlated effects | |
| 250 | 0.46 | 0.92 | 1.03 | 0.67 | 0.92 | 1.14 |
| 260 | 0.33 | 0.86 | 0.92 | 0.42 | 0.86 | 0.96 |
| 270 | 0.28 | 0.80 | 0.85 | 0.44 | 0.80 | 0.91 |
| 280 | 0.29 | 0.75 | 0.81 | 0.26 | 0.75 | 0.80 |
| 290 | 0.40 | 0.71 | 0.82 | 0.26 | 0.71 | 0.76 |
| 300 | 0.31 | 0.67 | 0.74 | 0.25 | 0.67 | 0.71 |
| 320 | 0.31 | 0.60 | 0.68 | 0.19 | 0.60 | 0.63 |
| 340 | 0.22 | 0.55 | 0.59 | 0.20 | 0.55 | 0.58 |
| 360 | 0.33 | 0.51 | 0.60 | 0.18 | 0.51 | 0.54 |
| 380 | 0.23 | 0.47 | 0.52 | 0.16 | 0.47 | 0.50 |
| 400 | 0.21 | 0.44 | 0.49 | 0.18 | 0.44 | 0.48 |
| 450 | 0.21 | 0.39 | 0.44 | 0.14 | 0.39 | 0.41 |
| 500 | 0.21 | 0.35 | 0.41 | 0.17 | 0.35 | 0.39 |
| 555 | 0.26 | 0.32 | 0.41 | 0.16 | 0.32 | 0.36 |
| 600 | 0.26 | 0.30 | 0.40 | 0.17 | 0.30 | 0.35 |
| 700 | 0.23 | 0.28 | 0.36 | 0.19 | 0.28 | 0.34 |
| 800 | 0.27 | 0.26 | 0.38 | 0.20 | 0.26 | 0.33 |
| 900 | 0.19 | 0.25 | 0.32 | 0.17 | 0.25 | 0.30 |
| 1000 | 0.19 | 0.25 | 0.31 | 0.17 | 0.25 | 0.30 |
| 1100 | 0.17 | 0.24 | 0.30 | 0.20 | 0.24 | 0.31 |
| 1300 | 0.17 | 0.24 | 0.29 | 0.16 | 0.24 | 0.29 |
| 1500 | 0.15 | 0.23 | 0.28 | 0.16 | 0.23 | 0.28 |
| 1700 | 0.29 | 0.23 | 0.37 | 0.29 | 0.23 | 0.37 |
| 2000 | 0.50 | 0.23 | 0.55 | 0.31 | 0.23 | 0.39 |
| 2200 | 0.65 | 0.23 | 0.69 | 0.40 | 0.23 | 0.46 |
| 2300 | 0.70 | 0.23 | 0.74 | 0.45 | 0.23 | 0.50 |
| 2400 | 0.72 | 0.23 | 0.75 | 0.48 | 0.23 | 0.53 |
| 2500 | 0.84 | 0.23 | 0.87 | 0.78 | 0.23 | 0.81 |

Table 5.3.5. Spectral Irradiance standard uncertainties (k=1) of the lamp **BN-9101-641**

| Wavelength, nm | Round 1 | | | Round 2 | | |
|---|---|---|---|---|---|---|
| | Uncertainties associated with, % | | Combined uncertainty, % | Uncertainties associated with, % | | Combined uncertainty, % |
| | Uncorrelated effects | Correlated effects | | Uncorrelated effects | Correlated effects | |
| 250 | 0.38 | 0.92 | 1.00 | 0.66 | 0.92 | 1.14 |
| 260 | 0.28 | 0.86 | 0.90 | 0.41 | 0.86 | 0.95 |
| 270 | 0.26 | 0.80 | 0.85 | 0.43 | 0.80 | 0.91 |
| 280 | 0.28 | 0.75 | 0.80 | 0.26 | 0.75 | 0.80 |
| 290 | 0.39 | 0.71 | 0.81 | 0.26 | 0.71 | 0.76 |
| 300 | 0.31 | 0.67 | 0.74 | 0.25 | 0.67 | 0.72 |
| 320 | 0.31 | 0.60 | 0.68 | 0.19 | 0.60 | 0.63 |
| 340 | 0.22 | 0.55 | 0.59 | 0.20 | 0.55 | 0.58 |
| 360 | 0.33 | 0.51 | 0.60 | 0.18 | 0.51 | 0.54 |
| 380 | 0.23 | 0.47 | 0.52 | 0.16 | 0.47 | 0.50 |
| 400 | 0.21 | 0.44 | 0.49 | 0.18 | 0.44 | 0.48 |
| 450 | 0.21 | 0.39 | 0.44 | 0.14 | 0.39 | 0.41 |
| 500 | 0.21 | 0.35 | 0.41 | 0.17 | 0.35 | 0.39 |
| 555 | 0.26 | 0.32 | 0.41 | 0.16 | 0.32 | 0.36 |
| 600 | 0.26 | 0.30 | 0.40 | 0.17 | 0.30 | 0.35 |
| 700 | 0.23 | 0.28 | 0.36 | 0.19 | 0.28 | 0.34 |
| 800 | 0.27 | 0.26 | 0.38 | 0.20 | 0.26 | 0.33 |
| 900 | 0.19 | 0.25 | 0.32 | 0.17 | 0.25 | 0.30 |
| 1000 | 0.19 | 0.25 | 0.31 | 0.17 | 0.25 | 0.30 |
| 1100 | 0.17 | 0.24 | 0.30 | 0.20 | 0.24 | 0.31 |
| 1300 | 0.17 | 0.24 | 0.29 | 0.16 | 0.24 | 0.29 |
| 1500 | 0.15 | 0.23 | 0.28 | 0.16 | 0.23 | 0.28 |
| 1700 | 0.29 | 0.23 | 0.37 | 0.29 | 0.23 | 0.37 |
| 2000 | 0.50 | 0.23 | 0.55 | 0.31 | 0.23 | 0.39 |
| 2200 | 0.64 | 0.23 | 0.68 | 0.40 | 0.23 | 0.46 |
| 2300 | 0.69 | 0.23 | 0.73 | 0.45 | 0.23 | 0.50 |
| 2400 | 0.71 | 0.23 | 0.74 | 0.48 | 0.23 | 0.53 |
| 2500 | 0.78 | 0.23 | 0.81 | 0.77 | 0.23 | 0.80 |

### 5.3.7. References to section 5.3

[19] S.N. Park, C.W. Park, D.H. Lee, and B.H. Kim "Consistency of the Temperature Scales above the Silver Freezing Point Realized at Four Different Spectral Bands", SICE-ICASE International Joint Conference 2006 Oct. 18-21, 2006 in Bexco, Busan, Korea (2006).

[20] Preston-Thomas H. “The International Scale of 1990 (ITS-90)”, *Metrologia*, 1990, **27**, 3-10.

## 5.4. LNE-CNAM, France

### 5.4.1. Primary scale realisation

The primary spectral irradiance scale at LNE-CNAM is based on the comparison of a light source with a primary standard high temperature black body (HTBB) at a given temperature. The calibration method is similar to others previously developed in other National Measurement Institutes [21,12]. The temperature of HTBB is accessed by measuring the spectral radiance at one wavelength with a filter radiometer [27]. The spectral responsivity of the radiometer is obtained by calibration of the trap detector with our cryogenic radiometer [23,24] and calibration of the spectral regular transmittance of the filter with our primary spectrophotometer [25]. The radiance at other wavelengths is calculated with the Planck's radiation law. The traceability of spectral irradiance with national realisation of watt and meter is schematized Figure 5.4.1. To minimize the uncertainty of this method, corrections due to the characteristics of the blackbody such as its temperature homogeneity and its emissivity are applied [26]. The high temperature blackbody (HTBB) used for the comparison was a BB3200pg supplied by VNIIOFI.

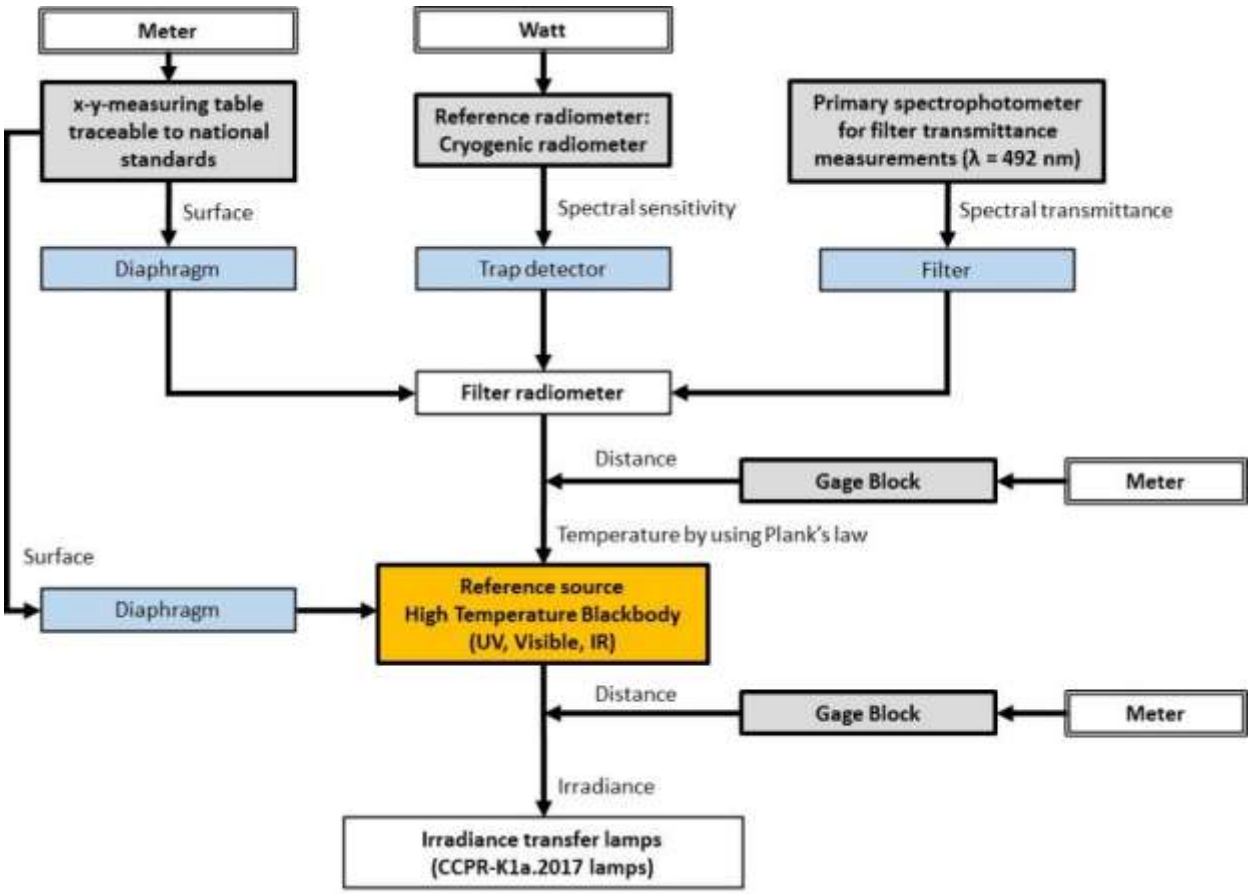


Figure 5.4.1. Traceability chain for the spectral irradiance calibration at LNE-CNAM (LCM)

### 5.4.2. Description of the calibration facility

The spectroradiometer of the LNE-CNAM is described in Figure 5.4.2. The HTBB is used as an irradiance reference for the calibration of transfer sources. For this purpose, a spectroradiometric system have been placed between the HTBB and transfer lamps (Lamp1 and Lamp2). The integrating sphere that receives the flux from the sources has an entrance port equipped with a circular calibrated diaphragm and an output port located at 90° with a rectangular slit shape of 2 mm x 15 mm. Two Ø 150 mm spherical mirrors focus the image of the sphere exit slit onto the entrance slit of a double monochromator.

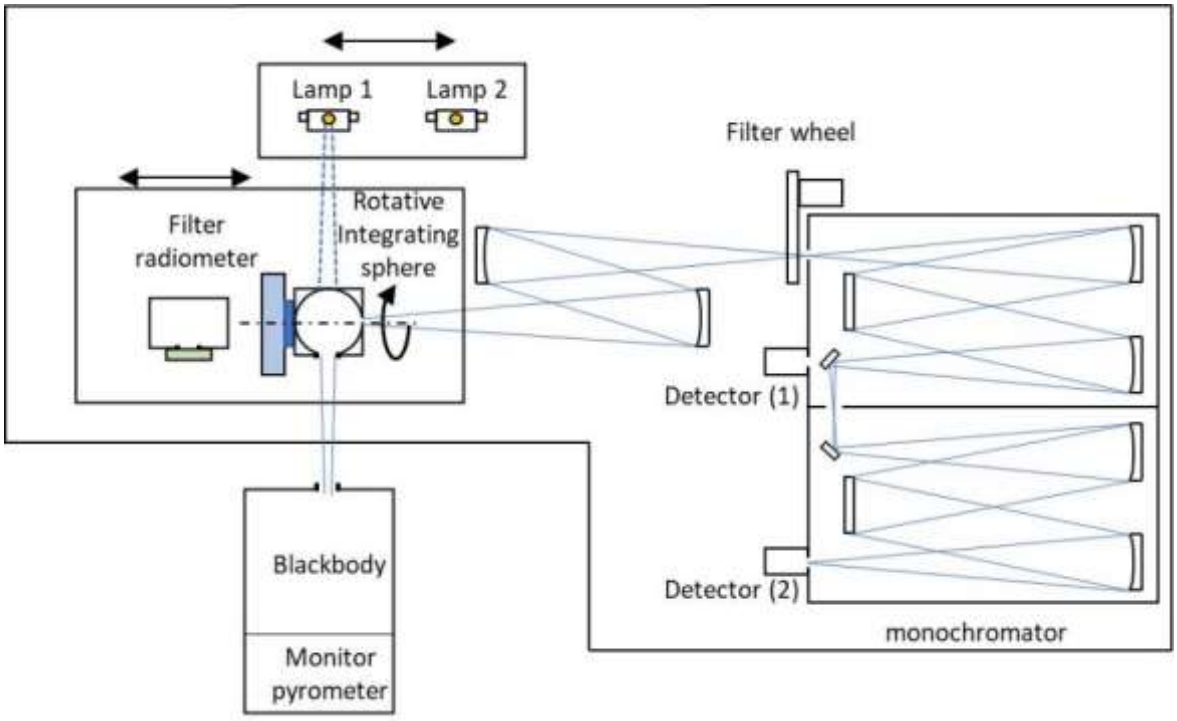


Figure 5.4.2. Diagram of LNE-CNAM calibration facility

The filter radiometer and the integrating sphere are placed on the same automated translation table. This allows the blackbody temperature to be automatically measured during the measurement cycle. The integrating sphere is mounted on a rotation stage that allows a 180° rotation around the axis centered on the exit slit. This allows the collection of either the flux of the HTBB (configuration represented in Figure 5.4.2), or the flux of the transfer lamps (not represented). The top and bottom of the exit slit are reversed but its position is the same. The flux is then guided by the 2 mirrors from the sphere to the input slit of the monochromator. This makes it possible to measure the spectral distribution of sources from 250 nm to 2500 nm.

The monochromator is a Jobin Yvon HRD1 which have been retrofitted. The manual wavelength selection mechanism has been replaced by a high precision motorized translation table. Three pairs of gratings are used to cover the wavelengths from 250 nm to 2500 nm. The gratings and detectors characteristics are described in Table 5.4.1.

Four detectors are used:

- Photomultiplier tube (PM R456 Hamamatsu) for the spectral range from 250 nm to 700 nm
- Silicium photodiode (S6337 Hamamatsu) for the spectral range from 475 nm to 1100 nm
- InGaAs photodiode (G6126 Hamamatsu) for the spectral range from 1000 nm to 1600 nm
- Extended InGaAs photodiode (J23TE2-66C-R03M-2.6 Teledyn) for the spectral range from 900 nm to 2500 nm

PM detector has been mounted in front of the second exit slit of monochromator (double monochromator). Other detectors have been mounted to first exit slit (single monochromator). The InGaAs extended detector is thermoelectrically cooled.

Table 5.4.1. Grating and detector used on spectroradiometer facility of LNE-CNAM

| Grating | Wavelength range, nm | Detector | Lines per mm | Blaze Wavelength | Monochromator |
|---|---|---|---|---|---|
| **UV** | 250 – 700 | PM R456 | 600 | 250 nm | Double |
| **Visible** | 475 – 1100 | Si95D | 1200 | 500 nm | Single |
| **IR** | 1000 – 1600 | InGaAs | 600 | 2 µm | Single |
| **IR** | 900 – 2500 (round 1)<br>1100 – 2500 (round 2) | InGaAs extended | 600 | 2 µm | Double (round 1)<br>Single (round 2) |

The entire facility is placed in a box with two compartments, one of which isolates the monochromator, in order to reduce stray light.

The bench is controlled by a program developed in LabView. This program allows moving of transfer lamps and radiometer, rotation of the sphere and control of monochromator. The program also allows the control of the whole protocol during a complete measurement cycle. Thanks to this facility it is possible to measure the absolute irradiance of transfer lamps and the spectral distribution in irradiance compared to HTBB with a direct traceability to cryogenic radiometer.

### 5.4.3. Measurement procedure

The calibration of a lamp consists in comparing its irradiance with that of the HTBB wavelength by wavelength. The diagram in Figure 5.4.3 describes the different steps of the measurement sequence for the calibration of two lamps L1 and L2. The blue boxes represent measurements made at the output of the monochromator.

### 5.4.4. Reporting of Results

The spectral irradiance of lamps is calculated as follows:

$$E_{lamp}(\lambda) = \frac{Signal\ lamp(\lambda)}{Signal\ HTBB(\lambda)} * E_{HTBB}(\lambda, T) \qquad (5.4.1)$$

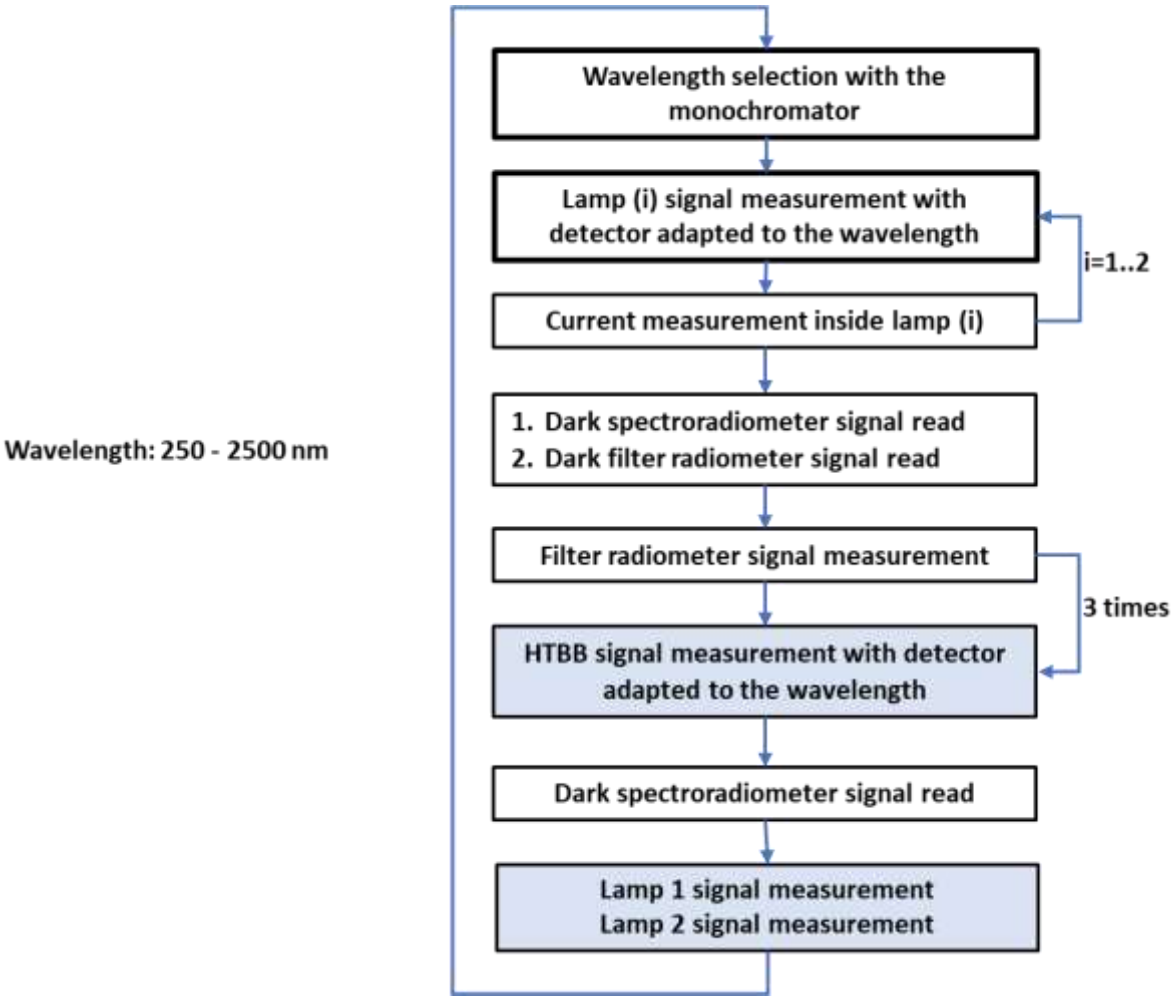


Figure 5.4.3. Measurement procedure at LNE-CNAM

## 5.4.5. Uncertainty determination

### *5.4.5.1. HTBB Temperature measurement uncertainty*

The temperature of the HTBB is obtained thanks to the following model:

$$T_{\lambda_0} = \frac{C_2}{n.\lambda_0.ln\left(\frac{C_1}{\pi.n^2.{\lambda_0}^5.\varepsilon.L_{\lambda_0}}+1\right)} \quad \text{and,} \quad L_{\lambda_0} = \frac{d^2}{A} * E_{\lambda_0} \tag{5.4.2}$$

with :

$T_{\lambda_0}$: temperature of the HTBB measured at $\lambda_0$

$C_1$ and $C_2$ : Planck constants

$n$: air refractive index. $n$ = 1.00027113 with a relative uncertainty of $2.4 \cdot 10^{-8}$, at room temperature, normal pressure and at 492 nm, according to the Ciddor model

$\lambda_0$: wavelength in vacuum used with filter radiometer (at 492 nm)

$\varepsilon$: emissivity of the HTBB

$L_{\lambda_0}$: Radiance of the HTBB measured at $\lambda_0$ with filter radiometer

*A*: Area of the precision HTBB diaphragm,

*d*: distance from the HTBB diaphragm to the filter radiometer diaphragm

$E_{\lambda_0}$: Irradiance of the HTBB measured at $\lambda_0$ with filter radiometer

Uncertainty budget of the temperature measurement during the spectral irradiance comparison is detailed in Table 5.4.2.

Table 5.4.2. Uncertainty budget of the temperature measurement

| | **Round 1** | | | **Round 2** | | | |
|---|---|---|---|---|---|---|---|
| **Parameters** | **Relative uncertainty (k=1)** | **Uncertainty at 3000 K (k=1) / K** | **Uncertainty at 3150 K (k=1) / K** | **Relative uncertainty (k=1)** | **Uncertainty at 2650 K (k=1) / K** | **Uncertainty at 3000 K (k=1) / K** | **Uncertainty at 3150 K (k=1) / K** |
| Standard deviation of measurements | 0.08% | 0.25 | 0.28 | 0.08% | 0.20 | 0.25 | 0.28 |
| Filter radiometer | 0.17% | 0.53 | 0.59 | 0.17% | 0.41 | 0.53 | 0.59 |
| Aperture area | 0.05% | 0.16 | 0.17 | 0.05% | 0.12 | 0.16 | 0.17 |
| Distance HTBB_filter radiometer (d=858 mm round 1, d=758 mm round 2) | 0.05% | 0.17 | 0.19 | 0.06% | 0.14 | 0.18 | 0.20 |
| Emissivity | 0.05% | 0.16 | 0.17 | 0.05% | 0.12 | 0.16 | 0.17 |
| Voltmeter, current, voltage converter | 0.01% | 0.02 | 0.02 | 0.01% | 0.02 | 0.02 | 0.02 |
| Stray light | 0.10% | 0.31 | 0.34 | 0.10% | 0.24 | 0.31 | 0.34 |
| **Combined standard uncertainty (k=1)** | 0.23% | **0.72** | **0.80** | 0.23% | **0.57** | **0.72** | **0.80** |

Standard deviation of measurements:

The standard deviations shown in Table 5.4.2 are calculated from the HTTB signal measured with the filter radiometer during measurement cycle. This relative uncertainty is 0.08 %.

Filter radiometer responsivity:

The spectral responsivity of the filter radiometer is expressed in $AW^{-1}m^2$. The global uncertainty on the filter radiometer responsivity comes from uncertainties associated to each filter radiometer component:

- The filter transmittance, calibrated with our primary spectrophotometer.
- The trap detector spectral responsivity, calibrated with the cryogenic radiometer.
- The aperture surface, calibrated with our XY measuring table.

The combination of these independent sources of uncertainty results in a relative standard uncertainty of 0.17 % for the measurement of absolute spectral irradiance.

The aperture surface:

The surface of the HTBB diaphragm is measured with an X-Y table,
$A = 50.250\ mm^2 \pm 0.024\ mm^2$. The relative uncertainty on the surface measurement is equal to 0.05 %.

Distance between the HTBB and the filter radiometer:

The distance between the HTBB and the filter radiometer is measured with a gage block. They are $d = 858$ mm in round 1 and $d = 758$ mm in round 2. The uncertainty associated to these distance measurements is equal to 0.23 mm. The relative uncertainty is equal to 0.05 % for first round and 0.06 % for second round.

Emissivity:

The emissivity value has been estimated with STEEP322 software. The estimated emissivity is equal to 0.9976 with a relative uncertainty of 0.05 %.

Voltmeter, Current, voltage converter:

The output current of the filter radiometer is converted into voltage by means of a current to voltage converter. The voltage is then measured with a voltmeter. The uncertainty associated with this measurement is the combination of the uncertainties associated with the converter and the voltmeter. The overall relative uncertainty is equal to 0.01 %.

The uncertainties of Planck constants $C_1$, $C_2$ and air refractive index n are negligible comparing with other components. So, these uncertainties have not considered in the budget.

**Combined uncertainty of the HTBB temperature measurement**:

The temperature is calculated from the different components according to equation (5.4.2), the combined uncertainty is:

- 0.57 K for HTBB at 2650 K
- 0.72 K for HTBB at 3000 K
- 0.80 K for HTBB at 3150 K

### 5.4.5.2. HTBB Spectral irradiance uncertainties

The spectral irradiance emitted by the HTBB is calculated as:

$$E_{HTBB}(\lambda,T) = \frac{A}{d^2} * \varepsilon * \frac{C_1}{\pi n^2 \lambda^5 \left(exp\left(\frac{C_2}{n\lambda T}\right) - 1\right)} \quad (5.4.3)$$

where
$\lambda$ : wavelength in vacuum
$T$ : temperature of the HTBB

Uncertainty budget of the HTBB spectral irradiance is shown in Table 5.4.3 for round 1 and in Table 5.4.4 for round 2. During the first round, HTBB has been used with a temperature set between 3000 K and 3100 K. And for the second round, temperature of the HTBB was set between 3000 K and 3150 K from 250 nm to 1100 nm, and about 2650 K from 1100 nm to 2500 nm.

Table 5.4.3. Uncertainty budget of the HTBB spectral irradiance during Round 1

| Round 1 | | | | | | |
|---|---|---|---|---|---|---|
| Wavelength / nm | Uncertainties associated with (k = 1) / (%) | | | | | Combined uncertainty (k = 1) / (%) |
| | Temperature 0.8 K | Blackbody stability 0.2 K | Emissivity | Aperture Area | Distance blackbody-sphere | |
| **250** | 0.48 | 0.12 | 0.05 | 0.05 | 0.06 | **0.51** |
| **260** | 0.47 | 0.12 | 0.05 | 0.05 | 0.06 | **0.49** |
| **270** | 0.45 | 0.11 | 0.05 | 0.05 | 0.06 | **0.47** |
| **280** | 0.43 | 0.11 | 0.05 | 0.05 | 0.06 | **0.45** |
| **290** | 0.42 | 0.10 | 0.05 | 0.05 | 0.06 | **0.44** |
| **300** | 0.40 | 0.10 | 0.05 | 0.05 | 0.06 | **0.43** |
| **320** | 0.38 | 0.09 | 0.05 | 0.05 | 0.06 | **0.40** |
| **340** | 0.36 | 0.09 | 0.05 | 0.05 | 0.06 | **0.38** |
| **360** | 0.34 | 0.08 | 0.05 | 0.05 | 0.06 | **0.36** |
| **380** | 0.32 | 0.08 | 0.05 | 0.05 | 0.06 | **0.34** |
| **400** | 0.30 | 0.08 | 0.05 | 0.05 | 0.06 | **0.32** |
| **450** | 0.27 | 0.07 | 0.05 | 0.05 | 0.06 | **0.29** |
| **500** | 0.24 | 0.06 | 0.05 | 0.05 | 0.06 | **0.27** |
| **555** | 0.22 | 0.05 | 0.05 | 0.05 | 0.06 | **0.24** |
| **600** | 0.20 | 0.05 | 0.05 | 0.05 | 0.06 | **0.23** |
| **700** | 0.17 | 0.04 | 0.05 | 0.05 | 0.06 | **0.20** |
| **800** | 0.17 | 0.04 | 0.05 | 0.05 | 0.06 | **0.20** |
| **900** | 0.13 | 0.03 | 0.05 | 0.05 | 0.06 | **0.16** |
| **1000** | 0.12 | 0.03 | 0.05 | 0.05 | 0.06 | **0.15** |
| **1100** | 0.12 | 0.03 | 0.05 | 0.05 | 0.06 | **0.15** |
| **1300** | 0.11 | 0.03 | 0.05 | 0.05 | 0.06 | **0.14** |
| **1500** | 0.08 | 0.02 | 0.05 | 0.05 | 0.06 | **0.12** |
| **1700** | 0.07 | 0.02 | 0.05 | 0.05 | 0.06 | **0.12** |
| **2000** | 0.06 | 0.02 | 0.05 | 0.05 | 0.06 | **0.11** |
| **2200** | 0.05 | 0.01 | 0.05 | 0.05 | 0.06 | **0.11** |
| **2300** | 0.05 | 0.01 | 0.05 | 0.05 | 0.06 | **0.11** |
| **2400** | 0.05 | 0.01 | 0.05 | 0.05 | 0.06 | **0.10** |
| **2500** | 0.05 | 0.01 | 0.05 | 0.05 | 0.06 | **0.10** |

Table 5.4.4. Uncertainty budget of the HTBB spectral irradiance during Round 2

| Round 2 | | | | | | |
|---|---|---|---|---|---|---|
| Wavelength / nm | Uncertainties associated with (k = 1) / (%) | | | | | Combined uncertainty (k = 1) / (%) |
| | Temperature | Blackbody stability | Emissivity | Aperture Area | Distance blackbody-sphere | |
| **250** | 0.48 | 0.34 | 0.05 | 0.05 | 0.06 | **0.60** |
| **260** | 0.47 | 0.24 | 0.05 | 0.05 | 0.06 | **0.53** |
| **270** | 0.45 | 0.23 | 0.05 | 0.05 | 0.06 | **0.51** |
| **280** | 0.43 | 0.17 | 0.05 | 0.05 | 0.06 | **0.47** |
| **290** | 0.42 | 0.17 | 0.05 | 0.05 | 0.06 | **0.46** |
| **300** | 0.40 | 0.26 | 0.05 | 0.05 | 0.06 | **0.49** |
| **320** | 0.38 | 0.16 | 0.05 | 0.05 | 0.06 | **0.42** |
| **340** | 0.36 | 0.15 | 0.05 | 0.05 | 0.06 | **0.40** |
| **360** | 0.34 | 0.17 | 0.05 | 0.05 | 0.06 | **0.39** |
| **380** | 0.32 | 0.13 | 0.05 | 0.05 | 0.06 | **0.36** |
| **400** | 0.30 | 0.13 | 0.05 | 0.05 | 0.06 | **0.34** |
| **450** | 0.27 | 0.11 | 0.05 | 0.05 | 0.06 | **0.30** |
| **500** | 0.24 | 0.15 | 0.05 | 0.05 | 0.06 | **0.30** |
| **555** | 0.22 | 0.13 | 0.05 | 0.05 | 0.06 | **0.27** |
| **600** | 0.20 | 0.15 | 0.05 | 0.05 | 0.06 | **0.27** |
| **700** | 0.17 | 0.18 | 0.05 | 0.05 | 0.06 | **0.26** |
| **800** | 0.17 | 0.24 | 0.05 | 0.05 | 0.06 | **0.31** |
| **900** | 0.13 | 0.09 | 0.05 | 0.05 | 0.06 | **0.18** |
| **1000** | 0.12 | 0.11 | 0.05 | 0.05 | 0.06 | **0.19** |
| **1100** | 0.11 | 0.11 | 0.05 | 0.05 | 0.06 | **0.18** |
| **1300** | 0.09 | 0.06 | 0.05 | 0.05 | 0.06 | **0.14** |
| **1500** | 0.08 | 0.07 | 0.05 | 0.05 | 0.06 | **0.14** |
| **1700** | 0.07 | 0.04 | 0.05 | 0.05 | 0.06 | **0.12** |
| **2000** | 0.06 | 0.04 | 0.05 | 0.05 | 0.06 | **0.11** |
| **2200** | 0.05 | 0.06 | 0.05 | 0.05 | 0.06 | **0.12** |
| **2300** | 0.05 | 0.06 | 0.05 | 0.05 | 0.06 | **0.12** |
| **2400** | 0.05 | 0.03 | 0.05 | 0.05 | 0.06 | **0.11** |
| **2500** | 0.05 | 0.05 | 0.05 | 0.05 | 0.06 | **0.11** |

In the first round (Table 5.4.3), the uncertainty on temperature measurement is 0.8 K. The stability of HTBB is the standard deviation of temperature measurement and estimated at 0.2 K. The surface of the HTBB diaphragm is measured with an X-Y table. The relative uncertainty on the surface measurement is equal to 0.05 %. The sixth column is the uncertainty on distance measurement between HTBB and integrating sphere. It is 0.23 mm for a distance between HTBB and integrating sphere of 824 mm.

In the second round (Table 5.4.4), the uncertainty of temperature measurement is varied from 0.57 K to 0.8 K. These values depended on the temperature used at 2650 K and around 3100 K. The stability of the HTBB during the measurement cycle, at a given wavelength, is the standard deviation obtained from three temperature measurements made with the filter radiometer. For each wavelength a standard deviation is calculated. HTBB stability is defined as the maximum of the calculated standard deviations. The uncertainties of aperture area and distance are the same values as the first round.

#### *5.4.5.3. Uncertainties of LNE-CNAM calibration of traveling standard lamps*

Three lamps were measured at LNE-CNAM: BN-9101-653, BN-9101-655 and BN-9101-656.

**Round 1**

Uncertainties components for the three lamps measured during the first round are shown in Table 5.4.5, Table 5.4.6 and Table 5.4.7.

In these tables the type A uncertainty combines the repeatability and the reproducibility of traveling standard lamps and the repeatability of the HTBB. We can find the uncertainty of the HTBB spectral irradiance calculated in Table 5.4.3. The third column is the uncertainty of distance measurement between lamp and integrating sphere. It is 0.16 mm for distance between lamp and integrating sphere of 500 mm. Lamp current uncertainty is 0.4 mA. Wavelength uncertainties are 0.01 nm with UV grating and 0.06 nm with IR grating.

In this round the irradiation spectrum is recalculated using the absolute measurement of each lamp at two wavelengths (492 nm and 575 nm) with a filter radiometer. Consequently, the uncertainty of this parameter was taken into account in the uncertainty budget for spectral irradiance of each lamp. It is combined uncertainty of absolutes values measurements at 492 nm and 575 nm.

During the first round failures occurred in our measurement set up that impacted results for the three lamps, at several wavelengths (from 800 nm to 1100 nm, and from 1700 to 2500 nm). We decided to remove those values from the comparison.

**Round 2**

Uncertainty budget of the three traveling lamps measured during second round is shown in Table 5.4.8, Table 5.4.9 and Table 5.4.10. Like for the first round, the type A uncertainty combines the repeatability and the reproducibility of traveling standard lamps and the repeatability of the HTBB. The uncertainty of the HTBB spectral irradiance is calculated in Table 5.4.4. The uncertainties on distance measurement between HTBB and integrating sphere and lamp current are the same values as the first round. Wavelength uncertainties are 0.012 nm with UV grating, 0.1 nm with VIS grating and 0.2 nm with IR grating. In the second round the spectral irradiance is measured directly in absolute value.

**Correlation**

The only correlated effects are the scale realisation with the HTBB and the wavelength accuracy of the monochromator during one round.

The measurements repeatability, lamp distance, current and alignment are uncorrelated.

The final uncertainty values submitted by LNE-CNAM to the pilot with the spectral irradiance data are presented in Tables 5.4.11 – 5.4.13.

### 5.4.6. References to section 5.4

[21] Yoon H W, Gibson C E and Barnes P Y 2003 The realization of the NIST detector-based spectral irradiance scale *Metrologia* **40** S172–S176

[22] W. Möller, P. Sperfeld, B. Nawo K H and J M 1998 Realization of the spectral irradiance scale in the air-ultraviolet using thermal radiators *Metrologia* **35** 261–5

[23] Coutin J and Rougie B 2016 Characterization and validation of a new cryogenic radiometer at the LNE-LCM *Rev. Française métrologie* 2016–1 11–20

[24] Bastie J 2005 Optical radiation measurements at CNAM-INM *ENGEVISTA* 7 4–18

[25] Obein G and Bastie J 2011 Report on the key comparison EUROMET-PR-K6: Spectral regular transmittance *Metrologia* **48** 39

[26] ROUGIÉ B., VALIN M. H., 2017 Thermodynamic measurement and validation of a high temperature blackbody for spectral radiance and irradiance reference, *NEWRAD 2017 Proceedings*, Tokyo, Japan.

[27] Valin M H 2019, Etalon d'éclairement et de luminance énergétique de l'ultraviolet à l'infrarouge basé sur un corps noir haute température raccordé aux références radiométriques, internal report.

Table 5.4.5. Uncertainty budget for spectral irradiance of the lamp BN-9101-653 in round 1

| BN-9101-653, Round 1 | | | | | | | | |
|---|---|---|---|---|---|---|---|---|
| | Uncertainty in spectral irradiance (k=1) / % | | | | | | | |
| **Wavelength / nm** | Type A Standard deviation of measurements | Uncertainty of the HTBB spectral irradiance | Distance Lamp to Sphere | Type B Lampe current | Wavelength | Alignment | absolute values | **Combined uncertainty** |
| **250** | 2.62 | 0.51 | 0.06 | 0.06 | 0.05 | 0.10 | 0.26 | **2.69** |
| **260** | 1.12 | 0.49 | 0.06 | 0.06 | 0.05 | 0.10 | 0.26 | **1.26** |
| **270** | 0.73 | 0.47 | 0.06 | 0.06 | 0.05 | 0.10 | 0.26 | **0.92** |
| **280** | 0.55 | 0.45 | 0.06 | 0.05 | 0.04 | 0.10 | 0.26 | **0.77** |
| **290** | 0.36 | 0.44 | 0.06 | 0.05 | 0.04 | 0.10 | 0.26 | **0.64** |
| **300** | 0.30 | 0.43 | 0.06 | 0.05 | 0.04 | 0.10 | 0.26 | **0.60** |
| **320** | 0.22 | 0.40 | 0.06 | 0.05 | 0.03 | 0.10 | 0.26 | **0.54** |
| **340** | 0.17 | 0.38 | 0.06 | 0.04 | 0.03 | 0.10 | 0.26 | **0.51** |
| **360** | 0.15 | 0.36 | 0.06 | 0.04 | 0.02 | 0.10 | 0.26 | **0.48** |
| **380** | 0.15 | 0.34 | 0.06 | 0.04 | 0.02 | 0.10 | 0.26 | **0.47** |
| **400** | 0.14 | 0.32 | 0.06 | 0.04 | 0.02 | 0.10 | 0.26 | **0.46** |
| **450** | 0.12 | 0.29 | 0.06 | 0.03 | 0.01 | 0.10 | 0.26 | **0.43** |
| **500** | 0.22 | 0.27 | 0.06 | 0.03 | 0.01 | 0.10 | 0.26 | **0.45** |
| **555** | 0.12 | 0.24 | 0.06 | 0.03 | 0.01 | 0.10 | 0.26 | **0.39** |
| **600** | 0.14 | 0.23 | 0.06 | 0.03 | 0.00 | 0.10 | 0.26 | **0.39** |
| **700** | 0.37 | 0.20 | 0.06 | 0.02 | 0.00 | 0.10 | 0.26 | **0.51** |
| **800** | | | | | | | | |
| **900** | | | | | | | | |
| **1000** | | | | | | | | |
| **1100** | | | | | | | | |
| **1300** | 0.65 | 0.14 | 0.06 | 0.01 | 0.00 | 0.10 | 0.26 | **0.72** |
| **1500** | 0.70 | 0.12 | 0.06 | 0.01 | 0.01 | 0.10 | 0.26 | **0.76** |
| **1700** | | | | | | | | |
| **2000** | | | | | | | | |
| **2200** | | | | | | | | |
| **2300** | | | | | | | | |
| **2400** | | | | | | | | |
| **2500** | | | | | | | | |

Table 5.4.6. Uncertainty budget for spectral irradiance of the lamp BN-9101-655 in round 1

| **BN-9101-655_ Round 1** | | | | | | | | |
|---|---|---|---|---|---|---|---|---|
| | **Uncertainty in spectral irradiance (k=1) / %** | | | | | | | |
| **Wavelength / nm** | Type A Standard deviation of measurements | Uncertainty of the HTBB spectral irradiance | Distance Lamp to Sphere | Type B Lampe current | Wavelength | Alignment | absolute values | **Combined standard uncertainty** |
| **250** | 2.77 | 0.51 | 0.06 | 0.06 | 0.05 | 0.10 | 0.26 | **2.83** |
| **260** | 1.24 | 0.49 | 0.06 | 0.06 | 0.05 | 0.10 | 0.26 | **1.36** |
| **270** | 1.04 | 0.47 | 0.06 | 0.06 | 0.05 | 0.10 | 0.26 | **1.18** |
| **280** | 0.66 | 0.45 | 0.06 | 0.05 | 0.04 | 0.10 | 0.26 | **0.86** |
| **290** | 0.58 | 0.44 | 0.06 | 0.05 | 0.04 | 0.10 | 0.26 | **0.79** |
| **300** | 0.37 | 0.43 | 0.06 | 0.05 | 0.04 | 0.10 | 0.26 | **0.63** |
| **320** | 0.47 | 0.40 | 0.06 | 0.05 | 0.03 | 0.10 | 0.26 | **0.68** |
| **340** | 0.36 | 0.38 | 0.06 | 0.04 | 0.03 | 0.10 | 0.26 | **0.60** |
| **360** | 0.20 | 0.36 | 0.06 | 0.04 | 0.02 | 0.10 | 0.26 | **0.50** |
| **380** | 0.27 | 0.34 | 0.06 | 0.04 | 0.02 | 0.10 | 0.26 | **0.52** |
| **400** | 0.28 | 0.32 | 0.06 | 0.04 | 0.02 | 0.10 | 0.26 | **0.52** |
| **450** | 0.16 | 0.29 | 0.06 | 0.03 | 0.01 | 0.10 | 0.26 | **0.44** |
| **500** | 0.13 | 0.27 | 0.06 | 0.03 | 0.01 | 0.10 | 0.26 | **0.41** |
| **555** | 0.23 | 0.24 | 0.06 | 0.03 | 0.01 | 0.10 | 0.26 | **0.44** |
| **600** | 0.16 | 0.23 | 0.06 | 0.03 | 0.00 | 0.10 | 0.26 | **0.40** |
| **700** | 0.34 | 0.20 | 0.06 | 0.02 | 0.00 | 0.10 | 0.26 | **0.48** |
| **800** | | | | | | | | |
| **900** | | | | | | | | |
| **1000** | | | | | | | | |
| **1100** | | | | | | | | |
| **1300** | 0.62 | 0.14 | 0.06 | 0.01 | 0.00 | 0.10 | 0.26 | **0.70** |
| **1500** | 0.71 | 0.12 | 0.06 | 0.01 | 0.01 | 0.10 | 0.26 | **0.78** |
| **1700** | | | | | | | | |
| **2000** | | | | | | | | |
| **2200** | | | | | | | | |
| **2300** | | | | | | | | |
| **2400** | | | | | | | | |
| **2500** | | | | | | | | |

Table 5.4.7. Uncertainty budget for spectral irradiance of the lamp BN-9101-656 in round 1

| **BN-9101-656_ Round 1** | | | | | | | | |
|---|---|---|---|---|---|---|---|---|
| | **Uncertainty in spectral irradiance (k=1) / %** | | | | | | | |
| | Type A | Type B | | | | | | |
| **Wavelength / nm** | Standard deviation of measurements | Uncertainty of the HTBB spectral irradiance | Distance Lamp to Sphere | Lampe current | Wavelength | Alignment | absolute values | **Combined standard uncertainty** |
| **250** | 7.32 | 0.51 | 0.06 | 0.06 | 0.05 | 0.10 | 0.26% | **7.34** |
| **260** | 2.15 | 0.49 | 0.06 | 0.06 | 0.05 | 0.10 | 0.26% | **2.21** |
| **270** | 1.75 | 0.47 | 0.06 | 0.06 | 0.05 | 0.10 | 0.26% | **1.82** |
| **280** | 0.89 | 0.45 | 0.06 | 0.05 | 0.04 | 0.10 | 0.26% | **1.01** |
| **290** | 0.91 | 0.44 | 0.06 | 0.05 | 0.04 | 0.10 | 0.26% | **1.02** |
| **300** | 0.44 | 0.43 | 0.06 | 0.05 | 0.04 | 0.10 | 0.26% | **0.63** |
| **320** | 0.38 | 0.40 | 0.06 | 0.05 | 0.03 | 0.10 | 0.26% | **0.57** |
| **340** | 0.32 | 0.38 | 0.06 | 0.04 | 0.03 | 0.10 | 0.26% | **0.51** |
| **360** | 0.30 | 0.36 | 0.06 | 0.04 | 0.02 | 0.10 | 0.26% | **0.48** |
| **380** | 0.26 | 0.34 | 0.06 | 0.04 | 0.02 | 0.10 | 0.26% | **0.45** |
| **400** | 0.27 | 0.32 | 0.06 | 0.04 | 0.02 | 0.10 | 0.26% | **0.44** |
| **450** | 0.35 | 0.29 | 0.06 | 0.03 | 0.01 | 0.10 | 0.26% | **0.47** |
| **500** | 0.43 | 0.27 | 0.06 | 0.03 | 0.01 | 0.10 | 0.26% | **0.52** |
| **555** | 0.26 | 0.24 | 0.06 | 0.03 | 0.01 | 0.10 | 0.26% | **0.37** |
| **600** | 0.25 | 0.23 | 0.06 | 0.03 | 0.00 | 0.10 | 0.26% | **0.36** |
| **700** | 0.53 | 0.20 | 0.06 | 0.02 | 0.00 | 0.10 | 0.26% | **0.58** |
| **800** | | | | | | | | |
| **900** | | | | | | | | |
| **1000** | | | | | | | | |
| **1100** | | | | | | | | |
| **1300** | 0.66 | 0.14 | 0.06 | 0.01 | 0.00 | 0.10 | 0.26% | **0.69** |
| **1500** | 0.70 | 0.12 | 0.06 | 0.01 | 0.01 | 0.10 | 0.26% | **0.72** |
| **1700** | | | | | | | | |
| **2000** | | | | | | | | |
| **2200** | | | | | | | | |
| **2300** | | | | | | | | |
| **2400** | | | | | | | | |
| **2500** | | | | | | | | |

Table 5.4.8. Uncertainty budget for spectral irradiance of the lamp BN-9101-653 in round 2

| **BN-9101-653_ Round 2** | | | | | | | |
|---|---|---|---|---|---|---|---|
| | **Uncertainty in spectral irradiance (k=1) / %** | | | | | | |
| | Type A | Type B | | | | | |
| **Wavelength / nm** | Standard deviation of measurements | Uncertainty of the HTBB spectral irradiance | Distance lamp to Sphere | Lampe current | Wavelength | Alignment | **Combined standard uncertainty** |
| **250** | 3.29 | 0.60 | 0.06 | 0.06 | 0.09 | 0.10 | **3.35** |
| **260** | 1.16 | 0.53 | 0.06 | 0.06 | 0.08 | 0.10 | **1.28** |
| **270** | 0.79 | 0.51 | 0.06 | 0.06 | 0.07 | 0.10 | **0.96** |
| **280** | 0.55 | 0.48 | 0.06 | 0.05 | 0.07 | 0.10 | **0.74** |
| **290** | 0.42 | 0.46 | 0.06 | 0.05 | 0.06 | 0.10 | **0.64** |
| **300** | 0.34 | 0.49 | 0.06 | 0.05 | 0.06 | 0.10 | **0.61** |
| **320** | 0.25 | 0.42 | 0.06 | 0.05 | 0.05 | 0.10 | **0.51** |
| **340** | 0.19 | 0.40 | 0.06 | 0.04 | 0.04 | 0.10 | **0.46** |
| **360** | 0.18 | 0.39 | 0.06 | 0.04 | 0.04 | 0.10 | **0.45** |
| **380** | 0.15 | 0.36 | 0.06 | 0.04 | 0.03 | 0.10 | **0.41** |
| **400** | 0.13 | 0.34 | 0.06 | 0.04 | 0.03 | 0.10 | **0.39** |
| **450** | 0.11 | 0.31 | 0.06 | 0.03 | 0.02 | 0.10 | **0.35** |
| **500** | 0.13 | 0.30 | 0.06 | 0.03 | 0.01 | 0.10 | **0.35** |
| **555** | 0.14 | 0.27 | 0.06 | 0.03 | 0.01 | 0.10 | **0.33** |
| **600** | 0.17 | 0.27 | 0.06 | 0.03 | 0.01 | 0.10 | **0.34** |
| **700** | 0.25 | 0.27 | 0.06 | 0.02 | 0.00 | 0.10 | **0.39** |
| **800** | 0.38 | 0.30 | 0.06 | 0.02 | 0.00 | 0.10 | **0.50** |
| **900** | 0.11 | 0.19 | 0.06 | 0.02 | 0.00 | 0.10 | **0.25** |
| **1000** | 0.04 | 0.19 | 0.06 | 0.02 | 0.00 | 0.10 | **0.23** |
| **1100** | 0.12 | 0.18 | 0.06 | 0.01 | 0.00 | 0.10 | **0.25** |
| **1300** | 0.10 | 0.14 | 0.06 | 0.01 | 0.01 | 0.10 | **0.21** |
| **1500** | 0.08 | 0.14 | 0.06 | 0.01 | 0.02 | 0.10 | **0.20** |
| **1700** | 0.09 | 0.12 | 0.06 | 0.01 | 0.02 | 0.10 | **0.19** |
| **2000** | 0.26 | 0.11 | 0.06 | 0.01 | 0.02 | 0.10 | **0.30** |
| **2200** | 0.42 | 0.12 | 0.06 | 0.01 | 0.02 | 0.10 | **0.45** |
| **2300** | 0.58 | 0.12 | 0.06 | 0.01 | 0.02 | 0.10 | **0.60** |
| **2400** | 1.01 | 0.11 | 0.06 | 0.01 | 0.02 | 0.10 | **1.02** |
| **2500** | 3.71 | 0.11 | 0.06 | 0.01 | 0.02 | 0.10 | **3.71** |

Table 5.4.9. Uncertainty budget for spectral irradiance of the lamp BN-9101-655 in round 2

| **BN-9101-655_ Round 2** | | | | | | | |
|---|---|---|---|---|---|---|---|
| | **Uncertainty in spectral irradiance (k=1) / %** | | | | | | |
| | Type A | Type B | | | | | |
| **Wavelength / nm** | Standard deviation of measurements | Uncertainty of the HTBB spectral irradiance | Distance Lamp to Sphere | Lampe current | Wavelength | Alignment | **Combined standard uncertainty** |
| **250** | 3.77 | 0.60 | 0.06 | 0.06 | 0.09 | 0.10 | **3.82** |
| **260** | 1.33 | 0.53 | 0.06 | 0.06 | 0.08 | 0.10 | **1.44** |
| **270** | 0.88 | 0.51 | 0.06 | 0.06 | 0.07 | 0.10 | **1.03** |
| **280** | 0.57 | 0.48 | 0.06 | 0.05 | 0.07 | 0.10 | **0.76** |
| **290** | 0.46 | 0.46 | 0.06 | 0.05 | 0.06 | 0.10 | **0.67** |
| **300** | 0.35 | 0.49 | 0.06 | 0.05 | 0.06 | 0.10 | **0.62** |
| **320** | 0.27 | 0.42 | 0.06 | 0.05 | 0.05 | 0.10 | **0.52** |
| **340** | 0.21 | 0.40 | 0.06 | 0.04 | 0.04 | 0.10 | **0.47** |
| **360** | 0.19 | 0.39 | 0.06 | 0.04 | 0.04 | 0.10 | **0.45** |
| **380** | 0.22 | 0.36 | 0.06 | 0.04 | 0.03 | 0.10 | **0.44** |
| **400** | 0.21 | 0.34 | 0.06 | 0.04 | 0.03 | 0.10 | **0.42** |
| **450** | 0.17 | 0.31 | 0.06 | 0.03 | 0.02 | 0.10 | **0.37** |
| **500** | 0.20 | 0.30 | 0.06 | 0.03 | 0.09 | 0.10 | **0.39** |
| **555** | 0.19 | 0.27 | 0.06 | 0.03 | 0.07 | 0.10 | **0.36** |
| **600** | 0.32 | 0.27 | 0.06 | 0.03 | 0.05 | 0.10 | **0.43** |
| **700** | 0.51 | 0.27 | 0.06 | 0.02 | 0.03 | 0.10 | **0.59** |
| **800** | 0.13 | 0.30 | 0.06 | 0.02 | 0.01 | 0.10 | **0.35** |
| **900** | 0.10 | 0.19 | 0.06 | 0.02 | 0.00 | 0.10 | **0.25** |
| **1000** | 0.14 | 0.19 | 0.06 | 0.02 | 0.00 | 0.10 | **0.26** |
| **1100** | 0.68 | 0.18 | 0.06 | 0.01 | 0.00 | 0.10 | **0.71** |
| **1300** | 0.14 | 0.14 | 0.06 | 0.01 | 0.01 | 0.10 | **0.23** |
| **1500** | 0.27 | 0.14 | 0.06 | 0.01 | 0.02 | 0.10 | **0.32** |
| **1700** | 0.35 | 0.12 | 0.06 | 0.01 | 0.02 | 0.10 | **0.39** |
| **2000** | 0.36 | 0.11 | 0.06 | 0.01 | 0.02 | 0.10 | **0.39** |
| **2200** | 0.72 | 0.12 | 0.06 | 0.01 | 0.02 | 0.10 | **0.74** |
| **2300** | 0.74 | 0.12 | 0.06 | 0.01 | 0.02 | 0.10 | **0.76** |
| **2400** | 1.31 | 0.11 | 0.06 | 0.01 | 0.02 | 0.10 | **1.32** |
| **2500** | 5.06 | 0.11 | 0.06 | 0.01 | 0.02 | 0.10 | **5.07** |

Table 5.4.10. Uncertainty budget for spectral irradiance of the lamp BN-9101-656 in round 2

| **BN-9101-656_ Round 2** | | | | | | | |
|---|---|---|---|---|---|---|---|
| | **Uncertainty in spectral irradiance (k=1) / %** | | | | | | |
| | Type A | Type B | | | | | |
| Wavelength / nm | Standard deviation of measurements | Uncertainty of the HTBB spectral irradiance | Distance Lamp to Sphere | Lampe current | Wavelength | Alignment | Combined standard uncertainty |
| **250** | 3.78 | 0.60 | 0.06 | 0.06 | 0.09 | 0.10 | **3.84** |
| **260** | 1.53 | 0.53 | 0.06 | 0.06 | 0.08 | 0.10 | **1.63** |
| **270** | 0.85 | 0.51 | 0.06 | 0.06 | 0.07 | 0.10 | **1.01** |
| **280** | 0.59 | 0.48 | 0.06 | 0.05 | 0.07 | 0.10 | **0.77** |
| **290** | 0.58 | 0.46 | 0.06 | 0.05 | 0.06 | 0.10 | **0.76** |
| **300** | 0.49 | 0.49 | 0.06 | 0.05 | 0.06 | 0.10 | **0.71** |
| **320** | 0.54 | 0.42 | 0.06 | 0.05 | 0.05 | 0.10 | **0.70** |
| **340** | 0.44 | 0.40 | 0.06 | 0.04 | 0.04 | 0.10 | **0.61** |
| **360** | 0.48 | 0.39 | 0.06 | 0.04 | 0.04 | 0.10 | **0.63** |
| **380** | 0.29 | 0.36 | 0.06 | 0.04 | 0.03 | 0.10 | **0.48** |
| **400** | 0.47 | 0.34 | 0.06 | 0.04 | 0.03 | 0.10 | **0.60** |
| **450** | 0.36 | 0.31 | 0.06 | 0.03 | 0.02 | 0.10 | **0.49** |
| **500** | 0.18 | 0.30 | 0.06 | 0.03 | 0.01 | 0.10 | **0.37** |
| **555** | 0.15 | 0.27 | 0.06 | 0.03 | 0.01 | 0.10 | **0.33** |
| **600** | 0.20 | 0.27 | 0.06 | 0.03 | 0.01 | 0.10 | **0.35** |
| **700** | 0.36 | 0.27 | 0.06 | 0.02 | 0.00 | 0.10 | **0.46** |
| **800** | 0.91 | 0.30 | 0.06 | 0.02 | 0.00 | 0.10 | **0.97** |

Table 5.4.11. Spectral Irradiance standard uncertainties (k=1) of the lamp **BN-9101-653**

| Wavelength, nm | Round 1 | | | Round 2 | | |
|---|---|---|---|---|---|---|
| | Uncertainties associated with, % | | Combined uncertainty, % | Uncertainties associated with, % | | Combined uncertainty, % |
| | Uncorrelated effects | Correlated effects | | Uncorrelated effects | Correlated effects | |
| 250 | 2.64 | 0.51 | 2.69 | 3.30 | 0.61 | 3.35 |
| 260 | 1.16 | 0.49 | 1.26 | 1.16 | 0.54 | 1.28 |
| 270 | 0.78 | 0.47 | 0.92 | 0.80 | 0.52 | 0.96 |
| 280 | 0.62 | 0.46 | 0.77 | 0.57 | 0.48 | 0.74 |
| 290 | 0.46 | 0.44 | 0.64 | 0.44 | 0.47 | 0.64 |
| 300 | 0.42 | 0.43 | 0.60 | 0.37 | 0.49 | 0.61 |
| 320 | 0.36 | 0.40 | 0.54 | 0.28 | 0.42 | 0.51 |
| 340 | 0.34 | 0.38 | 0.51 | 0.23 | 0.40 | 0.46 |
| 360 | 0.33 | 0.36 | 0.48 | 0.22 | 0.39 | 0.45 |
| 380 | 0.32 | 0.34 | 0.47 | 0.19 | 0.36 | 0.41 |
| 400 | 0.32 | 0.32 | 0.46 | 0.18 | 0.34 | 0.39 |
| 450 | 0.31 | 0.29 | 0.43 | 0.16 | 0.31 | 0.35 |
| 500 | 0.36 | 0.27 | 0.45 | 0.18 | 0.30 | 0.35 |
| 555 | 0.31 | 0.24 | 0.39 | 0.19 | 0.27 | 0.33 |
| 600 | 0.32 | 0.23 | 0.39 | 0.21 | 0.27 | 0.34 |
| 700 | 0.46 | 0.20 | 0.51 | 0.28 | 0.27 | 0.39 |
| 800 | | | | 0.40 | 0.30 | 0.50 |
| 900 | | | | 0.16 | 0.19 | 0.25 |
| 1000 | | | | 0.13 | 0.19 | 0.23 |
| 1100 | | | | 0.16 | 0.18 | 0.25 |
| 1300 | 0.71 | 0.14 | 0.72 | 0.16 | 0.14 | 0.21 |
| 1500 | 0.75 | 0.12 | 0.76 | 0.14 | 0.14 | 0.20 |
| 1700 | | | | 0.15 | 0.12 | 0.19 |
| 2000 | | | | 0.28 | 0.12 | 0.30 |
| 2200 | | | | 0.43 | 0.12 | 0.45 |
| 2300 | | | | 0.59 | 0.12 | 0.60 |
| 2400 | | | | 1.01 | 0.11 | 1.02 |
| 2500 | | | | 3.71 | 0.11 | 3.71 |

Table 5.4.12. Spectral Irradiance standard uncertainties (k=1) of the lamp **BN-9101-655**

| Wavelength, nm | Round 1 | | | Round 2 | | |
|---|---|---|---|---|---|---|
| | Uncertainties associated with, % | | Combined uncertainty, % | Uncertainties associated with, % | | Combined uncertainty, % |
| | Uncorrelated effects | Correlated effects | | Uncorrelated effects | Correlated effects | |
| 250 | 2.78 | 0.51 | 2.83 | 3.77 | 0.61 | 3.82 |
| 260 | 1.27 | 0.49 | 1.36 | 1.33 | 0.54 | 1.44 |
| 270 | 1.08 | 0.47 | 1.18 | 0.89 | 0.52 | 1.03 |
| 280 | 0.72 | 0.46 | 0.86 | 0.58 | 0.48 | 0.76 |
| 290 | 0.65 | 0.44 | 0.79 | 0.48 | 0.47 | 0.67 |
| 300 | 0.47 | 0.43 | 0.63 | 0.38 | 0.49 | 0.62 |
| 320 | 0.55 | 0.40 | 0.68 | 0.29 | 0.42 | 0.52 |
| 340 | 0.46 | 0.38 | 0.60 | 0.25 | 0.40 | 0.47 |
| 360 | 0.35 | 0.36 | 0.50 | 0.23 | 0.39 | 0.45 |
| 380 | 0.40 | 0.34 | 0.52 | 0.25 | 0.36 | 0.44 |
| 400 | 0.40 | 0.32 | 0.52 | 0.24 | 0.34 | 0.42 |
| 450 | 0.33 | 0.29 | 0.44 | 0.21 | 0.31 | 0.37 |
| 500 | 0.32 | 0.27 | 0.41 | 0.23 | 0.31 | 0.39 |
| 555 | 0.37 | 0.24 | 0.44 | 0.22 | 0.28 | 0.36 |
| 600 | 0.33 | 0.23 | 0.40 | 0.34 | 0.27 | 0.43 |
| 700 | 0.44 | 0.20 | 0.48 | 0.53 | 0.27 | 0.59 |
| 800 | | | | 0.18 | 0.30 | 0.35 |
| 900 | | | | 0.16 | 0.19 | 0.25 |
| 1000 | | | | 0.18 | 0.19 | 0.26 |
| 1100 | | | | 0.69 | 0.18 | 0.71 |
| 1300 | 0.68 | 0.14 | 0.70 | 0.18 | 0.14 | 0.23 |
| 1500 | 0.77 | 0.12 | 0.78 | 0.29 | 0.14 | 0.32 |
| 1700 | | | | 0.37 | 0.12 | 0.39 |
| 2000 | | | | 0.37 | 0.12 | 0.39 |
| 2200 | | | | 0.73 | 0.12 | 0.74 |
| 2300 | | | | 0.75 | 0.12 | 0.76 |
| 2400 | | | | 1.31 | 0.11 | 1.32 |
| 2500 | | | | 5.06 | 0.11 | 5.07 |

Table 5.4.11. Spectral Irradiance standard uncertainties (k=1) of the lamp **BN-9101-656**

| Wavelength, nm | Round 1 | | | Round 2 | | |
|---|---|---|---|---|---|---|
| | Uncertainties associated with, % | | Combined uncertainty, % | Uncertainties associated with, % | | Combined uncertainty, % |
| | Uncorrelated effects | Correlated effects | | Uncorrelated effects | Correlated effects | |
| 250 | 7.33 | 0.51 | 7.35 | 3.79 | 0.61 | 3.84 |
| 260 | 0.26 | 2.17 | 2.19 | 1.54 | 0.54 | 1.63 |
| 270 | 0.26 | 1.78 | 1.80 | 0.86 | 0.52 | 1.01 |
| 280 | 0.26 | 0.94 | 0.97 | 0.60 | 0.48 | 0.77 |
| 290 | 0.26 | 0.96 | 0.99 | 0.60 | 0.47 | 0.76 |
| 300 | 0.26 | 0.53 | 0.59 | 0.50 | 0.49 | 0.71 |
| 320 | 0.26 | 0.48 | 0.54 | 0.56 | 0.42 | 0.70 |
| 340 | 0.26 | 0.43 | 0.51 | 0.46 | 0.40 | 0.61 |
| 360 | 0.26 | 0.41 | 0.49 | 0.49 | 0.39 | 0.63 |
| 380 | 0.26 | 0.39 | 0.47 | 0.32 | 0.36 | 0.48 |
| 400 | 0.26 | 0.39 | 0.47 | 0.49 | 0.34 | 0.60 |
| 450 | 0.26 | 0.45 | 0.52 | 0.38 | 0.31 | 0.49 |
| 500 | 0.26 | 0.52 | 0.58 | 0.22 | 0.30 | 0.37 |
| 555 | 0.26 | 0.38 | 0.46 | 0.19 | 0.27 | 0.33 |
| 600 | 0.26 | 0.38 | 0.46 | 0.23 | 0.27 | 0.35 |
| 700 | 0.26 | 0.60 | 0.66 | 0.38 | 0.27 | 0.46 |
| 800 | | | | 0.92 | 0.30 | 0.97 |
| 900 | | | | | | |
| 1000 | | | | | | |
| 1100 | | | | | | |
| 1300 | 0.26 | 0.72 | 0.77 | | | |
| 1500 | 0.26 | 0.76 | 0.80 | | | |
| 1700 | | | | | | |
| 2000 | | | | | | |
| 2200 | | | | | | |
| 2300 | | | | | | |
| 2400 | | | | | | |
| 2500 | | | | | | |

## 5.5. NIM, China

### 5.5.1. Description of the NIM measurement facility

The spectral irradiance scale at NIM is realized using a high-temperature blackbody BB3500M. The cylindrical cavity of the BB3500M has a depth of 30 mm, an inner-wall diameter of 59 mm and an opening diameter of 15 mm. The BB3500M is a windowless blackbody, and the effective emissivity was estimated to be about 0.999 using a Monte-Carlo method calculation. The working temperature of the BB3500M is about 3000 K.

The comparison lamps were measured directly comparing with HTBB and no other transfer standards. The spectral irradiance measurement facility of NIM is illustrated in Figure 5.5.1.

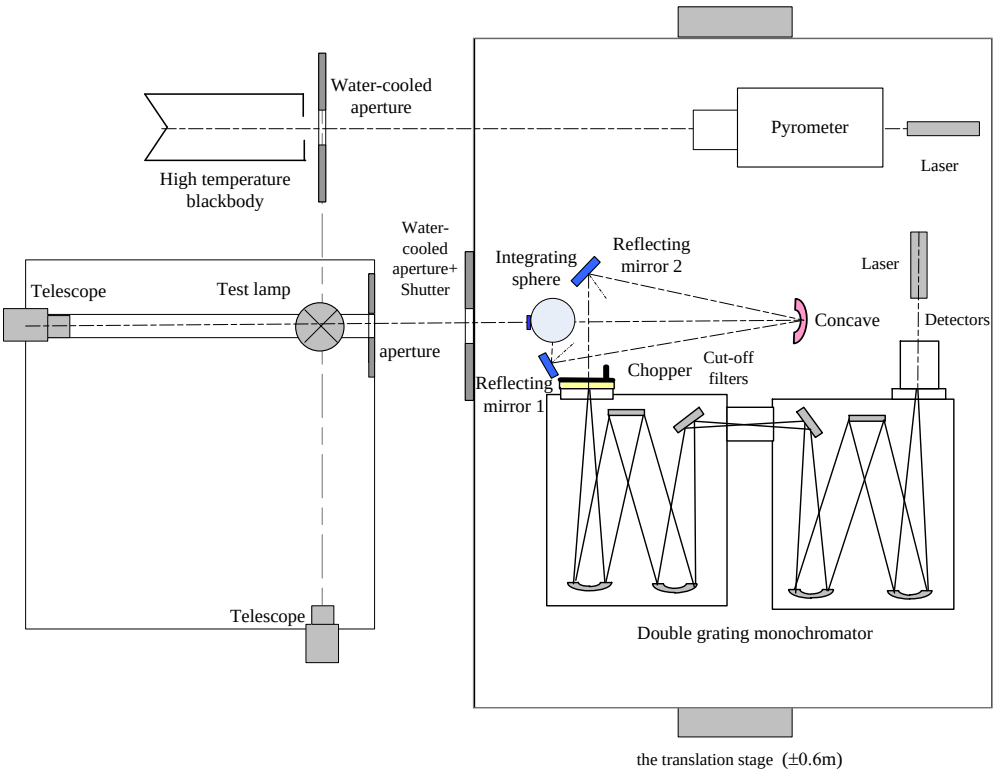


Figure 5.5.1. The spectral irradiance measurement facility of NIM.

The spectroradiometer of NIM is based on a double-grating monochromator (Model M207D, made by McPherson, Inc). The spectroradiometer is set up on the translation stage. The translation range of the stage is ±600 mm. Three pairs of gratings (1800, 1200 and 600 g/mm) are used to cover the wavelength range from 250 nm to 2500 nm. The focal length of the monochromator is 0.67 m; the f/No is 5.8; and the spectral dispersion is (0.83~2.48) nm/mm. The spectral bandwidth of the monochromator over the working wavelength range is from 0.50 nm to 1.49 nm. Three detectors are used for the working wavelength range: a R3896 photomultiplier, a Si detector and a thermo-electrically cooled InGaAs detector with a thermoelectric cooling temperature of –85°C. A 226 Hz chopper and two-phase lock in amplifier is used in infrared wavelength. The chopper is placed in front of the entrance slit of the monochromator, with limiting apertures to cut down stray radiation. A set of second order cut-off filters is mounted in front of the entrance slit.

The imaging optics consist of an integrating sphere with a diameter of 50 mm, a spherical concave mirror and two flat mirrors. The diameter of the entrance port of the integrating sphere is 12 mm.

The width and height of the exit port are 2.6 mm and 10 mm, respectively. The concave mirror had a diameter of 110 mm and a focal length of 550 mm. The image of the exit of the integrating sphere is focused on the entrance slit of the monochromator with a magnification of 1:1.

### 5.5.2. Measurement procedure

The measurement procedure of comparison lamps at NIM is described as follows:

First. the temperature of the BB3500M blackbody was measured by a LP5 pyrometer. the temperature of which was traced to the latest temperature scale realization of NIM.

Next. a water-cooled aperture with area of 20.479 $mm^2$ was set in front of the blackbody. the uniform radiation from the blackbody cavity passed through the aperture, and then irradiated on the entrance port of the integrating sphere. The exit port of the integrating sphere was imaged on the entrance slit of the double grating monochromator, and then the irradiance signal of the blackbody was measured over the specified wavelength range.

Then the translation stage was moved to the position to measure the lamp and the irradiance signal of the test lamp was measured over the specified wavelength range.

Finally, the spectral irradiance of the comparison lamp can be calculated according to the signal ratio of the blackbody and the lamp.

### 5.5.3. The transfer standard and traceability of NIM

The calibration uncertainty of the pyrometer is 0.50 K ($k$ = 2) at 2011.05 K and 0.95 K ($k$ = 2) at 2746.97 K, which is traceable to ITS-90. The transfer standards and traceability are listed in Table 5.5.1.

Table 5.5.1. The transfer standards and traceability

| No. | Device | Type | Manufacturer | Descriptions | Uncertainty | Traceability |
|---|---|---|---|---|---|---|
| 1 | Pyrometer | LP5 | Germany | Range: 900 ℃ ~3000 ℃ | $U$ = 0.50 ℃ ($k$ =2) @ $T$ = 1737.90 ℃. $U$ = 0.95 ℃ ($k$=2) @ $T$ = 2473.82 ℃ | the latest temperature scale realization of NIM |
| 2 | Digital voltage meter | 34420A | Agilent | Range: 0.01 V ~100 V; Accuracy: 0.005% | $U = 12\times10^{-6}$ V ~$6\times10^{-6}$ V ($k$=2) | the latest Ampere and volt scale realization of NIM |
| 3 | Standard resistance | BZ6 | Shanghai Ammeter Factory of China | 0.01 Ω, 0.01 class, 10 A | $U = 22\times10^{-6}$ Ω ($k$=2) | the latest Resistance scale realization of NIM |

### 5.5.4. Laboratory conditions

Temperature range: (20±1) ℃. Humidity: (30~65) %RH.

### 5.5.5. Measurement uncertainty for spectral irradiance realized at NIM

Table 5.5.2. Measurement uncertainty of spectral irradiance realization at NIM

| Wave length /nm | Uncorrelated effects | | | | | | | | Correlated effects | | | | | | |
|---|---|---|---|---|---|---|---|---|---|---|---|---|---|---|---|
| | Type A Uncertainty in Value /% | | Type B Uncertainty in Value /% | | | | | | | | | | | RMS total /% | % |
| | Repeatability $u_1$ | Reproducibility of realignment $u_2$ | Temperature Measurement of HTBB $u_3$ | Non-Uniformity of HTBB $u_4$ | Instability of HTBB $u_5$ | Emisivity $u_6$ | Area of water-cooled aperture $u_7$ | Current $u_8$ | Non-linearity of measurement system $u_9$ | Wavelength $u_{10}$ | Bandwidth $u_{11}$ | Distance $u_{12}$ | Stray light $u_{13}$ | Combined uncertainty $u_c$ | $U$ ($k$=2) |
| | Uncorrelated effects % | | | | | | | | Correlated effects % | | | | | | |
| **250** | 0.650 | 0.500 | 0.407 | 0.109 | 0.128 | 0.100 | 0.015 | 0.140 | 0.100 | 0.020 | 0.046 | 0.045 | 0.030 | **0.95** | **1.9** |
| **260** | 0.550 | 0.300 | 0.391 | 0.105 | 0.123 | 0.100 | 0.015 | 0.140 | 0.100 | 0.020 | 0.044 | 0.045 | 0.030 | **0.79** | **1.6** |
| **270** | 0.500 | 0.250 | 0.377 | 0.101 | 0.118 | 0.100 | 0.015 | 0.130 | 0.100 | 0.020 | 0.034 | 0.045 | 0.030 | **0.72** | **1.4** |
| **280** | 0.500 | 0.250 | 0.363 | 0.097 | 0.114 | 0.100 | 0.015 | 0.130 | 0.100 | 0.020 | 0.028 | 0.045 | 0.030 | **0.71** | **1.4** |
| **290** | 0.400 | 0.200 | 0.351 | 0.094 | 0.110 | 0.100 | 0.015 | 0.120 | 0.100 | 0.020 | 0.023 | 0.045 | 0.030 | **0.62** | **1.2** |
| **300** | 0.300 | 0.200 | 0.339 | 0.091 | 0.107 | 0.100 | 0.015 | 0.120 | 0.100 | 0.020 | 0.022 | 0.045 | 0.030 | **0.55** | **1.1** |
| **320** | 0.300 | 0.200 | 0.318 | 0.085 | 0.100 | 0.100 | 0.015 | 0.110 | 0.100 | 0.020 | 0.019 | 0.045 | 0.030 | **0.53** | **1.1** |
| **340** | 0.200 | 0.200 | 0.299 | 0.080 | 0.094 | 0.100 | 0.015 | 0.100 | 0.100 | 0.020 | 0.012 | 0.045 | 0.030 | **0.47** | **0.9** |
| **360** | 0.200 | 0.200 | 0.283 | 0.075 | 0.089 | 0.050 | 0.015 | 0.100 | 0.100 | 0.020 | 0.066 | 0.045 | 0.030 | **0.45** | **0.90** |
| **380** | 0.200 | 0.200 | 0.268 | 0.072 | 0.084 | 0.050 | 0.015 | 0.090 | 0.100 | 0.020 | 0.049 | 0.045 | 0.030 | **0.44** | **0.87** |
| **400** | 0.150 | 0.150 | 0.254 | 0.068 | 0.080 | 0.050 | 0.015 | 0.080 | 0.100 | 0.020 | 0.004 | 0.045 | 0.030 | **0.38** | **0.76** |
| **450** | 0.150 | 0.150 | 0.226 | 0.060 | 0.071 | 0.050 | 0.015 | 0.070 | 0.100 | 0.010 | 0.002 | 0.045 | 0.030 | **0.35** | **0.71** |
| **500** | 0.150 | 0.150 | 0.203 | 0.054 | 0.064 | 0.050 | 0.015 | 0.060 | 0.100 | 0.010 | 0.001 | 0.045 | 0.030 | **0.34** | **0.67** |
| **555** | 0.100 | 0.150 | 0.183 | 0.049 | 0.058 | 0.050 | 0.015 | 0.050 | 0.100 | 0.010 | 0.000 | 0.045 | 0.030 | **0.30** | **0.60** |
| **600** | 0.100 | 0.150 | 0.170 | 0.045 | 0.053 | 0.050 | 0.015 | 0.050 | 0.100 | 0.010 | 0.000 | 0.045 | 0.030 | **0.29** | **0.58** |
| **700** | 0.100 | 0.150 | 0.145 | 0.039 | 0.046 | 0.050 | 0.015 | 0.040 | 0.100 | 0.010 | 0.000 | 0.045 | 0.030 | **0.27** | **0.55** |
| **800** | 0.130 | 0.150 | 0.127 | 0.034 | 0.040 | 0.050 | 0.015 | 0.030 | 0.100 | 0.010 | 0.000 | 0.045 | 0.030 | **0.27** | **0.55** |
| **900** | 0.150 | 0.200 | 0.113 | 0.030 | 0.036 | 0.050 | 0.015 | 0.030 | 0.100 | 0.005 | 0.000 | 0.045 | 0.030 | **0.31** | **0.61** |
| **1000** | 0.150 | 0.200 | 0.102 | 0.027 | 0.032 | 0.050 | 0.015 | 0.020 | 0.100 | 0.005 | 0.000 | 0.045 | 0.030 | **0.30** | **0.60** |
| **1100** | 0.155 | 0.200 | 0.092 | 0.025 | 0.029 | 0.050 | 0.015 | 0.020 | 0.100 | 0.005 | 0.000 | 0.045 | 0.030 | **0.30** | **0.60** |
| **1300** | 0.150 | 0.200 | 0.078 | 0.021 | 0.025 | 0.050 | 0.015 | 0.020 | 0.100 | 0.005 | 0.000 | 0.045 | 0.030 | **0.29** | **0.59** |
| **1500** | 0.200 | 0.200 | 0.068 | 0.018 | 0.021 | 0.050 | 0.015 | 0.010 | 0.100 | 0.005 | 0.000 | 0.045 | 0.030 | **0.32** | **0.64** |
| **1700** | 0.200 | 0.200 | 0.060 | 0.016 | 0.019 | 0.050 | 0.015 | 0.010 | 0.100 | 0.005 | 0.000 | 0.045 | 0.030 | **0.32** | **0.63** |
| **2000** | 0.200 | 0.200 | 0.051 | 0.014 | 0.016 | 0.050 | 0.015 | 0.010 | 0.100 | 0.005 | 0.000 | 0.045 | 0.030 | **0.31** | **0.63** |
| **2200** | 0.300 | 0.200 | 0.046 | 0.012 | 0.015 | 0.050 | 0.015 | 0.010 | 0.100 | 0.005 | 0.000 | 0.045 | 0.030 | **0.39** | **0.77** |
| **2300** | 0.300 | 0.300 | 0.044 | 0.012 | 0.014 | 0.050 | 0.015 | 0.010 | 0.100 | 0.005 | 0.000 | 0.045 | 0.030 | **0.45** | **0.89** |
| **2400** | 0.500 | 0.600 | 0.042 | 0.011 | 0.013 | 0.050 | 0.015 | 0.010 | 0.100 | 0.005 | 0.000 | 0.045 | 0.030 | **0.79** | **1.6** |
| **2500** | 0.800 | 0.900 | 0.041 | 0.011 | 0.013 | 0.050 | 0.015 | 0.010 | 0.100 | 0.005 | 0.000 | 0.045 | 0.030 | **1.21** | **2.4** |

#### *5.5.5.1. The breakdown of the sources of uncertainty for spectral irradiance realized at NIM*

Spectral irradiance of the blackbody can be calculated according to the equation.

$$E_{\mathrm{BB}}(\lambda,T) = \varepsilon_{\mathrm{eff}} \cdot G \cdot \frac{c_1}{\mathrm{n}^2\lambda^5} \cdot \frac{1}{\mathrm{e}^{c_2/n\lambda T}-1} \qquad (5.5.1)$$

where $E_{BB}(\lambda,T)$ – spectral irradiance

$\varepsilon_{eff}$ – emissivity of the blackbody

G – geometric factor
$n$ – air refractive index
$\lambda$ – wavelength in air
$c_1$=3.741772×10$^{-16}$ Wm$^2$ – is the first radiation constant
$c_2$=1.438777×10$^4$ μm·K – is the second radiation constant
$T$ – is the thermodynamic temperature of blackbody

#### *5.5.5.1.1. Type A Uncertainty*

**1）Repeatability of measurement** $u_1$

The relative standard deviation is calculated as the type A uncertainty, see Table 5.5.3.

Table 5.5.3. Relative standard deviation of measurements

| Wavelength /nm | $u_1$ /% | Wavelength /nm | $u_1$ /% | Wavelength /nm | $u_1$ /% | Wavelength /nm | $u_1$ /% |
|---|---|---|---|---|---|---|---|
| **250** | 0.650 | **340** | 0.200 | **600** | 0.100 | **1500** | 0.200 |
| **260** | 0.550 | **360** | 0.200 | **700** | 0.100 | **1700** | 0.200 |
| **270** | 0.500 | **380** | 0.200 | **800** | 0.130 | **2000** | 0.200 |
| **280** | 0.500 | **400** | 0.150 | **900** | 0.150 | **2200** | 0.300 |
| **290** | 0.400 | **450** | 0.150 | **1000** | 0.150 | **2300** | 0.300 |
| **300** | 0.300 | **500** | 0.150 | **1100** | 0.155 | **2400** | 0.500 |
| **320** | 0.300 | **555** | 0.100 | **1300** | 0.150 | **2500** | 0.800 |

**2）Reproducibility of realignment of the lamp** $u_2$

The reproducibility of realignment of lamp is listed in Table 5.5.4.

Table 5.5.4. Reproducibility of realignment of the lamp

| Wavelength /nm | $u_2$ /% | Wavelength /nm | $u_2$ /% | Wavelength /nm | $u_2$ /% | Wavelength /nm | $u_2$ /% |
|---|---|---|---|---|---|---|---|
| **250** | 0.500 | **340** | 0.200 | **600** | 0.150 | **1500** | 0.200 |
| **260** | 0.300 | **360** | 0.200 | **700** | 0.150 | **1700** | 0.200 |
| **270** | 0.250 | **380** | 0.200 | **800** | 0.150 | **2000** | 0.200 |
| **280** | 0.250 | **400** | 0.150 | **900** | 0.200 | **2200** | 0.200 |
| **290** | 0.200 | **450** | 0.150 | **1000** | 0.200 | **2300** | 0.300 |
| **300** | 0.200 | **500** | 0.150 | **1100** | 0.200 | **2400** | 0.600 |
| **320** | 0.200 | **555** | 0.150 | **1300** | 0.200 | **2500** | 0.900 |

#### *5.5.5.1.2. Type B Uncertainty, Scale*

The sources of the uncertainty "Scale" include: temperature measurement of HTBB, non-uniformity of HTBB source, instability of HTBB source, area of the water-cooled aperture, non-linearity of the measurement system etc.

**1) Temperature Measurement of HTBB** $u_3$

A pyrometer was used to measure temperature of HTBB. The pyrometer calibration was traceable to the latest temperature scale realization of NIM.

The uncertainty of temperature measurement at 3000 K was $u_T$=0.636 K ($k$=1). The sources of uncertainty are the pyrometer uncertainty, instability of HTBB and repeatability of measurement.

Table 5.5.5. Uncertainty of HTBB temperature measurement

| Wavelength | Temperature of HTBB $T$ /K | Uncertainty of pyrometer $T$ /K | Instability of HTBB $T$ /K | Repeatability of measurement $T$ /K | Combined uncertainty $T$ /K |
|---|---|---|---|---|---|
| 250 nm ~2500 nm | 3000 K | 0.600 | 0.150 | 0.150 | 0.636 |

The relative uncertainty of spectral irradiance contributed by temperature measurement of HTBB is calculated according to the equation $u_3=u_T c_2/(\lambda T^2)$, see Table 5.5.6.

Table 5.5.6. Uncertainties of spectral irradiance associated with HTBB temperature measurement

| Wavelength /nm | $u_3$ /% | Wavelength /nm | $u_3$ /% | Wavelength /nm | $u_3$ /% | Wavelength /nm | $u_3$ /% |
|---|---|---|---|---|---|---|---|
| **250** | 0.407 | **340** | 0.299 | **600** | 0.170 | **1500** | 0.068 |
| **260** | 0.391 | **360** | 0.283 | **700** | 0.145 | **1700** | 0.060 |
| **270** | 0.377 | **380** | 0.268 | **800** | 0.127 | **2000** | 0.051 |
| **280** | 0.363 | **400** | 0.254 | **900** | 0.113 | **2200** | 0.046 |
| **290** | 0.351 | **450** | 0.226 | **1000** | 0.102 | **2300** | 0.044 |
| **300** | 0.339 | **500** | 0.203 | **1100** | 0.092 | **2400** | 0.042 |
| **320** | 0.318 | **555** | 0.183 | **1300** | 0.078 | **2500** | 0.041 |

**2) Non-uniformity of HTBB Source** $u_4$

Non-uniformity of HTBB source is measured at 3000 K. Non-uniformity of HTBB is less than 0.17 K in area of effective aperture. The relative uncertainty of spectral irradiance contributed by non-uniformity of HTBB source between every measurement is calculated according to the equation $u_4 = u_T c_2/(\lambda T^2)$, see Table 5.5.7.

Table 5.5.7. Uncertainty of spectral irradiance contributed by non-uniformity of HTBB

| Wavelength /nm | $u_4$ /% | Wavelength /nm | $u_4$ /% | Wavelength /nm | $u_4$ /% | Wavelength /nm | $u_4$ /% |
|---|---|---|---|---|---|---|---|
| **250** | 0.109 | **340** | 0.080 | **600** | 0.045 | **1500** | 0.018 |
| **260** | 0.105 | **360** | 0.075 | **700** | 0.039 | **1700** | 0.016 |
| **270** | 0.101 | **380** | 0.072 | **800** | 0.034 | **2000** | 0.014 |
| **280** | 0.097 | **400** | 0.068 | **900** | 0.030 | **2200** | 0.012 |
| **290** | 0.094 | **450** | 0.060 | **1000** | 0.027 | **2300** | 0.012 |
| **300** | 0.091 | **500** | 0.054 | **1100** | 0.025 | **2400** | 0.011 |
| **320** | 0.085 | **555** | 0.049 | **1300** | 0.021 | **2500** | 0.011 |

**3) Instability of HTBB Source** $u_5$

At the temperature of 3000 K the instability of HTBB was always less than 0.20 K. The associated relative uncertainty of spectral irradiance was calculated by $u_5=u_T c_2/(\lambda T^2)$, see Table 5.5.8.

Table 5.5.8. The uncertainty of spectral irradiance contributed by instability of HTBB

| Wavelength /nm | $u_5$ /% | Wavelength /nm | $u_5$ /% | Wavelength /nm | $u_5$ /% | Wavelength /nm | $u_5$ /% |
|---|---|---|---|---|---|---|---|
| **250** | 0.128 | **340** | 0.094 | **600** | 0.053 | **1500** | 0.021 |
| **260** | 0.123 | **360** | 0.089 | **700** | 0.046 | **1700** | 0.019 |
| **270** | 0.118 | **380** | 0.084 | **800** | 0.040 | **2000** | 0.016 |
| **280** | 0.114 | **400** | 0.080 | **900** | 0.036 | **2200** | 0.015 |
| **290** | 0.110 | **450** | 0.071 | **1000** | 0.032 | **2300** | 0.014 |
| **300** | 0.107 | **500** | 0.064 | **1100** | 0.029 | **2400** | 0.013 |
| **320** | 0.100 | **555** | 0.058 | **1300** | 0.025 | **2500** | 0.013 |

**4) Emissivity** $u_6$

Emissivity $\varepsilon_{\text{eff}}$ was estimated as 0.9995 with standard uncertainty of 0.0005 for the spectral range from 360 nm to 2500 nm, and increasing up to 0.001 for the spectral range from 250 nm to 350 nm. The estimation was based on modelling using the STEEP3 software. The spectral irradiance relative uncertainty is spectrally independent and equals to 0.1 % and 0.05 %, respectively.

Table 5.5.9. The uncertainty of spectral irradiance contributed by emissivity

| Wavelength /nm | $u_6$ /% | Wavelength /nm | $u_6$ /% | Wavelength /nm | $u_6$ /% | Wavelength /nm | $u_6$ /% |
|---|---|---|---|---|---|---|---|
| **250** | 0.100 | **340** | 0.100 | **600** | 0.050 | **1500** | 0.050 |
| **260** | 0.100 | **360** | 0.050 | **700** | 0.050 | **1700** | 0.050 |
| **270** | 0.100 | **380** | 0.050 | **800** | 0.050 | **2000** | 0.050 |
| **280** | 0.100 | **400** | 0.050 | **900** | 0.050 | **2200** | 0.050 |
| **290** | 0.100 | **450** | 0.050 | **1000** | 0.050 | **2300** | 0.050 |
| **300** | 0.100 | **500** | 0.050 | **1100** | 0.050 | **2400** | 0.050 |
| **320** | 0.100 | **555** | 0.050 | **1300** | 0.050 | **2500** | 0.050 |

**5) Area of the Water-cooled Aperture** $u_7$

The area of the water-cooled aperture is 20.479 mm$^2$, the measurement uncertainty is 0.003 mm$^2$, and then the relative uncertainty of spectral irradiance contributed by area of the water-cooled aperture is about 0.0146 %. Area of the water-cooled aperture is measured at Length Division of NIM.

Table 5.5.10. The uncertainty of water-cooled aperture

| | Measurement value | Measurement uncertainty $u_7$ |
|---|---|---|
| Area of water-cooled aperture $A$ | 20.479 mm$^2$ | 0.003 mm$^2$ |

**6) Current Passed through Transfer Standard** $u_8$

Sources of the uncertainty include power supply (drift of the current with time is less than $5\times10^{-5}$/hour), $7^{1/2}$ nanovoltmeter (uncertainty: $12\times10^{-6}$ V ~$6\times10^{-6}$ V, $k$=2), 0.01 Ω standard resistance (uncertainty: $2.2\times10^{-5}$ Ω, $k$=2) etc.

Current measurement and stability was estimated as 1 mA. The associated spectral irradiance uncertainties were evaluated comparing the measurements the FEL lamps at 8.1000 A current.

Table 5.5.11. The Current uncertainty passed through transfer standard

| Wavelength /nm | $u_8$ /% | Wavelength /nm | $u_8$ /% | Wavelength /nm | $u_8$ /% | Wavelength /nm | $u_8$ /% |
|---|---|---|---|---|---|---|---|
| **250** | 0.140 | **340** | 0.100 | **600** | 0.050 | **1500** | 0.010 |
| **260** | 0.140 | **360** | 0.100 | **700** | 0.040 | **1700** | 0.010 |
| **270** | 0.130 | **380** | 0.090 | **800** | 0.030 | **2000** | 0.010 |
| **280** | 0.130 | **400** | 0.080 | **900** | 0.030 | **2200** | 0.010 |
| **290** | 0.120 | **450** | 0.070 | **1000** | 0.020 | **2300** | 0.010 |
| **300** | 0.120 | **500** | 0.060 | **1100** | 0.020 | **2400** | 0.010 |
| **320** | 0.110 | **555** | 0.050 | **1300** | 0.020 | **2500** | 0.010 |

**7) Non-linearity of Measurement System for Spectral Irradiance** $u_9$

The relative uncertainty of spectral irradiance contributed by non-linearity of measurement system is 0.10%.

The non-linearity of the measurement system is less than 0.10%. which is tested by linearity system of NIM.

**8) Wavelength** $u_{10}$

A M207D double grating monochromator is adopted in the measurement system. Hg spectrum lamp and He-Ne laser are used to calibrate wavelength of the monochromator. The uncertainty of wavelength contributed by reproducibility and accuracy was listed in Table 5.5.12.

**T**able 5.5.12. The uncertainty of wavelength

| | Wavelength error $\Delta\lambda$ /nm | Temperature of Blackbody /K | $u_{\square}$/nm |
|---|---|---|---|
| 250nm~400nm | 0.02 | 3021 | 0.0115 |
| 380nm~1000nm | 0.03 | 3021 | 0.0173 |
| 1000nm~2500nm | 0.09 | 3021 | 0.0520 |

The relative uncertainty of spectral irradiance contributed by wavelength is calculated by the equation

$$u = (\frac{-5}{\lambda} + \frac{C_2}{\lambda^2 T})u_\lambda \qquad (5.5.2)$$

The results are listed in Table 5.5.13.

Table 5.5.13. Uncertainties of spectral irradiance contributed by wavelength

| Wavelength /nm | $u_{10}$ /% | Wavelength /nm | $u_{10}$ /% | Wavelength /nm | $u_{10}$ /% | Wavelength /nm | $u_{10}$ /% |
|---|---|---|---|---|---|---|---|
| **250** | 0.020 | **340** | 0.020 | **600** | 0.010 | **1500** | 0.005 |
| **260** | 0.020 | **360** | 0.020 | **700** | 0.010 | **1700** | 0.005 |
| **270** | 0.020 | **380** | 0.020 | **800** | 0.010 | **2000** | 0.005 |
| **280** | 0.020 | **400** | 0.020 | **900** | 0.005 | **2200** | 0.005 |
| **290** | 0.020 | **450** | 0.010 | **1000** | 0.005 | **2300** | 0.005 |
| **300** | 0.020 | **500** | 0.010 | **1100** | 0.005 | **2400** | 0.005 |
| **320** | 0.020 | **555** | 0.010 | **1300** | 0.005 | **2500** | 0.005 |

**9) Bandwidth** $u_{11}$

Table 5.5.14. Uncertainty of spectral irradiance contributed by bandwidth

| Wavelength /nm | $u_{11}$ /% | Wavelength /nm | $u_{11}$ /% | Wavelength /nm | $u_{11}$ /% | Wavelength /nm | $u_{11}$ /% |
|---|---|---|---|---|---|---|---|
| **250** | 0.0460 | **340** | 0.0120 | **600** | 0.0001 | **1500** | 0.0001 |
| **260** | 0.0440 | **360** | 0.0660 | **700** | 0.0001 | **1700** | 0.0001 |
| **270** | 0.0340 | **380** | 0.0490 | **800** | 0.0001 | **2000** | 0.0001 |
| **280** | 0.0283 | **400** | 0.0037 | **900** | 0.0001 | **2200** | 0.0001 |
| **290** | 0.0235 | **450** | 0.0018 | **1000** | 0.0001 | **2300** | 0.0001 |
| **300** | 0.0219 | **500** | 0.0009 | **1100** | 0.0001 | **2400** | 0.0001 |
| **320** | 0.0185 | **555** | 0.0001 | **1300** | 0.0001 | **2500** | 0.0001 |

**10) Distance to Transfer Standard** $u_{12}$

The distance was measured by a special micrometer with the measurement uncertainty 0.005 mm. When the micrometer was used to measure the distance. the measurement error is 0.0737 mm.

Distance between the test lamp and the diffuser is 500 mm. and the relative uncertainty of spectral irradiance contributed by distance is $u_l$=0.0295 %.

Distance between the water-cooled aperture and the diffuser is 433 mm. and the relative uncertainty of spectral irradiance contributed by distance is $u_a$=0.0340 %.

So the total relative uncertainty of spectral irradiance contributed by distance is 0.045%.

Table 5.5.15. Uncertainty of distance measurement

| Wavelength range /nm | Distance of lamp /mm | $u_l$ /% | Distance of water-cooled aperture /mm | $u_a$ /% | Combined Uncertainty% |
|---|---|---|---|---|---|
| 250nm~2500nm | 500 | 0.0295 | 433 | 0.0340 | 0.045 |

**11) Stray light** $u_{13}$

A cut-off filter was used to test the stray light of double grating monochromator. At 250 nm the influence of stray light was less than 0.03 %.

The final uncertainty values submitted by NIM to the pilot with the spectral irradiance data are presented in Tables 5.5.16. The uncertainties are the same for all three lamps and both rounds

Table 5.5.16. Spectral Irradiance standard uncertainties (k=1) of the NIM lamps

| Wavelength, nm | Round 1 & 2 | | |
|---|---|---|---|
| | Uncertainties associated with, % | | Combined uncertainty, % |
| | Uncorrelated effects | Correlated effects | |
| 250 | 0.947 | 0.124 | 0.95 |
| 260 | 0.776 | 0.124 | 0.79 |
| 270 | 0.711 | 0.120 | 0.72 |
| 280 | 0.703 | 0.119 | 0.71 |
| 290 | 0.607 | 0.118 | 0.62 |
| 300 | 0.538 | 0.117 | 0.55 |
| 320 | 0.520 | 0.117 | 0.53 |
| 340 | 0.453 | 0.116 | 0.47 |
| 360 | 0.431 | 0.133 | 0.45 |
| 380 | 0.418 | 0.125 | 0.44 |
| 400 | 0.360 | 0.115 | 0.38 |
| 450 | 0.335 | 0.114 | 0.35 |
| 500 | 0.316 | 0.114 | 0.34 |
| 555 | 0.278 | 0.114 | 0.30 |
| 600 | 0.267 | 0.114 | 0.29 |
| 700 | 0.248 | 0.114 | 0.27 |
| 800 | 0.249 | 0.114 | 0.27 |
| 900 | 0.285 | 0.114 | 0.31 |
| 1000 | 0.279 | 0.114 | 0.30 |
| 1100 | 0.278 | 0.114 | 0.30 |
| 1300 | 0.270 | 0.114 | 0.29 |
| 1500 | 0.297 | 0.114 | 0.32 |
| 1700 | 0.295 | 0.114 | 0.32 |
| 2000 | 0.293 | 0.114 | 0.31 |
| 2200 | 0.368 | 0.114 | 0.39 |
| 2300 | 0.430 | 0.114 | 0.45 |
| 2400 | 0.784 | 0.114 | 0.79 |
| 2500 | 1.206 | 0.114 | 1.21 |

## 5.6. NIST, USA

A group of working standard FEL lamps, F410, F423, F430 and F465 was calibrated at 8.2 A using the HTBB whose temperature was determined using filter radiometers. These calibrations, from 250 nm to 2500 nm, were performed just prior to our measurements of the comparison traveling standard lamps. These working standard lamps were then used to calibrate the CCPR-K1a.2017 traveling lamps for both rounds of the NIST measurements.

The comparison traveling lamps were hand carried to the pilot laboratory.

### 5.6.1. Description of the scale realization

At the NIST, the spectral irradiance scale is realized using a detector-based scale [28]. The NIST spectral irradiance scale is realized using filter radiometers (FR) calibrated for absolute spectral power responsivity traceable to the NIST cryogenic radiometer. The aperture areas which are needed for conversion of radiant power to irradiance are measured using interferometric techniques. The calibrated FRs are then used to determine the radiance temperature of a high-temperature blackbody (HTBB) operating near 3000 K. Although the spectral irradiance in the ultraviolet wavelength region could be increased with higher temperatures, the HTBB was operated at near 2950 K to avoid possible changes in the spectral emissivity of the blackbody due to the sublimation of graphite in the blackbody. The spectral irradiance of the HTBB is determined using the knowledge of the geometric factors and Planck radiance law and then is used to assign the spectral irradiances of a group of 1000 W FEL lamps using a calibrated spectroradiometer.

### 5.6.2. Description of the measurement facility and procedure

Figure 5.6.1 shows the physical layout of the FASCAL 2 facility [29]. The facility has four separate lamp mounts to calibrate the NIST disseminated spectral irradiance sources, FEL lamps, which are placed in kinematic lamp mounts with 6-axes of adjustments for alignment. The electrical power to the lamps is controlled using a calibrated shunt resistor with a temperature coefficient of resistance of 3 ppm / C°, and the lamp current is actively controlled using 16-bit current regulation. The lamp voltages are also recorded. All lamps are turned on to their operational currents over a 20 min period using computer control. Lamps are also turned off by slowly decreasing the lamp current.

The spectral irradiances of the sources are measured using an integrating sphere receiver (ISR) with a circular opening with 1 $cm^2$ aperture area. The ISR is a 2.54 cm diameter custom-packed polytetrafluoroethylene (PTFE) sphere for high transmittance throughout the spectral range of measurements. The ISR is placed on a kinematic mount and can be replaced with a mirror for alignment purposes. An additive-dispersive double monochromator (McPherson 2035D) with dual gratings placed in motorized grating turrets is used, and a combination of 5 different filters are used for second-order rejection from the grating and for further stray-light rejection. The monochromator is a Czerny-Turner design with a focal length of 0.35 m and an effective aperture of F/4.8 in the vertical direction and F/9.6 in the horizontal direction. The angular change of the grating is achieved using a sine-bar mechanism and driven with a DC servo motor with an absolute encoder. The temperatures of the monochromators are also monitored using platinum resistance thermometers and are also recorded during the spectral irradiance measurements. To avoid errors in the wavelength arising from thermal changes in the monochromator, the monochromator section is temperature stabilized using forced air from TE coolers set to the ambient temperature of the laboratory prior to turning on the FEL lamps. To avoid stray light, the entire monochromator system including the input optics and the detectors are covered using a light-tight box.

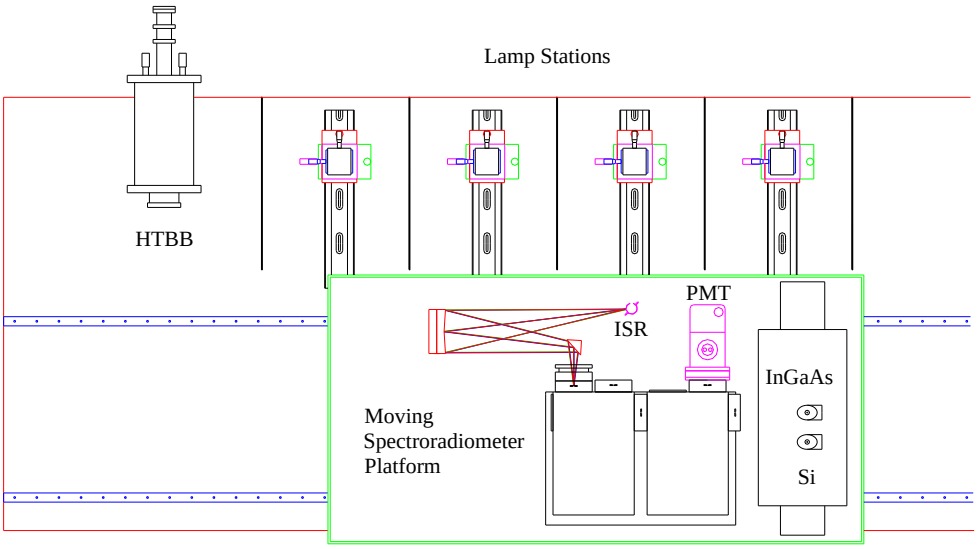


Figure 5.6.1. The optical layout showing the monochromator table with the positions of the input and the exit optics. A double monochromator in a Czerny-Turner design is used for dispersion and stray-light rejection. The CCPR lamps were measured in two stations farthest away from the HTBB. The two stations closer to the HTBB were used for the NIST bi-post mounted lamps.

Three separate detectors with two gratings and spectral selection filters are used for spectral coverage from 250 nm to 2500 nm. The spectral range of the gratings and the detectors are shown in Table 5.6.1, and although the blaze wavelength is outside the range of the Si diode wavelength region, the throughput of the monochromator is adequate. For measurements in the ultraviolet wavelength region, a Hamamatsu R106 low-noise bi-alkali side-on photomultiplier tube (PMT) is used.

Table 5.6.1. Wavelength ranges, bandpass and detector settings.

| Beginning Wavelength [nm] | End Wavelength [nm] | Grating [g/mm] | Grating Blaze [nm] | Dispersion [nm/mm] | Bandwidth [nm] | Type of Detector | Mode of Operation |
|---|---|---|---|---|---|---|---|
| 200 nm | 450 nm | 1200 | 300 | 2 | 4 | Bi-alkali PMT | DC |
| 350 nm | 1100 nm | 1200 | 300 | 2 | 4 | TE-cooled Si diode | DC |
| 900 nm | 2500 nm | 600 | 1250 | 4 | 8 | TE-cooled Extended-InGaAs diode | AC |

The temperature of the PMT is stabilized to - 26°C using a temperature-feedback controller, and the PMT is attached to the output port of the monochromator. A fused silica lens is attached to the PMT housing and focuses the image of the output slit onto the PMT with 2:1 de-magnification factor. Detectors are selected by the use of a motorized 45° mirror, internal to the monochromator. The 2.4 mm by 2.4 mm square silicon (Si) photodiode is temperature stabilized and cooled to -25 °C for low-noise operation. The 3 mm diameter indium gallium arsenide (InGaAs) photodiode is cooled to -80 °C using 4-stage TE coolers, and the InGaAs diode is selected for extended

responsivity to 2500 nm. In order to increase the InGaAs detector signals at 2500 nm, the detector was set at a temperature of -10 °C when measuring FELs at 2500 nm. Both the Si diode and the PMT are used in DC-current measurement mode, and the InGaAs detector is used with a frequency-stabilized tuning-fork chopper (not shown) and phase-sensitive detection techniques for better signal-to-noise ratios in the short-wave infrared wavelength region. The Si and the InGaAs photodiodes are placed on a computer-controlled translation stage for repeatability. The helium-neon laser (not shown) on the detector stage is used in the alignment of source to the optical axis of the spectroradiometer. For the long-term stability of the system responsivity, the monochromator and the detector stage are purged with dry nitrogen to increase the long-term stability of the internal mirrors and gratings, and the fore-optic section is purged using a dry-air generator which removes water vapors and carbon dioxide to reduce atmospheric absorption.

### 5.6.3. Uncertainty analysis

The uncertainty budget for NIST spectral irradiances is shown in Table 5.6.2 The uncertainties in rows B1 to B3 are associated with the operation of the HTBB. Row B4 accounts for uncertainties in aperture area, angular alignment of the apertures and distance measurements by grouping those terms into geometric factors. Since NIST working standard lamps are first calibrated directly using the HTBB and then these working standard lamps used for subsequent calibrations of the CCPR comparison lamps, uncertainties due to this intermediate step are listed in rows B5 to B7. The working standard FEL lamps, F410, F423, F430 and F465 which were calibrated at the beginning of the intercomparison and then used in-turn calibrate the CCPR K1.a lamps were not operated during this period. They were only used to calibrate the CCPR K1.a lamps after they came back. This uncertainty is based upon the spectrally dependent changes that we observe with burning hours on FEL lamps and are used as bases for rejecting working standards if their changes exceed these values. The uncertainty due to the temporal stability of the HTBB listed in A1 is measured from the optical feedback stabilization at the rear of the cavity confirmed by reproducibility of the filter radiometer measurements of the HTBB temperatures at the front of the HTBB. The alignment uncertainties of the both the NIST and the CCPR lamps are listed in row A2. The uncertainties in row A3 account for the stability and noise of the spectroradiometer system during the calibration sequence.

For the comparison data analysis the NIST Type B uncertainties were considered uncorrelated, and the Type A were considered correlated. The final uncertainty values used for the analysis are presented in Tables 5.6.4. The uncertainties are the same for all lamps and both rounds.

### 5.6.4. References to section 5.6

[28] H.W. Yoon, C.E. Gibson, P.Y. Barnes, **"**Realization of the National Institute of Standards and Technology detector-based spectral irradiance scale", *Applied Optics* **41**, 5879-5890 (2002)

[29] H.W. Yoon, J.E. Proctor, C.E. Gibson, "FASCAL 2: a New NIST facility for the calibration of the spectral irradiance of sources"*, Metrologia* **40** (2003) S30-S34

Table 5.6.2. NIST total uncertainty budget

| **Uncorrelated** | **Correlated** | **Type** | | **NIST Spectral Irradiance Scale Uncertainty (*k*=2) [%]** | | | | | | | | | | |
|---|---|---|---|---|---|---|---|---|---|---|---|---|---|---|
| | | | | **Wavelength [nm]** | | | | | | | | | | |
| | | | | **250** | **350** | **450** | **550** | **655** | **900** | **1600** | **2000** | **2300** | **2400** | **2500** |
| | x | B | B1) HTBB Temperature Uncertainty (0.86 K at 2950 K) | 0.57 | 0.41 | 0.32 | 0.26 | 0.22 | 0.16 | 0.09 | 0.08 | 0.07 | 0.07 | 0.07 |
| | x | B | B2) HTBB spectral emissivity | 0.10 | 0.10 | 0.10 | 0.10 | 0.10 | 0.10 | 0.10 | 0.10 | 0.10 | 0.10 | 0.10 |
| | x | B | B3) HTBB spatial uniformity | 0.10 | 0.10 | 0.10 | 0.10 | 0.10 | 0.10 | 0.10 | 0.10 | 0.10 | 0.10 | 0.10 |
| | x | B | B4) Geometric Factors in Irradiance Transfer | 0.10 | 0.10 | 0.10 | 0.10 | 0.10 | 0.10 | 0.10 | 0.10 | 0.10 | 0.10 | 0.10 |
| | x | B | B5) Lamp Current Stability | 0.07 | 0.05 | 0.04 | 0.03 | 0.03 | 0.02 | 0.02 | 0.01 | 0.01 | 0.01 | 0.01 |
| x | | B | B6) Wavelength accuracy (0.1 nm) | 0.58 | 0.26 | 0.13 | 0.07 | 0.04 | 0.005 | 0.011 | 0.013 | 0.011 | 0.011 | 0.011 |
| x | | B | B7) Long-term stability of working standards | 1.31 | 0.94 | 0.73 | 0.60 | 0.50 | 0.36 | 0.20 | 0.16 | 0.14 | 0.14 | 0.13 |
| | | | **Total Type B** | **1.55** | **1.07** | **0.82** | **0.68** | **0.57** | **0.43** | **0.28** | **0.25** | **0.23** | **0.23** | **0.23** |
| x | | A | A8) HTBB temporal stability (0.1K / hour) | 0.07 | 0.05 | 0.04 | 0.03 | 0.03 | 0.02 | 0.01 | 0.01 | 0.01 | 0.01 | 0.01 |
| | x | A | A9) Lamp / Spectroradiometer transfer | 0.10 | 0.10 | 0.10 | 0.10 | 0.10 | 0.10 | 0.10 | 0.10 | 0.10 | 0.10 | 0.10 |
| x | | A | A10) Spectroradiometer Responsivity Stability | 0.10 | 0.10 | 0.10 | 0.10 | 0.10 | 0.10 | 0.10 | 0.10 | 0.10 | 0.50 | 1.00 |
| | | | **Total Type A** | **0.16** | **0.15** | **0.15** | **0.14** | **0.14** | **0.14** | **0.14** | **0.14** | **0.14** | **0.51** | **1.01** |
| | | | **Total (A+B) (*k*=2)** | **1.56** | **1.08** | **0.84** | **0.69** | **0.59** | **0.46** | **0.32** | **0.29** | **0.27** | **0.56** | **1.03** |
| | | | | | | | | | | | | | | |
| | | | **Total Uncertainty of the issued standards (k=1)** | **0.78** | **0.54** | **0.42** | **0.35** | **0.30** | **0.23** | **0.16** | **0.14** | **0.14** | **0.28** | **0.52** |

Table 5.6.3. NIST standard uncertainties ($k$=1) of spectral irradiance measurement of comparison traveling lamps

| **Wavelength, nm** | **Round 1 & 2** | | |
|---|---|---|---|
| | **Uncertainties associated with, %** | | **Combined uncertainty, %** |
| | **Uncorrelated effects** | **Correlated effects** | |
| 250 | 0.080 | 0.775 | 0.78 |
| 260 | 0.080 | 0.751 | 0.76 |
| 270 | 0.080 | 0.727 | 0.73 |
| 280 | 0.080 | 0.703 | 0.71 |
| 290 | 0.080 | 0.679 | 0.68 |
| 300 | 0.075 | 0.655 | 0.66 |
| 320 | 0.075 | 0.607 | 0.61 |
| 340 | 0.075 | 0.559 | 0.56 |
| 360 | 0.075 | 0.523 | 0.53 |
| 380 | 0.075 | 0.499 | 0.50 |
| 400 | 0.075 | 0.475 | 0.48 |
| 450 | 0.075 | 0.415 | 0.42 |
| 500 | 0.073 | 0.380 | 0.39 |
| 555 | 0.070 | 0.340 | 0.35 |
| 600 | 0.070 | 0.320 | 0.33 |
| 700 | 0.070 | 0.280 | 0.29 |
| 800 | 0.070 | 0.246 | 0.26 |
| 900 | 0.070 | 0.215 | 0.23 |
| 1000 | 0.070 | 0.204 | 0.22 |
| 1100 | 0.070 | 0.194 | 0.21 |
| 1300 | 0.070 | 0.172 | 0.19 |
| 1500 | 0.070 | 0.151 | 0.17 |
| 1700 | 0.070 | 0.140 | 0.16 |
| 2000 | 0.070 | 0.125 | 0.14 |
| 2200 | 0.070 | 0.120 | 0.14 |
| 2300 | 0.071 | 0.115 | 0.14 |
| 2400 | 0.255 | 0.115 | 0.28 |
| 2500 | 0.505 | 0.115 | 0.52 |

## 5.7. NMC A*STAR, Singapore

### 5.7.1. Description of the scale realization

The NMC spectral irradiance measurement unit is realised using a variable high temperature black body radiator (HTBB) (shown in Figure 5.7.1(a)), with its thermodynamic temperature determined by a multi-wavelength filter radiometer (MWFR) (shown in Figure 5.7.1(b)). The MWFR contains a silicon trap detector, an InGaAs trap detector and 24 band pass filters with nominal centre wavelengths from 250 nm to 1600 nm. The spectral response of the trap detectors are traceable to the NMC primary standard cryogenic radiometer whereas the spectral transmittance of the filters are traceable to the NMC reference spectrophotometer. The traceability of the measurement is shown schematically in Figure 5.7.2. The structure of the MWFR is shown in Figure 5.7.3.

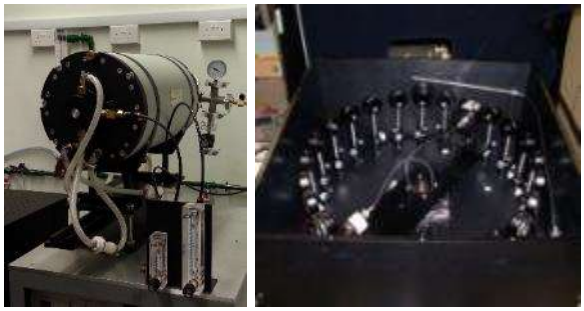

(a) (b)

Figure 5.7.1. (a) Variable high temperature black body radiator (HTBB).
(b) Multi-wavelength filter radiometer (MWFR)

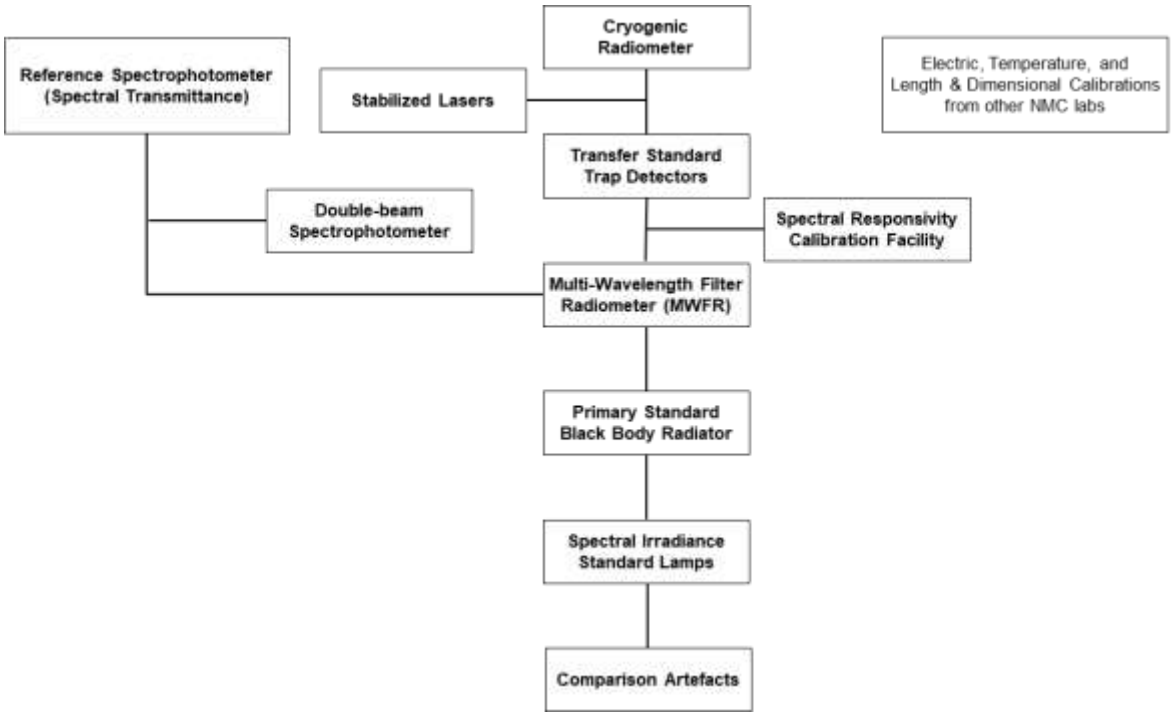


Figure 5.7.2. Traceability of spectral irradiance measurement

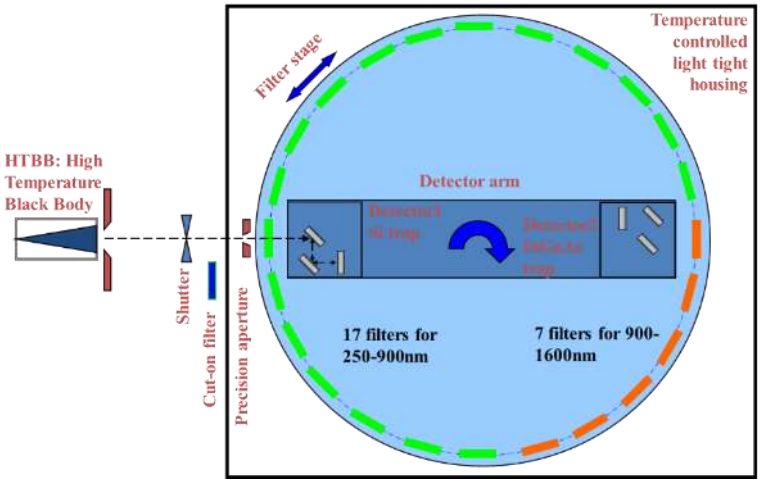


Figure 5.7.3. The multi-wavelength filter radiometer (MWFR)

The MWFR is housed in a light-tight casing with temperature controlled at 28˚C ± 0.1˚C. A precision aperture with a nominal diameter of 4 mm is mounted on the input port. Two detectors (a Si trap and an InGaAs trap) and 24 interference filters with nominal bandpass of 10 nm full width at half maximum (FWHM) are mounted on two motorised rotating stages separately to allow different filter-detector combinations. Mechanically any of these combinations is possible for measurement. The actual filter-detector arrangement for the measurement range of 250 nm to 1600 nm is shown in Table 5.7.1. In the range 900 nm to 1050 nm both detectors can be used so that counter checking of various effects due to alignment, beam geometry, stray light, inter-reflection, etc can be carried out.

The HTBB is a BB3500M blackbody radiator supplied by VNIIOFI. It has an effective emissivity of 0.9995 ± 0.0005. The diameter of the output port of the radiation cavity is 25 mm. A water-cooled precision aperture is used in front of the output port of the radiation cavity to provide a calculable spectral irradiance at a distance of 500 mm from spectral radiance obtained by the Planck's law once the thermodynamic temperature of HTBB is determined.

Table 5.7.1. Filter-detector combinations at each wavelength

| Filter nominal wavelength (nm) | Detector used |
|---|---|
| 254, 260, 280, 300, 310, 330, 340, 360, 380, 400, 450, 500, 550, 600, 650, 700, 800 | Si trap |
| 900, 1050 | Si trap & InGaAs trap |
| 1100, 1200, 1300, 1550, 1600 | InGaAs trap |

**Determination of blackbody radiator thermodynamic temperature**

In principle, one filter radiometer is sufficient to measure the thermodynamic temperature of the HTBB. However, multiple filter radiometers can be used to improve the reliability of the unit realization. Following is the process of determine thermodynamic temperature *T* of the HTBB.

$$E(\lambda) = \frac{H\varepsilon(\lambda)c_1}{\lambda^5[\exp(c_2/\lambda T)-1]} \qquad (1)$$

$$i(\lambda) = A_{FR}E(\lambda)\tau(\lambda)R(\lambda) \qquad (2)$$

For each filter $k$ :

$$i_k = A_{FR}\int E(\lambda)\tau_k(\lambda)R(\lambda)d\lambda$$

let: $$\lambda_{eff,k} = \frac{\int \lambda\, E(\lambda)\tau_k(\lambda)R(\lambda)d\lambda}{\int E(\lambda)\tau_k(\lambda)R(\lambda)d\lambda}$$

$$BW_{eff,k} = \frac{i_k}{i(\lambda_{eff,k})}$$

Then $$E(\lambda_{eff,k}) = \frac{i_k}{A_{FR}\tau(\lambda_{eff,k})R(\lambda_{eff,k})\,BW_{eff,k}}$$

From (1) $$E(\lambda_{eff,k,BB}) = \frac{Hc_1}{\lambda_{eff,k}^5[\exp(c_2/\lambda_{eff,k}T)-1]}$$

$$\Delta_k = \frac{E(\lambda_{eff,k})}{E(\lambda_{eff,k,BB})} - 1$$

**Adjusting $T$ and $T_k$ for filter k is determined when $\Delta_k$ is minimized**

$i(\lambda)$: photo current produced by $E(\lambda)$
$i_k$ : total FR photo current with filter k
$A_{FR}$ : aperture area of FR
$\tau_k(\lambda)$ : spectral transmittance of filter k
$\lambda_{eff,k}$ : effective wavelength of filter k
$BW_{eff,k}$: effective bandwidth of filter k
$\tau(\lambda_{eff,k})$: filter k spectral transmittance at effective wavelength of $\lambda_{eff,k}$
$R(\lambda_{eff,k})$ : Detector spectral responsivity at effective wavelength of $\lambda_{eff,k}$
$E(\lambda_{eff,k})$ : effective spectral irradiance of filter k calculated from measured $i_k$
$E(\lambda_{eff,k,BB})$ : Spectral irradiance of BB at effective wavelength of $\lambda_{eff,k}$ using equation (1)
H : geometry factor calculable from aperture areas of HTBB, FR and the distance in between

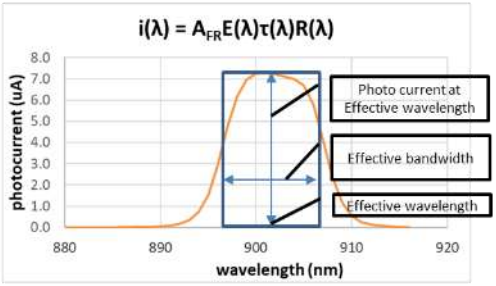


**For multi-filter results, perform a linear fitting for all the $\Delta$ values, adjusting $T$ and $T$ is determined when the slope of the fitted formula is minimized**

**The heating current of the blackbody is typically set so that its temperature is about 2970 K. With its built parameters and working distance the spectral irradiance it realised is close to the working standard of 1000 W tungsten lamp**

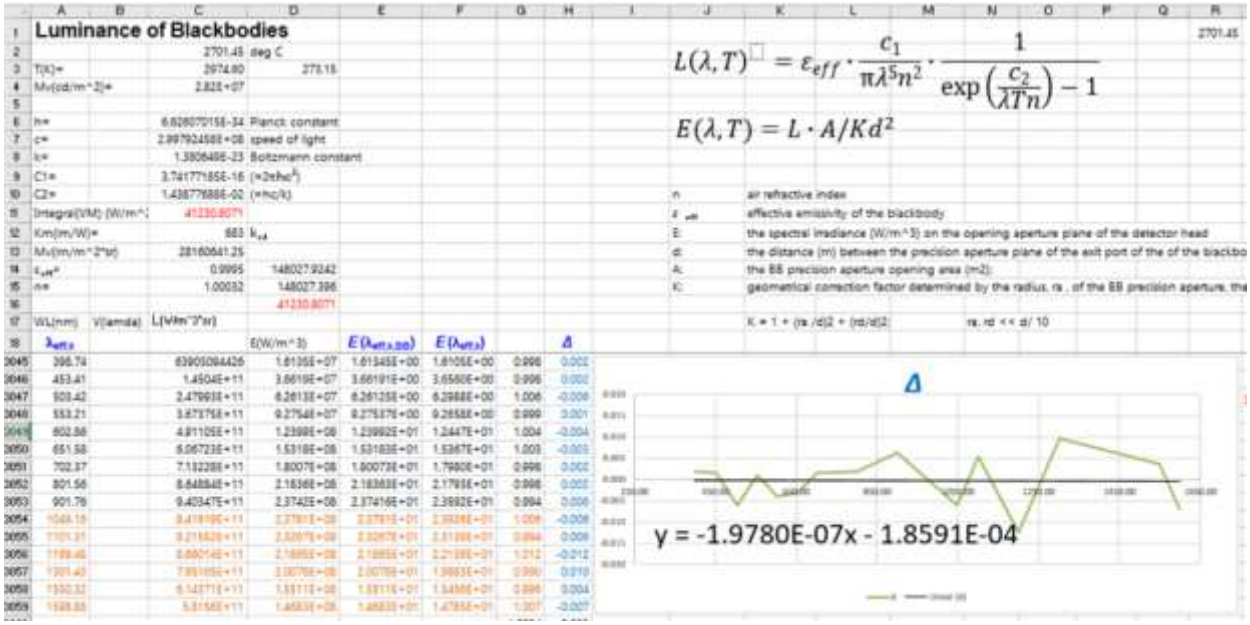


The data for filters in the UV wavelength range (filter nominal wavelength less than 400 nm) is not included for the determination of blackbody radiator thermodynamic temperature due to their higher deviations from other filters.

### 5.7.2. Description of the measurement facility and procedure

A schematic diagram of the measurement facility is shown in Figure 5.7.4. It is constructed to measure both spectral irradiance and radiance. The measuring instruments sit on a motorized optical table and the light sources are set up at fixed locations. After the thermodynamic temperature of the HTBB is measured by the MWFR, the spectral responsivity of the double grating monochromator based spectroradiometer is calibrated against the HTBB at the required wavelengths. The double grating monochromator employs 3 gratings with 2400 grooves/mm, 1200 grooves/mm and 400 grooves/mm respectively to cover the wavelength range of 250 nm to 2500 nm. For spectral irradiance measurement, a 2-inch integrating sphere is used to receive the irradiation from the light sources to minimise the polarisation effects. An optical chopper can be automatically inserted into the optical path for AC measurement using lock-in amplifier to increase the signal to noise ratio in the IR wavelength region. Both of the exit slits of the monochromator are used. One is directly coupled to a photomultiplier (PMT) detector for UV and VIS light measurement from 250 nm to 850 nm, and the other for the extended InGaAs detector for IR measurement from 850 nm to 2500 nm. A silicon detector can be included to cover the middle range if necessary. The He-Ne laser beside the PMT is used for optical alignment.

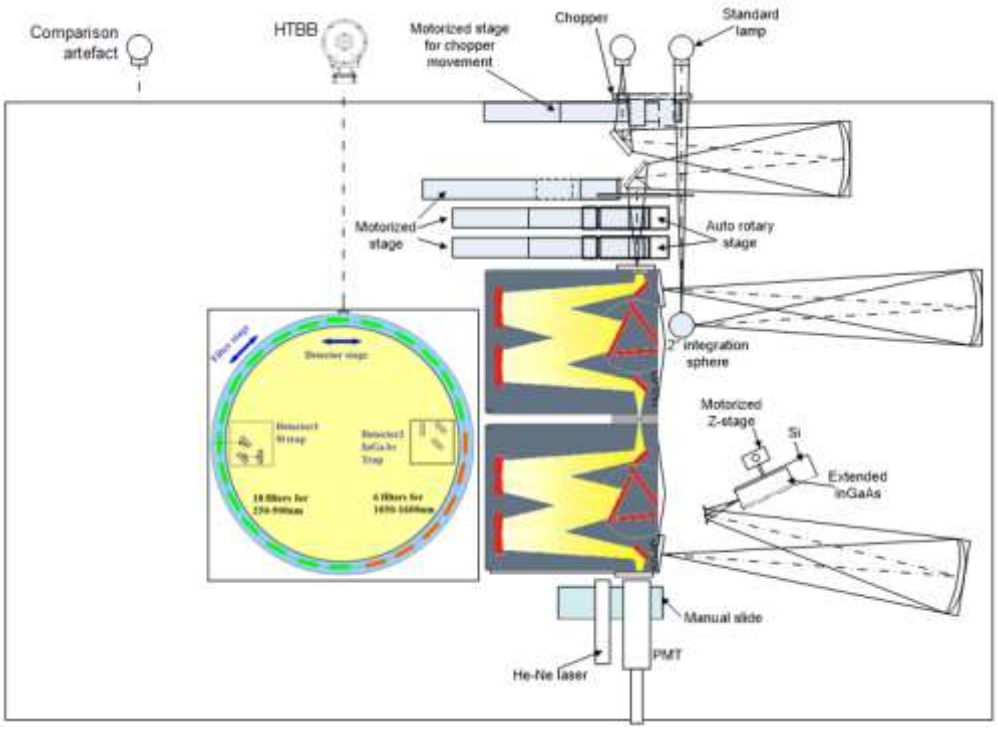


Figure 5.7.4. The spectral irradiance/radiance measurement facility

The measurement facility is used to calibrated working standard lamps against the HTBB. and used to calibrate the comparison artefacts against the working standards. The spectral irradiance of a test source is given by:

$$E_{T.\lambda} = (R_{T.\lambda} / R_{S.\lambda}) \cdot E_{S.\lambda} \quad (5.7.1)$$

where $E_{S.\lambda}$ : the spectral irradiance of the standard source at the measuring wavelength λ, and $R_{T.\lambda}$ and $R_{S.\lambda}$ are the spectral responses of the spectroradiometer for the test and the standard source respectively at the same wavelength.

For working standard lamp calibration, the test source is the working standard lamp whereas the standard source is the HTBB.

For comparison artefact calibration. the test source is the comparison artefact whereas the standard source is the working standard lamp.

### 5.7.3. Measurement uncertainty analysis

The measurement uncertainties of the base unit realisation and the calibration of working standards and comparison artefacts are listed in the following tables:

Table 5.7.2. The uncertainty budget of the primary scale realization for spectral irradiance measurement. All uncertainty components are standard uncertainties, k = 1

| WL (nm) | Temp (0.85K. R0.18%) | emissivity (0.1%/1.73) | air refractive index (0.00005 /1.73) | BB uniformity (0.3K/1.73) | BB stability (0.2K.4hrs/1.73) | aperture area (0.135%/1.73) | distance (0.25mm /1.73) | **Pri-Scale Realisation unc %** |
|---|---|---|---|---|---|---|---|---|
| 250 | 0.554 | 0.058 | 0.052 | 0.195 | 0.130 | 0.078 | 0.058 | **0.614** |
| 260 | 0.533 | 0.058 | 0.050 | 0.188 | 0.125 | 0.078 | 0.058 | **0.592** |
| 270 | 0.513 | 0.058 | 0.048 | 0.181 | 0.120 | 0.078 | 0.058 | **0.570** |
| 280 | 0.495 | 0.058 | 0.046 | 0.174 | 0.116 | 0.078 | 0.058 | **0.551** |
| 290 | 0.477 | 0.058 | 0.044 | 0.168 | 0.112 | 0.078 | 0.058 | **0.533** |
| 300 | 0.462 | 0.058 | 0.042 | 0.163 | 0.108 | 0.078 | 0.058 | **0.516** |
| 320 | 0.433 | 0.058 | 0.039 | 0.152 | 0.102 | 0.078 | 0.058 | **0.485** |
| 340 | 0.407 | 0.058 | 0.037 | 0.144 | 0.096 | 0.078 | 0.058 | **0.458** |
| 360 | 0.384 | 0.058 | 0.034 | 0.136 | 0.090 | 0.078 | 0.058 | **0.434** |
| 380 | 0.364 | 0.058 | 0.032 | 0.128 | 0.086 | 0.078 | 0.058 | **0.413** |
| 400 | 0.346 | 0.058 | 0.030 | 0.122 | 0.081 | 0.078 | 0.058 | **0.394** |
| 450 | 0.307 | 0.058 | 0.026 | 0.108 | 0.072 | 0.078 | 0.058 | **0.354** |
| 500 | 0.277 | 0.058 | 0.023 | 0.098 | 0.065 | 0.078 | 0.058 | **0.322** |
| 555 | 0.249 | 0.058 | 0.020 | 0.088 | 0.059 | 0.078 | 0.058 | **0.294** |
| 600 | 0.231 | 0.058 | 0.018 | 0.081 | 0.054 | 0.078 | 0.058 | **0.275** |
| 700 | 0.198 | 0.058 | 0.015 | 0.070 | 0.046 | 0.078 | 0.058 | **0.243** |
| 800 | 0.173 | 0.058 | 0.012 | 0.061 | 0.041 | 0.078 | 0.058 | **0.220** |
| 900 | 0.154 | 0.058 | 0.010 | 0.054 | 0.036 | 0.078 | 0.058 | **0.202** |
| 1000 | 0.139 | 0.058 | 0.009 | 0.049 | 0.033 | 0.078 | 0.058 | **0.189** |
| 1100 | 0.127 | 0.058 | 0.007 | 0.045 | 0.030 | 0.078 | 0.058 | **0.179** |
| 1300 | 0.109 | 0.058 | 0.005 | 0.038 | 0.026 | 0.078 | 0.058 | **0.164** |
| 1500 | 0.096 | 0.058 | 0.004 | 0.034 | 0.023 | 0.078 | 0.058 | **0.154** |
| 1700 | 0.086 | 0.058 | 0.003 | 0.030 | 0.020 | 0.078 | 0.058 | **0.147** |
| 2000 | 0.076 | 0.058 | 0.002 | 0.027 | 0.018 | 0.078 | 0.058 | **0.140** |
| 2200 | 0.071 | 0.058 | 0.001 | 0.025 | 0.017 | 0.078 | 0.058 | **0.137** |
| 2300 | 0.068 | 0.058 | 0.001 | 0.024 | 0.016 | 0.078 | 0.058 | **0.135** |
| 2400 | 0.066 | 0.058 | 0.001 | 0.023 | 0.016 | 0.078 | 0.058 | **0.134** |
| 2500 | 0.065 | 0.058 | 0.001 | 0.023 | 0.015 | 0.078 | 0.058 | **0.133** |

Table 5.7.3. The uncertainty budget of the Working Standard spectral irradiance calibration. All uncertainty components are standard uncertainties, k = 1

| WL (nm) | **Pri-Scale Realisation unc %** | distance WS (1/2) | Lamp current WS (0.01%)/1.73 | WL (0.1nm) /1.73 | Ex stray light/1.73 | **Cor related unc %** | Reproducibility | BB Repeatability | WS Repeatability | **Uncor related unc %** | **WS unc %** |
|---|---|---|---|---|---|---|---|---|---|---|---|
| 250 | **0.614** | 0.029 | 0.069 | 0.322 | 0.0009 | **0.698** | 0.440 | 0.140 | 0.111 | **0.475** | **0.844** |
| 260 | **0.592** | 0.029 | 0.067 | 0.293 | 0.0009 | **0.664** | 0.304 | 0.110 | 0.088 | **0.335** | **0.744** |
| 270 | **0.570** | 0.029 | 0.064 | 0.268 | 0.0009 | **0.634** | 0.190 | 0.081 | 0.069 | **0.218** | **0.670** |
| 280 | **0.551** | 0.029 | 0.062 | 0.245 | 0.0008 | **0.607** | 0.375 | 0.095 | 0.040 | **0.389** | **0.721** |
| 290 | **0.533** | 0.029 | 0.060 | 0.225 | 0.0008 | **0.582** | 0.136 | 0.070 | 0.041 | **0.159** | **0.603** |
| 300 | **0.516** | 0.029 | 0.058 | 0.207 | 0.0007 | **0.559** | 0.191 | 0.028 | 0.042 | **0.198** | **0.593** |
| 320 | **0.485** | 0.029 | 0.054 | 0.177 | 0.0007 | **0.520** | 0.187 | 0.032 | 0.039 | **0.194** | **0.555** |
| 340 | **0.458** | 0.029 | 0.051 | 0.151 | 0.0006 | **0.486** | 0.106 | 0.035 | 0.040 | **0.118** | **0.500** |
| 360 | **0.434** | 0.029 | 0.048 | 0.131 | 0.0005 | **0.457** | 0.108 | 0.017 | 0.026 | **0.112** | **0.470** |
| 380 | **0.413** | 0.029 | 0.046 | 0.113 | 0.0004 | **0.431** | 0.107 | 0.008 | 0.017 | **0.109** | **0.445** |
| 400 | **0.394** | 0.029 | 0.043 | 0.099 | 0.0004 | **0.409** | 0.088 | 0.013 | 0.016 | **0.091** | **0.419** |
| 450 | **0.354** | 0.029 | 0.039 | 0.071 | 0.0002 | **0.364** | 0.121 | 0.009 | 0.017 | **0.122** | **0.384** |
| 500 | **0.322** | 0.029 | 0.035 | 0.051 | 0.0000 | **0.329** | 0.093 | 0.011 | 0.018 | **0.095** | **0.343** |
| 555 | **0.294** | 0.029 | 0.031 | 0.037 | 0.0002 | **0.299** | 0.098 | 0.008 | 0.013 | **0.099** | **0.315** |
| 600 | **0.275** | 0.029 | 0.029 | 0.028 | 0.0004 | **0.280** | 0.114 | 0.007 | 0.012 | **0.115** | **0.303** |
| 700 | **0.243** | 0.029 | 0.025 | 0.014 | 0.0007 | **0.247** | 0.065 | 0.005 | 0.011 | **0.066** | **0.255** |
| 800 | **0.220** | 0.029 | 0.022 | 0.007 | 0.0011 | **0.223** | 0.135 | 0.012 | 0.024 | **0.138** | **0.262** |
| 900 | **0.202** | 0.029 | 0.019 | 0.002 | 0.0007 | **0.205** | 0.231 | 0.087 | 0.117 | **0.273** | **0.341** |
| 1000 | **0.189** | 0.029 | 0.017 | -0.002 | 0.0007 | **0.192** | 0.102 | 0.097 | 0.096 | **0.171** | **0.257** |
| 1100 | **0.179** | 0.029 | 0.016 | -0.004 | 0.0008 | **0.182** | 0.040 | 0.077 | 0.087 | **0.122** | **0.219** |
| 1300 | **0.164** | 0.029 | 0.013 | -0.006 | 0.0008 | **0.167** | 0.057 | 0.080 | 0.086 | **0.130** | **0.212** |
| 1500 | **0.154** | 0.029 | 0.012 | -0.007 | 0.0009 | **0.157** | 0.104 | 0.077 | 0.078 | **0.151** | **0.218** |
| 1700 | **0.147** | 0.029 | 0.010 | -0.008 | 0.0009 | **0.150** | 0.056 | 0.079 | 0.064 | **0.116** | **0.190** |
| 2000 | **0.140** | 0.029 | 0.009 | -0.008 | 0.0010 | **0.143** | 0.080 | 0.085 | 0.083 | **0.143** | **0.202** |
| 2200 | **0.137** | 0.029 | 0.008 | -0.007 | 0.0011 | **0.140** | 0.146 | 0.079 | 0.074 | **0.182** | **0.230** |
| 2300 | **0.135** | 0.029 | 0.008 | -0.007 | 0.0011 | **0.139** | 0.110 | 0.081 | 0.085 | **0.161** | **0.213** |
| 2400 | **0.134** | 0.029 | 0.007 | -0.007 | 0.0011 | **0.138** | 0.127 | 0.079 | 0.075 | **0.168** | **0.217** |
| 2500 | **0.133** | 0.029 | 0.007 | -0.007 | 0.0011 | **0.137** | 0.181 | 0.099 | 0.092 | **0.226** | **0.264** |

Table 5.7.4. The uncertainty budget of the comparison artefact spectral irradiance calibration. All uncertainty components are standard uncertainties, k = 1

| WL (nm) | **WS unc %** | distance CA (1/2) | Lamp current CA (0.01%)/1.73 | WL (0.1nm) /1.73 | Ex stray light/1.73 | **Cor related unc %** | Reproducibility | WS Repeatability | CA Repeatability | **Uncor related unc %** | **CA unc %** |
|---|---|---|---|---|---|---|---|---|---|---|---|
| 250 | **0.844** | 0.029 | 0.069 | 0.322 | 0.0009 | **0.906** | 0.122 | 0.130 | 0.038 | **0.182** | **0.925** |
| 260 | **0.744** | 0.029 | 0.067 | 0.293 | 0.0009 | **0.803** | 0.365 | 0.130 | 0.099 | **0.400** | **0.897** |
| 270 | **0.670** | 0.029 | 0.064 | 0.268 | 0.0009 | **0.725** | 0.213 | 0.037 | 0.034 | **0.219** | **0.758** |
| 280 | **0.721** | 0.029 | 0.062 | 0.245 | 0.0008 | **0.765** | 0.193 | 0.066 | 0.036 | **0.207** | **0.792** |
| 290 | **0.603** | 0.029 | 0.060 | 0.225 | 0.0008 | **0.647** | 0.253 | 0.038 | 0.045 | **0.260** | **0.698** |
| 300 | **0.593** | 0.029 | 0.058 | 0.207 | 0.0007 | **0.632** | 0.243 | 0.016 | 0.019 | **0.244** | **0.677** |
| 320 | **0.555** | 0.029 | 0.054 | 0.177 | 0.0007 | **0.585** | 0.224 | 0.025 | 0.010 | **0.225** | **0.627** |
| 340 | **0.500** | 0.029 | 0.051 | 0.151 | 0.0006 | **0.526** | 0.250 | 0.032 | 0.029 | **0.254** | **0.584** |
| 360 | **0.470** | 0.029 | 0.048 | 0.131 | 0.0005 | **0.491** | 0.235 | 0.009 | 0.005 | **0.236** | **0.545** |
| 380 | **0.445** | 0.029 | 0.046 | 0.113 | 0.0004 | **0.462** | 0.218 | 0.010 | 0.023 | **0.219** | **0.512** |
| 400 | **0.419** | 0.029 | 0.043 | 0.099 | 0.0004 | **0.433** | 0.214 | 0.007 | 0.003 | **0.214** | **0.483** |
| 450 | **0.384** | 0.029 | 0.039 | 0.071 | 0.0002 | **0.393** | 0.248 | 0.013 | 0.009 | **0.249** | **0.465** |
| 500 | **0.343** | 0.029 | 0.035 | 0.051 | 0.0000 | **0.349** | 0.193 | 0.010 | 0.008 | **0.194** | **0.400** |
| 555 | **0.315** | 0.029 | 0.031 | 0.037 | 0.0002 | **0.320** | 0.226 | 0.010 | 0.009 | **0.227** | **0.392** |
| 600 | **0.303** | 0.029 | 0.029 | 0.028 | 0.0004 | **0.307** | 0.235 | 0.008 | 0.008 | **0.236** | **0.387** |
| 700 | **0.255** | 0.029 | 0.025 | 0.014 | 0.0007 | **0.258** | 0.202 | 0.015 | 0.008 | **0.203** | **0.328** |
| 800 | **0.262** | 0.029 | 0.022 | 0.007 | 0.0011 | **0.265** | 0.262 | 0.018 | 0.010 | **0.263** | **0.373** |
| 900 | **0.341** | 0.029 | 0.019 | 0.002 | 0.0007 | **0.343** | 0.125 | 0.042 | 0.230 | **0.265** | **0.434** |
| 1000 | **0.257** | 0.029 | 0.017 | -0.002 | 0.0007 | **0.259** | 0.110 | 0.139 | 0.083 | **0.196** | **0.325** |
| 1100 | **0.219** | 0.029 | 0.016 | -0.004 | 0.0008 | **0.222** | 0.139 | 0.110 | 0.113 | **0.210** | **0.305** |
| 1300 | **0.212** | 0.029 | 0.013 | -0.006 | 0.0008 | **0.214** | 0.130 | 0.111 | 0.101 | **0.198** | **0.292** |
| 1500 | **0.218** | 0.029 | 0.012 | -0.007 | 0.0009 | **0.221** | 0.150 | 0.100 | 0.102 | **0.207** | **0.302** |
| 1700 | **0.190** | 0.029 | 0.010 | -0.008 | 0.0009 | **0.192** | 0.107 | 0.103 | 0.099 | **0.178** | **0.262** |
| 2000 | **0.202** | 0.029 | 0.009 | -0.008 | 0.0010 | **0.205** | 0.096 | 0.087 | 0.114 | **0.173** | **0.268** |
| 2200 | **0.230** | 0.029 | 0.008 | -0.007 | 0.0011 | **0.232** | 0.140 | 0.117 | 0.103 | **0.209** | **0.312** |
| 2300 | **0.213** | 0.029 | 0.008 | -0.007 | 0.0011 | **0.215** | 0.224 | 0.115 | 0.117 | **0.278** | **0.351** |
| 2400 | **0.217** | 0.029 | 0.007 | -0.007 | 0.0011 | **0.219** | 0.100 | 0.109 | 0.143 | **0.205** | **0.300** |
| 2500 | **0.264** | 0.029 | 0.007 | -0.007 | 0.0011 | **0.266** | 0.255 | 0.125 | 0.126 | **0.311** | **0.409** |

### *5.7.3.1. Uncertainties of the Comparison artefacts*

Table 5.7.5. Spectral Irradiance standard uncertainties (k=1) of the lamp **BN-9101-642**

| Wavelength, nm | Round 1 | | | Round 2 | | |
|---|---|---|---|---|---|---|
| | Uncertainties associated with, % | | Combined uncertainty, % | Uncertainties associated with, % | | Combined uncertainty, % |
| | Uncorrelated effects | Correlated effects | | Uncorrelated effects | Correlated effects | |
| 250 | 0.20 | 0.91 | 0.93 | 0.18 | 0.91 | 0.92 |
| 260 | 0.27 | 0.80 | 0.85 | 0.40 | 0.80 | 0.90 |
| 270 | 0.20 | 0.73 | 0.75 | 0.22 | 0.73 | 0.76 |
| 280 | 0.08 | 0.76 | 0.77 | 0.21 | 0.76 | 0.79 |
| 290 | 0.06 | 0.65 | 0.65 | 0.26 | 0.65 | 0.70 |
| 300 | 0.05 | 0.63 | 0.63 | 0.24 | 0.63 | 0.68 |
| 320 | 0.13 | 0.59 | 0.60 | 0.23 | 0.59 | 0.63 |
| 340 | 0.08 | 0.53 | 0.53 | 0.25 | 0.53 | 0.58 |
| 360 | 0.08 | 0.49 | 0.50 | 0.24 | 0.49 | 0.54 |
| 380 | 0.09 | 0.46 | 0.47 | 0.22 | 0.46 | 0.51 |
| 400 | 0.03 | 0.43 | 0.43 | 0.21 | 0.43 | 0.48 |
| 450 | 0.07 | 0.39 | 0.40 | 0.25 | 0.39 | 0.47 |
| 500 | 0.06 | 0.35 | 0.35 | 0.19 | 0.35 | 0.40 |
| 555 | 0.06 | 0.32 | 0.33 | 0.23 | 0.32 | 0.39 |
| 600 | 0.05 | 0.31 | 0.31 | 0.24 | 0.31 | 0.39 |
| 700 | 0.10 | 0.26 | 0.28 | 0.20 | 0.26 | 0.33 |
| 800 | 0.16 | 0.26 | 0.31 | 0.26 | 0.26 | 0.37 |
| 900 | 0.61 | 0.34 | 0.70 | 0.15 | 0.34 | 0.37 |
| 1000 | 0.11 | 0.26 | 0.28 | 0.20 | 0.26 | 0.32 |
| 1100 | 0.13 | 0.22 | 0.26 | 0.21 | 0.22 | 0.31 |
| 1300 | 0.09 | 0.21 | 0.23 | 0.20 | 0.21 | 0.29 |
| 1500 | 0.15 | 0.22 | 0.27 | 0.21 | 0.22 | 0.30 |
| 1700 | 0.11 | 0.19 | 0.22 | 0.18 | 0.19 | 0.26 |
| 2000 | 0.10 | 0.20 | 0.23 | 0.17 | 0.20 | 0.27 |
| 2200 | 0.12 | 0.23 | 0.26 | 0.21 | 0.23 | 0.31 |
| 2300 | 0.08 | 0.21 | 0.23 | 0.28 | 0.21 | 0.35 |
| 2400 | 0.22 | 0.22 | 0.31 | 0.21 | 0.22 | 0.30 |
| 2500 | 0.03 | 0.27 | 0.27 | 0.31 | 0.27 | 0.41 |

Table 5.7.6. Spectral Irradiance standard uncertainties (k=1) of the lamp **BN-9101-643**

| Wavelength, nm | Round 1 | | | Round 2 | | |
|---|---|---|---|---|---|---|
| | Uncertainties associated with, % | | Combined uncertainty, % | Uncertainties associated with, % | | Combined uncertainty, % |
| | Uncorrelated effects | Correlated effects | | Uncorrelated effects | Correlated effects | |
| 250 | 0.84 | 0.91 | 1.24 | 0.18 | 0.91 | 0.92 |
| 260 | 0.27 | 0.80 | 0.85 | 0.26 | 0.80 | 0.84 |
| 270 | 0.11 | 0.73 | 0.73 | 0.25 | 0.73 | 0.77 |
| 280 | 0.23 | 0.76 | 0.80 | 0.23 | 0.76 | 0.80 |
| 290 | 0.25 | 0.65 | 0.69 | 0.20 | 0.65 | 0.68 |
| 300 | 0.09 | 0.63 | 0.64 | 0.18 | 0.63 | 0.66 |
| 320 | 0.16 | 0.59 | 0.61 | 0.16 | 0.59 | 0.61 |
| 340 | 0.08 | 0.53 | 0.53 | 0.19 | 0.53 | 0.56 |
| 360 | 0.05 | 0.49 | 0.49 | 0.20 | 0.49 | 0.53 |
| 380 | 0.07 | 0.46 | 0.47 | 0.22 | 0.46 | 0.51 |
| 400 | 0.07 | 0.43 | 0.44 | 0.20 | 0.43 | 0.48 |
| 450 | 0.06 | 0.39 | 0.40 | 0.19 | 0.39 | 0.44 |
| 500 | 0.06 | 0.35 | 0.35 | 0.21 | 0.35 | 0.41 |
| 555 | 0.04 | 0.32 | 0.32 | 0.24 | 0.32 | 0.40 |
| 600 | 0.07 | 0.31 | 0.31 | 0.17 | 0.31 | 0.35 |
| 700 | 0.06 | 0.26 | 0.27 | 0.16 | 0.26 | 0.30 |
| 800 | 0.13 | 0.26 | 0.30 | 0.29 | 0.26 | 0.39 |
| 900 | 0.66 | 0.34 | 0.74 | 0.33 | 0.34 | 0.47 |
| 1000 | 0.13 | 0.26 | 0.29 | 0.16 | 0.26 | 0.30 |
| 1100 | 0.09 | 0.22 | 0.24 | 0.13 | 0.22 | 0.26 |
| 1300 | 0.12 | 0.21 | 0.25 | 0.15 | 0.21 | 0.26 |
| 1500 | 0.01 | 0.22 | 0.22 | 0.11 | 0.22 | 0.24 |
| 1700 | 0.05 | 0.19 | 0.20 | 0.14 | 0.19 | 0.24 |
| 2000 | 0.07 | 0.20 | 0.22 | 0.13 | 0.20 | 0.24 |
| 2200 | 0.09 | 0.23 | 0.25 | 0.19 | 0.23 | 0.30 |
| 2300 | 0.06 | 0.21 | 0.22 | 0.14 | 0.21 | 0.25 |
| 2400 | 0.19 | 0.22 | 0.29 | 0.13 | 0.22 | 0.25 |
| 2500 | 0.20 | 0.27 | 0.33 | 0.37 | 0.27 | 0.46 |

Table 5.7.7. Spectral Irradiance standard uncertainties (k=1) of the lamp **BN-9101-644**

| Wavelength, nm | Round 1 | | | Round 2 | | |
|---|---|---|---|---|---|---|
| | Uncertainties associated with, % | | Combined uncertainty, % | Uncertainties associated with, % | | Combined uncertainty, % |
| | Uncorrelated effects | Correlated effects | | Uncorrelated effects | Correlated effects | |
| 250 | 0.41 | 0.91 | 0.99 | 0.41 | 0.91 | 0.99 |
| 260 | 0.22 | 0.80 | 0.83 | 0.39 | 0.80 | 0.89 |
| 270 | 0.23 | 0.73 | 0.76 | 0.13 | 0.73 | 0.74 |
| 280 | 0.23 | 0.76 | 0.80 | 0.24 | 0.76 | 0.80 |
| 290 | 0.19 | 0.65 | 0.67 | 0.30 | 0.65 | 0.71 |
| 300 | 0.07 | 0.63 | 0.64 | 0.30 | 0.63 | 0.70 |
| 320 | 0.16 | 0.59 | 0.61 | 0.19 | 0.59 | 0.61 |
| 340 | 0.10 | 0.53 | 0.54 | 0.17 | 0.53 | 0.55 |
| 360 | 0.06 | 0.49 | 0.49 | 0.19 | 0.49 | 0.53 |
| 380 | 0.05 | 0.46 | 0.46 | 0.24 | 0.46 | 0.52 |
| 400 | 0.02 | 0.43 | 0.43 | 0.19 | 0.43 | 0.47 |
| 450 | 0.03 | 0.39 | 0.39 | 0.24 | 0.39 | 0.46 |
| 500 | 0.07 | 0.35 | 0.36 | 0.18 | 0.35 | 0.39 |
| 555 | 0.06 | 0.32 | 0.33 | 0.17 | 0.32 | 0.36 |
| 600 | 0.05 | 0.31 | 0.31 | 0.15 | 0.31 | 0.34 |
| 700 | 0.10 | 0.26 | 0.28 | 0.13 | 0.26 | 0.29 |
| 800 | 0.14 | 0.26 | 0.30 | 0.18 | 0.26 | 0.32 |
| 900 | 0.57 | 0.34 | 0.67 | 0.15 | 0.34 | 0.37 |
| 1000 | 0.02 | 0.26 | 0.26 | 0.15 | 0.26 | 0.30 |
| 1100 | 0.09 | 0.22 | 0.24 | 0.17 | 0.22 | 0.28 |
| 1300 | 0.11 | 0.21 | 0.24 | 0.13 | 0.21 | 0.25 |
| 1500 | 0.08 | 0.22 | 0.23 | 0.14 | 0.22 | 0.26 |
| 1700 | 0.12 | 0.19 | 0.23 | 0.14 | 0.19 | 0.24 |
| 2000 | 0.08 | 0.20 | 0.22 | 0.14 | 0.20 | 0.25 |
| 2200 | 0.05 | 0.23 | 0.24 | 0.09 | 0.23 | 0.25 |
| 2300 | 0.02 | 0.21 | 0.22 | 0.16 | 0.21 | 0.27 |
| 2400 | 0.13 | 0.22 | 0.26 | 0.12 | 0.22 | 0.25 |
| 2500 | 0.10 | 0.27 | 0.28 | 0.23 | 0.27 | 0.35 |

## 5.8. NMIA, Australia

### 5.8.1. Introduction

The NMIA spectral irradiance scale is based on two inputs:
- the NMIA 2018 and NMIA 2019 scales of relative spectral irradiance, and
- the NMIA 2016 unit of illuminance.

Measured values of relative spectral irradiance, when processed with V(λ) in the usual way, give a result that is proportional to the illuminance. The proportionality factor is determined by comparison with measured illuminance values at the required distance, and then used to scale the relative spectral irradiance to SI spectral irradiance units. The illuminance measurements are based on the NMIA 2016 illuminance scale, which has only a very weak correlation with the relative spectral irradiance scale.

### 5.8.2. Measurements and Calculations

#### *5.8.2.1. Summary of the Spectral Comparator System*

Figure 5.8.1 is a schematic diagram of the spectral comparator system, with reference numbers in the paragraphs below referring to the numbers on the diagram. Each travelling standard lamp (1) was compared spectrally with a windowless IKE graphite cavity blackbody radiator (2) operated at temperatures between 2350 K and 2750 K.

The lamps were mounted inside a spectrally non-selective matt black housing (3) of approximate diameter 310 mm and height 420 mm. An air gap approximately 40 mm high around the base of the housing allowed natural convective air flow around the lamp. Radiation from the rear of the lamp was contained by a conical light trap (4) and no part of the housing was directly visible from the spectroradiometer system.

Irradiance from the lamp and the blackbody was projected towards a small Halon diffuser plate (5), with pneumatically-controlled shutters used to select either blackbody radiation or lamp radiation at different stages of the measurement sequence.

During measurement of each source, the Halon plate was oriented normal to the direction of radiation from that source. The plate was held in a pivoting mount, and changes to the orientation needed to maintain normal incidence for both sources were made with a pneumatic actuator which rotated the mount between two fixed mechanical stops.

The irradiance from each source was spectrally resolved by two coupled Jobin-Yvon single monochromators (6) with order sorting filters. Light reflected from the Halon plate was imaged onto the entrance slit of the first monochromators using an off-axis spherical mirror (7). The mirror was positioned symmetrically between the incident directions of radiation from the two sources, maintaining the symmetry of the scattering process for the blackbody radiation and the lamp radiation. The magnification of the focussing system was designed so that only light reflected off the Halon plate entered the monochromators, i.e. reflections from the mount were excluded.

A detector housing (8), containing photomultiplier, silicon, InGaAs and long-wave InGaAs detectors, was mounted at the exit slit of the second monochromator. Pneumatically controlled actuators allowed automated selection of the appropriate detector for the spectral region in each measurement block, and an auxiliary focussing system (9) ensured a suitable spot size on each detector.

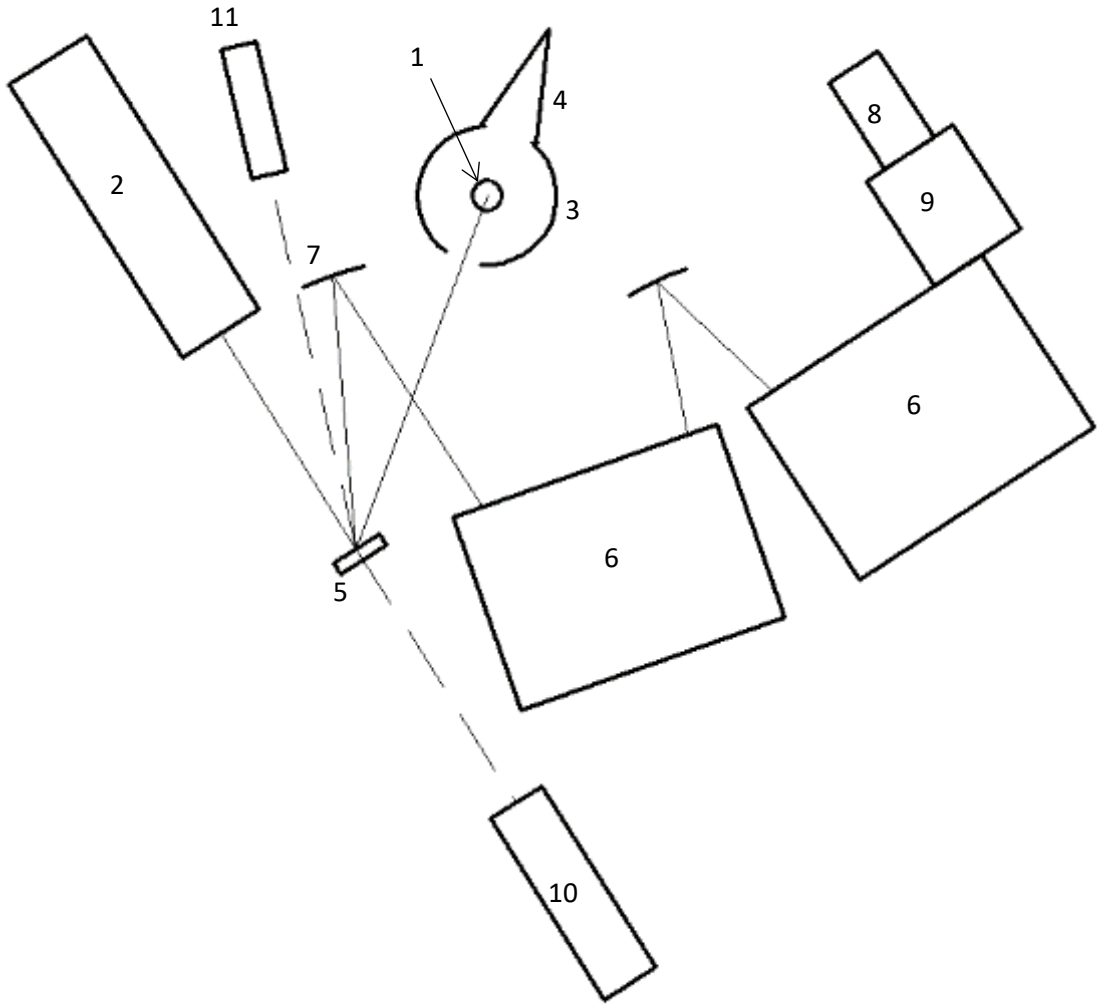


Figure 5.8.1. Schematic Diagram of the Spectral Comparator System

Lamp voltages were measured by Agilent 34410A digital multimeters and lamp currents measured by Agilent 34410A digital multimeters via standard resistors. All meters and standard resistors were calibrated by the NMIA Electrical Section. Detector signals were measured utilising calibrated Keithley 6485 picoammeters or, in the case of the long-wave InGaAs detector, a Stanford Research model SR810 DSP lock-in amplifier.

The blackbody cavity temperature was measured with a KE Technologies LP-5 linear pyrometer (10) which was calibrated by the NMIA Temperature Project. The line-of-sight of the pyrometer was aligned with the axis of the cavity, and it was focussed a few centimetres in front of the rear wall of the cavity to match the view of the monochromator system more closely. In order to complete measurements of the cavity temperature, which were made at the beginning and end of each run, it was necessary to move the Halon plate mount and pivot mechanism out of the beam. This was done manually, with a positive mechanical stop ensuring the plate was reliably positioned each time.

Some of the light scattered from the Halon plate was also imaged onto a filter radiometer (11) with central wavelength of approximately 455 nm. This radiometer allowed stability monitoring for each source, and was used in conjunction with the temperature measurements from the calibrated pyrometer to calculate the blackbody temperature corresponding to each measurement point.

Figure 5.8.2 is a photograph of the input side of the spectral comparator system, showing most of the input-side components. Individual components are identified using the same numbering system as used in Figure 5.8.1.

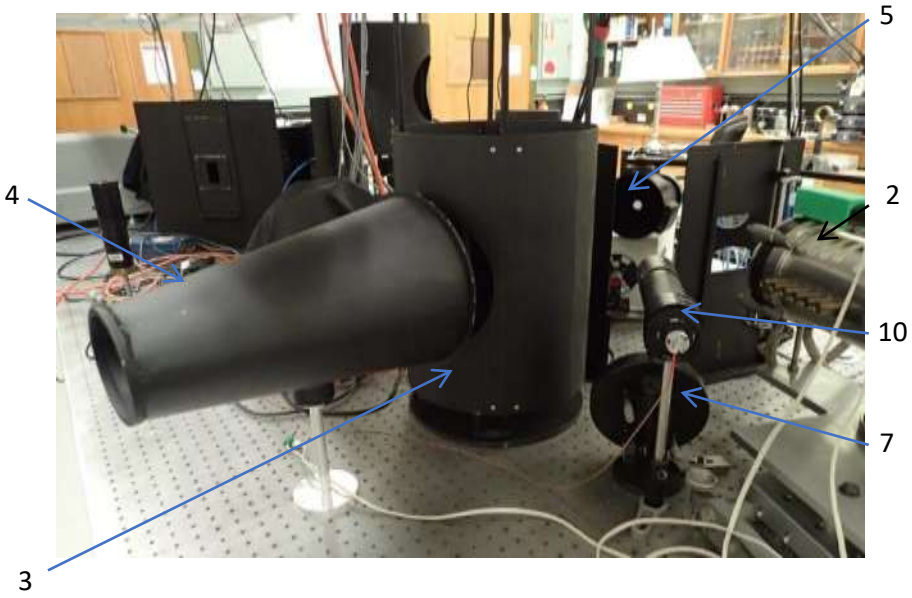


Figure 5.8.2. View of the Spectral Comparator System Showing most of the Components

### *5.8.2.2. Illuminance measurements*

For the measurements of illuminance, the travelling standard lamps were set up at the required distance of 500.0 mm from the photometer on an optical bench with suitable black curtains, screens and shutter and with a 200 mm-diameter gloss black-painted light-trap behind the lamp to eliminate background reflections. Stray light was controlled using baffles with apertures having edges designed to minimise the amount of light reflected towards the detection system. The photometer was calibrated for Illuminant A response against the ensemble of working standard lamps that carry the NMIA luminous intensity scale. Details of the system may be found in the CCPR-K3.2014 report.

### *5.8.2.3. Calculations*

Since the optical path is assumed to be equivalent for travelling standard lamp measurements and blackbody measurements and the same detector is used, the ratio of the detector signals for the two sources at any given wavelength is equal to the ratio of spectral irradiance values at that wavelength. If the temperature of the cavity radiator is known, the spectral shape of the blackbody emission can be calculated from Planck's Law, allowing calculation of the spectral shape of the lamp emission. Dividing the calculation result at each wavelength by the result at 555 nm (the normalising wavelength) gives the relative spectral irradiance of the lamp normalised to 555 nm, denoted by $\tilde{E}_{e,\lambda}(\lambda)$

Because the spectral irradiance is related to the normalised spectral irradiance by

$$E_{e,\lambda}(\lambda) = E_{e,\lambda}(555\text{ nm}) \times \tilde{E}_{e,\lambda}(\lambda)\,, \tag{5.8.1}$$

the spectral irradiance at 555 nm can be found from the illuminance, $E_v$, using

$$E_{e,\lambda}(555\text{ nm}) = E_v \Big/ \left( K_m \times \int_{360nm}^{830nm} \tilde{E}_{e,\lambda}(\lambda).V(\lambda)\,.d\lambda \right)$$

Once $E_{e,\lambda}(555\text{ nm})$ is known, it can be used to recover the spectral irradiance from the normalised spectral irradiance.

#### *5.8.2.4. Details of the Measurement Process*

***Round 1***

The spectral irradiance values submitted for each travelling standard in round 1 were measured for normalised spectral irradiance against the NMIA reference blackbody radiator with absolute spectral irradiance values derived from photometric measurements as described above.

The normalised spectral irradiance values were measured against the NMIA reference blackbody radiator with at least three separate runs on each lamp with the blackbody running in a different temperature range for each spectral run to enable checking of stray light levels. The wavelength range required by the protocol was divided into sections utilising a photomultiplier for wavelengths between 250 nm and 800 nm, overlapping with results from a silicon detector for wavelengths between 350 nm and 1000 nm, overlapping with results from an InGaAs detector for the wavelength range between 900 nm and 1700 nm, overlapping with results from a long-wave InGaAs detector from 1300 nm to 2500 nm. Final results were selected based on measurement sets having the lowest total uncertainty.

The photometric measurements used for scaling the normalised spectral results to absolute spectral irradiance values were obtained on the NMIA photometric bench with the lamp aligned and spaced according to section 3.4 of the comparison protocol. The area used for the irradiance measurements utilised a photometer having a circular area of 6.23 mm diameter with spatial responsivity uniformity across this area maintained within 0.7% of the mean responsivity value. The uncertainties derived for this calibration do not include a component for use of the lamp with different target areas.

***Round 2***

The measurement system employed for Round 2 used the same equipment and measurement practice as for Round 1. However, resupply of blackbody cavities for the NMIA blackbody used more dense graphite than for the blackbody cavities used in Round 1 of the comparison.

The new cavities required lower cavity voltage but significantly higher current than the older cavities to maintain a given distribution temperature. Although the original blackbody supply could drive the new cavities to the desired temperature, the stabilisation system was not able to operate with the higher currents. Consequently, the Round 2 results, even though corrected via monitoring the blackbody output using the filter radiometer, are significantly noisier than for Round 1.

***Scan method***

The blackbody was powered up and left to stabilise for a period of around 2 hours. The blackbody temperature was then checked using the calibrated pyrometer and set to a temperature suitable for transfer for the particular spectral range of the test undertaken. The blackbody was then allowed

another 10 minutes to stabilise at which time the temperature was rechecked and the spectroradiometer diffuser was rotated into place. The spectral comparison between the blackbody source and the test source was then started, selecting the first wavelength, taking reference signal measurements, reference zero measurements, reference monitor measurements, test signal measurements, test zero measurements and test monitor measurements before proceeding to the next wavelength. At the end of the spectral run, the spectroradiometer diffuser was rotated out of alignment so that the pyrometer could be used to determine any drift in the blackbody temperature during the spectral run and correlations between the monitor detector and pyrometer readings could be analysed. This process is automated for the full spectral range of the comparison, however to conserve blackbody cavity life spectral runs over selected wavelength ranges (particularly in the UV and IR spectral regions were performed using higher blackbody temperatures. The spectral distributions of the test sources were the same for any of the blackbody temperatures chosen, however, higher blackbody temperatures generally produced lower measurement noise.

As an additional measure to improve the signal to noise ratio in the UV and IR regions, the spectral comparator system was modified for use as a single monochromator by moving the detector to the output of the first monochromator. During the IR measurements a silicon pre-filter was used as an order-sorting filter, and in the UV region the zero offset was estimated from the 'signal' at wavelength settings where the rapid fall of the Planck spectrum means both the blackbody and the lamp would produce negligible output.

### 5.8.3. Corrections

#### *5.8.3.1. Current Setting*

There is a small but unavoidable difference between the current to which the travelling standard lamp is set and the target current specified by the protocol. Measured spectral irradiance values are therefore corrected to values corresponding to the target current. The correction factor is based on an equation (given in the section discussing uncertainty components) that has been developed from empirical observations of several different types of lamp operating at a number of temperatures.

#### *5.8.3.2. Source Spectrum for Illuminance Measurement*

The relative spectral responsivity of the photometer used for the illuminance measurements is well characterised. Raw illuminance measurements from this photometer were corrected for the effects of deviation from ideal V(λ) response in the usual way, based on the measured normalised spectral irradiance of each of the travelling standard lamps.

#### *5.8.3.3. Atmospheric Absorption*

Because the measurand for the comparison was the spectral irradiance of a lamp in a specified reference plane, consideration was given to correcting the measurements for the effects of atmospheric absorption over the propagation path. When determining the relative spectral irradiance of the travelling standard lamps, the reference was a theoretical spectral shape calculated from Planck's Law. Because any spectrally varying atmospheric absorption in the path between either source and the diffuser would apply equally to both (assuming the path lengths were equal), the normalised spectral irradiance of the lamp calculated from ratios of detector signals would not include the effect of the atmospheric absorption. The result would therefore not be the actual spectral irradiance of the lamp at the reference plane when the lamp was operated in a normal atmosphere.

Despite these considerations, no corrections for atmospheric absorption are included in the NMIA results. There are a number of reasons for this.

1. The magnitude of the correction appears to be small at all comparison wavelengths except possibly 2500 nm. Initial calculations derived an estimated correction of approximately 2% at this wavelength (but see the following two points).
2. The available data sources of which we are aware were not intended for use with the short path lengths used in the comparison.
3. Some rough measurements (at a different wavelength) appeared to contradict the prediction of the data source that we used.

It therefore appeared likely that including corrections for atmospheric absorption based on this data source would distort the results, and the corrected values would not be more reliable measurements of the measurand than the uncorrected values.

It could be argued that corrections for atmospheric absorption should be a part of measurement of spectral irradiance, since the actual spectral irradiance of any lamp when used by a client will be modified by the atmosphere. It would therefore be beneficial for the client if calibration results for the lamp included the effect. However, the converse argument is that the effect depends on the atmospheric conditions and the operating distance when the lamp is used, and it would be impossible to include all variations in calibration results. Finally, in the context of an international comparison it may not be appropriate to include effects such as this since the objective is comparison of international primary standards.

### 5.8.4. Uncertainties

This section lists the main contributions to the uncertainty in the NMIA measurements of the spectral irradiance of the travelling standard lamps. The components are separated into those contributing to the illuminance measurements and those contributing to the normalised spectral irradiance measurements.

The format of the entries in the list below depends on the nature of the uncertainty component. In some cases, for example “Reference Separation”, the form of the dependence of the final quantity (illuminance, $E_v$, in the example) on the parameter in question is specified and the contribution to the uncertainty in the final quantity is calculated in the normal way. In other cases, for example “Photometer Non-linearity”, an expression for the uncertainty is given directly. In these cases, the effect on the final quantity is a factor close to 1.0 and the uncertainty is calculated as described.

Each entry is given a descriptive label (e.g. “Base Illuminance Responsivity”) and that label is used in Tables 5.8.1 – 5.8.3 which list the numerical values of the components pertaining to the two measurement rounds.

#### *5.8.4.1. Illuminance:*

The uncertainties listed below follow the NMIA uncertainty budget for the CCPR-K3.2014 comparison.

- Base Illuminance Responsivity (Types A and B)
  The photometric scale is held on a number of photometric lamps. The primary derivation of the scale involves calibration of these lamps for illuminance at a specified distance.
- Agreement Between Reference Photometric Lamps (Type A)
  Four calibrated photometric reference lamps were used when calibrating the illuminance responsivity of the photometer, and the photometer calibration was repeated for each

independent set of measurements on the travelling standard lamps. The uncertainty budget includes a component calculated from the variability of these calibration results.

- Reference Separation (Type B)
  Derived from the uncertainty in the position of the photometer during its calibration relative to the nominal position for which the reference lamp illuminance is known,

$$E_{\mathrm{v}} \propto d^{-2}$$

  where d is the separation of the photometer and the reference lamp.

- Reference Current (Type B)
  Derived from the uncertainty in setting the reference lamp to the nominal current when calibrating the photometer.

$$E_{\mathrm{v}} \propto I^{j}$$

  where Ev is the illuminance. It is the lamp current in the region of the lamp target current and j has a value between 5.84 and 5.96 dependent on which reference lamp is in use. A value of j = 6.25 was actually used to cover the uncertainty in the current correction factor.

- Transfer to DUT (Type A)
  Transfer noise is typically a few parts in $10^5$, however this component also includes the variation between separate independent measurements made on each travelling standard lamp.

- DUT Separation (Type B)
  Derived from the uncertainty in the separation between the photometer and the travelling standard lamp.

$$E_{v} \propto d^{-2}$$

- DUT Current Setting (Type B)
  Derived from the uncertainty in setting the reference lamp to the specified current when measuring the illuminance at the specified measurement plane.

$$E_{\mathrm{v}} \propto I^{5.02}$$

  An exponent of 6.25 was actually used to cover the uncertainty in the current correction factor although this is not dominant so the factor is not critical in this case.

- V(λ) Spectral Mismatch Correction (Type B)
  Refers to the difference in the illuminance responsivity of the photometer to Illuminant A (against which it was calibrated) and the responsivity to the spectrum of the travelling standard lamp.

$$E_{\mathrm{v}} \propto \frac{\int_{\lambda} S(\lambda)V(\lambda)d\lambda}{\int_{\lambda} S(\lambda)\, s_{rel}(\lambda)d\lambda} \frac{\int_{\lambda} S_A(\lambda)s_{rel}(\lambda)d\lambda}{\int_{\lambda} S_A\,(\lambda)V(\lambda)d\lambda}$$

  In practice the correction is smaller than many other uncertainty components, so the uncertainty in the correction is assumed to be approximately 10% of the correction, resulting in an uncertainty contribution that is far from dominant.

- Photometer Non-linearity (Type B)
  Due to the difference in illuminance at which the photometer was calibrated and that produced by the travelling standard lamp.

$$u(E_v) = 0.0001 \times \log_{5.6}\left(\frac{E_v}{E_v'}\right)$$

where $E_v$ and $E_v'$ are irradiance values at the limits of the range over which non-linearity is being investigated. The base of the logarithm arises from the NMIA multi-aperture non-linearity testing system, which has an area ratio of 5.6. In practice the non-linearity of the photometer is very small so no correction is made and the associated uncertainty component is set equal to the measurement limit of the NMIA linearity measurement system.

- Drift in Reference Calibration (Type B)
  Due to the time elapsed from the most recent calibration of the photometric standard lamps to their use when calibrating the photometer immediately prior to making the illuminance measurement on the travelling standard lamps.

$$u(E_v) = 0.000215 \times t$$

  where *t* is the elapsed time in years. The drift rate value is based on more than 30 years of calibration of the photometric reference lamps. In practice, the drift rate is small so no correction is made and the drift is included as an uncertainty component.

- Reference Instrument Resolution (Type B)
  Refers to the resolution of instrumentation utilised for photometer signal current measurement.

- Baffle Edge Reflection/Diffraction Loss (Type B)
  Refers to the contribution to the radiation incident on the detector of light that is reflected at grazing incidence off the inside edge of any baffles in the optical path between the source and the detector. Depending on the source/baffle/detector geometry, ray paths from source to detector that follow such a geometry make spurious contributions to the signal since they would leave the system if the reflection did not occur.
- Consideration of the geometry leads to a model for the contributions to the uncertainty:

$$u(E_v) = G_1 G_2 G_3 G_4 G_5$$

  where $G_1$ is a geometric factor dependent on the angular distribution of the source, as observed from the baffle aperture edges, for a particular aperture position between the source and the photometer. $G_2$ is a geometric factor dependent on the geometry of the cross-sectional profile of baffle aperture edge. $G_3$ is a geometric factor related to the size of the aperture (where larger aperture, depending on source and detector geometries, tends to have less grazing incidence reflection). $G_4$ is the fraction of the baffle aperture edge which is tangential to the measurement axis (on the basis that at grazing incidence angles, reflections from baffle edges tend to be specular in nature) and $G_5$ is a geometric factor dependent of the size and spatial distribution of the responsivity of the detector system. The NMIA baffle aperture design attempts to reduce the value of $G_4$ as far as possible.

  Although the individual factors in the model have not been characterised separately, the estimates of the value given in Table 1 are based on empirical observations of the influence on measured illuminance values of a range of different aperture shapes and positions. During these observations, an uncertainty contribution of 0.08% was found for the worst-case design, with the contribution from the star-shaped apertures actually used being approximately 0.01%. These measurements were supported by visual observations. with no reflection off the inside edges of the apertures being visible at the detector position, in contrast to the readily visible reflection from the inside edge of circular apertures.

- Test Lamp Orientation (Type A)
  Already included in transfer noise uncertainty
- Temperature Effects (Type B)
  Refers to effects on lamp temperature and voltage and current characteristics due to differences in air flow when the lamp was operated inside a housing during the measurements of normalised spectral irradiance and without a housing during illuminance measurements. The effect is not characterised well enough to include a correction but an uncertainty contribution is included in the budget. The size of the contribution was estimated from observations of differences in illuminance measurements with and without the housing.
- Area Correction
  Refers to possible differences caused by irradiance non-uniformity of the travelling standard lamps combining with differences between the sensitive area of the photometer (i.e. a precision aperture) and the measurement area for the comparison.

  However, since the target area is undefined in the protocol, measurements were performed with the photometer aperture with which the reference photometer was calibrated. It was not possible to estimate a suitable value for this component to include in the budget. It would be preferable if future comparison protocols for spectral irradiance would specify the target area.

The components identified as "Reference Separation" and "DUT Separation" are correlated since they are based on the same bench scale and stick micrometer. However, both components are small (particularly the "Reference Separation" component) and the effect of any correlations is to reduce the combined contribution even further. For this reason, those correlations have not been included in the uncertainty calculations.

#### *5.8.4.2. Normalised spectral irradiance:*

- Pyrometer Calibration (Type A and B)
  Refers to the uncertainty in the calibration of the linear pyrometer used to measure the temperature of the blackbody cavity,

  $$u(T) \approx 2 \text{ K}$$

  From reports by the NMIA Temperature Project, referenced RN161736 and RN181313, on the calibration of KE-Technologie Linearpyrometer LP5 for measurement of the reference blackbody temperature.

  The uncertainty values in Tables 2 and 4 below are estimated by varying the temperature used to calculate the reference blackbody spectrum and determining the resultant change in the normalised spectral irradiance calculated from the measurement results.
- Blackbody Uniformity (Type B)
  Refers to the difference between different geometries of detector used to monitor the temperature of the reference blackbody. The LP5 reference pyrometer responds to a limited field size whereas the in-situ filter radiometer temperature monitor responds to the full blackbody distribution incident on the irradiance target area.

  $$u(T) \approx 3.5 \text{ K}$$
- Transfer Noise (Type A)
  The standard deviation of the transfer is evaluated at each wavelength based on the detector signal current noise for the reference blackbody and the source under test and the

detector zero current noise for the reference blackbody and the source. However, that effect was completely dominated by drift of the blackbody during runs, particularly during round 2 where the stabilisation system could not be used as described above. The Type A determination is based on multiple repeated measurements of different spectral regions.

- Lamp Current (Type B)
  The standard uncertainty in setting the lamp current is 0.0001 of the value.

  The NMIA correction for lamp current results in an uncertainty equation

$$\Delta E_\lambda(\lambda) = \Delta I \times 7.5 \times \left({}^{DT}/_{3150}\right) \times \left({}^{400}/_{\lambda}\right)$$

  where:

| Symbol | Definition |
|---|---|
| $\Delta E_\lambda(\lambda)$ | Fractional offset of spectral irradiance at wavelength λ |
| $\Delta I$ | Fractional offset for lamp current |
| $DT$ | Calculated distribution temperature of the source in K |
| $\lambda$ | Wavelength in nanometres |

- Wavelength Precision (Type B)

  Up to 400 nm: Δλ = 0.2 nm
  Up to 700 nm: Δλ = 0.4 nm
  Up to 2500 nm: Δλ = 0.8nm

$$u(\mathrm{E}_\lambda) = u(\lambda) \times \frac{\delta \mathrm{E}_\lambda}{\delta \lambda}$$

- Housing Thermal Effects (Type B)
  Refers to the difference in convection state between the housing used at NMIA and using the lamp without a housing.

$$u(T) \approx 1 \text{ K}$$

  The housing state was not specified in the protocol however using the lamp in free space with unforced air cooling seems reasonable.

- Housing Spectral Selectivity (Type B)
  Refers to reflection by the lamp housing/surrounds from the lamp back to the lamp envelope, introducing a spectral selectivity based on the reflectance of the housing/surrounds.

$$u(E_\lambda) = G \times R_{\Omega\lambda}$$

  This has been evaluated at NMIA based on a radiance propagation calculation with a spectrally flat diffuse reflector modelling the housing reflectance ($R_{\Omega\lambda}$). For cylindrical geometry, $G$ is assessed as approximately 0.000255 based on the lamp envelope reflecting approximately 0.08 of the incident reflected irradiance.

- Lamp Spectral Stabilisation (Type B)
  Allows for lamp settling between the minimum warm-up time of 20 minutes and the time for the lamp to reach thermal equilibrium at approximately 43 minutes after activation.

$$u(T) \approx 0.3 \text{ K}$$

- Air Refractive Index (Type B)
  Refers to the effect of refractive index on the reference blackbody spectrum calculated using the Planck equation.

  For simplicity, the calculations of the reference blackbody spectrum used a fixed refractive index value of $n_{air}$ = 1.00029, which is the refractive index of air at approximately 300 nm. The uncertainty estimate is based on a calculation with the Planck equation where the dispersion of air [30] was included. This is expected to encompass any differences to the actual refractive index of air during the measurements.

- Blackbody Emissivity
  Because the calculated blackbody spectrum is only used to determine the normalised spectral irradiance, the emissivity only affects the final result indirectly. As described above, the scaling factor is determined from photometric measurements and is therefore unaffected by imperfect emissivity.

  However, an emissivity that is less than 1.0 will affect the temperature measurement by the linear pyrometer, which then distorts the calculated blackbody spectrum. To determine the uncertainty component related to this effect, an emissivity value of 0.995 has been assumed and the effect on the measured temperature has been calculated to be 1.6 K (at a temperature of 2660 K). This value has been used to calculate the corresponding component at each comparison wavelength, and these values are included in Tables 5.8.2 and 5.8.3.

Table 5.8.1. Photometric Uncertainty Components used for converting normalised spectral data to absolute spectral data

| **Source of Uncertainty** | **Standard Uncertainty $u_i$ (%)** | | **Uncertainty Type** |
|---|---|---|---|
| | **Round 1** | **Round 2** | |
| Base Illuminance Responsivity | 0.100 | 0.100 | Systematic |
| Agreement Between Reference Photometric Lamps | 0.053 | 0.066 | Random |
| Reference Separation | 0.002 | 0.002 | Systematic |
| Reference Current | 0.010 | 0.010 | Systematic |
| Transfer to DUT | 0.068 | 0.089 | Random |
| DUT Separation | 0.012 | 0.012 | Systematic |
| DUT Current Setting | 0.010 | 0.010 | Systematic |
| $V(\lambda)$ Spectral Mismatch Correction | 0.007 | 0.007 | Systematic |
| Photometer Non-linearity | 0.031 | 0.031 | Systematic |
| Drift in Reference Calibration | 0.045 | 0.064 | Systematic |
| Reference Instrument Resolution | 0.003 | 0.003 | Systematic |
| Baffle Edge Reflection/Diffraction Loss | 0.010 | 0.010 | Systematic |
| Test Lamp Orientation | 0.000 | 0.000 | Systematic |
| Stray Light | 0.000 | 0.000 | Systematic |
| Temperature Effects | 0.010 | 0.010 | Systematic |
| Area Correction | 0.000 | 0.000 | Systematic |

Table 5.8.2. Round 1 Normalised Spectral Irradiance Standard Uncertainties of NMIA measurements, in %

| **Uncertainty Type** | **Systematic** | **Systematic** | **Random** | **Systematic** | **Systematic** | **Systematic** | **Systematic** | **Systematic** | **Systematic** | **Systematic** |
|---|---|---|---|---|---|---|---|---|---|---|
| **Wavelength (nm)** | **Pyrometer Calibration** | **Blackbody Uniformity** | **Transfer Noise** | **Lamp Current** | **Wavelength Precision** | **Housing Thermal Effects** | **Housing Spectral Selectivity** | **Lamp Spectral Stabilisation** | **Air Refractive Index** | **Blackbody Emissivity** |
| 250 | 0.7712 | 1.5694 | 1.9105 | 0.1175 | 0.0183 | 0.3329 | 0.0006 | 0.1796 | 0.0320 | 1.2089 |
| 260 | 0.7170 | 1.4587 | 1.1906 | 0.1129 | 0.1548 | 0.3096 | 0.0005 | 0.1726 | 0.0263 | 1.1538 |
| 270 | 0.6669 | 1.3564 | 1.0888 | 0.1088 | 0.1409 | 0.2880 | 0.0004 | 0.1662 | 0.0216 | 1.1025 |
| 280 | 0.6204 | 1.2615 | 0.3965 | 0.1049 | 0.1413 | 0.2679 | 0.0004 | 0.1603 | 0.0177 | 1.0545 |
| 290 | 0.5771 | 1.1732 | 0.4048 | 0.1013 | 0.1514 | 0.2492 | 0.0004 | 0.1548 | 0.0146 | 1.0095 |
| 300 | 0.5367 | 1.0908 | 0.1051 | 0.0979 | 0.1436 | 0.2318 | 0.0003 | 0.1496 | 0.0120 | 0.9672 |
| 320 | 0.4635 | 0.9417 | 0.1300 | 0.0918 | 0.1292 | 0.2003 | 0.0002 | 0.1403 | 0.0081 | 0.8894 |
| 340 | 0.3990 | 0.8104 | 0.0972 | 0.0864 | 0.1155 | 0.1724 | 0.0003 | 0.1320 | 0.0053 | 0.8194 |
| 360 | 0.3417 | 0.6937 | 0.1206 | 0.0816 | 0.1063 | 0.1476 | 0.0002 | 0.1247 | 0.0034 | 0.7558 |
| 380 | 0.2904 | 0.5895 | 0.1095 | 0.0773 | 0.0951 | 0.1255 | 0.0001 | 0.1181 | 0.0021 | 0.6976 |
| 400 | 0.2443 | 0.4958 | 0.0375 | 0.0734 | 0.0988 | 0.1056 | 0.0001 | 0.1122 | 0.0012 | 0.6437 |
| 450 | 0.1470 | 0.2982 | 0.0062 | 0.0653 | 0.1399 | 0.0636 | 0.0000 | 0.0997 | 0.0000 | 0.5236 |
| 500 | 0.0693 | 0.1405 | 0.0263 | 0.0587 | 0.1151 | 0.0299 | 0.0000 | 0.0897 | 0.0002 | 0.4171 |
| 555 | 0.0000 | 0.0000 | 0.0003 | 0.0529 | 0.0940 | 0.0000 | 0.0000 | 0.0809 | 0.0000 | 0.3060 |
| 600 | 0.0472 | 0.0956 | 0.0264 | 0.0489 | 0.0824 | 0.0204 | 0.0000 | 0.0748 | 0.0004 | 0.2091 |
| 700 | 0.1302 | 0.2637 | 0.0426 | 0.0420 | 0.0616 | 0.0562 | 0.0000 | 0.0642 | 0.0014 | 0.1861 |
| 800 | 0.1922 | 0.3892 | 0.0272 | 0.0367 | 0.1291 | 0.0829 | 0.0000 | 0.0562 | 0.0024 | 0.2921 |
| 900 | 0.2402 | 0.4862 | 0.0205 | 0.0326 | 0.0802 | 0.1035 | 0.0000 | 0.0501 | 0.0033 | 0.3463 |
| 1000 | 0.2783 | 0.5633 | 0.0126 | 0.0294 | 0.0568 | 0.1198 | 0.0000 | 0.0453 | 0.0041 | 0.3801 |
| 1100 | 0.3092 | 0.6258 | 0.0343 | 0.0267 | 0.0552 | 0.1330 | 0.0000 | 0.0414 | 0.0047 | 0.4032 |
| 1300 | 0.3560 | 0.7203 | 0.0328 | 0.0226 | 0.0468 | 0.1528 | 0.0000 | 0.0355 | 0.0058 | 0.4322 |
| 1500 | 0.3895 | 0.7879 | 0.0531 | 0.0196 | 0.0367 | 0.1669 | 0.0000 | 0.0313 | 0.0066 | 0.4492 |
| 1700 | 0.4144 | 0.8382 | 0.1632 | 0.0173 | 0.0309 | 0.1773 | 0.0001 | 0.0282 | 0.0073 | 0.4600 |
| 2000 | 0.4415 | 0.8928 | 0.2268 | 0.0147 | 0.0202 | 0.1886 | 0.0001 | 0.0248 | 0.0080 | 0.4702 |
| 2200 | 0.4550 | 0.9201 | 0.2462 | 0.0133 | 0.0118 | 0.1942 | 0.0002 | 0.0232 | 0.0083 | 0.4747 |
| 2300 | 0.4607 | 0.9317 | 0.2195 | 0.0128 | 0.0080 | 0.1966 | 0.0002 | 0.0225 | 0.0085 | 0.4765 |
| 2400 | 0.4659 | 0.9422 | 0.1650 | 0.0122 | 0.0066 | 0.1988 | 0.0002 | 0.0218 | 0.0086 | 0.4781 |
| 2500 | 0.4707 | 0.9517 | 0.5133 | 0.0117 | 0.0061 | 0.2008 | 0.0002 | 0.0212 | 0.0087 | 0.4794 |

Table 5.8.3. Round 2 Normalised Spectral Irradiance Standard Uncertainties of NMIA measurements, in %

| Uncertainty Type | Systematic | Systematic | Random | Systematic | Systematic | Systematic | Systematic | Systematic | Systematic | Systematic |
|---|---|---|---|---|---|---|---|---|---|---|
| Wavelength (nm) | Pyrometer Calibration | Blackbody Uniformity | Transfer Noise | Lamp Current | Wavelength Precision | Housing Thermal Effects | Housing Spectral Selectivity | Lamp Spectral Stabilisation | Air Refractive Index | Blackbody Emissivity |
| 250 | 0.7712 | 1.5694 | 9.1661 | 0.1175 | 0.0183 | 0.3329 | 0.0006 | 0.1796 | 0.0320 | 1.2089 |
| 260 | 0.7170 | 1.4587 | 6.1510 | 0.1130 | 0.1548 | 0.3096 | 0.0005 | 0.1727 | 0.0263 | 1.1538 |
| 270 | 0.6669 | 1.3564 | 3.5183 | 0.1088 | 0.1409 | 0.2880 | 0.0005 | 0.1663 | 0.0216 | 1.1025 |
| 280 | 0.6204 | 1.2615 | 2.1125 | 0.1049 | 0.1413 | 0.2679 | 0.0004 | 0.1603 | 0.0178 | 1.0546 |
| 290 | 0.5771 | 1.1732 | 7.1926 | 0.1013 | 0.1514 | 0.2493 | 0.0004 | 0.1548 | 0.0146 | 1.0095 |
| 300 | 0.5367 | 1.0908 | 2.4076 | 0.0979 | 0.1436 | 0.2318 | 0.0003 | 0.1496 | 0.0120 | 0.9672 |
| 320 | 0.4635 | 0.9417 | 1.1830 | 0.0918 | 0.1292 | 0.2003 | 0.0003 | 0.1403 | 0.0081 | 0.8894 |
| 340 | 0.3990 | 0.8104 | 0.4809 | 0.0864 | 0.1155 | 0.1724 | 0.0003 | 0.1320 | 0.0053 | 0.8194 |
| 360 | 0.3417 | 0.6937 | 0.2244 | 0.0816 | 0.1063 | 0.1477 | 0.0002 | 0.1247 | 0.0034 | 0.7558 |
| 380 | 0.2904 | 0.5895 | 0.3795 | 0.0773 | 0.0951 | 0.1255 | 0.0001 | 0.1181 | 0.0021 | 0.6976 |
| 400 | 0.2443 | 0.4958 | 0.3141 | 0.0734 | 0.0988 | 0.1056 | 0.0001 | 0.1122 | 0.0012 | 0.6437 |
| 450 | 0.1470 | 0.2982 | 1.3668 | 0.0653 | 0.1399 | 0.0636 | 0.0001 | 0.0997 | 0.0000 | 0.5236 |
| 500 | 0.0693 | 0.1405 | 0.4919 | 0.0587 | 0.1151 | 0.0299 | 0.0000 | 0.0898 | 0.0002 | 0.4171 |
| 555 | 0.0000 | 0.0000 | 0.4120 | 0.0529 | 0.0941 | 0.0000 | 0.0000 | 0.0809 | 0.0000 | 0.3060 |
| 600 | 0.0472 | 0.0956 | 0.6914 | 0.0489 | 0.0824 | 0.0204 | 0.0000 | 0.0748 | 0.0004 | 0.2091 |
| 700 | 0.1302 | 0.2637 | 0.3927 | 0.0420 | 0.0616 | 0.0562 | 0.0000 | 0.0642 | 0.0014 | 0.1861 |
| 800 | 0.1922 | 0.3892 | 0.1645 | 0.0367 | 0.1292 | 0.0829 | 0.0000 | 0.0562 | 0.0024 | 0.2921 |
| 900 | 0.2402 | 0.4863 | 0.1992 | 0.0326 | 0.0802 | 0.1035 | 0.0000 | 0.0501 | 0.0033 | 0.3463 |
| 1000 | 0.2783 | 0.5633 | 0.2497 | 0.0294 | 0.0568 | 0.1198 | 0.0000 | 0.0453 | 0.0041 | 0.3801 |
| 1100 | 0.3092 | 0.6258 | 0.1690 | 0.0267 | 0.0552 | 0.1330 | 0.0000 | 0.0414 | 0.0047 | 0.4032 |
| 1300 | 0.3560 | 0.7203 | 0.1674 | 0.0226 | 0.0468 | 0.1528 | 0.0000 | 0.0355 | 0.0058 | 0.4322 |
| 1500 | 0.3895 | 0.7879 | 0.2160 | 0.0196 | 0.0367 | 0.1669 | 0.0000 | 0.0313 | 0.0066 | 0.4492 |
| 1700 | 0.4144 | 0.8382 | 0.1844 | 0.0173 | 0.0309 | 0.1773 | 0.0001 | 0.0282 | 0.0073 | 0.4600 |
| 2000 | 0.4415 | 0.8928 | 0.1987 | 0.0147 | 0.0202 | 0.1886 | 0.0001 | 0.0248 | 0.0080 | 0.4702 |
| 2200 | 0.4550 | 0.9201 | 0.2582 | 0.0134 | 0.0118 | 0.1942 | 0.0001 | 0.0232 | 0.0083 | 0.4747 |
| 2300 | 0.4607 | 0.9317 | 0.2398 | 0.0128 | 0.0080 | 0.1966 | 0.0001 | 0.0225 | 0.0085 | 0.4765 |
| 2400 | 0.4660 | 0.9422 | 0.1877 | 0.0122 | 0.0066 | 0.1988 | 0.0001 | 0.0218 | 0.0086 | 0.4781 |
| 2500 | 0.4707 | 0.9517 | 0.3316 | 0.0118 | 0.0061 | 0.2008 | 0.0001 | 0.0212 | 0.0087 | 0.4794 |

### 5.8.5. NMIA reported uncertainties for comparison traveling standard lamps

Table 5.8.4. Spectral Irradiance standard uncertainties (k=1) of the lamp **BN-9101-657**

| Wavelength, nm | Round 1 | | | Round 2 | | |
|---|---|---|---|---|---|---|
| | Uncertainties associated with, % | | Combined uncertainty, % | Uncertainties associated with, % | | Combined uncertainty, % |
| | Uncorrelated effects | Correlated effects | | Uncorrelated effects | Correlated effects | |
| 250 | 1.91 | 2.17 | 2.89 | 9.17 | 2.17 | 9.42 |
| 260 | 1.19 | 2.04 | 2.36 | 6.15 | 2.04 | 6.48 |
| 270 | 1.09 | 1.91 | 2.20 | 3.52 | 1.91 | 4.01 |
| 280 | 0.41 | 1.80 | 1.84 | 2.12 | 1.80 | 2.78 |
| 290 | 0.41 | 1.69 | 1.74 | 7.19 | 1.69 | 7.39 |
| 300 | 0.14 | 1.59 | 1.60 | 2.41 | 1.59 | 2.89 |
| 320 | 0.16 | 1.41 | 1.42 | 1.19 | 1.41 | 1.85 |
| 340 | 0.13 | 1.26 | 1.26 | 0.49 | 1.26 | 1.35 |
| 360 | 0.15 | 1.12 | 1.13 | 0.25 | 1.12 | 1.14 |
| 380 | 0.14 | 0.99 | 1.00 | 0.40 | 0.99 | 1.07 |
| 400 | 0.09 | 0.88 | 0.89 | 0.33 | 0.88 | 0.95 |
| 450 | 0.09 | 0.67 | 0.67 | 1.37 | 0.67 | 1.53 |
| 500 | 0.09 | 0.50 | 0.50 | 0.50 | 0.50 | 0.71 |
| 555 | 0.09 | 0.37 | 0.38 | 0.43 | 0.37 | 0.56 |
| 600 | 0.09 | 0.30 | 0.32 | 0.70 | 0.31 | 0.76 |
| 700 | 0.10 | 0.39 | 0.41 | 0.41 | 0.40 | 0.57 |
| 800 | 0.09 | 0.57 | 0.58 | 0.20 | 0.57 | 0.60 |
| 900 | 0.09 | 0.68 | 0.68 | 0.23 | 0.68 | 0.71 |
| 1000 | 0.09 | 0.76 | 0.77 | 0.27 | 0.76 | 0.81 |
| 1100 | 0.09 | 0.83 | 0.84 | 0.20 | 0.83 | 0.86 |
| 1300 | 0.09 | 0.94 | 0.94 | 0.20 | 0.94 | 0.96 |
| 1500 | 0.10 | 1.01 | 1.02 | 0.24 | 1.01 | 1.04 |
| 1700 | 0.18 | 1.07 | 1.08 | 0.22 | 1.07 | 1.09 |
| 2000 | 0.24 | 1.13 | 1.15 | 0.23 | 1.13 | 1.15 |
| 2200 | 0.26 | 1.16 | 1.19 | 0.28 | 1.16 | 1.19 |
| 2300 | 0.24 | 1.17 | 1.19 | 0.26 | 1.17 | 1.20 |
| 2400 | 0.19 | 1.18 | 1.20 | 0.22 | 1.18 | 1.20 |
| 2500 | 0.52 | 1.19 | 1.30 | 0.35 | 1.19 | 1.24 |

Table 5.8.5. Spectral Irradiance standard uncertainties (k=1) of the lamp **BN-9101-658**

| Wavelength, nm | Round 1 | | | Round 2 | | |
|---|---|---|---|---|---|---|
| | Uncertainties associated with, % | | Combined uncertainty, % | Uncertainties associated with, % | | Combined uncertainty, % |
| | Uncorrelated effects | Correlated effects | | Uncorrelated effects | Correlated effects | |
| 250 | 1.63 | 2.17 | 2.71 | 9.32 | 2.17 | 9.57 |
| 260 | 1.30 | 2.04 | 2.42 | 5.13 | 2.04 | 5.52 |
| 270 | 0.42 | 1.91 | 1.96 | 2.49 | 1.91 | 3.14 |
| 280 | 0.38 | 1.80 | 1.84 | 1.55 | 1.80 | 2.37 |
| 290 | 0.48 | 1.69 | 1.76 | 1.33 | 1.69 | 2.15 |
| 300 | 0.57 | 1.59 | 1.69 | 1.27 | 1.59 | 2.04 |
| 320 | 0.32 | 1.41 | 1.45 | 1.31 | 1.41 | 1.93 |
| 340 | 0.32 | 1.26 | 1.30 | 0.91 | 1.26 | 1.55 |
| 360 | 0.27 | 1.12 | 1.15 | 0.56 | 1.12 | 1.25 |
| 380 | 0.27 | 0.99 | 1.03 | 0.93 | 0.99 | 1.36 |
| 400 | 0.25 | 0.88 | 0.92 | 0.42 | 0.88 | 0.98 |
| 450 | 0.24 | 0.67 | 0.71 | 0.28 | 0.67 | 0.73 |
| 500 | 0.25 | 0.50 | 0.55 | 0.23 | 0.50 | 0.55 |
| 555 | 0.24 | 0.37 | 0.44 | 0.15 | 0.37 | 0.40 |
| 600 | 0.25 | 0.30 | 0.39 | 0.17 | 0.31 | 0.35 |
| 700 | 0.24 | 0.39 | 0.46 | 0.22 | 0.40 | 0.45 |
| 800 | 0.24 | 0.57 | 0.62 | 0.18 | 0.57 | 0.60 |
| 900 | 0.24 | 0.68 | 0.72 | 0.18 | 0.68 | 0.70 |
| 1000 | 0.25 | 0.76 | 0.80 | 0.21 | 0.76 | 0.79 |
| 1100 | 0.25 | 0.83 | 0.87 | 0.27 | 0.83 | 0.88 |
| 1300 | 0.27 | 0.94 | 0.98 | 0.20 | 0.94 | 0.96 |
| 1500 | 0.27 | 1.01 | 1.05 | 0.23 | 1.01 | 1.04 |
| 1700 | 0.35 | 1.07 | 1.12 | 0.28 | 1.07 | 1.11 |
| 2000 | 0.92 | 1.13 | 1.46 | 0.40 | 1.13 | 1.20 |
| 2200 | 0.69 | 1.16 | 1.35 | 0.49 | 1.16 | 1.26 |
| 2300 | 0.36 | 1.17 | 1.22 | 0.51 | 1.17 | 1.28 |
| 2400 | 0.98 | 1.18 | 1.54 | 0.44 | 1.18 | 1.26 |
| 2500 | 0.32 | 1.19 | 1.23 | 0.41 | 1.19 | 1.26 |

Table 5.8.6. Spectral Irradiance standard uncertainties (k=1) of the lamp **BN-9101-659**

| Wavelength, nm | Round 1 | | | Round 2 | | |
|---|---|---|---|---|---|---|
| | Uncertainties associated with, % | | Combined uncertainty, % | Uncertainties associated with, % | | Combined uncertainty, % |
| | Uncorrelated effects | Correlated effects | | Uncorrelated effects | Correlated effects | |
| 250 | 2.00 | 2.17 | 2.95 | 21.23 | 1.80 | 21.30 |
| 260 | 1.15 | 2.04 | 2.34 | 11.85 | 1.68 | 11.97 |
| 270 | 0.68 | 1.91 | 2.03 | 6.30 | 1.57 | 6.50 |
| 280 | 0.80 | 1.80 | 1.97 | 3.66 | 1.46 | 3.94 |
| 290 | 0.75 | 1.69 | 1.85 | 2.04 | 1.36 | 2.45 |
| 300 | 0.52 | 1.59 | 1.68 | 1.64 | 1.27 | 2.07 |
| 320 | 0.55 | 1.41 | 1.52 | 1.17 | 1.10 | 1.60 |
| 340 | 0.43 | 1.26 | 1.33 | 0.71 | 0.95 | 1.19 |
| 360 | 0.39 | 1.12 | 1.18 | 0.99 | 0.82 | 1.29 |
| 380 | 0.29 | 0.99 | 1.03 | 0.72 | 0.71 | 1.01 |
| 400 | 0.29 | 0.88 | 0.93 | 0.49 | 0.61 | 0.78 |
| 450 | 0.18 | 0.67 | 0.69 | 0.37 | 0.41 | 0.56 |
| 500 | 0.15 | 0.50 | 0.52 | 0.20 | 0.27 | 0.34 |
| 555 | 0.11 | 0.37 | 0.38 | 0.20 | 0.20 | 0.29 |
| 600 | 0.13 | 0.30 | 0.33 | 0.10 | 0.22 | 0.24 |
| 700 | 0.17 | 0.39 | 0.43 | 0.59 | 0.35 | 0.69 |
| 800 | 0.18 | 0.57 | 0.60 | 0.20 | 0.49 | 0.53 |
| 900 | 0.24 | 0.68 | 0.72 | 0.21 | 0.58 | 0.62 |
| 1000 | 0.27 | 0.76 | 0.81 | 0.22 | 0.66 | 0.70 |
| 1100 | 0.31 | 0.83 | 0.89 | 0.25 | 0.73 | 0.77 |
| 1300 | 0.14 | 0.94 | 0.95 | 0.25 | 0.83 | 0.87 |
| 1500 | 0.25 | 1.01 | 1.04 | 0.24 | 0.91 | 0.94 |
| 1700 | 0.31 | 1.07 | 1.11 | 0.25 | 0.97 | 1.00 |
| 2000 | 1.16 | 1.13 | 1.62 | 0.53 | 1.03 | 1.15 |
| 2200 | 0.23 | 1.16 | 1.18 | 0.53 | 1.06 | 1.18 |
| 2300 | 0.85 | 1.17 | 1.44 | 0.53 | 1.07 | 1.19 |
| 2400 | 0.83 | 1.18 | 1.45 | 0.53 | 1.08 | 1.20 |
| 2500 | 0.48 | 1.19 | 1.29 | 0.53 | 1.09 | 1.21 |

### 5.8.6. References to section 5.8

[30] *Appl. Optics* 35, 1566 – 1573 (1996)

## 5.9. NMIJ, Japan

### 5.9.1. Scale realization

The NMIJ spectral irradiance scale was realized by using a high-temperature blackbody (HTBB) with a temperature stabilization system. A silica glass window was mounted on the exit port of the HTBB and the radiant flux passing through the window was used for the measurement. The stabilized temperature of HTBB, determined by a radiance comparison between the HTBB and a copper fixed-point blackbody (Cu-BB), was approximately 2900 K. The HTBB radiance scale was transferred to the spectral irradiance scale by using two precision apertures whose opening diameters were calibrated. One aperture was put in front of the exit port of the HTBB, and another one before the entrance opening of our measurement facility (See 5.9.2). The nominal diameters of these apertures are18 mm and 12 mm, respectively. The distance between two apertures is approximately 1.1 m. With the aperture arrangement shown above, the HTBB can be regarded as an almost uniform spectral irradiance source on the diffuser plate of the measurement facility, which is the reference plane of the spectral irradiance to be calibrated.

### 5.9.2. Measurement Facility and Measurement Procedure

Figure 5.9.1 shows our measurement facility and the measurement procedure.

The measurement facility consists of an entrance optics, a monochromator and a detector unit, Radiant flux passing from the HTBB and the lamps described below passed through the entrance optics and the monochromator is measured by the detector unit. A diffuser plate and a focusing optics are introduced as the entrance optics to the monochromator. The focusing optics installed between the diffuser plate and the monochromator forms the image of the diffuser plate on the entrance slit of the monochromator. The monochromator is a Czerny-Turner subtractive double-grating-type monochromator. The detector unit, that consists of a focusing optics, a photomultiplier tube (PMT), a Si-photodiode (Si-PD) and two InGaAs photodiodes (InGaAs-PD1 and InGaAs-PD2) with different spectral responsivity, is mounted at the exit slit of the monochromator. The focusing optics has the function to select one of the detectors and form the image of the exit slit of the monochromator on its sensing area. Each of the detector is connected to its own current-to-voltage converter. The photocurrent from each detector is detected as the voltage signal by a 8.5-digit digital multimeter.

In this comparison, the following detector arrangement was applied depending on the wavelength range.

1) PMT: from 250 nm to 380 nm. 2) Si-PD: from 380 nm to 1100 nm, 3) InGaAs-PD1: from 1100 nm to 2000 nm, and 4) InGaAs-PD2: from 2000 nm to 2500 nm

The direction of the incident radiant flux of the entrance optics can be selected as shown in Figure 5.9.1. The radiant flux A and B are introduced to the monochromator alternately by changing the angle of the diffuser plate. The spectral irradiances generated by the radiant flux A and B can be compared by the comparison of the signal from the detector unit.

As shown in 5.9.1, the spectral irradiance of the HTBB was determined with a calibrated thermodynamic temperature and a geometric factor derived from two apertures, and the HTBB was used as the light source realizing spectral irradiance scale. The measurement facility tentatively transferred the spectral irradiance scale from the HTBB to the working standard lamps (500 W type tungsten halogen lamp, see 5.9.4 for details) that were places at the opposite side of the HTBB across the diffuser plate, by the comparison of the detector signal when the radiation from the HTBB and the working standard lamps were measured. Then the measurement facility transferred the

tentative spectral irradiance scale from the working standard lamps to the test lamps in the same manner. In this comparison, three traveling standard lamps (BN-9101-695, BN-9101-696 and BN-9101-697) were placed at the position of the test lamps. In this calibration procedure, unsymmetrical effect due to the diffuser plate is cancelled out, because the HTBB and the test lamps are compared in the same direction with the same optical axes via the working standard lamps placed the opposite side across the diffuser plate.

When the spectral irradiance is compared, the wavelength is set up to the specified value and the direction of the diffuser plate alternately switched over to introduce the radiant flux A and the radiant flux B from each light source. Consequently, the wavelength setting error is correlated between the measurement of radiant flux A and the radiant flux B at each wavelength.

Three personal computers are equipped with the measurement facility. One is used to control the measurement facility in terms of the setting of the wavelength, optical parameters such as the selection of a grating, a detector and an order-sorting filter. The other two are used to controll two electrical feeding systems, one of which is for the test lamp and another for the working standard lamp. During the measurement of the traveling standard lamps for CCPR-K1.a, lamp current was controlled by the electrical feeding system to be 8.1 A DC according the protocol. For the working standard lamps, lamp voltage was stabilized to be 97 V DC because they become more stable when feeding constant DC voltage.

More specifically, each of the electrical feeding system consists of an electrical power supply, a precision shunt resistor and two digital multimeters. The shunt resistor and the digital multimeters were calibrated. The shunt resistor and one of the multimeters are used to measure the lamp feeding current. The other multimeter is used to measure the lamp feeding voltage. The measured lamp current or voltage of each lamp is feedbacked to the corresponding computer for stabilization.

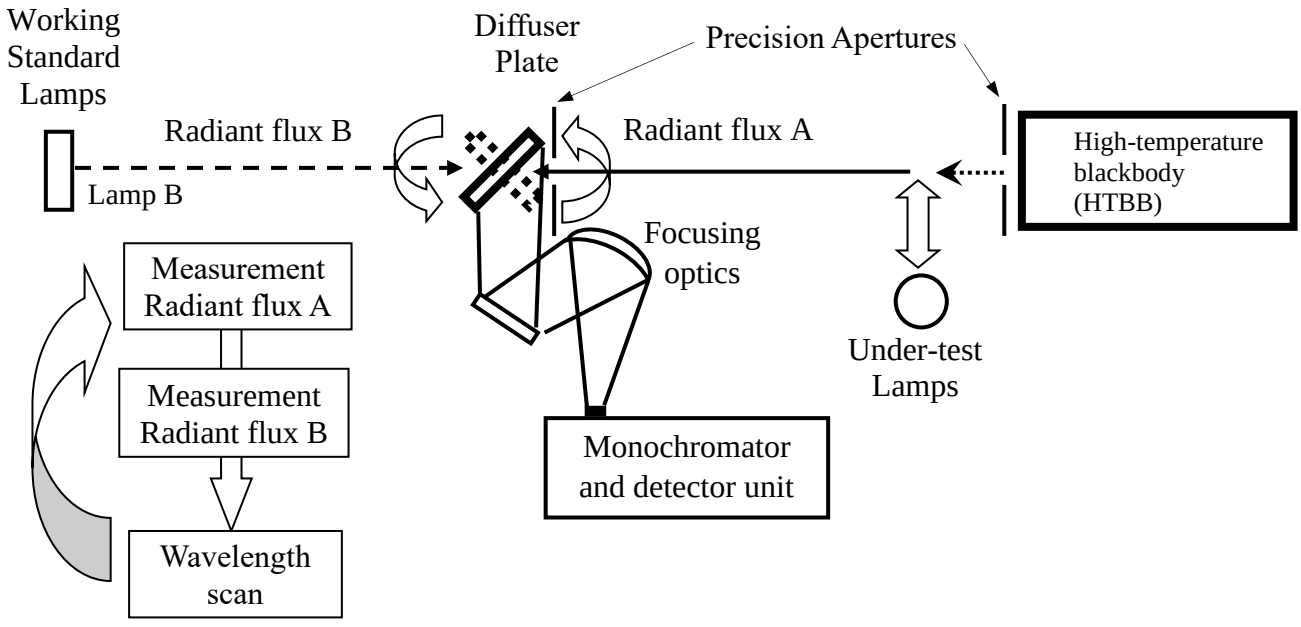


Figure 5.9.1. Measurement facility and the measurement procedure

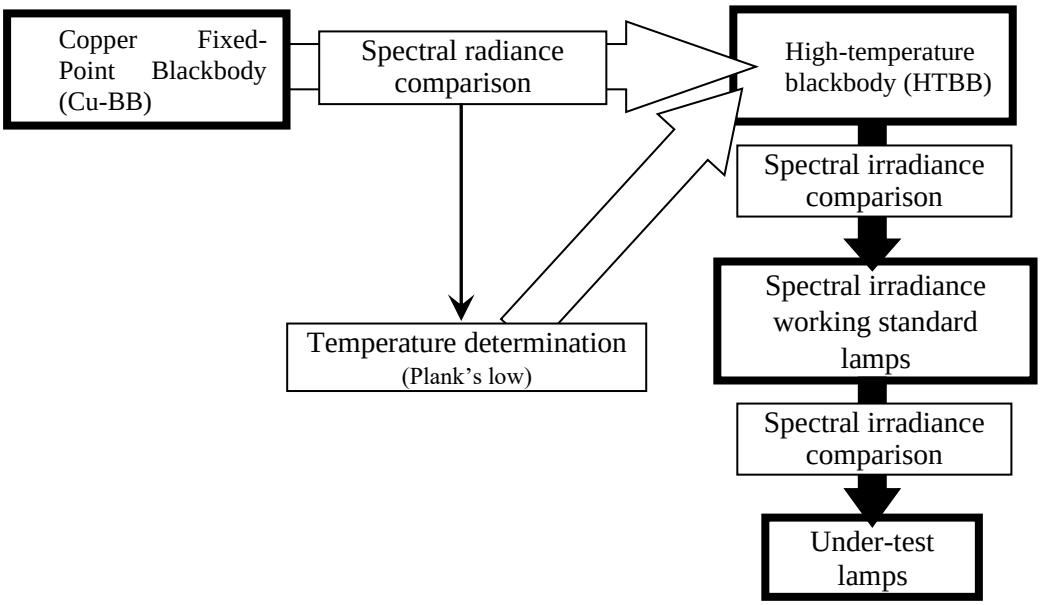


Figure 5.9.2. Diagram for the realization of the spectral irradiance scale

### 5.9.3. Laboratory Conditions

All the measurements were carried out in the darkroom. The temperature of the darkroom where the measurement facility is placed is controlled at 23 ºC ± 2 ºC and the relative humidity of the room is controlled at 50 % ±10 %.

### 5.9.4. Working standard used

ETL/NMIJ/Ushio quartz-bromine lamps, whose nominal operating voltage and nominal power consumption are 100 V and 500 W, were used as the working standard lamps in this comparison. These lamps were operated at 97 V DC with constant-voltage mode.

The scale transfer of spectral irradiance from the HTBB to the working standard lamps is just tentative because the setting on the diffuser plate might have a little asymmetry between the measurement of the radiant flux A and the radiant flux B. The unsymmetrical effect is cancelled out by re-transferring the tentative scale of the working standard lamps to the test lamps.

### 5.9.5. Uncertainty evaluation

The combined standard uncertainty of the spectral irradiance calibration is evaluated from the following uncertainty factors:

- The uncertainty of spectral radiance of HTBB caused by the temperature uncertainty was evaluated from the measurement repeatability of the spectral radiance comparison between the HTBB and the Cu-BB, the temperature uncertainty of the Cu-BB calibration, the wavelength uncertainty of the comparison, the size of source effect, the emissivity of the blackbody, and the uncertainty caused by the transmittance of the silica glass window mounted on the exit port of the HTBB. Since the wavelength range in which the spectral radiance comparison was carried

out was limited, the last uncertainty factor mentioned above was evaluated from the transmittance measurement in the limited wavelength range. The detail of the factor was composed of the repeatability of the transmittance measurement, the transmittance uniformity, and the change of transmittance before and after operation.

- The uncertainty of spectral irradiance of the HTBB caused by the silica glass window was evaluated from the repeatability of transmittance measurement, the transmittance uniformity, and the change of transmittance before and after operation. The uncertainty was determined in the full wavelength range in which the spectral irradiance comparison was carried out.
- Radiant flux passing through a circular aperture which is coaxial with a circular source having uniform radiance can be evaluated theoretically [50]. The geometric factor transferring the spectral radiance of HTBB to the spectral irradiance was determined based on the theory. The geometric factor calculated from the aperture sizes, the distance from the HTBB to the apertures and the distance from HTBB to the measurement facility (the diffuser plate). The HTBB radiance scale transferred to the spectral irradiance scale. The uncertainty of the geometric factor was evaluated from the uncertainty of aperture sizes, the uncertainty of the distance from HTBB to the apertures and the uncertainty of the distance from HTBB to the diffuser plate in the measurement facility.
- Uncertainty of the wavelength adjustment of the monochromator was based on the wavelength setting imperfection of the monochromator, determined by the comparison between reference lamp emissions with known wavelengths. As shown in the above, the wavelength setting error is correlated between the measurement of radiant flux A and radiant flux B at each wavelength. That is considered in evaluating the uncertainty induced by wavelength adjustment of the monochromator.
- For other uncertainty factors, the uncertainty induced by the input power was evaluated from the uncertainty of the electrical feeding system, that consists of the calibration uncertainty of the digital multimeters and the shunt resistors and reproducibility. The uncertainty of the distance adjustment of the lamps (500 mm) was based on the calibration uncertainty of an instrument for the distance measurement and reproducibility. The measurement repeatability of the comparison was evaluated based on type-A analysis for the comparison between radiant flux A and B.

Table 5.9.1 shows the typical uncertainty budget of our spectral irradiance calibration.

The total uncertainties of the NMIJ comparison lamps measurements are presented in Tables 5.9.2 – 5.9.4.

### 5.9.6. References to section 5.9

[50] J.W.T. Walsh, Photometry, Dover, New York, 1965

Table 5.9.1. Uncertainty budget of spectral irradiance calibration at NMIJ

Uncertainty Budget / Relative Standard Uncertainty (%) (k =1)

| Wavelength / nm | | | Source of Uncertainty | | | | | | | | | | | Relative combined standard uncertainty |
|---|---|---|---|---|---|---|---|---|---|---|---|---|---|---|
| | | | Blackbody | | | Working Standard lamp (WS) | | | | Lamp under-test (UT) | | | | |
| | | | Evaluation of Blackbody temperature | Evaluation of Blackbody Window Transmittance | Evaluation of Geometric Factors in Irradiance Transfer | Input Power | Distance adjustment | Wavelength Adjustment in Comparison between WS and Blackbody | Repeatability in Comparison between WS and Blackbody | Input Power | Distance adjustment | Wavelength Adjustment in Comparison between UT and WS | Repeatability in Comparison between UT and WS | |
| Type of Uncertainty | | | B | A | B | B | B | B | A | B | B | B | A | |
| Correlated | Fully Correlated | | | | ○ | | | | | | | | | |
| | Correlated while Round | | ○ | ○ | | ○ | ○ | ○ | ○ | | | | | |
| Un-correlated | | | | | | | | | | ○ | ○ | ○ | ○ | |
| 250 | | | 1.12% | 0.07% | 0.53% | 0.02% | 0.08% | 0.37% | 0.30% | 0.02% | 0.08% | 0.01% | 0.08% | 1.34% |
| 260 | | | 1.08% | 0.07% | 0.53% | 0.02% | 0.08% | 0.32% | 0.09% | 0.02% | 0.08% | 0.01% | 0.04% | 1.26% |
| 270 | | | 1.04% | 0.07% | 0.53% | 0.02% | 0.08% | 0.28% | 0.06% | 0.02% | 0.08% | 0.01% | 0.03% | 1.21% |
| 280 | | | 1.01% | 0.06% | 0.53% | 0.02% | 0.08% | 0.25% | 0.06% | 0.02% | 0.08% | 0.01% | 0.03% | 1.18% |
| 290 | | | 0.98% | 0.06% | 0.53% | 0.02% | 0.08% | 0.23% | 0.04% | 0.02% | 0.08% | 0.01% | 0.05% | 1.14% |
| 300 | | | 0.95% | 0.05% | 0.53% | 0.02% | 0.08% | 0.23% | 0.04% | 0.02% | 0.08% | 0.01% | 0.03% | 1.12% |
| 320 | | | 0.89% | 0.04% | 0.53% | 0.02% | 0.08% | 0.19% | 0.02% | 0.02% | 0.08% | 0.01% | 0.02% | 1.06% |
| 340 | | | 0.84% | 0.04% | 0.53% | 0.02% | 0.08% | 0.15% | 0.02% | 0.02% | 0.08% | 0.01% | 0.02% | 1.01% |
| 360 | | | 0.80% | 0.04% | 0.53% | 0.02% | 0.08% | 0.13% | 0.02% | 0.02% | 0.08% | 0.01% | 0.02% | 0.98% |
| 380 | | | 0.76% | 0.04% | 0.53% | 0.02% | 0.08% | 0.11% | 0.02% | 0.02% | 0.08% | 0.01% | 0.03% | 0.94% |
| 400 | | | 0.73% | 0.04% | 0.53% | 0.02% | 0.08% | 0.10% | 0.03% | 0.02% | 0.08% | 0.01% | 0.01% | 0.92% |
| 450 | | | 0.66% | 0.03% | 0.53% | 0.02% | 0.08% | 0.07% | 0.01% | 0.02% | 0.08% | 0.01% | 0.01% | 0.86% |
| 500 | | | 0.60% | 0.03% | 0.53% | 0.02% | 0.08% | 0.04% | 0.01% | 0.02% | 0.08% | 0.01% | 0.01% | 0.81% |
| 555 | | | 0.55% | 0.05% | 0.53% | 0.02% | 0.08% | 0.03% | 0.01% | 0.02% | 0.08% | 0.01% | 0.01% | 0.78% |
| 600 | | | 0.52% | 0.04% | 0.53% | 0.02% | 0.08% | 0.02% | 0.01% | 0.02% | 0.08% | 0.01% | 0.01% | 0.75% |
| 700 | | | 0.46% | 0.04% | 0.53% | 0.02% | 0.08% | 0.01% | 0.01% | 0.02% | 0.08% | 0.01% | 0.01% | 0.72% |
| 800 | | | 0.42% | 0.04% | 0.53% | 0.02% | 0.08% | 0.01% | 0.02% | 0.02% | 0.08% | 0.01% | 0.01% | 0.69% |
| 900 | | | 0.39% | 0.04% | 0.53% | 0.02% | 0.08% | 0.01% | 0.01% | 0.02% | 0.08% | 0.01% | 0.01% | 0.67% |
| 1000 | | | 0.37% | 0.03% | 0.53% | 0.02% | 0.08% | 0.01% | 0.01% | 0.02% | 0.08% | 0.01% | 0.01% | 0.66% |
| 1100 | | | 0.35% | 0.04% | 0.53% | 0.02% | 0.08% | 0.01% | 0.01% | 0.02% | 0.08% | 0.01% | 0.01% | 0.65% |
| 1300 | | | 0.33% | 0.04% | 0.53% | 0.02% | 0.08% | 0.01% | 0.01% | 0.02% | 0.08% | 0.01% | 0.01% | 0.64% |
| 1500 | | | 0.31% | 0.04% | 0.53% | 0.02% | 0.08% | 0.01% | 0.01% | 0.02% | 0.08% | 0.01% | 0.01% | 0.63% |
| 1700 | | | 0.30% | 0.05% | 0.53% | 0.02% | 0.08% | 0.01% | 0.01% | 0.02% | 0.08% | 0.01% | 0.01% | 0.62% |
| 2000 | | | 0.29% | 0.04% | 0.53% | 0.02% | 0.08% | 0.01% | 0.02% | 0.02% | 0.08% | 0.01% | 0.02% | 0.62% |
| 2200 | | | 0.28% | 0.04% | 0.53% | 0.02% | 0.08% | 0.01% | 0.04% | 0.02% | 0.08% | 0.01% | 0.03% | 0.61% |
| 2300 | | | 0.28% | 0.05% | 0.53% | 0.02% | 0.08% | 0.01% | 0.06% | 0.02% | 0.08% | 0.01% | 0.03% | 0.62% |
| 2400 | | | 0.28% | 0.04% | 0.53% | 0.02% | 0.08% | 0.01% | 0.13% | 0.02% | 0.08% | 0.01% | 0.08% | 0.63% |
| 2500 | | | 0.51% | 0.43% | 0.53% | 0.02% | 0.08% | 0.01% | 0.26% | 0.02% | 0.08% | 0.01% | 0.08% | 0.91% |

Table 5.9.2. Spectral Irradiance standard uncertainties (k=1) of the lamp **BN-9101-695**

| Wavelength, nm | Round 1 | | | Round 2 | | |
|---|---|---|---|---|---|---|
| | Uncertainties associated with, % | | Combined uncertainty, % | Uncertainties associated with, % | | Combined uncertainty, % |
| | Uncorrelated effects | Correlated effects | | Uncorrelated effects | Correlated effects | |
| 250 | 0.11% | 1.34% | 1.34% | 0.19% | 1.37% | 1.38% |
| 260 | 0.14% | 1.26% | 1.26% | 0.11% | 1.26% | 1.26% |
| 270 | 0.14% | 1.21% | 1.22% | 0.11% | 1.21% | 1.22% |
| 280 | 0.14% | 1.17% | 1.18% | 0.11% | 1.17% | 1.18% |
| 290 | 0.13% | 1.14% | 1.15% | 0.10% | 1.14% | 1.14% |
| 300 | 0.10% | 1.11% | 1.12% | 0.09% | 1.11% | 1.12% |
| 320 | 0.12% | 1.06% | 1.06% | 0.09% | 1.06% | 1.06% |
| 340 | 0.11% | 1.01% | 1.02% | 0.09% | 1.01% | 1.02% |
| 360 | 0.20% | 0.97% | 0.99% | 0.09% | 0.97% | 0.98% |
| 380 | 0.14% | 0.94% | 0.95% | 0.09% | 0.94% | 0.94% |
| 400 | 0.11% | 0.91% | 0.92% | 0.08% | 0.91% | 0.92% |
| 450 | 0.11% | 0.85% | 0.86% | 0.08% | 0.85% | 0.86% |
| 500 | 0.10% | 0.81% | 0.81% | 0.08% | 0.81% | 0.81% |
| 555 | 0.11% | 0.77% | 0.78% | 0.08% | 0.77% | 0.78% |
| 600 | 0.10% | 0.75% | 0.76% | 0.08% | 0.75% | 0.75% |
| 700 | 0.10% | 0.71% | 0.72% | 0.09% | 0.71% | 0.72% |
| 800 | 0.10% | 0.68% | 0.69% | 0.08% | 0.68% | 0.69% |
| 900 | 0.09% | 0.67% | 0.67% | 0.09% | 0.67% | 0.67% |
| 1000 | 0.09% | 0.65% | 0.66% | 0.08% | 0.65% | 0.66% |
| 1100 | 0.09% | 0.64% | 0.65% | 0.08% | 0.64% | 0.65% |
| 1300 | 0.10% | 0.63% | 0.64% | 0.08% | 0.63% | 0.64% |
| 1500 | 0.10% | 0.62% | 0.63% | 0.08% | 0.62% | 0.63% |
| 1700 | 0.09% | 0.62% | 0.62% | 0.08% | 0.62% | 0.62% |
| 2000 | 0.09% | 0.61% | 0.62% | 0.10% | 0.61% | 0.62% |
| 2200 | 0.10% | 0.61% | 0.62% | 0.13% | 0.61% | 0.62% |
| 2300 | 0.13% | 0.61% | 0.62% | 0.11% | 0.61% | 0.62% |
| 2400 | 0.14% | 0.62% | 0.63% | 0.23% | 0.63% | 0.68% |
| 2500 | 0.35% | 0.90% | 0.96% | 0.15% | 0.96% | 0.97% |

Table 5.9.3. Spectral Irradiance standard uncertainties (k=1) of the lamp **BN-9101-696**

| Wavelength, nm | Round 1 | | | Round 2 | | |
|---|---|---|---|---|---|---|
| | Uncertainties associated with, % | | Combined uncertainty, % | Uncertainties associated with, % | | Combined uncertainty, % |
| | Uncorrelated effects | Correlated effects | | Uncorrelated effects | Correlated effects | |
| 250 | 0.12% | 1.34% | 1.34% | 0.19% | 1.37% | 1.38% |
| 260 | 0.09% | 1.26% | 1.26% | 0.11% | 1.26% | 1.26% |
| 270 | 0.09% | 1.21% | 1.21% | 0.10% | 1.21% | 1.22% |
| 280 | 0.09% | 1.17% | 1.18% | 0.10% | 1.17% | 1.18% |
| 290 | 0.10% | 1.14% | 1.14% | 0.10% | 1.14% | 1.14% |
| 300 | 0.09% | 1.11% | 1.12% | 0.10% | 1.11% | 1.12% |
| 320 | 0.14% | 1.06% | 1.07% | 0.15% | 1.06% | 1.07% |
| 340 | 0.09% | 1.01% | 1.02% | 0.09% | 1.01% | 1.02% |
| 360 | 0.09% | 0.97% | 0.98% | 0.09% | 0.97% | 0.98% |
| 380 | 0.18% | 0.94% | 0.96% | 0.09% | 0.94% | 0.94% |
| 400 | 0.08% | 0.91% | 0.92% | 0.09% | 0.91% | 0.92% |
| 450 | 0.08% | 0.85% | 0.86% | 0.08% | 0.85% | 0.86% |
| 500 | 0.08% | 0.81% | 0.81% | 0.08% | 0.81% | 0.81% |
| 555 | 0.08% | 0.77% | 0.78% | 0.08% | 0.77% | 0.78% |
| 600 | 0.08% | 0.75% | 0.75% | 0.08% | 0.75% | 0.75% |
| 700 | 0.09% | 0.71% | 0.72% | 0.08% | 0.71% | 0.72% |
| 800 | 0.09% | 0.68% | 0.69% | 0.08% | 0.68% | 0.69% |
| 900 | 0.09% | 0.67% | 0.67% | 0.08% | 0.67% | 0.67% |
| 1000 | 0.09% | 0.65% | 0.66% | 0.08% | 0.65% | 0.66% |
| 1100 | 0.08% | 0.64% | 0.65% | 0.08% | 0.64% | 0.65% |
| 1300 | 0.09% | 0.63% | 0.64% | 0.08% | 0.63% | 0.64% |
| 1500 | 0.09% | 0.62% | 0.63% | 0.08% | 0.62% | 0.63% |
| 1700 | 0.09% | 0.62% | 0.62% | 0.08% | 0.62% | 0.62% |
| 2000 | 0.09% | 0.61% | 0.62% | 0.09% | 0.61% | 0.62% |
| 2200 | 0.09% | 0.61% | 0.62% | 0.09% | 0.61% | 0.62% |
| 2300 | 0.09% | 0.61% | 0.62% | 0.09% | 0.61% | 0.62% |
| 2400 | 0.15% | 0.62% | 0.64% | 0.12% | 0.63% | 0.65% |
| 2500 | 0.22% | 0.90% | 0.92% | 0.12% | 0.96% | 0.96% |

Table 5.9.4. Spectral Irradiance standard uncertainties (k=1) of the lamp **BN-9101-697**

| Wavelength, nm | Round 1 | | | Round 2 | | |
|---|---|---|---|---|---|---|
| | Uncertainties associated with, % | | Combined uncertainty, % | Uncertainties associated with, % | | Combined uncertainty, % |
| | Uncorrelated effects | Correlated effects | | Uncorrelated effects | Correlated effects | |
| 250 | 0.15% | 1.34% | 1.34% | 0.23% | 1.37% | 1.39% |
| 260 | 0.10% | 1.26% | 1.26% | 0.13% | 1.26% | 1.27% |
| 270 | 0.14% | 1.21% | 1.22% | 0.10% | 1.21% | 1.22% |
| 280 | 0.12% | 1.17% | 1.18% | 0.12% | 1.17% | 1.18% |
| 290 | 0.12% | 1.14% | 1.15% | 0.10% | 1.14% | 1.14% |
| 300 | 0.11% | 1.11% | 1.12% | 0.10% | 1.11% | 1.12% |
| 320 | 0.10% | 1.06% | 1.06% | 0.09% | 1.06% | 1.06% |
| 340 | 0.10% | 1.01% | 1.02% | 0.10% | 1.01% | 1.02% |
| 360 | 0.09% | 0.97% | 0.98% | 0.09% | 0.97% | 0.98% |
| 380 | 0.19% | 0.94% | 0.96% | 0.09% | 0.94% | 0.94% |
| 400 | 0.10% | 0.91% | 0.92% | 0.09% | 0.91% | 0.92% |
| 450 | 0.10% | 0.85% | 0.86% | 0.08% | 0.85% | 0.86% |
| 500 | 0.09% | 0.81% | 0.81% | 0.08% | 0.81% | 0.81% |
| 555 | 0.09% | 0.77% | 0.78% | 0.08% | 0.77% | 0.78% |
| 600 | 0.09% | 0.75% | 0.75% | 0.08% | 0.75% | 0.75% |
| 700 | 0.09% | 0.71% | 0.72% | 0.08% | 0.71% | 0.72% |
| 800 | 0.09% | 0.68% | 0.69% | 0.08% | 0.68% | 0.69% |
| 900 | 0.09% | 0.67% | 0.67% | 0.08% | 0.67% | 0.67% |
| 1000 | 0.09% | 0.65% | 0.66% | 0.08% | 0.65% | 0.66% |
| 1100 | 0.09% | 0.64% | 0.65% | 0.08% | 0.64% | 0.65% |
| 1300 | 0.09% | 0.63% | 0.64% | 0.08% | 0.63% | 0.64% |
| 1500 | 0.08% | 0.62% | 0.63% | 0.08% | 0.62% | 0.63% |
| 1700 | 0.08% | 0.62% | 0.62% | 0.08% | 0.62% | 0.62% |
| 2000 | 0.09% | 0.61% | 0.62% | 0.09% | 0.61% | 0.62% |
| 2200 | 0.09% | 0.61% | 0.61% | 0.09% | 0.61% | 0.62% |
| 2300 | 0.11% | 0.61% | 0.62% | 0.14% | 0.61% | 0.63% |
| 2400 | 0.16% | 0.62% | 0.64% | 0.17% | 0.63% | 0.66% |
| 2500 | 0.17% | 0.90% | 0.91% | 0.29% | 0.96% | 1.00% |

## 5.10. NPL, UK

This section describes the measurement facility and uncertainties used for the NPL measurements for the CCPR-K1a.2017 comparison of spectral irradiance.

### 5.10.1. Primary scale realisation

The NPL spectral irradiance scale is based on the use of a high temperature blackbody operating at a known (measured) temperature and Planck's law. The traceability to SI comes from the determination of the thermodynamic temperature of the blackbody using a filter radiometer whose spectral responsivity is directly traceable to the NPL primary standard cryogenic radiometer. This traceability chain is shown schematically in Figure 5.10.1.

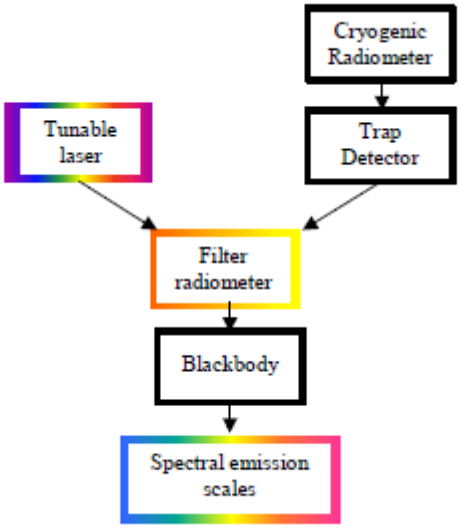


Figure 5.10.1. Traceability chain for the primary spectral irradiance scale at NPL

The blackbody is model BB3500, supplied to NPL by VNIIOFI in early 1999, similar in design to the BB3200pg used at a number of other laboratories [31]. It consists of a cavity made from pyrolytic graphite rings that are directly heated by an electrical current of around 650 A. Measurements at NPL [32] showed the uniformity of the cavity to be < ± 0.05 % and, under active optical stabilisation from the front, a long-term average stability of < ± 0.005 % and short term stability of ± 0.2 % (in radiance) at 800 nm were achieved. Investigations have shown [33] that this blackbody suffers from the same ultraviolet absorption around 380 nm as has been observed with the BB3200pg [34]. For this reason, the blackbody temperature was kept relatively low, around 3050 K.

The spectral radiance of the blackbody was determined from Planck's law, based on a measure of its thermodynamic temperature via filter radiometers, and the geometry defined by a water-cooled, brass, diamond-turned, aperture in front of the blackbody and the aperture on the integrating sphere at the front of the monochromator. The filter radiometer comprised a diamond-turned brass aperture, a wedged 10 nm bandwidth interference filter and a silicon photodiode with transimpedance amplifier, which was all housed in a water-cooled jacket. A 300 mm focal length lens was used at a distance of 600 mm to image light from the blackbody aperture so as to overfill the filter radiometer aperture. This aperture, and a thin-film aperture on the lens, defined the geometry of the measurement. The filter radiometer was used in the same f/55 geometry in which

it had been calibrated. The lens transmittance was calculated using the Fresnel equations. which had previously [5] been shown to agree within 0.05 % of the measured value at this wavelength. A correction was also applied for differences in "size-of-source" based on measurements using similar techniques to those described previously [6].

### 5.10.2. Description of the NPL spectral irradiance calibration facility

The NPL Spectral Radiance and Irradiance Primary Scales (SRIPS) facility, shown schematically in Figure 10.2, was used not only for establishing the NPL spectral irradiance scale, but also for NPL's measurements of lamps for this Key Comparison. The primary source was a BB3500 blackbody source purchased from VNIIOFI, typically operated at temperatures around 3050 K. For each measurement the thermodynamic temperature of the blackbody was determined absolutely using one of a group of two 800 nm filter radiometers built at NPL. The filter radiometers were calibrated by reference to two trap detectors using a tuneable laser illuminated integrating sphere source, with measurements being made in approximately 0.1 nm intervals across the full responsivity range of the radiometer. The trap detectors, in turn, were calibrated against the NPL cryogenic radiometer at a number of fixed wavelengths using a well-stabilised laser as the source. A calibrated aperture on the trap detector was used to convert spectral power responsivity to spectral irradiance responsivity. A more detailed description of this process can be found in the literature [36].

Wavelength selection for measurements of the lamps against the blackbody reference source was using a Bentham double grating monochromator operating in subtractive mode, with a triple grating turret to cover the range 200 nm to 2500 nm. An encoder was fitted to the grating turret in the first half to control its position and improve wavelength setting accuracy and repeatability. Measurements were made using a PMT (operating in photon-counting mode) or a silicon, InGaAs or extended-InGaAs photodiode, depending on the wavelength. The monochromator and detectors were mounted on a large translation stage that could be moved in front of each source in turn. The entire facility was computer controlled. The facility is shown schematically in Figure 5.10.2.

A major refurbishment of the facility was begun shortly after the first round of measurements, which involved replacing the monochromator, overhauling all the optical and mechanical components (including the detectors), updating the control and data analysis software for the measurement system. and updating the control and safety systems and software for the blackbody. The feedback system for the blackbody was moved to the backplate as part of this work, as recommended by VNIIOFI, but no other significant changes to the blackbody itself were needed. During this refurbishment it was discovered that the blackbody emits significant quantities of nanoparticles when running at normal operating temperature and this, coupled with the effects of the Covid-19 pandemic, meant that progress was significantly delayed. As a result, it has not yet been possible to carry out the second round NPL measurements on the lamps for the comparison.

### 5.10.3. Laboratory conditions

The laboratory ambient temperature during the measurements was 22 °C ± 2 °C and the relative humidity varied between about 40 % and 60 %.

### 5.10.4. Laboratory transfer standard

No intermediate transfer standards were used; the lamps used for the comparison were measured directly against the NPL primary reference blackbody.

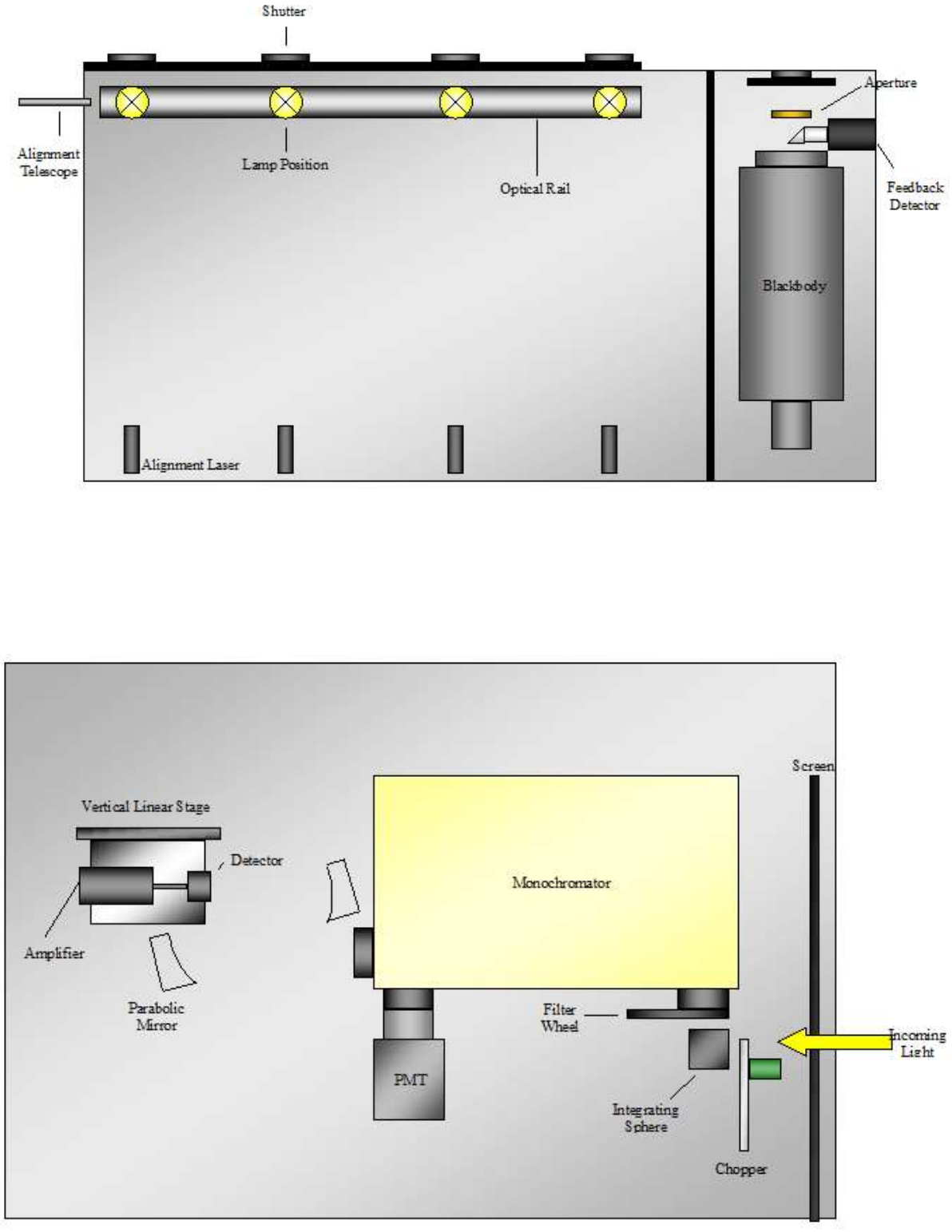


Figure 5.10.2. Measurement facility, showing source bench layout (top) and measurement bench layout (bottom). The measurement bench is mounted on a translation stage enabling it to be positioned in front of each source in turn.

### 5.10.5. Measurement procedure

For the purposes of measurement, the full spectral range (250 nm to 2500 nm) was split into several spectral regions, each of which used a different combination of grating and detector, as detailed in Table 5.10.1. At least three independent measurements were made at each wavelength, with the lamp being switched off, moved to a different position on the lamp optical rail and realigned between each measurement, and with the blackbody being switched off but not realigned. The measurement sequence for each independent measurement was:

i. blackbody temperature (using filter radiometer)
ii. blackbody spectral measurement across specified range (typically either 250 nm to 1500 nm or 1700 nm to 2500 nm)
iii. blackbody temperature (using filter radiometer)
iv. lamp spectral measurement across specified range (typically three lamps in each measurement sequence, with only the lamp actually being measured switched on in each case)
v. blackbody temperature (using filter radiometer)
vi. blackbody spectral measurement across specified range
vii. blackbody temperature (using filter radiometer)

Table 5.10.1. Detector, grating and filter combinations for each wavelength range

| **Wavelength range** | **Detector** | **Grating** | **Second order or ND filter** |
|---|---|---|---|
| 250 nm to 280 nm | PMT | 2400 g / mm, 250 nm blaze | None |
| 290 nm – 340 nm | PMT | 2400 g / mm, 250 nm blaze | ND filter |
| 360 nm – 400 nm | PMT | 2400 g / mm, 250 nm blaze | Higher density ND filter |
| 450 nm – 595 nm | Si | 1200 g / mm, 500 nm blaze | 400 nm cut-on |
| 600 nm – 800 nm | Si | 1200 g / mm, 500 nm blaze | 600 nm cut-on |
| 900 nm | Si | 1200 g / mm, 500 nm blaze | 900 nm cut-on |
| 1000 nm | Si | 600 g / mm, 1600 nm blaze | 900 nm cut-on |
| 1000 nm – 1200 nm | InGaAs | 600 g / mm, 1600 nm blaze | 900 nm cut-on |
| 1300 nm – 1500 nm | InGaAs | 600 g / mm, 1600 nm blaze | 1250 nm cut-on |
| 1700 nm – 1900 nm | Extended InGaAs | 600 g / mm, 1600 nm blaze | 1250 nm cut-on |
| 2000 nm – 2500 nm | Extended InGaAs | 600 g / mm, 1600blaze | 2000 nm cut-on |

### 5.10.6. Measurement equations

The SRIPS facility is used to measure both the blackbody and the lamp. The signal when measuring the blackbody is:

$$V^{\mathrm{BB}}(\lambda) = \pi\, g \cdot \int R^{\mathrm{SRIPS,BB}}(l) \cdot L^{BB}(T,l) \cdot S(l,\lambda) \cdot dl + \text{stray light} + \text{electronic noise} \qquad (5.10.1)$$

$g$ is the geometric factor (described below);

$V^{\mathrm{BB}}$ is the signal measured by the SRIPS detector;

$R^{\mathrm{SRIPS.BB}}$ is the responsivity of the SRIPS facility during the blackbody measurements;

$L^{\mathrm{BB}}$ is the radiance of the blackbody as given by Planck's law;

$S$ is the slit function of the monochromator. normalised to have a unit area;

$l$ is an integration constant, equivalent to wavelength, but only over the slit width.

The integral is over the extent of the slit function. usually 5–10 nm. Over this wavelength range there will be a small change in the blackbody radiance and also a (usually small) change in the SRIPS responsivity, therefore these functions lie inside the integral. Stray light and electrical noise were determined using a shutter.

The signal SRIPS measures when calibrating the lamp is given by a similar equation (in this equation, $A$ is the area of the integrating sphere aperture):

$$V^{\mathrm{lamp}}(\lambda) = A \cdot \int R^{\mathrm{SRIPS,lamp}}(l) \cdot E^{\mathrm{lamp}}(\lambda) \cdot S(l,\lambda) \cdot dl + \text{stray light} + \text{electronic noise} \qquad (5.10.2)$$

When the second blackbody scan is made, the signal is given by Equation 5.10.1 again, although the stray-light and electrical noise may be different and the responsivity of SRIPS may have drifted a small amount.

If the sources can be considered to be varying only slowly with wavelength over the slit function, then the integrals can be removed. This approximation is reasonable when the two sources are spectrally similar, as for a blackbody and lamp. Taking this approximation, the two equations can be combined to give the measured lamp irradiance. $E^{\mathrm{lamp}}$:

$$E^{\mathrm{lamp}}(\lambda) = K\kappa(\lambda)\frac{\pi g}{A} L^{\mathrm{BB}}(\lambda;T)\frac{V^{\mathrm{lamp}}(\lambda)}{V^{\mathrm{BB}}(\lambda)}\frac{R^{\mathrm{SRIPS,BB}}(\lambda)}{R^{\mathrm{SRIPS,lamp}}(\lambda)} \qquad (5.10.3)$$

If there is no drift in the SRIPS facility, then the final term is unity; it is left in at this stage for the purposes of uncertainty calculations. The constant $K$ is introduced to account for any difference between the measured lamp geometry (alignment distance, tilt etc) and the defined lamp geometry at which the lamp should be measured. This constant is unity but has an associated uncertainty. Similarly $\kappa(\lambda)$ is a term introduced to account for any difference between the measured lamp current and the defined lamp current at which the lamp should be measured, $\kappa(\lambda)$ has a value of nominally unity, but has a small wavelength dependent uncertainty.

In practice the two measurements of the blackbody have been made at potentially different temperatures. The average of the two ratios $L^{\mathrm{BB}}/V^{\mathrm{BB}}$ is therefore used, where $L^{\mathrm{BB}}$ is calculated for the average of the blackbody temperature measured before and after the relevant monochromator scan.

The geometric factor *g* comes from the form factor for radiative transfer between two coaxial circular discs, but is multiplied by the area of the emitting aperture in order to make a version that is symmetrical from one disc to the other:

$$g = \frac{2\pi r_1^2 r_2^2}{(r_1^2 + r_2^2 + d^2) + \sqrt{(r_1^2 + r_2^2 + d^2)^2 - 4r_1^2 r_2^2}} \tag{5.10.4}$$

Here $r_1$ and $r_2$ are the radii of the two discs and *d* is the distance between them. For SRIPS measurements these are the radii of the blackbody and the integrating sphere aperture making the entrance aperture to the monochromator system.

The radiance of a blackbody in air is given by Planck's law using air wavelengths and the refractive index of air. $n$:

$$L_{BB} = \frac{2h(c/n)^2}{\lambda^5(\exp[hc/n\lambda kT]-1)} \tag{5.10.5}$$

where *h* is the Planck constant, 6.626 0693(11)×10-34 J s, *c* is the speed of light, 299792458 m $s^{-1}$ (exact), *k* is the Boltzmann constant, 1.380 6505(24) × 10-23 J $K^{-1}$, *n* is the air refractive index, 1.00029 ± 0.00005, and *e* is the emissivity of the blackbody, which is 0.99988 ± 0.00010.

### 5.10.7. Uncertainties

#### *5.10.7.1. Uncertainty in constants*

This section discusses the uncertainty in the constants in Equation 5.10.3 i.e. *K*, *k*(*l*), *g* and *A*. These constants are the same for all measurements and hence the uncertainties are correlated.

*K* is a measure of the quality of the alignment of the lamp compared with the defined lamp geometry at which the lamp should be measured. It is wavelength independent and has a value that is nominally taken as unity. It is a systematic effect and has been evaluated based on the uncertainty associated with the measurement of the distance and the ability to set the alignment jig perpendicular to measurement axis. *K* has a value of 1 ± 0.0014. Additional uncertainties associated with the reproducibility of the alignment from one measurement to another are included as part of the overall lamp reproducibility (random effect) and are therefore not included here.

*k*(*l*) is a measure of the quality of the lamp current compared with the defined current at which it should be measured. The current supplied to the lamp directly relates to the power output of the lamp. The uncertainty in the lamp's current arises from uncertainties associated with: the calibration of the standard resistor; possible drift in the resistance since the time of calibration of the standard resistor; temperature changes in the resistor during use (the resistor is in an oil bath so temperature changes are minimal); the calibration of the DVM used to measure the voltage across the standard resistor; and drift in the DVM since its calibration. The overall effect is an uncertainty of 0.002 % in the current. To convert this to an uncertainty in lamp irradiance at a given wavelength we need to consider that the lamp approximates to a blackbody and therefore the spectral effect of this current uncertainty can be evaluated using the Planck equation by considering the change in temperature caused by a 0.002 % change in current. From the Stefan-Boltzmann law, the power output of the lamp is proportional to $T^4$ and from basic electrical laws the input power is proportional to $I^2$. Therefore, the temperature is proportional to $I^{0.5}$. At a temperature of approximately 3000 K, this leads to an uncertainty in the blackbody temperature of 0.03 K (corresponding to an irradiance uncertainty of 0.02 % at 250 nm and less than 0.01 % for 500 nm and above). An additional uncertainty arises from the stability of the lamp current during

the calibration, due to noise on the power supply. The uncertainty in the stability of the current is 0.0035 % or better, leading to a temperature uncertainty of 0.05 K and an irradiance uncertainty of 0.04 % at 250 nm, falling to less than 0.01 % at 900 nm.

The uncertainty associated with the value of $\pi g / A$ is due to geometry. It is a constant at all wavelengths and for all individual lamp measurements made within a few months of each other. The effect is taken as a Type B uncertainty of 0.05% based on the calibration uncertainties for the apertures and the uncertainty in the distance between them.

#### *5.10.7.2. Uncertainty in blackbody radiance*

The blackbody spectral radiance at temperature $T$ is given by a modified version of the Planck equation:

$$L^{BB}(\lambda;T) = \alpha(\lambda)\varepsilon \frac{2h(c/n)^2}{\lambda^5(\exp[hc/n\lambda kT]-1)} \qquad (5.10.6)$$

The additional term $a(\lambda)$ allows for the absorption of the blackbody. For a small region around 380 nm the carbon gas emitted by the blackbody absorbs the radiation and the blackbody does not obey the Planck equation. No correction is made for this, but an additional wavelength dependent uncertainty applies in this narrow spectral region to account for the absorption.

The uncertainty components to consider for the blackbody spectral radiance therefore come from: the temperature (factors contributing to this are detailed below); the absorption due to carbon at wavelengths around 380 nm; and the uncertainty in the emissivity correction (this is very small). The majority of these components are the same for all measurements and hence the associated uncertainties are correlated.

#### *5.10.7.3. Uncertainty in blackbody temperature*

The temperature of the blackbody is measured using a filter radiometer whose spectral responsivity, $R(\lambda)$, has been calibrated. The filter radiometer is placed in front of the blackbody and light is focussed onto it using a lens. A light reading, $V^{\text{light}}$, and a dark reading, $V^{\text{dark}}$, are taken and combined with an out-of-band reading $V^{\text{OOB}}$ (with a long-pass filter in front of the filter radiometer, to account for any filter radiometer responsivity at wavelengths longer than the longest calibration wavelength) and a dark out-of-band reading $V^{\text{OOB, Dark}}$ (with the long pass filter and the shutter) and the resultant signal, $V$, can be compared with the expected signal using the following equation:

$$\begin{aligned} V &= V^{\text{light}} - V^{\text{dark}} - V^{\text{OOB}} + V^{\text{OOB,Dark}} \\ &= sGUS \cdot g\pi R \cdot \int_{\lambda_0}^{\lambda_1} r(\lambda)\,\tau(\lambda)\,L(\lambda;T)\,d\lambda \end{aligned} \qquad (5.10.7)$$

Here $L$ is the radiance of the blackbody given by Equation 5.10.6, $t$ is the wavelength-dependent lens transmittance, $g$ is the geometric factor, given by Equation 4, but this time with the lens and filter radiometer apertures, $G$ is the electronic gain of the amplifier and $s$ is the size-of-source effect (SSE), a measure of the amount of light scattered by imperfections in the lens, $U$ is the uniformity of the blackbody i.e. the difference between the signal measured and the signal that would be measured if a larger area of the blackbody were observed (needed because the spectral irradiance calibration facility sees a larger area of blackbody than the filter radiometer). $S$ is a measure of the blackbody stability between the time when the temperature is measured and the time when the

spectral irradiance is measured; this has a value of unity, but an associated uncertainty. The responsivity of the filter radiometer has been split into two components. The absolute responsivity, $R$ (in A $W^{-1}$) has been separated from the relative spectral responsivity $r$ to simplify the uncertainty analysis ($R$ is the component correlated at all wavelengths, $r$ is entirely uncorrelated from one wavelength to the next).

The filter radiometer responsivity has been calibrated at discrete wavelengths; therefore Equation 5.10.7 is replaced by a discrete version, using the trapezium rule:

$$V(T) = C\sum_{j=1}^{N} r_j L(\lambda_j, T)\cdot\delta\lambda_j \qquad (5.10.8)$$

Here $C$ combines all the uncertainties on the outside of the integral in Equation 5.10.7, $\delta\lambda_j$ is $\left(\lambda_{j+1}-\lambda_{j-1}\right)/2$ for all but the first $\left(\left(\lambda_2-\lambda_1\right)/2\right)$ and last $\left(\left(\lambda_N-\lambda_{N-1}\right)/2\right)$ values.

The Newton-Raphson technique is used to determine the temperature of the blackbody given the signal. This is robust for this calculation because only one value of temperature can be associated with each signal.

According to normal uncertainty analysis, as described in the Guide to the Uncertainty of Measurement (GUM) [37], given a function $f(x_1,x_2,x_3\ldots)$, the uncertainty associated with the function should be derived from the uncertainties calculated from the individual parts. However, here the temperature cannot be described as a function of the other variables. Instead we must use the techniques for a "multivariate, implicit, real valued model" as described in section 6.3.4 of the 6th best practice guide from the Software Support for Metrology programme at NPL [38]. This requires Equation 5.10.8 to be written in the form:

$$h(T,C,V,r_1\ldots r_N,\tau_1\ldots\tau_N) = \left[C\sum_{j=1}^{N} r_j L(\lambda_j,T)\cdot\delta\lambda_j\right] - V = 0 \qquad (5.10.9)$$

The best practice guide supplies methods for determining the uncertainty in T due to the uncertainties in all the other components. The following equations are therefore needed to determine the uncertainty in temperature due to uncertainties in each of the components:

$$\left(\frac{\partial h}{\partial T}\right)^2 u^2(T) = u^2(V)\left(\frac{\partial h}{\partial V}\right)^2 + u^2(C)\left(\frac{\partial h}{\partial C}\right)^2 + \sum_{i=1}^{N} u^2(r_i)\left(\frac{\partial h}{\partial r_i}\right)^2 \qquad (5.10.10)$$

$$\left(\frac{\partial h}{\partial T}\right)^2 = \left[C\sum_{j=1}^{N}\left(r_j\,\tau_j\,\delta\lambda_j\,\frac{\partial L(\lambda_j;T)}{\partial T}\right)\right]^2 \qquad (5.10.11)$$

$$\left(\frac{\partial h}{\partial V}\right)^2 = 1 \qquad (5.10.12)$$

$$\left(\frac{\partial h}{\partial C}\right)^2 = \left(\frac{V}{C}\right)^2 \qquad (5.10.13)$$

$$\sum_{j=1}^{N}\left(\frac{\partial h}{\partial r_j}\right)^2 u^2(r_j) = \sum_{j=1}^{N}\left[C\,\tau_j\,L(\lambda_j;T)\delta\lambda_j\right]^2 u^2(r_j) \qquad (5.10.14)$$

$$\frac{\partial L(\lambda_j;T)}{\partial T} = \frac{2h^2c^3 \exp[hc/n\lambda kT]}{n^3\lambda^6 kT^2 \left(\exp[hc/n\lambda kT]-1\right)^2} \qquad (5.10.15)$$

These equations assume no correlation and there are no correlations between $V$ and $C$ (although there may be some correlations within $C$), nor between either of these and the $r_j$ terms.

#### *5.10.7.4. Uncertainty in signal levels*

The signal level used in Equation 5.10.7 is the light signal level minus the dark signal and minus the out-of-band. This is treated as a Type B uncertainty and comes dominantly from the uncertainty in the calibration of the voltmeter and the electrical noise in the dark reading. The uncertainty in the out-of-band comes from the quality of the filter used for the out-of-band measurements together with any differences between the temperature of the blackbody during out-of-band measurements and during blackbody temperature measurements.

The uncertainty in the measured signal is:

$$u_V^2 = u_{V^{\text{light}}}^2 + u_{V^{\text{dark}}}^2 + u_{V^{\text{OOB}}}^2 + u_{V^{\text{OOB, dark}}}^2 + \left(\frac{V}{K}\right)^2 u_K^2 \qquad (5.10.16)$$

The final term represents the calibration uncertainty of the voltmeter. It assumes that it is the same for all four measurements and that they should all be multiplied by a, nominally unity, correction factor $K$. In practice, voltmeter non-linearities are negligible and $K$ is 1 with an uncertainty of 0.005 %. Typically, $V$ is about 1.8 V with an uncertainty of about 0.76 mV corresponding to a temperature uncertainty of 0.08 K.

#### *5.10.7.5. Uncertainty in SSE*

The size-of-source effect is (0.22 ± 0.06) %. From Equations 5.10.13 and 5.10.10, this corresponds to a temperature uncertainty of 0.31 K.

#### *5.10.7.6. Uncertainty in amplifier gain*

The uncertainty on the amplifier gain calibration is 0.02 % at 95 % confidence, or a standard uncertainty of 0.01 %. From Equations 5.10.13 and 5.10.10, this corresponds to a temperature uncertainty of 0.05 K.

#### *5.10.7.7. Uncertainty in lens transmittance*

The lens transmittance was calculated using the Fresnel equations, which had previously been shown to agree within 0.05 % of the measured value at this wavelength. This is used as the base uncertainty in the lens transmittance and an additional 0.05 % is added to allow for possible degradation with time, both components being treated as having a rectangular distribution function. From Equations 5.10.13 and 5.10.10, this corresponds to a temperature uncertainty of 0.31 K.

Although the lens transmittance is a wavelength dependent quantity and therefore inside the integral, the values are entirely correlated and therefore the uncertainty is considered in $C$.

#### *5.10.7.8. Uncertainty in geometric factor*

The geometric factor is derived from the size of the apertures on the filter radiometer and lens and the distance between them. The uncertainty calculation is the same as that for the geometric factor

in the spectral irradiance measurement i.e. *g*/*A* has a standard uncertainty of 0.05 %. which corresponds to a temperature uncertainty of 0.26 K.

#### *5.10.7.9. Uncertainty in FR responsivity*

The standard uncertainty associated with the responsivity of the filter radiometer has been assessed as 0.16 %, with the major contributions to this being possible drift in the response since calibration, non-uniformity of the sphere source used during calibration and uncertainties in the measured areas of the apertures used during calibration. This corresponds to a temperature uncertainty of 0.83 K.

#### *5.10.7.10. Uncertainty associated with properties of the blackbody*

The blackbody stability, uniformity and emissivity have been evaluated and the impact of these parameters on the assigned temperature has been determined as 0.32 K.

#### *5.10.7.11. Uncertainty in lamp-blackbody signal ratios*

The final uncertainty that needs to be considered is the uncertainty in the final two terms of Equation 3. i.e. the uncertainty in:

$$\frac{V^{\text{lamp}}(\lambda)}{V^{\text{BB}}(\lambda)} \frac{R^{\text{SRIPS,BB}}(\lambda)}{R^{\text{SRIPS,lamp}}(\lambda)} \tag{5.10.17}$$

The uncertainty in the ratios comes from any non-linearity in the response of the system or the measurement of the signals and in any drift in the facility between the measurement of the blackbody and the measurement of the lamp, along with the noise on the signals. Linearity and detector noise effects are better than 0.001 % and therefore entirely negligible, and drift is assessed through repeat measurements of the lamp and blackbody and therefore included through a Type A analysis that varies for each specific measurement but is set to a "typical" minimum value to ensure the uncertainties for abnormally "good" measurements are not underestimated. These uncertainties are uncorrelated between measurements.

There is an additional uncertainty due to whether this measured ratio is really the desired ratio, which comes from the wavelength accuracy and the effect of the monochromator bandwidth. This is evaluated through modelling and is negligibly small due to the closely-similar spectral shapes of the blackbody and the lamp.

### 5.10.8. References to section 5.10

[31] Sperfeld P., Metzdorf J., Harrison N.J., Fox N. P., Khlevnoy B.B., Khromchenko V.B., Mekhontsev S. N., Shapoval V.I., Zelener M.F.. Sapritsky V.I., Investigation of high-temperature blackbody BB3200, *Metrologia*, 1998, **35**, 419–422

[32] Woolliams E. R., Harrison N. J., Fox N. P., Preliminary results of the investigation of a 3500 K black body, *Metrologia*, 2000, **37(5)**, 501-504

[33] Woolliams E. R., Harrison N. J., Khlevnoy B.B., Rogers L.J., Fox N.P., Realisation and dissemination of spectral irradiance at NPL, *UV News*, 2002, **7**, 39-42

[34] Sperfeld P., Galal Yousef S., Metzdorf J., Nawo B., Möller W., The use of self-consistent calibrations to recover absorption bands in the black-body spectrum, *Metrologia*, 2000, **37(5)**, 373-376

[35] Woolliams E.R., Pollard D.F., Harrison N.J., Theocharous E., Fox N.P., New facility for the high-accuracy measurement of lens transmission, *Metrologia*, 2000, **37(5)**, 603-605

[36] Fox N.P., Martin J.E., Nettleton D.H., Absolute spectral radiometric determination of the thermodynamic temperatures of the melting/freezing points of gold, silver and aluminium, *Metrologia*, **28**, 1991, 357-374

[37] Guide to the Expression of Uncertainty in Measurement, Geneva, International Organization for Standardization, 1993

[38] Cox M.G., Dainton P.M., Harris P.M., Software Support for Metrology. Best Practice Guide No. 6: Uncertainty and statistical modelling", March 2001, available at: http://www.npl.co.uk/ssfm/download/

### 5.10.9. Final uncertainties submitted by NPL with the measurement results

Table 5.10.2. Spectral Irradiance standard uncertainties (k=1) of the lamp **BN-9101-636**

| Wavelength, nm | Round 1 | | | Round 2 | | |
|---|---|---|---|---|---|---|
| | Uncertainties associated with, % | | Combined uncertainty, % | Uncertainties associated with, % | | Combined uncertainty, % |
| | Uncorrelated effects | Correlated effects | | Uncorrelated effects | Correlated effects | |
| 250 | 0.314 | 0.841 | 0.898 | | | |
| 260 | 0.279 | 0.867 | 0.911 | | | |
| 270 | 0.265 | 0.892 | 0.930 | | | |
| 280 | 0.284 | 0.852 | 0.898 | | | |
| 290 | 0.252 | 0.787 | 0.826 | | | |
| 300 | 0.240 | 0.747 | 0.785 | | | |
| 320 | 0.203 | 0.759 | 0.786 | | | |
| 340 | 0.243 | 0.735 | 0.774 | | | |
| 360 | 0.243 | 0.708 | 0.749 | | | |
| 380 | 0.222 | 0.723 | 0.756 | | | |
| 400 | 0.259 | 0.680 | 0.728 | | | |
| 450 | 0.198 | 0.429 | 0.472 | | | |
| 500 | 0.109 | 0.388 | 0.403 | | | |
| 555 | 0.106 | 0.351 | 0.367 | | | |
| 600 | 0.104 | 0.327 | 0.343 | | | |
| 700 | 0.102 | 0.284 | 0.302 | | | |
| 800 | 0.120 | 0.253 | 0.280 | | | |
| 900 | 0.104 | 0.229 | 0.251 | | | |
| 1000 | 0.096 | 0.210 | 0.231 | | | |
| 1100 | 0.098 | 0.196 | 0.219 | | | |
| 1300 | 0.091 | 0.174 | 0.196 | | | |
| 1500 | 0.090 | 0.159 | 0.183 | | | |
| 1700 | 0.165 | 0.205 | 0.263 | | | |
| 2000 | 0.180 | 0.197 | 0.267 | | | |
| 2200 | 0.192 | 0.193 | 0.272 | | | |
| 2300 | 0.203 | 0.192 | 0.279 | | | |
| 2400 | 0.210 | 0.190 | 0.284 | | | |
| 2500 | 0.825 | 0.191 | 0.847 | | | |

Table 5.10.3. Spectral Irradiance standard uncertainties (k=1) of the lamp **BN-9101-637**

| Wavelength, nm | Round 1 | | | Round 2 | | |
|---|---|---|---|---|---|---|
| | Uncertainties associated with, % | | Combined uncertainty, % | Uncertainties associated with, % | | Combined uncertainty, % |
| | Uncorrelated effects | Correlated effects | | Uncorrelated effects | Correlated effects | |
| 250 | 0.301 | 0.841 | 0.893 | | | |
| 260 | 0.284 | 0.867 | 0.912 | | | |
| 270 | 0.276 | 0.892 | 0.934 | | | |
| 280 | 0.333 | 0.852 | 0.915 | | | |
| 290 | 0.267 | 0.787 | 0.831 | | | |
| 300 | 0.220 | 0.747 | 0.779 | | | |
| 320 | 0.234 | 0.759 | 0.795 | | | |
| 340 | 0.204 | 0.735 | 0.763 | | | |
| 360 | 0.196 | 0.708 | 0.735 | | | |
| 380 | 0.284 | 0.723 | 0.776 | | | |
| 400 | 0.283 | 0.680 | 0.737 | | | |
| 450 | 0.195 | 0.429 | 0.471 | | | |
| 500 | 0.104 | 0.388 | 0.401 | | | |
| 555 | 0.092 | 0.351 | 0.363 | | | |
| 600 | 0.092 | 0.327 | 0.339 | | | |
| 700 | 0.089 | 0.284 | 0.298 | | | |
| 800 | 0.104 | 0.253 | 0.273 | | | |
| 900 | 0.104 | 0.229 | 0.251 | | | |
| 1000 | 0.087 | 0.210 | 0.228 | | | |
| 1100 | 0.101 | 0.196 | 0.220 | | | |
| 1300 | 0.094 | 0.174 | 0.198 | | | |
| 1500 | 0.103 | 0.159 | 0.190 | | | |
| 1700 | 0.147 | 0.205 | 0.252 | | | |
| 2000 | 0.161 | 0.197 | 0.254 | | | |
| 2200 | 0.172 | 0.193 | 0.258 | | | |
| 2300 | 0.178 | 0.192 | 0.261 | | | |
| 2400 | 0.185 | 0.190 | 0.265 | | | |
| 2500 | 0.601 | 0.191 | 0.631 | | | |

Table 5.10.4. Spectral Irradiance standard uncertainties (k=1) of the lamp **BN-9101-553**

| Wavelength, nm | Round 1 | | | Round 2 | | |
|---|---|---|---|---|---|---|
| | Uncertainties associated with, % | | Combined uncertainty, % | Uncertainties associated with, % | | Combined uncertainty, % |
| | Uncorrelated effects | Correlated effects | | Uncorrelated effects | Correlated effects | |
| 250 | 0.509 | 0.841 | 0.983 | | | |
| 260 | 0.596 | 0.867 | 1.052 | | | |
| 270 | 0.730 | 0.892 | 1.152 | | | |
| 280 | 0.553 | 0.852 | 1.016 | | | |
| 290 | 0.367 | 0.787 | 0.868 | | | |
| 300 | 0.483 | 0.747 | 0.890 | | | |
| 320 | 0.588 | 0.759 | 0.960 | | | |
| 340 | 0.364 | 0.735 | 0.821 | | | |
| 360 | 0.432 | 0.708 | 0.830 | | | |
| 380 | 0.373 | 0.723 | 0.813 | | | |
| 400 | 0.355 | 0.680 | 0.767 | | | |
| 450 | 0.230 | 0.429 | 0.486 | | | |
| 500 | 0.201 | 0.388 | 0.436 | | | |
| 555 | 0.245 | 0.351 | 0.428 | | | |
| 600 | 0.221 | 0.327 | 0.395 | | | |
| 700 | 0.189 | 0.284 | 0.341 | | | |
| 800 | 0.156 | 0.253 | 0.297 | | | |
| 900 | 0.135 | 0.229 | 0.266 | | | |
| 1000 | 0.123 | 0.210 | 0.244 | | | |
| 1100 | 0.127 | 0.196 | 0.233 | | | |
| 1300 | 0.111 | 0.174 | 0.207 | | | |
| 1500 | 0.111 | 0.159 | 0.194 | | | |
| 1700 | 0.269 | 0.205 | 0.338 | | | |
| 2000 | 0.294 | 0.197 | 0.354 | | | |
| 2200 | 0.313 | 0.193 | 0.368 | | | |
| 2300 | 0.324 | 0.192 | 0.377 | | | |
| 2400 | 0.338 | 0.190 | 0.388 | | | |
| 2500 | 1.082 | 0.191 | 1.099 | | | |

## 5.11. NRC, Canada

### 5.11.1. Primary scale realisation

The primary spectral irradiance scale at the National Research Council Canada (NRC) is a source and detector-based scale from 250 nm to 2500 nm. A high temperature black body (HTBB) is implemented as a standard radiometric source and an NRC-designed wideband filter radiometer [39], with spectral responsivity traceable to the NRC optical power scale, is utilized to measure the thermodynamic temperature of the HTBB. The SI traceability chain of this scale realisation is shown in Figure 5.11.1. The spectral response of the filter radiometer implemented in the determination of the HTBB temperature was calibrated using a detector comparison method with a monochromator-based apparatus [40]. The HTBB temperature, Planck's Law, and geometric factors including the HTBB and filter radiometer aperture sizes and distance to the reference plane, are used to calculate the spectral irradiance of the HTBB. The spectral irradiance of an FEL transfer standard lamp is then determined by implementing a spectroradiometer system to collect spectral data from the HTBB and the FEL lamp. The irradiance of the FEL lamp at a given wavelength is then calculated by multiplying the HTBB irradiance and the ratio of the FEL lamp and HTBB photodetector signals. This calculation is described in further detail in section 5.11.4. For this key comparison, three travelling standard FEL lamps were calibrated using the HTBB at a thermodynamic temperature of approximately 2950 K.

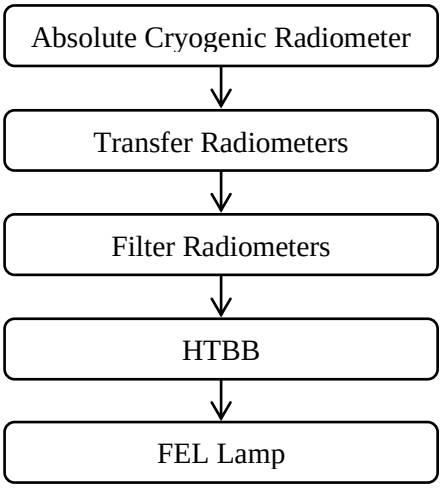


Figure 5.11.1. Traceability chain for NRC spectral irradiance scale.

### 5.11.2. Description of Measurement Facility

The NRC primary spectral irradiance measurement facility is shown in Figure 5.11.2. The monochromator in this facility is a one metre focal length GCS McPherson Model 2051 which has a single grating Czerny-Turner design. An integrating sphere with a 6 mm input port is mounted to a prism pre-disperser at the monochromator input. The entrance and exit slits to the monochromator were adjusted such that the maximum bandwidth was attained. A light-tight box with a 3 cm aperture was installed around the integrating sphere to reduce stray light. A beam blocker on a motorized flip mount was used to block the incident light for dark signal measurements. Combinations of two diffraction gratings and three photodetectors were used for the measurements in order to cover the complete spectral range of 250 nm to 2500 nm and are summarized in Table 5.11.1. For this spectroradiometer system, the monochromator diffraction gratings and photodetectors are changed manually with subsequent verification of wavelength calibration and detector alignment. During measurements, spectral data from the HTBB and all

FEL transfer standard lamps was collected using the same grating and photodetector combinations to cover one spectral range (e.g. 250 nm to 1100 nm). After the first measurement range was completed for all lamps, the grating and photodetectors were changed for the second spectral range (e.g. 1300 nm to 2500 nm). The monochromator was purged with dry air for the duration of the measurements.

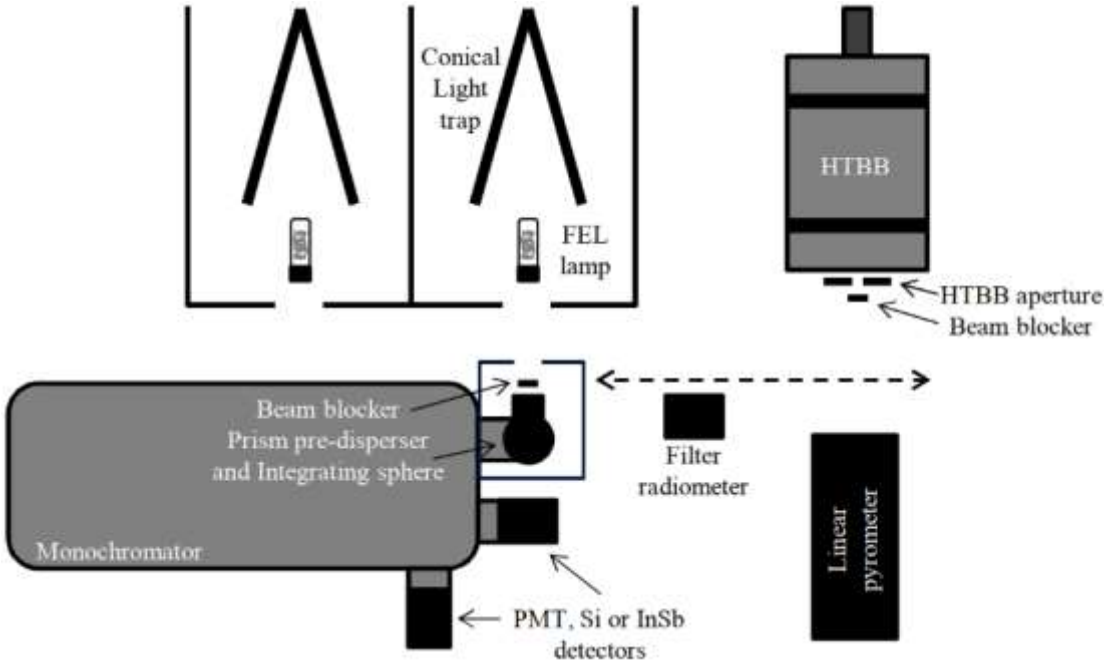


Figure 5.11.2. Schematic diagram of the NRC spectral irradiance facility.

Table 5.11.1. Grating and detector types used for spectral measurements.

| Wavelength range (nm) | Detector | Grating | | Bandwidth FWHM |
|---|---|---|---|---|
| | | Blaze | Grooves/mm | |
| 250 - 380 | PMT | 400 nm | 600 | 3 nm |
| 400 - 1100 | Si | 400 nm | 600 | 3 nm |
| 1300 - 2500 | InSb | 2700 nm | 600 | 3 mm |

This facility has two FEL lamp stations equipped with translation, rotation, and goniometer stages for lamp alignment. Stray light from the FEL lamps is mitigated by black side panels and front panels with a 7.5 cm aperture, as well as conical light traps installed behind the FEL lamps to capture the optical radiation emitted in the backward direction. Each lamp station is connected to a DC power supply (Agilent Technologies N6977A) and calibrated shunt resistor. For the first round of measurements, the same power supply and 0.01 ohm shunt resistor were used for all measurements on both lamp stations. For the second round of measurements, each lamp station was equipped with its own power supply and shunt resistor. Each station has the same model of power supply, but different models of calibrated shunt resistor (0.01 ohm and 0.1 ohm). In each

case the temperature of the shunt resistor was monitored and the power supply output current was corrected to maintain a value of 8.100 A.

The HTBB in this facility (model BB3500M, manufactured by VNIIOFI) has a water-cooled aperture at the output. A beam blocker on a motorized flip mount was placed after the water-cooled HTBB aperture to perform dark signal measurements with the filter radiometer. A linear pyrometer was used to monitor the temperature stability of the HTBB before the start of data collection, but was not used in the temperature determination of the HTBB for these measurements.

In this facility, the FEL lamp stations and HTBB are installed on separate optical tables. The monochromator system, filter radiometer, and linear pyrometer are all installed on the same optical table equipped with a rail and lead screw system as well as a linear encoder which facilitates 2 m of translation. A custom software program enables the automation of the positioning and data collection of different sources and detectors: alignment positioning of the HTBB and filter radiometer, the HTBB and spectroradiometer, and of the FEL lamps and spectroradiometer. All spectral data from the HTBB and FEL lamps was collected using the same measurement apparatus settings (i.e. with the same monochromator diffraction grating, photodetector, and transimpedance amplifier combination).

### 5.11.3. Measurement Procedure

The FEL transfer standard lamp measurements were conducted according to the measurement instructions in the CCPR-K1a.2017 Spectral Irradiance 250 nm to 2500 nm Technical Protocol. The distance between the front plate of the lamp and the entrance aperture of the integrating sphere on the monochromator was set using the lamp translation stage and a stainless-steel calibrated length bar (499.945 mm). The same calibrated length bar was used to set the distance between the HTBB and the filter radiometer apertures. After the first round of measurements was complete, it was found that the micrometre on one lamp station translation stage had a discrepancy of 4.45 mm for the distance measurement. This change has been incorporated in the measurement results for round one using the equation:

$$\boldsymbol{E_2 = E_1(d_1/d_2)^2} \qquad (5.11.1)$$

where $\boldsymbol{E_2}$ is the calculated irradiance at distance $\boldsymbol{d_2}$ of 499.945 mm, and $\boldsymbol{E_1}$ is the irradiance measured at distance $\boldsymbol{d_1}$ of 504.395 mm.

The lamp alignment was performed by placing the alignment jig on the side of the lamp base facing the measurement facility. An alignment laser was used to position the lamp such that the laser hit the target on the jig and the back reflection was aligned back to the laser using rotation and goniometer stages. A spirit level was used to verify that the alignment jig was level. All lamps were turned on using a current slew rate of 0.066 A/s and were warmed up for a minimum of 20 minutes at 8.100 A before measurements commenced.
A custom software program was used to control the alignment positions of the sources and photodetectors using the optical table and lead screw system, to control the monochromator wavelength, and to collect data from the filter radiometer and other photodetectors. After setting the distances of the HTBB and filter radiometer apertures, the HTBB and monochromator aperture, and the FEL lamps and monochromator aperture, the following measurement procedure was used:

1. Verify temperature stability of HTBB with linear pyrometer.
2. Move the optical table to the predetermined position where the filter radiometer is aligned to the HTBB output and measure the thermodynamic temperature of the HTBB.

3. Translate the optical table to align the monochromator integrating sphere input to the HTBB. Collect spectral data from the HTBB over a specified range.
4. Move the optical table, aligning the filter radiometer to the HTBB output to measure the thermodynamic temperature of HTBB for a second time to verify temperature stability.
5. Translate the optical table to align the monochromator integrating sphere input to an FEL lamp. Collect data in the same spectral range as step 3. For the FEL lamp measurements, the spectral data was collected three times to give an indication of measurement repeatability.
6. Repeat step 5 for the second FEL lamp.

As described in section 5.11.2, the monochromator diffraction gratings and photodetectors were changed manually to facilitate measurements from 250 nm to 2500 nm. Table 5.11.2 gives a summary of when measurements for each spectral range were performed for each round. All FEL transfer standard lamps were re-aligned before each measurements commenced, for a total of three complete measurements from 250 nm to 2500 nm in each round.

Table 5.11.2. Summary of measurement timeline per spectral range.

| Round | Measurement dates | Wavelength range |
|---|---|---|
| 1 | 28-Nov-2017 to 01-Dec-2017 | 250 nm – 1100 nm |
| 1 | 04-Dec-2017 to 06-Dec-2017 | 1300 nm – 2500 nm |
| 2 | 22-May-2018 to 03-Jun-2019 | 1300 nm – 2500 nm |
| 2 | 11-Jun-2019 to 26-Jun-2019 | 250 nm – 1100 nm |

### 5.11.4. Measurement Uncertainty

The uncertainty budget for the NRC spectral irradiance primary scale realisation is given in Table 5.11.3. The spectral irradiance of an FEL transfer standard lamp, $E_{\lambda.FEL}$, at a given wavelength, $\lambda$, was calculated using

$$\boldsymbol{E_{\lambda,FEL} = E_{\lambda,HTBB}\frac{S_{\lambda,FEL}}{S_{\lambda,HTBB}}} \tag{5.11.2}$$

where $E_{\lambda.HTBB}$ is the irradiance of the HTBB, and $S_{\lambda,FEL}$ and $S_{\lambda,HTBB}$ are the measured FEL lamp and HTBB photodetector signals from the spectroradiometer, respectively.

The HTBB irradiance is given by:

$$\boldsymbol{E_{\lambda,HTBB} = \left(\frac{\pi r_{HTBB}^2}{(d^2+r_{FR}^2+r_{HTBB}^2)}\right)\left(\frac{2\varepsilon hc^2}{\lambda^5 n^2 e^{hc/n\lambda kT}-1}\right)} \tag{5.11.3}$$

where $r_{HTBB}$ and $r_{FR}$ are the radii of the HTBB and filter radiometer precision apertures, $d$ is the distance between the HTBB and filter radiometer precision apertures, $\varepsilon$ is the HTBB emissivity, $h$ is the Planck constant, $c$ is the speed of light, $n$ is the refractive index of air [41, 42], $k$ is the Boltzmann constant, and $T$ is the thermodynamic temperature of the HTBB.

The determination of $T$ using NRC filter radiometers is described in [39]. The evaluation of the uncertainty components for this type of measurement have been most recently discussed in [10], where a sensitivity coefficient was used to convert the relative value of each uncertainty component to an uncertainty in temperature. A similar approach was taken here, where a sensitivity coefficient was determined for HTBB temperature measurements at 2950 K, and the relative values of the filter radiometer calibration, which includes the filter radiometer aperture area, filter radiometer to HTBB aperture distance, HTBB aperture area, HTBB radiance non-uniformity,

HTBB emissivity, and the refractive index of air have been taken into account. To determine the effect on $E_{\lambda,FEL}$, $E_{\lambda.HTBB}$ was calculated using values of $T$ with the incorporated temperature uncertainties. The resulting differences in $E_{\lambda,FEL}$ due to these components are given in Table 5.11.3. The uncertainty components related to the geometric factors, $\varepsilon$, and $n$ in Eq. 3 are included in the measurement of $T$ and as such are not counted again in the calculation of the HTBB irradiance.

The uncertainty in spectral irradiance due to the lamp distance measurement was calculated using Eqn. 5.11.1, where the uncertainty of the calibrated length bar (17 μm) and the repeatability of the lamp translation stage micrometre (0.05 mm) were taken into account. The uncertainties in the lamp distance and the filter radiometer to HTBB aperture distance are correlated as the same calibrated length bar and micrometres with the same resolution were used for these measurements.

The monochromator wavelength calibration uncertainty is proportional to the derivative of the ratio of the measured FEL lamp and HTBB photodetector signals:

$$u\big(S(\lambda)\big) = \frac{d\left(\frac{S_{\lambda,FEL}}{S_{\lambda,HTBB}}\right)}{d\lambda} \times \mathrm{u}(\lambda) \tag{5.11.4}$$

where $\mathrm{u}(\lambda)$ is the residual wavelength uncertainty obtained after wavelength correction curves have been applied to the monochromator system (±0.1 nm). The resulting effect of the wavelength uncertainty on $E_{\lambda,FEL}$ is listed in Table 5.11.3.

The HTBB temperature stability was determined by calculating the change in temperature from steps 2 and 4 in the measurement procedure described in section 5.11.3. The largest change in temperature was found to be 0.2 K. A rectangular distribution was used to evaluate this drift as a temperature uncertainty. and the effect on $E_{\lambda.FEL}$ was found using Equations 5.11.2 and 5.11.3.

The lamp current was monitored throughout all measurements. The repeatability of the lamp current measurement was converted to a standard uncertainty using a rectangular distribution. The calibration of the shunt resistors for both lamp stations, the calibration of the digital multimeters used for these measurements, and the repeatability of the lamp current measurements have a combined uncertainty of 572 μA. To convert this combined uncertainty in current to an uncertainty in spectral irradiance, the FEL lamp current, $I$, is taken to be proportional to the FEL lamp output power, $P$, and $P$ is taken to be proportional to the lamp radiance. Differentiating and rearranging the Stefan-Boltzmann law, where $\sigma$ is the Stefan-Boltzmann constant, one can write:

$$\begin{aligned} \boldsymbol{P} &= \boldsymbol{\sigma T^4} \\ \frac{\boldsymbol{dT}}{\boldsymbol{T}} &= \frac{\boldsymbol{dP}}{\boldsymbol{4\sigma T^4}} \\ \frac{\boldsymbol{dP}}{\boldsymbol{P}} &= \frac{\boldsymbol{4dT}}{\boldsymbol{T}} \end{aligned} \tag{5.11.5}$$

Similarly, differentiating and rearranging an expression for electrical power:

$$\begin{aligned} \boldsymbol{P} &= \boldsymbol{I^2 R} \\ \frac{\boldsymbol{dP}}{\boldsymbol{P}} &= \frac{\boldsymbol{2RIdI}}{\boldsymbol{RI^2}} \\ \frac{dP}{P} &= \frac{2IdI}{I} \end{aligned} \tag{5.11.6}$$

Combining equations 5.11.5 and 5.11.6:

$$dT = \frac{TdI}{2I} \quad (5.11.7)$$

The change in temperature, *dT*, was calculated using the distribution temperature of the FEL lamp [43] and the combined uncertainty in the current measurement. This change in temperature was applied to the HTBB thermodynamic temperature to calculate the effect on spectral irradiance.

Tables 5.11.4, 5.11.5 and 5.11.6 list the combined uncertainties for rounds 1 and 2 of the FEL traveling transfer standard lamp measurements. The uncertainty due to lamp measurement repeatability ($u^2_{repeatability}$) was determined using the standard deviation of the mean calculated from a set of three consecutive measurements using the spectroradiometer system. The uncertainty due to lamp measurement reproducibility ($u^2_{reproducibility}$) is the standard deviation of the mean calculated from the results of three independent measurements after each lamp re-alignment. Since the lamp measurement reproducibility partly includes repeatability, as described in section 6.4.12 of the CCPR-K1a.2017 Spectral Irradiance 250 nm to 2500 nm Technical Protocol, these Type A uncertainties have been combined using the equation:

$$u_A = \sqrt{\left(u^2_{repeatability}/n\right) + u^2_{reproducibility}} \quad (5.11.8)$$

where *n*=3 independent measurements.

The estimation of uncertainties in Tables 5.11.3 to 5.11.6 as well as the calculation of combined correlated and uncorrelated uncertainties have been analysed according to the Guide to the expression of uncertainty in measurement (GUM) [44].

### 5.11.5. Acknowledgments

The authors would like to thank A. A. Gaertner for his comments and contributions to the uncertainty analysis in this work.

### 5.11.6. References to section 5.11

[39] L. P. Boivin, C. Bamber, A. A. Gaertner, R. K. Gerson, D. J. Woods, and E. R. Woolliams, J. Mod. Opt, **57** 1648 – 1660 (2010).

[40] A. D. W. Todd and D. J. Woods, Metrologia **50** 20-60 (2013).

[41] K. P. Birch and M. J. Downs, Metrologia, **31** 315–316 (1994).

[42] A. A. Gaertner, Consultative Committee for Thermometry Working Document CCT/10-11 (2010). https://www.bipm.org/cc/CCT/Allowed/25/D11_CCTdraftAAG.pdf.

[10] E. R. Woolliams, *et. al*, Phil. Trans. R. Soc. A **374** 20150044 (2016) (Supplementary Material)

[43] CIE (International Commission on Illumination) Term 17-341, distribution temperature http://eilv.cie.co.at/term/341.

[44] JCGM 100:2008. Joint Committee for Guides in Metrology (September 2008). Evaluation of Measurement Data.

Table 5.11.3. Relative standard ($k$=1) uncertainties for the NRC primary spectral irradiance scale realisation, in %

| λ (nm) | Filter radiometer calibration | HTBB aperture area | HTBB radiance non-uniformity | HTBB Emissivity | Refractive index of air | Filter radiometer to HTBB aperture distance | Lamp distance | Monochromator wavelength (±0.1 nm) | HTBB Temperature stability (0.2 K) | Lamp current | Total correlated uncertainty (%) | Total uncorrelated uncertainty (%) | Total standard uncertainty (%) |
|---|---|---|---|---|---|---|---|---|---|---|---|---|---|
| | Components of HTBB temperature measurement | | | | | | | | | | | | |
| | Uncorrelated | | | | | Correlated | | Uncorrelated | | | | | |
| Type | B | B | B | B | B | B | B | B | B | B | | | |
| 250 | 0.177 | 0.040 | 0.075 | 0.028 | 0.004 | 0.020 | 0.021 | 0.062 | 0.038 | 0.525 | 0.04 | 0.57 | 0.57 |
| 260 | 0.170 | 0.039 | 0.072 | 0.027 | 0.004 | 0.019 | 0.021 | 0.028 | 0.037 | 0.505 | 0.04 | 0.54 | 0.54 |
| 270 | 0.164 | 0.037 | 0.070 | 0.026 | 0.004 | 0.018 | 0.021 | 0.013 | 0.036 | 0.487 | 0.04 | 0.52 | 0.52 |
| 280 | 0.158 | 0.036 | 0.067 | 0.025 | 0.004 | 0.018 | 0.021 | 0.007 | 0.034 | 0.469 | 0.04 | 0.50 | 0.50 |
| 290 | 0.152 | 0.035 | 0.065 | 0.024 | 0.003 | 0.017 | 0.021 | 0.004 | 0.033 | 0.453 | 0.04 | 0.49 | 0.49 |
| 300 | 0.147 | 0.034 | 0.063 | 0.023 | 0.003 | 0.017 | 0.021 | 0.009 | 0.032 | 0.438 | 0.04 | 0.47 | 0.47 |
| 320 | 0.138 | 0.032 | 0.059 | 0.022 | 0.003 | 0.015 | 0.021 | 0.016 | 0.030 | 0.411 | 0.04 | 0.44 | 0.44 |
| 340 | 0.130 | 0.030 | 0.055 | 0.020 | 0.003 | 0.015 | 0.021 | 0.009 | 0.028 | 0.386 | 0.04 | 0.41 | 0.42 |
| 360 | 0.123 | 0.028 | 0.052 | 0.019 | 0.003 | 0.014 | 0.021 | 0.010 | 0.027 | 0.365 | 0.03 | 0.39 | 0.39 |
| 380 | 0.116 | 0.027 | 0.050 | 0.018 | 0.003 | 0.013 | 0.021 | 0.012 | 0.025 | 0.346 | 0.03 | 0.37 | 0.37 |
| 400 | 0.110 | 0.025 | 0.047 | 0.017 | 0.002 | 0.012 | 0.021 | 0.014 | 0.024 | 0.328 | 0.03 | 0.35 | 0.35 |
| 450 | 0.098 | 0.022 | 0.042 | 0.015 | 0.002 | 0.011 | 0.021 | 0.008 | 0.021 | 0.292 | 0.03 | 0.31 | 0.31 |
| 500 | 0.088 | 0.020 | 0.038 | 0.014 | 0.002 | 0.010 | 0.021 | 0.008 | 0.019 | 0.263 | 0.03 | 0.28 | 0.28 |
| 555 | 0.080 | 0.018 | 0.034 | 0.013 | 0.002 | 0.009 | 0.021 | 0.006 | 0.017 | 0.237 | 0.03 | 0.25 | 0.26 |
| 600 | 0.074 | 0.017 | 0.031 | 0.012 | 0.002 | 0.008 | 0.021 | 0.006 | 0.016 | 0.219 | 0.03 | 0.23 | 0.24 |
| 700 | 0.063 | 0.014 | 0.027 | 0.010 | 0.001 | 0.007 | 0.021 | 0.005 | 0.014 | 0.188 | 0.03 | 0.20 | 0.20 |
| 800 | 0.055 | 0.013 | 0.024 | 0.009 | 0.001 | 0.006 | 0.021 | 0.004 | 0.012 | 0.165 | 0.03 | 0.18 | 0.18 |
| 900 | 0.049 | 0.011 | 0.021 | 0.008 | 0.001 | 0.006 | 0.021 | 0.004 | 0.011 | 0.147 | 0.03 | 0.16 | 0.16 |
| 1000 | 0.045 | 0.010 | 0.019 | 0.007 | 0.001 | 0.005 | 0.021 | 0.003 | 0.010 | 0.133 | 0.03 | 0.14 | 0.14 |
| 1100 | 0.041 | 0.009 | 0.017 | 0.006 | 0.001 | 0.005 | 0.021 | 0.003 | 0.009 | 0.121 | 0.03 | 0.13 | 0.13 |
| 1300 | 0.035 | 0.008 | 0.015 | 0.005 | 0.001 | 0.004 | 0.021 | 0.004 | 0.008 | 0.104 | 0.03 | 0.11 | 0.11 |
| 1500 | 0.031 | 0.007 | 0.013 | 0.005 | 0.001 | 0.003 | 0.021 | 0.001 | 0.007 | 0.092 | 0.02 | 0.10 | 0.10 |
| 1700 | 0.028 | 0.006 | 0.012 | 0.004 | 0.001 | 0.003 | 0.021 | 0.002 | 0.006 | 0.083 | 0.02 | 0.09 | 0.09 |
| 2000 | 0.024 | 0.006 | 0.010 | 0.004 | 0.001 | 0.003 | 0.021 | 0.001 | 0.005 | 0.073 | 0.02 | 0.08 | 0.08 |
| 2200 | 0.023 | 0.005 | 0.010 | 0.004 | 0.001 | 0.003 | 0.021 | 0.004 | 0.005 | 0.068 | 0.02 | 0.07 | 0.08 |
| 2300 | 0.022 | 0.005 | 0.009 | 0.003 | 0.000 | 0.002 | 0.021 | 0.003 | 0.005 | 0.066 | 0.02 | 0.07 | 0.07 |
| 2400 | 0.021 | 0.005 | 0.009 | 0.003 | 0.000 | 0.002 | 0.021 | 0.007 | 0.005 | 0.064 | 0.02 | 0.07 | 0.07 |
| 2500 | 0.021 | 0.005 | 0.009 | 0.003 | 0.000 | 0.002 | 0.021 | 0.032 | 0.004 | 0.062 | 0.02 | 0.07 | 0.08 |

Table 5. 11.4. Relative standard (*k*=1) uncertainties for NRC spectral irradiance measurements for lamp **BN-9101-668**, in %

| λ (nm) | Round 1 | | | | | Round 2 | | | | |
|---|---|---|---|---|---|---|---|---|---|---|
| | Primary scale realisation | Lamp measurement repeatability | Lamp measurement reproducibility | Total Type A uncertainty (%) | Combined standard uncertainty (total A+B) (%) | Primary scale realisation | Lamp measurement repeatability | Lamp measurement reproducibility | Total Type A uncertainty (%) | Combined standard uncertainty (total A+B) (%) |
| | Correlated | Uncorrelated | | | | Correlated | Uncorrelated | | | |
| Type | B | A | A | | | B | A | A | | |
| 250 | 0.57 | 1.46 | 1.18 | 1.45 | 1.55 | 0.57 | 1.25 | 0.34 | 0.80 | 0.98 |
| 260 | 0.54 | 1.19 | 0.85 | 1.10 | 1.22 | 0.54 | 1.44 | 1.97 | 2.14 | 2.20 |
| 270 | 0.52 | 0.77 | 0.61 | 0.75 | 0.91 | 0.52 | 0.70 | 0.22 | 0.46 | 0.70 |
| 280 | 0.50 | 0.53 | 0.62 | 0.69 | 0.85 | 0.50 | 0.27 | 0.17 | 0.23 | 0.55 |
| 290 | 0.49 | 0.61 | 0.65 | 0.74 | 0.89 | 0.49 | 0.10 | 0.26 | 0.27 | 0.56 |
| 300 | 0.47 | 0.54 | 0.59 | 0.67 | 0.82 | 0.47 | 0.09 | 0.33 | 0.34 | 0.58 |
| 320 | 0.44 | 0.43 | 0.50 | 0.56 | 0.71 | 0.44 | 0.08 | 0.28 | 0.28 | 0.52 |
| 340 | 0.42 | 0.37 | 0.48 | 0.52 | 0.67 | 0.42 | 0.09 | 0.23 | 0.23 | 0.48 |
| 360 | 0.39 | 0.33 | 0.43 | 0.47 | 0.61 | 0.39 | 0.09 | 0.24 | 0.24 | 0.46 |
| 380 | 0.37 | 0.34 | 0.43 | 0.47 | 0.60 | 0.37 | 0.10 | 0.21 | 0.22 | 0.43 |
| 400 | 0.35 | 0.10 | 0.11 | 0.12 | 0.37 | 0.35 | 0.03 | 0.11 | 0.11 | 0.37 |
| 450 | 0.31 | 0.15 | 0.10 | 0.13 | 0.34 | 0.31 | 0.03 | 0.13 | 0.13 | 0.34 |
| 500 | 0.28 | 0.06 | 0.07 | 0.08 | 0.29 | 0.28 | 0.05 | 0.15 | 0.15 | 0.32 |
| 555 | 0.26 | 0.08 | 0.07 | 0.08 | 0.27 | 0.26 | 0.03 | 0.10 | 0.10 | 0.27 |
| 600 | 0.24 | 0.04 | 0.06 | 0.06 | 0.24 | 0.24 | 0.02 | 0.09 | 0.09 | 0.25 |
| 700 | 0.20 | 0.04 | 0.06 | 0.07 | 0.21 | 0.20 | 0.04 | 0.10 | 0.11 | 0.23 |
| 800 | 0.18 | 0.05 | 0.17 | 0.17 | 0.25 | 0.18 | 0.05 | 0.07 | 0.07 | 0.19 |
| 900 | 0.16 | 0.05 | 0.09 | 0.10 | 0.19 | 0.16 | 0.06 | 0.08 | 0.08 | 0.18 |
| 1000 | 0.14 | 0.07 | 0.11 | 0.12 | 0.19 | 0.14 | 0.07 | 0.07 | 0.08 | 0.16 |
| 1100 | 0.13 | 0.08 | 0.14 | 0.14 | 0.20 | 0.13 | 0.06 | 0.04 | 0.05 | 0.14 |
| 1300 | 0.11 | 0.30 | 0.56 | 0.58 | 0.59 | 0.11 | 0.34 | 0.21 | 0.29 | 0.31 |
| 1500 | 0.10 | 0.70 | 0.56 | 0.69 | 0.70 | 0.10 | 0.70 | 0.49 | 0.63 | 0.64 |
| 1700 | 0.09 | 0.85 | 0.85 | 0.98 | 0.98 | 0.09 | 0.84 | 0.39 | 0.62 | 0.63 |
| 2000 | 0.08 | 1.17 | 1.15 | 1.33 | 1.33 | 0.08 | 1.38 | 0.66 | 1.03 | 1.04 |
| 2200 | 0.08 | 3.75 | 1.37 | 2.56 | 2.56 | 0.08 | 2.42 | 1.44 | 2.01 | 2.01 |
| 2300 | 0.07 | 2.94 | 2.15 | 2.74 | 2.74 | 0.07 | 2.50 | 3.29 | 3.60 | 3.60 |
| 2400 | 0.07 | 4.45 | 3.76 | 4.55 | 4.55 | 0.07 | 3.40 | 2.10 | 2.88 | 2.88 |
| 2500 | 0.08 | 13.50 | 7.30 | 10.68 | 10.68 | 0.08 | 14.72 | 4.23 | 9.49 | 9.49 |

Table 5.11.5. Relative standard (k=1) uncertainties for NRC spectral irradiance measurements for lamp **BN-9101-669**, in %

| λ (nm) | Round 1 | | | | | Round 2 | | | | |
|---|---|---|---|---|---|---|---|---|---|---|
| | Primary scale realisation | Lamp measurement repeatability | Lamp measurement reproducibility | Total Type A uncertainty (%) | Combined standard uncertainty (total A+B) (%) | Primary scale realisation | Lamp measurement repeatability | Lamp measurement reproducibility | Total Type A uncertainty (%) | Combined standard uncertainty (total A+B) (%) |
| | Correlated | Uncorrelated | | | | Correlated | Uncorrelated | | | |
| Type | B | A | A | | | B | A | A | | |
| 250 | 0.57 | 1.24 | 0.71 | 1.01 | 1.16 | 0.57 | 4.29 | 2.01 | 3.19 | 3.24 |
| 260 | 0.54 | 0.71 | 0.33 | 0.52 | 0.76 | 0.54 | 1.81 | 2.04 | 2.29 | 2.36 |
| 270 | 0.52 | 0.26 | 0.32 | 0.35 | 0.63 | 0.52 | 2.09 | 1.22 | 1.71 | 1.79 |
| 280 | 0.50 | 0.17 | 0.42 | 0.43 | 0.66 | 0.50 | 2.04 | 0.88 | 1.47 | 1.56 |
| 290 | 0.49 | 0.17 | 0.24 | 0.26 | 0.55 | 0.49 | 1.93 | 0.83 | 1.39 | 1.47 |
| 300 | 0.47 | 0.10 | 0.24 | 0.25 | 0.53 | 0.47 | 1.85 | 0.80 | 1.33 | 1.41 |
| 320 | 0.44 | 0.08 | 0.22 | 0.22 | 0.49 | 0.44 | 1.70 | 0.72 | 1.22 | 1.29 |
| 340 | 0.42 | 0.09 | 0.16 | 0.17 | 0.45 | 0.42 | 1.57 | 0.73 | 1.16 | 1.24 |
| 360 | 0.39 | 0.06 | 0.17 | 0.17 | 0.43 | 0.39 | 1.57 | 0.69 | 1.14 | 1.20 |
| 380 | 0.37 | 0.07 | 0.14 | 0.15 | 0.40 | 0.37 | 1.49 | 0.68 | 1.10 | 1.16 |
| 400 | 0.35 | 0.06 | 0.02 | 0.04 | 0.36 | 0.35 | 0.11 | 0.16 | 0.17 | 0.39 |
| 450 | 0.31 | 0.06 | 0.03 | 0.05 | 0.32 | 0.31 | 0.06 | 0.14 | 0.14 | 0.34 |
| 500 | 0.28 | 0.05 | 0.03 | 0.04 | 0.29 | 0.28 | 0.06 | 0.14 | 0.14 | 0.32 |
| 555 | 0.26 | 0.05 | 0.04 | 0.04 | 0.26 | 0.26 | 0.06 | 0.09 | 0.10 | 0.27 |
| 600 | 0.24 | 0.04 | 0.03 | 0.04 | 0.24 | 0.24 | 0.08 | 0.10 | 0.11 | 0.26 |
| 700 | 0.20 | 0.04 | 0.04 | 0.04 | 0.21 | 0.20 | 0.09 | 0.08 | 0.09 | 0.22 |
| 800 | 0.18 | 0.07 | 0.04 | 0.06 | 0.19 | 0.18 | 0.09 | 0.11 | 0.12 | 0.22 |
| 900 | 0.16 | 0.03 | 0.04 | 0.04 | 0.16 | 0.16 | 0.19 | 0.07 | 0.13 | 0.20 |
| 1000 | 0.14 | 0.04 | 0.04 | 0.04 | 0.15 | 0.14 | 0.22 | 0.06 | 0.14 | 0.20 |
| 1100 | 0.13 | 0.03 | 0.04 | 0.05 | 0.14 | 0.13 | 0.23 | 0.04 | 0.14 | 0.19 |
| 1300 | 0.11 | 0.71 | 0.16 | 0.44 | 0.45 | 0.11 | 0.94 | 0.12 | 0.56 | 0.57 |
| 1500 | 0.10 | 0.35 | 0.14 | 0.25 | 0.27 | 0.10 | 1.30 | 0.27 | 0.80 | 0.80 |
| 1700 | 0.09 | 0.51 | 0.26 | 0.39 | 0.40 | 0.09 | 1.54 | 0.17 | 0.91 | 0.91 |
| 2000 | 0.08 | 0.62 | 0.70 | 0.79 | 0.79 | 0.08 | 1.54 | 0.92 | 1.28 | 1.28 |
| 2200 | 0.08 | 2.33 | 1.51 | 2.02 | 2.02 | 0.08 | 4.99 | 1.38 | 3.20 | 3.20 |
| 2300 | 0.07 | 3.03 | 1.80 | 2.51 | 2.51 | 0.07 | 5.37 | 0.81 | 3.20 | 3.20 |
| 2400 | 0.07 | 3.93 | 0.82 | 2.41 | 2.41 | 0.07 | 1.85 | 1.80 | 2.09 | 2.09 |
| 2500 | 0.08 | 7.36 | 2.30 | 4.83 | 4.83 | 0.08 | 8.58 | 10.12 | 11.27 | 11.27 |

Table 5.11.6. Relative standard ($k$=1) uncertainties for NRC spectral irradiance measurements for lamp **BN-9101-670**, in %

| λ (nm) | Round 1 | | | | | Round 2 | | | | |
|---|---|---|---|---|---|---|---|---|---|---|
| | Primary scale realisation | Lamp measurement repeatability | Lamp measurement reproducibility | Total Type A uncertainty (%) | Combined standard uncertainty (total A+B) (%) | Primary scale realisation | Lamp measurement repeatability | Lamp measurement reproducibility | Total Type A uncertainty (%) | Combined standard uncertainty (total A+B) (%) |
| | Correlated | Uncorrelated | | | | Correlated | Uncorrelated | | | |
| Type | B | A | A | | | B | A | A | | |
| 250 | 0.57 | 0.59 | 0.61 | 0.70 | 0.90 | 0.57 | 3.35 | 2.40 | 3.09 | 3.14 |
| 260 | 0.54 | 0.67 | 1.19 | 1.26 | 1.37 | 0.54 | 1.21 | 1.00 | 1.22 | 1.33 |
| 270 | 0.52 | 0.87 | 1.08 | 1.19 | 1.30 | 0.52 | 0.61 | 0.44 | 0.57 | 0.77 |
| 280 | 0.50 | 0.73 | 1.06 | 1.14 | 1.25 | 0.50 | 0.32 | 0.06 | 0.20 | 0.54 |
| 290 | 0.49 | 0.73 | 0.97 | 1.05 | 1.16 | 0.49 | 0.29 | 0.13 | 0.21 | 0.53 |
| 300 | 0.47 | 0.70 | 0.86 | 0.95 | 1.06 | 0.47 | 0.28 | 0.13 | 0.21 | 0.52 |
| 320 | 0.44 | 0.55 | 0.73 | 0.79 | 0.91 | 0.44 | 0.15 | 0.04 | 0.10 | 0.45 |
| 340 | 0.42 | 0.57 | 0.65 | 0.73 | 0.84 | 0.42 | 0.14 | 0.05 | 0.10 | 0.43 |
| 360 | 0.39 | 0.52 | 0.61 | 0.68 | 0.78 | 0.39 | 0.14 | 0.08 | 0.11 | 0.41 |
| 380 | 0.37 | 0.49 | 0.58 | 0.65 | 0.75 | 0.37 | 0.15 | 0.04 | 0.10 | 0.38 |
| 400 | 0.35 | 0.06 | 0.06 | 0.07 | 0.36 | 0.35 | 0.03 | 0.03 | 0.03 | 0.36 |
| 450 | 0.31 | 0.06 | 0.07 | 0.08 | 0.32 | 0.31 | 0.02 | 0.03 | 0.03 | 0.32 |
| 500 | 0.28 | 0.04 | 0.06 | 0.07 | 0.29 | 0.28 | 0.04 | 0.01 | 0.03 | 0.28 |
| 555 | 0.26 | 0.05 | 0.04 | 0.05 | 0.26 | 0.26 | 0.01 | 0.01 | 0.01 | 0.26 |
| 600 | 0.24 | 0.05 | 0.05 | 0.06 | 0.24 | 0.24 | 0.05 | 0.01 | 0.03 | 0.24 |
| 700 | 0.20 | 0.05 | 0.05 | 0.05 | 0.21 | 0.20 | 0.05 | 0.01 | 0.03 | 0.21 |
| 800 | 0.18 | 0.06 | 0.14 | 0.14 | 0.23 | 0.18 | 0.04 | 0.01 | 0.02 | 0.18 |
| 900 | 0.16 | 0.10 | 0.04 | 0.07 | 0.17 | 0.16 | 0.08 | 0.04 | 0.06 | 0.17 |
| 1000 | 0.14 | 0.12 | 0.06 | 0.09 | 0.17 | 0.14 | 0.08 | 0.04 | 0.06 | 0.16 |
| 1100 | 0.13 | 0.14 | 0.07 | 0.11 | 0.17 | 0.13 | 0.08 | 0.02 | 0.05 | 0.14 |
| 1300 | 0.11 | 0.55 | 0.34 | 0.47 | 0.48 | 0.11 | 0.31 | 0.69 | 0.71 | 0.72 |
| 1500 | 0.10 | 0.47 | 0.35 | 0.44 | 0.45 | 0.10 | 0.36 | 0.51 | 0.55 | 0.56 |
| 1700 | 0.09 | 0.59 | 0.32 | 0.47 | 0.48 | 0.09 | 0.80 | 0.76 | 0.89 | 0.89 |
| 2000 | 0.08 | 0.94 | 0.51 | 0.75 | 0.75 | 0.08 | 0.75 | 1.54 | 1.60 | 1.60 |
| 2200 | 0.08 | 4.84 | 2.78 | 3.94 | 3.94 | 0.08 | 3.38 | 3.08 | 3.65 | 3.65 |
| 2300 | 0.07 | 2.70 | 2.81 | 3.22 | 3.22 | 0.07 | 6.24 | 2.76 | 4.54 | 4.54 |
| 2400 | 0.07 | 3.76 | 3.90 | 4.46 | 4.46 | 0.07 | 9.41 | 3.18 | 6.30 | 6.30 |
| 2500 | 0.08 | 9.43 | 2.89 | 6.17 | 6.17 | 0.08 | 13.58 | 3.95 | 8.78 | 8.78 |

### 5.11.7. Final uncertainties submitted by NRC with the measurement results

Table 5.11.7. Spectral irradiance standard uncertainties ($k$=1) of the NRC lamp **BN-9101-668** as used for the comparison analysis.

| Wavelength, nm | Round 1 | | | Round 2 | | |
|---|---|---|---|---|---|---|
| | Uncertainties associated with, % | | Combined uncertainty, % | Uncertainties associated with, % | | Combined uncertainty, % |
| | Uncorrelated effects | Correlated effects | | Uncorrelated effects | Correlated effects | |
| 250 | 1.45 | 0.57 | 1.55 | 0.80 | 0.57 | 0.98 |
| 260 | 1.10 | 0.54 | 1.22 | 2.14 | 0.54 | 2.20 |
| 270 | 0.75 | 0.52 | 0.91 | 0.46 | 0.52 | 0.70 |
| 280 | 0.69 | 0.50 | 0.85 | 0.23 | 0.50 | 0.55 |
| 290 | 0.74 | 0.49 | 0.89 | 0.27 | 0.49 | 0.56 |
| 300 | 0.67 | 0.47 | 0.82 | 0.34 | 0.47 | 0.58 |
| 320 | 0.56 | 0.44 | 0.71 | 0.28 | 0.44 | 0.52 |
| 340 | 0.52 | 0.42 | 0.67 | 0.23 | 0.42 | 0.48 |
| 360 | 0.47 | 0.39 | 0.61 | 0.24 | 0.39 | 0.46 |
| 380 | 0.47 | 0.37 | 0.60 | 0.22 | 0.37 | 0.43 |
| 400 | 0.12 | 0.35 | 0.37 | 0.11 | 0.35 | 0.37 |
| 450 | 0.13 | 0.31 | 0.34 | 0.13 | 0.31 | 0.34 |
| 500 | 0.08 | 0.28 | 0.29 | 0.15 | 0.28 | 0.32 |
| 555 | 0.08 | 0.26 | 0.27 | 0.10 | 0.26 | 0.27 |
| 600 | 0.06 | 0.24 | 0.24 | 0.09 | 0.24 | 0.25 |
| 700 | 0.07 | 0.20 | 0.21 | 0.11 | 0.20 | 0.23 |
| 800 | 0.17 | 0.18 | 0.25 | 0.07 | 0.18 | 0.19 |
| 900 | 0.10 | 0.16 | 0.19 | 0.08 | 0.16 | 0.18 |
| 1000 | 0.12 | 0.14 | 0.19 | 0.08 | 0.14 | 0.16 |
| 1100 | 0.14 | 0.13 | 0.20 | 0.05 | 0.13 | 0.14 |
| 1300 | 0.58 | 0.11 | 0.59 | 0.29 | 0.11 | 0.31 |
| 1500 | 0.69 | 0.10 | 0.70 | 0.63 | 0.10 | 0.64 |
| 1700 | 0.98 | 0.09 | 0.98 | 0.62 | 0.09 | 0.63 |
| 2000 | 1.33 | 0.08 | 1.33 | 1.03 | 0.08 | 1.04 |
| 2200 | 2.56 | 0.08 | 2.56 | 2.01 | 0.08 | 2.01 |
| 2300 | 2.74 | 0.07 | 2.74 | 3.60 | 0.07 | 3.60 |
| 2400 | 4.55 | 0.07 | 4.55 | 2.88 | 0.07 | 2.88 |
| 2500 | 10.68 | 0.08 | 10.68 | 9.49 | 0.08 | 9.49 |

Table 5.11.8. Spectral irradiance standard uncertainties ($k$=1) of the NRC lamp **BN-9101-669** as used for the comparison analysis.

| Wavelength, nm | Round 1 | | | Round 2 | | |
|---|---|---|---|---|---|---|
| | Uncertainties associated with, % | | Combined uncertainty, % | Uncertainties associated with, % | | Combined uncertainty, % |
| | Uncorrelated effects | Correlated effects | | Uncorrelated effects | Correlated effects | |
| 250 | 1.01 | 0.57 | 1.16 | 3.19 | 0.57 | 3.24 |
| 260 | 0.52 | 0.54 | 0.76 | 2.29 | 0.54 | 2.36 |
| 270 | 0.35 | 0.52 | 0.63 | 1.71 | 0.52 | 1.79 |
| 280 | 0.43 | 0.50 | 0.66 | 1.47 | 0.50 | 1.56 |
| 290 | 0.26 | 0.49 | 0.55 | 1.39 | 0.49 | 1.47 |
| 300 | 0.25 | 0.47 | 0.53 | 1.33 | 0.47 | 1.41 |
| 320 | 0.22 | 0.44 | 0.49 | 1.22 | 0.44 | 1.29 |
| 340 | 0.17 | 0.42 | 0.45 | 1.16 | 0.42 | 1.24 |
| 360 | 0.17 | 0.39 | 0.43 | 1.14 | 0.39 | 1.20 |
| 380 | 0.15 | 0.37 | 0.40 | 1.10 | 0.37 | 1.16 |
| 400 | 0.04 | 0.35 | 0.36 | 0.17 | 0.35 | 0.39 |
| 450 | 0.05 | 0.31 | 0.32 | 0.14 | 0.31 | 0.34 |
| 500 | 0.04 | 0.28 | 0.29 | 0.14 | 0.28 | 0.32 |
| 555 | 0.04 | 0.26 | 0.26 | 0.10 | 0.26 | 0.27 |
| 600 | 0.04 | 0.24 | 0.24 | 0.11 | 0.24 | 0.26 |
| 700 | 0.04 | 0.20 | 0.21 | 0.09 | 0.20 | 0.22 |
| 800 | 0.06 | 0.18 | 0.19 | 0.12 | 0.18 | 0.22 |
| 900 | 0.04 | 0.16 | 0.16 | 0.13 | 0.16 | 0.20 |
| 1000 | 0.04 | 0.14 | 0.15 | 0.14 | 0.14 | 0.20 |
| 1100 | 0.05 | 0.13 | 0.14 | 0.14 | 0.13 | 0.19 |
| 1300 | 0.44 | 0.11 | 0.45 | 0.56 | 0.11 | 0.57 |
| 1500 | 0.25 | 0.10 | 0.27 | 0.80 | 0.10 | 0.80 |
| 1700 | 0.39 | 0.09 | 0.40 | 0.91 | 0.09 | 0.91 |
| 2000 | 0.79 | 0.08 | 0.79 | 1.28 | 0.08 | 1.28 |
| 2200 | 2.02 | 0.08 | 2.02 | 3.20 | 0.08 | 3.20 |
| 2300 | 2.51 | 0.07 | 2.51 | 3.20 | 0.07 | 3.20 |
| 2400 | 2.41 | 0.07 | 2.41 | 2.09 | 0.07 | 2.09 |
| 2500 | 4.83 | 0.08 | 4.83 | 11.27 | 0.08 | 11.27 |

Table 5.11.9. Spectral irradiance standard uncertainties ($k$=1) of the NRC lamp **BN-9101-670** as used for the comparison analysis.

| Wavelength, nm | Round 1 | | | Round 2 | | |
|---|---|---|---|---|---|---|
| | Uncertainties associated with, % | | Combined uncertainty, % | Uncertainties associated with, % | | Combined uncertainty, % |
| | Uncorrelated effects | Correlated effects | | Uncorrelated effects | Correlated effects | |
| 250 | 0.70 | 0.57 | 0.90 | 3.09 | 0.57 | 3.14 |
| 260 | 1.26 | 0.54 | 1.37 | 1.22 | 0.54 | 1.33 |
| 270 | 1.19 | 0.52 | 1.30 | 0.57 | 0.52 | 0.77 |
| 280 | 1.14 | 0.50 | 1.25 | 0.20 | 0.50 | 0.54 |
| 290 | 1.05 | 0.49 | 1.16 | 0.21 | 0.49 | 0.53 |
| 300 | 0.95 | 0.47 | 1.06 | 0.21 | 0.47 | 0.52 |
| 320 | 0.79 | 0.44 | 0.91 | 0.10 | 0.44 | 0.45 |
| 340 | 0.73 | 0.42 | 0.84 | 0.10 | 0.42 | 0.43 |
| 360 | 0.68 | 0.39 | 0.78 | 0.11 | 0.39 | 0.41 |
| 380 | 0.65 | 0.37 | 0.75 | 0.10 | 0.37 | 0.38 |
| 400 | 0.07 | 0.35 | 0.36 | 0.03 | 0.35 | 0.36 |
| 450 | 0.08 | 0.31 | 0.32 | 0.03 | 0.31 | 0.32 |
| 500 | 0.07 | 0.28 | 0.29 | 0.03 | 0.28 | 0.28 |
| 555 | 0.05 | 0.26 | 0.26 | 0.01 | 0.26 | 0.26 |
| 600 | 0.06 | 0.24 | 0.24 | 0.03 | 0.24 | 0.24 |
| 700 | 0.05 | 0.20 | 0.21 | 0.03 | 0.20 | 0.21 |
| 800 | 0.14 | 0.18 | 0.23 | 0.02 | 0.18 | 0.18 |
| 900 | 0.07 | 0.16 | 0.17 | 0.06 | 0.16 | 0.17 |
| 1000 | 0.09 | 0.14 | 0.17 | 0.06 | 0.14 | 0.16 |
| 1100 | 0.11 | 0.13 | 0.17 | 0.05 | 0.13 | 0.14 |
| 1300 | 0.47 | 0.11 | 0.48 | 0.71 | 0.11 | 0.72 |
| 1500 | 0.44 | 0.10 | 0.45 | 0.55 | 0.10 | 0.56 |
| 1700 | 0.47 | 0.09 | 0.48 | 0.89 | 0.09 | 0.89 |
| 2000 | 0.75 | 0.08 | 0.75 | 1.60 | 0.08 | 1.60 |
| 2200 | 3.94 | 0.08 | 3.94 | 3.65 | 0.08 | 3.65 |
| 2300 | 3.22 | 0.07 | 3.22 | 4.54 | 0.07 | 4.54 |
| 2400 | 4.46 | 0.07 | 4.46 | 6.30 | 0.07 | 6.30 |
| 2500 | 6.17 | 0.08 | 6.17 | 8.78 | 0.08 | 8.78 |

## 5.12. PTB, Germany

### 5.12.1. Description of the measurement facility and primary scale realization

#### *5.12.1.1. Primary scale realisation*

The spectral irradiance scale at the Physikalisch-Technische Bundesanstalt (PTB) in Braunschweig is realized, maintained and disseminated [45] using a high temperature blackbody radiator of type BB3200pg [6]. The various radiometric parameters of this black body have been characterized in detail and it has been found very suitable for use as a primary standard of spectral irradiance [46, 31, 47]. The main parameter of a black body, the temperature, has to be determined very accurately. At the PTB in Braunschweig, broadband-filter detectors are well established for the detector-based determination of the so-called radiometric temperature [46]. Improvements of this procedure and comparisons with other methods have been carried out [47, 48].

The spectral irradiance at the reference plane of the spectroradiometer was calculated according to Planck's law using the geometric parameters and the measured radiometric temperatures of the blackbody.

For the intercomparison the blackbody has been used at different distances around 880 mm and at different temperatures between 2930 K and 3075 K. The measuring aperture 4.14-8 with an aperture size of 111.37 mm² ± 0.02 mm² was used to define the source area of the blackbody. The spectral irradiance at the reference plane of the spectroradiometer was then calculated according to Planck's law using the geometric parameters and the measured radiometric temperatures of the blackbody. The measurement procedure is described within the PTB quality-management system in document QM-AA-4.11-01 (spectral irradiance scale realization).

Since the last CCPR-K1.a intercomparison [2], the primary scale realization and the measurement procedure for dissemination of spectral irradiance has not been changed.

#### *5.12.1.2. Measurement facility*

The PTB spectroradiometer for spectral irradiance calibrations consists of an integrating sphere as entrance optics, an Acton-Research Spectra-Pro$^{TM}$-500 double monochromator system with triple grating turrets and three detectors to cover the spectral range from 250 nm to 2500 nm [49]. The grating turrets are equipped with three gratings with 1200 l/mm for the spectral range from 250 nm up to 1100 nm and 300 l/mm for the infrared spectral range above 1100 nm. The spectral bandwidth of the system is controlled by 8 motorized slits and varies for different spectral regions (Table 5.12.1)

The entrance port of the integrating sphere is formed by a precise aperture with 11 mm diameter which defines the reference plane for spectral irradiance measurements. The detectors at the exit ports of the monochromators are a photomultiplier tube (PMT) for the spectral range from 250 nm to 670 nm, a Si-Photodiode (680 nm to 1100 nm) and an extended InGaAs-detector (1200 nm to 2500 nm). A built-in monitor lamp is used to monitor the stability of the spectroradiometer-system during extended measurement campaigns. The system is placed on a translation stage to allow the quasi-simultaneous measurement of a group of lamps with respect to the blackbody radiation.

The measurement facility is located in the Albert-Einstein building at the PTB Braunschweig. The building has been finished in 2003 and contains air-conditioned labs with a constant relative humidity of 50 % ±5 % at 22 °C ±0.5 °C

Table 5.12.1. Spectral bandwidth expressed as Full width at half maximum (FWHM) for different spectral regions

| Spectral range | FWHM |
|---|---|
| 250 nm – 315 nm | 4.5 nm |
| 320 nm – 470 nm | 2.5 nm |
| 480 nm – 660 nm | 1.0 nm |
| 670 nm – 1100 nm | 2.5 nm |
| 1150 nm – 1350 nm | 5 nm |
| 1400 nm – 2250 nm | 8 nm |
| 2300 nm – 2500 nm | 14 nm |

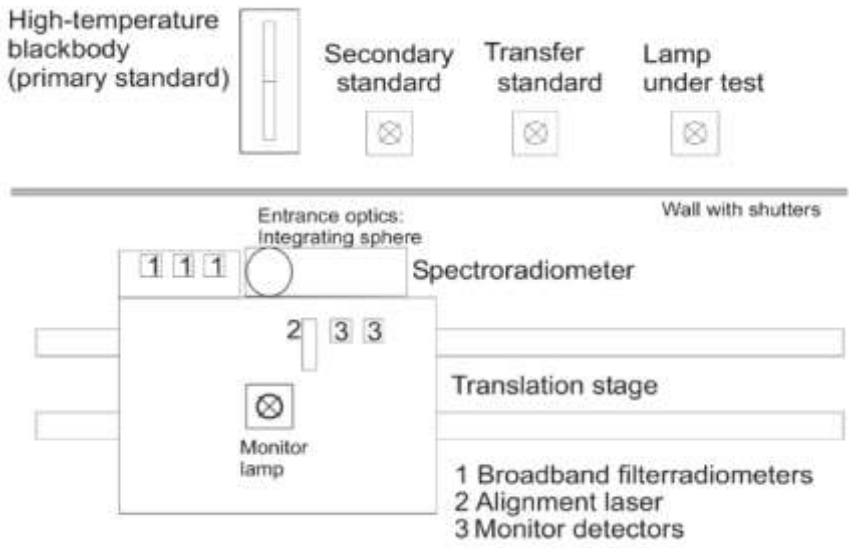


Figure 5.12.1. Set-up of the spectroradiometer facility

### *5.12.1.3. Measurement procedure*

The black body, working standards, or lamps under test, have been measured in nearly identical optical configurations of the system in different successive measurement cycles covering each the whole recommended wavelength range. The stability of the system was assured using the monitor lamp during each measurement cycle such that the photosignal caused by the blackbody source, the standard lamp, or the test lamp was directly compared to the photosignal caused by the monitor lamp at each wavelength position by opening two different entrance ports of the integrating sphere. The stability of the monitor lamp is known to be better than $1 \cdot 10^{-3}\,h^{-1}$ in the UV spectral region.

During each measurement campaign for spectral irradiance realization the standard lamps have been measured repeatedly in alternation with blackbody measurements and measurements of the PTB working standards. The spectral irradiance scale disseminated was averaged over multiple blackbody calibrations using the Photosignal ratio to the monitor lamp. The results were compared to earlier scale realizations using selected standard lamps.

The measurement procedure is as follows: The entire spectral range was always recorded for each source. Between the measurements with the black body, the comparison lamps and other working standards were measured. A total of eight measurements were taken with the blackbody in each round and at least three measurements were taken for each lamp. This interleaving and the use of the monitor lamp made it possible to compare all measurements directly with each other.

At each wavelength setting. the measurements were performed in the following order:

1. wavelength setting
2. adjustment of the slit width
3. setting a higher order filter
4. opening the shutter for the monitor lamp
5. recording of several averages of the photo signal for the monitor lamp
6. closing the shutter for the monitor lamp
7. measurement of the dark photo signal
8. opening the shutter for the standard lamp
9. recording of several averages of the photo signal for the standard lamp
10. closing the shutter of the standard lamp
11. measurement of lamp current and voltage and of ambient parameters

The detailed measurement procedure is documented within the PTB quality-management system in document QM-AA-4.11-02 (spectral irradiance calibrations).

### 5.12.2. Uncertainty budget

In this document the mathematical functions and the input quantities as well as their associated uncertainties are presented. Due to its complexity. the derivation and detailed description of all components of the mathematical models is not described in this document.

The complete measurement uncertainty budgets for the blackbody radiator temperature measurement. the spectral irradiance scale realization and the calibration procedure are described in detail in [6] and in the PTB quality-management system in documents QM-AA-4.11-01 and QM-AA-4.11-02.

The evaluation of uncertainty propagation was performed using Monte Carlo simulation.

#### *5.12.2.1. Black-body radiator temperature measurements*

The broadband-filter detectors measure the irradiance of the blackbody radiator weighted according to their spectral responsivity. Their photosignal is a measure for the temperature of the blackbody radiator.

This relationship can be described as follows:

$$U_{FB}(T_{BB}) = \varepsilon \cdot (V_{iU} + \delta V_{iU}) \cdot \cos\epsilon_1 \cdot \cos\epsilon_2 \cdot \frac{A_{BB}+\delta A_{BB}}{d_{FD}^2} \cdot (s_{abs} + \delta s_{abs}) \int s_{rel}(\lambda) \frac{c_1}{\pi \cdot \mathrm{n}^2 \cdot \lambda^5} \frac{1}{\exp\left(\frac{c2}{n \cdot \lambda \cdot T_{BB}}\right) - 1} d\lambda \quad (5.12.1)$$

The quantities used in this equation are

- $U_{\mathrm{FD}}$ photosignal of the broadband-filter detector measured in Volts
- $\varepsilon$ effective emissivity of the blackbody radiator
- $V_{\mathrm{iU}}$, $\delta V_{\mathrm{iU}}$ gain of the electrical measurements and its drift
- cos $\varepsilon_1$. cos $\varepsilon_2$ misalignment of filter detector to the optical axis of the black body

- $A_{BB}$, $\delta A_{BB}$ size of the blackbody opening aperture and its drift
- $d_{FD}$ distance of the filter detector to the blackbody aperture
- $s_{abs}$, $\delta s_{abs}$ absolute spectral responsivity of the filter detector and its drift
- $s_{rel}$ relative spectral responsivity distribution of the filter detector
- $\lambda$ wavelength used for calculation
- $T_{BB}$ radiometric temperature of the blackbody radiator
- $c_1$, $c_2$ the first and second radiation constants
- $n$ refractive index of air

Table 5.12.2. Standard measurement uncertainties for blackbody radiator temperature measurements

| Quantity | | Type A Uncertainty | Type B Uncertainty | Uncertainty of Temperature / K @ 3000 K |
|---|---|---|---|---|
| effective blackbody emissivity | $\varepsilon$ | | 0.01 % | 0.04 |
| blackbody alignment | cos $\varepsilon_1$ | | 1 ° | 0.05 |
| detector alignment | cos $\varepsilon_2$ | | 1 ° | 0.05 |
| blackbody aperture | $A_{BB}$ | | 0.02 mm² | 0.12 |
| aperture contamination during operation | $A_{BB}$ | | 0.02 % | 0.04 |
| distance detector to blackbody | $d_{FD}$ | | 0.05 mm | 0.07 |
| absolute detector responsivity | $s_{abs}$ | | 0.25 % | 0.89 |
| relative detector responsivity | $s_{rel}$ | | 0.01 % | 0.04 |
| responsivity drift between calibrations | $\delta s_{abs}$ | | 0.1 % | 0.38 |
| detector signal readings | $U_{FD}$ | 0.01 % | | 0.04 |
| gain and drift of electrical measurements | $V_{iU}.\delta V_{iU}$ | | 0.001 % | < 0.01 |
| Total standard measurement uncertainty | | | | 0.97 |
| Expanded uncertainty (k=2) | | | | 1.9 |

### *5.12.2.2. Primary spectral irradiance scale realisation*

With the temperature of the blackbody-radiator known, its spectral irradiance can directly be calculated as follows

$$E_{\lambda.BB}(\lambda, T_P) = \varepsilon \cdot \cos\epsilon_{diff1} \cdot \cos\epsilon_{diff2} \cdot \frac{A_{BB}+\delta A_{BB}}{{d_{diff}}^2} \cdot \frac{c_1}{\pi \cdot n^2 \cdot \lambda^5} \cdot \frac{1}{\exp\left(\frac{c_2}{n \cdot \lambda \cdot (T_P + \delta T_{BB} + \Delta T_{BB})}\right) - 1} \quad (5.12.2)$$

The quantities used in this equation are

- $E_{\lambda.BB}$ calculated spectral irradiance of the blackbody-radiator
- $\varepsilon$ emissivity of the blackbody radiator
- cos $\varepsilon_{diff1}$, cos $\varepsilon_{diff2}$ alignment of the integrating sphere opening to the optical axis of the black body
- $A_{BB}$, $\delta A_{BB}$ size and its drift of the black body opening aperture
- $d_{diff}$ distance of the integrating sphere opening to the black body aperture
- $\lambda$ calculated wavelength

- $T_P$ radiometric temperature of the blackbody radiator determined by the filter detectors
- $\delta T_{BB}$ correction for blackbody temperature drift during measurement
- $\Delta T_{BB}$ correction for blackbody nonuniformity
- $c_1$, $c_2$ the first and second radiation constants
- $n$ refractive index of air

The input quantities have the following uncertainty contributions to the calculated spectral irradiance:

- The **emissivity** $\varepsilon$ is determined with a standard uncertainty of $u(\varepsilon) = 0.05$ % and is fully correlated for all measurements and all wavelengths.
- The **alignment of the blackbody and the entrance optics cos** $\varepsilon_{diff1}$ **and cos** $\varepsilon_{diff2}$ is considered uncorrelated for all measurements with a standard uncertainty of 0.02 % each.
- The **size of the blackbody opening aperture** $A_{BB} = 111.37$ mm² is determined with an uncertainty of 0.02 mm² corresponding to a fully correlated relative uncertainty of 0.02 %.
- The **drift of the blackbody opening aperture** $\delta A_{BB}$ due to contamination of the aperture during is assigned to be zero with an uncorrelated uncertainty contribution of 0.01 %.
- The uncertainty for the **distance between blackbody opening and entrance optics** $d_{diff}$ is split into a fully correlated part for the gauge calibration of 0.05 mm and an uncorrelated part for the distance measurement of 0.05 mm corresponding to relative uncertainties of 0.01 % each.
- The **wavelength** $\lambda$ has no associated uncertainty because it is used as an exact calculation parameter.

The emissivity $\varepsilon$, the size of the black body opening aperture $A_{BB}$ and its drift $\delta A_{BB}$ in the mathematical model for the spectral irradiance are strongly correlated with the same input quantities that were used to determine the blackbody radiator temperature $T_{BB}$. The correlation slightly reduces the associated uncertainty for **the radiometric temperature of the blackbody** $T_P$ used to calculate the spectral irradiance. A standard measurement uncertainty is 0.7 K is considered that is correlated for all measurements and all wavelengths.

Although the blackbody temperature is determined separately for each wavelength setting, a slight **blackbody temperature drift** $\delta T_{BB}$ might occur. It is considered to be zero with an uncertainty of 0.05 K uncorrelated for all wavelengths and all measurements.

The spectral irradiance of the blackbody comes with a slight nonuniformity. The effect can be expressed by a temperature nonuniformity over the irradiated area and thus the **correction for the blackbody nonuniformity** $\Delta T_{BB}$ is the average temperature correction. It is considered to be zero with an uncorrelated uncertainty of 0.15 K.

### *5.12.2.3. Calibration procedure*

The mathematical model of the calibration procedure considers that separate measurements of the monitor lamp against the working standard $B$ (at the time $t_1$) and the transfer standard $S$ (at the time $t_2$) have to be combined. Several adjustment factors $\alpha$ have to be considered under varying conditions. The spectral irradiance of the transfer standard can be expressed as follows

$$E_{\lambda,S}(\lambda,t_2,T_S) = \frac{v_S(\lambda_2,b,t_2,T_S)}{v_M(\lambda_2,b,t_2,T_M)} \cdot \alpha_{\lambda,S,M}(\lambda,\lambda_2,t_2) \cdot \alpha_{L,S,M}(t_2) \cdot \alpha_{\epsilon,S}(t_2) \cdot \alpha_{d,S}(t_2) \frac{\alpha_{I,S}(t_2)}{\alpha_{I,M}(t_2)} \cdot \frac{1}{\alpha_{t,M}(\lambda,t_2,t_1)} \cdot \frac{v_M(\lambda_1,b,t_1,T_M)}{v_B(\lambda_1,b,t_1,T_B)} \cdot \alpha_{\lambda,B,M}(\lambda,\lambda_1,t_1) \cdot \alpha_{L,B,M}(t_1) \cdot \frac{1}{\alpha_{\epsilon,B}(t_1)\cdot\alpha_{d,B}(t_1)} \cdot \frac{\alpha_{I,M}(t_1)}{\alpha_{I,B}(t_1)} \cdot \frac{1}{\alpha_{t,B}(\lambda,t_2,t_1)} \cdot E_{\lambda,B}(\lambda,t_0,T_B) \quad (5.12.3)$$

The quantities used in this equation are

- $E_{\lambda,S}$ calibrated spectral irradiance of the transfer standard
- $t_0$, $t_1$ and $t_2$ times of measurements/calibrations
- $\lambda$ calculated wavelength
- $\lambda_1$, $\lambda_2$ wavelengths set at the monochromator system at times $t_1$ and $t_2$
- $T_S$, $T_B$, $T_M$ distributions temperatures of the transfer standard, the working standard and the monitor lamp
- $b$ spectral bandwidth of the monochromator system
- $v_S$, $v_B$, $v_M$ photosignals of the detectors for the different lamps
- $\alpha_{\lambda,S,M}$, $\alpha_{\lambda,B,M}$ combined adjustment factors for wavelength settings at times $t_1$ and $t_2$
- $\alpha_{L,S,M}$, $\alpha_{L,B,M}$ combined adjustment factors for nonlinearity of the measurement electronics at times $t_1$ and $t_2$
- $\alpha_{d,S}$, $\alpha_{d,B}$ adjustment factors for distance settings of the transfer standard and the working standard
- $\alpha_{\varepsilon,S}$, $\alpha_{\varepsilon,B}$ adjustment factors for alignment of the transfer standard and the working standard
- $\alpha_{I,S}$, $\alpha_{I,B}$, $\alpha_{I,M}$ adjustment factors for electrical current settings of any of the lamps
- $\alpha_{t,B}$, $\alpha_{t,M}$ adjustment factors for the drift of the working standard and the monitor lamp / measurement facility since the last measurement or calibration
- $E_{\lambda,B}$ spectral irradiance of the working standard

All adjustment factors and form factors are selected to be unity under the ideal conditions of the defined calibration procedures. Their associated uncertainties are considered for these conditions.

The combined adjustment factors take into account, that a misadjustment of a quantity (e.g. the spectral bandwidth $b$ or the wavelength $\lambda$) has the same effect on the monitor lamp and the other lamp measured at the same time. If for instance the distribution temperatures of the two lamps are similar, a misadjustment of the wavelength has a negligible effect on the ratio of the photosignals measured at the same time. Therefore the associated measurement uncertainty of these quantities for the spectral irradiance calibration can be significantly lower than usually assumed.

The input quantities have the following uncertainty contributions to the calculated spectral irradiance:

The **distribution temperatures $T_S$, $T_B$, $T_M$** for all lamps used are nearly identical around 3100 K. They do not need to be exactly known. Therefore, the lamps considered to be Planckian like radiators all have a very similar relative spectral distribution. The effect of changes in temperature can be evaluated by calculating the ratio of two Planckian radiators at the different temperatures. Changes of electrical parameters could be expressed as changes in distribution temperatures and the resulting spectral changes can be calculated. Figure 5.12.2 shows the relative spectral change of the spectral irradiance due to temperature changes of 0.02 % (0.7 K), 0.05 % (1.5 K) and 0.1 % (3 K).

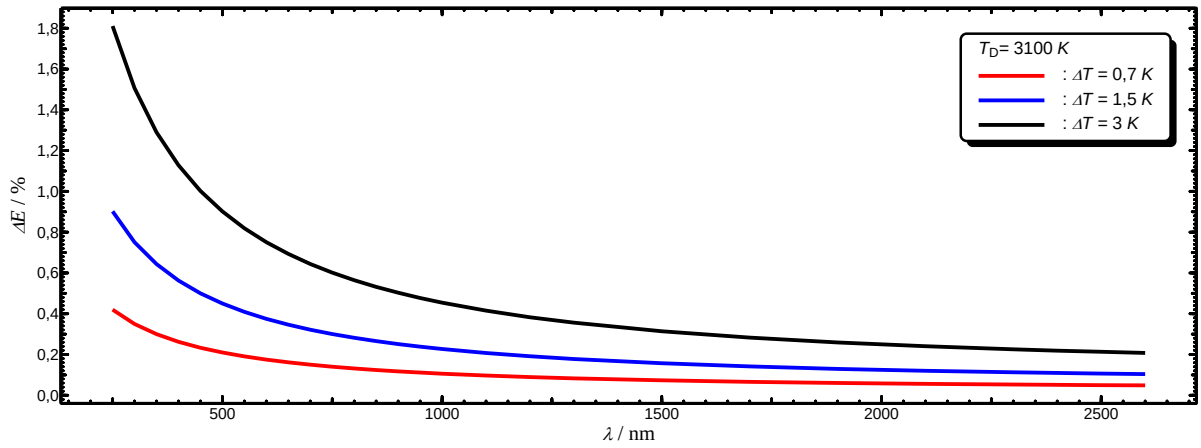


Figure 5.12.2. Relative spectral change of a Planckian radiator due to distribution temperature changes

The **spectral bandwidth** ***b*** of the monochromator system controlled by the slit width at the entrance and exit ports varies with wavelength. The slit width is individually set for every measuring point and is identical for monitor lamp and working standard or blackbody. Due to the application of the substitution method, the similar shape of the spectral irradiance distributions for all radiometric sources and the use of the monitor lamp, any possible corrections are considered to be 1 with an uncertainty <0.01% for all wavelengths.

The **photosignals** $v_S$, $v_B$, $v_M$ of the detectors are dark-signal corrected. Multiple readings are taken at every wavelength setting. The uncertainty of the mean of the readings depends on the spectral region and on the detectors used. In Figure 5.12.3 the typical uncertainty contribution for one measurement run of BN-9101-661 and for the monitor lamp is shown. It is wavelength dependent and considered uncorrelated for all wavelengths and all measurement runs.

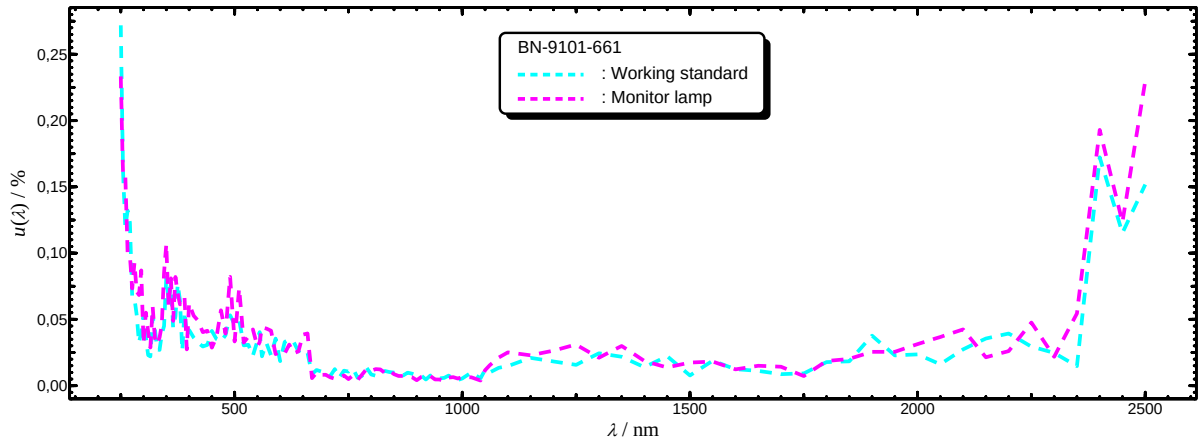


Figure 5.12.3. Typical uncertainty component of the mean for photosignals for working standard and monitor lamps

The wavelengths set at the monochromator system $\lambda_1, \lambda_2$ have an uncertainty of 0.1 nm. The relative change of the assigned spectral irradiance of lamp due to a wavelength error of 0.1 nm is shown in Figure 5.12.4. As both the monitor lamp and the working standard or the transfer standard will always be at identical wavelength settings. the changes in photocurrent for both will be nearly

the same and therefore the **combined adjustment factors for wavelength settings** $\alpha_{\lambda,S,M}, \alpha_{\lambda,B,M}$ will be 1 with an uncertainty <0.01% for all wavelengths.

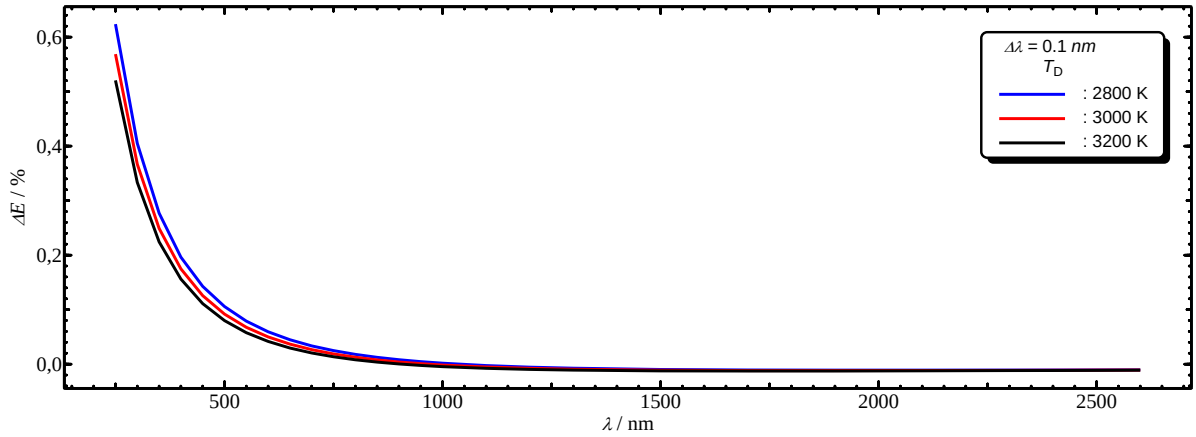


Figure 5.12.4. Relative spectral change of lamp spectral irradiance due to a wavelength error of 0.1 nm at different distribution temperatures.

The nonlinearity of the measurement electronics depends on the detectors used. It is assumed to be less than 0.1 % for the PMT and the Si-photodiode and less than 0.5 % for the InGaAs-detector. As both monitor lamp and working standard or transfer standard generate similar photosignals, effects of nonlinearity are nearly cancelled out and the **combined adjustment factors** $\alpha_{L,S,M}, \alpha_{L,B,M}$ **for nonlinearity** of the measurement electronics are considered to be 1 with an uncertainty of <0.01 %.

The distance of the standards to the entrance optics of the monochromator system is measured using a calibrated tubular inside micrometer. All distance measurements are to a certain extent correlated with each other. The absolute uncertainty for the distance measurements is estimated to be 0.05 mm. In addition, an uncorrelated part of each individual distance measurement of another 0.05 mm is assumed. Thus, the measurement uncertainty contributions of the **adjustment factors for distance settings** $\alpha_{d,s}, \alpha_{d,B}$ are partially correlated. but spectrally independent.

The electrical current with which a lamp is operated is a critical parameter for spectroradiometric quantities. For the standards, the lamp current of 8.1 A is fixed. This is set with an absolute measurement uncertainty of 0.0003 A. According to Stefan-Boltzmann's law, the radiated power of a temperature radiator is proportional to the fourth power of the temperature. Although the lamps have a temperature-dependent resistance. Ohm's law can be assumed for small changes and the electrical power is thus proportional to the square of the lamp current. Thus, a change $\Delta I$ in the lamp current is transformed into a quadratic change in the distribution temperature.

$$\frac{I+\Delta I}{I} = \left(\frac{T+\Delta T}{T}\right)^2 \tag{5.12.4}$$

Therefore. the uncertainty of 0.0003 A at a lamp current of 8.1 A leads to an uncertainty of 0.7 K for the distribution temperature of 3100 K for the lamp. The associated relative measurement uncertainty for the **adjustment factors for electrical current** $\alpha_{I,S}, \alpha_{I,B}, \alpha_{I,M}$ is similar to the curves shown in Figure 5.12.2. It is important, that these assumptions are valid only for very low variations of the electric parameters of the lamp. It is also assumed, that the electrical current is stabilized to better than 0.0003 A which results in an additional uncorrelated uncertainty contribution.

The uncertainty of the **adjustment factor for drift of the working standards and the repeatability of the measurement facility** $\alpha_{t,B}$ can be estimated as shown in Figure 5.12.5 based on many years of experience. These uncertainties are considered to be uncorrelated for the lamps and wavelengths. The increase of the measurement uncertainty at 2500 nm is attributed to the low sensitivity of the InGaAs detector and the resulting deviations and necessary corrections.

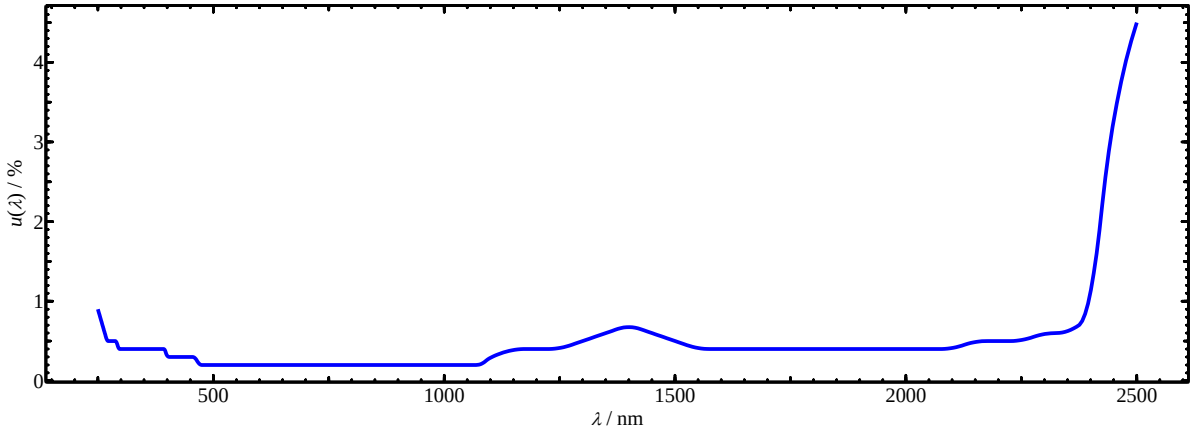


Figure 5.12.5. Uncertainty component due to drift of working standards and repeatability of measurement facility based on long-term experiences

The temporal stability and drift of the monitor lamp can be taken into account by the **adjustment factor for drift of the monitor lamp** $\alpha_{t,M}$. The monitor lamp is used to correct for short term changes of the measurement facility. Its drift is registered and compensated by the repeated measurements with the black body. Therefore an additional correction is not necessary and the uncertainty of the correction factor is assumed to be uncorrelated at 0.1 %.

#### *5.12.2.4. Uncertainty budget summary*

The multiple uncertainty contributions have been described in detail. Monte-Carlo simulation is used to determine the measurement uncertainties of the spectral irradiance of the individual lamps. The resulting correlated and uncorrelated measurement uncertainty contributions and the combined standard measurement uncertainty are shown exemplarily for the lamp BN-9101-661 in Table 5.12.3.

### 5.12.3. Working standards and Comparison lamps

A set of working standards (all 1000 W FEL-type tungsten halogen lamps) was calibrated simultaneously with the traveling lamps for the CCPR-K1.a.2017 intercomparison. So it is ensured that lamps for customers, which are calibrated against the PTB working standards, are linked to the same scale realization as the standards for the CCPR-K1.a.2017 intercomparison. The laboratory standards used for customer calibrations are documented in the PTB quality-management system.

Table 5.12.3. Standard Measurement uncertainties for lamp BN-9101-661

| $\lambda$ nm | Uncorrelated (k=1) | Correlated (k=1) | Combined (k=1) | Expanded (k=2) |
|---|---|---|---|---|
| 250 | 0.64% | 0.59% | 0.87% | 1.74% |
| 260 | 0.53% | 0.57% | 0.78% | 1.56% |
| 270 | 0.44% | 0.55% | 0.70% | 1.40% |
| 280 | 0.43% | 0.53% | 0.69% | 1.38% |
| 290 | 0.42% | 0.51% | 0.66% | 1.32% |
| 300 | 0.38% | 0.50% | 0.63% | 1.26% |
| 320 | 0.37% | 0.47% | 0.60% | 1.20% |
| 340 | 0.35% | 0.45% | 0.57% | 1.14% |
| 360 | 0.35% | 0.43% | 0.55% | 1.10% |
| 380 | 0.34% | 0.41% | 0.53% | 1.06% |
| 400 | 0.30% | 0.39% | 0.50% | 1.00% |
| 450 | 0.28% | 0.35% | 0.46% | 0.92% |
| 500 | 0.25% | 0.33% | 0.42% | 0.84% |
| 555 | 0.24% | 0.30% | 0.39% | 0.78% |
| 600 | 0.23% | 0.29% | 0.37% | 0.74% |
| 700 | 0.22% | 0.26% | 0.34% | 0.68% |
| 800 | 0.21% | 0.24% | 0.32% | 0.64% |
| 900 | 0.20% | 0.23% | 0.31% | 0.62% |
| 1000 | 0.20% | 0.22% | 0.30% | 0.60% |
| 1100 | 0.24% | 0.21% | 0.32% | 0.64% |
| 1300 | 0.31% | 0.20% | 0.37% | 0.74% |
| 1500 | 0.30% | 0.19% | 0.36% | 0.72% |
| 1700 | 0.26% | 0.19% | 0.32% | 0.64% |
| 2000 | 0.27% | 0.18% | 0.32% | 0.64% |
| 2200 | 0.35% | 0.18% | 0.39% | 0.78% |
| 2300 | 0.36% | 0.18% | 0.40% | 0.80% |
| 2400 | 0.49% | 0.18% | 0.52% | 1.04% |
| 2500 | 3.03% | 0.18% | 3.02% | 6.04% |

The following traveling lamps have been used for the CCPR-K1.a.2017 intercomparison: BN-9101-661, BN-9101-662 and BN-9101-681.

All lamps are 1000 W FEL-type quartz-halogen lamps. The lamps were adjusted in a distance of 500 mm with respect to the front plate of their mount using alignment jigs supplied with the lamps.

The lamps were all operated at 8.1 A constant DC current. The polarity is marked at the lamps mount. The lamps showed no significant voltage changes during their operations. Measurements were made in the sequence PTB-VNIIOFI-PTB. The details of the voltage, burning time and the measurement sequence are summarized in the trebles below.

The lamps have been hand-carried between the NMIs.

| BN-9101-661 | | lamp voltage | burning time |
|---|---|---|---|
| PTB | June 2017 | 108.74 V | 09:20 h |
| VNIIOFI | April-July 2018 | 108.75 V | 10:50 h |
| PTB | December 2018 | 108.76 V | 06:50 h |

| BN-9101-662 | | lamp voltage | burning time |
|---|---|---|---|
| PTB | June 2017 | 108.61 V | 08:25 h |
| VNIIOFI | April-June 2018 | 108.64 V | 12:10 h |
| PTB | December 2018 | 108.64 V | 06:20 h |

| BN-9101-681 | | lamp voltage | burning time |
|---|---|---|---|
| PTB | June 2017 | 109.21 V | 06:20 h |
| VNIIOFI | April-July 2018 | 109.25 V | 13:30 h |
| PTB | December 2018 | 109.30 V | 04:55 h |

### 5.12.4. References to section 5.12

[2] E.R. Woolliams, N.P. Fox, M.G. Cox, P.M. Harris and N.J. Harrison, *Final report on CCPR K1-a: Spectral Irradiance from 250 nm to 2500 nm*, Metrologia, 43 (1A Tech. Suppl.). (2006) S98-S104.

[45] Metzdorf J., Metrologia, 1993, 30, 403-408.

[6] Sapritsky V. I., Khlevnoy B. B., Khromchenko V. B., Lisiansky B. E., Mekhontsev S. N., Melenevsky U. A., Morozova S. P., Prokhorov A. V., Samoilov L. N., Shapoval V. I., Sudarev K. A., Zelener M. F., Appl. Opt., 1997, 36, 5403-5408.

[46] Sperfeld P., Metzdorf J., Galal Yousef S., Stock K. D., Möller W., Metrologia, 1998, 35, 267-271.

[31] Sperfeld P., Metzdorf J., Harrison N. J., Fox N. P., Khlevnoy B. B., Khromchenko V. B. Mekhontsev S. N., Shapoval V. I., Zelener M. F., Sapritsky V. I., Metrologia, 1998, 35, 419-422.

[47] Sperfeld P., Entwicklung einer empfängergestützten spektralen Bestrahlungs-stärkeskala, Braunschweig, 1999. http://www.biblio.tu-bs.de/ediss/data/19990628a/19990628a.html

[48] Khlevnoy B.B., Harrison N.J., Rogers L.J., Pollard D.F., Fox N.P., Sperfeld P., Fischer J., Friedrich R., Metzdorf J., Seidel J., Samoylov M.L., Stolyarevskaya R.I., Khromchenko V.B., Ogarev S.A., Sapritsky V.I., Metrologia, 2003, 40, S39–S44

[49] P. Sperfeld, S. Pape and B. Barton, *From Primary Standard to Mobile Measurements - Overview of the Spectral Irradiance Calibration Equipment at PTB,* MAPAN- Journal of Metrology Society of India, 25 (2010) 11-19.

### 5.12.5. Final uncertainties submitted by PTB with the measurement results

Table 5.12.4. PTB Spectral Irradiance standard uncertainties (k=1) of the lamp **BN-9101-661**

| Wavelength, nm | Round 1 | | | Round 2 | | |
|---|---|---|---|---|---|---|
| | Uncertainties associated with, % | | Combined uncertainty, % | Uncertainties associated with, % | | Combined uncertainty, % |
| | Uncorrelated effects | Correlated effects | | Uncorrelated effects | Correlated effects | |
| 250 | 0.61% | 0.57% | 0.84% | 0.64% | 0.59% | 0.87% |
| 260 | 0.50% | 0.55% | 0.74% | 0.53% | 0.57% | 0.78% |
| 270 | 0.42% | 0.53% | 0.67% | 0.44% | 0.55% | 0.70% |
| 280 | 0.41% | 0.51% | 0.65% | 0.43% | 0.53% | 0.69% |
| 290 | 0.40% | 0.49% | 0.64% | 0.42% | 0.51% | 0.66% |
| 300 | 0.36% | 0.48% | 0.60% | 0.38% | 0.50% | 0.63% |
| 320 | 0.35% | 0.45% | 0.57% | 0.37% | 0.47% | 0.60% |
| 340 | 0.34% | 0.43% | 0.55% | 0.35% | 0.45% | 0.57% |
| 360 | 0.33% | 0.41% | 0.53% | 0.35% | 0.43% | 0.55% |
| 380 | 0.32% | 0.39% | 0.51% | 0.34% | 0.41% | 0.53% |
| 400 | 0.29% | 0.38% | 0.47% | 0.30% | 0.39% | 0.50% |
| 450 | 0.27% | 0.34% | 0.44% | 0.28% | 0.35% | 0.46% |
| 500 | 0.24% | 0.32% | 0.40% | 0.25% | 0.33% | 0.42% |
| 555 | 0.23% | 0.29% | 0.37% | 0.24% | 0.30% | 0.39% |
| 600 | 0.22% | 0.28% | 0.35% | 0.23% | 0.29% | 0.37% |
| 700 | 0.21% | 0.25% | 0.33% | 0.22% | 0.26% | 0.34% |
| 800 | 0.20% | 0.24% | 0.31% | 0.21% | 0.24% | 0.32% |
| 900 | 0.19% | 0.22% | 0.30% | 0.20% | 0.23% | 0.31% |
| 1000 | 0.19% | 0.22% | 0.29% | 0.20% | 0.22% | 0.30% |
| 1100 | 0.23% | 0.21% | 0.31% | 0.24% | 0.21% | 0.32% |
| 1300 | 0.32% | 0.20% | 0.38% | 0.31% | 0.20% | 0.37% |
| 1500 | 0.30% | 0.19% | 0.36% | 0.30% | 0.19% | 0.36% |
| 1700 | 0.26% | 0.19% | 0.32% | 0.26% | 0.19% | 0.32% |
| 2000 | 0.31% | 0.18% | 0.36% | 0.27% | 0.18% | 0.32% |
| 2200 | 0.50% | 0.18% | 0.53% | 0.35% | 0.18% | 0.39% |
| 2300 | 0.42% | 0.18% | 0.46% | 0.36% | 0.18% | 0.40% |
| 2400 | 0.60% | 0.18% | 0.63% | 0.49% | 0.18% | 0.52% |
| 2500 | 4.32% | 0.18% | 4.35% | 3.03% | 0.18% | 3.02% |

Table 5.12.5. PTB Spectral Irradiance standard uncertainties (k=1) of the lamp **BN-9101-662**

| Wavelength, nm | Round 1 | | | Round 2 | | |
|---|---|---|---|---|---|---|
| | Uncertainties associated with, % | | Combined uncertainty, % | Uncertainties associated with, % | | Combined uncertainty, % |
| | Uncorrelated effects | Correlated effects | | Uncorrelated effects | Correlated effects | |
| 250 | 0.61% | 0.57% | 0.83% | 0.65% | 0.59% | 0.87% |
| 260 | 0.50% | 0.55% | 0.74% | 0.53% | 0.56% | 0.77% |
| 270 | 0.42% | 0.52% | 0.67% | 0.45% | 0.55% | 0.70% |
| 280 | 0.41% | 0.51% | 0.66% | 0.43% | 0.53% | 0.68% |
| 290 | 0.39% | 0.49% | 0.64% | 0.42% | 0.51% | 0.66% |
| 300 | 0.36% | 0.48% | 0.60% | 0.38% | 0.50% | 0.63% |
| 320 | 0.35% | 0.45% | 0.57% | 0.37% | 0.47% | 0.60% |
| 340 | 0.34% | 0.43% | 0.55% | 0.36% | 0.45% | 0.57% |
| 360 | 0.33% | 0.41% | 0.53% | 0.35% | 0.42% | 0.55% |
| 380 | 0.32% | 0.39% | 0.51% | 0.34% | 0.40% | 0.53% |
| 400 | 0.29% | 0.37% | 0.47% | 0.30% | 0.39% | 0.49% |
| 450 | 0.27% | 0.34% | 0.44% | 0.29% | 0.35% | 0.46% |
| 500 | 0.24% | 0.32% | 0.39% | 0.25% | 0.33% | 0.41% |
| 555 | 0.22% | 0.29% | 0.37% | 0.24% | 0.30% | 0.39% |
| 600 | 0.22% | 0.28% | 0.35% | 0.23% | 0.29% | 0.37% |
| 700 | 0.20% | 0.25% | 0.32% | 0.22% | 0.26% | 0.34% |
| 800 | 0.20% | 0.24% | 0.31% | 0.21% | 0.24% | 0.32% |
| 900 | 0.19% | 0.22% | 0.30% | 0.20% | 0.23% | 0.31% |
| 1000 | 0.19% | 0.21% | 0.29% | 0.20% | 0.22% | 0.30% |
| 1100 | 0.22% | 0.21% | 0.30% | 0.24% | 0.21% | 0.32% |
| 1300 | 0.34% | 0.20% | 0.39% | 0.34% | 0.20% | 0.40% |
| 1500 | 0.30% | 0.19% | 0.36% | 0.30% | 0.19% | 0.36% |
| 1700 | 0.26% | 0.19% | 0.32% | 0.27% | 0.19% | 0.32% |
| 2000 | 0.34% | 0.18% | 0.38% | 0.32% | 0.18% | 0.37% |
| 2200 | 0.55% | 0.18% | 0.58% | 0.44% | 0.18% | 0.48% |
| 2300 | 0.45% | 0.18% | 0.48% | 0.48% | 0.18% | 0.51% |
| 2400 | 0.54% | 0.18% | 0.57% | 0.49% | 0.18% | 0.53% |
| 2500 | 3.80% | 0.18% | 3.81% | 3.00% | 0.18% | 3.02% |

Table 5.12.6. Spectral Irradiance standard uncertainties (k=1) of the lamp **BN-9101-681**

| Wavelength, nm | Round 1 | | | Round 2 | | |
|---|---|---|---|---|---|---|
| | Uncertainties associated with, % | | Combined uncertainty, % | Uncertainties associated with, % | | Combined uncertainty, % |
| | Uncorrelated effects | Correlated effects | | Uncorrelated effects | Correlated effects | |
| 250 | 0.62% | 0.59% | 0.86% | 0.63% | 0.59% | 0.87% |
| 260 | 0.52% | 0.57% | 0.77% | 0.52% | 0.57% | 0.77% |
| 270 | 0.44% | 0.55% | 0.70% | 0.44% | 0.55% | 0.71% |
| 280 | 0.43% | 0.53% | 0.68% | 0.43% | 0.53% | 0.69% |
| 290 | 0.41% | 0.52% | 0.66% | 0.42% | 0.52% | 0.67% |
| 300 | 0.37% | 0.50% | 0.62% | 0.38% | 0.50% | 0.63% |
| 320 | 0.36% | 0.47% | 0.60% | 0.37% | 0.47% | 0.61% |
| 340 | 0.35% | 0.45% | 0.57% | 0.35% | 0.45% | 0.57% |
| 360 | 0.35% | 0.43% | 0.55% | 0.35% | 0.43% | 0.55% |
| 380 | 0.34% | 0.41% | 0.53% | 0.34% | 0.41% | 0.53% |
| 400 | 0.30% | 0.39% | 0.49% | 0.30% | 0.39% | 0.50% |
| 450 | 0.28% | 0.35% | 0.46% | 0.28% | 0.36% | 0.46% |
| 500 | 0.25% | 0.33% | 0.41% | 0.25% | 0.33% | 0.42% |
| 555 | 0.24% | 0.30% | 0.39% | 0.24% | 0.30% | 0.39% |
| 600 | 0.23% | 0.29% | 0.37% | 0.23% | 0.29% | 0.37% |
| 700 | 0.22% | 0.26% | 0.34% | 0.22% | 0.26% | 0.34% |
| 800 | 0.21% | 0.24% | 0.32% | 0.21% | 0.24% | 0.32% |
| 900 | 0.20% | 0.23% | 0.30% | 0.20% | 0.23% | 0.31% |
| 1000 | 0.20% | 0.22% | 0.30% | 0.20% | 0.22% | 0.30% |
| 1100 | 0.23% | 0.21% | 0.31% | 0.24% | 0.21% | 0.32% |
| 1300 | 0.37% | 0.20% | 0.42% | 0.31% | 0.20% | 0.37% |
| 1500 | 0.32% | 0.19% | 0.37% | 0.30% | 0.19% | 0.36% |
| 1700 | 0.29% | 0.19% | 0.34% | 0.26% | 0.19% | 0.32% |
| 2000 | 0.36% | 0.18% | 0.40% | 0.27% | 0.18% | 0.33% |
| 2200 | 0.70% | 0.18% | 0.73% | 0.34% | 0.18% | 0.38% |
| 2300 | 0.52% | 0.18% | 0.55% | 0.36% | 0.18% | 0.41% |
| 2400 | 0.62% | 0.18% | 0.65% | 0.45% | 0.18% | 0.49% |
| 2500 | 6.62% | 0.18% | 6.58% | 2.59% | 0.18% | 2.56% |

# 6. Measurement results

This section presents Spectral Irradiance values, reported by participants for their lamps and that obtained by the pilot. Only combined standard uncertainties of measurements are presented in this section. More details of uncertainty budgets can be found in the section 5.

## 6.1. VNIIOFI lamps data

VNIIOFI, as a participant, used for the comparison three lamps: BN-9101-664, BN-9101-665 and BN-9101-666. VNIIOFI had three campaigns of measuring these lamps. First measurements, Round 1, were done by VNIIOFI as a participant, not as a pilot, before the other participant's lamps arrived. Then the lamps were measured at VNIIOFI as a pilot together with lamps of other participants (the Pilot Round). Finally, VNIIOFI performed the Round 2 measurements of its lamps, again as a participant, after the pilot measurements were completed.

Table 6.1.1. Spectral Irradiance of VNIIOFI lamp **BN-9101-664**

| Wavelength, nm | Participant Data | | | | Pilot Data | |
|---|---|---|---|---|---|---|
| | Round 1 | | Round 2 | | | |
| | Spectral Irradiance, W m$^{-2}$ nm$^{-1}$ | Combined uncertainty ($k$=1), % | Spectral Irradiance, W m$^{-2}$ nm$^{-1}$ | Combined uncertainty ($k$=1), % | Spectral Irradiance, W m$^{-2}$ nm$^{-1}$ | Combined uncertainty ($k$=1), % |
| 250 | 1.579E-04 | 0.43 | 1.571E-04 | 0.43 | 1.571E-04 | 0.37 |
| 260 | 2.789E-04 | 0.38 | 2.779E-04 | 0.38 | 2.781E-04 | 0.34 |
| 270 | 4.652E-04 | 0.36 | 4.640E-04 | 0.36 | 4.637E-04 | 0.32 |
| 280 | 7.332E-04 | 0.34 | 7.312E-04 | 0.34 | 7.313E-04 | 0.30 |
| 290 | 1.108E-03 | 0.32 | 1.107E-03 | 0.32 | 1.106E-03 | 0.29 |
| 300 | 1.615E-03 | 0.31 | 1.612E-03 | 0.31 | 1.611E-03 | 0.29 |
| 320 | 3.146E-03 | 0.30 | 3.138E-03 | 0.30 | 3.135E-03 | 0.28 |
| 340 | 5.523E-03 | 0.29 | 5.511E-03 | 0.29 | 5.513E-03 | 0.27 |
| 360 | 8.958E-03 | 0.27 | 8.931E-03 | 0.27 | 8.933E-03 | 0.26 |
| 380 | 1.360E-02 | 0.28 | 1.354E-02 | 0.28 | 1.356E-02 | 0.26 |
| 400 | 1.951E-02 | 0.25 | 1.943E-02 | 0.25 | 1.944E-02 | 0.25 |
| 450 | 3.967E-02 | 0.22 | 3.955E-02 | 0.22 | 3.953E-02 | 0.22 |
| 500 | 6.608E-02 | 0.21 | 6.585E-02 | 0.21 | 6.588E-02 | 0.21 |
| 555 | 9.857E-02 | 0.19 | 9.832E-02 | 0.19 | 9.833E-02 | 0.18 |
| 600 | 1.250E-01 | 0.16 | 1.247E-01 | 0.16 | 1.246E-01 | 0.16 |
| 700 | 1.739E-01 | 0.16 | 1.735E-01 | 0.16 | 1.734E-01 | 0.16 |
| 800 | 2.027E-01 | 0.15 | 2.022E-01 | 0.15 | 2.021E-01 | 0.15 |
| 900 | 2.119E-01 | 0.14 | 2.117E-01 | 0.14 | 2.114E-01 | 0.14 |
| 1000 | 2.072E-01 | 0.13 | 2.071E-01 | 0.13 | 2.067E-01 | 0.13 |
| 1100 | 1.943E-01 | 0.13 | 1.940E-01 | 0.13 | 1.938E-01 | 0.13 |
| 1300 | 1.581E-01 | 0.13 | 1.580E-01 | 0.13 | 1.578E-01 | 0.13 |
| 1500 | 1.228E-01 | 0.12 | 1.227E-01 | 0.12 | 1.225E-01 | 0.12 |
| 1700 | 9.353E-02 | 0.13 | 9.353E-02 | 0.13 | 9.348E-02 | 0.12 |
| 2000 | 6.228E-02 | 0.18 | 6.202E-02 | 0.18 | 6.205E-02 | 0.14 |
| 2200 | 4.764E-02 | 0.19 | 4.751E-02 | 0.19 | 4.751E-02 | 0.16 |
| 2300 | 4.173E-02 | 0.23 | 4.172E-02 | 0.23 | 4.180E-02 | 0.19 |
| 2400 | 3.697E-02 | 0.28 | 3.666E-02 | 0.28 | 3.665E-02 | 0.21 |
| 2500 | 3.258E-02 | 0.34 | 3.225E-02 | 0.34 | 3.232E-02 | 0.23 |

Table 6.1.2. Spectral Irradiance of VNIIOFI lamp **BN-9101-665**

| Wavelength, nm | Participant Data | | | | Pilot Data | |
|---|---|---|---|---|---|---|
| | Round 1 | | Round 2 | | | |
| | Spectral Irradiance, W m$^{-2}$ nm$^{-1}$ | Combined uncertainty ($k$=1), % | Spectral Irradiance, W m$^{-2}$ nm$^{-1}$ | Combined uncertainty ($k$=1), % | Spectral Irradiance, W m$^{-2}$ nm$^{-1}$ | Combined uncertainty ($k$=1), % |
| 250 | 1.473E-04 | 0.43 | 1.472E-04 | 0.43 | 1.468E-04 | 0.37 |
| 260 | 2.620E-04 | 0.38 | 2.615E-04 | 0.38 | 2.610E-04 | 0.34 |
| 270 | 4.377E-04 | 0.36 | 4.382E-04 | 0.36 | 4.380E-04 | 0.32 |
| 280 | 6.902E-04 | 0.34 | 6.901E-04 | 0.34 | 6.887E-04 | 0.30 |
| 290 | 1.049E-03 | 0.32 | 1.048E-03 | 0.32 | 1.048E-03 | 0.29 |
| 300 | 1.533E-03 | 0.31 | 1.533E-03 | 0.31 | 1.533E-03 | 0.29 |
| 320 | 2.998E-03 | 0.30 | 2.995E-03 | 0.30 | 2.990E-03 | 0.28 |
| 340 | 5.284E-03 | 0.29 | 5.280E-03 | 0.29 | 5.270E-03 | 0.27 |
| 360 | 8.588E-03 | 0.27 | 8.578E-03 | 0.27 | 8.571E-03 | 0.26 |
| 380 | 1.306E-02 | 0.28 | 1.305E-02 | 0.28 | 1.304E-02 | 0.26 |
| 400 | 1.879E-02 | 0.25 | 1.876E-02 | 0.25 | 1.874E-02 | 0.25 |
| 450 | 3.841E-02 | 0.22 | 3.835E-02 | 0.22 | 3.829E-02 | 0.22 |
| 500 | 6.421E-02 | 0.21 | 6.409E-02 | 0.21 | 6.401E-02 | 0.21 |
| 555 | 9.609E-02 | 0.19 | 9.592E-02 | 0.19 | 9.583E-02 | 0.18 |
| 600 | 1.221E-01 | 0.16 | 1.219E-01 | 0.16 | 1.217E-01 | 0.16 |
| 700 | 1.705E-01 | 0.16 | 1.702E-01 | 0.16 | 1.700E-01 | 0.16 |
| 800 | 1.993E-01 | 0.15 | 1.989E-01 | 0.15 | 1.987E-01 | 0.15 |
| 900 | 2.089E-01 | 0.14 | 2.087E-01 | 0.14 | 2.084E-01 | 0.14 |
| 1000 | 2.047E-01 | 0.13 | 2.045E-01 | 0.13 | 2.041E-01 | 0.13 |
| 1100 | 1.920E-01 | 0.13 | 1.919E-01 | 0.13 | 1.915E-01 | 0.13 |
| 1300 | 1.565E-01 | 0.13 | 1.565E-01 | 0.13 | 1.562E-01 | 0.13 |
| 1500 | 1.216E-01 | 0.12 | 1.216E-01 | 0.12 | 1.213E-01 | 0.12 |
| 1700 | 9.273E-02 | 0.13 | 9.266E-02 | 0.13 | 9.251E-02 | 0.12 |
| 2000 | 6.169E-02 | 0.18 | 6.150E-02 | 0.18 | 6.148E-02 | 0.14 |
| 2200 | 4.717E-02 | 0.19 | 4.704E-02 | 0.19 | 4.704E-02 | 0.16 |
| 2300 | 4.140E-02 | 0.23 | 4.125E-02 | 0.23 | 4.134E-02 | 0.19 |
| 2400 | 3.645E-02 | 0.28 | 3.626E-02 | 0.28 | 3.634E-02 | 0.21 |
| 2500 | 3.191E-02 | 0.34 | 3.180E-02 | 0.34 | 3.177E-02 | 0.23 |

Table 6.1.3. Spectral Irradiance of VNIIOFI lamp **BN-9101-666**

| Wavelength, nm | Participant Data | | | | Pilot Data | |
|---|---|---|---|---|---|---|
| | Round 1 | | Round 2 | | | |
| | Spectral Irradiance, W $m^{-2}$ $nm^{-1}$ | Combined uncertainty ($k$=1), % | Spectral Irradiance, W $m^{-2}$ $nm^{-1}$ | Combined uncertainty ($k$=1), % | Spectral Irradiance, W $m^{-2}$ $nm^{-1}$ | Combined uncertainty ($k$=1), % |
| 250 | 1.353E-04 | 0.43 | 1.352E-04 | 0.43 | 1.348E-04 | 0.37 |
| 260 | 2.414E-04 | 0.38 | 2.418E-04 | 0.38 | 2.414E-04 | 0.34 |
| 270 | 4.050E-04 | 0.36 | 4.045E-04 | 0.36 | 4.043E-04 | 0.32 |
| 280 | 6.430E-04 | 0.34 | 6.410E-04 | 0.34 | 6.400E-04 | 0.30 |
| 290 | 9.761E-04 | 0.32 | 9.742E-04 | 0.32 | 9.725E-04 | 0.29 |
| 300 | 1.429E-03 | 0.31 | 1.426E-03 | 0.31 | 1.425E-03 | 0.29 |
| 320 | 2.804E-03 | 0.30 | 2.797E-03 | 0.30 | 2.795E-03 | 0.28 |
| 340 | 4.963E-03 | 0.29 | 4.940E-03 | 0.29 | 4.937E-03 | 0.27 |
| 360 | 8.089E-03 | 0.27 | 8.064E-03 | 0.27 | 8.052E-03 | 0.26 |
| 380 | 1.235E-02 | 0.28 | 1.230E-02 | 0.28 | 1.228E-02 | 0.26 |
| 400 | 1.778E-02 | 0.25 | 1.772E-02 | 0.25 | 1.769E-02 | 0.25 |
| 450 | 3.652E-02 | 0.22 | 3.636E-02 | 0.22 | 3.635E-02 | 0.22 |
| 500 | 6.130E-02 | 0.21 | 6.103E-02 | 0.21 | 6.102E-02 | 0.21 |
| 555 | 9.212E-02 | 0.19 | 9.174E-02 | 0.19 | 9.174E-02 | 0.18 |
| 600 | 1.173E-01 | 0.16 | 1.169E-01 | 0.16 | 1.168E-01 | 0.16 |
| 700 | 1.645E-01 | 0.16 | 1.640E-01 | 0.16 | 1.639E-01 | 0.16 |
| 800 | 1.929E-01 | 0.15 | 1.923E-01 | 0.15 | 1.922E-01 | 0.15 |
| 900 | 2.028E-01 | 0.14 | 2.022E-01 | 0.14 | 2.020E-01 | 0.14 |
| 1000 | 1.990E-01 | 0.13 | 1.985E-01 | 0.13 | 1.984E-01 | 0.13 |
| 1100 | 1.871E-01 | 0.13 | 1.866E-01 | 0.13 | 1.864E-01 | 0.13 |
| 1300 | 1.530E-01 | 0.13 | 1.526E-01 | 0.13 | 1.525E-01 | 0.13 |
| 1500 | 1.192E-01 | 0.12 | 1.190E-01 | 0.12 | 1.188E-01 | 0.12 |
| 1700 | 9.094E-02 | 0.13 | 9.073E-02 | 0.13 | 9.073E-02 | 0.12 |
| 2000 | 6.069E-02 | 0.18 | 6.042E-02 | 0.18 | 6.047E-02 | 0.14 |
| 2200 | 4.655E-02 | 0.19 | 4.635E-02 | 0.19 | 4.633E-02 | 0.16 |
| 2300 | 4.095E-02 | 0.23 | 4.071E-02 | 0.23 | 4.074E-02 | 0.19 |
| 2400 | 3.607E-02 | 0.28 | 3.574E-02 | 0.28 | 3.583E-02 | 0.21 |
| 2500 | 3.168E-02 | 0.34 | 3.143E-02 | 0.34 | 3.151E-02 | 0.23 |

## 6.2. IO-CSIC lamps data

Originally IO-CSIC calibrated for the comparison three traveling lamps: BN-9101-610, BN-9101-611 and BN-9101-612.

Unfortunately, lamp BN9101-610 arrived at the pilot laboratory (VNIIOFI) with the filament broken. Therefore, only two lamps, BN9101-611 and BN9101-612, from IO-CSIC were used in the comparison.

Table 6.2.1. Spectral Irradiance of IO-CSIC lamp **BN-9101-611**

| Wavelength, nm | Participant Data | | | | Pilot Data | |
|---|---|---|---|---|---|---|
| | Round 1 | | Round 2 | | | |
| | Spectral Irradiance, W $m^{-2}$ $nm^{-1}$ | Combined uncertainty ($k$=1), % | Spectral Irradiance, W $m^{-2}$ $nm^{-1}$ | Combined uncertainty ($k$=1), % | Spectral Irradiance, W $m^{-2}$ $nm^{-1}$ | Combined uncertainty ($k$=1), % |
| 250 | 1.306E-04 | 2.6 | 1.261E-04 | 2.6 | 1.334E-04 | 0.37 |
| 260 | 2.295E-04 | 2.5 | 2.217E-04 | 2.5 | 2.370E-04 | 0.34 |
| 270 | 3.823E-04 | 2.5 | 3.681E-04 | 2.5 | 3.960E-04 | 0.32 |
| 280 | 6.062E-04 | 2.3 | 5.902E-04 | 2.3 | 6.274E-04 | 0.30 |
| 290 | 9.315E-04 | 2.3 | 9.064E-04 | 2.3 | 9.534E-04 | 0.29 |
| 300 | 1.412E-03 | 2.6 | 1.366E-03 | 2.6 | 1.395E-03 | 0.29 |
| 320 | 2.801E-03 | 2.0 | 2.737E-03 | 2.0 | 2.737E-03 | 0.28 |
| 340 | 4.966E-03 | 1.8 | 4.855E-03 | 1.8 | 4.832E-03 | 0.27 |
| 360 | 8.112E-03 | 1.7 | 7.929E-03 | 1.7 | 7.875E-03 | 0.26 |
| 380 | 1.237E-02 | 1.6 | 1.210E-02 | 1.6 | 1.202E-02 | 0.26 |
| 400 | 1.794E-02 | 1.6 | 1.734E-02 | 1.6 | 1.732E-02 | 0.25 |
| 450 | 3.679E-02 | 1.6 | 3.562E-02 | 1.6 | 3.561E-02 | 0.22 |
| 500 | 6.168E-02 | 1.7 | 5.967E-02 | 1.7 | 5.975E-02 | 0.21 |
| 555 | 9.271E-02 | 1.8 | 8.965E-02 | 1.8 | 8.987E-02 | 0.18 |
| 600 | 1.182E-01 | 1.7 | 1.143E-01 | 1.7 | 1.145E-01 | 0.16 |
| 700 | 1.662E-01 | 1.6 | 1.637E-01 | 1.6 | 1.607E-01 | 0.16 |
| 800 | 1.917E-01 | 1.6 | 1.915E-01 | 1.6 | 1.886E-01 | 0.15 |
| 900 | 1.989E-01 | 1.9 | 2.012E-01 | 1.9 | 1.985E-01 | 0.14 |
| 1000 | 1.942E-01 | 1.9 | 1.937E-01 | 1.9 | 1.950E-01 | 0.13 |
| 1100 | 1.837E-01 | 2.3 | 1.813E-01 | 2.3 | 1.833E-01 | 0.13 |
| 1300 | 1.510E-01 | 2.0 | 1.475E-01 | 2.0 | 1.502E-01 | 0.13 |
| 1500 | 1.174E-01 | 2.1 | 1.132E-01 | 2.1 | 1.171E-01 | 0.12 |
| 1700 | 8.686E-02 | 2.1 | 8.559E-02 | 2.1 | 8.955E-02 | 0.12 |
| 2000 | | | | | | |
| 2200 | | | | | | |
| 2300 | | | | | | |
| 2400 | | | | | | |
| 2500 | | | | | | |

Table 6.2.2. Spectral Irradiance of IO-CSIC lamp **BN-9101-612**

| Wavelength, nm | Participant Data | | | | Pilot Data | |
|---|---|---|---|---|---|---|
| | Round 1 | | Round 2 | | | |
| | Spectral Irradiance, W $m^{-2}$ $nm^{-1}$ | Combined uncertainty ($k$=1), % | Spectral Irradiance, W $m^{-2}$ $nm^{-1}$ | Combined uncertainty ($k$=1), % | Spectral Irradiance, W $m^{-2}$ $nm^{-1}$ | Combined uncertainty ($k$=1), % |
| 250 | 1.266E-04 | 2.6 | 1.249E-04 | 2.6 | 1.290E-04 | 0.37 |
| 260 | 2.228E-04 | 2.5 | 2.189E-04 | 2.5 | 2.296E-04 | 0.34 |
| 270 | 3.705E-04 | 2.5 | 3.632E-04 | 2.5 | 3.856E-04 | 0.32 |
| 280 | 5.870E-04 | 2.3 | 5.813E-04 | 2.3 | 6.119E-04 | 0.30 |
| 290 | 9.024E-04 | 2.3 | 8.962E-04 | 2.3 | 9.297E-04 | 0.29 |
| 300 | 1.365E-03 | 2.6 | 1.352E-03 | 2.6 | 1.364E-03 | 0.29 |
| 320 | 2.708E-03 | 2.0 | 2.683E-03 | 2.0 | 2.680E-03 | 0.28 |
| 340 | 4.800E-03 | 1.8 | 4.762E-03 | 1.8 | 4.743E-03 | 0.27 |
| 360 | 7.861E-03 | 1.7 | 7.766E-03 | 1.7 | 7.747E-03 | 0.26 |
| 380 | 1.201E-02 | 1.6 | 1.186E-02 | 1.6 | 1.184E-02 | 0.26 |
| 400 | 1.737E-02 | 1.6 | 1.706E-02 | 1.6 | 1.709E-02 | 0.25 |
| 450 | 3.567E-02 | 1.6 | 3.517E-02 | 1.6 | 3.519E-02 | 0.22 |
| 500 | 5.989E-02 | 1.7 | 5.901E-02 | 1.7 | 5.922E-02 | 0.21 |
| 555 | 9.015E-02 | 1.8 | 8.883E-02 | 1.8 | 8.920E-02 | 0.18 |
| 600 | 1.151E-01 | 1.7 | 1.133E-01 | 1.7 | 1.138E-01 | 0.16 |
| 700 | 1.620E-01 | 1.6 | 1.607E-01 | 1.6 | 1.600E-01 | 0.16 |
| 800 | 1.881E-01 | 1.6 | 1.889E-01 | 1.6 | 1.880E-01 | 0.15 |
| 900 | 1.981E-01 | 1.9 | 1.982E-01 | 1.9 | 1.980E-01 | 0.14 |
| 1000 | 1.941E-01 | 1.9 | 1.945E-01 | 1.9 | 1.947E-01 | 0.13 |
| 1100 | 1.816E-01 | 2.3 | 1.827E-01 | 2.3 | 1.831E-01 | 0.13 |
| 1300 | 1.510E-01 | 2.0 | 1.521E-01 | 2.0 | 1.501E-01 | 0.13 |
| 1500 | 1.172E-01 | 2.1 | 1.172E-01 | 2.1 | 1.170E-01 | 0.12 |
| 1700 | 8.037E-02 | 2.1 | 7.969E-02 | 2.1 | 8.931E-02 | 0.12 |
| 2000 | | | | | | |
| 2200 | | | | | | |
| 2300 | | | | | | |
| 2400 | | | | | | |
| 2500 | | | | | | |

## 6.3. KRISS lamps data

KRISS traveling lamps: BN-9101-639, BN-9101-640 and BN-9101-641.

Note: at the stage of Data Verification of the Pre-Draft A process KRISS requested withdrawing from the comparison the lamp BN-9101-641 because it demonstrated significant difference between the 1st and 2nd Rounds. The request was agreed by the participants. Therefore, although all three lamps data were reported by KRISS and are presented in this section, only two lamps data, BN-9101-639, BN-9101-640, were finally used for the comparison analysis.

Table 6.3.1. Spectral Irradiance of KRISS lamp **BN-9101-639**

| Wavelength, nm | Participant Data | | | | Pilot Data | |
|---|---|---|---|---|---|---|
| | Round 1 | | Round 2 | | | |
| | Spectral Irradiance, W m$^{-2}$ nm$^{-1}$ | Combined uncertainty ($k$=1), % | Spectral Irradiance, W m$^{-2}$ nm$^{-1}$ | Combined uncertainty ($k$=1), % | Spectral Irradiance, W m$^{-2}$ nm$^{-1}$ | Combined uncertainty ($k$=1), % |
| 250 | 1.350E-04 | 1.02 | 1.345E-04 | 1.15 | 1.338E-04 | 0.37 |
| 260 | 2.390E-04 | 0.91 | 2.405E-04 | 0.96 | 2.381E-04 | 0.34 |
| 270 | 4.008E-04 | 0.85 | 4.028E-04 | 0.92 | 3.990E-04 | 0.32 |
| 280 | 6.344E-04 | 0.81 | 6.364E-04 | 0.80 | 6.334E-04 | 0.30 |
| 290 | 9.616E-04 | 0.81 | 9.672E-04 | 0.76 | 9.603E-04 | 0.29 |
| 300 | 1.406E-03 | 0.74 | 1.413E-03 | 0.72 | 1.405E-03 | 0.29 |
| 320 | 2.753E-03 | 0.68 | 2.758E-03 | 0.63 | 2.754E-03 | 0.28 |
| 340 | 4.877E-03 | 0.59 | 4.884E-03 | 0.58 | 4.872E-03 | 0.27 |
| 360 | 7.958E-03 | 0.60 | 7.970E-03 | 0.54 | 7.941E-03 | 0.26 |
| 380 | 1.213E-02 | 0.52 | 1.217E-02 | 0.50 | 1.212E-02 | 0.26 |
| 400 | 1.748E-02 | 0.49 | 1.753E-02 | 0.48 | 1.748E-02 | 0.25 |
| 450 | 3.586E-02 | 0.44 | 3.596E-02 | 0.41 | 3.591E-02 | 0.22 |
| 500 | 6.024E-02 | 0.41 | 6.035E-02 | 0.39 | 6.031E-02 | 0.21 |
| 555 | 9.060E-02 | 0.41 | 9.081E-02 | 0.36 | 9.070E-02 | 0.18 |
| 600 | 1.155E-01 | 0.40 | 1.158E-01 | 0.35 | 1.156E-01 | 0.16 |
| 700 | 1.623E-01 | 0.36 | 1.628E-01 | 0.34 | 1.623E-01 | 0.16 |
| 800 | 1.912E-01 | 0.38 | 1.919E-01 | 0.33 | 1.905E-01 | 0.15 |
| 900 | 2.004E-01 | 0.32 | 2.006E-01 | 0.30 | 2.004E-01 | 0.14 |
| 1000 | 1.969E-01 | 0.31 | 1.971E-01 | 0.30 | 1.970E-01 | 0.13 |
| 1100 | 1.852E-01 | 0.30 | 1.855E-01 | 0.31 | 1.854E-01 | 0.13 |
| 1300 | 1.518E-01 | 0.29 | 1.521E-01 | 0.29 | 1.518E-01 | 0.13 |
| 1500 | 1.182E-01 | 0.28 | 1.187E-01 | 0.28 | 1.183E-01 | 0.12 |
| 1700 | 8.995E-02 | 0.37 | 9.077E-02 | 0.37 | 9.040E-02 | 0.12 |
| 2000 | 6.002E-02 | 0.55 | 6.038E-02 | 0.39 | 6.023E-02 | 0.14 |
| 2200 | 4.563E-02 | 0.69 | 4.586E-02 | 0.44 | 4.623E-02 | 0.16 |
| 2300 | 4.057E-02 | 0.74 | 4.076E-02 | 0.49 | 4.063E-02 | 0.19 |
| 2400 | 3.562E-02 | 0.75 | 3.575E-02 | 0.52 | 3.560E-02 | 0.21 |
| 2500 | 3.153E-02 | 0.90 | 3.130E-02 | 0.81 | 3.143E-02 | 0.23 |

Table 6.3.2. Spectral Irradiance of KRISS lamp **BN-9101-640**

| Wavelength, nm | Participant Data | | | | Pilot Data | |
|---|---|---|---|---|---|---|
| | Round 1 | | Round 2 | | | |
| | Spectral Irradiance, W $m^{-2}$ $nm^{-1}$ | Combined uncertainty ($k$=1), % | Spectral Irradiance, W $m^{-2}$ $nm^{-1}$ | Combined uncertainty ($k$=1), % | Spectral Irradiance, W $m^{-2}$ $nm^{-1}$ | Combined uncertainty ($k$=1), % |
| 250 | 1.331E-04 | 1.03 | 1.336E-04 | 1.14 | 1.319E-04 | 0.37 |
| 260 | 2.369E-04 | 0.92 | 2.382E-04 | 0.96 | 2.350E-04 | 0.34 |
| 270 | 3.968E-04 | 0.85 | 3.990E-04 | 0.91 | 3.945E-04 | 0.32 |
| 280 | 6.294E-04 | 0.81 | 6.297E-04 | 0.80 | 6.264E-04 | 0.30 |
| 290 | 9.540E-04 | 0.82 | 9.554E-04 | 0.76 | 9.510E-04 | 0.29 |
| 300 | 1.397E-03 | 0.74 | 1.399E-03 | 0.71 | 1.393E-03 | 0.29 |
| 320 | 2.735E-03 | 0.68 | 2.733E-03 | 0.63 | 2.733E-03 | 0.28 |
| 340 | 4.839E-03 | 0.59 | 4.837E-03 | 0.58 | 4.831E-03 | 0.27 |
| 360 | 7.893E-03 | 0.60 | 7.898E-03 | 0.54 | 7.875E-03 | 0.26 |
| 380 | 1.204E-02 | 0.52 | 1.205E-02 | 0.50 | 1.202E-02 | 0.26 |
| 400 | 1.735E-02 | 0.49 | 1.736E-02 | 0.48 | 1.732E-02 | 0.25 |
| 450 | 3.559E-02 | 0.44 | 3.562E-02 | 0.41 | 3.562E-02 | 0.22 |
| 500 | 5.979E-02 | 0.41 | 5.983E-02 | 0.39 | 5.984E-02 | 0.21 |
| 555 | 9.004E-02 | 0.41 | 9.004E-02 | 0.36 | 9.008E-02 | 0.18 |
| 600 | 1.148E-01 | 0.40 | 1.149E-01 | 0.35 | 1.149E-01 | 0.16 |
| 700 | 1.616E-01 | 0.36 | 1.618E-01 | 0.34 | 1.616E-01 | 0.16 |
| 800 | 1.907E-01 | 0.38 | 1.909E-01 | 0.33 | 1.899E-01 | 0.15 |
| 900 | 2.001E-01 | 0.32 | 1.999E-01 | 0.30 | 2.002E-01 | 0.14 |
| 1000 | 1.969E-01 | 0.31 | 1.967E-01 | 0.30 | 1.969E-01 | 0.13 |
| 1100 | 1.854E-01 | 0.30 | 1.854E-01 | 0.31 | 1.855E-01 | 0.13 |
| 1300 | 1.522E-01 | 0.29 | 1.523E-01 | 0.29 | 1.523E-01 | 0.13 |
| 1500 | 1.188E-01 | 0.28 | 1.190E-01 | 0.28 | 1.189E-01 | 0.12 |
| 1700 | 9.032E-02 | 0.37 | 9.116E-02 | 0.37 | 9.101E-02 | 0.12 |
| 2000 | 6.035E-02 | 0.55 | 6.079E-02 | 0.39 | 6.073E-02 | 0.14 |
| 2200 | 4.615E-02 | 0.69 | 4.616E-02 | 0.46 | 4.651E-02 | 0.16 |
| 2300 | 4.060E-02 | 0.74 | 4.094E-02 | 0.50 | 4.103E-02 | 0.19 |
| 2400 | 3.606E-02 | 0.75 | 3.623E-02 | 0.53 | 3.595E-02 | 0.21 |
| 2500 | 3.162E-02 | 0.87 | 3.181E-02 | 0.81 | 3.169E-02 | 0.23 |

Table 6.3.3. Spectral Irradiance of KRISS lamp **BN-9101-641**

| Wavelength, nm | Participant Data | | | | Pilot Data | |
|---|---|---|---|---|---|---|
| | Round 1 | | Round 2 | | | |
| | Spectral Irradiance, W $m^{-2}$ $nm^{-1}$ | Combined uncertainty ($k$=1), % | Spectral Irradiance, W $m^{-2}$ $nm^{-1}$ | Combined uncertainty ($k$=1), % | Spectral Irradiance, W $m^{-2}$ $nm^{-1}$ | Combined uncertainty ($k$=1), % |
| 250 | 1.419E-04 | 1.00 | 1.374E-04 | 1.14 | 1.390E-04 | 0.37 |
| 260 | 2.506E-04 | 0.90 | 2.455E-04 | 0.95 | 2.474E-04 | 0.34 |
| 270 | 4.188E-04 | 0.85 | 4.104E-04 | 0.91 | 4.136E-04 | 0.32 |
| 280 | 6.635E-04 | 0.80 | 6.506E-04 | 0.80 | 6.554E-04 | 0.30 |
| 290 | 1.005E-03 | 0.81 | 9.865E-04 | 0.76 | 9.955E-04 | 0.29 |
| 300 | 1.465E-03 | 0.74 | 1.442E-03 | 0.72 | 1.455E-03 | 0.29 |
| 320 | 2.865E-03 | 0.68 | 2.814E-03 | 0.63 | 2.850E-03 | 0.28 |
| 340 | 5.063E-03 | 0.59 | 4.972E-03 | 0.58 | 5.030E-03 | 0.27 |
| 360 | 8.245E-03 | 0.60 | 8.099E-03 | 0.54 | 8.193E-03 | 0.26 |
| 380 | 1.255E-02 | 0.52 | 1.236E-02 | 0.50 | 1.248E-02 | 0.26 |
| 400 | 1.807E-02 | 0.49 | 1.779E-02 | 0.48 | 1.798E-02 | 0.25 |
| 450 | 3.696E-02 | 0.44 | 3.647E-02 | 0.41 | 3.687E-02 | 0.22 |
| 500 | 6.194E-02 | 0.41 | 6.120E-02 | 0.39 | 6.181E-02 | 0.21 |
| 555 | 9.308E-02 | 0.41 | 9.206E-02 | 0.36 | 9.287E-02 | 0.18 |
| 600 | 1.184E-01 | 0.40 | 1.174E-01 | 0.35 | 1.183E-01 | 0.16 |
| 700 | 1.662E-01 | 0.36 | 1.650E-01 | 0.34 | 1.660E-01 | 0.16 |
| 800 | 1.958E-01 | 0.38 | 1.945E-01 | 0.33 | 1.947E-01 | 0.15 |
| 900 | 2.053E-01 | 0.32 | 2.035E-01 | 0.30 | 2.049E-01 | 0.14 |
| 1000 | 2.017E-01 | 0.31 | 2.001E-01 | 0.30 | 2.015E-01 | 0.13 |
| 1100 | 1.897E-01 | 0.30 | 1.886E-01 | 0.31 | 1.896E-01 | 0.13 |
| 1300 | 1.555E-01 | 0.29 | 1.549E-01 | 0.29 | 1.554E-01 | 0.13 |
| 1500 | 1.212E-01 | 0.28 | 1.210E-01 | 0.28 | 1.212E-01 | 0.12 |
| 1700 | 9.215E-02 | 0.37 | 9.271E-02 | 0.37 | 9.269E-02 | 0.12 |
| 2000 | 6.172E-02 | 0.55 | 6.164E-02 | 0.39 | 6.172E-02 | 0.14 |
| 2200 | 4.713E-02 | 0.68 | 4.683E-02 | 0.46 | 4.732E-02 | 0.16 |
| 2300 | 4.148E-02 | 0.73 | 4.163E-02 | 0.50 | 4.165E-02 | 0.19 |
| 2400 | 3.663E-02 | 0.74 | 3.669E-02 | 0.53 | 3.668E-02 | 0.21 |
| 2500 | 3.199E-02 | 0.81 | 3.233E-02 | 0.80 | 3.217E-02 | 0.23 |

## 6.4. LNE-CNAM lamps data

Three lamps were measured at LNE-CNAM: BN-9101-653, BN-9101-655 and BN-9101-656.

In the Round 1 LNE-CNAM was not able to do measurements in the whole wavelength range because of problems with the blackbody. Only data for wavelengths from 250 nm to 700 nm and from 1300 nm to 1500 nm were submitted.

In the Round 2 measurements were done in the whole range from 250 nm to 2500 nm. However, the lamp BN-9101-656, when was measured up to 800 nm, showed significant difference, of about 2 % or 3 %, compared to the first round data; therefore, measurement of this lamp stopped and the lamp was excluded from the comparison. LNE-CNAM wrote in its Measurement report: "*Lamp **BN-9101-656** has been measured only up to 800 nm because it showed a difference of about 2 % or 3 % compared to the first round. In addition, we observed a lot of white spots on the bulb. This defect appeared after fourth use in the first round. **This lamp is out of our set of lamps**. The results of the lamps BN-9101-653, BN-9101-655 and BN-9101-656 (**this lamp is removed from the comparison**) are shown below…*".

Note: LNE-CNAM required withdrawing from the comparison the lamp BN-9101-656 at the moment of submitting the Measurement Report, i.e. before the stage Pre-Draft A started.

Table 6.4.1. Spectral Irradiance of LNE-CNAM lamp **BN-9101-653**

| Wavelength, nm | Participant Data | | | | Pilot Data | |
|---|---|---|---|---|---|---|
| | Round 1 | | Round 2 | | | |
| | Spectral Irradiance, W m$^{-2}$ nm$^{-1}$ | Combined uncertainty ($k$=1), % | Spectral Irradiance, W m$^{-2}$ nm$^{-1}$ | Combined uncertainty ($k$=1), % | Spectral Irradiance, W m$^{-2}$ nm$^{-1}$ | Combined uncertainty ($k$=1), % |
| 250 | 1.374E-04 | 2.69 | 1.283E-04 | 3.35 | 1.262E-04 | 0.37 |
| 260 | 2.307E-04 | 1.26 | 2.259E-04 | 1.28 | 2.249E-04 | 0.34 |
| 270 | 3.804E-04 | 0.92 | 3.833E-04 | 0.96 | 3.786E-04 | 0.32 |
| 280 | 6.008E-04 | 0.77 | 6.035E-04 | 0.74 | 5.978E-04 | 0.30 |
| 290 | 9.186E-04 | 0.64 | 9.193E-04 | 0.64 | 9.131E-04 | 0.29 |
| 300 | 1.341E-03 | 0.60 | 1.359E-03 | 0.61 | 1.338E-03 | 0.29 |
| 320 | 2.656E-03 | 0.54 | 2.663E-03 | 0.51 | 2.629E-03 | 0.28 |
| 340 | 4.714E-03 | 0.51 | 4.713E-03 | **0.46** | 4.658E-03 | 0.27 |
| 360 | 7.700E-03 | 0.48 | 7.717E-03 | **0.45** | 7.612E-03 | 0.26 |
| 380 | 1.179E-02 | 0.47 | 1.180E-02 | **0.41** | 1.163E-02 | 0.26 |
| 400 | 1.700E-02 | 0.46 | 1.702E-02 | 0.39 | 1.679E-02 | 0.25 |
| 450 | 3.480E-02 | 0.43 | 3.491E-02 | 0.35 | 3.461E-02 | 0.22 |
| 500 | 5.851E-02 | 0.45 | 5.872E-02 | 0.35 | 5.830E-02 | 0.21 |
| 555 | 8.823E-02 | 0.39 | 8.855E-02 | 0.33 | 8.789E-02 | 0.18 |
| 600 | 1.126E-01 | 0.39 | 1.129E-01 | 0.34 | 1.122E-01 | 0.16 |
| 700 | 1.574E-01 | 0.51 | 1.593E-01 | 0.39 | 1.581E-01 | 0.16 |
| 800 | | | 1.879E-01 | 0.50 | 1.860E-01 | 0.15 |
| 900 | | | 1.977E-01 | 0.25 | 1.962E-01 | 0.14 |
| 1000 | | | 1.950E-01 | 0.23 | 1.931E-01 | 0.13 |
| 1100 | | | 1.834E-01 | 0.25 | 1.820E-01 | 0.13 |
| 1300 | 1.509E-01 | 0.72 | 1.515E-01 | 0.21 | 1.494E-01 | 0.13 |
| 1500 | 1.177E-01 | 0.76 | 1.182E-01 | 0.20 | 1.167E-01 | 0.12 |
| 1700 | | | 9.128E-02 | 0.19 | 8.935E-02 | 0.12 |

| | | | | | | |
|---|---|---|---|---|---|---|
| 2000 | | | 6.133E-02 | 0.30 | 5.968E-02 | 0.14 |
| 2200 | | | 4.744E-02 | 0.45 | 4.575E-02 | 0.16 |
| 2300 | | | 4.229E-02 | 0.60 | 4.032E-02 | 0.19 |
| 2400 | | | 3.805E-02 | 1.02 | 3.538E-02 | 0.21 |
| 2500 | | | 3.322E-02 | 3.71 | 3.127E-02 | 0.23 |

Table 6.4.2. Spectral Irradiance of LNE-CNAM lamp **BN-9101-655**

| **Wavelength, nm** | **Participant Data** | | | | **Pilot Data** | |
|---|---|---|---|---|---|---|
| | **Round 1** | | **Round 2** | | | |
| | **Spectral Irradiance, W m$^{-2}$ nm$^{-1}$** | **Combined uncertainty ($k$=1), %** | **Spectral Irradiance, W m$^{-2}$ nm$^{-1}$** | **Combined uncertainty ($k$=1), %** | **Spectral Irradiance, W m$^{-2}$ nm$^{-1}$** | **Combined uncertainty ($k$=1), %** |
| 250 | 1.372E-04 | 2.83 | 1.263E-04 | 3.82 | 1.252E-04 | 0.37 |
| 260 | 2.292E-04 | 1.36 | 2.252E-04 | 1.44 | 2.231E-04 | 0.34 |
| 270 | 3.783E-04 | 1.18 | 3.756E-04 | 1.03 | 3.742E-04 | 0.32 |
| 280 | 6.005E-04 | 0.86 | 5.988E-04 | 0.76 | 5.951E-04 | 0.30 |
| 290 | 9.156E-04 | 0.79 | 9.113E-04 | 0.67 | 9.059E-04 | 0.29 |
| 300 | 1.331E-03 | 0.63 | 1.344E-03 | 0.62 | 1.327E-03 | 0.29 |
| 320 | 2.650E-03 | 0.68 | 2.643E-03 | 0.52 | 2.614E-03 | 0.28 |
| 340 | 4.704E-03 | 0.60 | 4.676E-03 | 0.47 | 4.633E-03 | 0.27 |
| 360 | 7.695E-03 | 0.50 | 7.667E-03 | 0.45 | 7.582E-03 | 0.26 |
| 380 | 1.179E-02 | 0.52 | 1.177E-02 | 0.44 | 1.160E-02 | 0.26 |
| 400 | 1.700E-02 | 0.52 | 1.696E-02 | 0.42 | 1.675E-02 | 0.25 |
| 450 | 3.489E-02 | 0.44 | 3.480E-02 | 0.37 | 3.461E-02 | 0.22 |
| 500 | 5.870E-02 | 0.41 | 5.864E-02 | 0.39 | 5.834E-02 | 0.21 |
| 555 | 8.861E-02 | 0.44 | 8.850E-02 | 0.36 | 8.804E-02 | 0.18 |
| 600 | 1.131E-01 | 0.40 | 1.130E-01 | 0.43 | 1.125E-01 | 0.16 |
| 700 | 1.582E-01 | 0.48 | 1.593E-01 | 0.59 | 1.586E-01 | 0.16 |
| 800 | | | 1.873E-01 | 0.35 | 1.867E-01 | 0.15 |
| 900 | | | 1.981E-01 | 0.25 | 1.969E-01 | 0.14 |
| 1000 | | | 1.951E-01 | 0.26 | 1.938E-01 | 0.13 |
| 1100 | | | 1.842E-01 | 0.71 | 1.826E-01 | 0.13 |
| 1300 | 1.526E-01 | 0.70 | 1.513E-01 | 0.23 | 1.499E-01 | 0.13 |
| 1500 | 1.193E-01 | 0.78 | 1.181E-01 | 0.32 | 1.170E-01 | 0.12 |
| 1700 | | | 9.092E-02 | 0.39 | 8.956E-02 | 0.12 |
| 2000 | | | 6.119E-02 | 0.39 | 5.974E-02 | 0.14 |
| 2200 | | | 4.721E-02 | 0.74 | 4.584E-02 | 0.16 |
| 2300 | | | 4.190E-02 | 0.76 | 4.023E-02 | 0.19 |
| 2400 | | | 3.787E-02 | 1.32 | 3.544E-02 | 0.21 |
| 2500 | | | 3.434E-02 | 5.07 | 3.129E-02 | 0.23 |

Table 6.4.2. Spectral Irradiance of LNE-CNAM lamp **BN-9101-656**

| Wavelength, nm | Participant Data | | | | Pilot Data | |
|---|---|---|---|---|---|---|
| | Round 1 | | Round 2 | | | |
| | Spectral Irradiance, W $m^{-2}$ $nm^{-1}$ | Combined uncertainty ($k$=1), % | Spectral Irradiance, W $m^{-2}$ $nm^{-1}$ | Combined uncertainty ($k$=1), % | Spectral Irradiance, W $m^{-2}$ $nm^{-1}$ | Combined uncertainty ($k$=1), % |
| 250 | 1.31E-04 | 7.35 | 1.280E-04 | 3.84 | 1.285E-04 | 0.37 |
| 260 | 2.34E-04 | 2.19 | 2.260E-04 | 1.63 | 2.289E-04 | 0.34 |
| 270 | 3.93E-04 | 1.80 | 3.830E-04 | 1.01 | 3.843E-04 | 0.32 |
| 280 | 6.26E-04 | 0.97 | 6.070E-04 | 0.77 | 6.110E-04 | 0.30 |
| 290 | 9.54E-04 | 0.99 | 9.230E-04 | 0.76 | 9.282E-04 | 0.29 |
| 300 | 1.39E-03 | 0.59 | 1.360E-03 | 0.71 | 1.360E-03 | 0.29 |
| 320 | 2.75E-03 | 0.54 | 2.660E-03 | 0.70 | 2.668E-03 | 0.28 |
| 340 | 4.85E-03 | 0.51 | 4.710E-03 | 0.61 | 4.718E-03 | 0.27 |
| 360 | 7.93E-03 | 0.49 | 7.700E-03 | 0.63 | 7.702E-03 | 0.26 |
| 380 | 1.21E-02 | 0.47 | 1.180E-02 | 0.48 | 1.175E-02 | 0.26 |
| 400 | 1.75E-02 | 0.47 | 1.700E-02 | 0.60 | 1.696E-02 | 0.25 |
| 450 | 3.56E-02 | 0.52 | 3.480E-02 | 0.49 | 3.488E-02 | 0.22 |
| 500 | 5.98E-02 | 0.58 | 5.860E-02 | 0.37 | 5.862E-02 | 0.21 |
| 555 | 9.00E-02 | 0.46 | 8.830E-02 | 0.33 | 8.827E-02 | 0.18 |
| 600 | 1.15E-01 | 0.46 | 1.130E-01 | 0.35 | 1.126E-01 | 0.16 |
| 700 | 1.61E-01 | 0.66 | 1.580E-01 | 0.46 | 1.584E-01 | 0.16 |
| 800 | | | 1.860E-01 | 0.97 | 1.861E-01 | 0.15 |
| 900 | | | | | | |
| 1000 | | | | | | |
| 1100 | | | | | | |
| 1300 | 1.51E-01 | 0.77 | | | | |
| 1500 | 1.18E-01 | 0.80 | | | | |
| 1700 | | | | | | |
| 2000 | | | | | | |
| 2200 | | | | | | |
| 2300 | | | | | | |
| 2400 | | | | | | |
| 2500 | | | | | | |

## 6.5. NIM lamps data

NIM traveling lamps: BN-9101-650, BN-9101-651 and BN-9101-652.

Table 6.5.1. Spectral Irradiance of NIM lamp **BN-9101-650**

| Wavelength, nm | Participant Data | | | | Pilot Data | |
|---|---|---|---|---|---|---|
| | Round 1 | | Round 2 | | | |
| | Spectral Irradiance, W m$^{-2}$ nm$^{-1}$ | Combined uncertainty ($k$=1), % | Spectral Irradiance, W m$^{-2}$ nm$^{-1}$ | Combined uncertainty ($k$=1), % | Spectral Irradiance, W m$^{-2}$ nm$^{-1}$ | Combined uncertainty ($k$=1), % |
| 250 | 1.382E-04 | 0.95 | 1.379E-04 | 0.95 | 1.366E-04 | 0.37 |
| 260 | 2.449E-04 | 0.79 | 2.455E-04 | 0.79 | 2.434E-04 | 0.34 |
| 270 | 4.092E-04 | 0.72 | 4.108E-04 | 0.72 | 4.077E-04 | 0.32 |
| 280 | 6.500E-04 | 0.71 | 6.523E-04 | 0.71 | 6.469E-04 | 0.30 |
| 290 | 9.874E-04 | 0.62 | 9.891E-04 | 0.62 | 9.817E-04 | 0.29 |
| 300 | 1.445E-03 | 0.55 | 1.446E-03 | 0.55 | 1.438E-03 | 0.29 |
| 320 | 2.822E-03 | 0.53 | 2.831E-03 | 0.53 | 2.814E-03 | 0.28 |
| 340 | 4.996E-03 | 0.47 | 5.010E-03 | 0.47 | 4.972E-03 | 0.27 |
| 360 | 8.143E-03 | 0.45 | 8.172E-03 | 0.45 | 8.109E-03 | 0.26 |
| 380 | 1.242E-02 | 0.44 | 1.245E-02 | 0.44 | 1.236E-02 | 0.26 |
| 400 | 1.791E-02 | 0.38 | 1.793E-02 | 0.38 | 1.782E-02 | 0.25 |
| 450 | 3.684E-02 | 0.35 | 3.682E-02 | 0.35 | 3.657E-02 | 0.22 |
| 500 | 6.168E-02 | 0.34 | 6.171E-02 | 0.34 | 6.136E-02 | 0.21 |
| 555 | 9.280E-02 | 0.30 | 9.274E-02 | 0.30 | 9.223E-02 | 0.18 |
| 600 | 1.181E-01 | 0.29 | 1.181E-01 | 0.29 | 1.175E-01 | 0.16 |
| 700 | 1.657E-01 | 0.27 | 1.656E-01 | 0.27 | 1.647E-01 | 0.16 |
| 800 | 1.945E-01 | 0.27 | 1.944E-01 | 0.27 | 1.931E-01 | 0.15 |
| 900 | 2.042E-01 | 0.31 | 2.038E-01 | 0.31 | 2.030E-01 | 0.14 |
| 1000 | 2.001E-01 | 0.30 | 2.003E-01 | 0.30 | 1.993E-01 | 0.13 |
| 1100 | 1.875E-01 | 0.30 | 1.877E-01 | 0.30 | 1.874E-01 | 0.13 |
| 1300 | 1.537E-01 | 0.29 | 1.538E-01 | 0.29 | 1.532E-01 | 0.13 |
| 1500 | 1.197E-01 | 0.32 | 1.198E-01 | 0.32 | 1.193E-01 | 0.12 |
| 1700 | 9.150E-02 | 0.32 | 9.151E-02 | 0.32 | 9.122E-02 | 0.12 |
| 2000 | 6.084E-02 | 0.31 | 6.083E-02 | 0.31 | 6.064E-02 | 0.14 |
| 2200 | 4.667E-02 | 0.39 | 4.678E-02 | 0.39 | 4.649E-02 | 0.16 |
| 2300 | 4.104E-02 | 0.45 | 4.113E-02 | 0.45 | 4.093E-02 | 0.19 |
| 2400 | 3.602E-02 | 0.79 | 3.620E-02 | 0.79 | 3.591E-02 | 0.21 |
| 2500 | 3.185E-02 | 1.21 | 3.198E-02 | 1.21 | 3.156E-02 | 0.23 |

Table 6.5.2. Spectral Irradiance of NIM lamp **BN-9101-651**

| Wavelength, nm | Participant Data | | | | Pilot Data | |
|---|---|---|---|---|---|---|
| | Round 1 | | Round 2 | | | |
| | Spectral Irradiance, W $m^{-2}$ $nm^{-1}$ | Combined uncertainty ($k$=1), % | Spectral Irradiance, W $m^{-2}$ $nm^{-1}$ | Combined uncertainty ($k$=1), % | Spectral Irradiance, W $m^{-2}$ $nm^{-1}$ | Combined uncertainty ($k$=1), % |
| 250 | 1.354E-04 | 0.95 | 1.365E-04 | 0.95 | 1.338E-04 | 0.37 |
| 260 | 2.392E-04 | 0.79 | 2.407E-04 | 0.79 | 2.377E-04 | 0.34 |
| 270 | 4.016E-04 | 0.72 | 4.003E-04 | 0.72 | 3.996E-04 | 0.32 |
| 280 | 6.376E-04 | 0.71 | 6.360E-04 | 0.71 | 6.339E-04 | 0.30 |
| 290 | 9.684E-04 | 0.62 | 9.683E-04 | 0.62 | 9.628E-04 | 0.29 |
| 300 | 1.418E-03 | 0.55 | 1.417E-03 | 0.55 | 1.409E-03 | 0.29 |
| 320 | 2.776E-03 | 0.53 | 2.775E-03 | 0.53 | 2.765E-03 | 0.28 |
| 340 | 4.920E-03 | 0.47 | 4.924E-03 | 0.47 | 4.889E-03 | 0.27 |
| 360 | 8.027E-03 | 0.45 | 8.045E-03 | 0.45 | 7.991E-03 | 0.26 |
| 380 | 1.224E-02 | 0.44 | 1.228E-02 | 0.44 | 1.220E-02 | 0.26 |
| 400 | 1.766E-02 | 0.38 | 1.768E-02 | 0.38 | 1.758E-02 | 0.25 |
| 450 | 3.635E-02 | 0.35 | 3.638E-02 | 0.35 | 3.617E-02 | 0.22 |
| 500 | 6.104E-02 | 0.34 | 6.101E-02 | 0.34 | 6.076E-02 | 0.21 |
| 555 | 9.193E-02 | 0.30 | 9.180E-02 | 0.30 | 9.143E-02 | 0.18 |
| 600 | 1.172E-01 | 0.29 | 1.170E-01 | 0.29 | 1.165E-01 | 0.16 |
| 700 | 1.644E-01 | 0.27 | 1.643E-01 | 0.27 | 1.636E-01 | 0.16 |
| 800 | 1.929E-01 | 0.27 | 1.929E-01 | 0.27 | 1.919E-01 | 0.15 |
| 900 | 2.028E-01 | 0.31 | 2.026E-01 | 0.31 | 2.019E-01 | 0.14 |
| 1000 | 1.990E-01 | 0.30 | 1.990E-01 | 0.30 | 1.982E-01 | 0.13 |
| 1100 | 1.865E-01 | 0.30 | 1.867E-01 | 0.30 | 1.863E-01 | 0.13 |
| 1300 | 1.529E-01 | 0.29 | 1.529E-01 | 0.29 | 1.524E-01 | 0.13 |
| 1500 | 1.192E-01 | 0.32 | 1.192E-01 | 0.32 | 1.187E-01 | 0.12 |
| 1700 | 9.111E-02 | 0.32 | 9.125E-02 | 0.32 | 9.068E-02 | 0.12 |
| 2000 | 6.067E-02 | 0.31 | 6.066E-02 | 0.31 | 6.043E-02 | 0.14 |
| 2200 | 4.648E-02 | 0.39 | 4.651E-02 | 0.39 | 4.632E-02 | 0.16 |
| 2300 | 4.084E-02 | 0.45 | 4.083E-02 | 0.45 | 4.071E-02 | 0.19 |
| 2400 | 3.583E-02 | 0.79 | 3.588E-02 | 0.79 | 3.573E-02 | 0.21 |
| 2500 | 3.150E-02 | 1.21 | 3.166E-02 | 1.21 | 3.147E-02 | 0.23 |

Table 6.5.3. Spectral Irradiance of NIM lamp **BN-9101-652**

| Wavelength, nm | Participant Data | | | | Pilot Data | |
|---|---|---|---|---|---|---|
| | Round 1 | | Round 2 | | | |
| | Spectral Irradiance, W $m^{-2}$ $nm^{-1}$ | Combined uncertainty ($k$=1), % | Spectral Irradiance, W $m^{-2}$ $nm^{-1}$ | Combined uncertainty ($k$=1), % | Spectral Irradiance, W $m^{-2}$ $nm^{-1}$ | Combined uncertainty ($k$=1), % |
| 250 | 1.209E-04 | 0.95 | 1.210E-04 | 0.95 | 1.200E-04 | 0.37 |
| 260 | 2.137E-04 | 0.79 | 2.155E-04 | 0.79 | 2.135E-04 | 0.34 |
| 270 | 3.607E-04 | 0.72 | 3.614E-04 | 0.72 | 3.600E-04 | 0.32 |
| 280 | 5.743E-04 | 0.71 | 5.759E-04 | 0.71 | 5.736E-04 | 0.30 |
| 290 | 8.772E-04 | 0.62 | 8.775E-04 | 0.62 | 8.744E-04 | 0.29 |
| 300 | 1.286E-03 | 0.55 | 1.291E-03 | 0.55 | 1.286E-03 | 0.29 |
| 320 | 2.533E-03 | 0.53 | 2.543E-03 | 0.53 | 2.536E-03 | 0.28 |
| 340 | 4.513E-03 | 0.47 | 4.530E-03 | 0.47 | 4.507E-03 | 0.27 |
| 360 | 7.397E-03 | 0.45 | 7.431E-03 | 0.45 | 7.391E-03 | 0.26 |
| 380 | 1.134E-02 | 0.44 | 1.138E-02 | 0.44 | 1.130E-02 | 0.26 |
| 400 | 1.640E-02 | 0.38 | 1.644E-02 | 0.38 | 1.637E-02 | 0.25 |
| 450 | 3.398E-02 | 0.35 | 3.399E-02 | 0.35 | 3.389E-02 | 0.22 |
| 500 | 5.738E-02 | 0.34 | 5.734E-02 | 0.34 | 5.720E-02 | 0.21 |
| 555 | 8.680E-02 | 0.30 | 8.670E-02 | 0.30 | 8.646E-02 | 0.18 |
| 600 | 1.110E-01 | 0.29 | 1.109E-01 | 0.29 | 1.106E-01 | 0.16 |
| 700 | 1.567E-01 | 0.27 | 1.567E-01 | 0.27 | 1.562E-01 | 0.16 |
| 800 | 1.848E-01 | 0.27 | 1.849E-01 | 0.27 | 1.843E-01 | 0.15 |
| 900 | 1.956E-01 | 0.31 | 1.953E-01 | 0.31 | 1.946E-01 | 0.14 |
| 1000 | 1.920E-01 | 0.30 | 1.924E-01 | 0.30 | 1.917E-01 | 0.13 |
| 1100 | 1.804E-01 | 0.30 | 1.811E-01 | 0.30 | 1.810E-01 | 0.13 |
| 1300 | 1.483E-01 | 0.29 | 1.487E-01 | 0.29 | 1.486E-01 | 0.13 |
| 1500 | 1.161E-01 | 0.32 | 1.164E-01 | 0.32 | 1.161E-01 | 0.12 |
| 1700 | 8.889E-02 | 0.32 | 8.910E-02 | 0.32 | 8.879E-02 | 0.12 |
| 2000 | 5.919E-02 | 0.31 | 5.936E-02 | 0.31 | 5.927E-02 | 0.14 |
| 2200 | 4.548E-02 | 0.39 | 4.551E-02 | 0.39 | 4.554E-02 | 0.16 |
| 2300 | 3.997E-02 | 0.45 | 4.000E-02 | 0.45 | 4.000E-02 | 0.19 |
| 2400 | 3.499E-02 | 0.79 | 3.513E-02 | 0.79 | 3.516E-02 | 0.21 |
| 2500 | 3.087E-02 | 1.21 | 3.101E-02 | 1.21 | 3.098E-02 | 0.23 |

## 6.6. NIST lamps data

NIST measured four lamps: GO-N34, GO-N51, GO-N60 and GO-N44. Three lams, GO-N34, GO-N51 and GO-N60, were used as the comparison traveling standard lamps and were send to the pilot. The lamps GO-N44 was calibrated with the other three lamps but kept at NIST to be used as a control standard. This control lamp was used to check for reproducibility between the two rounds of measurements. The lamp voltages and cumulative operational times are listed in Table 6.6.1. There is no evidence of large changes in lamp voltages between the first round of measurements and the second round which occurred after these lamps were returned from the pilot lab.

The operational hours reflect how the lamps were operated at NIST. Each group of three measurements during few days denote periods where the lamp was turned off and repositioned to a different lamp measurement station. These lamps were calibrated for the wavelength range from 250 nm to 2400 nm. Equipment settings were changed to perform measurements at 2500 nm. All the measurements were performed at laboratory temperatures between 18 °C and 19 °C and relative humidity values between 65 % and 70 %. The laboratory temperatures are set lower than the typical ambient lab temperatures in order to thermally stabilize the cooled detectors in our facility.

Table 6.6.1. CCPR lamp operational hours and voltages. The lamps were hand carried to the pilot lab between the 1st and 2nd round of measurements.

| **Lamp** | **Date** | **Total hours /h** | **Lamp voltage /V** | **Date** | **Total hours /h** | **Lamp voltage /V** |
|---|---|---|---|---|---|---|
| | CCPR 1st Round | | | CCPR 2nd Round | | |
| GO-N34 | 6/16/2018 | 15.11 | 108.13 | 8/27/2019 | 39.53 | 108.28 |
| GO-N51 | 6/12/2018 | 6.50 | 104.97 | 8/27/2019 | 26.71 | 105.09 |
| GO-N60 | 6/12/2018 | 6.47 | 105.96 | 8/27/2019 | 19.61 | 106.05 |

The NIST spectral irradiances measurements of both rounds along with the ratios of the second round to the first round are listed in the tables below. Immediately, the spectrally flat changes in the spectral irradiances of GO-N34 can be observed in Figure 6.6.1. The other two lamps repeated to within the total ($k$=1) standard uncertainties of the NIST measurements. Spectrally flat changes of spectral irradiance can occur with filament unwinding which can come from physical shock to the lamp. A white patch on lamp GO-N34, which was not evident during the 1st round of measurements, could be seen after the lamp was returned from the pilot lab.

In order to account for any anomalous changes of the CCPR transfer standard lamps, lamp GO-N44 was calibrated along with the other CCPR lamps but kept at NIST. Figure 6.2 shows a comparison of this lamp which was kept at NIST to the others which were sent to the pilot lab. This lamp, GO-N44, and the other lamps do not display the changes observed in lamp GO-N34. At NIST these lamps were calibrated at more wavelengths than the ones specified for the CCPR comparison. One the basis of the changes seen in lamp GO-N34. This lamp has been excluded from the comparison by mutual agreement between the pilot lab and NIST, which later was approved by other participants.

Note: withdrawing from the comparison of the NIST lamp GO-N34 was requested at the stage of submitting the NIST Measurement report.

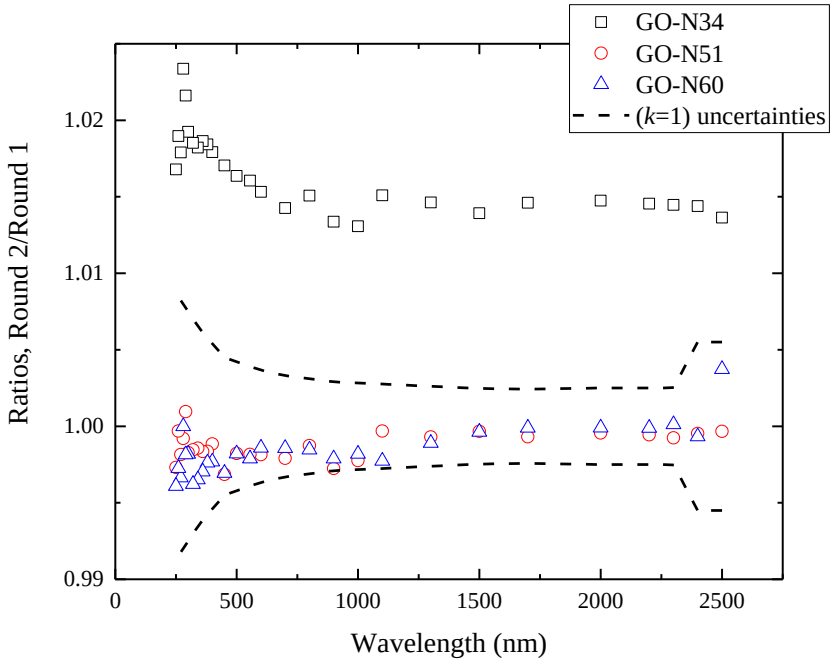


**Figure 6.6.1.** Spectral irradiance ratios between the 1st and 2nd round NIST measurements, at only the wavelengths specified for the CCPR key comparison. Lamp GO-N34 showed a spectrally flat change between the two rounds. Due to the observed changes, NIST and the pilot lab have agreed to remove GO-N34 from the intercomparison.

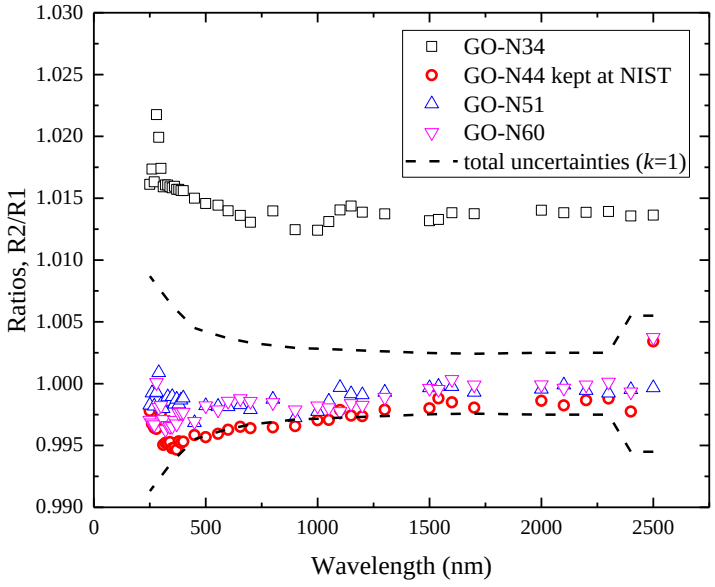


**Figure 6.6.2.** Spectral irradiance ratios at all the wavelengths measured at NIST including wavelengths which were not specified in the CCPR key comparison for the 1st and 2nd rounds. One of the lamps, GO-N44, was kept at NIST as a check standard. This lamp and the others do not show the large spectrally flat change observed with GO-N34.

Table 6.6.2. Spectral Irradiance of NIST lamp **GO-N34**

| Wavelength, nm | Participant Data | | | | Pilot Data | |
|---|---|---|---|---|---|---|
| | Round 1 | | Round 2 | | | |
| | Spectral Irradiance, W $m^{-2}$ $nm^{-1}$ | Combined uncertainty ($k$=1), % | Spectral Irradiance, W $m^{-2}$ $nm^{-1}$ | Combined uncertainty ($k$=1), % | Spectral Irradiance, W $m^{-2}$ $nm^{-1}$ | Combined uncertainty ($k$=1), % |
| 250 | 1.444E-04 | 0.78 | 1.468E-04 | 0.78 | 1.441E-04 | 0.37 |
| 260 | 2.563E-04 | 0.76 | 2.612E-04 | 0.76 | 2.565E-04 | 0.34 |
| 270 | 4.259E-04 | 0.73 | 4.336E-04 | 0.73 | 4.296E-04 | 0.32 |
| 280 | 6.729E-04 | 0.71 | 6.886E-04 | 0.71 | 6.744E-04 | 0.30 |
| 290 | 1.031E-03 | 0.68 | 1.053E-03 | 0.68 | 1.033E-03 | 0.29 |
| 300 | 1.514E-03 | 0.66 | 1.543E-03 | 0.66 | 1.513E-03 | 0.29 |
| 320 | 2.961E-03 | 0.61 | 3.015E-03 | 0.61 | 2.961E-03 | 0.28 |
| 340 | 5.227E-03 | 0.56 | 5.322E-03 | 0.56 | 5.227E-03 | 0.27 |
| 360 | 8.485E-03 | 0.53 | 8.643E-03 | 0.53 | 8.499E-03 | 0.26 |
| 380 | 1.290E-02 | 0.50 | 1.314E-02 | 0.50 | 1.294E-02 | 0.26 |
| 400 | 1.856E-02 | 0.48 | 1.890E-02 | 0.48 | 1.859E-02 | 0.25 |
| 450 | 3.798E-02 | 0.42 | 3.862E-02 | 0.42 | 3.798E-02 | 0.22 |
| 500 | 6.345E-02 | 0.39 | 6.449E-02 | 0.39 | 6.341E-02 | 0.21 |
| 555 | 9.487E-02 | 0.35 | 9.639E-02 | 0.35 | 9.483E-02 | 0.18 |
| 600 | 1.205E-01 | 0.33 | 1.224E-01 | 0.33 | 1.204E-01 | 0.16 |
| 700 | 1.680E-01 | 0.29 | 1.704E-01 | 0.29 | 1.680E-01 | 0.16 |
| 800 | 1.958E-01 | 0.26 | 1.987E-01 | 0.26 | 1.962E-01 | 0.15 |
| 900 | 2.059E-01 | 0.23 | 2.087E-01 | 0.23 | 2.057E-01 | 0.14 |
| 1000 | 2.017E-01 | 0.22 | 2.043E-01 | 0.22 | 2.016E-01 | 0.13 |
| 1100 | 1.886E-01 | 0.21 | 1.915E-01 | 0.21 | 1.891E-01 | 0.13 |
| 1300 | 1.540E-01 | 0.19 | 1.563E-01 | 0.19 | 1.545E-01 | 0.13 |
| 1500 | 1.198E-01 | 0.17 | 1.214E-01 | 0.17 | 1.202E-01 | 0.12 |
| 1700 | 9.150E-02 | 0.16 | 9.283E-02 | 0.16 | 9.180E-02 | 0.12 |
| 2000 | 6.086E-02 | 0.14 | 6.176E-02 | 0.14 | 6.102E-02 | 0.14 |
| 2200 | 4.665E-02 | 0.14 | 4.733E-02 | 0.14 | 4.677E-02 | 0.16 |
| 2300 | 4.098E-02 | 0.14 | 4.157E-02 | 0.14 | 4.114E-02 | 0.19 |
| 2400 | 3.593E-02 | 0.28 | 3.645E-02 | 0.28 | 3.615E-02 | 0.21 |
| 2500 | 3.186E-02 | 0.52 | 3.229E-02 | 0.52 | 3.175E-02 | 0.23 |

Table 6.6.3. Spectral Irradiance of NIST lamp **GO-N51**

| Wavelength, nm | Participant Data | | | | Pilot Data | |
|---|---|---|---|---|---|---|
| | Round 1 | | Round 2 | | | |
| | Spectral Irradiance, W $m^{-2}$ $nm^{-1}$ | Combined uncertainty ($k$=1), % | Spectral Irradiance, W $m^{-2}$ $nm^{-1}$ | Combined uncertainty ($k$=1), % | Spectral Irradiance, W $m^{-2}$ $nm^{-1}$ | Combined uncertainty ($k$=1), % |
| 250 | 1.223E-04 | 0.78 | 1.220E-04 | 0.78 | 1.215E-04 | 0.37 |
| 260 | 2.177E-04 | 0.76 | 2.177E-04 | 0.76 | 2.165E-04 | 0.34 |
| 270 | 3.644E-04 | 0.73 | 3.637E-04 | 0.73 | 3.634E-04 | 0.32 |
| 280 | 5.816E-04 | 0.71 | 5.811E-04 | 0.71 | 5.786E-04 | 0.30 |
| 290 | 8.872E-04 | 0.68 | 8.880E-04 | 0.68 | 8.833E-04 | 0.29 |
| 300 | 1.307E-03 | 0.66 | 1.305E-03 | 0.66 | 1.297E-03 | 0.29 |
| 320 | 2.576E-03 | 0.61 | 2.572E-03 | 0.61 | 2.559E-03 | 0.28 |
| 340 | 4.579E-03 | 0.56 | 4.573E-03 | 0.56 | 4.549E-03 | 0.27 |
| 360 | 7.485E-03 | 0.53 | 7.473E-03 | 0.53 | 7.452E-03 | 0.26 |
| 380 | 1.146E-02 | 0.50 | 1.144E-02 | 0.50 | 1.142E-02 | 0.26 |
| 400 | 1.657E-02 | 0.48 | 1.655E-02 | 0.48 | 1.651E-02 | 0.25 |
| 450 | 3.436E-02 | 0.42 | 3.425E-02 | 0.42 | 3.414E-02 | 0.22 |
| 500 | 5.789E-02 | 0.39 | 5.779E-02 | 0.39 | 5.757E-02 | 0.21 |
| 555 | 8.732E-02 | 0.35 | 8.716E-02 | 0.35 | 8.692E-02 | 0.18 |
| 600 | 1.116E-01 | 0.33 | 1.114E-01 | 0.33 | 1.111E-01 | 0.16 |
| 700 | 1.571E-01 | 0.29 | 1.568E-01 | 0.29 | 1.566E-01 | 0.16 |
| 800 | 1.844E-01 | 0.26 | 1.842E-01 | 0.26 | 1.843E-01 | 0.15 |
| 900 | 1.951E-01 | 0.23 | 1.946E-01 | 0.23 | 1.944E-01 | 0.14 |
| 1000 | 1.919E-01 | 0.22 | 1.914E-01 | 0.22 | 1.912E-01 | 0.13 |
| 1100 | 1.800E-01 | 0.21 | 1.800E-01 | 0.21 | 1.799E-01 | 0.13 |
| 1300 | 1.477E-01 | 0.19 | 1.476E-01 | 0.19 | 1.477E-01 | 0.13 |
| 1500 | 1.151E-01 | 0.17 | 1.151E-01 | 0.17 | 1.153E-01 | 0.12 |
| 1700 | 8.824E-02 | 0.16 | 8.818E-02 | 0.16 | 8.823E-02 | 0.12 |
| 2000 | 5.883E-02 | 0.14 | 5.881E-02 | 0.14 | 5.883E-02 | 0.14 |
| 2200 | 4.515E-02 | 0.14 | 4.513E-02 | 0.14 | 4.517E-02 | 0.16 |
| 2300 | 3.971E-02 | 0.14 | 3.968E-02 | 0.14 | 3.967E-02 | 0.19 |
| 2400 | 3.483E-02 | 0.28 | 3.481E-02 | 0.28 | 3.492E-02 | 0.21 |
| 2500 | 3.082E-02 | 0.52 | 3.081E-02 | 0.52 | 3.074E-02 | 0.23 |

Table 6.6.4. Spectral Irradiance of NIST lamp **GO-N60**

| Wavelength, nm | Participant Data | | | | Pilot Data | |
|---|---|---|---|---|---|---|
| | Round 1 | | Round 2 | | | |
| | Spectral Irradiance, W $m^{-2}$ $nm^{-1}$ | Combined uncertainty ($k$=1), % | Spectral Irradiance, W $m^{-2}$ $nm^{-1}$ | Combined uncertainty ($k$=1), % | Spectral Irradiance, W $m^{-2}$ $nm^{-1}$ | Combined uncertainty ($k$=1), % |
| 250 | 1.413E-04 | 0.78 | 1.408E-04 | 0.78 | 1.397E-04 | 0.37 |
| 260 | 2.494E-04 | 0.76 | 2.488E-04 | 0.76 | 2.482E-04 | 0.34 |
| 270 | 4.134E-04 | 0.73 | 4.120E-04 | 0.73 | 4.137E-04 | 0.32 |
| 280 | 6.431E-04 | 0.71 | 6.431E-04 | 0.71 | 6.432E-04 | 0.30 |
| 290 | 9.974E-04 | 0.68 | 9.955E-04 | 0.68 | 9.915E-04 | 0.29 |
| 300 | 1.463E-03 | 0.66 | 1.460E-03 | 0.66 | 1.451E-03 | 0.29 |
| 320 | 2.861E-03 | 0.61 | 2.850E-03 | 0.61 | 2.841E-03 | 0.28 |
| 340 | 5.053E-03 | 0.56 | 5.035E-03 | 0.56 | 5.027E-03 | 0.27 |
| 360 | 8.220E-03 | 0.53 | 8.196E-03 | 0.53 | 8.186E-03 | 0.26 |
| 380 | 1.252E-02 | 0.50 | 1.249E-02 | 0.50 | 1.248E-02 | 0.26 |
| 400 | 1.803E-02 | 0.48 | 1.799E-02 | 0.48 | 1.797E-02 | 0.25 |
| 450 | 3.705E-02 | 0.42 | 3.694E-02 | 0.42 | 3.681E-02 | 0.22 |
| 500 | 6.200E-02 | 0.39 | 6.189E-02 | 0.39 | 6.167E-02 | 0.21 |
| 555 | 9.300E-02 | 0.35 | 9.280E-02 | 0.35 | 9.255E-02 | 0.18 |
| 600 | 1.183E-01 | 0.33 | 1.182E-01 | 0.33 | 1.178E-01 | 0.16 |
| 700 | 1.656E-01 | 0.29 | 1.653E-01 | 0.29 | 1.650E-01 | 0.16 |
| 800 | 1.936E-01 | 0.26 | 1.933E-01 | 0.26 | 1.933E-01 | 0.15 |
| 900 | 2.040E-01 | 0.23 | 2.036E-01 | 0.23 | 2.032E-01 | 0.14 |
| 1000 | 2.001E-01 | 0.22 | 1.998E-01 | 0.22 | 1.995E-01 | 0.13 |
| 1100 | 1.875E-01 | 0.21 | 1.871E-01 | 0.21 | 1.875E-01 | 0.13 |
| 1300 | 1.534E-01 | 0.19 | 1.532E-01 | 0.19 | 1.535E-01 | 0.13 |
| 1500 | 1.194E-01 | 0.17 | 1.194E-01 | 0.17 | 1.196E-01 | 0.12 |
| 1700 | 9.143E-02 | 0.16 | 9.142E-02 | 0.16 | 9.163E-02 | 0.12 |
| 2000 | 6.090E-02 | 0.14 | 6.089E-02 | 0.14 | 6.099E-02 | 0.14 |
| 2200 | 4.672E-02 | 0.14 | 4.671E-02 | 0.14 | 4.675E-02 | 0.16 |
| 2300 | 4.107E-02 | 0.14 | 4.107E-02 | 0.14 | 4.105E-02 | 0.19 |
| 2400 | 3.602E-02 | 0.28 | 3.600E-02 | 0.28 | 3.619E-02 | 0.21 |
| 2500 | 3.181E-02 | 0.52 | 3.193E-02 | 0.52 | 3.177E-02 | 0.23 |

## 6.7. NMC A*STAR lamps data

NMC A*STAR traveling lamps: BN-9101-642, BN-9101-643 and BN-9101-644.

Table 6.7.1. Spectral Irradiance of NMC A*STAR lamp **BN-9101-642**

| Wavelength, nm | Participant Data | | | | Pilot Data | |
|---|---|---|---|---|---|---|
| | Round 1 | | Round 2 | | | |
| | Spectral Irradiance, W $m^{-2}$ $nm^{-1}$ | Combined uncertainty ($k$=1), % | Spectral Irradiance, W $m^{-2}$ $nm^{-1}$ | Combined uncertainty ($k$=1), % | Spectral Irradiance, W $m^{-2}$ $nm^{-1}$ | Combined uncertainty ($k$=1), % |
| 250 | 1.611E-04 | 0.93 | 1.609E-04 | 0.92 | 1.622E-04 | 0.37 |
| 260 | 2.841E-04 | 0.85 | 2.857E-04 | 0.90 | 2.865E-04 | 0.34 |
| 270 | 4.761E-04 | 0.75 | 4.773E-04 | 0.76 | 4.770E-04 | 0.32 |
| 280 | 7.496E-04 | 0.77 | 7.534E-04 | 0.79 | 7.530E-04 | 0.30 |
| 290 | 1.128E-03 | 0.65 | 1.132E-03 | 0.70 | 1.136E-03 | 0.29 |
| 300 | 1.647E-03 | 0.63 | 1.650E-03 | 0.68 | 1.655E-03 | 0.29 |
| 320 | 3.188E-03 | 0.60 | 3.199E-03 | 0.63 | 3.210E-03 | 0.28 |
| 340 | 5.614E-03 | 0.53 | 5.627E-03 | 0.58 | 5.636E-03 | 0.27 |
| 360 | 9.091E-03 | 0.50 | 9.117E-03 | 0.54 | 9.122E-03 | 0.26 |
| 380 | 1.379E-02 | 0.47 | 1.381E-02 | 0.51 | 1.382E-02 | 0.26 |
| 400 | 1.974E-02 | 0.43 | 1.980E-02 | 0.48 | 1.980E-02 | 0.25 |
| 450 | 3.993E-02 | 0.40 | 4.000E-02 | 0.47 | 4.015E-02 | 0.22 |
| 500 | 6.625E-02 | 0.35 | 6.637E-02 | 0.40 | 6.671E-02 | 0.21 |
| 555 | 9.890E-02 | 0.33 | 9.897E-02 | 0.39 | 9.934E-02 | 0.18 |
| 600 | 1.251E-01 | 0.31 | 1.254E-01 | 0.39 | 1.258E-01 | 0.16 |
| 700 | 1.739E-01 | 0.28 | 1.741E-01 | 0.33 | 1.746E-01 | 0.16 |
| 800 | 2.049E-01 | 0.31 | 2.045E-01 | 0.37 | 2.033E-01 | 0.15 |
| 900 | 2.140E-01 | 0.70 | 2.145E-01 | 0.37 | 2.128E-01 | 0.14 |
| 1000 | 2.091E-01 | 0.28 | 2.100E-01 | 0.32 | 2.081E-01 | 0.13 |
| 1100 | 1.965E-01 | 0.26 | 1.970E-01 | 0.31 | 1.951E-01 | 0.13 |
| 1300 | 1.604E-01 | 0.23 | 1.607E-01 | 0.29 | 1.591E-01 | 0.13 |
| 1500 | 1.247E-01 | 0.27 | 1.252E-01 | 0.30 | 1.236E-01 | 0.12 |
| 1700 | 9.527E-02 | 0.22 | 9.556E-02 | 0.26 | 9.434E-02 | 0.12 |
| 2000 | 6.328E-02 | 0.23 | 6.338E-02 | 0.27 | 6.267E-02 | 0.14 |
| 2200 | 4.845E-02 | 0.26 | 4.861E-02 | 0.31 | 4.802E-02 | 0.16 |
| 2300 | 4.258E-02 | 0.23 | 4.266E-02 | 0.35 | 4.217E-02 | 0.19 |
| 2400 | 3.748E-02 | 0.31 | 3.757E-02 | 0.30 | 3.711E-02 | 0.21 |
| 2500 | 3.305E-02 | 0.27 | 3.313E-02 | 0.41 | 3.265E-02 | 0.23 |

Table 6.7.2. Spectral Irradiance of NMC A*STAR lamp **BN-9101-643**

| Wavelength, nm | Participant Data | | | | Pilot Data | |
|---|---|---|---|---|---|---|
| | Round 1 | | Round 2 | | | |
| | Spectral Irradiance, W $m^{-2}$ $nm^{-1}$ | Combined uncertainty ($k$=1), % | Spectral Irradiance, W $m^{-2}$ $nm^{-1}$ | Combined uncertainty ($k$=1), % | Spectral Irradiance, W $m^{-2}$ $nm^{-1}$ | Combined uncertainty ($k$=1), % |
| 250 | 1.453E-04 | 1.24 | 1.461E-04 | 0.92 | 1.459E-04 | 0.37 |
| 260 | 2.580E-04 | 0.85 | 2.612E-04 | 0.84 | 2.609E-04 | 0.34 |
| 270 | 4.341E-04 | 0.73 | 4.385E-04 | 0.77 | 4.361E-04 | 0.32 |
| 280 | 6.741E-04 | 0.80 | 6.816E-04 | 0.80 | 6.824E-04 | 0.30 |
| 290 | 1.040E-03 | 0.69 | 1.048E-03 | 0.68 | 1.046E-03 | 0.29 |
| 300 | 1.523E-03 | 0.64 | 1.536E-03 | 0.66 | 1.531E-03 | 0.29 |
| 320 | 2.969E-03 | 0.61 | 2.992E-03 | 0.61 | 2.991E-03 | 0.28 |
| 340 | 5.248E-03 | 0.53 | 5.290E-03 | 0.56 | 5.275E-03 | 0.27 |
| 360 | 8.552E-03 | 0.49 | 8.610E-03 | 0.53 | 8.569E-03 | 0.26 |
| 380 | 1.300E-02 | 0.47 | 1.308E-02 | 0.51 | 1.304E-02 | 0.26 |
| 400 | 1.869E-02 | 0.44 | 1.880E-02 | 0.48 | 1.875E-02 | 0.25 |
| 450 | 3.805E-02 | 0.40 | 3.827E-02 | 0.44 | 3.830E-02 | 0.22 |
| 500 | 6.357E-02 | 0.35 | 6.384E-02 | 0.41 | 6.398E-02 | 0.21 |
| 555 | 9.534E-02 | 0.32 | 9.565E-02 | 0.40 | 9.575E-02 | 0.18 |
| 600 | 1.212E-01 | 0.31 | 1.214E-01 | 0.35 | 1.216E-01 | 0.16 |
| 700 | 1.693E-01 | 0.27 | 1.696E-01 | 0.30 | 1.698E-01 | 0.16 |
| 800 | 2.003E-01 | 0.30 | 2.002E-01 | 0.39 | 1.985E-01 | 0.15 |
| 900 | 2.112E-01 | 0.74 | 2.103E-01 | 0.47 | 2.082E-01 | 0.14 |
| 1000 | 2.053E-01 | 0.29 | 2.064E-01 | 0.30 | 2.041E-01 | 0.13 |
| 1100 | 1.930E-01 | 0.24 | 1.935E-01 | 0.26 | 1.916E-01 | 0.13 |
| 1300 | 1.581E-01 | 0.25 | 1.583E-01 | 0.26 | 1.566E-01 | 0.13 |
| 1500 | 1.231E-01 | 0.22 | 1.233E-01 | 0.24 | 1.219E-01 | 0.12 |
| 1700 | 9.424E-02 | 0.20 | 9.418E-02 | 0.24 | 9.306E-02 | 0.12 |
| 2000 | 6.271E-02 | 0.22 | 6.266E-02 | 0.24 | 6.194E-02 | 0.14 |
| 2200 | 4.809E-02 | 0.25 | 4.804E-02 | 0.30 | 4.753E-02 | 0.16 |
| 2300 | 4.227E-02 | 0.22 | 4.220E-02 | 0.25 | 4.178E-02 | 0.19 |
| 2400 | 3.718E-02 | 0.29 | 3.718E-02 | 0.25 | 3.670E-02 | 0.21 |
| 2500 | 3.280E-02 | 0.33 | 3.284E-02 | 0.46 | 3.236E-02 | 0.23 |

Table 6.7.3. Spectral Irradiance of NMC A*STAR lamp **BN-9101-644**

| Wavelength, nm | Participant Data | | | | Pilot Data | |
|---|---|---|---|---|---|---|
| | Round 1 | | Round 2 | | | |
| | Spectral Irradiance, W $m^{-2}$ $nm^{-1}$ | Combined uncertainty ($k$=1), % | Spectral Irradiance, W $m^{-2}$ $nm^{-1}$ | Combined uncertainty ($k$=1), % | Spectral Irradiance, W $m^{-2}$ $nm^{-1}$ | Combined uncertainty ($k$=1), % |
| 250 | 1.466E-04 | 0.99 | 1.473E-04 | 0.99 | 1.479E-04 | 0.37 |
| 260 | 2.606E-04 | 0.83 | 2.633E-04 | 0.89 | 2.634E-04 | 0.34 |
| 270 | 4.379E-04 | 0.76 | 4.415E-04 | 0.74 | 4.409E-04 | 0.32 |
| 280 | 6.830E-04 | 0.80 | 6.888E-04 | 0.80 | 6.894E-04 | 0.30 |
| 290 | 1.049E-03 | 0.67 | 1.056E-03 | 0.71 | 1.057E-03 | 0.29 |
| 300 | 1.536E-03 | 0.64 | 1.547E-03 | 0.70 | 1.546E-03 | 0.29 |
| 320 | 2.996E-03 | 0.61 | 3.015E-03 | 0.61 | 3.022E-03 | 0.28 |
| 340 | 5.306E-03 | 0.54 | 5.327E-03 | 0.55 | 5.325E-03 | 0.27 |
| 360 | 8.617E-03 | 0.49 | 8.670E-03 | 0.53 | 8.657E-03 | 0.26 |
| 380 | 1.312E-02 | 0.46 | 1.318E-02 | 0.52 | 1.318E-02 | 0.26 |
| 400 | 1.885E-02 | 0.43 | 1.895E-02 | 0.47 | 1.894E-02 | 0.25 |
| 450 | 3.839E-02 | 0.39 | 3.859E-02 | 0.46 | 3.866E-02 | 0.22 |
| 500 | 6.407E-02 | 0.36 | 6.436E-02 | 0.39 | 6.456E-02 | 0.21 |
| 555 | 9.608E-02 | 0.33 | 9.639E-02 | 0.36 | 9.661E-02 | 0.18 |
| 600 | 1.220E-01 | 0.31 | 1.225E-01 | 0.34 | 1.227E-01 | 0.16 |
| 700 | 1.706E-01 | 0.28 | 1.709E-01 | 0.29 | 1.713E-01 | 0.16 |
| 800 | 2.014E-01 | 0.30 | 2.015E-01 | 0.32 | 2.001E-01 | 0.15 |
| 900 | 2.096E-01 | 0.67 | 2.126E-01 | 0.37 | 2.099E-01 | 0.14 |
| 1000 | 2.071E-01 | 0.26 | 2.078E-01 | 0.30 | 2.057E-01 | 0.13 |
| 1100 | 1.948E-01 | 0.24 | 1.947E-01 | 0.28 | 1.930E-01 | 0.13 |
| 1300 | 1.593E-01 | 0.24 | 1.594E-01 | 0.25 | 1.577E-01 | 0.13 |
| 1500 | 1.240E-01 | 0.23 | 1.240E-01 | 0.26 | 1.227E-01 | 0.12 |
| 1700 | 9.482E-02 | 0.23 | 9.490E-02 | 0.24 | 9.372E-02 | 0.12 |
| 2000 | 6.304E-02 | 0.22 | 6.300E-02 | 0.25 | 6.239E-02 | 0.14 |
| 2200 | 4.831E-02 | 0.24 | 4.833E-02 | 0.25 | 4.780E-02 | 0.16 |
| 2300 | 4.246E-02 | 0.22 | 4.244E-02 | 0.27 | 4.210E-02 | 0.19 |
| 2400 | 3.737E-02 | 0.26 | 3.737E-02 | 0.25 | 3.694E-02 | 0.21 |
| 2500 | 3.290E-02 | 0.28 | 3.296E-02 | 0.35 | 3.265E-02 | 0.23 |

## 6.8. NMIA lamps data

NMIA traveling lamps: BN-9101-657, BN-9101-658 and BN-9101-659.

Note: NMIA submitted the measurement data for both rounds. But, later, at the stage of the Relative Data analysis of Pre-Draft A process, NMIA requested withdrawing the Round 2 data for all three lamps. The request was agreed. Therefore, the NMIA Round 2 data were not used for comparison analysis. In the tables below the Round 2 data marked in grey courol.

Table 6.8.1. Spectral Irradiance of NMIA lamp **BN-9101-657**

| Wavelength, nm | Participant Data | | | | Pilot Data | |
|---|---|---|---|---|---|---|
| | Round 1 | | Round 2 | | | |
| | Spectral Irradiance, W m$^{-2}$ nm$^{-1}$ | Combined uncertainty ($k$=1), % | Spectral Irradiance, W m$^{-2}$ nm$^{-1}$ | Combined uncertainty ($k$=1), % | Spectral Irradiance, W m$^{-2}$ nm$^{-1}$ | Combined uncertainty ($k$=1), % |
| 250 | 1.392E-04 | 2.89 | 1.400E-04 | 9.42 | 1.436E-04 | 0.37 |
| 260 | 2.510E-04 | 2.36 | 2.530E-04 | 6.48 | 2.545E-04 | 0.34 |
| 270 | 4.140E-04 | 2.20 | 4.120E-04 | 4.01 | 4.267E-04 | 0.32 |
| 280 | 6.610E-04 | 1.84 | 6.380E-04 | 2.78 | 6.758E-04 | 0.30 |
| 290 | 1.001E-03 | 1.74 | 9.300E-04 | 7.39 | 1.026E-03 | 0.29 |
| 300 | 1.463E-03 | 1.60 | 1.373E-03 | 2.89 | 1.499E-03 | 0.29 |
| 320 | 2.855E-03 | 1.42 | 2.740E-03 | 1.85 | 2.930E-03 | 0.28 |
| 340 | 5.040E-03 | 1.26 | 4.870E-03 | 1.35 | 5.163E-03 | 0.27 |
| 360 | 8.220E-03 | 1.13 | 8.030E-03 | 1.14 | 8.407E-03 | 0.26 |
| 380 | 1.252E-02 | 1.00 | 1.227E-02 | 1.07 | 1.280E-02 | 0.26 |
| 400 | 1.803E-02 | 0.89 | 1.775E-02 | 0.95 | 1.840E-02 | 0.25 |
| 450 | 3.707E-02 | 0.67 | 3.700E-02 | 1.53 | 3.761E-02 | 0.22 |
| 500 | 6.235E-02 | 0.50 | 6.221E-02 | 0.71 | 6.289E-02 | 0.21 |
| 555 | 9.388E-02 | 0.38 | 9.378E-02 | 0.56 | 9.428E-02 | 0.18 |
| 600 | 1.197E-01 | 0.32 | 1.196E-01 | 0.76 | 1.199E-01 | 0.16 |
| 700 | 1.681E-01 | 0.41 | 1.685E-01 | 0.57 | 1.676E-01 | 0.16 |
| 800 | 1.977E-01 | 0.58 | 1.987E-01 | 0.60 | 1.961E-01 | 0.15 |
| 900 | 2.085E-01 | 0.68 | 2.104E-01 | 0.71 | 2.059E-01 | 0.14 |
| 1000 | 2.050E-01 | 0.77 | 2.073E-01 | 0.81 | 2.018E-01 | 0.13 |
| 1100 | 1.930E-01 | 0.84 | 1.952E-01 | 0.86 | 1.896E-01 | 0.13 |
| 1300 | 1.583E-01 | 0.94 | 1.608E-01 | 0.96 | 1.550E-01 | 0.13 |
| 1500 | 1.236E-01 | 1.02 | 1.258E-01 | 1.04 | 1.207E-01 | 0.12 |
| 1700 | 9.470E-02 | 1.08 | 9.650E-02 | 1.09 | 9.213E-02 | 0.12 |
| 2000 | 6.340E-02 | 1.15 | 6.420E-02 | 1.15 | 6.140E-02 | 0.14 |
| 2200 | 4.890E-02 | 1.19 | 4.920E-02 | 1.19 | 4.706E-02 | 0.16 |
| 2300 | 4.359E-02 | 1.19 | 4.363E-02 | 1.20 | 4.136E-02 | 0.19 |
| 2400 | 3.886E-02 | 1.20 | 3.893E-02 | 1.20 | 3.640E-02 | 0.21 |
| 2500 | 3.486E-02 | 1.30 | 3.484E-02 | 1.24 | 3.202E-02 | 0.23 |

Table 6.8.2. Spectral Irradiance of NMIA lamp **BN-9101-658**

| Wavelength, nm | Participant Data | | | | Pilot Data | |
|---|---|---|---|---|---|---|
| | Round 1 | | Round 2 | | | |
| | Spectral Irradiance, W $m^{-2}$ $nm^{-1}$ | Combined uncertainty ($k$=1), % | Spectral Irradiance, W $m^{-2}$ $nm^{-1}$ | Combined uncertainty ($k$=1), % | Spectral Irradiance, W $m^{-2}$ $nm^{-1}$ | Combined uncertainty ($k$=1), % |
| 250 | 1.333E-04 | 2.71 | 1.330E-04 | 9.57 | 1.378E-04 | 0.37 |
| 260 | 2.385E-04 | 2.42 | 2.430E-04 | 5.52 | 2.459E-04 | 0.34 |
| 270 | 4.050E-04 | 1.96 | 4.020E-04 | 3.14 | 4.141E-04 | 0.32 |
| 280 | 6.430E-04 | 1.84 | 6.290E-04 | 2.37 | 6.548E-04 | 0.30 |
| 290 | 9.780E-04 | 1.76 | 9.490E-04 | 2.15 | 9.951E-04 | 0.29 |
| 300 | 1.430E-03 | 1.69 | 1.371E-03 | 2.04 | 1.457E-03 | 0.29 |
| 320 | 2.793E-03 | 1.45 | 2.652E-03 | 1.93 | 2.853E-03 | 0.28 |
| 340 | 4.935E-03 | 1.30 | 4.800E-03 | 1.55 | 5.047E-03 | 0.27 |
| 360 | 8.060E-03 | 1.15 | 7.880E-03 | 1.25 | 8.224E-03 | 0.26 |
| 380 | 1.231E-02 | 1.03 | 1.205E-02 | 1.36 | 1.254E-02 | 0.26 |
| 400 | 1.775E-02 | 0.92 | 1.741E-02 | 0.98 | 1.806E-02 | 0.25 |
| 450 | 3.655E-02 | 0.71 | 3.625E-02 | 0.73 | 3.705E-02 | 0.22 |
| 500 | 6.154E-02 | 0.55 | 6.136E-02 | 0.55 | 6.212E-02 | 0.21 |
| 555 | 9.281E-02 | 0.44 | 9.294E-02 | 0.40 | 9.334E-02 | 0.18 |
| 600 | 1.184E-01 | 0.39 | 1.188E-01 | 0.35 | 1.188E-01 | 0.16 |
| 700 | 1.664E-01 | 0.46 | 1.676E-01 | 0.45 | 1.666E-01 | 0.16 |
| 800 | 1.960E-01 | 0.62 | 1.984E-01 | 0.60 | 1.952E-01 | 0.15 |
| 900 | 2.067E-01 | 0.72 | 2.099E-01 | 0.70 | 2.052E-01 | 0.14 |
| 1000 | 2.030E-01 | 0.80 | 2.069E-01 | 0.79 | 2.014E-01 | 0.13 |
| 1100 | 1.914E-01 | 0.87 | 1.953E-01 | 0.88 | 1.892E-01 | 0.13 |
| 1300 | 1.569E-01 | 0.98 | 1.608E-01 | 0.96 | 1.548E-01 | 0.13 |
| 1500 | 1.225E-01 | 1.05 | 1.259E-01 | 1.04 | 1.206E-01 | 0.12 |
| 1700 | 9.380E-02 | 1.12 | 9.670E-02 | 1.11 | 9.219E-02 | 0.12 |
| 2000 | 6.320E-02 | 1.46 | 6.430E-02 | 1.20 | 6.135E-02 | 0.14 |
| 2200 | 4.850E-02 | 1.35 | 4.940E-02 | 1.26 | 4.704E-02 | 0.16 |
| 2300 | 4.313E-02 | 1.22 | 4.360E-02 | 1.28 | 4.134E-02 | 0.19 |
| 2400 | 3.840E-02 | 1.54 | 3.897E-02 | 1.26 | 3.646E-02 | 0.21 |
| 2500 | 3.487E-02 | 1.23 | 3.483E-02 | 1.26 | 3.197E-02 | 0.23 |

Table 6.8.3. Spectral Irradiance of NMIA lamp **BN-9101-659**

| Wavelength, nm | Participant Data | | | | Pilot Data | |
|---|---|---|---|---|---|---|
| | Round 1 | | Round 2 | | | |
| | Spectral Irradiance, W $m^{-2}$ $nm^{-1}$ | Combined uncertainty ($k$=1), % | Spectral Irradiance, W $m^{-2}$ $nm^{-1}$ | Combined uncertainty ($k$=1), % | Spectral Irradiance, W $m^{-2}$ $nm^{-1}$ | Combined uncertainty ($k$=1), % |
| 250 | 1.547E-04 | 2.95 | 1.720E-04 | 21.30 | 1.497E-04 | 0.37 |
| 260 | 2.630E-04 | 2.34 | 2.840E-04 | 11.97 | 2.661E-04 | 0.34 |
| 270 | 4.410E-04 | 2.03 | 4.380E-04 | 6.50 | 4.448E-04 | 0.32 |
| 280 | 6.830E-04 | 1.97 | 6.670E-04 | 3.94 | 6.892E-04 | 0.30 |
| 290 | 1.053E-03 | 1.85 | 1.005E-03 | 2.45 | 1.063E-03 | 0.29 |
| 300 | 1.538E-03 | 1.68 | 1.449E-03 | 2.07 | 1.553E-03 | 0.29 |
| 320 | 2.985E-03 | 1.52 | 2.801E-03 | 1.60 | 3.031E-03 | 0.28 |
| 340 | 5.250E-03 | 1.33 | 4.860E-03 | 1.19 | 5.331E-03 | 0.27 |
| 360 | 8.540E-03 | 1.18 | 7.930E-03 | 1.29 | 8.653E-03 | 0.26 |
| 380 | 1.296E-02 | 1.03 | 1.218E-02 | 1.01 | 1.315E-02 | 0.26 |
| 400 | 1.855E-02 | 0.93 | 1.770E-02 | 0.78 | 1.888E-02 | 0.25 |
| 450 | 3.807E-02 | 0.69 | 3.715E-02 | 0.56 | 3.848E-02 | 0.22 |
| 500 | 6.370E-02 | 0.52 | 6.296E-02 | 0.34 | 6.422E-02 | 0.21 |
| 555 | 9.553E-02 | 0.38 | 9.551E-02 | 0.29 | 9.601E-02 | 0.18 |
| 600 | 1.214E-01 | 0.33 | 1.219E-01 | 0.24 | 1.219E-01 | 0.16 |
| 700 | 1.695E-01 | 0.43 | 1.716E-01 | 0.69 | 1.699E-01 | 0.16 |
| 800 | 1.986E-01 | 0.60 | 2.031E-01 | 0.53 | 1.982E-01 | 0.15 |
| 900 | 2.085E-01 | 0.72 | 2.147E-01 | 0.62 | 2.077E-01 | 0.14 |
| 1000 | 2.044E-01 | 0.81 | 2.115E-01 | 0.70 | 2.033E-01 | 0.13 |
| 1100 | 1.921E-01 | 0.89 | 1.993E-01 | 0.77 | 1.906E-01 | 0.13 |
| 1300 | 1.569E-01 | 0.95 | 1.639E-01 | 0.87 | 1.555E-01 | 0.13 |
| 1500 | 1.222E-01 | 1.04 | 1.283E-01 | 0.94 | 1.210E-01 | 0.12 |
| 1700 | 9.360E-02 | 1.11 | 9.850E-02 | 1.00 | 9.234E-02 | 0.12 |
| 2000 | 6.220E-02 | 1.62 | 6.510E-02 | 1.15 | 6.137E-02 | 0.14 |
| 2200 | 4.820E-02 | 1.18 | 5.010E-02 | 1.18 | 4.707E-02 | 0.16 |
| 2300 | 4.320E-02 | 1.44 | 4.420E-02 | 1.19 | 4.139E-02 | 0.19 |
| 2400 | 3.840E-02 | 1.45 | 3.951E-02 | 1.20 | 3.641E-02 | 0.21 |
| 2500 | 3.471E-02 | 1.29 | 3.533E-02 | 1.21 | 3.191E-02 | 0.23 |

## 6.9. NMJ lamps data

NMIJ traveling lamps: BN-9101-695, BN-9101-696 and BN-9101-697.

Table 6.9.1. Spectral Irradiance of NMIJ lamp **BN-9101-695**

| Wavelength, nm | Participant Data | | | | Pilot Data | |
|---|---|---|---|---|---|---|
| | Round 1 | | Round 2 | | | |
| | Spectral Irradiance, W $m^{-2}$ $nm^{-1}$ | Combined uncertainty ($k$=1), % | Spectral Irradiance, W $m^{-2}$ $nm^{-1}$ | Combined uncertainty ($k$=1), % | Spectral Irradiance, W $m^{-2}$ $nm^{-1}$ | Combined uncertainty ($k$=1), % |
| 250 | 1.291E-04 | 1.34 | 1.293E-04 | 1.38 | 1.285E-04 | 0.37 |
| 260 | 2.315E-04 | 1.26 | 2.310E-04 | 1.26 | 2.296E-04 | 0.34 |
| 270 | 3.891E-04 | 1.22 | 3.893E-04 | 1.22 | 3.850E-04 | 0.32 |
| 280 | 5.998E-04 | 1.18 | 5.995E-04 | 1.18 | 5.948E-04 | 0.30 |
| 290 | 9.393E-04 | 1.15 | 9.399E-04 | 1.14 | 9.310E-04 | 0.29 |
| 300 | 1.381E-03 | 1.12 | 1.383E-03 | 1.12 | 1.367E-03 | 0.29 |
| 320 | 2.708E-03 | 1.06 | 2.712E-03 | 1.06 | 2.686E-03 | 0.28 |
| 340 | 4.807E-03 | 1.02 | 4.809E-03 | 1.02 | 4.762E-03 | 0.27 |
| 360 | 7.874E-03 | 0.99 | 7.858E-03 | 0.98 | 7.784E-03 | 0.26 |
| 380 | 1.205E-02 | 0.95 | 1.202E-02 | 0.94 | 1.191E-02 | 0.26 |
| 400 | 1.748E-02 | 0.92 | 1.745E-02 | 0.92 | 1.719E-02 | 0.25 |
| 450 | 3.594E-02 | 0.86 | 3.584E-02 | 0.86 | 3.546E-02 | 0.22 |
| 500 | 6.048E-02 | 0.81 | 6.034E-02 | 0.81 | 5.974E-02 | 0.21 |
| 555 | 9.110E-02 | 0.78 | 9.094E-02 | 0.78 | 9.008E-02 | 0.18 |
| 600 | 1.162E-01 | 0.76 | 1.160E-01 | 0.75 | 1.150E-01 | 0.16 |
| 700 | 1.633E-01 | 0.72 | 1.631E-01 | 0.72 | 1.620E-01 | 0.16 |
| 800 | 1.922E-01 | 0.69 | 1.921E-01 | 0.69 | 1.905E-01 | 0.15 |
| 900 | 2.028E-01 | 0.67 | 2.027E-01 | 0.67 | 2.007E-01 | 0.14 |
| 1000 | 1.986E-01 | 0,66 | 1.984E-01 | 0,66 | 1.974E-01 | 0.13 |
| 1100 | 1.866E-01 | 0,65 | 1.859E-01 | 0,65 | 1.859E-01 | 0.13 |
| 1300 | 1.526E-01 | 0,64 | 1.524E-01 | 0,64 | 1.522E-01 | 0.13 |
| 1500 | 1.186E-01 | 0,63 | 1.185E-01 | 0,63 | 1.188E-01 | 0.12 |
| 1700 | 9.049E-02 | 0,62 | 9.040E-02 | 0,62 | 9.096E-02 | 0.12 |
| 2000 | 6.002E-02 | 0,62 | 5.988E-02 | 0,62 | 6.078E-02 | 0.14 |
| 2200 | 4.576E-02 | 0,62 | 4.582E-02 | 0,62 | 4.672E-02 | 0.16 |
| 2300 | 4.041E-02 | 0,62 | 4.061E-02 | 0,62 | 4.098E-02 | 0.19 |
| 2400 | 3.571E-02 | 0,63 | 3.571E-02 | 0,68 | 3.622E-02 | 0.21 |
| 2500 | 3.172E-02 | 0,96 | 3.201E-02 | 0,97 | 3.177E-02 | 0.23 |

Table 6.9.2. Spectral Irradiance of NMIJ lamp **BN-9101-696**

| Wavelength, nm | Participant Data | | | | Pilot Data | |
|---|---|---|---|---|---|---|
| | Round 1 | | Round 2 | | | |
| | Spectral Irradiance, W $m^{-2}$ $nm^{-1}$ | Combined uncertainty ($k$=1), % | Spectral Irradiance, W $m^{-2}$ $nm^{-1}$ | Combined uncertainty ($k$=1), % | Spectral Irradiance, W $m^{-2}$ $nm^{-1}$ | Combined uncertainty ($k$=1), % |
| 250 | 1.409E-04 | 1.34 | 1.416E-04 | 1.38 | 1.405E-04 | 0.37 |
| 260 | 2.518E-04 | 1.26 | 2.524E-04 | 1.26 | 2.501E-04 | 0.34 |
| 270 | 4.219E-04 | 1.21 | 4.230E-04 | 1.22 | 4.188E-04 | 0.32 |
| 280 | 6.678E-04 | 1.18 | 6.695E-04 | 1.18 | 6.622E-04 | 0.30 |
| 290 | 1.012E-03 | 1.14 | 1.013E-03 | 1.14 | 1.005E-03 | 0.29 |
| 300 | 1.480E-03 | 1.12 | 1.485E-03 | 1.12 | 1.469E-03 | 0.29 |
| 320 | 2.885E-03 | 1.07 | 2.893E-03 | 1.07 | 2.870E-03 | 0.28 |
| 340 | 5.099E-03 | 1.02 | 5.099E-03 | 1.02 | 5.059E-03 | 0.27 |
| 360 | 8.269E-03 | 0.98 | 8.288E-03 | 0.98 | 8.223E-03 | 0.26 |
| 380 | 1.260E-02 | 0.96 | 1.262E-02 | 0.94 | 1.251E-02 | 0.26 |
| 400 | 1.824E-02 | 0.92 | 1.821E-02 | 0.92 | 1.799E-02 | 0.25 |
| 450 | 3.717E-02 | 0.86 | 3.708E-02 | 0.86 | 3.679E-02 | 0.22 |
| 500 | 6.206E-02 | 0.81 | 6.192E-02 | 0.81 | 6.147E-02 | 0.21 |
| 555 | 9.288E-02 | 0.78 | 9.268E-02 | 0.78 | 9.206E-02 | 0.18 |
| 600 | 1.179E-01 | 0.75 | 1.176E-01 | 0.75 | 1.169E-01 | 0.16 |
| 700 | 1.643E-01 | 0.72 | 1.639E-01 | 0.72 | 1.633E-01 | 0.16 |
| 800 | 1.922E-01 | 0.69 | 1.918E-01 | 0.69 | 1.908E-01 | 0.15 |
| 900 | 2.018E-01 | 0.67 | 2.015E-01 | 0.67 | 2.001E-01 | 0.14 |
| 1000 | 1.968E-01 | 0.66 | 1.964E-01 | 0.66 | 1.959E-01 | 0.13 |
| 1100 | 1.841E-01 | 0.65 | 1.831E-01 | 0.65 | 1.839E-01 | 0.13 |
| 1300 | 1.500E-01 | 0.64 | 1.495E-01 | 0.64 | 1.501E-01 | 0.13 |
| 1500 | 1.163E-01 | 0.63 | 1.158E-01 | 0.63 | 1.167E-01 | 0.12 |
| 1700 | 8.857E-02 | 0.62 | 8.824E-02 | 0.62 | 8.895E-02 | 0.12 |
| 2000 | 5.856E-02 | 0.62 | 5.847E-02 | 0.62 | 5.929E-02 | 0.14 |
| 2200 | 4.457E-02 | 0.62 | 4.438E-02 | 0.62 | 4.543E-02 | 0.16 |
| 2300 | 3.938E-02 | 0.62 | 3.925E-02 | 0.62 | 3.993E-02 | 0.19 |
| 2400 | 3.458E-02 | 0.64 | 3.430E-02 | 0.65 | 3.530E-02 | 0.21 |
| 2500 | 3.036E-02 | 0.92 | 2.964E-02 | 0.96 | 3.096E-02 | 0.23 |

Table 6.9.3. Spectral Irradiance of NMIJ lamp **BN-9101-697**

| Wavelength, nm | Participant Data | | | | Pilot Data | |
|---|---|---|---|---|---|---|
| | Round 1 | | Round 2 | | | |
| | Spectral Irradiance, W m$^{-2}$ nm$^{-1}$ | Combined uncertainty ($k$=1), % | Spectral Irradiance, W m$^{-2}$ nm$^{-1}$ | Combined uncertainty ($k$=1), % | Spectral Irradiance, W m$^{-2}$ nm$^{-1}$ | Combined uncertainty ($k$=1), % |
| 250 | 1.450E-04 | 1.34 | 1.459E-04 | 1.39 | 1.451E-04 | 0.37 |
| 260 | 2.589E-04 | 1.26 | 2.606E-04 | 1.27 | 2.574E-04 | 0.34 |
| 270 | 4.342E-04 | 1.22 | 4.371E-04 | 1.22 | 4.316E-04 | 0.32 |
| 280 | 6.881E-04 | 1.18 | 6.926E-04 | 1.18 | 6.840E-04 | 0.30 |
| 290 | 1.042E-03 | 1.15 | 1.048E-03 | 1.14 | 1.036E-03 | 0.29 |
| 300 | 1.526E-03 | 1.12 | 1.535E-03 | 1.12 | 1.515E-03 | 0.29 |
| 320 | 2.973E-03 | 1.06 | 2.992E-03 | 1.06 | 2.959E-03 | 0.28 |
| 340 | 5.242E-03 | 1.02 | 5.267E-03 | 1.02 | 5.219E-03 | 0.27 |
| 360 | 8.517E-03 | 0.98 | 8.561E-03 | 0.98 | 8.485E-03 | 0.26 |
| 380 | 1.298E-02 | 0.96 | 1.302E-02 | 0.94 | 1.291E-02 | 0.26 |
| 400 | 1.879E-02 | 0.92 | 1.883E-02 | 0.92 | 1.856E-02 | 0.25 |
| 450 | 3.832E-02 | 0.86 | 3.836E-02 | 0.86 | 3.795E-02 | 0.22 |
| 500 | 6.402E-02 | 0.81 | 6.410E-02 | 0.81 | 6.349E-02 | 0.21 |
| 555 | 9.586E-02 | 0.78 | 9.595E-02 | 0.78 | 9.511E-02 | 0.18 |
| 600 | 1.217E-01 | 0.75 | 1.219E-01 | 0.75 | 1.209E-01 | 0.16 |
| 700 | 1.698E-01 | 0.72 | 1.699E-01 | 0.72 | 1.689E-01 | 0.16 |
| 800 | 1.986E-01 | 0.69 | 1.989E-01 | 0.69 | 1.975E-01 | 0.15 |
| 900 | 2.086E-01 | 0.67 | 2.089E-01 | 0.67 | 2.071E-01 | 0.14 |
| 1000 | 2.034E-01 | 0.66 | 2.036E-01 | 0.66 | 2.029E-01 | 0.13 |
| 1100 | 1.904E-01 | 0.65 | 1.899E-01 | 0.65 | 1.904E-01 | 0.13 |
| 1300 | 1.553E-01 | 0.64 | 1.552E-01 | 0.64 | 1.555E-01 | 0.13 |
| 1500 | 1.204E-01 | 0.63 | 1.203E-01 | 0.63 | 1.209E-01 | 0.12 |
| 1700 | 9.183E-02 | 0.62 | 9.170E-02 | 0.62 | 9.215E-02 | 0.12 |
| 2000 | 6.077E-02 | 0.62 | 6.055E-02 | 0.62 | 6.149E-02 | 0.14 |
| 2200 | 4.626E-02 | 0.61 | 4.619E-02 | 0.62 | 4.713E-02 | 0.16 |
| 2300 | 4.081E-02 | 0.62 | 4.055E-02 | 0.63 | 4.152E-02 | 0.19 |
| 2400 | 3.596E-02 | 0.64 | 3.593E-02 | 0.66 | 3.644E-02 | 0.21 |
| 2500 | 3.114E-02 | 0.91 | 3.187E-02 | 1.00 | 3.223E-02 | 0.23 |

## 6.10. NPL lamps data

NPL traveling lamps: BN-9101-636, BN-9101-637 and BN-9101-553.

Note: NPL submitted data for the Round 1 only.

Table 6.10.1. Spectral Irradiance of NPL lamp **BN-9101-636**

| Wavelength, nm | Participant Data | | | | Pilot Data | |
|---|---|---|---|---|---|---|
| | Round 1 | | Round 2 | | | |
| | Spectral Irradiance, W m$^{-2}$ nm$^{-1}$ | Combined uncertainty ($k$=1), % | Spectral Irradiance, W m$^{-2}$ nm$^{-1}$ | Combined uncertainty ($k$=1), % | Spectral Irradiance, W m$^{-2}$ nm$^{-1}$ | Combined uncertainty ($k$=1), % |
| 250 | 1.321E-04 | 0.898 | | | 1.328E-04 | 0.37 |
| 260 | 2.336E-04 | 0.911 | | | 2.369E-04 | 0.34 |
| 270 | 3.901E-04 | 0.930 | | | 3.965E-04 | 0.32 |
| 280 | 6.162E-04 | 0.898 | | | 6.275E-04 | 0.30 |
| 290 | 9.462E-04 | 0.826 | | | 9.556E-04 | 0.29 |
| 300 | 1.387E-03 | 0.785 | | | 1.400E-03 | 0.29 |
| 320 | 2.701E-03 | 0.786 | | | 2.746E-03 | 0.28 |
| 340 | 4.800E-03 | 0.774 | | | 4.861E-03 | 0.27 |
| 360 | 7.857E-03 | 0.749 | | | 7.926E-03 | 0.26 |
| 380 | 1.202E-02 | 0.756 | | | 1.210E-02 | 0.26 |
| 400 | 1.732E-02 | 0.728 | | | 1.745E-02 | 0.25 |
| 450 | 3.568E-02 | 0.472 | | | 3.591E-02 | 0.22 |
| 500 | 6.007E-02 | 0.403 | | | 6.036E-02 | 0.21 |
| 555 | 9.043E-02 | 0.367 | | | 9.085E-02 | 0.18 |
| 600 | 1.153E-01 | 0.343 | | | 1.158E-01 | 0.16 |
| 700 | 1.620E-01 | 0.302 | | | 1.628E-01 | 0.16 |
| 800 | 1.903E-01 | 0.280 | | | 1.912E-01 | 0.15 |
| 900 | 2.003E-01 | 0.251 | | | 2.014E-01 | 0.14 |
| 1000 | 1.970E-01 | 0.231 | | | 1.980E-01 | 0.13 |
| 1100 | 1.856E-01 | 0.219 | | | 1.863E-01 | 0.13 |
| 1300 | 1.522E-01 | 0.196 | | | 1.527E-01 | 0.13 |
| 1500 | 1.187E-01 | 0.183 | | | 1.191E-01 | 0.12 |
| 1700 | 9.079E-02 | 0.263 | | | 9.109E-02 | 0.12 |
| 2000 | 6.054E-02 | 0.267 | | | 6.067E-02 | 0.14 |
| 2200 | 4.650E-02 | 0.272 | | | 4.655E-02 | 0.16 |
| 2300 | 4.085E-02 | 0.279 | | | 4.090E-02 | 0.19 |
| 2400 | 3.603E-02 | 0.284 | | | 3.592E-02 | 0.21 |
| 2500 | 3.154E-02 | 0.847 | | | 3.185E-02 | 0.23 |

Table 6.10.2. Spectral Irradiance of NPL lamp **BN-9101-637**

| Wavelength, nm | Participant Data | | | | Pilot Data | |
|---|---|---|---|---|---|---|
| | Round 1 | | Round 2 | | | |
| | Spectral Irradiance, W $m^{-2}$ $nm^{-1}$ | Combined uncertainty ($k$=1), % | Spectral Irradiance, W $m^{-2}$ $nm^{-1}$ | Combined uncertainty ($k$=1), % | Spectral Irradiance, W $m^{-2}$ $nm^{-1}$ | Combined uncertainty ($k$=1), % |
| 250 | 1.260E-04 | 0.893 | | | 1.272E-04 | 0.37 |
| 260 | 2.226E-04 | 0.912 | | | 2.265E-04 | 0.34 |
| 270 | 3.726E-04 | 0.934 | | | 3.796E-04 | 0.32 |
| 280 | 5.935E-04 | 0.915 | | | 6.049E-04 | 0.30 |
| 290 | 9.060E-04 | 0.831 | | | 9.198E-04 | 0.29 |
| 300 | 1.332E-03 | 0.779 | | | 1.349E-03 | 0.29 |
| 320 | 2.603E-03 | 0.795 | | | 2.652E-03 | 0.28 |
| 340 | 4.633E-03 | 0.763 | | | 4.705E-03 | 0.27 |
| 360 | 7.592E-03 | 0.735 | | | 7.697E-03 | 0.26 |
| 380 | 1.163E-02 | 0.776 | | | 1.176E-02 | 0.26 |
| 400 | 1.678E-02 | 0.737 | | | 1.698E-02 | 0.25 |
| 450 | 3.479E-02 | 0.471 | | | 3.506E-02 | 0.22 |
| 500 | 5.876E-02 | 0.401 | | | 5.908E-02 | 0.21 |
| 555 | 8.867E-02 | 0.363 | | | 8.914E-02 | 0.18 |
| 600 | 1.133E-01 | 0.339 | | | 1.139E-01 | 0.16 |
| 700 | 1.598E-01 | 0.298 | | | 1.606E-01 | 0.16 |
| 800 | 1.884E-01 | 0.273 | | | 1.891E-01 | 0.15 |
| 900 | 1.986E-01 | 0.251 | | | 1.996E-01 | 0.14 |
| 1000 | 1.957E-01 | 0.228 | | | 1.965E-01 | 0.13 |
| 1100 | 1.845E-01 | 0.220 | | | 1.852E-01 | 0.13 |
| 1300 | 1.516E-01 | 0.198 | | | 1.521E-01 | 0.13 |
| 1500 | 1.183E-01 | 0.190 | | | 1.187E-01 | 0.12 |
| 1700 | 9.056E-02 | 0.252 | | | 9.079E-02 | 0.12 |
| 2000 | 6.042E-02 | 0.254 | | | 6.060E-02 | 0.14 |
| 2200 | 4.641E-02 | 0.258 | | | 4.655E-02 | 0.16 |
| 2300 | 4.081E-02 | 0.261 | | | 4.082E-02 | 0.19 |
| 2400 | 3.594E-02 | 0.265 | | | 3.592E-02 | 0.21 |
| 2500 | 3.184E-02 | 0.631 | | | 3.182E-02 | 0.23 |

Table 6.10.3. Spectral Irradiance of NPL lamp **BN-9101-553**

| Wavelength, nm | Participant Data | | | | Pilot Data | |
|---|---|---|---|---|---|---|
| | Round 1 | | Round 2 | | | |
| | Spectral Irradiance, W $m^{-2}$ $nm^{-1}$ | Combined uncertainty ($k$=1), % | Spectral Irradiance, W $m^{-2}$ $nm^{-1}$ | Combined uncertainty ($k$=1), % | Spectral Irradiance, W $m^{-2}$ $nm^{-1}$ | Combined uncertainty ($k$=1), % |
| 250 | 1.309E-04 | 0.983 | | | 1.316E-04 | 0.37 |
| 260 | 2.305E-04 | 1.052 | | | 2.343E-04 | 0.34 |
| 270 | 3.864E-04 | 1.152 | | | 3.930E-04 | 0.32 |
| 280 | 6.074E-04 | 1.016 | | | 6.191E-04 | 0.30 |
| 290 | 9.340E-04 | 0.868 | | | 9.442E-04 | 0.29 |
| 300 | 1.372E-03 | 0.890 | | | 1.382E-03 | 0.29 |
| 320 | 2.681E-03 | 0.960 | | | 2.710E-03 | 0.28 |
| 340 | 4.752E-03 | 0.821 | | | 4.795E-03 | 0.27 |
| 360 | 7.764E-03 | 0.830 | | | 7.825E-03 | 0.26 |
| 380 | 1.185E-02 | 0.813 | | | 1.194E-02 | 0.26 |
| 400 | 1.708E-02 | 0.767 | | | 1.722E-02 | 0.25 |
| 450 | 3.526E-02 | 0.486 | | | 3.540E-02 | 0.22 |
| 500 | 5.927E-02 | 0.436 | | | 5.946E-02 | 0.21 |
| 555 | 8.917E-02 | 0.428 | | | 8.944E-02 | 0.18 |
| 600 | 1.136E-01 | 0.395 | | | 1.141E-01 | 0.16 |
| 700 | 1.596E-01 | 0.341 | | | 1.602E-01 | 0.16 |
| 800 | 1.874E-01 | 0.297 | | | 1.880E-01 | 0.15 |
| 900 | 1.971E-01 | 0.266 | | | 1.978E-01 | 0.14 |
| 1000 | 1.937E-01 | 0.244 | | | 1.942E-01 | 0.13 |
| 1100 | 1.821E-01 | 0.233 | | | 1.826E-01 | 0.13 |
| 1300 | 1.490E-01 | 0.207 | | | 1.494E-01 | 0.13 |
| 1500 | 1.161E-01 | 0.194 | | | 1.164E-01 | 0.12 |
| 1700 | 8.818E-02 | 0.338 | | | 8.899E-02 | 0.12 |
| 2000 | 5.880E-02 | 0.354 | | | 5.918E-02 | 0.14 |
| 2200 | 4.500E-02 | 0.368 | | | 4.539E-02 | 0.16 |
| 2300 | 3.964E-02 | 0.377 | | | 3.992E-02 | 0.19 |
| 2400 | 3.480E-02 | 0.388 | | | 3.499E-02 | 0.21 |
| 2500 | 3.028E-02 | 1.099 | | | 3.073E-02 | 0.23 |

## 6.11. NRC lamps data

NRC traveling lamps: BN-9101-668, BN-9101-669 and BN-9101-670.

Table 6.11.1. Spectral Irradiance of NRC lamp **BN-9101-668**

| Wavelength, nm | Participant Data | | | | Pilot Data | |
|---|---|---|---|---|---|---|
| | Round 1 | | Round 2 | | | |
| | Spectral Irradiance, W m$^{-2}$ nm$^{-1}$ | Combined uncertainty ($k$=1), % | Spectral Irradiance, W m$^{-2}$ nm$^{-1}$ | Combined uncertainty ($k$=1), % | Spectral Irradiance, W m$^{-2}$ nm$^{-1}$ | Combined uncertainty ($k$=1), % |
| 250 | 1.246E-04 | 1.55 | 1.257E-04 | 0.98 | 1.255E-04 | 0.37 |
| 260 | 2.226E-04 | 1.22 | 2.247E-04 | 2.20 | 2.244E-04 | 0.34 |
| 270 | 3.759E-04 | 0.91 | 3.794E-04 | 0.70 | 3.778E-04 | 0.32 |
| 280 | 5.947E-04 | 0.85 | 5.978E-04 | 0.55 | 5.972E-04 | 0.30 |
| 290 | 9.128E-04 | 0.89 | 9.166E-04 | 0.56 | 9.146E-04 | 0.29 |
| 300 | 1.341E-03 | 0.82 | 1.347E-03 | 0.58 | 1.342E-03 | 0.29 |
| 320 | 2.632E-03 | 0.71 | 2.646E-03 | 0.52 | 2.644E-03 | 0.28 |
| 340 | 4.673E-03 | 0.67 | 4.700E-03 | 0.48 | 4.680E-03 | 0.27 |
| 360 | 7.655E-03 | 0.61 | 7.693E-03 | 0.46 | 7.655E-03 | 0.26 |
| 380 | 1.171E-02 | 0.60 | 1.176E-02 | 0.43 | 1.171E-02 | 0.26 |
| 400 | 1.680E-02 | 0.37 | 1.694E-02 | 0.37 | 1.691E-02 | 0.25 |
| 450 | 3.461E-02 | 0.34 | 3.487E-02 | 0.34 | 3.486E-02 | 0.22 |
| 500 | 5.834E-02 | 0.29 | 5.869E-02 | 0.32 | 5.868E-02 | 0.21 |
| 555 | 8.793E-02 | 0.27 | 8.839E-02 | 0.27 | 8.844E-02 | 0.18 |
| 600 | 1.123E-01 | 0.24 | 1.127E-01 | 0.25 | 1.129E-01 | 0.16 |
| 700 | 1.579E-01 | 0.21 | 1.585E-01 | 0.23 | 1.588E-01 | 0.16 |
| 800 | 1.856E-01 | 0.25 | 1.865E-01 | 0.19 | 1.867E-01 | 0.15 |
| 900 | 1.952E-01 | 0.19 | 1.959E-01 | 0.18 | 1.967E-01 | 0.14 |
| 1000 | 1.922E-01 | 0.19 | 1.926E-01 | 0.16 | 1.933E-01 | 0.13 |
| 1100 | 1.814E-01 | 0.20 | 1.813E-01 | 0.14 | 1.819E-01 | 0.13 |
| 1300 | 1.509E-01 | 0.59 | 1.478E-01 | 0.31 | 1.491E-01 | 0.13 |
| 1500 | 1.174E-01 | 0.70 | 1.148E-01 | 0.64 | 1.162E-01 | 0.12 |
| 1700 | 8.989E-02 | 0.98 | 8.856E-02 | 0.63 | 8.883E-02 | 0.12 |
| 2000 | 5.931E-02 | 1.33 | 5.899E-02 | 1.04 | 5.913E-02 | 0.14 |
| 2200 | 4.611E-02 | 2.56 | 4.531E-02 | 2.01 | 4.544E-02 | 0.16 |
| 2300 | 4.073E-02 | 2.74 | 3.799E-02 | 3.60 | 3.993E-02 | 0.19 |
| 2400 | 3.485E-02 | 4.55 | 3.611E-02 | 2.88 | 3.492E-02 | 0.21 |
| 2500 | 3.164E-02 | 10.68 | 3.007E-02 | 9.49 | 3.073E-02 | 0.23 |

Table 6.11.2. Spectral Irradiance of NRC lamp **BN-9101-669**

| Wavelength, nm | Participant Data | | | | Pilot Data | |
|---|---|---|---|---|---|---|
| | Round 1 | | Round 2 | | | |
| | Spectral Irradiance, W $m^{-2}$ $nm^{-1}$ | Combined uncertainty ($k$=1), % | Spectral Irradiance, W $m^{-2}$ $nm^{-1}$ | Combined uncertainty ($k$=1), % | Spectral Irradiance, W $m^{-2}$ $nm^{-1}$ | Combined uncertainty ($k$=1), % |
| 250 | 1.421E-04 | 1.16 | 1.465E-04 | 3.24 | 1.416E-04 | 0.37 |
| 260 | 2.538E-04 | 0.76 | 2.629E-04 | 2.36 | 2.533E-04 | 0.34 |
| 270 | 4.246E-04 | 0.63 | 4.421E-04 | 1.79 | 4.240E-04 | 0.32 |
| 280 | 6.589E-04 | 0.66 | 6.872E-04 | 1.56 | 6.617E-04 | 0.30 |
| 290 | 1.020E-03 | 0.55 | 1.059E-03 | 1.47 | 1.019E-03 | 0.29 |
| 300 | 1.492E-03 | 0.53 | 1.549E-03 | 1.41 | 1.491E-03 | 0.29 |
| 320 | 2.908E-03 | 0.49 | 3.016E-03 | 1.29 | 2.911E-03 | 0.28 |
| 340 | 5.139E-03 | 0.45 | 5.326E-03 | 1.24 | 5.139E-03 | 0.27 |
| 360 | 8.379E-03 | 0.43 | 8.674E-03 | 1.20 | 8.364E-03 | 0.26 |
| 380 | 1.276E-02 | 0.40 | 1.320E-02 | 1.16 | 1.273E-02 | 0.26 |
| 400 | 1.837E-02 | 0.36 | 1.850E-02 | 0.39 | 1.832E-02 | 0.25 |
| 450 | 3.755E-02 | 0.32 | 3.782E-02 | 0.34 | 3.748E-02 | 0.22 |
| 500 | 6.287E-02 | 0.29 | 6.331E-02 | 0.32 | 6.273E-02 | 0.21 |
| 555 | 9.423E-02 | 0.26 | 9.483E-02 | 0.27 | 9.404E-02 | 0.18 |
| 600 | 1.199E-01 | 0.24 | 1.206E-01 | 0.26 | 1.196E-01 | 0.16 |
| 700 | 1.675E-01 | 0.21 | 1.684E-01 | 0.22 | 1.673E-01 | 0.16 |
| 800 | 1.964E-01 | 0.19 | 1.968E-01 | 0.22 | 1.958E-01 | 0.15 |
| 900 | 2.052E-01 | 0.16 | 2.069E-01 | 0.20 | 2.055E-01 | 0.14 |
| 1000 | 2.015E-01 | 0.15 | 2.031E-01 | 0.20 | 2.016E-01 | 0.13 |
| 1100 | 1.897E-01 | 0.14 | 1.910E-01 | 0.19 | 1.894E-01 | 0.13 |
| 1300 | 1.555E-01 | 0.45 | 1.600E-01 | 0.57 | 1.548E-01 | 0.13 |
| 1500 | 1.208E-01 | 0.27 | 1.242E-01 | 0.80 | 1.206E-01 | 0.12 |
| 1700 | 9.241E-02 | 0.40 | 9.550E-02 | 0.91 | 9.194E-02 | 0.12 |
| 2000 | 6.097E-02 | 0.79 | 6.368E-02 | 1.28 | 6.125E-02 | 0.14 |
| 2200 | 4.687E-02 | 2.02 | 4.960E-02 | 3.20 | 4.693E-02 | 0.16 |
| 2300 | 4.184E-02 | 2.51 | 4.243E-02 | 3.20 | 4.124E-02 | 0.19 |
| 2400 | 3.602E-02 | 2.41 | 4.095E-02 | 2.09 | 3.642E-02 | 0.21 |
| 2500 | 3.589E-02 | 4.83 | 3.256E-02 | 11.27 | 3.189E-02 | 0.23 |

Table 6.11.3. Spectral Irradiance of NRC lamp **BN-9101-670**

| Wavelength, nm | Participant Data | | | | Pilot Data | |
|---|---|---|---|---|---|---|
| | Round 1 | | Round 2 | | | |
| | Spectral Irradiance, W $m^{-2}$ $nm^{-1}$ | Combined uncertainty ($k$=1), % | Spectral Irradiance, W $m^{-2}$ $nm^{-1}$ | Combined uncertainty ($k$=1), % | Spectral Irradiance, W $m^{-2}$ $nm^{-1}$ | Combined uncertainty ($k$=1), % |
| 250 | 1.453E-04 | 0.90 | 1.469E-04 | 3.14 | 1.447E-04 | 0.37 |
| 260 | 2.622E-04 | 1.37 | 2.597E-04 | 1.33 | 2.574E-04 | 0.34 |
| 270 | 4.379E-04 | 1.30 | 4.350E-04 | 0.77 | 4.324E-04 | 0.32 |
| 280 | 6.880E-04 | 1.25 | 6.862E-04 | 0.54 | 6.817E-04 | 0.30 |
| 290 | 1.050E-03 | 1.16 | 1.043E-03 | 0.53 | 1.039E-03 | 0.29 |
| 300 | 1.534E-03 | 1.06 | 1.524E-03 | 0.52 | 1.518E-03 | 0.29 |
| 320 | 2.987E-03 | 0.91 | 2.979E-03 | 0.45 | 2.973E-03 | 0.28 |
| 340 | 5.282E-03 | 0.84 | 5.265E-03 | 0.43 | 5.241E-03 | 0.27 |
| 360 | 8.609E-03 | 0.78 | 8.585E-03 | 0.41 | 8.535E-03 | 0.26 |
| 380 | 1.311E-02 | 0.75 | 1.307E-02 | 0.38 | 1.301E-02 | 0.26 |
| 400 | 1.870E-02 | 0.36 | 1.877E-02 | 0.36 | 1.873E-02 | 0.25 |
| 450 | 3.825E-02 | 0.32 | 3.838E-02 | 0.32 | 3.834E-02 | 0.22 |
| 500 | 6.408E-02 | 0.29 | 6.422E-02 | 0.28 | 6.417E-02 | 0.21 |
| 555 | 9.609E-02 | 0.26 | 9.627E-02 | 0.26 | 9.626E-02 | 0.18 |
| 600 | 1.222E-01 | 0.24 | 1.224E-01 | 0.24 | 1.224E-01 | 0.16 |
| 700 | 1.708E-01 | 0.21 | 1.711E-01 | 0.21 | 1.713E-01 | 0.16 |
| 800 | 1.997E-01 | 0.23 | 2.004E-01 | 0.18 | 2.005E-01 | 0.15 |
| 900 | 2.093E-01 | 0.17 | 2.097E-01 | 0.17 | 2.104E-01 | 0.14 |
| 1000 | 2.054E-01 | 0.17 | 2.055E-01 | 0.16 | 2.061E-01 | 0.13 |
| 1100 | 1.931E-01 | 0.17 | 1.928E-01 | 0.14 | 1.935E-01 | 0.13 |
| 1300 | 1.604E-01 | 0.48 | 1.557E-01 | 0.72 | 1.578E-01 | 0.13 |
| 1500 | 1.245E-01 | 0.45 | 1.216E-01 | 0.56 | 1.226E-01 | 0.12 |
| 1700 | 9.516E-02 | 0.48 | 9.255E-02 | 0.89 | 9.333E-02 | 0.12 |
| 2000 | 6.334E-02 | 0.75 | 6.083E-02 | 1.60 | 6.199E-02 | 0.14 |
| 2200 | 4.856E-02 | 3.94 | 4.842E-02 | 3.65 | 4.747E-02 | 0.16 |
| 2300 | 4.290E-02 | 3.22 | 4.211E-02 | 4.54 | 4.163E-02 | 0.19 |
| 2400 | 3.686E-02 | 4.46 | 3.813E-02 | 6.30 | 3.682E-02 | 0.21 |
| 2500 | 3.274E-02 | 6.17 | 3.400E-02 | 8.78 | 3.227E-02 | 0.23 |

## 6.12. PTB lamps data

PTB traveling lamps: BN-9101-661, BN-9101-662 and BN-9101-681.

Table 6.12.1. Spectral Irradiance of PTB lamp **BN-9101-661**

| Wavelength, nm | Participant Data | | | | Pilot Data | |
|---|---|---|---|---|---|---|
| | Round 1 | | Round 2 | | | |
| | Spectral Irradiance, W m$^{-2}$ nm$^{-1}$ | Combined uncertainty ($k$=1), % | Spectral Irradiance, W m$^{-2}$ nm$^{-1}$ | Combined uncertainty ($k$=1), % | Spectral Irradiance, W m$^{-2}$ nm$^{-1}$ | Combined uncertainty ($k$=1), % |
| 250 | 1.483E-04 | 0.84 | 1.501E-04 | 0.87 | 1.473E-04 | 0.37 |
| 260 | 2.644E-04 | 0.74 | 2.677E-04 | 0.78 | 2.619E-04 | 0.34 |
| 270 | 4.422E-04 | 0.67 | 4.473E-04 | 0.70 | 4.383E-04 | 0.32 |
| 280 | 6.885E-04 | 0.65 | 6.961E-04 | 0.69 | 6.846E-04 | 0.30 |
| 290 | 1.062E-03 | 0.64 | 1.071E-03 | 0.66 | 1.050E-03 | 0.29 |
| 300 | 1.550E-03 | 0.60 | 1.562E-03 | 0.63 | 1.536E-03 | 0.29 |
| 320 | 3.024E-03 | 0.57 | 3.043E-03 | 0.60 | 3.000E-03 | 0.28 |
| 340 | 5.336E-03 | 0.55 | 5.376E-03 | 0.57 | 5.289E-03 | 0.27 |
| 360 | 8.685E-03 | 0.53 | 8.741E-03 | 0.55 | 8.605E-03 | 0.26 |
| 380 | 1.321E-02 | 0.51 | 1.329E-02 | 0.53 | 1.309E-02 | 0.26 |
| 400 | 1.897E-02 | 0.47 | 1.908E-02 | 0.50 | 1.881E-02 | 0.25 |
| 450 | 3.864E-02 | 0.44 | 3.887E-02 | 0.46 | 3.847E-02 | 0.22 |
| 500 | 6.455E-02 | 0.40 | 6.491E-02 | 0.42 | 6.434E-02 | 0.21 |
| 555 | 9.674E-02 | 0.37 | 9.703E-02 | 0.39 | 9.647E-02 | 0.18 |
| 600 | 1.229E-01 | 0.35 | 1.232E-01 | 0.37 | 1.226E-01 | 0.16 |
| 700 | 1.716E-01 | 0.33 | 1.722E-01 | 0.34 | 1.716E-01 | 0.16 |
| 800 | 2.009E-01 | 0.31 | 2.014E-01 | 0.32 | 2.009E-01 | 0.15 |
| 900 | 2.110E-01 | 0.30 | 2.114E-01 | 0.31 | 2.110E-01 | 0.14 |
| 1000 | 2.069E-01 | 0.29 | 2.073E-01 | 0.30 | 2.070E-01 | 0.13 |
| 1100 | 1.949E-01 | 0.31 | 1.954E-01 | 0.32 | 1.945E-01 | 0.13 |
| 1300 | 1.590E-01 | 0.38 | 1.593E-01 | 0.37 | 1.591E-01 | 0.13 |
| 1500 | 1.240E-01 | 0.36 | 1.242E-01 | 0.36 | 1.240E-01 | 0.12 |
| 1700 | 9.486E-02 | 0.32 | 9.468E-02 | 0.32 | 9.471E-02 | 0.12 |
| 2000 | 6.310E-02 | 0.36 | 6.315E-02 | 0.32 | 6.311E-02 | 0.14 |
| 2200 | 4.852E-02 | 0.53 | 4.842E-02 | 0.39 | 4.833E-02 | 0.16 |
| 2300 | 4.250E-02 | 0.46 | 4.247E-02 | 0.40 | 4.247E-02 | 0.19 |
| 2400 | 3.740E-02 | 0.63 | 3.749E-02 | 0.52 | 3.738E-02 | 0.21 |
| 2500 | 3.290E-02 | 4.35 | 3.310E-02 | 3.02 | 3.303E-02 | 0.23 |

Table 6.12.2. Spectral Irradiance of PTB lamp **BN-9101-662**

| Wavelength, nm | Participant Data | | | | Pilot Data | |
|---|---|---|---|---|---|---|
| | Round 1 | | Round 2 | | | |
| | Spectral Irradiance, W $m^{-2}$ $nm^{-1}$ | Combined uncertainty ($k$=1), % | Spectral Irradiance, W $m^{-2}$ $nm^{-1}$ | Combined uncertainty ($k$=1), % | Spectral Irradiance, W $m^{-2}$ $nm^{-1}$ | Combined uncertainty ($k$=1), % |
| 250 | 1.472E-04 | 0.83 | 1.486E-04 | 0.87 | 1.454E-04 | 0.37 |
| 260 | 2.622E-04 | 0.74 | 2.642E-04 | 0.77 | 2.582E-04 | 0.34 |
| 270 | 4.383E-04 | 0.67 | 4.422E-04 | 0.70 | 4.322E-04 | 0.32 |
| 280 | 6.856E-04 | 0.66 | 6.916E-04 | 0.68 | 6.786E-04 | 0.30 |
| 290 | 1.052E-03 | 0.64 | 1.059E-03 | 0.66 | 1.039E-03 | 0.29 |
| 300 | 1.536E-03 | 0.60 | 1.544E-03 | 0.63 | 1.517E-03 | 0.29 |
| 320 | 2.995E-03 | 0.57 | 3.012E-03 | 0.60 | 2.964E-03 | 0.28 |
| 340 | 5.286E-03 | 0.55 | 5.313E-03 | 0.57 | 5.227E-03 | 0.27 |
| 360 | 8.612E-03 | 0.53 | 8.653E-03 | 0.55 | 8.504E-03 | 0.26 |
| 380 | 1.309E-02 | 0.51 | 1.316E-02 | 0.53 | 1.294E-02 | 0.26 |
| 400 | 1.882E-02 | 0.47 | 1.890E-02 | 0.49 | 1.862E-02 | 0.25 |
| 450 | 3.830E-02 | 0.44 | 3.846E-02 | 0.46 | 3.807E-02 | 0.22 |
| 500 | 6.399E-02 | 0.39 | 6.419E-02 | 0.41 | 6.367E-02 | 0.21 |
| 555 | 9.580E-02 | 0.37 | 9.603E-02 | 0.39 | 9.539E-02 | 0.18 |
| 600 | 1.217E-01 | 0.35 | 1.219E-01 | 0.37 | 1.213E-01 | 0.16 |
| 700 | 1.697E-01 | 0.32 | 1.702E-01 | 0.34 | 1.694E-01 | 0.16 |
| 800 | 1.982E-01 | 0.31 | 1.987E-01 | 0.32 | 1.980E-01 | 0.15 |
| 900 | 2.078E-01 | 0.30 | 2.082E-01 | 0.31 | 2.077E-01 | 0.14 |
| 1000 | 2.035E-01 | 0.29 | 2.039E-01 | 0.30 | 2.035E-01 | 0.13 |
| 1100 | 1.913E-01 | 0.30 | 1.921E-01 | 0.32 | 1.910E-01 | 0.13 |
| 1300 | 1.557E-01 | 0.39 | 1.557E-01 | 0.40 | 1.557E-01 | 0.13 |
| 1500 | 1.212E-01 | 0.36 | 1.214E-01 | 0.36 | 1.210E-01 | 0.12 |
| 1700 | 9.232E-02 | 0.32 | 9.243E-02 | 0.32 | 9.231E-02 | 0.12 |
| 2000 | 6.139E-02 | 0.38 | 6.141E-02 | 0.37 | 6.139E-02 | 0.14 |
| 2200 | 4.699E-02 | 0.58 | 4.724E-02 | 0.48 | 4.707E-02 | 0.16 |
| 2300 | 4.132E-02 | 0.48 | 4.145E-02 | 0.51 | 4.133E-02 | 0.19 |
| 2400 | 3.631E-02 | 0.57 | 3.668E-02 | 0.53 | 3.632E-02 | 0.21 |
| 2500 | 3.190E-02 | 3.81 | 3.230E-02 | 3.02 | 3.188E-02 | 0.23 |

Table 6.12.3. Spectral Irradiance of PTB lamp **BN-9101-681**

| Wavelength, nm | Participant Data | | | | Pilot Data | |
|---|---|---|---|---|---|---|
| | Round 1 | | Round 2 | | | |
| | Spectral Irradiance, W $m^{-2}$ $nm^{-1}$ | Combined uncertainty ($k$=1), % | Spectral Irradiance, W $m^{-2}$ $nm^{-1}$ | Combined uncertainty ($k$=1), % | Spectral Irradiance, W $m^{-2}$ $nm^{-1}$ | Combined uncertainty ($k$=1), % |
| 250 | 1.539E-04 | 0.86 | 1.556E-04 | 0.87 | 1.513E-04 | 0.37 |
| 260 | 2.721E-04 | 0.77 | 2.756E-04 | 0.77 | 2.689E-04 | 0.34 |
| 270 | 4.542E-04 | 0.70 | 4.591E-04 | 0.71 | 4.491E-04 | 0.32 |
| 280 | 7.177E-04 | 0.68 | 7.250E-04 | 0.69 | 7.111E-04 | 0.30 |
| 290 | 1.085E-03 | 0.66 | 1.094E-03 | 0.67 | 1.074E-03 | 0.29 |
| 300 | 1.583E-03 | 0.62 | 1.594E-03 | 0.63 | 1.566E-03 | 0.29 |
| 320 | 3.077E-03 | 0.60 | 3.098E-03 | 0.61 | 3.055E-03 | 0.28 |
| 340 | 5.415E-03 | 0.57 | 5.454E-03 | 0.57 | 5.364E-03 | 0.27 |
| 360 | 8.793E-03 | 0.55 | 8.859E-03 | 0.55 | 8.708E-03 | 0.26 |
| 380 | 1.335E-02 | 0.53 | 1.344E-02 | 0.53 | 1.321E-02 | 0.26 |
| 400 | 1.913E-02 | 0.49 | 1.927E-02 | 0.50 | 1.897E-02 | 0.25 |
| 450 | 3.877E-02 | 0.46 | 3.903E-02 | 0.46 | 3.865E-02 | 0.22 |
| 500 | 6.457E-02 | 0.41 | 6.499E-02 | 0.42 | 6.441E-02 | 0.21 |
| 555 | 9.640E-02 | 0.39 | 9.687E-02 | 0.39 | 9.623E-02 | 0.18 |
| 600 | 1.222E-01 | 0.37 | 1.227E-01 | 0.37 | 1.221E-01 | 0.16 |
| 700 | 1.699E-01 | 0.34 | 1.707E-01 | 0.34 | 1.700E-01 | 0.16 |
| 800 | 1.981E-01 | 0.32 | 1.990E-01 | 0.32 | 1.983E-01 | 0.15 |
| 900 | 2.075E-01 | 0.30 | 2.082E-01 | 0.31 | 2.078E-01 | 0.14 |
| 1000 | 2.031E-01 | 0.30 | 2.038E-01 | 0.30 | 2.034E-01 | 0.13 |
| 1100 | 1.909E-01 | 0.31 | 1.919E-01 | 0.32 | 1.908E-01 | 0.13 |
| 1300 | 1.555E-01 | 0.42 | 1.557E-01 | 0.37 | 1.556E-01 | 0.13 |
| 1500 | 1.212E-01 | 0.37 | 1.213E-01 | 0.36 | 1.211E-01 | 0.12 |
| 1700 | 9.242E-02 | 0.34 | 9.237E-02 | 0.32 | 9.243E-02 | 0.12 |
| 2000 | 6.127E-02 | 0.40 | 6.148E-02 | 0.33 | 6.138E-02 | 0.14 |
| 2200 | 4.720E-02 | 0.73 | 4.705E-02 | 0.38 | 4.705E-02 | 0.16 |
| 2300 | 4.139E-02 | 0.55 | 4.132E-02 | 0.41 | 4.136E-02 | 0.19 |
| 2400 | 3.627E-02 | 0.65 | 3.670E-02 | 0.49 | 3.641E-02 | 0.21 |
| 2500 | 3.190E-02 | 6.58 | 3.227E-02 | 2.56 | 3.196E-02 | 0.23 |

# 7. Pre-Draft A procedure

The following Pre-Draft A processes were carried out:

- Pre-Draft-A Process 1: Verification of reported results;
- Pre-Draft-A Process 2: Review of uncertainty budgets and descriptions of measurement techniques and facilities;
- Pre-Draft-A Process 3: Review of Relative Data;
- Pre-Draft-A Process 4: Identification of outliers and consistency check.

Relative Data were calculated separately for each lamp & round combination by the equation:

$$Rel.Data = \left(\frac{E_{NMI,j,R}(\lambda)}{E_{p,j,R}(\lambda)} - 1\right) - \frac{1}{N_L N_R}\sum_{j,R}\left(\frac{E_{NMI,j,R}(\lambda)}{E_{p,j,R}(\lambda)} - 1\right)$$

where:

$E_{NMI,j,R}(\lambda)$ – value of spectral irradiance of the lamp *j* reported by participating NMI for the round *R* at the wavelength $\lambda$;

$E_{p,j,R}(\lambda)$ – value of spectral irradiance reported by the pilot for the same lamp, round and wavelength;

$N_L$ – total number of lamps used by the participating NMI (usually 3 or 2);

$N_R = 2$ – number rounds.

The relative data are presented in graphic form in Appendix A.

## 7.1. Data Corrections at the Pre-Draft A stage

At the stage of **Data Verification** the following requests were made:

- KRISS requested withdrawing the lamp BN-9101-641 "because it showed big differences between the 1st and 2nd round measurement results".

- NMIJ found an error on calculation of uncertainties values originally submitted to the pilot. NMIJ requested the pilot to replace the NMIJ reported uncertainties for new, correct, values. Note, table in sections 5 and 6 for the NMIJ lamps present the correct values.

- NPL found an error on calculation of spectral irradiance values of the lamp BN-9101-553. NPL requested the pilot to replace the BN-9101-553 lamp data for new, correct, values. Note, the Table 6.10.3 in section 6.10 for the lamp presents the correct values.

At the stage of **Relative Data Review** the following requests / statements were made:

- KRISS confirmed withdrawing the lamp BN-9101-641 that was requested first at the Data Verification stage;

- LNE-CNAM confirmed withdrawing the lamp BN-9101-656 that was requested first at the time of submitting the measurement report;

- NIST confirmed withdrawing the lamp GO-N34 that was requested first at the time of submitting the measurement report; NIST added the following information: "We noticed that the behaviour of GO-N34 in both rounds is different from the other two NIST lamps. When we got the GO-N34 lamp back, we also noticed that there was a large white mark on the surface which was baked into

the surface indicating that some change had occurred. We confirm that we would like both rounds of GO-N34 removed from further consideration in the comparison".

- NMIA requested withdrawing the results from NMIA's second round measurements. The arguments were:

"1. The NMIA measurements of each of the lamps is performed using two separate systems: absolute irradiance obtained from photometry and spectral shape determined by comparison with the NMIA reference blackbody.

2. The photometric results for each of the lamps matched extremely well between the first and second measurement rounds at NMIA, indicating that the lamps were stable.

3. For the first round the blackbody cavity output could be stabilised.

4. For the second round the blackbody cavity output could not be stabilised for the reason outlined below. Unfortunately, the relative data clearly show that there is a significant problem with our results. As we discussed in our report, the cavity-temperature stabilisation system for our blackbody could not be used during the measurements for the second round, due to different characteristics of a new batch of cavities from the manufacturer. We were not able to get our blackbody upgraded in time to make measurements with a fully operational system, at least partially because of the Covid situation. So, we had to submit data that were obtained without cavity-temperature stabilisation. There were no problems with the illuminance measurements, and the photometric results for each of the lamps matched extremely well between the first and second measurement rounds. We believe that this indicates that the lamps were stable, and the issues shown up by the relative data are entirely due to the cavity-temperature stabilisation issue. This means that our second-round data are not representative of our measurement system when it is operating normally. On the other hand, during the first round, the system was operating normally. So, if it is possible**, we would prefer to use only the results from the first round** as our data for the comparison".

- NMIJ requested correction of the spectral irradiance value of the lamp BN-9101-695 for the Round 1 at the wavelength 360 nm. NMIJ gave thew following explanation: "We found that the "BN695 round 1" measurement result would have an error at 360 nm. We checked our measurement data and found that some measurement signals at 360 nm was apparently shifted in the BN695 round 1 measurement. That would be caused by a temporary adjustment error of our measurement instrument or something. So, it is desirable to remove the shifted signals". NMIJ requested to correct the spectral irradiance of the lamp BN-9101-695, Round 1 at 360 nm for the new value: 7,8743E-03 W $m^{-2}$ $nm^{-1}$ (the old value was 7,7921E-03 W $m^{-2}$ $nm^{-1}$). Note: the table 6.9.1 presents the corrected value.

All requests of withdrawing and corrections were agreed by the participants.

# 8. Comparison data analysis

## 8.1. Completeness of the data for analysis

The participants agreed, by signing the Technical protocol, that each participant would use three lamps, measured in the spectral range 250 nm to 2500 nm in two rounds. Actually, some participants, for some reasons, submitted not complete data sets: not full wavelength set, or not both rounds, or two lamps instead three. Later some more data were withdrawn during the Pre-Draft A Procedure. Table 8.1 shows the amount of measurement data (how many lamps, rounds and wavelengths) that were available for the analysis.

Table 8.1. Summary of amount of measurement data available for the analysis

| NMI | Number of lamps | Lamp identifications | Wavelengths & Rounds | |
|---|---|---|---|---|
| | | | Round 1 | Round 2 |
| VNIIOFI (pilot) | 3 | BN-9101-664<br>BN-9101-665<br>BN-9101-666 | 250 nm – 2500 nm (Full set) | 250 nm – 2500 nm (Full set) |
| IO-CSIC | 2 | BN-9101-611<br>BN-9101-612 | 250 nm – 1700 nm | 250 nm – 1700 nm |
| KRISS | 2 | BN-9101-639<br>BN-9101-640 | 250 nm – 2500 nm (Full set) | 250 nm – 2500 nm (Full set) |
| LNE-CNAM | 2 | BN-9101-653<br>BN-9101-655 | 250 nm – 700 nm, 1300 nm, 1500 nm | 250 nm – 2500 nm (Full set) |
| NIM | 3 | BN-9101-650<br>BN-9101-651<br>BN-9101-652 | 250 nm – 2500 nm (Full set) | 250 nm – 2500 nm (Full set) |
| NIST | 2 | GO-N51<br>GO-N60 | 250 nm – 2500 nm (Full set) | 250 nm – 2500 nm (Full set) |
| NMC, A*STAR | 3 | BN-9101-642<br>BN-9101-643<br>BN-9101-644 | 250 nm – 2500 nm (Full set) | 250 nm – 2500 nm (Full set) |
| NMIA | 3 | BN-9101-657<br>BN-9101-658<br>BN-9101-659 | 250 nm – 2500 nm (Full set) | - |
| NMIJ | 3 | BN-9101-695<br>BN-9101-696<br>BN-9101-697 | 250 nm – 2500 nm (Full set) | 250 nm – 2500 nm (Full set) |
| NPL | 3 | BN-9101-636<br>BN-9101-637<br>BN-9101-553 | 250 nm – 2500 nm (Full set) | - |
| NRC | 3 | BN-9101-668<br>BN-9101-669<br>BN-9101-670 | 250 nm – 2500 nm (Full set) | 250 nm – 2500 nm (Full set) |
| PTB | 3 | BN-9101-661<br>BN-9101-662<br>BN-9101-681 | 250 nm – 2500 nm (Full set) | 250 nm – 2500 nm (Full set) |

## 8.2. Discussions before analysis

NIST initiated discussions about whether the data from all participants should be used for evaluating the Key comparison reference value (KCRV). The NIST's concern was supported by PTB.

Howard Yoon (NIST): "I am somewhat troubled by the request from NMIA because they state that their second-round results should be withdrawn since they were using nonconforming equipment. I do not understand why the second-round measurements were submitted at all in this case. Why were these measurements not validated using check standards? This is a clear failure of the internal quality system at NMIA under 17025 and requires further explanation".

Peter Sperfeld (PTB): "…we should not ignore the fact that this is a star comparison with three measurement steps (participant-pilot-participant). Two participant rounds have intention to detect possible changes in artifacts… If participants completely withdraw all measurement results of a round or do not deliver any data for one round, all data of these participants should be treated separately, because no complete participation in the key comparison has taken place. Therefore, the NMIA and NPL results should not be used to calculate the KCRV because of their incompliance with the technical protocol of the comparison. Unfortunately, the case of participants not providing any data for one round of the comparison is not explicitly mentioned in the CCPR guidelines. However, as already stated, the technical protocol of the intercomparison was not fulfilled. Therefore, we need to consult within the CCPR".

Howard Yoon (NIST): "NIST agrees that the NPL and NMIA results should be removed from the calculation of the KCRV. I think that the results from these NMIs should be included in the appendix but without the calculations of DOEs. The appendix should include also the second round of NMIA's measurements for the record".

Errol Atkinson (NMIA): "We think that excluding NMIA's results from the calculations of the KCRV is a reasonable way of dealing with this situation, and agree to that course of action. We are assuming that, as Peter (Sperfeld) mentions, the NMIA results, DoE, $D_i$ and $U_i$ would be included in the report".

Teresa Goodman (NPL): "I think I should clarify a few points regarding the NPL situation, as well as replying to some of the other points that have been raised.

Our primary spectral irradiance facility is currently not operational, but this is only due to health and safety concerns relating to the blackbody and severe delays in work to address these health and safety issues due to the Covid situation. This is the reason that we were not able to carry out the second round of measurements on our lamps. And whilst it is true that we are not currently able to measure spectral irradiance lamps on request on our primary system, this certainly isn't a unique situation. Indeed all of our measurement services at NPL have periods of time when they are not available for various reasons, such as closure for lab or facility maintenance, recalibration of working standards, staff availability etc. I suspect the same is true for any other NMI as well. So the fact our system is not operational at present isn't, in my view, a reason not to calculate DOEs for NPL or to include our results in the KCRV.

Regarding the purpose of comparisons, of course Howard is right that they are intended to support CMCs. But we need to remember that a comparison can only ever demonstrate the agreement between the participants (i.e. validate the CMCs) at the time the measurements are actually made. The ongoing validity of the CMCs between comparisons relies on each NMI having suitable systems in place to ensure that the disseminated results are still compliant with these

CMCs i.e. that the scale has not drifted and that the uncertainties are still valid. That is why the CMCs also require each NMI to have a robust quality system in place. At NPL we have several ways in which to confirm whether any spectral irradiance measurements that we perform are consistent with those we have performed previously, going back to even before the last K1.a comparison. These checks are carried out on a regular basis and obviously they will be carried out as soon as we are able to operate our facility again. In other words, our internal checks will confirm whether our scale is unchanged and ensure that our CMCs, as demonstrated in this comparison, are still valid.

Regarding whether or not NPL's results should be included in the KCRV because we only submitted results from one round of measurements, we will of course accept whatever the majority recommend and the CCPR WG-KC decides. However I would like to point out that the reason for having two rounds of measurements is to help identify any potential problems associated with changes in the transfer standards, either due to use or transportation (the latter is more likely in the case of lamps). Two independent sets of results provide for some redundancy and the possibility to exclude some results if inconsistencies are observed. There is the risk with using just one set of measurements that any changes that may have occurred in the lamps are not clearly revealed in the measurements. However it is very unlikely that changes due to transportation would occur in the same way for all the lamps involved and therefore the consistency between the lamps also gives a good indication of stability.

In NPL's case we took the approach of hand carriage of the lamps to and from VNIIOFI, which minimises the risk of any changes during transportation. We therefore feel that there is a good argument to include NPL's results in the KCRV since there is (a) little risk of unexpected changes in the lamps used by NPL and (b) the possibility to confirm the stability of the lamps through the degree of consistency in the ratio between the values assigned by NPL and VNIIOFI".

Teresa Goodman (NPL): "…looking at the NMIA relative data… I realised that the agreement between the 3 lamps in round 1 was good, and that the large spread shown in the graph was due to a clear difference between the rounds rather than differences between lamps within each round. For that reason I believe the NMIA results from round 1 are acceptable for the KCRV, because there is good evidence to support that the lamps were unlikely to have changed in transportation and because NMIA have given a clear explanation for the differences between their two sets of measurements".

The participant opinions on the issue were collected by voting and presented in Tables 8.2 and 8.3.

As can be seen from Table 8.2, most participants agreed with excluding NMIA data from KCRV, but opinions were divided about the exclusion of NPL data. Therefore, the situation was reported to CCPR-WG-KC, and the discussion was continued on the WG on-line meeting on 30 November 2021.

The WG could not reach an agreement and make a final decision on the issue. Therefore, the Pilot suggested a compromise: to make two versions of the comparison result analysis, including NPL data to KCRV and excluding, and later select one version as a final. NPL and NRC suggested to analyse the third version where all participants are included to KCRV.

Table 8.2. Summary of voting for/against excluding NPL and NMIA data from KCRV

| Participant | NPL | | NMIA | |
|---|---|---|---|---|
| | **Exclude NPL** data from KCRV | **Do not exclude NPL** data from KCRV | **Exclude NMIA** data from KCRV | **Do not exclude NMIA** data from KCRV |
| CSIC | YES | | YES | |
| KRISS | ABSTAIN (The pilot could consider NPL as the pilot of the previous CCPR-K1a.) | | YES | |
| LNE-CNAM | | Do NOT (taking into account experience NPL in Spectral irradiance) | YES | |
| NIM | | Do NOT (on condition that the ratio between the values assigned by NPL and the pilot show good consistency) | YES | |
| NIST | YES | | YES | |
| NMC A-STAR | YES | | YES | |
| NMIA | | Do NOT | YES | |
| NMIJ | YES | | YES | |
| NPL | | Do NOT | | Do NOT |
| NRC | | Do NOT (if lamp stability is confirmed) | | their first-round results could be included if lamp stability is confirmed. |
| PTB | YES | | YES | |
| VNIIOFI | | Do NOT (taking into account experience NPL in Spectral irradiance) | YES | |

Table 8.3. Summary of voting of the question "If a participant is excluded from KCRV shall we calculate its DoE and where should we show it?"

| Participant | **Do not calculate DoE**. Show the measurement results in appendix | **Calculate DoE** and **show it in appendix** | **Calculate DoE** and **show it in main part of the report** (as for other participants) |
|---|---|---|---|
| CSIC | | | X |
| KRISS | | | X |
| LNE-CNAM | | | X (in the main comparison report but separate from the main table) |
| NIM | | | |
| NIST | X | | |
| NMC A-STAR | | | X |
| NMIA | | X | |
| NMIJ | | | X |
| NPL | | | X |
| NRC | | | X |
| PTB | | | X |
| VNIIOFI | | | X |

Therefore, three versions of analysis were carried out:

**Version 1**: NMIA data excluded from calculation of KCRV. All other participants included.

**Version 2**: NMIA, NPL and LNE-CNAM for wavelengths (800-1200) nm and (1700-2500) nm data excluded from calculation of KCRV. All other participants included. *Note: although LNE-CNAM exclusion was not discussed before, it must be excluded for the above-mentioned wavelengths because LNE-CNAM submitted only one round measurement data for these wavelengths and, therefore, was at the same situation as NPL.*

**Version 3**: All participants included in calculation of KCRV.

Method of analysis was the same for all three versions.

## 8.3. Method of comparison data analysis

Analysis of the comparison data was done independently for each wavelength. The analysis follows the approach described in the Appendix B of the Guidelines for CCPR Key Comparison Report Preparation, version CCPR-G2 Rev.4 [4].

1. For each NMI *i* for each lamp *j*, the Spectral Irradiance NMI measured values $E_{i,j,r}$ of two rounds *r* are averaged:

$$E_{i,j} = \frac{1}{2}\sum_{r=1}^{2} E_{i,j,r} \tag{8.1}$$

Note: NPL has not submitted the second-round data, and NMIA has withdrawn its second-round data. Therefore, for NPL and NMIA $E_{i,j} = E_{i,j,1}$. LNE-Cnam for wavelength ranges (800 – 1100) nm and (1700 – 2500) nm has not submitted the first-round data. Therefore, for LNE-CNAM at the specified wavelengths $E_{i,j} = E_{i,j,2}$.

The standard uncertainty of $E_{i,j}$ are given by:

- for NPL, NMIA and LNE-CNAM at above mentioned wavelengths

$$u(E_{i,j}) = u(E_{i,j,r}) \tag{8.2}$$

where $u(E_{i,j,r})$ is reported combined standard uncertainty of the first round for NPL and NMIA, and the second round for LNE-CNAM;

- for other NMIs

$$u(E_{i,j}) = \sqrt{\left(\frac{1}{2}\sum_{r=1}^{2} u_{\mathrm{corr}}(E_{i,j,r})\right)^2 + \frac{1}{4}\sum_{r=1}^{2} u^2_{\mathrm{uncorr}}(E_{i,j,r})} \tag{8.3}$$

where $u_{\mathrm{corr}}(E_{i,j,r})$ and $u_{\mathrm{uncorr}}(E_{i,j,r})$ are reported total correlated and uncorrelated components of standard uncertainty.

Note: Eq.8.3 corresponds to Eq.3 of the Appendix B of CCPR-G2; we use average of $u_{\mathrm{corr}}(E_{i,j,1})$ and $u_{\mathrm{corr}}(E_{i,j,2})$ instead $u_{\mathrm{rel}}(\bar{E}_i^S)$, and $u_{\mathrm{uncorr}}(E_{i,j,r})$ instead $u_{\mathrm{rel}}(E_{i,j,r}^{\mathrm{T}})$. All uncertainties in this analysis are relative. Therefore, we omit the subscript "rel" in this text.

2. For each NMI *i* for each lamp *j*, the relative difference between NMI measurement (as an average of two rounds) and Pilot measurement is given by

$$\Delta_{i,j} = \frac{E_{i,j}}{E^{\mathrm{P}}_{i,j}} - 1\,, \tag{8.4}$$

and its uncertainty by

$$u(\Delta_{i,j}) = \sqrt{u^2(E_{i,j}) + u^2_{\mathrm{uncorr}}(E^{\mathrm{P}}_{i,j})} \tag{8.5}$$

where $u_{\mathrm{uncorr}}(E^{\mathrm{P}}_{i,j})$ is the uncorrelated (random) component of the pilot uncertainty. This component is considered the same for all NMIs and all lamps. Therefore, $u_{\mathrm{uncorr}}(E^{\mathrm{P}}_{i,j}) = u_{\mathrm{uncorr}}(E^{\mathrm{P}})$. These values are presented in Table 8.4.

3. For each NMI *i*, the relative differences (average of the three lamps) is obtained by

$$\Delta_i = \frac{1}{m}\sum_{j=1}^{3} \Delta_{i,j}\,, \tag{8.6}$$

and its uncertainty by

$$u(\Delta_i) = \frac{1}{m}\sum_{j=1}^{m} u(\Delta_{i,j})\,, \tag{8.7}$$

where *m* is a number of lamps: *m*=3 for most NMIs, and *m*=2 for CSIC, KRISS, LNE-CNAM and NIST.

Table 8.4. Uncorrelated (random) component of the pilot uncertainty

| $\lambda$ , nm | $u_{\mathrm{uncorr}}(E^{\mathrm{P}})$, % | $\lambda$ , nm | $u_{\mathrm{uncorr}}(E^{\mathrm{P}})$, % | $\lambda$ , nm | $u_{\mathrm{uncorr}}(E^{\mathrm{P}})$, % | $\lambda$ , nm | $u_{\mathrm{uncorr}}(E^{\mathrm{P}})$, % |
|---|---|---|---|---|---|---|---|
| 250 | 0.21 | 340 | 0.12 | 600 | 0.10 | 1500 | 0.09 |
| 260 | 0.17 | 360 | 0.12 | 700 | 0.10 | 1700 | 0.09 |
| 270 | 0.16 | 380 | 0.11 | 800 | 0.10 | 2000 | 0.12 |
| 280 | 0.15 | 400 | 0.11 | 900 | 0.09 | 2200 | 0.14 |
| 290 | 0.14 | 450 | 0.11 | 1000 | 0.09 | 2300 | 0.18 |
| 300 | 0.14 | 500 | 0.10 | 1100 | 0.09 | 2400 | 0.20 |
| 320 | 0.12 | 555 | 0.10 | 1300 | 0.09 | 2500 | 0.22 |

### 8.3.1. Calculation of KCRV

4. The relative uncertainty of measurements of NMI *i*, averaged for all lamps, is determined by

$$u(E_i) = \frac{1}{m}\sum_{j=1}^{m} u(E_{i,j})\,, \tag{8.10}$$

Note: numbering of equations here is the same as at the CCPR-G2, Appendix B.

5. The KCRV is calculated using weighted mean with cut-off. The cut-off value $u_{\mathrm{cut-off}}$ is calculated by

$$u_{\mathrm{cut-off}} = \text{average}\,\{u(E_i)\} \text{ for } u(E_i) \le \text{median}\{u(E_i)\} \tag{8.12}$$

The reported uncertainty of each NMI *i* is adjusted by the cut-off:

$$\begin{aligned} u_{\mathrm{adj}}(E_i) &= u(E_i) \text{ for } u(E_i) \ge u_{\mathrm{cut-off}} \\ u_{\mathrm{adj}}(E_i) &= u_{\mathrm{cut-off}} \text{ for } u(E_i) < u_{\mathrm{cut-off}} \end{aligned} \tag{8.13}$$

The uncertainty of after cut-off is given by

$$u_{\mathrm{adj}}(\Delta_i) = \sqrt{u_{\mathrm{adj}}^2(E_i) + u_{\mathrm{uncorr}}^2\left(E_{i,j}^{\mathrm{P}}\right) + s^2} \tag{8.15, 20}$$

where *s* is the Mandel-Paule addition (see below). At the first step *s* = 0.

The weights $w_i$ for NMI *i* is determined by

$$w_i = u_{\mathrm{adj}}^{-2}(\Delta_i) \Big/ \sum_{i=1}^{N} u_{\mathrm{adj}}^{-2}(\Delta_i) \tag{8.16}$$

where *N* is the number of participants, whose results are included in calculating KCRV.

The KCRV, $\Delta_{\mathrm{KCRV}}$, is determined by

$$\Delta_{\mathrm{KCRV}} = \sum_{i=1}^{N} w_i \Delta_i \tag{8.17}$$

The uncertainty of the KCRV (weighted mean with cut-off) is given by

$$u(\Delta_{\mathrm{KCRV}}) = \sqrt{\sum_{i=1}^{N} \frac{u^2(\Delta_i)}{u_{\mathrm{adj}}^4(\Delta_i)}} \Big/ \sum_{i=1}^{N} u_{\mathrm{adj}}^{-2}(\Delta_i) \tag{8.18}$$

### 8.3.2. Consistency check

6. Calculate the Chi-square value $\chi_{\mathrm{obs}}^2$ for consistency check:

$$\chi_{\mathrm{obs}}^2 = \sum_{i=1}^{N} \frac{(\Delta_i - \Delta_{\mathrm{KCRV}})^2}{u_{\mathrm{adj}}^2(\Delta_i)} \tag{8.19}$$

Determine $\chi_{0.05}^2(\nu)$ value from the Table 8.5. $\nu = N - 1$

Table 8.5. $\chi_{0.05}^2(\nu)$ value

| $\nu$ | 5 | 6 | 7 | 8 | 9 | 10 | 11 |
|---|---|---|---|---|---|---|---|
| $\chi_{0.05}^2(\nu)$ | 11.070 | 12.592 | 14.067 | 15.507 | 16.919 | 18.307 | 19.675 |

If $\chi_{\mathrm{obs}}^2 > \chi_{0.05}^2(\nu)$, consistency fails. In this case, following the Mandel-Paule method, add the $s^2$ term in eq. (8.15). The value of *s* can be determined by iterative process so that $\chi_{\mathrm{obs}}^2 = \chi_{0.05}^2(\nu)$.

If $\chi_{\mathrm{obs}}^2 \le \chi_{0.05}^2(\nu)$, consistency is satisfied, *s* = 0.

### 8.3.3. Calculation of Degrees of Equivalence

7. The unilateral DoE of NMI *i* is given by

$$D_i = \Delta_i - \Delta_{\mathrm{KCRV}} \tag{8.21}$$

$$U_i = k\sqrt{u^2(\Delta_i) + u^2(\Delta_{\mathrm{KCRV}}) - 2\left(\frac{u^2(\Delta_i)}{u_{\mathrm{adj}}^2(\Delta_i)}\Big/\sum_{i=1}^{N} u_{\mathrm{adj}}^{-2}(\Delta_i)\right)};\ \ k = 2 \tag{8.22}$$

Equation (8.22) takes into account the effect of correlation between $\Delta_i$ and $\Delta_{\mathrm{KCRV}}$. For any labs that are excluded from KCRV calculation, the uncertainty $U_i$ is given by:

$$U_i = k\sqrt{u^2(\Delta_i) + u^2(\Delta_{\mathrm{KCRV}})};\ \ k = 2 \tag{8.23}$$

## 8.4. Results of comparison data analysis

Analysis was done for three versions mentioned above and circulated to the participants.

Comparison of the versions results showed insignificant difference. For instance, the change of KCRV, $\Delta_{\mathrm{KCRV}}$ , from version to version is less than the standard uncertainty of KCRV, $u(\Delta_{\mathrm{KCRV}})$, and the uncertainty, $u(\Delta_{\mathrm{KCRV}})$, does not change at the most of the wavelengths.

The participants agreed to accept as the final the Version 3, where all participants are used for calculation of KCRV. Therefore, this section presents the final version (the version 3) results only. The results for version 1 and 2 are presented in Appendices B and C.

### 8.4.1. Calculation of Differences from Pilot

The **relative average differences** $\boldsymbol{\Delta_i}$ of NMI Spectral Irradiance data to the Pilot Spectral Irradiance data (Eq. 8.6) and **uncertainties** $\boldsymbol{u(\Delta_i)}$ of these differences (Eq. 8.7) are presented in Table 8.6 and Table 8.7, respectively.

Table 8.6. Relative average differences $\boldsymbol{\Delta_i}$ of NMI-to-Pilot data (Eq.8.6 of the Section 8.3)

| λ, | $\Delta_i$, % | | | | | | | | | | | |
|---|---|---|---|---|---|---|---|---|---|---|---|---|
| nm | CSIC | KRISS | LNE | NIM | NIST | NMC | NMIA | NMIJ | NPL | NRC | PTB | VNIIOFI |
| 250 | -3.16 | 0.92 | 5.26 | 1.17 | 0.72 | -0.50 | -0.99 | 0.43 | -0.67 | 0.87 | 1.76 | 0.20 |
| 260 | -4.30 | 0.88 | 1.67 | 0.74 | 0.47 | -0.54 | -1.85 | 0.81 | -1.58 | 1.01 | 1.79 | 0.18 |
| 270 | -5.06 | 0.78 | 0.78 | 0.39 | -0.04 | -0.10 | -2.01 | 0.96 | -1.72 | 1.03 | 1.67 | 0.11 |
| 280 | -4.59 | 0.41 | 0.75 | 0.46 | 0.23 | -0.46 | -1.63 | 0.91 | -1.85 | 0.78 | 1.35 | 0.18 |
| 290 | -3.44 | 0.41 | 0.73 | 0.53 | 0.49 | -0.40 | -1.70 | 0.83 | -1.19 | 0.94 | 1.50 | 0.15 |
| 300 | -0.42 | 0.35 | 0.85 | 0.47 | 0.70 | -0.26 | -1.75 | 1.02 | -0.96 | 0.94 | 1.41 | 0.10 |
| 320 | 0.88 | 0.05 | 1.20 | 0.30 | 0.55 | -0.46 | -2.05 | 0.79 | -1.51 | 0.63 | 1.18 | 0.18 |
| 340 | 1.21 | 0.17 | 1.21 | 0.54 | 0.47 | -0.18 | -2.04 | 0.81 | -1.23 | 0.86 | 1.32 | 0.14 |
| 360 | 1.35 | 0.27 | 1.29 | 0.49 | 0.31 | -0.07 | -1.84 | 0.79 | -1.01 | 0.97 | 1.37 | 0.14 |
| 380 | 1.30 | 0.24 | 1.50 | 0.53 | 0.26 | -0.13 | -1.81 | 0.84 | -0.86 | 0.92 | 1.35 | 0.14 |
| 400 | 1.29 | 0.18 | 1.32 | 0.46 | 0.28 | -0.13 | -1.82 | 1.40 | -0.91 | 0.15 | 1.22 | 0.18 |
| 450 | 1.17 | -0.03 | 0.69 | 0.51 | 0.49 | -0.42 | -1.29 | 1.05 | -0.60 | 0.04 | 0.74 | 0.16 |
| 500 | 0.97 | -0.04 | 0.56 | 0.42 | 0.46 | -0.52 | -0.87 | 0.96 | -0.45 | 0.09 | 0.61 | 0.15 |
| 555 | 0.90 | -0.02 | 0.58 | 0.47 | 0.37 | -0.35 | -0.50 | 0.88 | -0.43 | 0.04 | 0.47 | 0.13 |
| 600 | 0.95 | 0.01 | 0.52 | 0.46 | 0.39 | -0.35 | -0.32 | 0.78 | -0.46 | 0.04 | 0.35 | 0.16 |
| 700 | 1.72 | 0.10 | 0.15 | 0.44 | 0.24 | -0.29 | -0.01 | 0.59 | -0.46 | -0.06 | 0.21 | 0.14 |
| 800 | 0.92 | 0.50 | 0.68 | 0.50 | 0.03 | 0.74 | 0.47 | 0.72 | -0.40 | -0.04 | 0.15 | 0.17 |
| 900 | 0.43 | -0.03 | 0.70 | 0.43 | 0.28 | 0.84 | 0.80 | 0.85 | -0.45 | -0.24 | 0.07 | 0.18 |
| 1000 | -0.37 | -0.01 | 0.81 | 0.38 | 0.24 | 0.81 | 0.97 | 0.39 | -0.38 | -0.14 | 0.05 | 0.15 |
| 1100 | -0.47 | -0.02 | 0.82 | 0.04 | -0.05 | 0.86 | 1.25 | -0.05 | -0.33 | -0.04 | 0.35 | 0.17 |
| 1300 | 0.17 | 0.05 | 1.29 | 0.20 | -0.09 | 1.02 | 1.45 | -0.05 | -0.30 | 0.75 | -0.02 | 0.17 |
| 1500 | -0.70 | 0.04 | 1.26 | 0.29 | -0.19 | 1.07 | 1.66 | -0.39 | -0.33 | 0.62 | 0.16 | 0.18 |
| 1700 | -7.05 | -0.17 | 1.84 | 0.37 | -0.12 | 1.20 | 1.97 | -0.53 | -0.50 | 1.07 | 0.03 | 0.14 |
| 2000 | | -0.15 | 2.59 | 0.23 | -0.09 | 1.09 | 2.54 | -1.34 | -0.39 | 0.65 | 0.01 | 0.16 |
| 2200 | | -0.90 | 3.34 | 0.26 | -0.07 | 1.09 | 3.14 | -2.01 | -0.43 | 1.84 | 0.19 | 0.15 |
| 2300 | | -0.28 | 4.52 | 0.22 | 0.06 | 0.99 | 4.71 | -1.57 | -0.29 | 0.95 | 0.06 | -0.04 |
| 2400 | | 0.39 | 7.20 | 0.20 | -0.38 | 1.20 | 5.85 | -1.73 | -0.05 | 3.03 | 0.29 | 0.26 |
| 2500 | | 0.02 | 8.00 | 0.45 | 0.29 | 1.33 | 8.91 | -1.69 | -0.79 | 3.72 | 0.33 | 0.22 |

Table 8.7. Uncertainties $u(\Delta_i)$ of relative average differences (Eq. 8.7)

| λ, nm | $u(\Delta_i)$, % | | | | | | | | | | | |
|---|---|---|---|---|---|---|---|---|---|---|---|---|
| | CSIC | KRISS | LNE | NIM | NIST | NMC | NMIA | NMIJ | NPL | NRC | PTB | VNIIOFI |
| 250 | 2.53 | 1.03 | 2.31 | 0.79 | 0.80 | 0.98 | 2.86 | 1.38 | 0.95 | 1.50 | 0.76 | 0.43 |
| 260 | 2.45 | 0.92 | 1.03 | 0.67 | 0.77 | 0.85 | 2.38 | 1.27 | 0.97 | 1.23 | 0.69 | 0.38 |
| 270 | 2.43 | 0.86 | 0.82 | 0.62 | 0.75 | 0.76 | 2.07 | 1.22 | 1.02 | 0.86 | 0.64 | 0.36 |
| 280 | 2.23 | 0.79 | 0.66 | 0.61 | 0.72 | 0.79 | 1.89 | 1.18 | 0.95 | 0.78 | 0.62 | 0.34 |
| 290 | 2.21 | 0.76 | 0.60 | 0.55 | 0.70 | 0.68 | 1.79 | 1.15 | 0.85 | 0.75 | 0.60 | 0.32 |
| 300 | 2.49 | 0.71 | 0.56 | 0.51 | 0.67 | 0.66 | 1.66 | 1.12 | 0.83 | 0.71 | 0.58 | 0.32 |
| 320 | 1.95 | 0.64 | 0.51 | 0.48 | 0.62 | 0.61 | 1.47 | 1.07 | 0.86 | 0.64 | 0.54 | 0.30 |
| 340 | 1.83 | 0.58 | 0.47 | 0.44 | 0.57 | 0.55 | 1.30 | 1.02 | 0.80 | 0.61 | 0.52 | 0.29 |
| 360 | 1.72 | 0.56 | 0.44 | 0.42 | 0.54 | 0.52 | 1.16 | 0.98 | 0.78 | 0.58 | 0.50 | 0.28 |
| 380 | 1.62 | 0.50 | 0.42 | 0.40 | 0.51 | 0.49 | 1.03 | 0.95 | 0.79 | 0.55 | 0.48 | 0.28 |
| 400 | 1.62 | 0.47 | 0.41 | 0.36 | 0.49 | 0.46 | 0.92 | 0.92 | 0.75 | 0.37 | 0.45 | 0.26 |
| 450 | 1.61 | 0.42 | 0.37 | 0.34 | 0.43 | 0.42 | 0.70 | 0.86 | 0.49 | 0.34 | 0.41 | 0.24 |
| 500 | 1.70 | 0.39 | 0.36 | 0.32 | 0.40 | 0.38 | 0.53 | 0.82 | 0.43 | 0.31 | 0.38 | 0.22 |
| 555 | 1.80 | 0.37 | 0.34 | 0.29 | 0.36 | 0.35 | 0.41 | 0.78 | 0.40 | 0.28 | 0.35 | 0.20 |
| 600 | 1.70 | 0.35 | 0.34 | 0.28 | 0.34 | 0.34 | 0.36 | 0.76 | 0.37 | 0.26 | 0.34 | 0.18 |
| 700 | 1.60 | 0.33 | 0.40 | 0.26 | 0.30 | 0.29 | 0.44 | 0.72 | 0.33 | 0.23 | 0.31 | 0.17 |
| 800 | 1.61 | 0.33 | 0.44 | 0.26 | 0.27 | 0.31 | 0.61 | 0.69 | 0.30 | 0.22 | 0.30 | 0.16 |
| 900 | 1.90 | 0.29 | 0.27 | 0.27 | 0.24 | 0.48 | 0.71 | 0.68 | 0.27 | 0.19 | 0.28 | 0.16 |
| 1000 | 1.90 | 0.29 | 0.26 | 0.26 | 0.23 | 0.29 | 0.80 | 0.66 | 0.25 | 0.18 | 0.27 | 0.15 |
| 1100 | 2.30 | 0.29 | 0.49 | 0.26 | 0.22 | 0.26 | 0.87 | 0.65 | 0.24 | 0.17 | 0.28 | 0.14 |
| 1300 | 2.02 | 0.28 | 0.39 | 0.25 | 0.20 | 0.25 | 0.96 | 0.64 | 0.22 | 0.40 | 0.32 | 0.14 |
| 1500 | 2.12 | 0.27 | 0.43 | 0.26 | 0.18 | 0.26 | 1.04 | 0.63 | 0.21 | 0.43 | 0.30 | 0.14 |
| 1700 | 2.12 | 0.32 | 0.31 | 0.26 | 0.17 | 0.23 | 1.11 | 0.63 | 0.30 | 0.54 | 0.28 | 0.14 |
| 2000 | | 0.39 | 0.37 | 0.27 | 0.18 | 0.25 | 1.42 | 0.63 | 0.32 | 0.84 | 0.31 | 0.18 |
| 2200 | | 0.46 | 0.61 | 0.32 | 0.19 | 0.29 | 1.25 | 0.63 | 0.33 | 2.07 | 0.42 | 0.20 |
| 2300 | | 0.51 | 0.70 | 0.37 | 0.22 | 0.30 | 1.30 | 0.64 | 0.36 | 2.37 | 0.40 | 0.25 |
| 2400 | | 0.53 | 1.19 | 0.60 | 0.29 | 0.32 | 1.41 | 0.67 | 0.37 | 2.73 | 0.46 | 0.29 |
| 2500 | | 0.66 | 4.40 | 0.89 | 0.43 | 0.39 | 1.29 | 0.97 | 0.89 | 6.22 | 2.89 | 0.33 |

### 8.4.2. Calculation of KCRV

**Cut-off** values were calculated following Eq. 8.10 – 8.12. Values of relative average uncertainties of spectral irradiance $u(E_i)$, Median and Cut-off are presented in Table 8.8. Red-marked values in the table are the uncertainties, which are less or equal to Median.

**Uncertainties $u_{\mathbf{adj}}(\Delta_i)$ after cut-off** of relative average differences (Eq. 8.15,8.20) are presented in Table 8.9. At this stage $s = 0$.

Table 8.10 presents the **weights $w_i$, KCRV $\Delta_{\mathbf{KCRV}}$ and uncertainty of KCR $u(\Delta_{\mathbf{KCRV}})$,** determined by Equations 8.16, 8.17 and 8.18, respectively.

### 8.4.3. Calculation of preliminary values of Degrees of Equivalence

Degrees of Equivalence, i.e. Deviations from KCRV, $D_i$, and their associated expanded uncertainties, $U_i$, (Eq. 8.21 and 8.22, respectively) are presented in Table 8.11. These are preliminary (the first-step approach) values. They were calculated before carrying out consistency check, identifying outlies and applying the Mandel-Paule method.

Table 8.8. Relative average uncertainties of spectral irradiance $u(E_i)$, Median and Cut-off in %. Red-marked values in the table are the uncertainties, which are less or equal to Median.

| λ, nm | $u(E_i)$, % | | | | | | | | | | | | Median | **Cut-off** |
|---|---|---|---|---|---|---|---|---|---|---|---|---|---|---|
| | CSIC | KRISS | LNE | NIM | NIST | NMC | NMIA | NMIJ | NPL | NRC | PTB | VNII OFI | | |
| 250 | 2.52 | 1.00 | 2.30 | 0.76 | 0.78 | 0.96 | 2.85 | 1.36 | 0.92 | 1.49 | 0.73 | 0.37 | 0.98 | **0.75** |
| 260 | 2.44 | 0.90 | 1.01 | 0.65 | 0.75 | 0.83 | 2.37 | 1.26 | 0.96 | 1.21 | 0.67 | 0.34 | 0.93 | **0.69** |
| 270 | 2.42 | 0.84 | 0.80 | 0.60 | 0.73 | 0.74 | 2.06 | 1.21 | 1.01 | 0.85 | 0.62 | 0.32 | 0.82 | **0.64** |
| 280 | 2.22 | 0.775 | 0.65 | 0.59 | 0.71 | 0.775 | 1.88 | 1.17 | 0.94 | 0.766 | 0.60 | 0.30 | 0.77 | **0.60** |
| 290 | 2.21 | 0.75 | 0.58 | 0.53 | 0.68 | 0.67 | 1.78 | 1.14 | 0.84 | 0.74 | 0.58 | 0.29 | 0.71 | **0.57** |
| 300 | 2.49 | 0.70 | 0.54 | 0.49 | 0.66 | 0.64 | 1.66 | 1.11 | 0.82 | 0.70 | 0.56 | 0.28 | 0.68 | **0.53** |
| 320 | 1.95 | 0.63 | 0.49 | 0.47 | 0.61 | 0.60 | 1.46 | 1.06 | 0.85 | 0.63 | 0.53 | 0.27 | 0.62 | **0.50** |
| 340 | 1.82 | 0.57 | 0.46 | 0.42 | 0.56 | 0.54 | 1.30 | 1.01 | 0.79 | 0.60 | 0.51 | 0.27 | 0.565 | **0.46** |
| 360 | 1.71 | 0.54 | 0.43 | 0.41 | 0.53 | 0.50 | 1.15 | 0.97 | 0.77 | 0.56 | 0.49 | 0.25 | 0.535 | **0.43** |
| 380 | 1.61 | 0.49 | 0.41 | 0.39 | 0.50 | 0.48 | 1.02 | 0.94 | 0.78 | 0.54 | 0.47 | 0.26 | 0.496 | **0.41** |
| 400 | 1.61 | 0.46 | 0.39 | 0.35 | 0.48 | 0.44 | 0.91 | 0.91 | 0.74 | 0.36 | 0.44 | 0.24 | 0.45 | **0.37** |
| 450 | 1.60 | 0.41 | 0.35 | 0.32 | 0.42 | 0.407 | 0.69 | 0.85 | 0.48 | 0.32 | 0.40 | 0.21 | 0.409 | **0.33** |
| 500 | 1.70 | 0.38 | 0.35 | 0.30 | 0.38 | 0.36 | 0.52 | 0.81 | 0.41 | 0.29 | 0.37 | 0.20 | 0.37 | **0.31** |
| 555 | 1.80 | 0.35 | 0.33 | 0.27 | 0.344 | 0.34 | 0.40 | 0.77 | 0.39 | 0.26 | 0.34 | 0.17 | 0.342 | **0.28** |
| 600 | 1.70 | 0.34 | 0.330 | 0.26 | 0.32 | 0.326 | 0.35 | 0.75 | 0.36 | 0.25 | 0.328 | 0.15 | 0.329 | **0.27** |
| 700 | 1.60 | 0.32 | 0.39 | 0.24 | 0.28 | 0.28 | 0.43 | 0.71 | 0.31 | 0.21 | 0.30 | 0.14 | 0.306 | **0.24** |
| 800 | 1.60 | 0.31 | 0.43 | 0.24 | 0.25 | 0.30 | 0.60 | 0.68 | 0.28 | 0.20 | 0.28 | 0.13 | 0.29 | **0.23** |
| 900 | 1.90 | 0.28 | 0.25 | 0.25 | 0.22 | 0.47 | 0.71 | 0.67 | 0.26 | 0.17 | 0.27 | 0.13 | 0.26 | **0.21** |
| 1000 | 1.90 | 0.28 | 0.25 | 0.24 | 0.21 | 0.28 | 0.79 | 0.65 | 0.23 | 0.16 | 0.26 | 0.12 | 0.25 | **0.21** |
| 1100 | 2.30 | 0.27 | 0.48 | 0.24 | 0.20 | 0.24 | 0.87 | 0.64 | 0.22 | 0.15 | 0.27 | 0.11 | 0.25 | **0.19** |
| 1300 | 2.02 | 0.27 | 0.38 | 0.23 | 0.18 | 0.23 | 0.96 | 0.63 | 0.20 | 0.38 | 0.31 | 0.11 | 0.29 | **0.20** |
| 1500 | 2.12 | 0.25 | 0.42 | 0.25 | 0.16 | 0.24 | 1.04 | 0.62 | 0.19 | 0.42 | 0.29 | 0.10 | 0.27 | **0.20** |
| 1700 | 2.12 | 0.31 | 0.29 | 0.24 | 0.15 | 0.21 | 1.10 | 0.62 | 0.28 | 0.53 | 0.27 | 0.11 | 0.287 | **0.21** |
| 2000 | | 0.37 | 0.35 | 0.24 | 0.13 | 0.22 | 1.41 | 0.61 | 0.29 | 0.83 | 0.29 | 0.14 | 0.29 | **0.22** |
| 2200 | | 0.44 | 0.60 | 0.29 | 0.13 | 0.25 | 1.24 | 0.61 | 0.30 | 2.07 | 0.39 | 0.15 | 0.39 | **0.25** |
| 2300 | | 0.48 | 0.68 | 0.33 | 0.13 | 0.23 | 1.28 | 0.62 | 0.31 | 2.36 | 0.36 | 0.17 | 0.36 | **0.25** |
| 2400 | | 0.49 | 1.17 | 0.57 | 0.21 | 0.25 | 1.40 | 0.64 | 0.31 | 2.72 | 0.42 | 0.20 | 0.49 | **0.28** |
| 2500 | | 0.62 | 4.39 | 0.86 | 0.38 | 0.32 | 1.27 | 0.94 | 0.86 | 6.21 | 2.88 | 0.24 | 0.86 | **0.55** |

Table 8.9. Uncertainties $\boldsymbol{u_{adj}(\Delta_i)}$ after cut-off of relative average differences (Eq. 8.15). $s = 0$.

| λ, nm | $u_{adj}(\Delta_i)$, % | | | | | | | | | | | |
|---|---|---|---|---|---|---|---|---|---|---|---|---|
| | CSIC | KRISS | LNE | NIM | NIST | NMC | NMA | NMIJ | NPL | NRC | PTB | VNIIOFI |
| 250 | 2.53 | 1.03 | 2.31 | 0.79 | 0.80 | 0.98 | 2.86 | 1.38 | 0.95 | 1.50 | 0.78 | 0.78 |
| 260 | 2.45 | 0.92 | 1.03 | 0.71 | 0.77 | 0.85 | 2.38 | 1.27 | 0.97 | 1.23 | 0.71 | 0.71 |
| 270 | 2.43 | 0.86 | 0.82 | 0.66 | 0.75 | 0.76 | 2.07 | 1.22 | 1.02 | 0.86 | 0.66 | 0.66 |
| 280 | 2.23 | 0.79 | 0.66 | 0.62 | 0.72 | 0.79 | 1.89 | 1.18 | 0.95 | 0.78 | 0.62 | 0.62 |
| 290 | 2.21 | 0.76 | 0.60 | 0.59 | 0.70 | 0.68 | 1.79 | 1.15 | 0.85 | 0.75 | 0.60 | 0.59 |
| 300 | 2.49 | 0.71 | 0.56 | 0.55 | 0.67 | 0.66 | 1.66 | 1.12 | 0.83 | 0.71 | 0.58 | 0.55 |
| 320 | 1.95 | 0.64 | 0.51 | 0.51 | 0.62 | 0.61 | 1.47 | 1.07 | 0.86 | 0.64 | 0.54 | 0.51 |
| 340 | 1.83 | 0.58 | 0.47 | 0.47 | 0.57 | 0.55 | 1.30 | 1.02 | 0.80 | 0.61 | 0.52 | 0.47 |
| 360 | 1.72 | 0.56 | 0.45 | 0.45 | 0.54 | 0.52 | 1.16 | 0.98 | 0.78 | 0.58 | 0.50 | 0.45 |
| 380 | 1.62 | 0.50 | 0.43 | 0.43 | 0.51 | 0.49 | 1.03 | 0.95 | 0.79 | 0.55 | 0.48 | 0.43 |
| 400 | 1.62 | 0.47 | 0.41 | 0.38 | 0.49 | 0.46 | 0.92 | 0.92 | 0.75 | 0.38 | 0.45 | 0.38 |
| 450 | 1.61 | 0.42 | 0.37 | 0.35 | 0.43 | 0.42 | 0.70 | 0.86 | 0.49 | 0.35 | 0.41 | 0.35 |
| 500 | 1.70 | 0.39 | 0.36 | 0.33 | 0.40 | 0.38 | 0.53 | 0.82 | 0.43 | 0.33 | 0.38 | 0.33 |
| 555 | 1.80 | 0.37 | 0.34 | 0.30 | 0.36 | 0.35 | 0.41 | 0.78 | 0.40 | 0.30 | 0.35 | 0.30 |
| 600 | 1.70 | 0.35 | 0.34 | 0.29 | 0.34 | 0.34 | 0.36 | 0.76 | 0.37 | 0.29 | 0.34 | 0.29 |
| 700 | 1.60 | 0.33 | 0.40 | 0.26 | 0.30 | 0.29 | 0.44 | 0.72 | 0.33 | 0.26 | 0.31 | 0.26 |
| 800 | 1.61 | 0.33 | 0.44 | 0.26 | 0.27 | 0.31 | 0.61 | 0.69 | 0.30 | 0.25 | 0.30 | 0.25 |
| 900 | 1.90 | 0.29 | 0.27 | 0.27 | 0.24 | 0.48 | 0.71 | 0.68 | 0.27 | 0.23 | 0.28 | 0.23 |
| 1000 | 1.90 | 0.29 | 0.26 | 0.26 | 0.23 | 0.29 | 0.80 | 0.66 | 0.25 | 0.23 | 0.27 | 0.23 |
| 1100 | 2.30 | 0.29 | 0.49 | 0.26 | 0.22 | 0.26 | 0.87 | 0.65 | 0.24 | 0.21 | 0.28 | 0.21 |
| 1300 | 2.02 | 0.28 | 0.39 | 0.25 | 0.22 | 0.25 | 0.96 | 0.64 | 0.22 | 0.40 | 0.32 | 0.22 |
| 1500 | 2.12 | 0.27 | 0.43 | 0.26 | 0.22 | 0.26 | 1.04 | 0.63 | 0.22 | 0.43 | 0.30 | 0.22 |
| 1700 | 2.12 | 0.32 | 0.30 | 0.26 | 0.23 | 0.23 | 1.11 | 0.63 | 0.30 | 0.54 | 0.28 | 0.23 |
| 2000 | | 0.39 | 0.37 | 0.27 | 0.25 | 0.25 | 1.42 | 0.63 | 0.32 | 0.84 | 0.31 | 0.25 |
| 2200 | | 0.46 | 0.61 | 0.32 | 0.29 | 0.29 | 1.25 | 0.63 | 0.33 | 2.07 | 0.42 | 0.29 |
| 2300 | | 0.51 | 0.70 | 0.37 | 0.31 | 0.31 | 1.30 | 0.64 | 0.35 | 2.37 | 0.40 | 0.31 |
| 2400 | | 0.53 | 1.19 | 0.60 | 0.37 | 0.37 | 1.41 | 0.67 | 0.37 | 2.72 | 0.46 | 0.37 |
| 2500 | | 0.66 | 4.40 | 0.89 | 0.59 | 0.59 | 1.29 | 0.97 | 0.89 | 6.22 | 2.89 | 0.59 |

Table 8.10. Weights, $w_i$ , KCRV, $\Delta_{\mathrm{KCRV}}$, and uncertainty of KCR, $u(\Delta_{\mathrm{KCRV}})$

| λ, nm | $w_i$ | | | | | | | | | | | | $\Delta_{\mathrm{KCRV}}$ % | $u(\Delta_{\mathrm{KCRV}})$ % |
|---|---|---|---|---|---|---|---|---|---|---|---|---|---|---|
| | CSIC | KRISS | LNE | NIM | NIST | NMC | NMIA | NMIJ | NPL | NRC | PTB | VNII OFI | | |
| 250 | 0.014 | 0.087 | 0.017 | 0.147 | 0.141 | 0.094 | 0.011 | 0.048 | 0.102 | 0.041 | 0.149 | 0.149 | **0.62** | **0.28** |
| 260 | 0.012 | 0.086 | 0.069 | 0.143 | 0.121 | 0.101 | 0.013 | 0.044 | 0.076 | 0.048 | 0.143 | 0.143 | **0.47** | **0.25** |
| 270 | 0.010 | 0.082 | 0.089 | 0.139 | 0.107 | 0.103 | 0.014 | 0.040 | 0.058 | 0.081 | 0.139 | 0.139 | **0.36** | **0.23** |
| 280 | 0.011 | 0.084 | 0.119 | 0.136 | 0.101 | 0.084 | 0.015 | 0.037 | 0.057 | 0.086 | 0.135 | 0.136 | **0.30** | **0.22** |
| 290 | 0.009 | 0.080 | 0.129 | 0.133 | 0.095 | 0.099 | 0.014 | 0.035 | 0.063 | 0.082 | 0.128 | 0.133 | **0.39** | **0.20** |
| 300 | 0.007 | 0.082 | 0.131 | 0.139 | 0.092 | 0.096 | 0.015 | 0.033 | 0.060 | 0.081 | 0.125 | 0.139 | **0.46** | **0.19** |
| 320 | 0.009 | 0.088 | 0.137 | 0.137 | 0.093 | 0.095 | 0.017 | 0.031 | 0.049 | 0.087 | 0.121 | 0.137 | **0.36** | **0.18** |
| 340 | 0.009 | 0.091 | 0.137 | 0.137 | 0.094 | 0.100 | 0.018 | 0.030 | 0.049 | 0.084 | 0.114 | 0.137 | **0.46** | **0.17** |
| 360 | 0.009 | 0.090 | 0.137 | 0.137 | 0.095 | 0.104 | 0.021 | 0.029 | 0.046 | 0.084 | 0.111 | 0.137 | **0.50** | **0.16** |
| 380 | 0.010 | 0.099 | 0.136 | 0.136 | 0.095 | 0.105 | 0.024 | 0.028 | 0.040 | 0.083 | 0.109 | 0.136 | **0.51** | **0.15** |
| 400 | 0.008 | 0.090 | 0.123 | 0.137 | 0.085 | 0.098 | 0.024 | 0.024 | 0.036 | 0.137 | 0.100 | 0.137 | **0.39** | **0.14** |
| 450 | 0.006 | 0.090 | 0.119 | 0.130 | 0.086 | 0.091 | 0.033 | 0.022 | 0.068 | 0.130 | 0.094 | 0.130 | **0.19** | **0.12** |
| 500 | 0.005 | 0.091 | 0.103 | 0.128 | 0.087 | 0.096 | 0.048 | 0.020 | 0.075 | 0.128 | 0.093 | 0.128 | **0.13** | **0.11** |
| 555 | 0.004 | 0.085 | 0.099 | 0.126 | 0.090 | 0.092 | 0.068 | 0.019 | 0.072 | 0.126 | 0.092 | 0.126 | **0.14** | **0.10** |
| 600 | 0.004 | 0.085 | 0.089 | 0.125 | 0.092 | 0.091 | 0.081 | 0.018 | 0.076 | 0.125 | 0.089 | 0.125 | **0.12** | **0.10** |
| 700 | 0.004 | 0.083 | 0.058 | 0.135 | 0.101 | 0.107 | 0.047 | 0.018 | 0.085 | 0.135 | 0.093 | 0.135 | **0.08** | **0.09** |
| 800 | 0.003 | 0.083 | 0.046 | 0.135 | 0.121 | 0.090 | 0.024 | 0.019 | 0.098 | 0.141 | 0.099 | 0.141 | **0.23** | **0.09** |
| 900 | 0.002 | 0.089 | 0.109 | 0.109 | 0.136 | 0.033 | 0.015 | 0.017 | 0.104 | 0.144 | 0.098 | 0.144 | **0.16** | **0.08** |
| 1000 | 0.002 | 0.081 | 0.103 | 0.104 | 0.132 | 0.082 | 0.011 | 0.016 | 0.111 | 0.132 | 0.093 | 0.132 | **0.20** | **0.08** |
| 1100 | 0.001 | 0.083 | 0.029 | 0.105 | 0.144 | 0.104 | 0.009 | 0.016 | 0.119 | 0.151 | 0.087 | 0.151 | **0.13** | **0.08** |
| 1300 | 0.002 | 0.096 | 0.049 | 0.121 | 0.153 | 0.123 | 0.008 | 0.019 | 0.153 | 0.049 | 0.074 | 0.153 | **0.23** | **0.08** |
| 1500 | 0.002 | 0.104 | 0.042 | 0.109 | 0.159 | 0.116 | 0.007 | 0.019 | 0.159 | 0.040 | 0.084 | 0.159 | **0.20** | **0.08** |
| 1700 | 0.002 | 0.079 | 0.088 | 0.119 | 0.155 | 0.154 | 0.007 | 0.021 | 0.091 | 0.028 | 0.102 | 0.155 | **0.36** | **0.08** |
| 2000 | 0.000 | 0.064 | 0.074 | 0.135 | 0.160 | 0.160 | 0.005 | 0.025 | 0.100 | 0.014 | 0.103 | 0.160 | **0.35** | **0.09** |
| 2200 | 0.000 | 0.065 | 0.037 | 0.136 | 0.169 | 0.169 | 0.009 | 0.035 | 0.128 | 0.003 | 0.080 | 0.169 | **0.22** | **0.11** |
| 2300 | 0.000 | 0.063 | 0.033 | 0.116 | 0.168 | 0.168 | 0.010 | 0.040 | 0.129 | 0.003 | 0.102 | 0.168 | **0.28** | **0.12** |
| 2400 | 0.000 | 0.083 | 0.016 | 0.063 | 0.166 | 0.166 | 0.012 | 0.052 | 0.166 | 0.003 | 0.107 | 0.166 | **0.35** | **0.14** |
| 2500 | 0.000 | 0.149 | 0.003 | 0.082 | 0.188 | 0.188 | 0.039 | 0.069 | 0.083 | 0.002 | 0.008 | 0.188 | **0.59** | **0.21** |

Table 8.11. Preliminary Degrees of Equivalence: Deviations from KCRV, $D_i$, and their associated expanded Uncertainties, $U_i$, (Eq.8.21 and 8.22), in %

| λ, nm | CSIC | | KRISS | | LNE | | NIM | | NIST | | NMC | | NMIA | | NMIJ | | NPL | | NRC | | PTB | | VNIIOFI | |
|---|---|---|---|---|---|---|---|---|---|---|---|---|---|---|---|---|---|---|---|---|---|---|---|---|
| | $D_i$ | $U_i$ | $D_i$ | $U_i$ | $D_i$ | $U_i$ | $D_i$ | $U_i$ | $D_i$ | $U_i$ | $D_i$ | $U_i$ | $D_i$ | $U_i$ | $D_i$ | $U_i$ | $D_i$ | $U_i$ | $D_i$ | $U_i$ | $D_i$ | $U_i$ | $D_i$ | $U_i$ |
| 250 | -3.78 | 5.02 | 0.30 | 1.95 | 4.64 | 4.57 | 0.55 | 1.44 | 0.10 | 1.48 | -1.12 | 1.86 | -1.61 | 5.68 | -0.19 | 2.68 | -1.29 | 1.79 | 0.25 | 2.93 | 1.14 | 1.40 | -0.42 | 0.91 |
| 260 | -4.77 | 4.86 | 0.41 | 1.74 | 1.20 | 1.97 | 0.27 | 1.24 | 0.00 | 1.44 | -1.01 | 1.59 | -2.32 | 4.72 | 0.34 | 2.48 | -2.05 | 1.86 | 0.54 | 2.38 | 1.32 | 1.27 | -0.29 | 0.81 |
| 270 | -5.42 | 4.83 | 0.42 | 1.63 | 0.42 | 1.55 | 0.03 | 1.16 | -0.40 | 1.40 | -0.47 | 1.43 | -2.37 | 4.11 | 0.60 | 2.39 | -2.08 | 1.97 | 0.67 | 1.64 | 1.30 | 1.19 | -0.25 | 0.76 |
| 280 | -4.89 | 4.43 | 0.11 | 1.50 | 0.45 | 1.23 | 0.16 | 1.13 | -0.07 | 1.36 | -0.76 | 1.50 | -1.93 | 3.75 | 0.61 | 2.32 | -2.15 | 1.85 | 0.48 | 1.49 | 1.05 | 1.15 | -0.12 | 0.72 |
| 290 | -3.83 | 4.41 | 0.02 | 1.45 | 0.34 | 1.11 | 0.14 | 1.03 | 0.10 | 1.32 | -0.79 | 1.29 | -2.09 | 3.55 | 0.44 | 2.26 | -1.58 | 1.65 | 0.55 | 1.43 | 1.11 | 1.11 | -0.24 | 0.68 |
| 300 | -0.88 | 4.96 | -0.11 | 1.36 | 0.39 | 1.04 | 0.01 | 0.94 | 0.24 | 1.27 | -0.72 | 1.24 | -2.21 | 3.30 | 0.56 | 2.20 | -1.42 | 1.60 | 0.48 | 1.36 | 0.95 | 1.07 | -0.36 | 0.66 |
| 320 | 0.51 | 3.88 | -0.32 | 1.21 | 0.84 | 0.93 | -0.07 | 0.90 | 0.19 | 1.18 | -0.82 | 1.16 | -2.42 | 2.91 | 0.42 | 2.10 | -1.88 | 1.66 | 0.27 | 1.22 | 0.81 | 1.01 | -0.19 | 0.62 |
| 340 | 0.75 | 3.64 | -0.30 | 1.10 | 0.75 | 0.87 | 0.08 | 0.82 | 0.01 | 1.09 | -0.64 | 1.05 | -2.50 | 2.58 | 0.35 | 2.01 | -1.69 | 1.55 | 0.40 | 1.16 | 0.86 | 0.97 | -0.32 | 0.60 |
| 360 | 0.86 | 3.42 | -0.23 | 1.06 | 0.79 | 0.82 | 0.00 | 0.79 | -0.18 | 1.02 | -0.57 | 0.97 | -2.34 | 2.29 | 0.29 | 1.93 | -1.50 | 1.52 | 0.48 | 1.10 | 0.88 | 0.94 | -0.35 | 0.57 |
| 380 | 0.79 | 3.22 | -0.27 | 0.95 | 0.99 | 0.78 | 0.02 | 0.75 | -0.25 | 0.97 | -0.64 | 0.92 | -2.32 | 2.02 | 0.33 | 1.87 | -1.37 | 1.54 | 0.41 | 1.05 | 0.84 | 0.90 | -0.37 | 0.57 |
| 400 | 0.91 | 3.22 | -0.21 | 0.90 | 0.93 | 0.76 | 0.08 | 0.68 | -0.10 | 0.93 | -0.52 | 0.86 | -2.21 | 1.82 | 1.02 | 1.81 | -1.30 | 1.47 | -0.24 | 0.69 | 0.83 | 0.85 | -0.20 | 0.52 |
| 450 | 0.98 | 3.20 | -0.22 | 0.81 | 0.50 | 0.69 | 0.32 | 0.63 | 0.30 | 0.82 | -0.62 | 0.80 | -1.48 | 1.37 | 0.85 | 1.70 | -0.79 | 0.94 | -0.15 | 0.63 | 0.54 | 0.79 | -0.03 | 0.47 |
| 500 | 0.84 | 3.40 | -0.17 | 0.74 | 0.42 | 0.69 | 0.29 | 0.59 | 0.33 | 0.75 | -0.65 | 0.72 | -1.00 | 1.04 | 0.83 | 1.62 | -0.58 | 0.81 | -0.05 | 0.57 | 0.48 | 0.73 | 0.01 | 0.44 |
| 555 | 0.76 | 3.60 | -0.15 | 0.70 | 0.44 | 0.64 | 0.33 | 0.54 | 0.24 | 0.68 | -0.49 | 0.67 | -0.63 | 0.79 | 0.75 | 1.54 | -0.57 | 0.77 | -0.09 | 0.53 | 0.33 | 0.67 | -0.01 | 0.40 |
| 600 | 0.83 | 3.40 | -0.11 | 0.67 | 0.40 | 0.65 | 0.33 | 0.52 | 0.27 | 0.64 | -0.47 | 0.65 | -0.44 | 0.69 | 0.66 | 1.50 | -0.58 | 0.71 | -0.08 | 0.50 | 0.23 | 0.65 | 0.04 | 0.36 |
| 700 | 1.65 | 3.20 | 0.03 | 0.63 | 0.07 | 0.77 | 0.36 | 0.48 | 0.17 | 0.57 | -0.37 | 0.55 | -0.08 | 0.87 | 0.52 | 1.43 | -0.54 | 0.63 | -0.14 | 0.43 | 0.13 | 0.60 | 0.06 | 0.34 |
| 800 | 0.68 | 3.21 | 0.27 | 0.62 | 0.44 | 0.85 | 0.27 | 0.47 | -0.20 | 0.50 | 0.51 | 0.59 | 0.23 | 1.20 | 0.49 | 1.37 | -0.63 | 0.57 | -0.27 | 0.41 | -0.08 | 0.56 | -0.07 | 0.33 |
| 900 | 0.26 | 3.80 | -0.19 | 0.56 | 0.54 | 0.50 | 0.27 | 0.50 | 0.12 | 0.44 | 0.68 | 0.94 | 0.63 | 1.41 | 0.68 | 1.34 | -0.62 | 0.51 | -0.41 | 0.36 | -0.09 | 0.53 | 0.02 | 0.31 |
| 1000 | -0.57 | 3.80 | -0.21 | 0.56 | 0.61 | 0.49 | 0.18 | 0.49 | 0.04 | 0.42 | 0.61 | 0.56 | 0.77 | 1.59 | 0.19 | 1.31 | -0.58 | 0.47 | -0.34 | 0.35 | -0.15 | 0.52 | -0.05 | 0.30 |
| 1100 | -0.60 | 4.60 | -0.15 | 0.55 | 0.69 | 0.96 | -0.09 | 0.48 | -0.18 | 0.40 | 0.73 | 0.49 | 1.12 | 1.73 | -0.18 | 1.29 | -0.46 | 0.45 | -0.17 | 0.33 | 0.22 | 0.54 | 0.04 | 0.28 |
| 1300 | -0.06 | 4.03 | -0.18 | 0.53 | 1.06 | 0.77 | -0.03 | 0.46 | -0.32 | 0.37 | 0.79 | 0.46 | 1.22 | 1.91 | -0.28 | 1.27 | -0.53 | 0.40 | 0.52 | 0.77 | -0.25 | 0.62 | -0.06 | 0.29 |
| 1500 | -0.90 | 4.24 | -0.16 | 0.51 | 1.06 | 0.83 | 0.09 | 0.49 | -0.39 | 0.34 | 0.87 | 0.47 | 1.46 | 2.07 | -0.59 | 1.24 | -0.53 | 0.38 | 0.42 | 0.85 | -0.04 | 0.57 | -0.02 | 0.28 |
| 1700 | -7.41 | 4.24 | -0.53 | 0.61 | 1.49 | 0.58 | 0.01 | 0.48 | -0.48 | 0.33 | 0.84 | 0.42 | 1.61 | 2.21 | -0.89 | 1.24 | -0.85 | 0.56 | 0.71 | 1.06 | -0.33 | 0.53 | -0.22 | 0.28 |
| 2000 | | | -0.50 | 0.75 | 2.24 | 0.70 | -0.12 | 0.50 | -0.44 | 0.35 | 0.74 | 0.45 | 2.19 | 2.82 | -1.69 | 1.23 | -0.74 | 0.59 | 0.30 | 1.66 | -0.34 | 0.58 | -0.19 | 0.35 |
| 2200 | | | -1.12 | 0.89 | 3.12 | 1.20 | 0.04 | 0.59 | -0.30 | 0.38 | 0.87 | 0.51 | 2.92 | 2.48 | -2.23 | 1.23 | -0.65 | 0.61 | 1.62 | 4.14 | -0.04 | 0.79 | -0.07 | 0.39 |
| 2300 | | | -0.56 | 0.98 | 4.23 | 1.38 | -0.06 | 0.70 | -0.22 | 0.43 | 0.71 | 0.54 | 4.42 | 2.58 | -1.86 | 1.25 | -0.57 | 0.66 | 0.67 | 4.73 | -0.23 | 0.75 | -0.32 | 0.47 |
| 2400 | | | 0.03 | 1.00 | 6.85 | 2.35 | -0.15 | 1.16 | -0.73 | 0.55 | 0.85 | 0.59 | 5.50 | 2.80 | -2.08 | 1.29 | -0.40 | 0.67 | 2.68 | 5.44 | -0.06 | 0.87 | -0.09 | 0.54 |
| 2500 | | | -0.57 | 1.18 | 7.41 | 8.77 | -0.14 | 1.68 | -0.30 | 0.81 | 0.74 | 0.74 | 8.32 | 2.52 | -2.28 | 1.85 | -1.38 | 1.68 | 3.13 | 12.4 | -0.26 | 5.74 | -0.36 | 0.67 |

### 8.4.4. Consistency check (preliminary)

Table 8.12 presents Chi-square values $\chi^2_{\text{obs}}$ for consistency check, calculated by Eq.8.19 of the Section 8.3 "Method of comparison data analysis", as well as the $\chi^2_{0.05}(\nu)$ value for ν = *N*-1, where *N* is the number of NMIs contribute to KCRV, and the results of the consistency check.

Table 8.12. Chi-square values $\chi^2_{\text{obs}}$ and the consistency check (preliminary)

| λ, nm | $\chi^2_{\text{obs}}$ | ν = *N*-1 | $\chi^2_{0.05}(\nu)$ | Result of the consistency check |
|---|---|---|---|---|
| 250 | 12.81 | 11 | 19.675 | satisfied |
| 260 | 16.21 | 11 | 19.675 | satisfied |
| 270 | 16.57 | 11 | 19.675 | satisfied |
| 280 | 15.95 | 11 | 19.675 | satisfied |
| 290 | 13.76 | 11 | 19.675 | satisfied |
| 300 | 10.49 | 11 | 19.675 | satisfied |
| 320 | 15.16 | 11 | 19.675 | satisfied |
| 340 | 16.21 | 11 | 19.675 | satisfied |
| 360 | 17.07 | 11 | 19.675 | satisfied |
| 380 | **20.39** | 11 | 19.675 | **failed** |
| 400 | **21.13** | 11 | 19.675 | **failed** |
| 450 | 15.90 | 11 | 19.675 | satisfied |
| 500 | 14.20 | 11 | 19.675 | satisfied |
| 555 | 11.89 | 11 | 19.675 | satisfied |
| 600 | 10.78 | 11 | 19.675 | satisfied |
| 700 | 8.57 | 11 | 19.675 | satisfied |
| 800 | 12.48 | 11 | 19.675 | satisfied |
| 900 | 17.95 | 11 | 19.675 | satisfied |
| 1000 | **19.77** | 11 | 19.675 | **failed** |
| 1100 | 17.90 | 11 | 19.675 | satisfied |
| 1300 | **29.77** | 11 | 19.675 | **failed** |
| 1500 | **31.33** | 11 | 19.675 | **failed** |
| 1700 | **72.99** | 11 | 19.675 | **failed** |
| 2000 | **68.45** | 10 | 18.307 | **failed** |
| 2200 | **64.64** | 10 | 18.307 | **failed** |
| 2300 | **67.30** | 10 | 18.307 | **failed** |
| 2400 | **69.55** | 10 | 18.307 | **failed** |
| 2500 | **55.51** | 10 | 18.307 | **failed** |

### 8.4.5. Outliers

Table 8.13 shows the ratios of absolute values of Deviation from KCRV (DoE), $|D_i|$, to their associated expanded uncertainties, $U_i$, and the Fig.8.1 shows the values $D_i$.

Pilot suggests the following outliers (marked red bold in Table 8.13):

1) Points for which the Ratios $|D_i|/U_i$ is larger than 2.5. There are 6 such points: wavelengths 1700 nm to 2400 nm of LNE/CNAM, and wavelength 2500 nm of NMIA.
2) Point of CSIC at wavelength 1700 nm. Even the ratio $|D_i|/U_i$ for this point is less than 2.0, it looks like obvious outlier in Fig.8.1 (marked with red circle)

The suggested outliers were agreed by the participants.

Table 8.13. Ratios $|D_i|/U_i$. Red bold points are suggested outliers.

| λ, nm | Ratios $\|D_i\|/U_i$ | | | | | | | | | | | |
|---|---|---|---|---|---|---|---|---|---|---|---|---|
| | CSIC | KRISS | LNE | NIM | NIST | NMC | NMIA | NMIJ | NPL | NRC | PTB | VNIIOFI |
| 250 | 0.75 | 0.15 | 1.01 | 0.38 | 0.07 | 0.60 | 0.28 | 0.07 | 0.72 | 0.08 | 0.81 | 0.46 |
| 260 | 0.98 | 0.24 | 0.61 | 0.21 | 0.00 | 0.63 | 0.49 | 0.14 | 1.10 | 0.23 | 1.04 | 0.36 |
| 270 | 1.12 | 0.26 | 0.27 | 0.03 | 0.28 | 0.33 | 0.58 | 0.25 | 1.06 | 0.41 | 1.10 | 0.33 |
| 280 | 1.10 | 0.07 | 0.36 | 0.14 | 0.05 | 0.50 | 0.51 | 0.26 | 1.16 | 0.32 | 0.91 | 0.16 |
| 290 | 0.87 | 0.01 | 0.31 | 0.13 | 0.08 | 0.61 | 0.59 | 0.20 | 0.96 | 0.39 | 0.99 | 0.35 |
| 300 | 0.18 | 0.08 | 0.38 | 0.01 | 0.19 | 0.58 | 0.67 | 0.26 | 0.89 | 0.35 | 0.89 | 0.54 |
| 320 | 0.13 | 0.26 | 0.90 | 0.07 | 0.16 | 0.71 | 0.83 | 0.20 | 1.13 | 0.22 | 0.80 | 0.30 |
| 340 | 0.21 | 0.27 | 0.87 | 0.09 | 0.01 | 0.62 | 0.97 | 0.17 | 1.09 | 0.35 | 0.88 | 0.53 |
| 360 | 0.25 | 0.21 | 0.97 | 0.00 | 0.18 | 0.58 | 1.02 | 0.15 | 0.99 | 0.44 | 0.94 | 0.62 |
| 380 | 0.25 | 0.29 | 1.26 | 0.02 | 0.25 | 0.70 | 1.14 | 0.18 | 0.89 | 0.39 | 0.93 | 0.65 |
| 400 | 0.28 | 0.23 | 1.23 | 0.11 | 0.11 | 0.60 | 1.22 | 0.56 | 0.88 | 0.35 | 0.97 | 0.39 |
| 450 | 0.31 | 0.28 | 0.72 | 0.51 | 0.36 | 0.77 | 1.08 | 0.50 | 0.84 | 0.24 | 0.69 | 0.06 |
| 500 | 0.25 | 0.23 | 0.62 | 0.49 | 0.43 | 0.91 | 0.97 | 0.51 | 0.71 | 0.08 | 0.65 | 0.03 |
| 555 | 0.21 | 0.22 | 0.69 | 0.62 | 0.35 | 0.73 | 0.80 | 0.49 | 0.74 | 0.18 | 0.49 | 0.02 |
| 600 | 0.24 | 0.17 | 0.61 | 0.64 | 0.43 | 0.73 | 0.63 | 0.44 | 0.81 | 0.17 | 0.35 | 0.11 |
| 700 | 0.51 | 0.04 | 0.09 | 0.74 | 0.29 | 0.66 | 0.10 | 0.36 | 0.86 | 0.32 | 0.22 | 0.18 |
| 800 | 0.21 | 0.43 | 0.52 | 0.57 | 0.40 | 0.85 | 0.19 | 0.36 | 1.11 | 0.66 | 0.15 | 0.20 |
| 900 | 0.07 | 0.34 | 1.08 | 0.54 | 0.26 | 0.72 | 0.45 | 0.51 | 1.21 | 1.12 | 0.18 | 0.05 |
| 1000 | 0.15 | 0.38 | 1.24 | 0.36 | 0.10 | 1.10 | 0.48 | 0.14 | 1.23 | 1.00 | 0.28 | 0.16 |
| 1100 | 0.13 | 0.28 | 0.72 | 0.18 | 0.45 | 1.51 | 0.64 | 0.14 | 1.03 | 0.51 | 0.42 | 0.13 |
| 1300 | 0.02 | 0.34 | 1.39 | 0.06 | 0.86 | 1.71 | 0.64 | 0.22 | 1.33 | 0.68 | 0.41 | 0.21 |
| 1500 | 0.21 | 0.31 | 1.27 | 0.18 | 1.14 | 1.83 | 0.71 | 0.48 | 1.40 | 0.49 | 0.06 | 0.07 |
| 1700 | **1.75** | 0.86 | **2.57** | 0.02 | 1.44 | 2.02 | 0.73 | 0.71 | 1.51 | 0.67 | 0.62 | 0.77 |
| 2000 | | 0.67 | **3.21** | 0.23 | 1.27 | 1.64 | 0.78 | 1.37 | 1.24 | 0.18 | 0.58 | 0.53 |
| 2200 | | 1.26 | **2.61** | 0.07 | 0.78 | 1.69 | 1.17 | 1.81 | 1.06 | 0.39 | 0.05 | 0.19 |
| 2300 | | 0.57 | **3.07** | 0.09 | 0.52 | 1.33 | 1.72 | 1.48 | 0.87 | 0.14 | 0.30 | 0.68 |
| 2400 | | 0.03 | **2.91** | 0.13 | 1.33 | 1.43 | 1.96 | 1.61 | 0.60 | 0.49 | 0.07 | 0.17 |
| 2500 | | 0.48 | 0.84 | 0.08 | 0.37 | 1.00 | **3.31** | 1.23 | 0.82 | 0.25 | 0.04 | 0.54 |

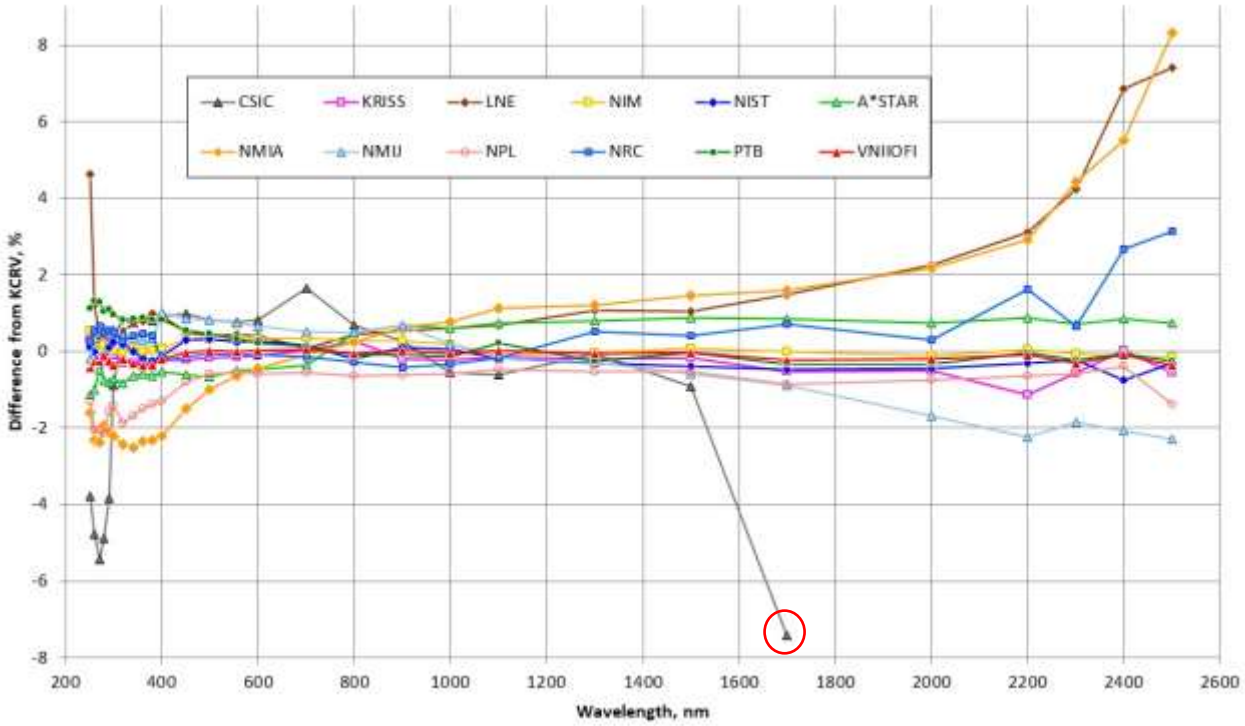


Figure 8.1. Deviations from KCRV, $D_i$, in %

### 8.4.6. Consistency check (preliminary) after excluding outliers

Note that after excluding the outliers number *N* of NMI contribute to KCRV was changed as follows:

*N* = 12 for wavelengths 250 nm to 1500 nm;
*N* = 10 for wavelengths 1700 nm to 2500 nm;

Table 8.14 presents the Chi-square values $\chi^2_{\text{obs}}$, $\chi^2_{0.05}(\nu)$ values for ν = *N*-1 and the results of the consistency check after excluding the outliers. Red figures indicate changes from the Table 8.12.

### 8.4.7. Applying Mandel-Paule method. Final consistency check

For the wavelengths where $\chi^2_{\text{obs}} > \chi^2_{0.05}(\nu)$ (the consistency check failed) the Mandel-Paule method was applied, i.e. the $s^2$ term is added in the Eq. (8.15, 8.20) for calculation of $u_{\text{adj}}(\Delta_i)$. The values of *s* are determined by iterative process so that $\chi^2_{\text{obs}} = \chi^2_{0.05}(\nu)$.

Table 8.15 shows the final consistency check results after the Mandel-Paule method, as well as the *s* values applied. Table 8.16 presents the $\boldsymbol{u_{\text{adj}}(\Delta_i)}$ uncertainties after applying the Mandel-Paule method. Red colour indicates differences from the Table 8.9.

Table 8.14. Chi-square values $\chi^2_{obs}$ and the consistency check after excluding the outliers

| λ, nm | $\chi^2_{obs}$ | ν = *N*-1 | $\chi^2_{0.05}(\nu)$ | Result of the consistency check |
|---|---|---|---|---|
| 250 | 12.81 | 11 | 19.675 | satisfied |
| 260 | 16.21 | 11 | 19.675 | satisfied |
| 270 | 16.57 | 11 | 19.675 | satisfied |
| 280 | 15.95 | 11 | 19.675 | satisfied |
| 290 | 13.76 | 11 | 19.675 | satisfied |
| 300 | 10.49 | 11 | 19.675 | satisfied |
| 320 | 15.16 | 11 | 19.675 | satisfied |
| 340 | 16.21 | 11 | 19.675 | satisfied |
| 360 | 17.07 | 11 | 19.675 | satisfied |
| 380 | **20.39** | 11 | 19.675 | **failed** |
| 400 | **21.13** | 11 | 19.675 | **failed** |
| 450 | 15.90 | 11 | 19.675 | satisfied |
| 500 | 14.20 | 11 | 19.675 | satisfied |
| 555 | 11.89 | 11 | 19.675 | satisfied |
| 600 | 10.78 | 11 | 19.675 | satisfied |
| 700 | 8.57 | 11 | 19.675 | satisfied |
| 800 | 12.48 | 11 | 19.675 | satisfied |
| 900 | 17.95 | 11 | 19.675 | satisfied |
| 1000 | **19.77** | 11 | 19.675 | **failed** |
| 1100 | 17.90 | 11 | 19.675 | satisfied |
| 1300 | **29.77** | 11 | 19.675 | **failed** |
| 1500 | **31.33** | 11 | 19.675 | **failed** |
| 1700 | **35.26** | 9 | 16.919 | **failed** |
| 2000 | **27.87** | 9 | 16.919 | **failed** |
| 2200 | **37.77** | 9 | 16.919 | **failed** |
| 2300 | **30.69** | 9 | 16.919 | **failed** |
| 2400 | **37.33** | 9 | 16.919 | **failed** |
| 2500 | 13.09 | 9 | 16.919 | satisfied |

Table 8.15. Result of the final consistency check after applying Mandel-Paule method, and *s* values.

| λ, nm | *s*, % | $\chi^2_{obs}$ | ν = *N*-1 | $\chi^2_{0.05}(\nu)$ | Result of the consistency check |
|---|---|---|---|---|---|
| 250 | 0.00 | 12.808 | 11 | 19.675 | satisfied |
| 260 | 0.00 | 16.206 | 11 | 19.675 | satisfied |
| 270 | 0.00 | 16.572 | 11 | 19.675 | satisfied |
| 280 | 0.00 | 15.948 | 11 | 19.675 | satisfied |
| 290 | 0.00 | 13.759 | 11 | 19.675 | satisfied |
| 300 | 0.00 | 10.494 | 11 | 19.675 | satisfied |
| 320 | 0.00 | 15.155 | 11 | 19.675 | satisfied |
| 340 | 0.00 | 16.213 | 11 | 19.675 | satisfied |
| 360 | 0.00 | 17.074 | 11 | 19.675 | satisfied |
| 380 | **0.11** | **19.616** | 11 | 19.675 | **satisfied** |
| 400 | **0.15** | **19.624** | 11 | 19.675 | **satisfied** |
| 450 | 0.00 | 15.902 | 11 | 19.675 | satisfied |
| 500 | 0.00 | 14.201 | 11 | 19.675 | satisfied |
| 555 | 0.00 | 11.887 | 11 | 19.675 | satisfied |
| 600 | 0.00 | 10.784 | 11 | 19.675 | satisfied |
| 700 | 0.00 | 8.572 | 11 | 19.675 | satisfied |
| 800 | 0.00 | 12.481 | 11 | 19.675 | satisfied |
| 900 | 0.00 | 17.948 | 11 | 19.675 | satisfied |
| 1000 | **0.02** | 19.663 | 11 | 19.675 | **satisfied** |
| 1100 | 0.00 | 17.899 | 11 | 19.675 | satisfied |
| 1300 | **0.21** | **19.358** | 11 | 19.675 | **satisfied** |
| 1500 | **0.23** | **19.186** | 11 | 19.675 | **satisfied** |
| 1700 | **0.31** | **16.478** | 9 | 16.919 | **satisfied** |
| 2000 | **0.28** | **16.611** | 9 | 16.919 | **satisfied** |
| 2200 | **0.57** | **16.686** | 9 | 16.919 | **satisfied** |
| 2300 | **0.58** | **16.912** | 9 | 16.919 | **satisfied** |
| 2400 | **0.89** | **16.815** | 9 | 16.919 | **satisfied** |
| 2500 | 0.00 | 13.091 | 9 | 16.919 | satisfied |

Table 8.16. Uncertainties $u_{adj}(\Delta_i)$ after Mandel-Paule method (Eq. 8.20).

| λ, nm | $u_{adj}(\Delta_i)$, % | | | | | | | | | | | |
|---|---|---|---|---|---|---|---|---|---|---|---|---|
| | CSIC | KRISS | LNE | NIM | NIST | NMC | NMIA | NMIJ | NPL | NRC | PTB | VNIIOFI |
| 250 | 2.53 | 1.03 | 2.31 | 0.79 | 0.80 | 0.98 | 2.86 | 1.38 | 0.95 | 1.50 | 0.78 | 0.78 |
| 260 | 2.45 | 0.92 | 1.03 | 0.71 | 0.77 | 0.85 | 2.38 | 1.27 | 0.97 | 1.23 | 0.71 | 0.71 |
| 270 | 2.43 | 0.86 | 0.82 | 0.66 | 0.75 | 0.76 | 2.07 | 1.22 | 1.02 | 0.86 | 0.66 | 0.66 |
| 280 | 2.23 | 0.79 | 0.66 | 0.62 | 0.72 | 0.79 | 1.89 | 1.18 | 0.95 | 0.78 | 0.62 | 0.62 |
| 290 | 2.21 | 0.76 | 0.60 | 0.59 | 0.70 | 0.68 | 1.79 | 1.15 | 0.85 | 0.75 | 0.60 | 0.59 |
| 300 | 2.49 | 0.71 | 0.56 | 0.55 | 0.67 | 0.66 | 1.66 | 1.12 | 0.83 | 0.71 | 0.58 | 0.55 |
| 320 | 1.95 | 0.64 | 0.51 | 0.51 | 0.62 | 0.61 | 1.47 | 1.07 | 0.86 | 0.64 | 0.54 | 0.51 |
| 340 | 1.83 | 0.58 | 0.47 | 0.47 | 0.57 | 0.55 | 1.30 | 1.02 | 0.80 | 0.61 | 0.52 | 0.47 |
| 360 | 1.72 | 0.56 | 0.45 | 0.45 | 0.54 | 0.52 | 1.16 | 0.98 | 0.78 | 0.58 | 0.50 | 0.45 |
| 380 | 1.62 | 0.51 | 0.44 | 0.44 | 0.53 | 0.50 | 1.03 | 0.96 | 0.80 | 0.56 | 0.49 | 0.44 |
| 400 | 1.62 | 0.50 | 0.43 | 0.41 | 0.51 | 0.48 | 0.93 | 0.93 | 0.77 | 0.41 | 0.48 | 0.41 |
| 450 | 1.61 | 0.42 | 0.37 | 0.35 | 0.43 | 0.42 | 0.70 | 0.86 | 0.49 | 0.35 | 0.41 | 0.35 |
| 500 | 1.70 | 0.39 | 0.36 | 0.33 | 0.40 | 0.38 | 0.53 | 0.82 | 0.43 | 0.33 | 0.38 | 0.33 |
| 555 | 1.80 | 0.37 | 0.34 | 0.30 | 0.36 | 0.35 | 0.41 | 0.78 | 0.40 | 0.30 | 0.35 | 0.30 |
| 600 | 1.70 | 0.35 | 0.34 | 0.29 | 0.34 | 0.34 | 0.36 | 0.76 | 0.37 | 0.29 | 0.34 | 0.29 |
| 700 | 1.60 | 0.33 | 0.40 | 0.26 | 0.30 | 0.29 | 0.44 | 0.72 | 0.33 | 0.26 | 0.31 | 0.26 |
| 800 | 1.61 | 0.33 | 0.44 | 0.26 | 0.27 | 0.31 | 0.61 | 0.69 | 0.30 | 0.25 | 0.30 | 0.25 |
| 900 | 1.90 | 0.29 | 0.27 | 0.27 | 0.24 | 0.48 | 0.71 | 0.68 | 0.27 | 0.23 | 0.28 | 0.23 |
| 1000 | 1.90 | 0.30 | 0.26 | 0.26 | 0.23 | 0.29 | 0.80 | 0.66 | 0.25 | 0.23 | 0.27 | 0.23 |
| 1100 | 2.30 | 0.29 | 0.49 | 0.26 | 0.22 | 0.26 | 0.87 | 0.65 | 0.24 | 0.21 | 0.28 | 0.21 |
| 1300 | 2.03 | 0.35 | 0.45 | 0.33 | 0.31 | 0.33 | 0.98 | 0.67 | 0.31 | 0.45 | 0.38 | 0.31 |
| 1500 | 2.14 | 0.35 | 0.48 | 0.35 | 0.32 | 0.34 | 1.07 | 0.67 | 0.32 | 0.49 | 0.38 | 0.32 |
| 1700 | 2.15 | 0.45 | 0.43 | 0.41 | 0.38 | 0.39 | 1.15 | 0.70 | 0.43 | 0.62 | 0.42 | 0.38 |
| 2000 | | 0.48 | 0.46 | 0.39 | 0.37 | 0.37 | 1.44 | 0.68 | 0.42 | 0.88 | 0.42 | 0.37 |
| 2200 | | 0.73 | 0.84 | 0.65 | 0.63 | 0.64 | 1.37 | 0.85 | 0.66 | 2.15 | 0.71 | 0.63 |
| 2300 | | 0.77 | 0.91 | 0.69 | 0.65 | 0.65 | 1.42 | 0.86 | 0.68 | 2.44 | 0.70 | 0.65 |
| 2400 | | 1.03 | 1.48 | 1.07 | 0.95 | 0.95 | 1.67 | 1.11 | 0.96 | 2.87 | 1.00 | 0.95 |
| 2500 | | 0.66 | 4.40 | 0.89 | 0.53 | 0.53 | 1.29 | 0.97 | 0.89 | 6.22 | 2.89 | 0.53 |

### 8.4.8. Final results

The final values of KCRV and DoEs after excluding outliers and applying the Mandel-Paule method are presented in section 9.

# 9. Comparison results

This section presents the final (after excluding outliers and applying the Mandel-Paule method) values of KCRV, additional *s* term added during a Mandel-Paule approach and Degrees of Equivalence (DoEs).

## 9.1. KCRV and Mandel-Paule *s* term

The CCPR-K1.a.2017 values of KCRV, $\Delta_{\mathrm{KCRV}}$, and uncertainty of KCRV, $u(\Delta_{\mathrm{KCRV}})$, are presented in Table 9.1. The table also presents the additional ***s*** term added during a Mandel-Paule approach.

Table 9.1. CCPR-K1.a.2017 values of KCRV, $\Delta_{\mathrm{KCRV}}$, uncertainty of KCR, $u(\Delta_{\mathrm{KCRV}})$ and additional ***s*** term added during a Mandel-Paule approach

| λ, nm | $\Delta_{\mathrm{KCRV}}$, % | $u(\Delta_{\mathrm{KCRV}})$, % | *s*, % | λ, nm | $\Delta_{\mathrm{KCRV}}$, % | $u(\Delta_{\mathrm{KCRV}})$, % | *s*, % |
|---|---|---|---|---|---|---|---|
| 250 | 0.62 | 0.28 | 0.00 | 600 | 0.12 | 0.10 | 0.00 |
| 260 | 0.47 | 0.25 | 0.00 | 700 | 0.08 | 0.09 | 0.00 |
| 270 | 0.36 | 0.23 | 0.00 | 800 | 0.23 | 0.09 | 0.00 |
| 280 | 0.30 | 0.22 | 0.00 | 900 | 0.16 | 0.08 | 0.00 |
| 290 | 0.39 | 0.20 | 0.00 | 1000 | 0.20 | 0.08 | 0.02 |
| 300 | 0.46 | 0.19 | 0.00 | 1100 | 0.13 | 0.08 | 0.00 |
| 320 | 0.36 | 0.18 | 0.00 | 1300 | 0.27 | 0.08 | 0.21 |
| 340 | 0.46 | 0.17 | 0.00 | 1500 | 0.25 | 0.08 | 0.23 |
| 360 | 0.50 | 0.16 | 0.00 | 1700 | 0.21 | 0.09 | 0.31 |
| 380 | 0.51 | 0.15 | 0.11 | 2000 | 0.13 | 0.10 | 0.28 |
| 400 | 0.38 | 0.14 | 0.15 | 2200 | 0.03 | 0.12 | 0.57 |
| 450 | 0.19 | 0.12 | 0.00 | 2300 | 0.13 | 0.13 | 0.58 |
| 500 | 0.13 | 0.11 | 0.00 | 2400 | 0.36 | 0.16 | 0.89 |
| 555 | 0.14 | 0.10 | 0.00 | 2500 | 0.29 | 0.20 | 0.00 |

## 9.2. Degrees of Equivalence (DoEs)

The CCPR-K1.a.2017 unilateral Degrees of Equivalence (DoEs), i.e. deviations from KCRV, $D_i$, and their associated expanded uncertainties, $U_i$, calculated by Eq.8.21 and 8.22, are listed in Table 9.2. In Fig.9.1 and Fig.9.1a the DoEs for all participants are presented. Fig.9.2 – Fig.9.13 show the DoEs individually for each participant as well as their associated expanded uncertainties.

Bilateral DoEs are not listed in this report since they are no longer required by the guidance CCPR-G2 for CCPR Key Comparison Report Preparation [4]. Bilateral DOEs can be determined from the individual NMI's unilateral DoE.

Table 9.2. CCPR-K1.a.2017 values of Degrees of Equivalence: Deviations from KCRV, $D_i$, and their associated Uncertainties, $U_i$, (Eq.8.21 and 8.22), in %

| λ, nm | CSIC | | KRISS | | LNE | | NIM | | NIST | | NMC | | NMIA | | NMIJ | | NPL | | NRC | | PTB | | VNIIOFI | |
|---|---|---|---|---|---|---|---|---|---|---|---|---|---|---|---|---|---|---|---|---|---|---|---|---|
| | $D_i$ | $U_i$ | $D_i$ | $U_i$ | $D_i$ | $U_i$ | $D_i$ | $U_i$ | $D_i$ | $U_i$ | $D_i$ | $U_i$ | $D_i$ | $U_i$ | $D_i$ | $U_i$ | $D_i$ | $U_i$ | $D_i$ | $U_i$ | $D_i$ | $U_i$ | $D_i$ | $U_i$ |
| 250 | -3.78 | 5.02 | 0.30 | 1.95 | 4.64 | 4.57 | 0.55 | 1.44 | 0.10 | 1.48 | -1.12 | 1.86 | -1.61 | 5.68 | -0.19 | 2.68 | -1.29 | 1.79 | 0.25 | 2.93 | 1.14 | 1.40 | -0.42 | 0.91 |
| 260 | -4.77 | 4.86 | 0.41 | 1.74 | 1.20 | 1.97 | 0.27 | 1.24 | 0.00 | 1.44 | -1.01 | 1.59 | -2.32 | 4.72 | 0.34 | 2.48 | -2.05 | 1.86 | 0.54 | 2.38 | 1.32 | 1.27 | -0.29 | 0.81 |
| 270 | -5.42 | 4.83 | 0.42 | 1.63 | 0.42 | 1.55 | 0.03 | 1.16 | -0.40 | 1.40 | -0.47 | 1.43 | -2.37 | 4.11 | 0.60 | 2.39 | -2.08 | 1.97 | 0.67 | 1.64 | 1.30 | 1.19 | -0.25 | 0.76 |
| 280 | -4.89 | 4.43 | 0.11 | 1.50 | 0.45 | 1.23 | 0.16 | 1.13 | -0.07 | 1.36 | -0.76 | 1.50 | -1.93 | 3.75 | 0.61 | 2.32 | -2.15 | 1.85 | 0.48 | 1.49 | 1.05 | 1.15 | -0.12 | 0.72 |
| 290 | -3.83 | 4.41 | 0.02 | 1.45 | 0.34 | 1.11 | 0.14 | 1.03 | 0.10 | 1.32 | -0.79 | 1.29 | -2.09 | 3.55 | 0.44 | 2.26 | -1.58 | 1.65 | 0.55 | 1.43 | 1.11 | 1.11 | -0.24 | 0.68 |
| 300 | -0.88 | 4.96 | -0.11 | 1.36 | 0.39 | 1.04 | 0.01 | 0.94 | 0.24 | 1.27 | -0.72 | 1.24 | -2.21 | 3.30 | 0.56 | 2.20 | -1.42 | 1.60 | 0.48 | 1.36 | 0.95 | 1.07 | -0.36 | 0.66 |
| 320 | 0.51 | 3.88 | -0.32 | 1.21 | 0.84 | 0.93 | -0.07 | 0.90 | 0.19 | 1.18 | -0.82 | 1.16 | -2.42 | 2.91 | 0.42 | 2.10 | -1.88 | 1.66 | 0.27 | 1.22 | 0.81 | 1.01 | -0.19 | 0.62 |
| 340 | 0.75 | 3.64 | -0.30 | 1.10 | 0.75 | 0.87 | 0.08 | 0.82 | 0.01 | 1.09 | -0.64 | 1.05 | -2.50 | 2.58 | 0.35 | 2.01 | -1.69 | 1.55 | 0.40 | 1.16 | 0.86 | 0.97 | -0.32 | 0.60 |
| 360 | 0.86 | 3.42 | -0.23 | 1.06 | 0.79 | 0.82 | 0.00 | 0.79 | -0.18 | 1.02 | -0.57 | 0.97 | -2.34 | 2.29 | 0.29 | 1.93 | -1.50 | 1.52 | 0.48 | 1.10 | 0.88 | 0.94 | -0.35 | 0.57 |
| 380 | 0.79 | 3.21 | -0.27 | 0.95 | 0.99 | 0.79 | 0.02 | 0.75 | -0.24 | 0.97 | -0.64 | 0.92 | -2.31 | 2.02 | 0.34 | 1.87 | -1.37 | 1.54 | 0.42 | 1.05 | 0.84 | 0.90 | -0.37 | 0.57 |
| 400 | 0.91 | 3.22 | -0.20 | 0.90 | 0.94 | 0.76 | 0.08 | 0.68 | -0.10 | 0.93 | -0.51 | 0.86 | -2.20 | 1.81 | 1.02 | 1.81 | -1.29 | 1.47 | -0.23 | 0.70 | 0.84 | 0.85 | -0.20 | 0.52 |
| 450 | 0.98 | 3.20 | -0.22 | 0.81 | 0.50 | 0.69 | 0.32 | 0.63 | 0.30 | 0.82 | -0.62 | 0.80 | -1.48 | 1.37 | 0.85 | 1.70 | -0.79 | 0.94 | -0.15 | 0.63 | 0.54 | 0.79 | -0.03 | 0.47 |
| 500 | 0.84 | 3.40 | -0.17 | 0.74 | 0.42 | 0.69 | 0.29 | 0.59 | 0.33 | 0.75 | -0.65 | 0.72 | -1.00 | 1.04 | 0.83 | 1.62 | -0.58 | 0.81 | -0.05 | 0.57 | 0.48 | 0.73 | 0.01 | 0.44 |
| 555 | 0.76 | 3.60 | -0.15 | 0.70 | 0.44 | 0.64 | 0.33 | 0.54 | 0.24 | 0.68 | -0.49 | 0.67 | -0.63 | 0.79 | 0.75 | 1.54 | -0.57 | 0.77 | -0.09 | 0.53 | 0.33 | 0.67 | -0.01 | 0.40 |
| 600 | 0.83 | 3.40 | -0.11 | 0.67 | 0.40 | 0.65 | 0.33 | 0.52 | 0.27 | 0.64 | -0.47 | 0.65 | -0.44 | 0.69 | 0.66 | 1.50 | -0.58 | 0.71 | -0.08 | 0.50 | 0.23 | 0.65 | 0.04 | 0.36 |
| 700 | 1.65 | 3.20 | 0.03 | 0.63 | 0.07 | 0.77 | 0.36 | 0.48 | 0.17 | 0.57 | -0.37 | 0.55 | -0.08 | 0.87 | 0.52 | 1.43 | -0.54 | 0.63 | -0.14 | 0.43 | 0.13 | 0.60 | 0.06 | 0.34 |
| 800 | 0.68 | 3.21 | 0.27 | 0.62 | 0.44 | 0.85 | 0.27 | 0.47 | -0.20 | 0.50 | 0.51 | 0.59 | 0.23 | 1.20 | 0.49 | 1.37 | -0.63 | 0.57 | -0.27 | 0.41 | -0.08 | 0.56 | -0.07 | 0.33 |
| 900 | 0.26 | 3.80 | -0.19 | 0.56 | 0.54 | 0.50 | 0.27 | 0.50 | 0.12 | 0.44 | 0.68 | 0.94 | 0.63 | 1.41 | 0.68 | 1.34 | -0.62 | 0.51 | -0.41 | 0.36 | -0.09 | 0.53 | 0.02 | 0.31 |
| 1000 | -0.57 | 3.80 | -0.21 | 0.56 | 0.61 | 0.49 | 0.18 | 0.49 | 0.04 | 0.42 | 0.61 | 0.56 | 0.77 | 1.59 | 0.19 | 1.31 | -0.58 | 0.47 | -0.34 | 0.35 | -0.15 | 0.52 | -0.05 | 0.30 |
| 1100 | -0.60 | 4.60 | -0.15 | 0.55 | 0.69 | 0.96 | -0.09 | 0.48 | -0.18 | 0.40 | 0.73 | 0.49 | 1.12 | 1.73 | -0.18 | 1.29 | -0.46 | 0.45 | -0.17 | 0.33 | 0.22 | 0.54 | 0.04 | 0.28 |
| 1300 | -0.10 | 4.03 | -0.22 | 0.53 | 1.03 | 0.76 | -0.06 | 0.47 | -0.35 | 0.38 | 0.75 | 0.46 | 1.18 | 1.90 | -0.32 | 1.25 | -0.57 | 0.41 | 0.49 | 0.76 | -0.29 | 0.61 | -0.10 | 0.30 |
| 1500 | -0.94 | 4.24 | -0.20 | 0.51 | 1.01 | 0.82 | 0.05 | 0.49 | -0.43 | 0.35 | 0.82 | 0.48 | 1.42 | 2.06 | -0.64 | 1.23 | -0.58 | 0.39 | 0.37 | 0.84 | -0.08 | 0.57 | -0.06 | 0.29 |
| 1700 | -7.26 | 4.23 | -0.38 | 0.60 | 1.63 | 0.57 | 0.16 | 0.49 | -0.33 | 0.34 | 0.99 | 0.43 | 1.76 | 2.19 | -0.74 | 1.22 | -0.71 | 0.56 | 0.86 | 1.04 | -0.18 | 0.53 | -0.07 | 0.30 |
| 2000 | | | -0.28 | 0.74 | 2.46 | 0.68 | 0.10 | 0.50 | -0.22 | 0.36 | 0.95 | 0.46 | 2.41 | 2.81 | -1.47 | 1.21 | -0.52 | 0.59 | 0.52 | 1.64 | -0.12 | 0.58 | 0.03 | 0.36 |
| 2200 | | | -0.93 | 0.86 | 3.31 | 1.15 | 0.24 | 0.60 | -0.10 | 0.41 | 1.06 | 0.55 | 3.11 | 2.43 | -2.04 | 1.19 | -0.45 | 0.62 | 1.81 | 4.11 | 0.16 | 0.78 | 0.12 | 0.42 |
| 2300 | | | -0.41 | 0.95 | 4.38 | 1.33 | 0.08 | 0.70 | -0.07 | 0.46 | 0.86 | 0.57 | 4.57 | 2.53 | -1.71 | 1.21 | -0.42 | 0.67 | 0.82 | 4.70 | -0.08 | 0.75 | -0.17 | 0.50 |
| 2400 | | | 0.03 | 0.98 | 6.84 | 2.27 | -0.16 | 1.12 | -0.74 | 0.60 | 0.84 | 0.64 | 5.49 | 2.72 | -2.09 | 1.24 | -0.41 | 0.72 | 2.67 | 5.38 | -0.07 | 0.87 | -0.10 | 0.59 |
| 2500 | | | -0.27 | 1.20 | 7.71 | 8.77 | 0.16 | 1.69 | 0.00 | 0.78 | 1.04 | 0.71 | 8.62 | 2.52 | -1.98 | 1.86 | -1.09 | 1.69 | 3.43 | 12.4 | 0.04 | 5.74 | -0.07 | 0.64 |

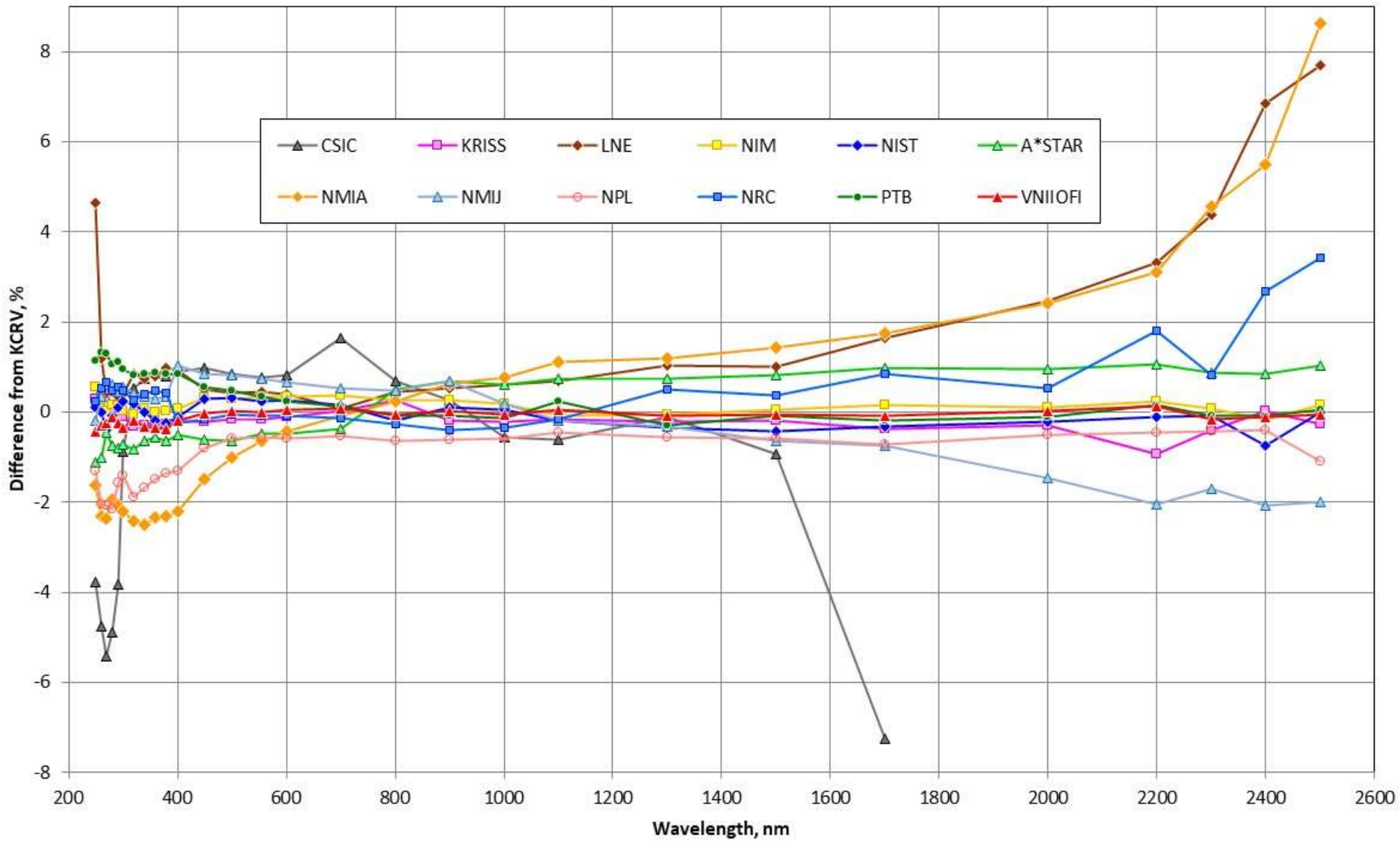


Figure 9.1. DoEs: Deviations from KCRV, $D_i$.

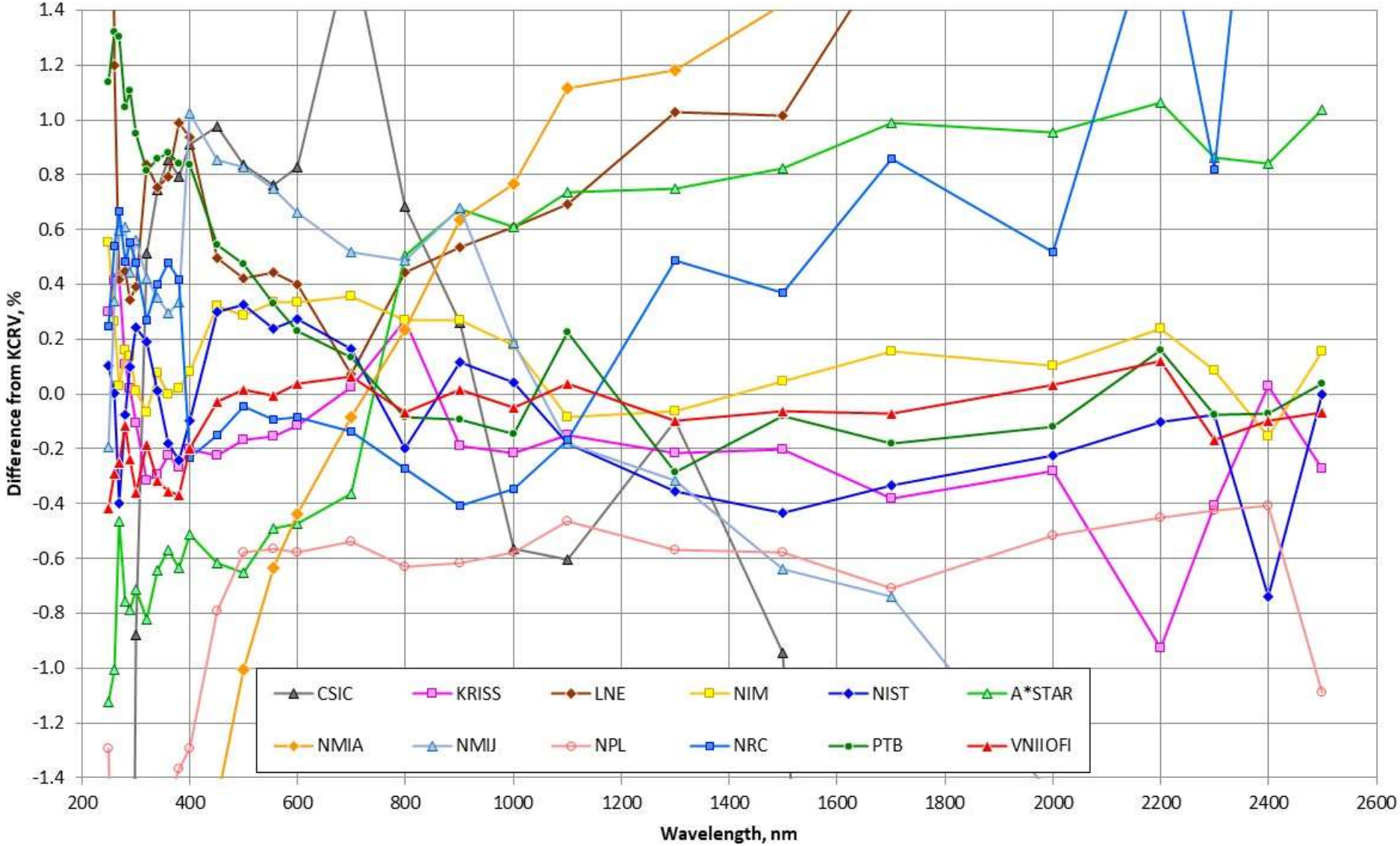


Figure 9.1a. DoEs: Deviations from KCRV, $D_i$. Central part.

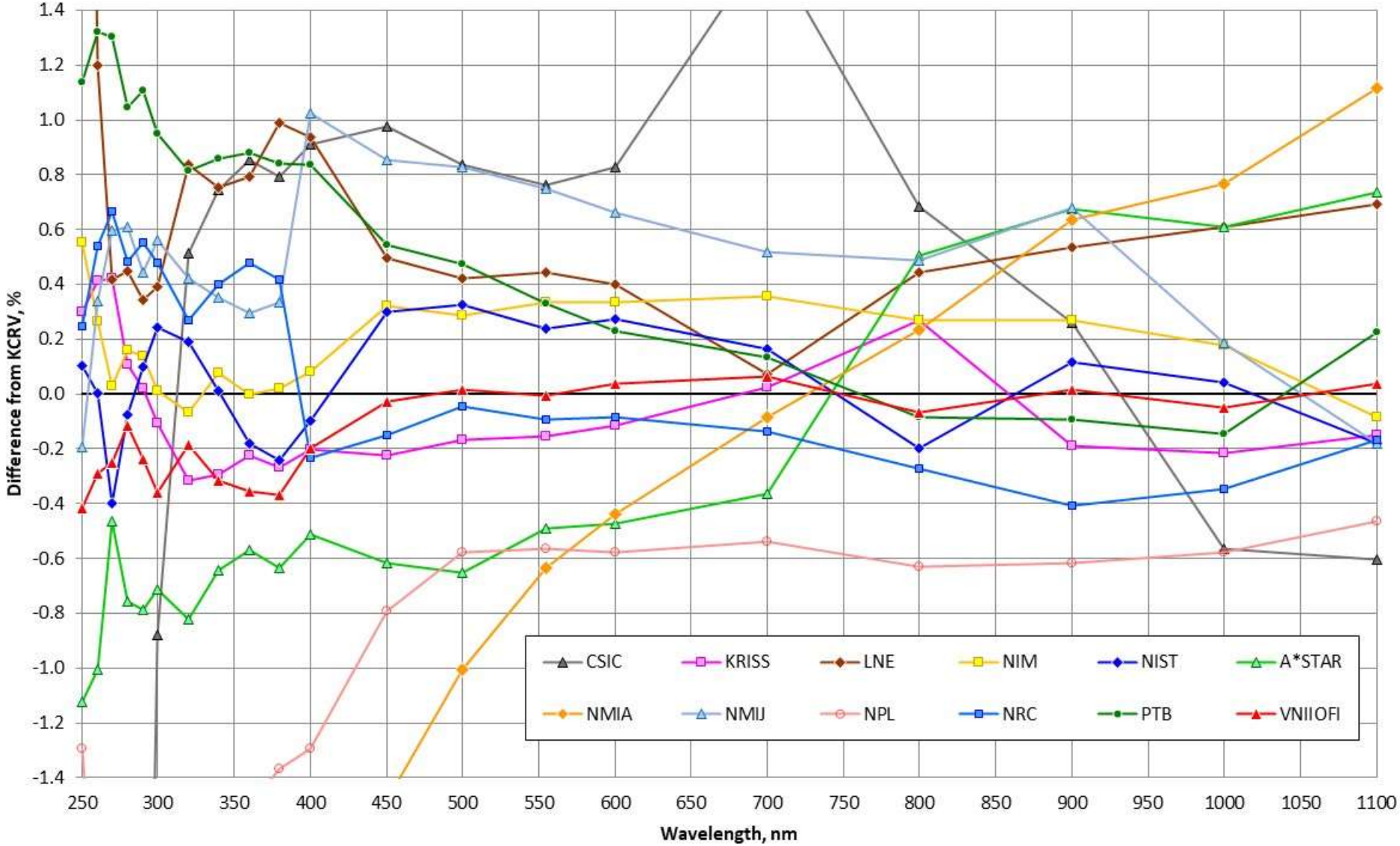


Figure 9.1b. DoEs: Deviations from KCRV, $D_i$. Central part in wavelength range 250 nm to 1100 nm

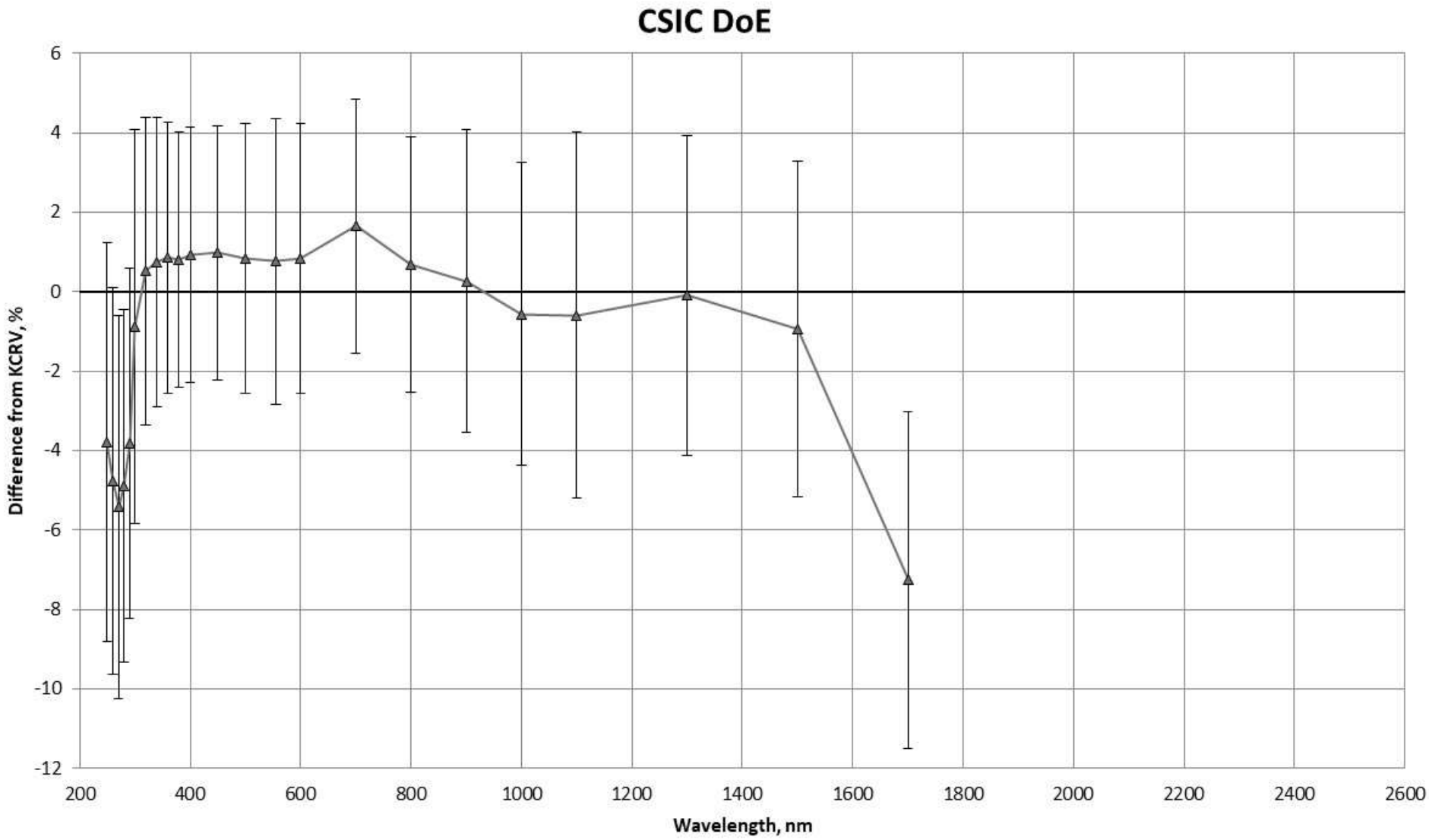


Figure 9.2. DoEs of CSIC

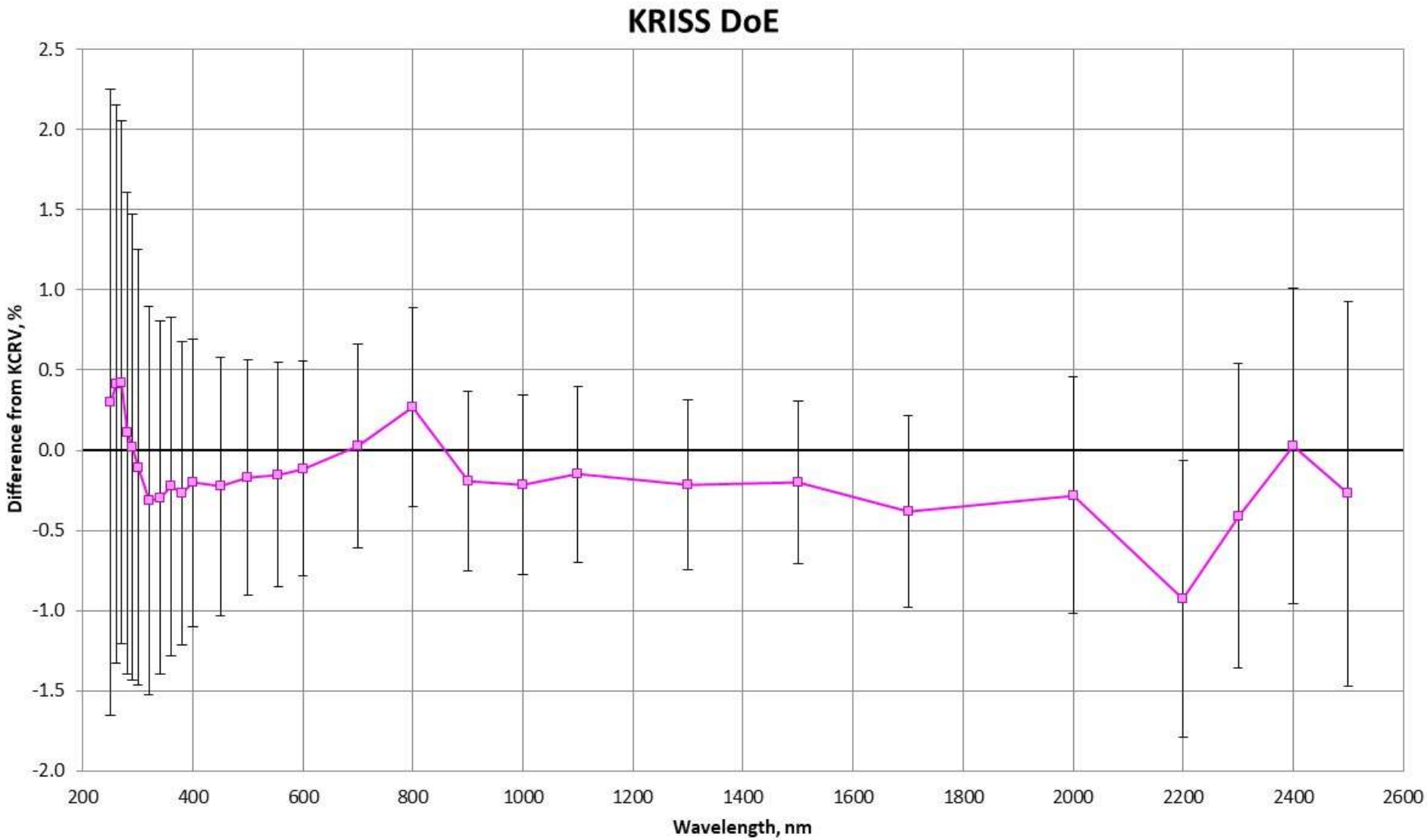


Figure 9.3. DoEs of KRIS

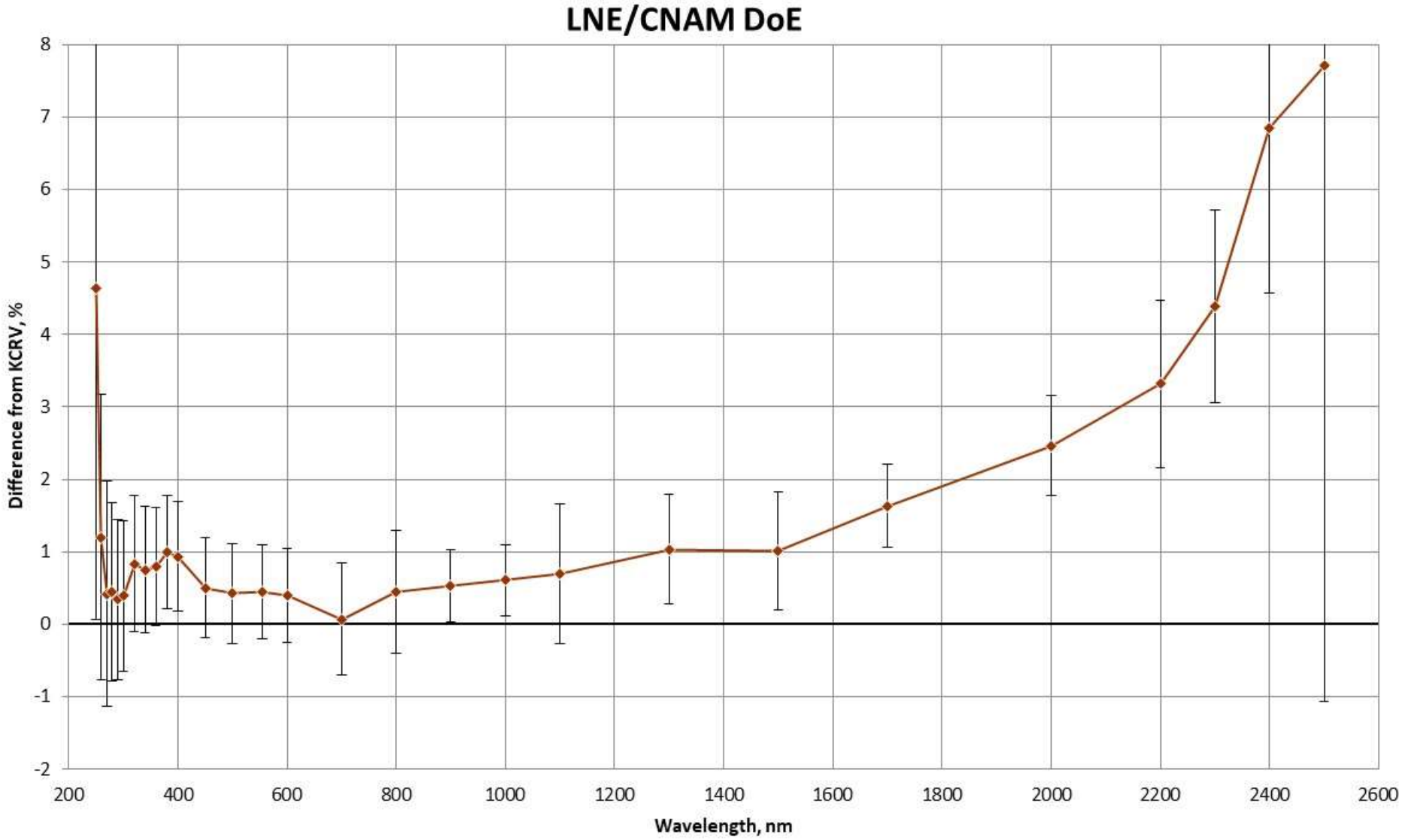


Figure 9.4. DoEs of LNE/CNAM

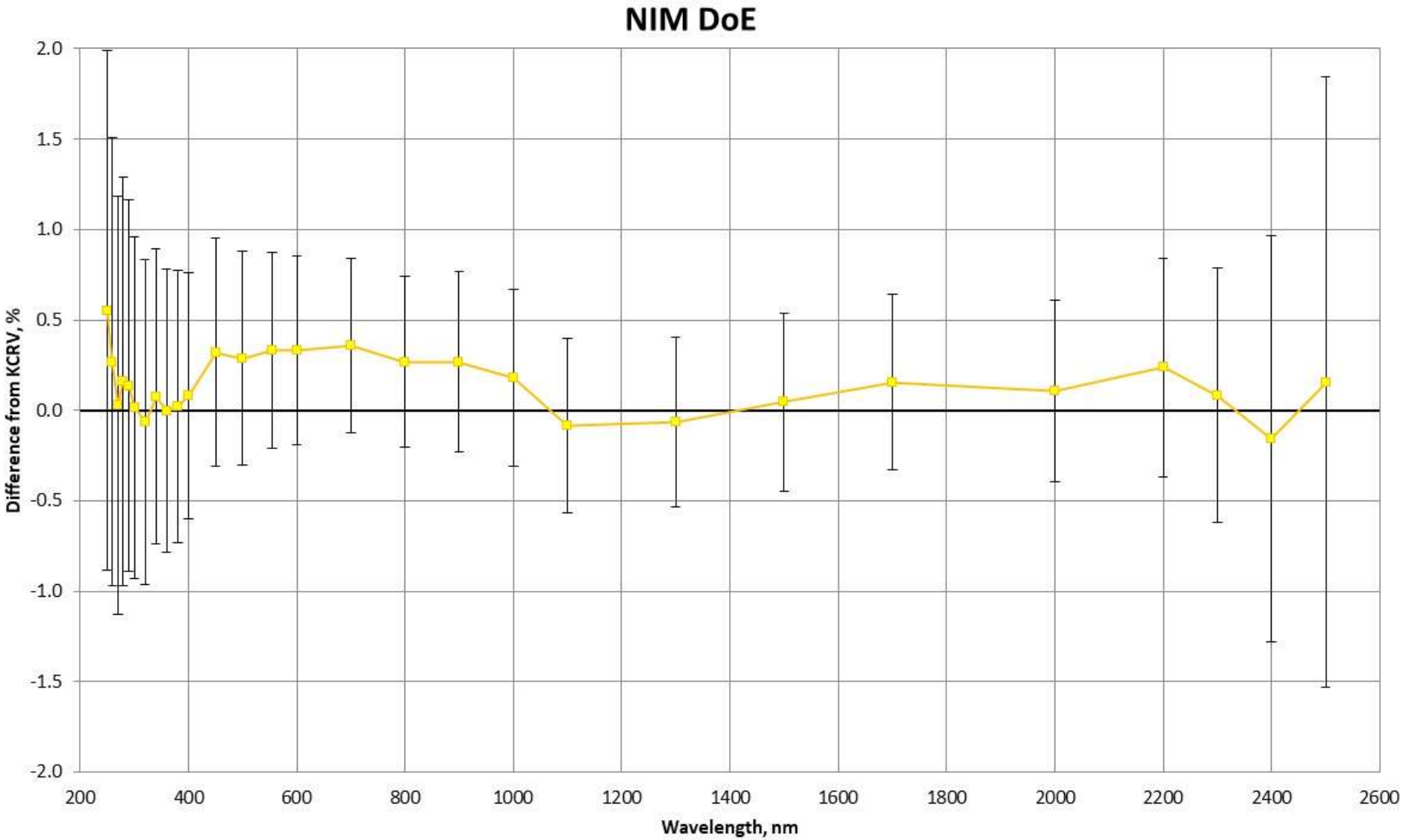


Figure 9.5. DoEs of NIM

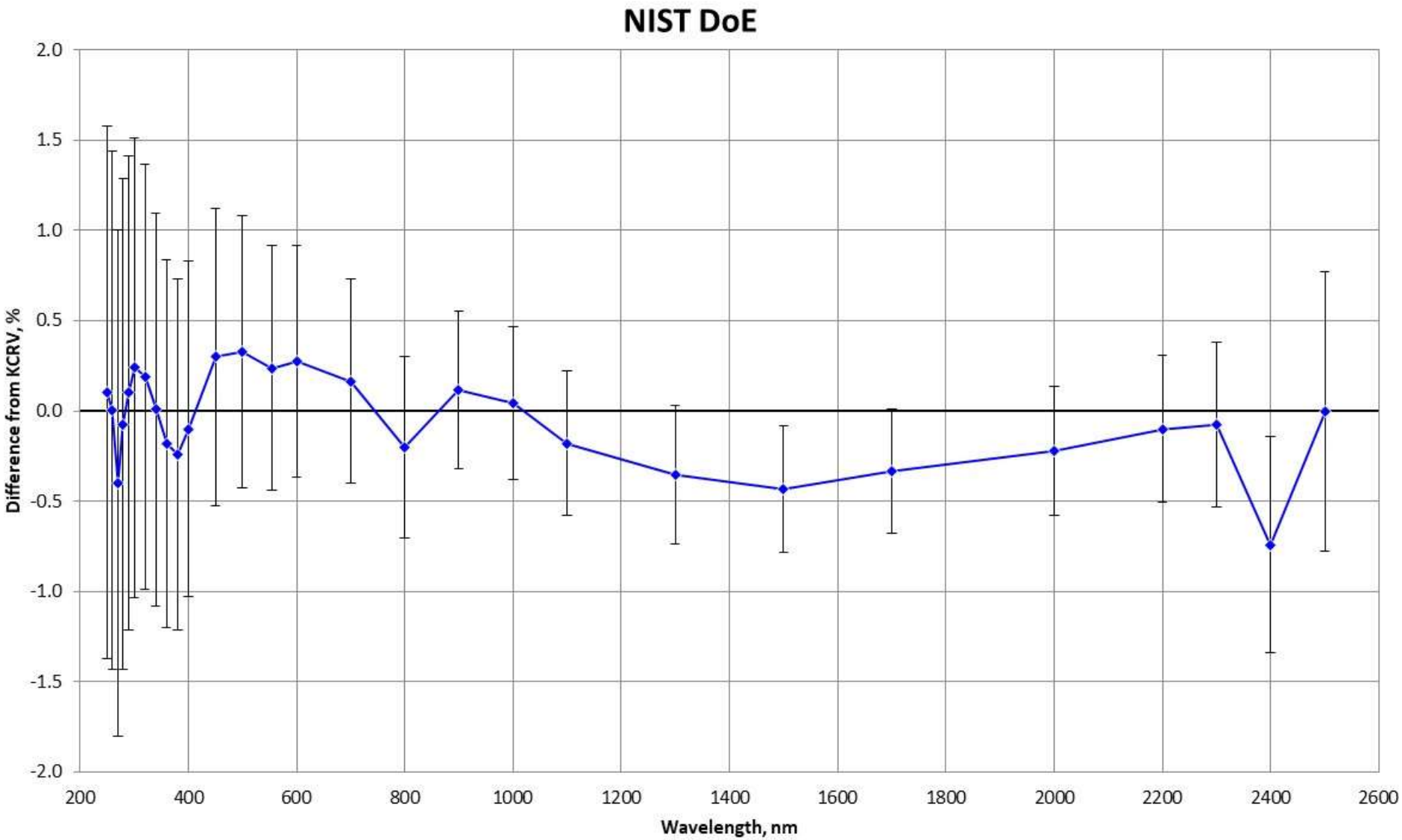


Figure 9.6. DoEs of NIST

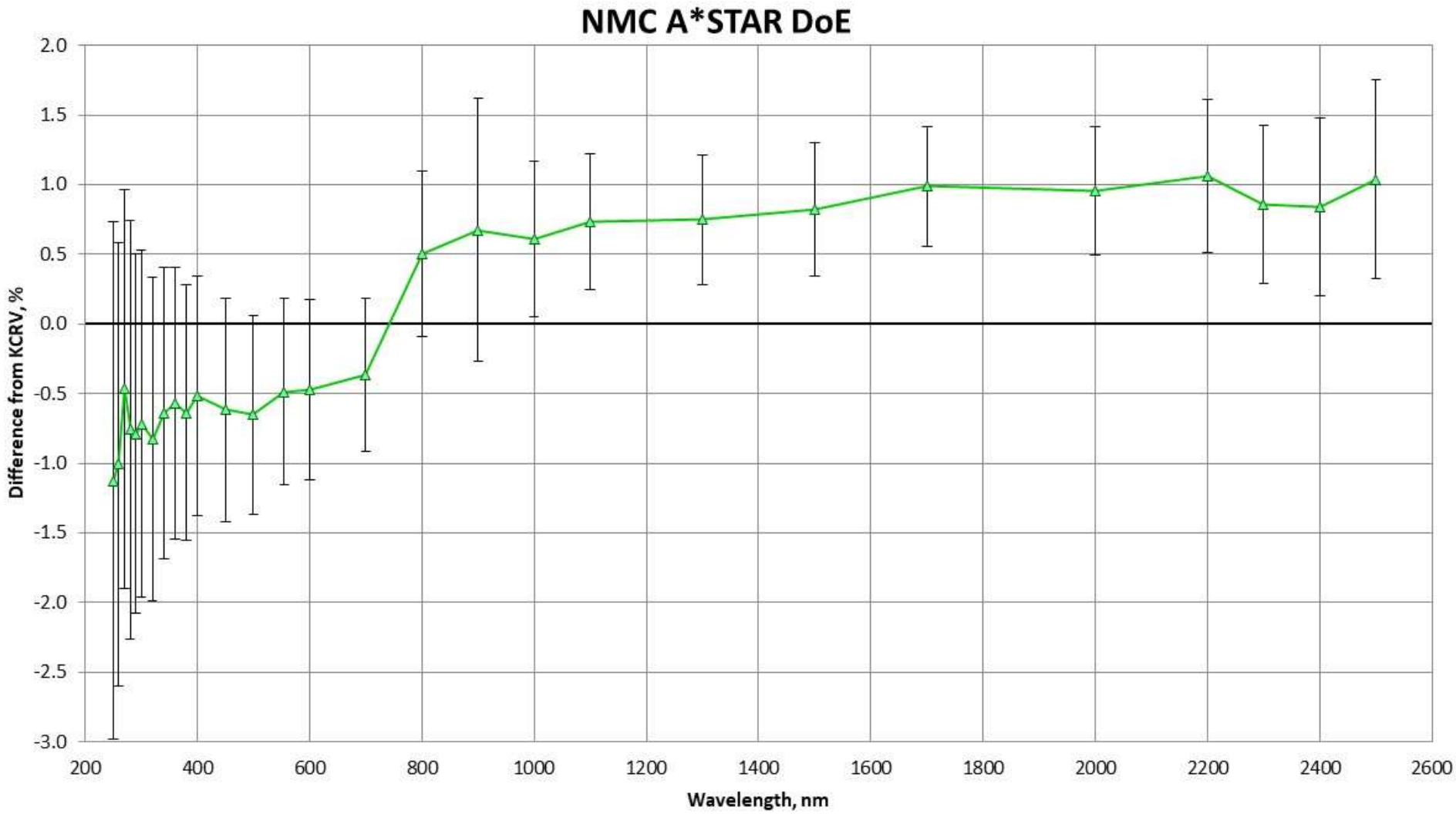


Figure 9.7. DoEs of NMC A*STAR

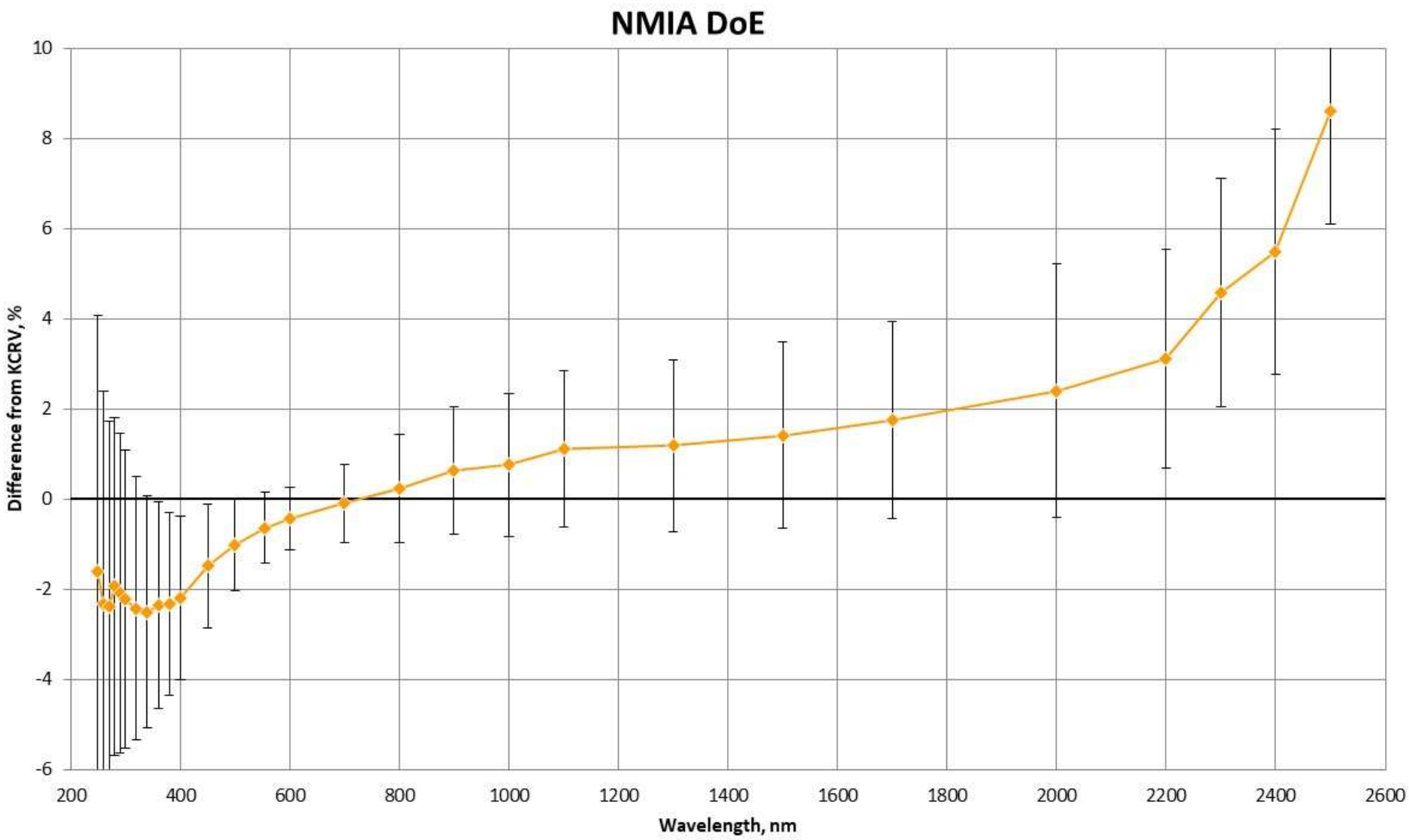


Figure 9.8. DoEs of NMIA

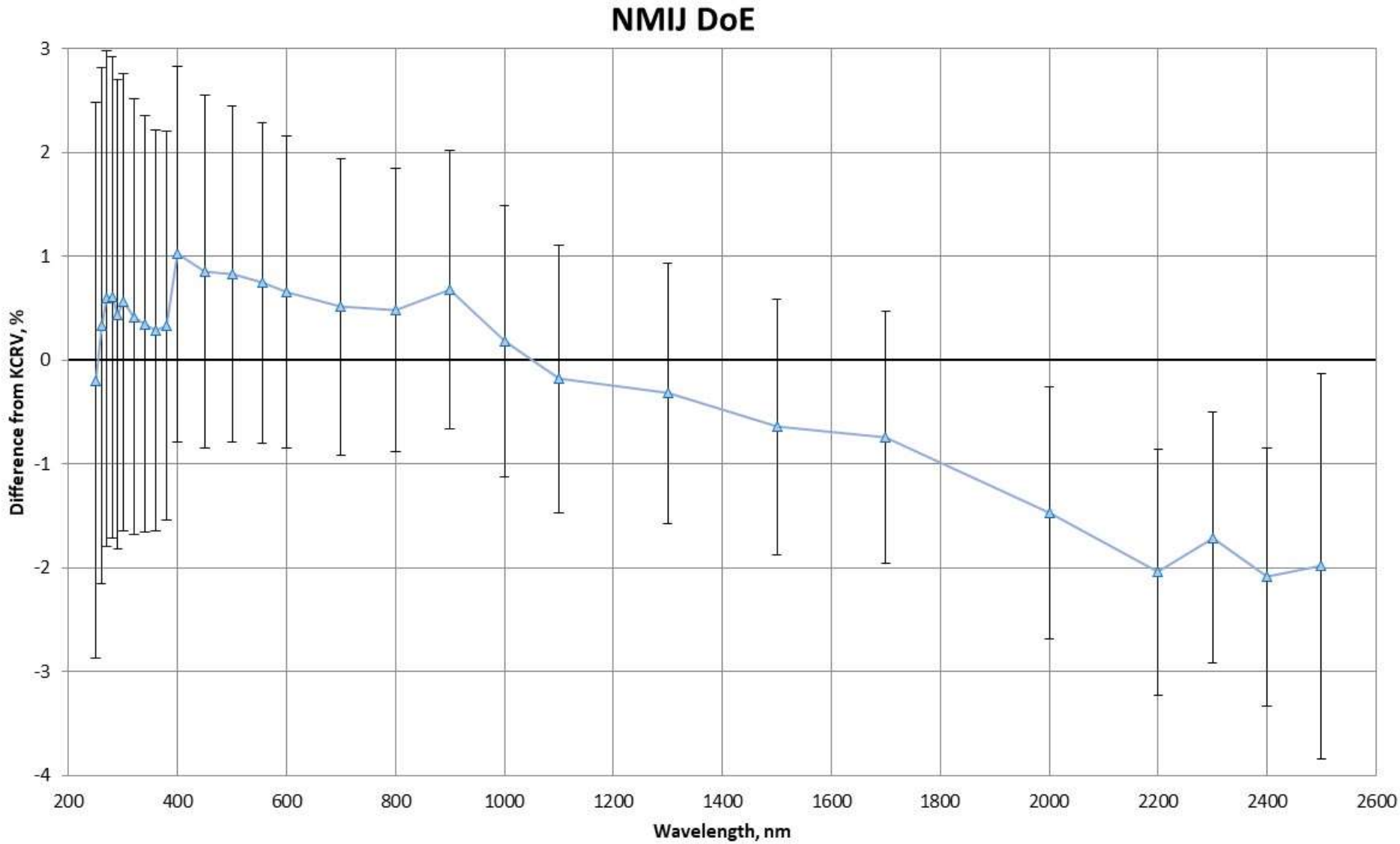


Figure 9.9. DoEs of NMIJ

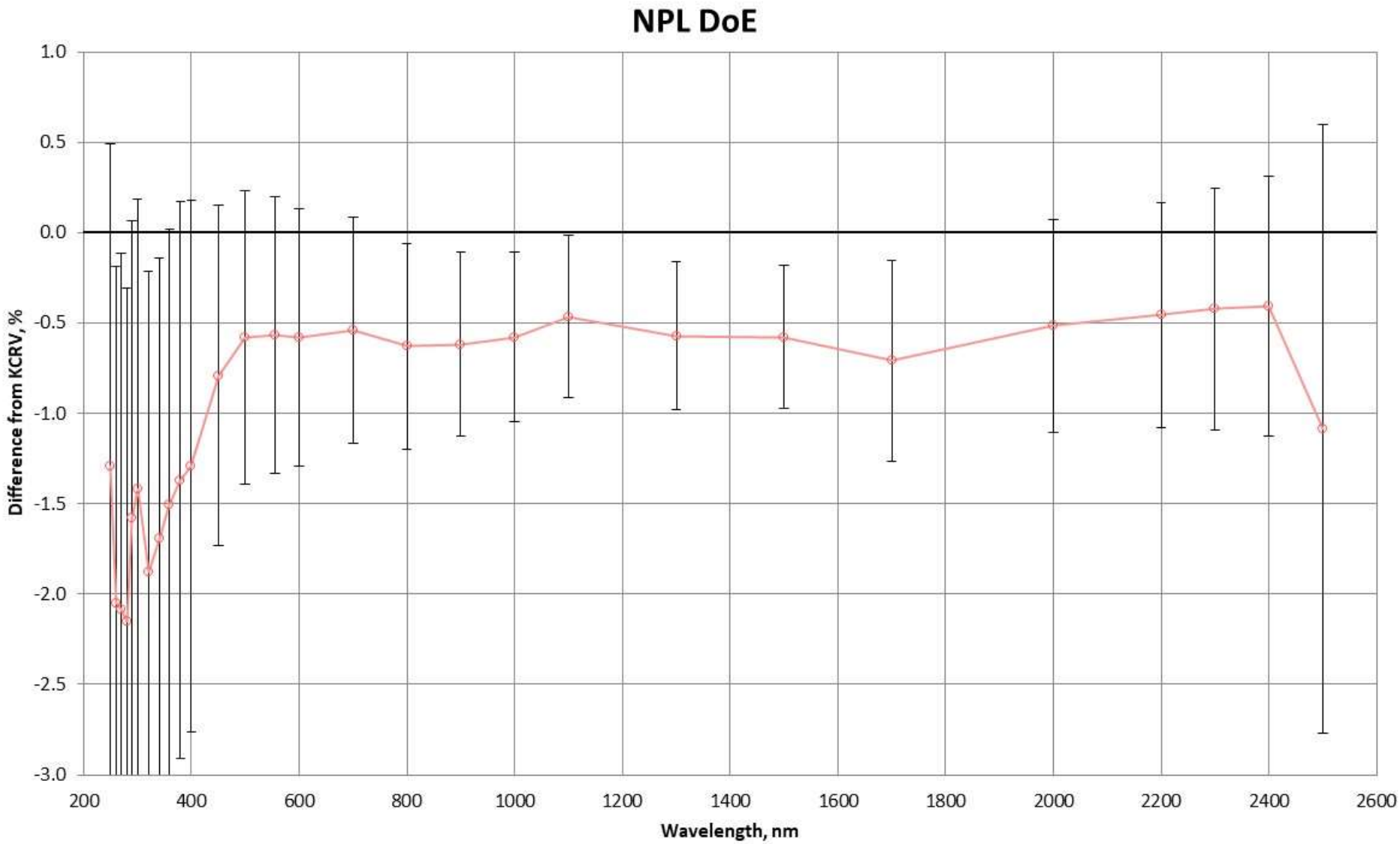


Figure 9.10. DoEs of NPL

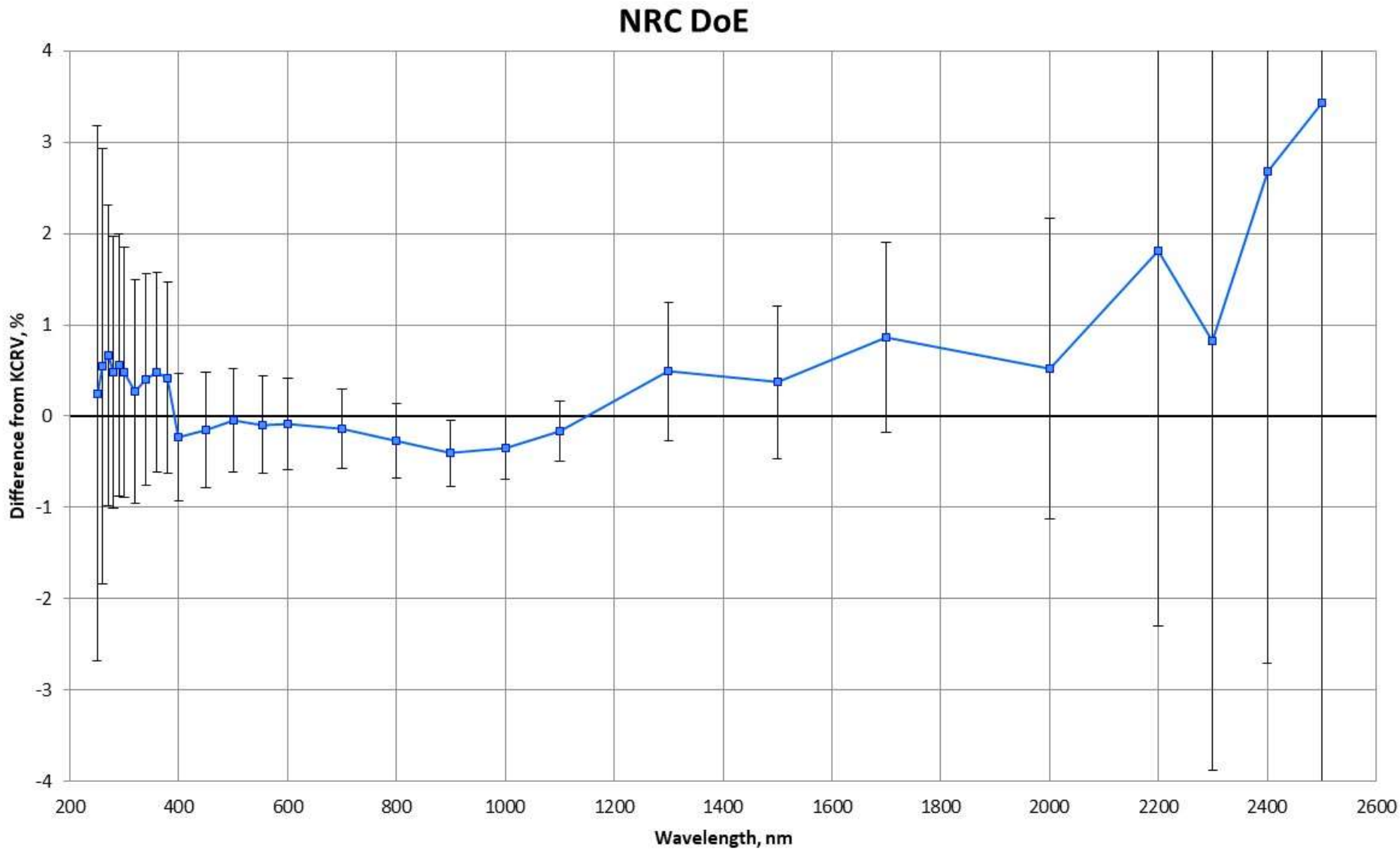


Figure 9.11. DoEs of NRC

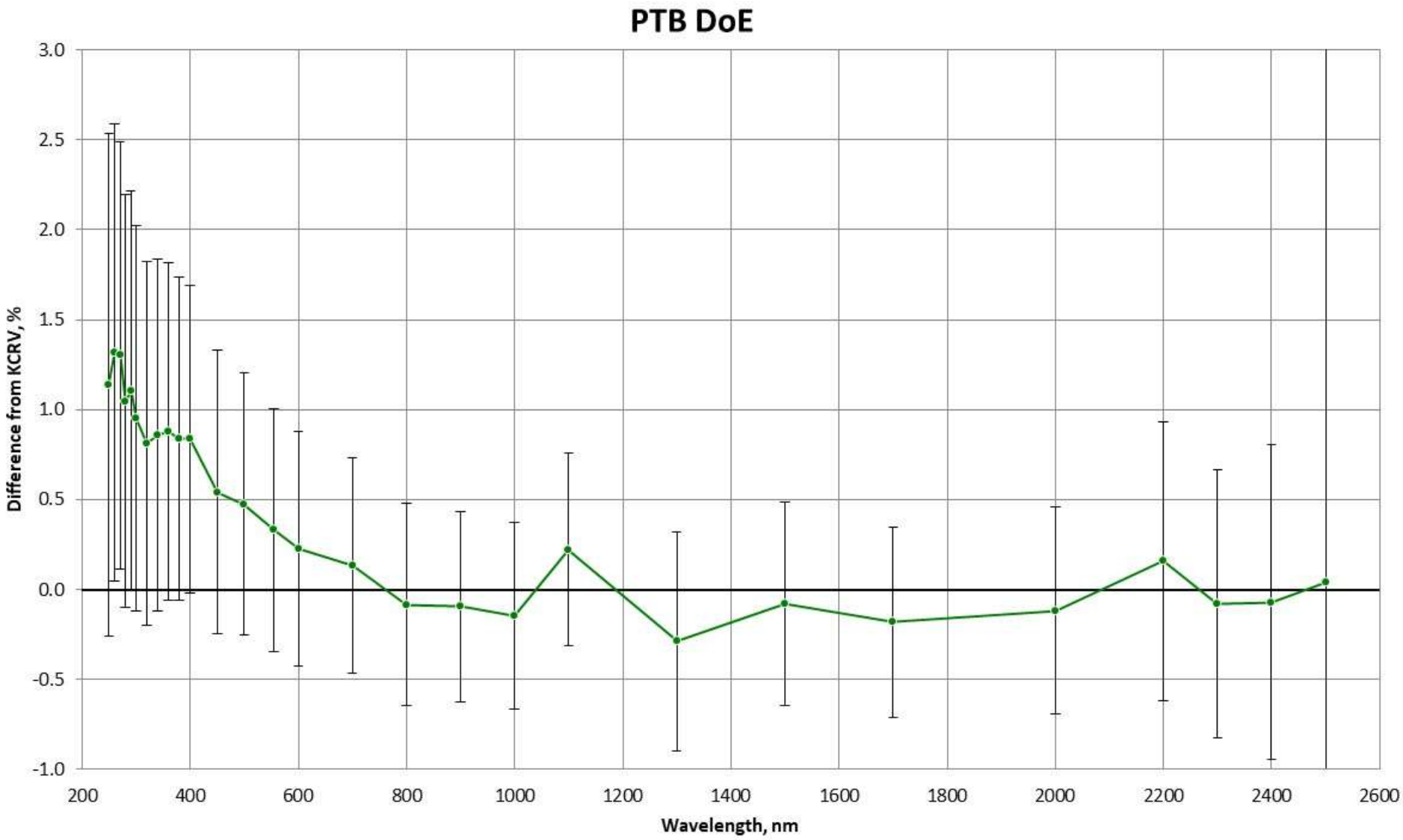


Figure 9.12. DoEs of PTB

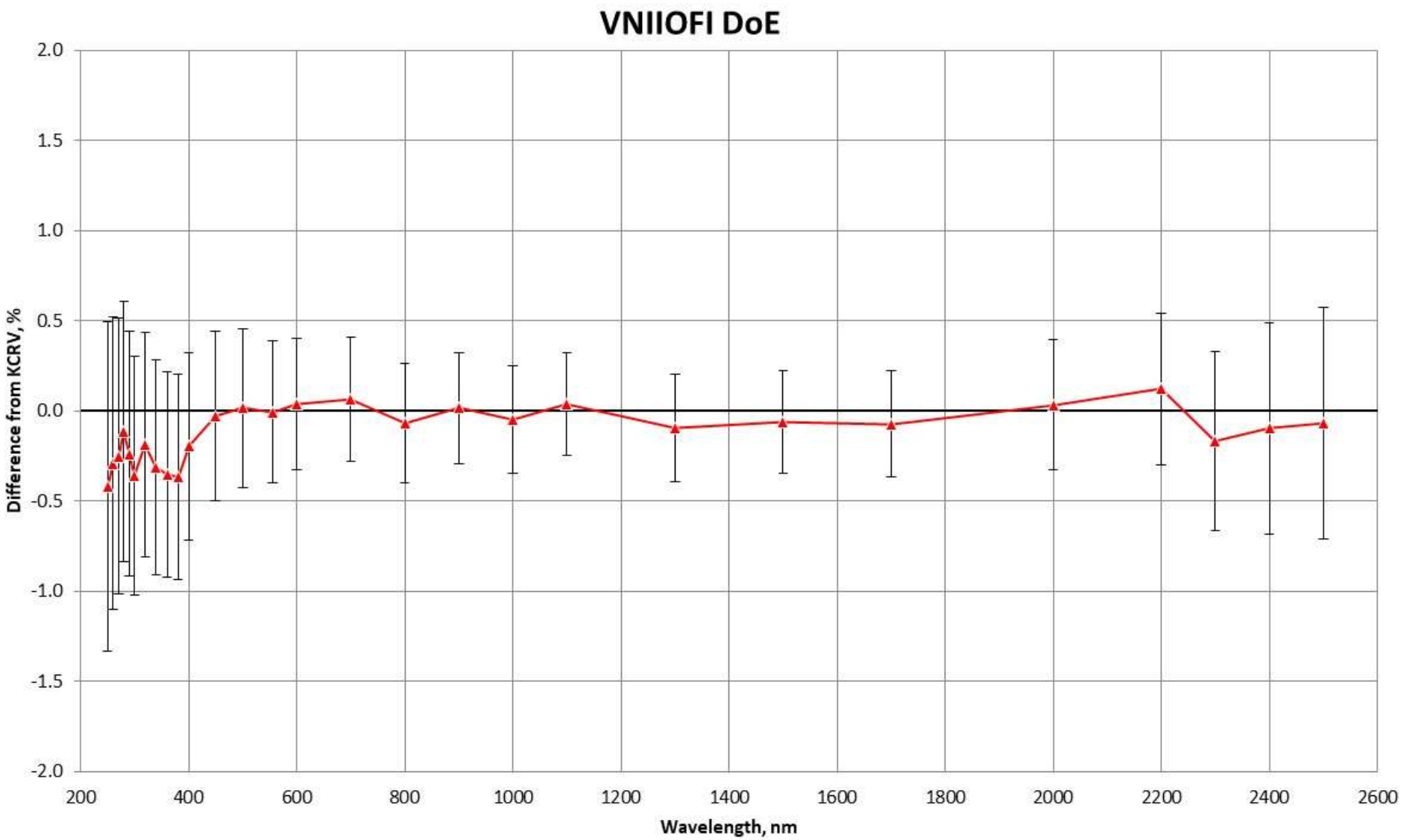


Figure 9.13. DoEs of VNIIOFI

# 10. REFERENCES


[1] https://www.bipm.org/en/cipm-mra

[2] Emma R Woolliams, Nigel P Fox, Maurice G Cox, Peter M Harris and Neil J Harrison, Final report on CCPR K1-a: Spectral irradiance from 250 nm to 2500 nm, *Metrologia*, 2006, **43**, Tech. Suppl., 02003.

[3] Dong-Joo Shin, Chul-Woung Park, Svetlana S Kolesnikova and Boris B Khlevnoy , Final report on bilateral comparison APMP.PR-K1.a.1-2008 between KRISS (Korea) and VNIIOFI (Russia): Spectral irradiance from 250 nm to 2500 nm, *Metrologia*, 2010, **47**, Tech. Suppl., 02005.

[4] Guidelines for CCPR Comparison Report Preparation, ***CCPR-G2***, Rev.4, January 2019 available from www.bipm.org.

[5] Guidelines for preparing CCPR Key Comparisons, ***CCPR-G4***, July 2013 available from www.bipm.org.

[6] Sapritsky V. I., Khlevnoy B. B., Khromchenko V. B., Lisiansky B. E., Mekhontsev S. N., Melenevsky U. A., Morozova S. P., Prokhorov A. V., Samoilov L. N., Shapoval V. I., Sudarev K. A., Zelener M. F., *Appl. Opt.*, 1997, 36, 5403-5408.

[7] http://www.virial.com/steep321.html

[8] Prokhorov A., Effective emissivities of isothermal blackbody cavities calculated by the Monte Carlo method using the three-component BRDF Model, *Appl. Opt.,* 2012, V. 51, No.13, 2322-2332.

[9] Samoylov M. L., Ogarev S. A., Khlevnoy B. B., Khromchenko V. B., Mekhontsev S. N., Sapritsky V. I., High Accuracy Radiation TSP-type Thermometers for Radiometric Scale Realization in Temperature Range from 600 to 3200 °C, *Temperature: It´s Measurement and Control in Science and Industry: Proc. 8th Symposium on Temperature*, 2003, V. 7, 583–588.

[10] Woolliams E. R., Anhalt K., Ballico M., Bloembergen P., Bourson F., Briaudeau S., Campos J., Cox M. G., Campo D., Dong W., Dury M. R., Gavrilov V., Grigoryeva I., Hernanz M. L., Jahan F., Khlevnoy B., Khromchenko V., Lowe D. H., Lu X., Machin G., Mantilla J. M., Martin M. J., McEvoy H. C., Rougié B., Sadli M., Salim S. G. R., Sasajima N., Taubert D. R., Todd A. D. W., Van den Bossche R., Van der Ham E., Wang T., Whittam A., Wilthan B., Woods D. J., Woodward J. T., Yamada Y., Yamaguchi Y., Yoon H. W. and Yuan Z., Thermodynamic temperature assignment to the point of inflection of the melting curve of high-temperature fixed points, *Phil.Trans.R.Soc.A* **374**: 20150044

[11] B.B. Khlevnoy, I.A. Grigoryeva, D.A. Otryaskin, Development and investigation of WC–C fixed-point cells, *Metrologia* **49**, S59 (2012).

[12] B. B. Khlevnoy and I. A. Grigoryeva, Long-Term Stability of WC-C Peritectic Fixed Point, *Int J Thermophys* (2015) **36**:367–373

[13] I. A. Grigoryeva, B. B. Khlevnoy and M. V. Solodilov, Reproducibility of WC–C High-Temperature Fixed Point, *Int J Thermophys* (2017) **38**:69, DOI 10.1007/s10765-017-2203-0

[14] P. Sperfeld, Final report on the CIPM key comparison CCPR-K1.b: Spectral irradiance 200 nm to 350 nm, *Metrologia*, 2008, **45**, *Tech. Suppl.*, 02002, doi:10.1088/0026-1394/45/1A/02002. (http://iopscience.iop.org/article/10.1088/0026-1394/45/1A/02002/meta)

[15] A.D.W. Todd, K. Anhalt, P. Bloembergen, B.B. Khlevnoy, D.H. Lowe, G. Machin, M. Sadli, N. Sasajima and P. Saunders, On the uncertainties in the realization of the kelvin based on thermodynamic temperatures of high-temperature fixed-point cells, *Metrologia* **58,** 035007

[16] P. Sperfeld, S. Pape, B. Khlevnoy and A. Burdakin, Performance limitations of carbon-cavity blackbodies due to absorption bands at the highest temperatures, *Metrologia*, **46** (2009) S170–S173.

[17] C. Carreras and A. Corróns, Absolute spectroradiometric and photometric scales based on an electrically calibrated pyroelectric radiometer, *Appl. Opt*., 1981, 20.

[18] P. Corredera, A. Corróns, A. Pons and J. Campos, Absolute spectral irradiance scale in the 700-2400 nm spectral range, *Appl. Opt*., 1990, 29.

[19] S.N. Park, C.W. Park, D.H. Lee, and B.H. Kim,"Consistency of the Temperature Scales above the Silver Freezing Point Realized at Four Different Spectral Bands", *SICE-ICASE International Joint Conference* 2006 Oct., 18-21, 2006 in Bexco, Busan, Korea (2006).

[20] Preston-Thomas H., "The International Scale of 1990 (ITS-90)", Metrologia, 1990, 27, 3-10.

[21] Yoon H W, Gibson C E and Barnes P Y 2003 The realization of the NIST detector-based spectral irradiance scale *Metrologia* **40** S172–S176

[22] W. Möller, P. Sperfeld, B. Nawo K H and J M 1998 Realization of the spectral irradiance scale in the air-ultraviolet using thermal radiators *Metrologia* **35** 261–5

[23] Coutin J and Rougie B 2016 Characterization and validation of a new cryogenic radiometer at the LNE-LCM *Rev. Française métrologie* 2016–1 11–20

[24] Bastie J 2005 Optical radiation measurements at CNAM-INM *ENGEVISTA* 7 4–18

[25] Obein G and Bastie J 2011 Report on the key comparison EUROMET-PR-K6: Spectral regular transmittance *Metrologia* **48** 39

[26] ROUGIÉ B., VALIN M. H., 2017 Thermodynamic measurement and validation of a high temperature blackbody for spectral radiance and irradiance reference, *NEWRAD 2017 Proceedings*, Tokyo, Japan.

[27] Valin M H 2019, Etalon d'éclairement et de luminance énergétique de l'ultraviolet à l'infrarouge basé sur un corps noir haute température raccordé aux références radiométriques, internal report.

[28] H. W. Yoon, C. E. Gibson, P. Y. Barnes, "Realization of the National Institute of Standards and Technology detector-based spectral irradiance scale", *Applied Optics* **41**, 5879-5890 (2002).

[29] H. W. Yoon, J.E. Proctor, C.E. Gibson, "FASCAL 2: A New NIST Facility for the Spectral Irradiance Calibrations of Sources", *Metrologia* **40**, S30-S34 (2003).

[30] P. E. Ciddor, Refractive index of air: new equations for the visible and near infrared, *Applied Optics* **35**, 1566-1573 (1996).

[31] Sperfeld P., Metzdorf J., Harrison N.J., Fox N. P., Khlevnoy B.B., Khromchenko V.B., Mekhontsev S. N., Shapoval V.I., Zelener M.F.. Sapritsky V.I., Investigation of high-temperature blackbody BB3200, *Metrologia*, 1998, **35**, 419–42

[32] Woolliams E. R., Harrison N. J., Fox N. P., Preliminary results of the investigation of a 3500 K black body, *Metrologia*, 2000, **37(5)**, 501-50

[33] Woolliams E. R., Harrison N. J., Khlevnoy B.B., Rogers L.J., Fox N.P., Realisation and dissemination of spectral irradiance at NPL, *UV News*, 2002, **7**, 39-4

[34] Sperfeld P., Galal Yousef S., Metzdorf J., Nawo B., Möller W., The use of self-consistent calibrations to recover absorption bands in the black-body spectrum, *Metrologia*, 2000, **37(5)**, 373-376

[35] Woolliams E.R., Pollard D.F., Harrison N.J., Theocharous E., Fox N.P., New facility for the high-accuracy measurement of lens transmission, *Metrologia*, 2000, **37(5)**, 603-605

[36] Fox N.P., Martin J.E., Nettleton D.H., Absolute spectral radiometric determination of the thermodynamic temperatures of the melting/freezing points of gold, silver and aluminium, *Metrologia*, **28**, 1991, 357-374

[37] Guide to the Expression of Uncertainty in Measurement, Geneva, International Organization for Standardization, 1993

[38] Cox M.G., Dainton P.M., Harris P.M., Software Support for Metrology. Best Practice Guide No. 6: Uncertainty and statistical modelling", March 2001, available at: http://www.npl.co.uk/ssfm/download/

[39] L. P. Boivin, C. Bamber, A. A. Gaertner, R. K. Gerson, D. J. Woods, and E. R. Woolliams, J. Mod. Opt, **57** 1648 – 1660 (2010).

[40] A. D. W. Todd and D. J. Woods, Metrologia **50** 20-60 (2013).

[41] K. P. Birch and M. J. Downs, Metrologia, **31** 315–316 (1994).

[42] A. A. Gaertner, Consultative Committee for Thermometry Working Document CCT/10-11 (2010). https://www.bipm.org/cc/CCT/Allowed/25/D11_CCTdraftAAG.pdf.

[43] CIE (International Commission on Illumination) Term 17-341, distribution temperature http://eilv.cie.co.at/term/341.

[44] JCGM 100:2008. Joint Committee for Guides in Metrology (September 2008). Evaluation of Measurement Data.

[45] Metzdorf J., Metrologia, 1993, 30, 403-408.

[46] Sperfeld P., Metzdorf J., Galal Yousef S., Stock K. D., Möller W., Metrologia, 1998, 35, 267-271.

[47] Sperfeld P., Entwicklung einer empfängergestützten spektralen Bestrahlungs-stärkeskala, Braunschweig, 1999. http://www.biblio.tu-bs.de/ediss/data/19990628a/19990628a.html

[48] Khlevnoy B.B., Harrison N.J., Rogers L.J., Pollard D.F., Fox N.P., Sperfeld P., Fischer J., Friedrich R., Metzdorf J., Seidel J., Samoylov M.L., Stolyarevskaya R.I., Khromchenko V.B., Ogarev S.A., Sapritsky V.I., Metrologia, 2003, 40, S39–S44

[49] P. Sperfeld, S. Pape and B. Barton, *From Primary Standard to Mobile Measurements - Overview of the Spectral Irradiance Calibration Equipment at PTB,* MAPAN- Journal of Metrology Society of India, 25 (2010) 11-19.

[50] J.W.T. Walsh, Photometry, Dover, New York, 1965

# Appendix A

## Relative Data

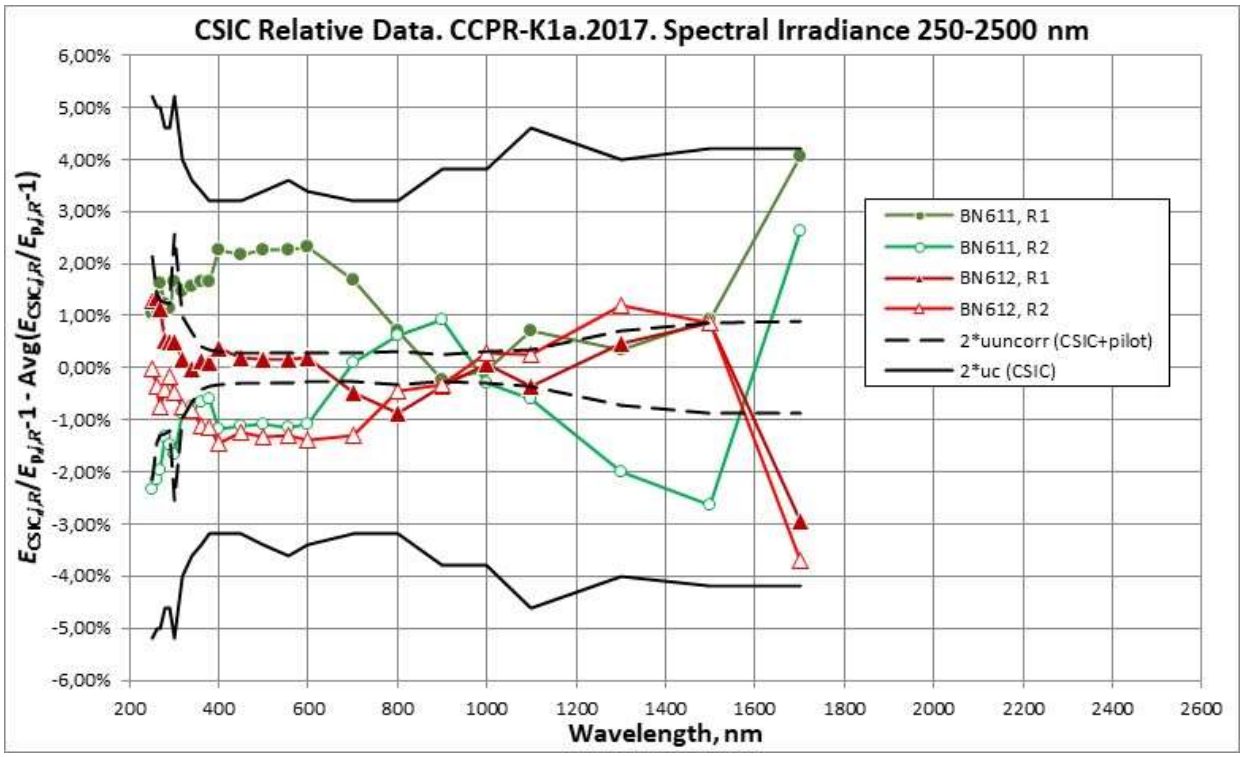


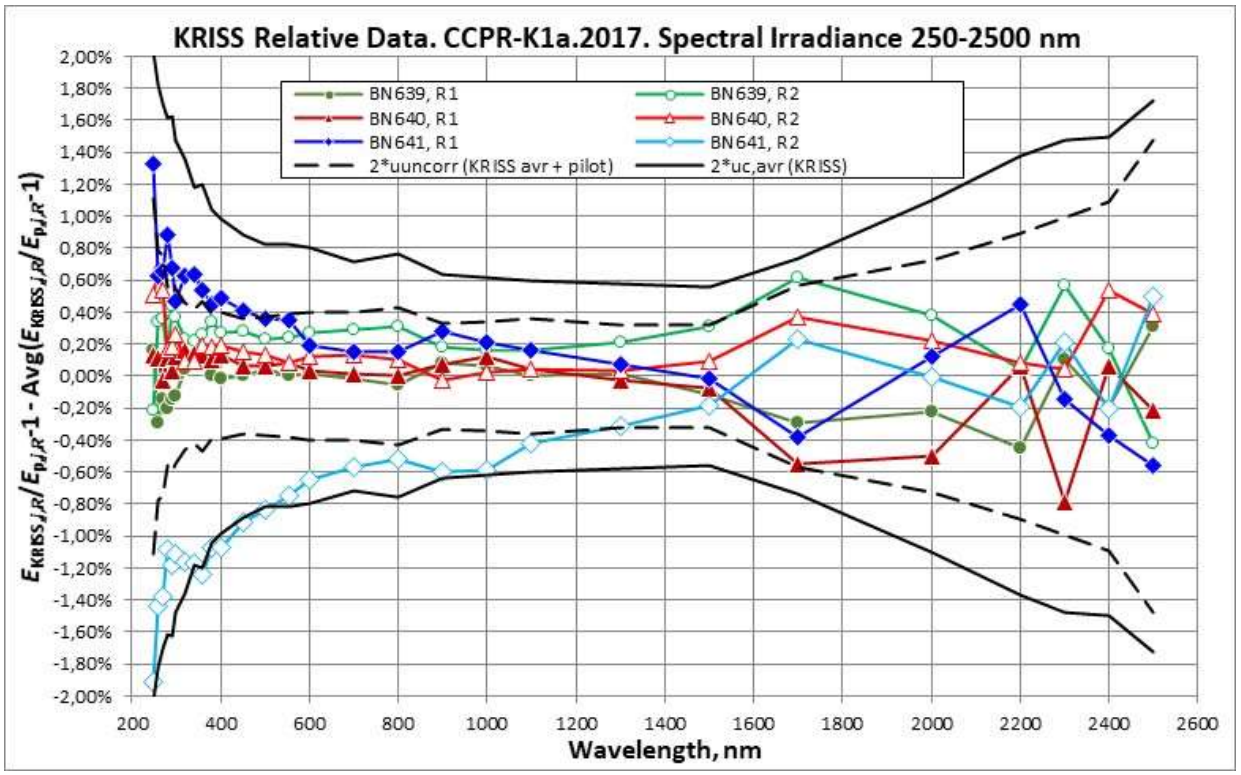

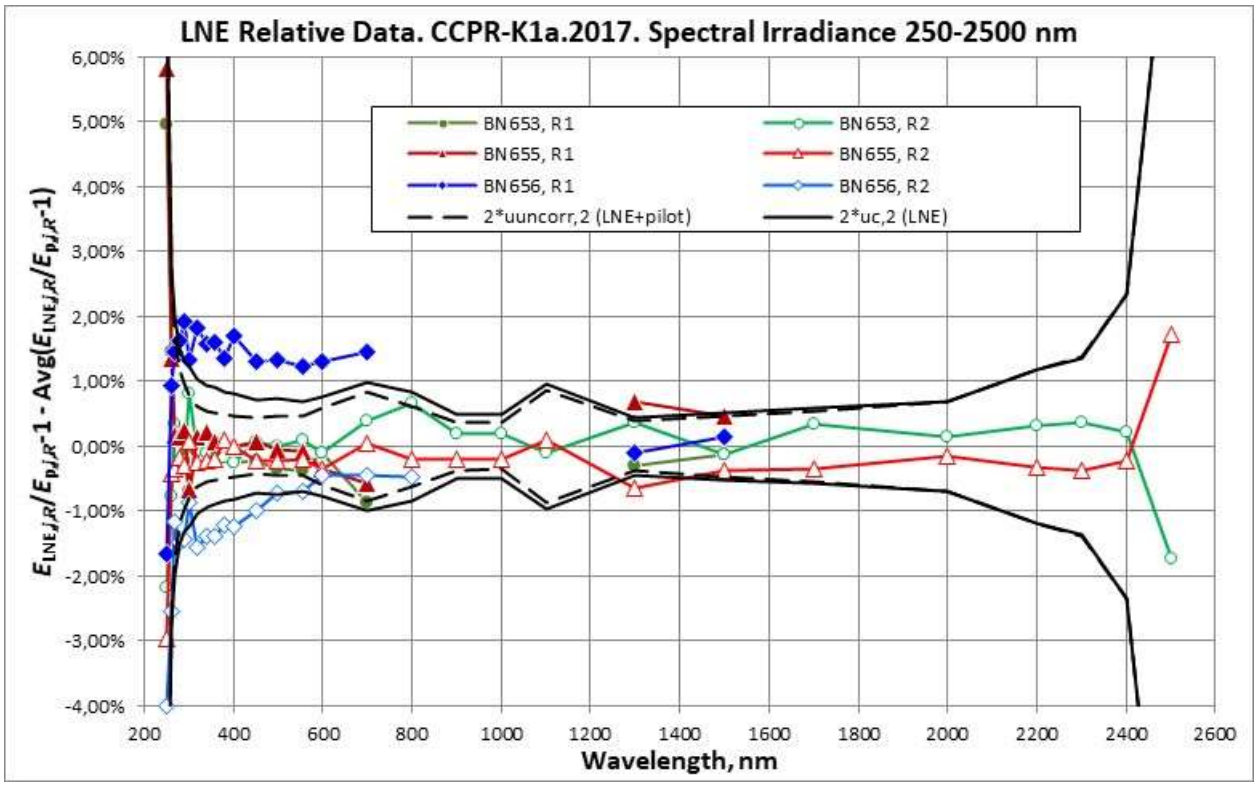
LNE Relative Data. CCPR-K1a.2017. Spectral Irradiance 250-2500 nm
BN653, R1
BN653, R2
BN655, R1
BN655, R2
BN656, R1
BN656, R2
2*uuncorr,2 (LNE+pilot)
2*uc,2 (LNE)
Wavelength, nm

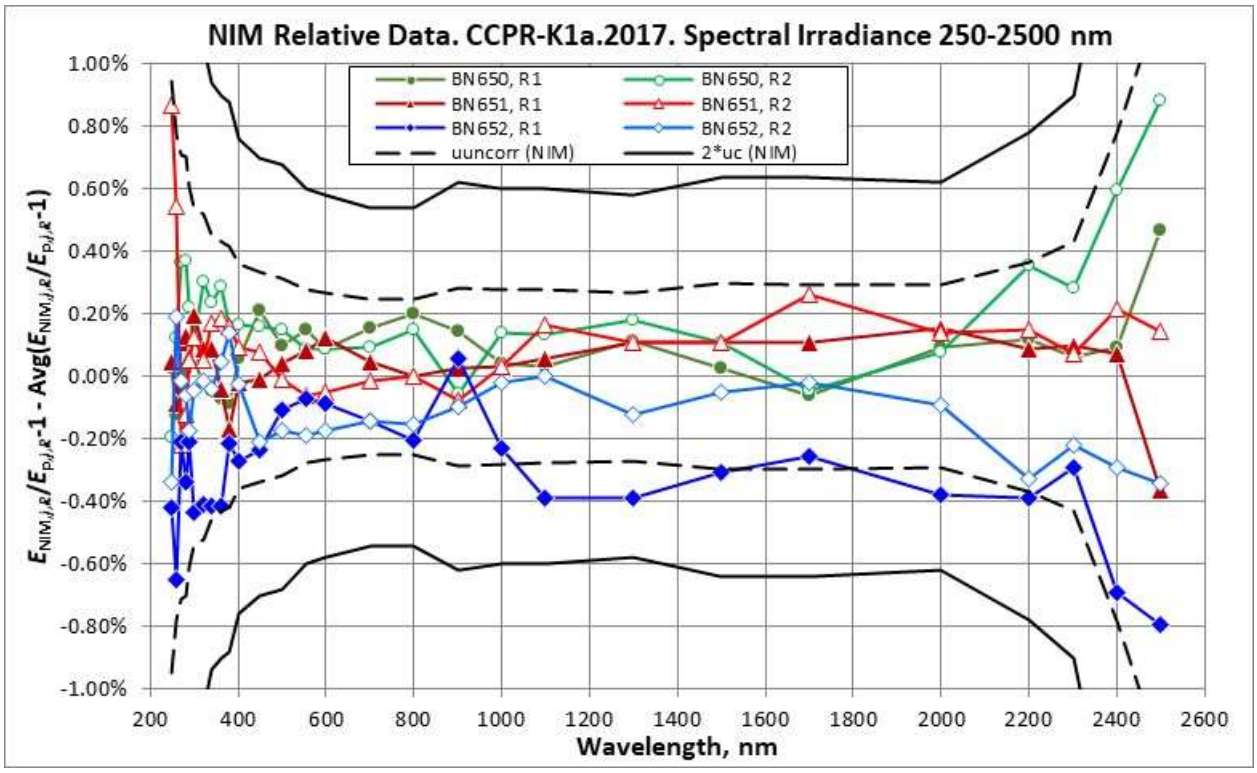
NIM Relative Data. CCPR-K1a.2017. Spectral Irradiance 250-2500 nm
BN650, R1
BN650, R2
BN651, R1
BN651, R2
BN652, R1
BN652, R2
uuncorr (NIM)
2*uc (NIM)
Wavelength, nm

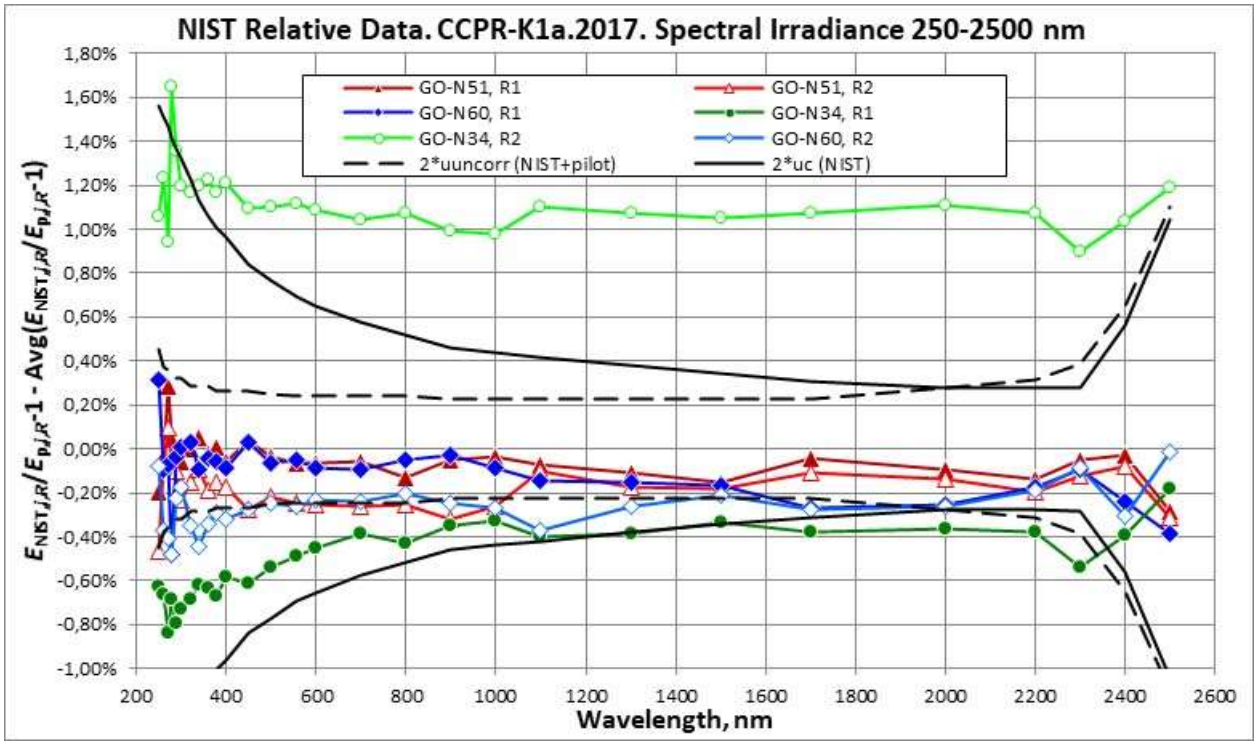
NIST Relative Data. CCPR-K1a.2017. Spectral Irradiance 250-2500 nm
GO-N51, R1
GO-N51, R2
GO-N60, R1
GO-N34, R1
GO-N34, R2
GO-N60, R2
2*uuncorr (NIST+pilot)
2*uc (NIST)
Wavelength, nm

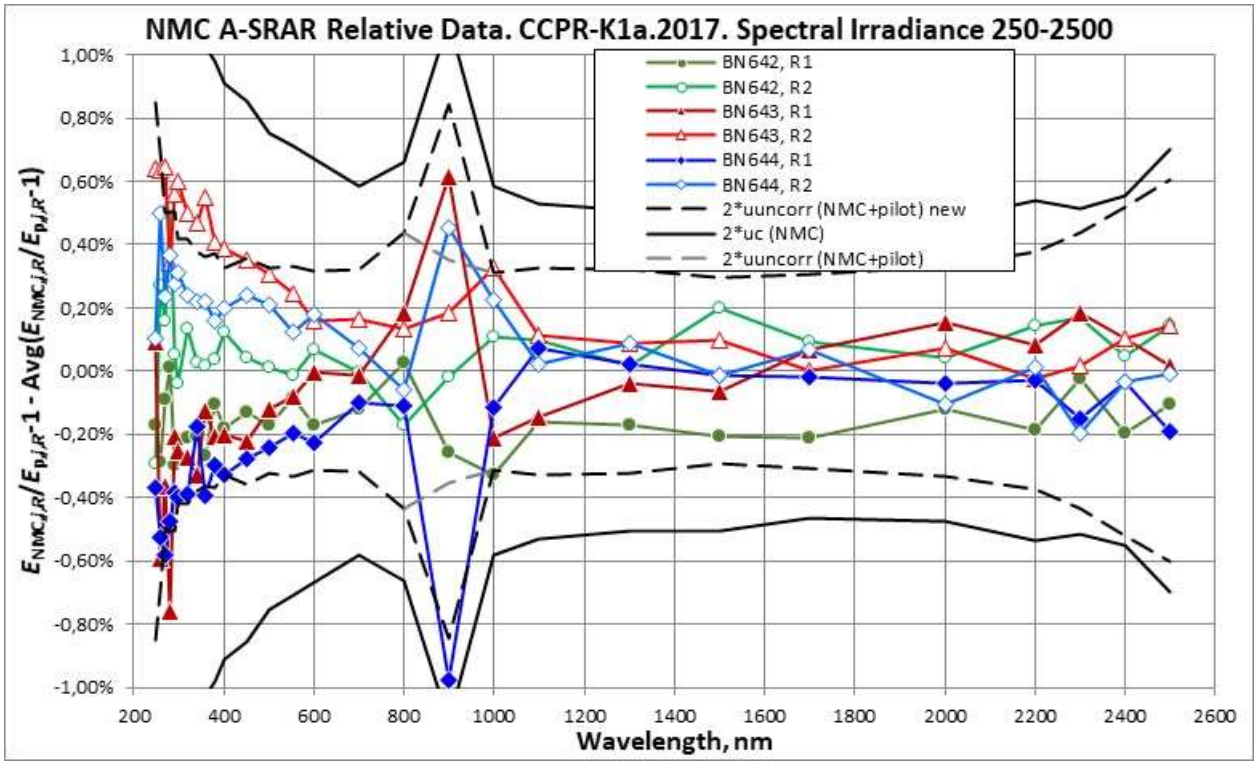
NMC A-SRAR Relative Data. CCPR-K1a.2017. Spectral Irradiance 250-2500
BN642, R1
BN642, R2
BN643, R1
BN643, R2
BN644, R1
BN644, R2
2*uuncorr (NMC+pilot) new
2*uc (NMC)
2*uuncorr (NMC+pilot)
Wavelength, nm

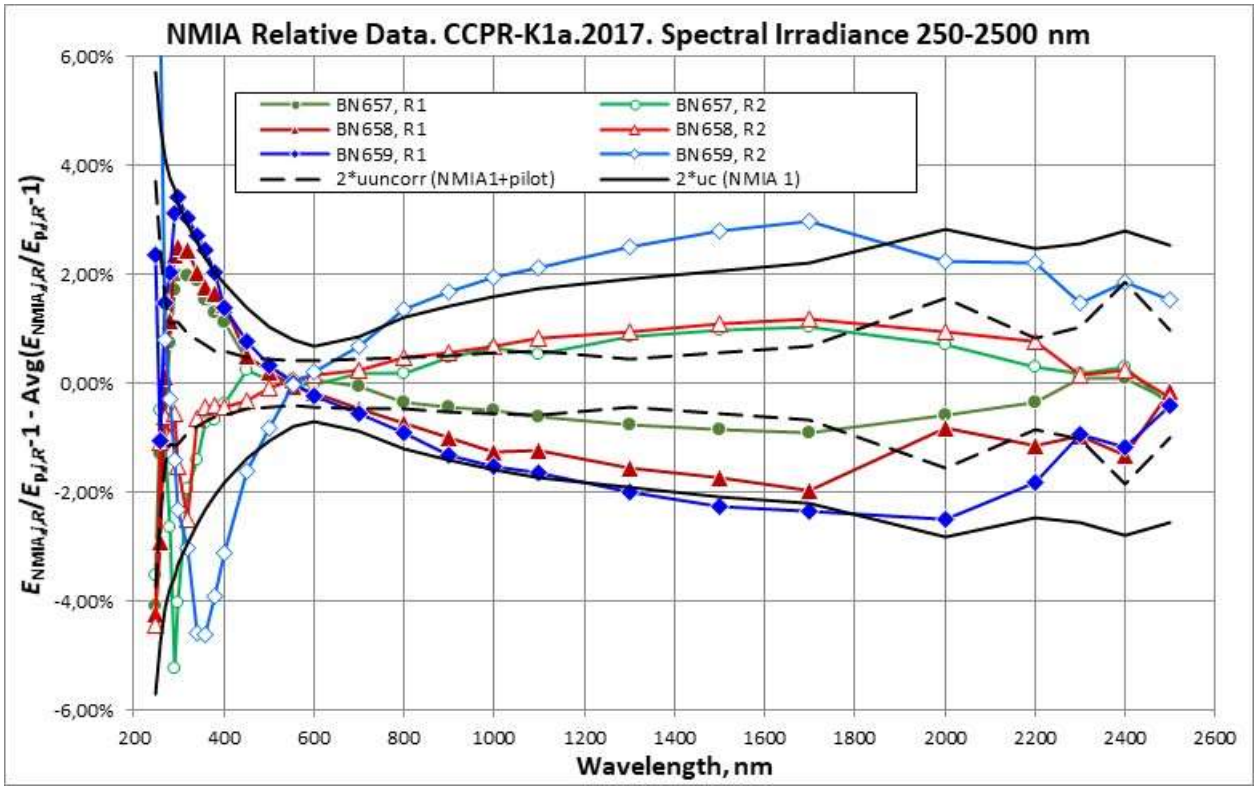
NMIA Relative Data. CCPR-K1a.2017. Spectral Irradiance 250-2500 nm
BN657, R1
BN658, R1
BN659, R1
2*uuncorr (NMIA1+pilot)
BN657, R2
BN658, R2
BN659, R2
2*uc (NMIA 1)
6,00%
4,00%
2,00%
0,00%
-2,00%
-4,00%
-6,00%
200
400
600
800
1000
1200
1400
1600
1800
2000
2200
2400
2600
Wavelength, nm

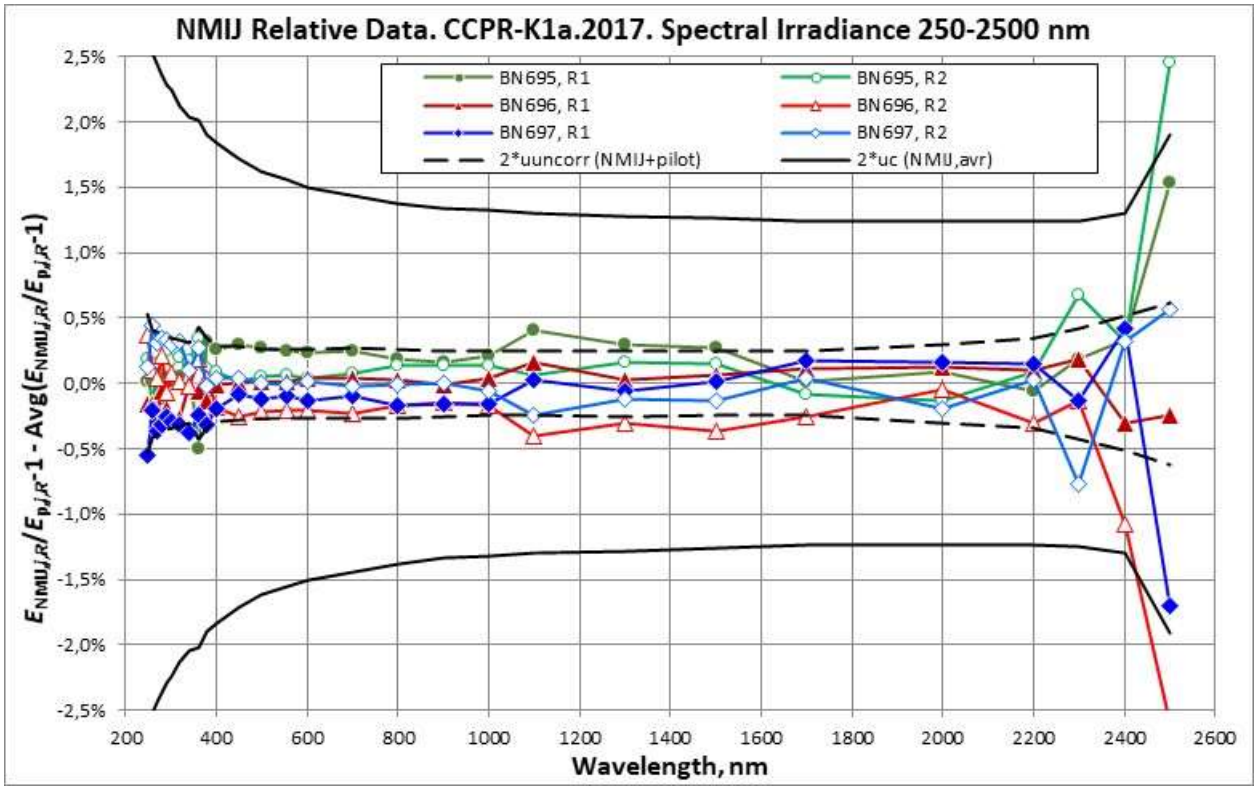
NMIJ Relative Data. CCPR-K1a.2017. Spectral Irradiance 250-2500 nm
BN695, R1
BN696, R1
BN697, R1
2*uuncorr (NMIJ+pilot)
BN695, R2
BN696, R2
BN697, R2
2*uc (NMIJ,avr)
2,5%
2,0%
1,5%
1,0%
0,5%
0,0%
-0,5%
-1,0%
-1,5%
-2,0%
-2,5%
200
400
600
800
1000
1200
1400
1600
1800
2000
2200
2400
2600
Wavelength, nm

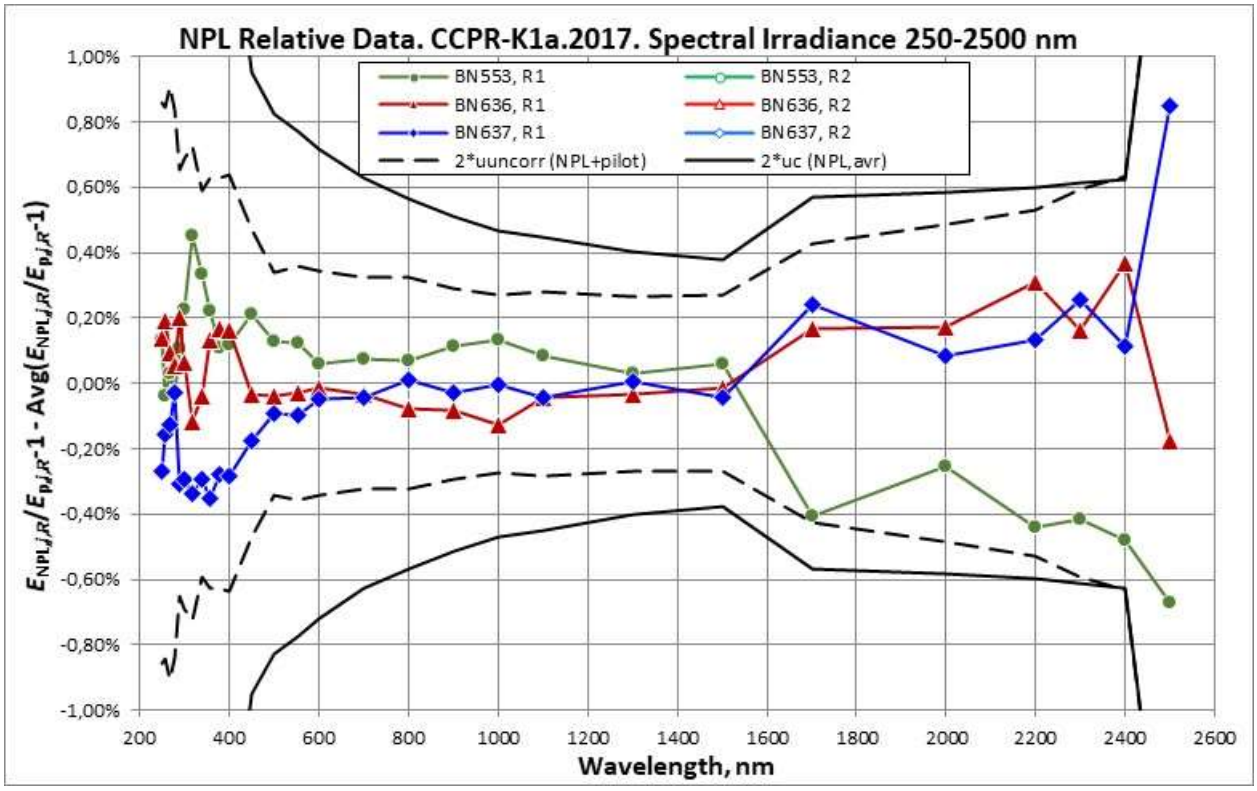
NPL Relative Data. CCPR-K1a.2017. Spectral Irradiance 250-2500 nm
BN553, R1
BN553, R2
BN636, R1
BN636, R2
BN637, R1
BN637, R2
2*uuncorr (NPL+pilot)
2*uc (NPL,avr)
Wavelength, nm

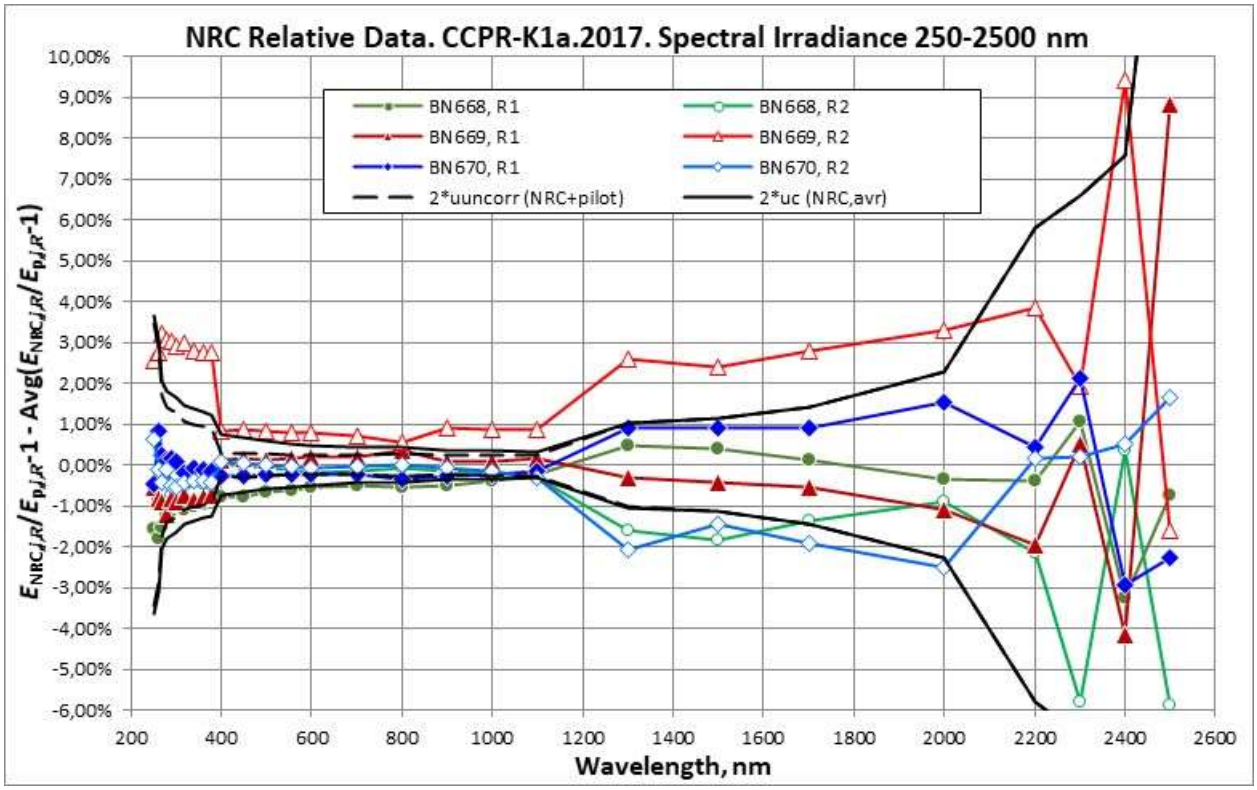
NRC Relative Data. CCPR-K1a.2017. Spectral Irradiance 250-2500 nm
BN668, R1
BN668, R2
BN669, R1
BN669, R2
BN670, R1
BN670, R2
2*uuncorr (NRC+pilot)
2*uc (NRC,avr)
Wavelength, nm

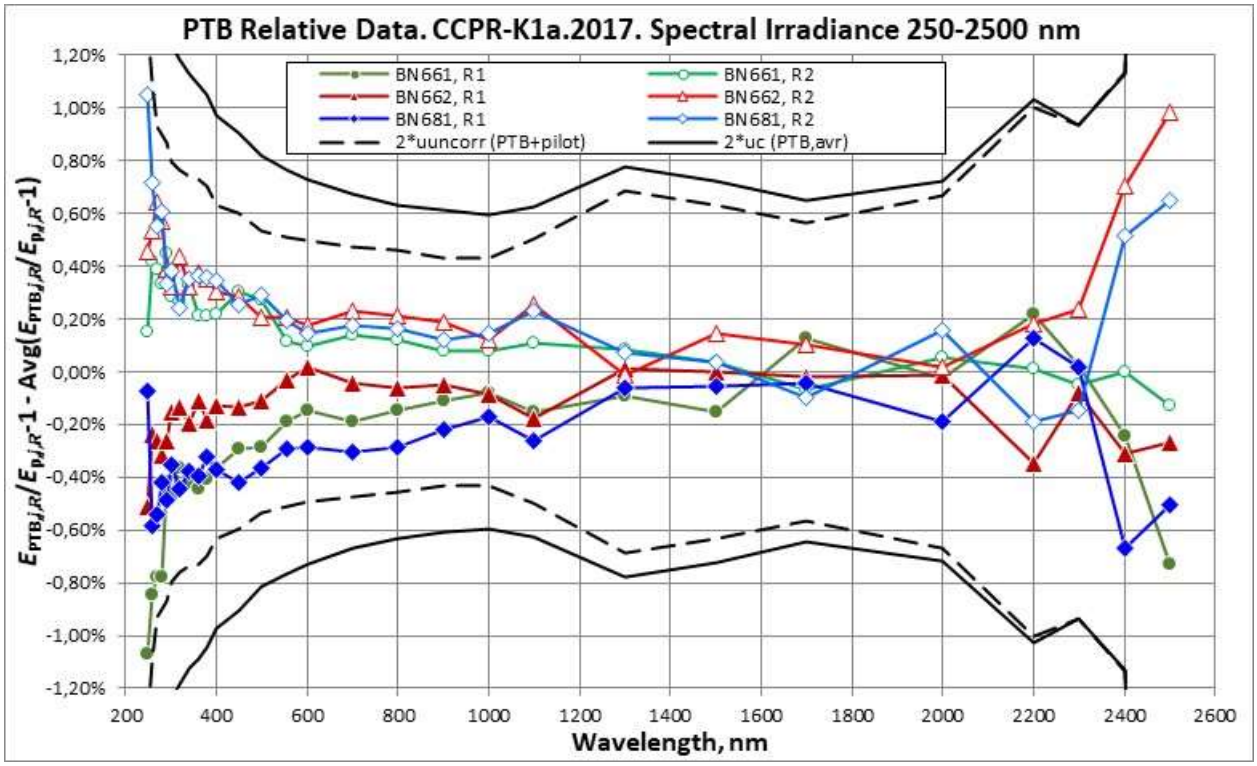
PTB Relative Data. CCPR-K1a.2017. Spectral Irradiance 250-2500 nm
BN661, R1
BN661, R2
BN662, R1
BN662, R2
BN681, R1
BN681, R2
2*uuncorr (PTB+pilot)
2*uc (PTB,avr)
Wavelength, nm

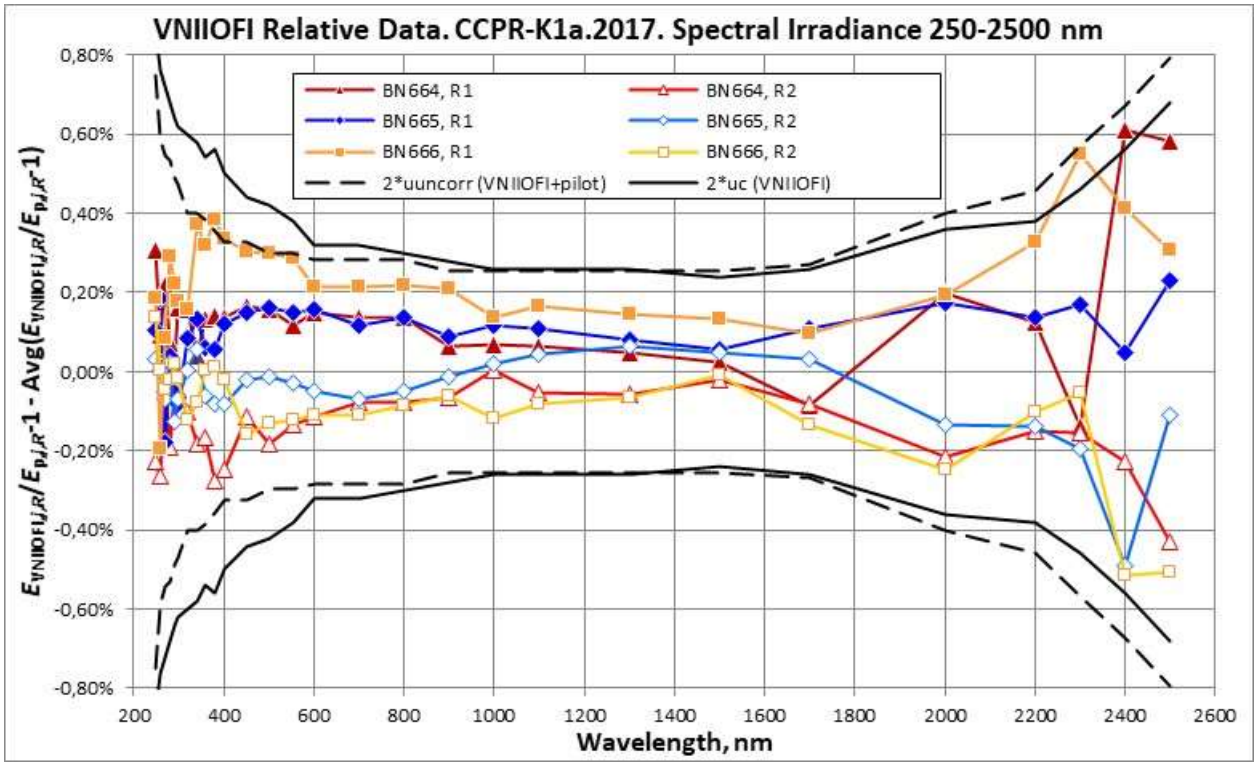
VNIIOFI Relative Data. CCPR-K1a.2017. Spectral Irradiance 250-2500 nm
BN664, R1
BN664, R2
BN665, R1
BN665, R2
BN666, R1
BN666, R2
2*uuncorr (VNIIOFI+pilot)
2*uc (VNIIOFI)
Wavelength, nm

# Appendix B

## Data Analysis Results. Version 1 (not final)

**NMIA data is excluded from calculation of KCRV**.

**NPL, as well as all other participants, are INCLUDED.**

Note that CSIC submitted measurement data for the wavelength rage from 250 nm to 1700 nm only. Therefore, the total number, *N*, of NMIs contribute to KCRV is:

*N* = 11 for the range from 250 nm to 1700 nm;
*N* = 10 for the range from 2000 nm to 2500 nm.

### B.1. Calculation of Differences from Pilot

The **relative average differences** $\Delta_i$ of NMI Spectral Irradiance data to the Pilot Spectral Irradiance data and the **uncertainties** $u(\Delta_i)$ of these differences (Eq.8.6 and Eq.8.7 of the Section 8.3 "Method of comparison data analysis", respectively) are presented in Table B1 and Table B2, respectively.

Table B1. Relative average differences $\Delta_i$ of NMI-to-Pilot data (Eq.8.6 of the Section 8.3)

| λ, nm | $\Delta_i$, % | | | | | | | | | | | |
|---|---|---|---|---|---|---|---|---|---|---|---|---|
| | CSIC | KRISS | LNE | NIM | NIST | NMC | NMIA | NMIJ | NPL | NRC | PTB | VNIIOFI |
| 250 | -3.16 | 0.92 | 5.26 | 1.17 | 0.72 | -0.50 | -0.99 | 0.43 | -0.67 | 0.87 | 1.76 | 0.20 |
| 260 | -4.30 | 0.88 | 1.67 | 0.74 | 0.47 | -0.54 | -1.85 | 0.81 | -1.58 | 1.01 | 1.79 | 0.18 |
| 270 | -5.06 | 0.78 | 0.78 | 0.39 | -0.04 | -0.10 | -2.01 | 0.96 | -1.72 | 1.03 | 1.67 | 0.11 |
| 280 | -4.59 | 0.41 | 0.75 | 0.46 | 0.23 | -0.46 | -1.63 | 0.91 | -1.85 | 0.78 | 1.35 | 0.18 |
| 290 | -3.44 | 0.41 | 0.73 | 0.53 | 0.49 | -0.40 | -1.70 | 0.83 | -1.19 | 0.94 | 1.50 | 0.15 |
| 300 | -0.42 | 0.35 | 0.85 | 0.47 | 0.70 | -0.26 | -1.75 | 1.02 | -0.96 | 0.94 | 1.41 | 0.10 |
| 320 | 0.88 | 0.05 | 1.20 | 0.30 | 0.55 | -0.46 | -2.05 | 0.79 | -1.51 | 0.63 | 1.18 | 0.18 |
| 340 | 1.21 | 0.17 | 1.21 | 0.54 | 0.47 | -0.18 | -2.04 | 0.81 | -1.23 | 0.86 | 1.32 | 0.14 |
| 360 | 1.35 | 0.27 | 1.29 | 0.49 | 0.31 | -0.07 | -1.84 | 0.79 | -1.01 | 0.97 | 1.37 | 0.14 |
| 380 | 1.30 | 0.24 | 1.50 | 0.53 | 0.26 | -0.13 | -1.81 | 0.84 | -0.86 | 0.92 | 1.35 | 0.14 |
| 400 | 1.29 | 0.18 | 1.32 | 0.46 | 0.28 | -0.13 | -1.82 | 1.40 | -0.91 | 0.15 | 1.22 | 0.18 |
| 450 | 1.17 | -0.03 | 0.69 | 0.51 | 0.49 | -0.42 | -1.29 | 1.05 | -0.60 | 0.04 | 0.74 | 0.16 |
| 500 | 0.97 | -0.04 | 0.56 | 0.42 | 0.46 | -0.52 | -0.87 | 0.96 | -0.45 | 0.09 | 0.61 | 0.15 |
| 555 | 0.90 | -0.02 | 0.58 | 0.47 | 0.37 | -0.35 | -0.50 | 0.88 | -0.43 | 0.04 | 0.47 | 0.13 |
| 600 | 0.95 | 0.01 | 0.52 | 0.46 | 0.39 | -0.35 | -0.32 | 0.78 | -0.46 | 0.04 | 0.35 | 0.16 |
| 700 | 1.72 | 0.10 | 0.15 | 0.44 | 0.24 | -0.29 | -0.01 | 0.59 | -0.46 | -0.06 | 0.21 | 0.14 |
| 800 | 0.92 | 0.50 | 0.68 | 0.50 | 0.03 | 0.74 | 0.47 | 0.72 | -0.40 | -0.04 | 0.15 | 0.17 |
| 900 | 0.43 | -0.03 | 0.70 | 0.43 | 0.28 | 0.84 | 0.80 | 0.85 | -0.45 | -0.24 | 0.07 | 0.18 |
| 1000 | -0.37 | -0.01 | 0.81 | 0.38 | 0.24 | 0.81 | 0.97 | 0.39 | -0.38 | -0.14 | 0.05 | 0.15 |
| 1100 | -0.47 | -0.02 | 0.82 | 0.04 | -0.05 | 0.86 | 1.25 | -0.05 | -0.33 | -0.04 | 0.35 | 0.17 |
| 1300 | 0.17 | 0.05 | 1.29 | 0.20 | -0.09 | 1.02 | 1.45 | -0.05 | -0.30 | 0.75 | -0.02 | 0.17 |
| 1500 | -0.70 | 0.04 | 1.26 | 0.29 | -0.19 | 1.07 | 1.66 | -0.39 | -0.33 | 0.62 | 0.16 | 0.18 |
| 1700 | -7.05 | -0.17 | 1.84 | 0.37 | -0.12 | 1.20 | 1.97 | -0.53 | -0.50 | 1.07 | 0.03 | 0.14 |
| 2000 | | -0.15 | 2.59 | 0.23 | -0.09 | 1.09 | 2.54 | -1.34 | -0.39 | 0.65 | 0.01 | 0.16 |
| 2200 | | -0.90 | 3.34 | 0.26 | -0.07 | 1.09 | 3.14 | -2.01 | -0.43 | 1.84 | 0.19 | 0.15 |
| 2300 | | -0.28 | 4.52 | 0.22 | 0.06 | 0.99 | 4.71 | -1.57 | -0.29 | 0.95 | 0.06 | -0.04 |
| 2400 | | 0.39 | 7.20 | 0.20 | -0.38 | 1.20 | 5.85 | -1.73 | -0.05 | 3.03 | 0.29 | 0.26 |
| 2500 | | 0.02 | 8.00 | 0.45 | 0.29 | 1.33 | 8.91 | -1.69 | -0.79 | 3.72 | 0.33 | 0.22 |

Table B2. Uncertainties $u(\Delta_i)$ of relative average differences (Eq.8.7 of the Section 8.3)

| λ, nm | $u(\Delta_i)$, % | | | | | | | | | | | |
|---|---|---|---|---|---|---|---|---|---|---|---|---|
| | CSIC | KRISS | LNE | NIM | NIST | NMC | NMIA | NMIJ | NPL | NRC | PTB | VNIIOFI |
| 250 | 2.53 | 1.03 | 2.31 | 0.79 | 0.80 | 0.98 | 2.86 | 1.38 | 0.95 | 1.50 | 0.76 | 0.43 |
| 260 | 2.45 | 0.92 | 1.03 | 0.67 | 0.77 | 0.85 | 2.38 | 1.27 | 0.97 | 1.23 | 0.69 | 0.38 |
| 270 | 2.43 | 0.86 | 0.82 | 0.62 | 0.75 | 0.76 | 2.07 | 1.22 | 1.02 | 0.86 | 0.64 | 0.36 |
| 280 | 2.23 | 0.79 | 0.66 | 0.61 | 0.72 | 0.79 | 1.89 | 1.18 | 0.95 | 0.78 | 0.62 | 0.34 |
| 290 | 2.21 | 0.76 | 0.60 | 0.55 | 0.70 | 0.68 | 1.79 | 1.15 | 0.85 | 0.75 | 0.60 | 0.32 |
| 300 | 2.49 | 0.71 | 0.56 | 0.51 | 0.67 | 0.66 | 1.66 | 1.12 | 0.83 | 0.71 | 0.58 | 0.32 |
| 320 | 1.95 | 0.64 | 0.51 | 0.48 | 0.62 | 0.61 | 1.47 | 1.07 | 0.86 | 0.64 | 0.54 | 0.30 |
| 340 | 1.83 | 0.58 | 0.47 | 0.44 | 0.57 | 0.55 | 1.30 | 1.02 | 0.80 | 0.61 | 0.52 | 0.29 |
| 360 | 1.72 | 0.56 | 0.44 | 0.42 | 0.54 | 0.52 | 1.16 | 0.98 | 0.78 | 0.58 | 0.50 | 0.28 |
| 380 | 1.62 | 0.50 | 0.42 | 0.40 | 0.51 | 0.49 | 1.03 | 0.95 | 0.79 | 0.55 | 0.48 | 0.28 |
| 400 | 1.62 | 0.47 | 0.41 | 0.36 | 0.49 | 0.46 | 0.92 | 0.92 | 0.75 | 0.37 | 0.45 | 0.26 |
| 450 | 1.61 | 0.42 | 0.37 | 0.34 | 0.43 | 0.42 | 0.70 | 0.86 | 0.49 | 0.34 | 0.41 | 0.24 |
| 500 | 1.70 | 0.39 | 0.36 | 0.32 | 0.40 | 0.38 | 0.53 | 0.82 | 0.43 | 0.31 | 0.38 | 0.22 |
| 555 | 1.80 | 0.37 | 0.34 | 0.29 | 0.36 | 0.35 | 0.41 | 0.78 | 0.40 | 0.28 | 0.35 | 0.20 |
| 600 | 1.70 | 0.35 | 0.34 | 0.28 | 0.34 | 0.34 | 0.36 | 0.76 | 0.37 | 0.26 | 0.34 | 0.18 |
| 700 | 1.60 | 0.33 | 0.40 | 0.26 | 0.30 | 0.29 | 0.44 | 0.72 | 0.33 | 0.23 | 0.31 | 0.17 |
| 800 | 1.61 | 0.33 | 0.44 | 0.26 | 0.27 | 0.31 | 0.61 | 0.69 | 0.30 | 0.22 | 0.30 | 0.16 |
| 900 | 1.90 | 0.29 | 0.27 | 0.27 | 0.24 | 0.48 | 0.71 | 0.68 | 0.27 | 0.19 | 0.28 | 0.16 |
| 1000 | 1.90 | 0.29 | 0.26 | 0.26 | 0.23 | 0.29 | 0.80 | 0.66 | 0.25 | 0.18 | 0.27 | 0.15 |
| 1100 | 2.30 | 0.29 | 0.49 | 0.26 | 0.22 | 0.26 | 0.87 | 0.65 | 0.24 | 0.17 | 0.28 | 0.14 |
| 1300 | 2.02 | 0.28 | 0.39 | 0.25 | 0.20 | 0.25 | 0.96 | 0.64 | 0.22 | 0.40 | 0.32 | 0.14 |
| 1500 | 2.12 | 0.27 | 0.43 | 0.26 | 0.18 | 0.26 | 1.04 | 0.63 | 0.21 | 0.43 | 0.30 | 0.14 |
| 1700 | 2.12 | 0.32 | 0.31 | 0.26 | 0.17 | 0.23 | 1.11 | 0.63 | 0.30 | 0.54 | 0.28 | 0.14 |
| 2000 | | 0.39 | 0.37 | 0.27 | 0.18 | 0.25 | 1.42 | 0.63 | 0.32 | 0.84 | 0.31 | 0.18 |
| 2200 | | 0.46 | 0.61 | 0.32 | 0.19 | 0.29 | 1.25 | 0.63 | 0.33 | 2.07 | 0.42 | 0.20 |
| 2300 | | 0.51 | 0.70 | 0.37 | 0.22 | 0.30 | 1.30 | 0.64 | 0.36 | 2.37 | 0.40 | 0.25 |
| 2400 | | 0.53 | 1.19 | 0.60 | 0.29 | 0.32 | 1.41 | 0.67 | 0.37 | 2.73 | 0.46 | 0.29 |
| 2500 | | 0.66 | 4.40 | 0.89 | 0.43 | 0.39 | 1.29 | 0.97 | 0.89 | 6.22 | 2.89 | 0.33 |

## B.2. Calculation of KCRV

**Cut-off** is calculated following Eq.8.10 – 8.12 of the Section 8.3 "Method of comparison data analysis". Values of relative average uncertainties of spectral irradiance $u(E_i)$, Median and Cut-off are presented in Table B3.

**Uncertainties $u_{\mathbf{adj}}(\Delta_i)$ after cut-off** of relative average differences (Eq.8.15, 8.20) are presented in Table B4. At this stage $s = 0$.

Table 5 presents the **weights $w_i$ , KCRV $\Delta_{\mathbf{KCRV}}$ and uncertainty of KCR $u(\Delta_{\mathbf{KCRV}})$,** determent by Equations 8.16, 8.17 and 8.18, respectively.

## B3. Calculation of preliminary values of Degrees of Equivalence

Preliminary Degrees of Equivalence, i.e. Deviations from KCRV, $D_i$, and their associated expanded uncertainties, $U_i$, (Eq.8.21 and 8.22-8.23, respectively) are presented in Table B6.

Table B3. Relative average uncertainties of spectral irradiance $u(E_i)$, Median and Cut-off in %

| λ, nm | $u(E_i)$, % | | | | | | | | | | | Median | **Cut-off** |
|---|---|---|---|---|---|---|---|---|---|---|---|---|---|
| | CSIC | KRISS | LNE | NIM | NIST | NMC | NMIJ | NPL | NRC | PTB | VNII OFI | | |
| 250 | 2.52 | 1.00 | 2.30 | 0.76 | 0.78 | 0.96 | 1.36 | 0.92 | 1.49 | 0.73 | 0.37 | 0.96 | **0.75** |
| 260 | 2.44 | 0.90 | 1.01 | 0.65 | 0.75 | 0.83 | 1.26 | 0.96 | 1.21 | 0.67 | 0.34 | 0.90 | **0.69** |
| 270 | 2.42 | 0.84 | 0.80 | 0.60 | 0.73 | 0.74 | 1.21 | 1.01 | 0.85 | 0.62 | 0.32 | 0.80 | **0.64** |
| 280 | 2.22 | 0.775 | 0.65 | 0.59 | 0.71 | 0.775 | 1.17 | 0.94 | 0.766 | 0.60 | 0.30 | 0.766 | **0.60** |
| 290 | 2.21 | 0.75 | 0.58 | 0.53 | 0.68 | 0.67 | 1.14 | 0.84 | 0.74 | 0.58 | 0.29 | 0.68 | **0.57** |
| 300 | 2.49 | 0.70 | 0.54 | 0.49 | 0.66 | 0.64 | 1.11 | 0.82 | 0.70 | 0.56 | 0.28 | 0.66 | **0.53** |
| 320 | 1.95 | 0.63 | 0.49 | 0.47 | 0.61 | 0.60 | 1.06 | 0.85 | 0.63 | 0.53 | 0.27 | 0.61 | **0.50** |
| 340 | 1.82 | 0.57 | 0.46 | 0.42 | 0.56 | 0.54 | 1.01 | 0.79 | 0.60 | 0.51 | 0.27 | 0.56 | **0.46** |
| 360 | 1.71 | 0.54 | 0.43 | 0.41 | 0.53 | 0.50 | 0.97 | 0.77 | 0.56 | 0.49 | 0.25 | 0.53 | **0.43** |
| 380 | 1.61 | 0.49 | 0.41 | 0.39 | 0.50 | 0.48 | 0.94 | 0.78 | 0.54 | 0.47 | 0.26 | 0.49 | **0.41** |
| 400 | 1.61 | 0.46 | 0.39 | 0.35 | 0.48 | 0.44 | 0.91 | 0.74 | 0.36 | 0.44 | 0.24 | 0.44 | **0.37** |
| 450 | 1.60 | 0.410 | 0.35 | 0.32 | 0.42 | 0.407 | 0.85 | 0.48 | 0.32 | 0.40 | 0.21 | 0.407 | **0.33** |
| 500 | 1.70 | 0.38 | 0.35 | 0.30 | 0.38 | 0.36 | 0.81 | 0.41 | 0.29 | 0.37 | 0.20 | 0.37 | **0.31** |
| 555 | 1.80 | 0.35 | 0.33 | 0.27 | 0.344 | 0.339 | 0.77 | 0.39 | 0.26 | 0.340 | 0.17 | 0.340 | **0.28** |
| 600 | 1.70 | 0.34 | 0.330 | 0.26 | 0.32 | 0.326 | 0.75 | 0.36 | 0.25 | 0.328 | 0.15 | 0.328 | **0.27** |
| 700 | 1.60 | 0.32 | 0.39 | 0.24 | 0.28 | 0.28 | 0.71 | 0.31 | 0.21 | 0.30 | 0.14 | 0.30 | **0.24** |
| 800 | 1.60 | 0.31 | 0.43 | 0.24 | 0.25 | 0.30 | 0.68 | 0.28 | 0.20 | 0.28 | 0.13 | 0.28 | **0.23** |
| 900 | 1.90 | 0.28 | 0.25 | 0.25 | 0.22 | 0.47 | 0.67 | 0.26 | 0.17 | 0.27 | 0.13 | 0.26 | **0.21** |
| 1000 | 1.90 | 0.28 | 0.25 | 0.24 | 0.21 | 0.28 | 0.65 | 0.23 | 0.16 | 0.26 | 0.12 | 0.25 | **0.20** |
| 1100 | 2.30 | 0.27 | 0.48 | 0.24 | 0.20 | 0.24 | 0.64 | 0.22 | 0.15 | 0.27 | 0.11 | 0.24 | **0.19** |
| 1300 | 2.02 | 0.27 | 0.38 | 0.23 | 0.18 | 0.23 | 0.63 | 0.20 | 0.38 | 0.31 | 0.11 | 0.27 | **0.20** |
| 1500 | 2.12 | 0.25 | 0.42 | 0.25 | 0.16 | 0.24 | 0.62 | 0.19 | 0.42 | 0.29 | 0.10 | 0.25 | **0.20** |
| 1700 | 2.12 | 0.31 | 0.29 | 0.24 | 0.15 | 0.21 | 0.62 | 0.28 | 0.53 | 0.27 | 0.11 | 0.28 | **0.21** |
| 2000 | | 0.37 | 0.35 | 0.24 | 0.13 | 0.22 | 0.61 | 0.292 | 0.83 | 0.285 | 0.14 | 0.289 | **0.20** |
| 2200 | | 0.44 | 0.60 | 0.29 | 0.13 | 0.25 | 0.61 | 0.30 | 2.07 | 0.39 | 0.15 | 0.35 | **0.22** |
| 2300 | | 0.48 | 0.68 | 0.33 | 0.13 | 0.23 | 0.62 | 0.31 | 2.36 | 0.36 | 0.17 | 0.34 | **0.23** |
| 2400 | | 0.49 | 1.17 | 0.57 | 0.21 | 0.25 | 0.64 | 0.31 | 2.72 | 0.42 | 0.20 | 0.45 | **0.28** |
| 2500 | | 0.62 | 4.39 | 0.862 | 0.38 | 0.32 | 0.94 | 0.859 | 6.21 | 2.88 | 0.24 | 0.860 | **0.48** |

Table B4. Uncertainties $\boldsymbol{u_{adj}(\Delta_i)}$ after cut-off of relative average differences (Eq. 8.15)

| λ, nm | $u_{adj}(\Delta_i)$, % | | | | | | | | | | |
|---|---|---|---|---|---|---|---|---|---|---|---|
| | CSIC | KRISS | LNE | NIM | NIST | NMC | NMIJ | NPL | NRC | PTB | VNIIOFI |
| 250 | 2.53 | 1.03 | 2.31 | 0.79 | 0.80 | 0.98 | 1.38 | 0.95 | 1.50 | 0.78 | 0.78 |
| 260 | 2.45 | 0.92 | 1.03 | 0.71 | 0.77 | 0.85 | 1.27 | 0.97 | 1.23 | 0.71 | 0.71 |
| 270 | 2.43 | 0.86 | 0.82 | 0.66 | 0.75 | 0.76 | 1.22 | 1.02 | 0.86 | 0.66 | 0.66 |
| 280 | 2.23 | 0.79 | 0.66 | 0.62 | 0.72 | 0.79 | 1.18 | 0.95 | 0.78 | 0.62 | 0.62 |
| 290 | 2.21 | 0.76 | 0.60 | 0.59 | 0.70 | 0.68 | 1.15 | 0.85 | 0.75 | 0.60 | 0.59 |
| 300 | 2.49 | 0.71 | 0.56 | 0.55 | 0.67 | 0.66 | 1.12 | 0.83 | 0.71 | 0.58 | 0.55 |
| 320 | 1.95 | 0.64 | 0.51 | 0.51 | 0.62 | 0.61 | 1.07 | 0.86 | 0.64 | 0.54 | 0.51 |
| 340 | 1.83 | 0.58 | 0.47 | 0.47 | 0.57 | 0.55 | 1.02 | 0.80 | 0.61 | 0.52 | 0.47 |
| 360 | 1.72 | 0.56 | 0.45 | 0.45 | 0.54 | 0.52 | 0.98 | 0.78 | 0.58 | 0.50 | 0.45 |
| 380 | 1.62 | 0.50 | 0.43 | 0.43 | 0.51 | 0.49 | 0.95 | 0.79 | 0.55 | 0.48 | 0.43 |
| 400 | 1.62 | 0.47 | 0.41 | 0.38 | 0.49 | 0.46 | 0.92 | 0.75 | 0.38 | 0.45 | 0.38 |

| | | | | | | | | | | | |
|---|---|---|---|---|---|---|---|---|---|---|---|
| 450 | 1.61 | 0.42 | 0.37 | 0.35 | 0.43 | 0.42 | 0.86 | 0.49 | 0.35 | 0.41 | 0.35 |
| 500 | 1.70 | 0.39 | 0.36 | 0.33 | 0.40 | 0.38 | 0.82 | 0.43 | 0.33 | 0.38 | 0.33 |
| 555 | 1.80 | 0.37 | 0.34 | 0.30 | 0.36 | 0.35 | 0.78 | 0.40 | 0.30 | 0.35 | 0.30 |
| 600 | 1.70 | 0.35 | 0.34 | 0.29 | 0.34 | 0.34 | 0.76 | 0.37 | 0.29 | 0.34 | 0.29 |
| 700 | 1.60 | 0.33 | 0.40 | 0.26 | 0.30 | 0.29 | 0.72 | 0.33 | 0.26 | 0.31 | 0.26 |
| 800 | 1.61 | 0.33 | 0.44 | 0.26 | 0.27 | 0.31 | 0.69 | 0.30 | 0.25 | 0.30 | 0.25 |
| 900 | 1.90 | 0.29 | 0.27 | 0.27 | 0.24 | 0.48 | 0.68 | 0.27 | 0.23 | 0.28 | 0.23 |
| 1000 | 1.90 | 0.29 | 0.26 | 0.26 | 0.23 | 0.29 | 0.66 | 0.25 | 0.22 | 0.27 | 0.22 |
| 1100 | 2.30 | 0.29 | 0.49 | 0.26 | 0.22 | 0.26 | 0.65 | 0.24 | 0.21 | 0.28 | 0.21 |
| 1300 | 2.02 | 0.28 | 0.39 | 0.25 | 0.22 | 0.25 | 0.64 | 0.22 | 0.40 | 0.32 | 0.22 |
| 1500 | 2.12 | 0.27 | 0.43 | 0.26 | 0.22 | 0.26 | 0.63 | 0.22 | 0.43 | 0.30 | 0.22 |
| 1700 | 2.12 | 0.32 | 0.30 | 0.26 | 0.23 | 0.23 | 0.63 | 0.30 | 0.54 | 0.28 | 0.23 |
| 2000 | | 0.39 | 0.37 | 0.27 | 0.24 | 0.25 | 0.63 | 0.32 | 0.84 | 0.31 | 0.24 |
| 2200 | | 0.46 | 0.61 | 0.32 | 0.26 | 0.29 | 0.63 | 0.33 | 2.07 | 0.42 | 0.26 |
| 2300 | | 0.51 | 0.70 | 0.37 | 0.29 | 0.30 | 0.64 | 0.35 | 2.37 | 0.40 | 0.29 |
| 2400 | | 0.53 | 1.19 | 0.60 | 0.34 | 0.34 | 0.67 | 0.37 | 2.72 | 0.46 | 0.34 |
| 2500 | | 0.66 | 4.40 | 0.89 | 0.53 | 0.53 | 0.97 | 0.89 | 6.22 | 2.89 | 0.53 |

**Table B5**. Weights, $w_i$ , KCRV, $\Delta_{\mathrm{KCRV}}$, and uncertainty of KCR, $u(\Delta_{\mathrm{KCRV}})$

| λ, nm | $w_i$ | | | | | | | | | | | $\Delta_{\mathrm{KCRV}}$, % | $u(\Delta_{\mathrm{KCRV}})$ % |
|---|---|---|---|---|---|---|---|---|---|---|---|---|---|
| | CSIC | KRISS | LNE | NIM | NIST | NMC | NMIJ | NPL | NRC | PTB | VNII OFI | | |
| 250 | 0.014 | 0.088 | 0.017 | 0.149 | 0.142 | 0.096 | 0.049 | 0.103 | 0.041 | 0.151 | 0.151 | **0.64** | **0.29** |
| 260 | 0.012 | 0.087 | 0.070 | 0.145 | 0.123 | 0.102 | 0.045 | 0.077 | 0.049 | 0.145 | 0.145 | **0.50** | **0.25** |
| 270 | 0.010 | 0.083 | 0.091 | 0.141 | 0.109 | 0.105 | 0.041 | 0.058 | 0.082 | 0.141 | 0.141 | **0.40** | **0.23** |
| 280 | 0.011 | 0.085 | 0.121 | 0.138 | 0.102 | 0.085 | 0.038 | 0.058 | 0.087 | 0.137 | 0.138 | **0.33** | **0.22** |
| 290 | 0.010 | 0.081 | 0.131 | 0.135 | 0.097 | 0.100 | 0.035 | 0.064 | 0.083 | 0.130 | 0.135 | **0.42** | **0.20** |
| 300 | 0.007 | 0.083 | 0.133 | 0.141 | 0.093 | 0.097 | 0.034 | 0.061 | 0.083 | 0.127 | 0.141 | **0.49** | **0.19** |
| 320 | 0.010 | 0.089 | 0.139 | 0.139 | 0.094 | 0.096 | 0.032 | 0.050 | 0.088 | 0.123 | 0.139 | **0.41** | **0.18** |
| 340 | 0.009 | 0.093 | 0.140 | 0.140 | 0.095 | 0.102 | 0.030 | 0.050 | 0.085 | 0.116 | 0.140 | **0.51** | **0.17** |
| 360 | 0.010 | 0.091 | 0.140 | 0.140 | 0.097 | 0.106 | 0.029 | 0.047 | 0.086 | 0.113 | 0.140 | **0.54** | **0.16** |
| 380 | 0.010 | 0.101 | 0.139 | 0.139 | 0.097 | 0.108 | 0.028 | 0.041 | 0.085 | 0.112 | 0.139 | **0.57** | **0.15** |
| 400 | 0.008 | 0.093 | 0.126 | 0.141 | 0.087 | 0.100 | 0.025 | 0.037 | 0.141 | 0.102 | 0.141 | **0.44** | **0.14** |
| 450 | 0.006 | 0.093 | 0.123 | 0.135 | 0.089 | 0.094 | 0.023 | 0.070 | 0.135 | 0.097 | 0.135 | **0.24** | **0.12** |
| 500 | 0.005 | 0.095 | 0.108 | 0.134 | 0.091 | 0.100 | 0.021 | 0.079 | 0.134 | 0.097 | 0.134 | **0.18** | **0.11** |
| 555 | 0.004 | 0.091 | 0.107 | 0.136 | 0.096 | 0.099 | 0.020 | 0.078 | 0.136 | 0.098 | 0.136 | **0.18** | **0.11** |
| 600 | 0.004 | 0.092 | 0.097 | 0.136 | 0.100 | 0.099 | 0.020 | 0.082 | 0.136 | 0.097 | 0.136 | **0.16** | **0.10** |
| 700 | 0.004 | 0.087 | 0.060 | 0.141 | 0.106 | 0.112 | 0.019 | 0.089 | 0.142 | 0.098 | 0.142 | **0.08** | **0.09** |
| 800 | 0.004 | 0.085 | 0.047 | 0.138 | 0.124 | 0.092 | 0.019 | 0.100 | 0.144 | 0.102 | 0.144 | **0.23** | **0.09** |
| 900 | 0.002 | 0.090 | 0.111 | 0.110 | 0.138 | 0.034 | 0.017 | 0.106 | 0.147 | 0.099 | 0.147 | **0.16** | **0.08** |
| 1000 | 0.002 | 0.080 | 0.101 | 0.102 | 0.132 | 0.081 | 0.016 | 0.110 | 0.142 | 0.092 | 0.142 | **0.19** | **0.08** |
| 1100 | 0.001 | 0.084 | 0.029 | 0.106 | 0.145 | 0.105 | 0.017 | 0.120 | 0.153 | 0.088 | 0.153 | **0.12** | **0.08** |
| 1300 | 0.002 | 0.097 | 0.049 | 0.122 | 0.155 | 0.124 | 0.019 | 0.155 | 0.049 | 0.074 | 0.155 | **0.22** | **0.08** |
| 1500 | 0.002 | 0.104 | 0.042 | 0.110 | 0.160 | 0.117 | 0.019 | 0.160 | 0.040 | 0.084 | 0.160 | **0.19** | **0.08** |
| 1700 | 0.002 | 0.079 | 0.089 | 0.120 | 0.156 | 0.156 | 0.021 | 0.092 | 0.028 | 0.102 | 0.156 | **0.35** | **0.08** |
| 2000 | 0.000 | 0.062 | 0.072 | 0.131 | 0.172 | 0.156 | 0.025 | 0.097 | 0.014 | 0.100 | 0.172 | **0.33** | **0.09** |
| 2200 | 0.000 | 0.061 | 0.035 | 0.128 | 0.191 | 0.161 | 0.033 | 0.121 | 0.003 | 0.076 | 0.191 | **0.19** | **0.10** |
| 2300 | 0.000 | 0.060 | 0.031 | 0.111 | 0.179 | 0.178 | 0.038 | 0.124 | 0.003 | 0.098 | 0.179 | **0.24** | **0.12** |
| 2400 | 0.000 | 0.077 | 0.015 | 0.059 | 0.181 | 0.181 | 0.048 | 0.156 | 0.003 | 0.099 | 0.181 | **0.29** | **0.14** |
| 2500 | 0.000 | 0.137 | 0.003 | 0.076 | 0.212 | 0.212 | 0.064 | 0.076 | 0.002 | 0.007 | 0.212 | **0.29** | **0.20** |

Table B6. Version 1. Preliminary Degrees of Equivalence: Deviations from KCRV $D_i$ and their associated expanded Uncertainties $U_i$ (Eq. 8.21 and 8.22-8.23), in %

| λ, nm | CSIC | | KRISS | | LNE | | NIM | | NIST | | NMC | | NMIA | | NMIJ | | NPL | | NRC | | PTB | | VNIIOFI | |
|---|---|---|---|---|---|---|---|---|---|---|---|---|---|---|---|---|---|---|---|---|---|---|---|---|
| | $D_i$ | $U_i$ | $D_i$ | $U_i$ | $D_i$ | $U_i$ | $D_i$ | $U_i$ | $D_i$ | $U_i$ | $D_i$ | $U_i$ | $D_i$ | $U_i$ | $D_i$ | $U_i$ | $D_i$ | $U_i$ | $D_i$ | $U_i$ | $D_i$ | $U_i$ | $D_i$ | $U_i$ |
| 250 | -3.80 | 5.02 | 0.28 | 1.95 | 4.62 | 4.57 | 0.53 | 1.44 | 0.09 | 1.48 | -1.14 | 1.86 | -1.63 | 5.68 | -0.21 | 2.68 | -1.31 | 1.78 | 0.23 | 2.93 | 1.12 | 1.40 | -0.44 | 0.91 |
| 260 | -4.80 | 4.86 | 0.38 | 1.74 | 1.17 | 1.97 | 0.24 | 1.24 | -0.03 | 1.43 | -1.04 | 1.59 | -2.35 | 4.72 | 0.31 | 2.48 | -2.08 | 1.86 | 0.51 | 2.38 | 1.29 | 1.27 | -0.32 | 0.81 |
| 270 | -5.45 | 4.83 | 0.39 | 1.63 | 0.38 | 1.55 | 0.00 | 1.16 | -0.43 | 1.40 | -0.50 | 1.43 | -2.41 | 4.11 | 0.56 | 2.39 | -2.12 | 1.97 | 0.63 | 1.64 | 1.27 | 1.18 | -0.29 | 0.76 |
| 280 | -4.92 | 4.43 | 0.08 | 1.50 | 0.42 | 1.23 | 0.13 | 1.13 | -0.10 | 1.36 | -0.79 | 1.50 | -1.96 | 3.75 | 0.58 | 2.31 | -2.18 | 1.85 | 0.45 | 1.48 | 1.02 | 1.14 | -0.14 | 0.72 |
| 290 | -3.86 | 4.40 | -0.01 | 1.45 | 0.31 | 1.11 | 0.11 | 1.02 | 0.07 | 1.31 | -0.82 | 1.29 | -2.12 | 3.55 | 0.41 | 2.26 | -1.61 | 1.64 | 0.52 | 1.43 | 1.08 | 1.11 | -0.27 | 0.68 |
| 300 | -0.91 | 4.96 | -0.14 | 1.36 | 0.36 | 1.04 | -0.02 | 0.94 | 0.21 | 1.27 | -0.75 | 1.24 | -2.24 | 3.30 | 0.53 | 2.20 | -1.45 | 1.60 | 0.45 | 1.36 | 0.92 | 1.07 | -0.39 | 0.66 |
| 320 | 0.47 | 3.88 | -0.36 | 1.21 | 0.80 | 0.93 | -0.11 | 0.90 | 0.15 | 1.18 | -0.87 | 1.16 | -2.46 | 2.91 | 0.38 | 2.10 | -1.92 | 1.66 | 0.23 | 1.22 | 0.77 | 1.01 | -0.23 | 0.62 |
| 340 | 0.70 | 3.64 | -0.34 | 1.10 | 0.71 | 0.87 | 0.03 | 0.82 | -0.04 | 1.09 | -0.69 | 1.04 | -2.55 | 2.58 | 0.30 | 2.00 | -1.73 | 1.55 | 0.35 | 1.16 | 0.81 | 0.97 | -0.36 | 0.60 |
| 360 | 0.81 | 3.42 | -0.28 | 1.06 | 0.74 | 0.82 | -0.05 | 0.78 | -0.23 | 1.02 | -0.62 | 0.97 | -2.39 | 2.29 | 0.24 | 1.93 | -1.55 | 1.52 | 0.43 | 1.09 | 0.83 | 0.94 | -0.40 | 0.57 |
| 380 | 0.73 | 3.22 | -0.33 | 0.95 | 0.93 | 0.78 | -0.04 | 0.75 | -0.30 | 0.97 | -0.70 | 0.92 | -2.37 | 2.02 | 0.28 | 1.87 | -1.43 | 1.54 | 0.36 | 1.05 | 0.78 | 0.90 | -0.43 | 0.57 |
| 400 | 0.85 | 3.22 | -0.26 | 0.90 | 0.88 | 0.75 | 0.02 | 0.68 | -0.16 | 0.93 | -0.57 | 0.86 | -2.26 | 1.81 | 0.96 | 1.81 | -1.35 | 1.47 | -0.29 | 0.69 | 0.78 | 0.85 | -0.26 | 0.52 |
| 450 | 0.93 | 3.20 | -0.28 | 0.80 | 0.45 | 0.69 | 0.27 | 0.63 | 0.25 | 0.82 | -0.67 | 0.80 | -1.53 | 1.37 | 0.80 | 1.70 | -0.84 | 0.94 | -0.20 | 0.63 | 0.49 | 0.78 | -0.08 | 0.47 |
| 500 | 0.79 | 3.40 | -0.22 | 0.73 | 0.37 | 0.68 | 0.24 | 0.59 | 0.28 | 0.75 | -0.70 | 0.71 | -1.06 | 1.04 | 0.78 | 1.62 | -0.63 | 0.81 | -0.10 | 0.57 | 0.42 | 0.72 | -0.04 | 0.44 |
| 555 | 0.71 | 3.60 | -0.20 | 0.70 | 0.40 | 0.64 | 0.29 | 0.54 | 0.19 | 0.68 | -0.53 | 0.67 | -0.68 | 0.79 | 0.70 | 1.54 | -0.61 | 0.76 | -0.14 | 0.53 | 0.28 | 0.67 | -0.05 | 0.40 |
| 600 | 0.79 | 3.40 | -0.15 | 0.67 | 0.36 | 0.65 | 0.30 | 0.52 | 0.24 | 0.64 | -0.51 | 0.64 | -0.48 | 0.69 | 0.62 | 1.50 | -0.62 | 0.71 | -0.12 | 0.49 | 0.19 | 0.65 | 0.00 | 0.37 |
| 700 | 1.64 | 3.20 | 0.02 | 0.63 | 0.07 | 0.77 | 0.35 | 0.48 | 0.16 | 0.57 | -0.37 | 0.55 | -0.09 | 0.86 | 0.51 | 1.42 | -0.54 | 0.63 | -0.14 | 0.43 | 0.13 | 0.59 | 0.06 | 0.34 |
| 800 | 0.69 | 3.21 | 0.27 | 0.62 | 0.45 | 0.85 | 0.27 | 0.47 | -0.19 | 0.50 | 0.51 | 0.59 | 0.24 | 1.20 | 0.49 | 1.37 | -0.62 | 0.57 | -0.26 | 0.41 | -0.08 | 0.56 | -0.06 | 0.33 |
| 900 | 0.27 | 3.80 | -0.18 | 0.56 | 0.55 | 0.50 | 0.28 | 0.50 | 0.13 | 0.44 | 0.69 | 0.94 | 0.64 | 1.41 | 0.69 | 1.34 | -0.61 | 0.51 | -0.40 | 0.36 | -0.08 | 0.53 | 0.02 | 0.31 |
| 1000 | -0.55 | 3.80 | -0.20 | 0.56 | 0.62 | 0.49 | 0.19 | 0.49 | 0.06 | 0.42 | 0.62 | 0.56 | 0.78 | 1.59 | 0.20 | 1.31 | -0.57 | 0.47 | -0.33 | 0.34 | -0.13 | 0.52 | -0.03 | 0.30 |
| 1100 | -0.59 | 4.60 | -0.14 | 0.55 | 0.70 | 0.96 | -0.08 | 0.48 | -0.17 | 0.40 | 0.74 | 0.48 | 1.13 | 1.73 | -0.17 | 1.29 | -0.45 | 0.45 | -0.16 | 0.33 | 0.23 | 0.53 | 0.05 | 0.28 |
| 1300 | -0.05 | 4.03 | -0.17 | 0.53 | 1.07 | 0.77 | -0.02 | 0.46 | -0.31 | 0.37 | 0.80 | 0.46 | 1.23 | 1.91 | -0.27 | 1.27 | -0.52 | 0.40 | 0.53 | 0.77 | -0.24 | 0.62 | -0.05 | 0.29 |
| 1500 | -0.89 | 4.24 | -0.15 | 0.51 | 1.07 | 0.83 | 0.10 | 0.49 | -0.38 | 0.34 | 0.88 | 0.47 | 1.47 | 2.07 | -0.58 | 1.24 | -0.52 | 0.38 | 0.43 | 0.85 | -0.03 | 0.57 | -0.01 | 0.28 |
| 1700 | -7.40 | 4.24 | -0.52 | 0.61 | 1.50 | 0.58 | 0.02 | 0.48 | -0.47 | 0.33 | 0.85 | 0.41 | 1.62 | 2.21 | -0.88 | 1.24 | -0.84 | 0.56 | 0.72 | 1.06 | -0.32 | 0.53 | -0.21 | 0.28 |
| 2000 | | | -0.48 | 0.76 | 2.27 | 0.70 | -0.09 | 0.50 | -0.42 | 0.34 | 0.76 | 0.45 | 2.21 | 2.82 | -1.67 | 1.23 | -0.71 | 0.60 | 0.32 | 1.66 | -0.32 | 0.58 | -0.17 | 0.35 |
| 2200 | | | -1.09 | 0.89 | 3.15 | 1.20 | 0.08 | 0.59 | -0.26 | 0.37 | 0.90 | 0.52 | 2.95 | 2.48 | -2.20 | 1.23 | -0.61 | 0.61 | 1.65 | 4.14 | 0.00 | 0.80 | -0.04 | 0.38 |
| 2300 | | | -0.52 | 0.98 | 4.27 | 1.38 | -0.03 | 0.70 | -0.18 | 0.42 | 0.75 | 0.53 | 4.46 | 2.58 | -1.82 | 1.25 | -0.53 | 0.66 | 0.71 | 4.73 | -0.19 | 0.75 | -0.28 | 0.46 |
| 2400 | | | 0.09 | 1.01 | 6.91 | 2.35 | -0.09 | 1.16 | -0.68 | 0.54 | 0.91 | 0.58 | 5.55 | 2.80 | -2.02 | 1.30 | -0.34 | 0.68 | 2.74 | 5.44 | 0.00 | 0.87 | -0.03 | 0.53 |
| 2500 | | | -0.27 | 1.20 | 7.71 | 8.77 | 0.16 | 1.69 | 0.00 | 0.78 | 1.04 | 0.71 | 8.62 | 2.52 | -1.98 | 1.86 | -1.09 | 1.69 | 3.43 | 12.4 | 0.04 | 5.74 | -0.07 | 0.64 |

### B.4. Consistency check (preliminary)

Table B7 presents Chi-square values $\chi^2_{\text{obs}}$ for consistency check calculated by Eq.8.19 of the Section 8.3 "Method of comparison data analysis", as well as the $\chi^2_{0.05}(\nu)$ value for ν = *N*-1, where *N* is the number of NMIs contribute to KCRV, and the results of the consistency check.

Table B7. Chi-square values $\chi^2_{\text{obs}}$ and the consistency check

| λ, nm | $\chi^2_{\text{obs}}$ | ν = *N*-1 | $\chi^2_{0.05}(\nu)$ | Result of the consistency check |
|---|---|---|---|---|
| 250 | 12.49 | 10 | 18.307 | satisfied |
| 260 | 15.24 | 10 | 18.307 | satisfied |
| 270 | 15.24 | 10 | 18.307 | satisfied |
| 280 | 14.89 | 10 | 18.307 | satisfied |
| 290 | 12.38 | 10 | 18.307 | satisfied |
| 300 | 8.70 | 10 | 18.307 | satisfied |
| 320 | 12.40 | 10 | 18.307 | satisfied |
| 340 | 12.46 | 10 | 18.307 | satisfied |
| 360 | 12.92 | 10 | 18.307 | satisfied |
| 380 | 15.16 | 10 | 18.307 | satisfied |
| 400 | 15.23 | 10 | 18.307 | satisfied |
| 450 | 11.24 | 10 | 18.307 | satisfied |
| 500 | 10.47 | 10 | 18.307 | satisfied |
| 555 | 9.35 | 10 | 18.307 | satisfied |
| 600 | 9.19 | 10 | 18.307 | satisfied |
| 700 | 8.53 | 10 | 18.307 | satisfied |
| 800 | 12.33 | 10 | 18.307 | satisfied |
| 900 | 17.14 | 10 | 18.307 | satisfied |
| 1000 | **19.04** | 10 | 18.307 | **failed** |
| 1100 | 16.24 | 10 | 18.307 | satisfied |
| 1300 | **28.15** | 10 | 18.307 | **failed** |
| 1500 | **29.34** | 10 | 18.307 | **failed** |
| 1700 | **70.86** | 10 | 18.307 | **failed** |
| 2000 | **66.49** | 9 | 16.919 | **failed** |
| 2200 | **59.39** | 9 | 16.919 | **failed** |
| 2300 | **56.28** | 9 | 16.919 | **failed** |
| 2400 | **55.81** | 9 | 16.919 | **failed** |
| 2500 | 13.09 | 9 | 16.919 | satisfied |

### B5. Outliers

Table B8 shows the ratios of absolute values of Deviation from KCRV (DoE), $|D_i|$, to their associated expanded uncertainties, $U_i$, (except NMIA) and the Fig.1 shows the values $D_i$.

Pilot suggests the following outliers:

1) Points for which the Ratios $|D_i|/U_i$ is larger than 2.5. There are 5 such points: LNE/CNAM for wavelengths from 1700 nm to 2400 nm;
2) Point of CSIC at wavelength 1700 nm. Even the ratio $|D_i|/U_i$ for this point is less than 2.0, it looks like obvious outlier at the Fig.B1 (marked with red circle)

Table B8. Ratios $|D_i|/U_i$. Red points are suggested outliers. Bold points indicate the ratios >1

| λ, nm | Ratios $\|D_i\|/U_i$ | | | | | | | | | | |
|---|---|---|---|---|---|---|---|---|---|---|---|
| | CSIC | KRISS | LNE | NIM | NIST | NMC | NMIJ | NPL | NRC | PTB | VNIIOFI |
| 250 | 0.76 | 0.14 | 1.01 | 0.37 | 0.06 | 0.61 | 0.08 | 0.73 | 0.08 | 0.80 | 0.48 |
| 260 | 0.99 | 0.22 | 0.59 | 0.19 | 0.02 | 0.65 | 0.12 | 1.12 | 0.21 | 1.02 | 0.40 |
| 270 | 1.13 | 0.24 | 0.25 | 0.00 | 0.31 | 0.35 | 0.24 | 1.08 | 0.39 | 1.07 | 0.37 |
| 280 | 1.11 | 0.05 | 0.34 | 0.12 | 0.08 | 0.52 | 0.25 | 1.18 | 0.30 | 0.89 | 0.20 |
| 290 | 0.88 | 0.01 | 0.28 | 0.10 | 0.05 | 0.64 | 0.18 | 0.98 | 0.37 | 0.97 | 0.39 |
| 300 | 0.18 | 0.10 | 0.34 | 0.02 | 0.16 | 0.60 | 0.24 | 0.91 | 0.33 | 0.86 | 0.59 |
| 320 | 0.12 | 0.29 | 0.85 | 0.12 | 0.13 | 0.74 | 0.18 | 1.15 | 0.19 | 0.77 | 0.36 |
| 340 | 0.19 | 0.31 | 0.81 | 0.04 | 0.03 | 0.66 | 0.15 | 1.12 | 0.31 | 0.83 | 0.61 |
| 360 | 0.24 | 0.26 | 0.91 | 0.07 | 0.23 | 0.64 | 0.13 | 1.02 | 0.39 | 0.88 | 0.70 |
| 380 | 0.23 | 0.35 | 1.19 | 0.05 | 0.31 | 0.76 | 0.15 | 0.93 | 0.34 | 0.87 | 0.75 |
| 400 | 0.26 | 0.29 | 1.16 | 0.03 | 0.17 | 0.67 | 0.53 | 0.92 | 0.43 | 0.91 | 0.50 |
| 450 | 0.29 | 0.34 | 0.65 | 0.43 | 0.30 | 0.84 | 0.47 | 0.90 | 0.32 | 0.63 | 0.17 |
| 500 | 0.23 | 0.30 | 0.55 | 0.40 | 0.37 | 0.98 | 0.48 | 0.78 | 0.17 | 0.59 | 0.08 |
| 555 | 0.20 | 0.29 | 0.62 | 0.53 | 0.28 | 0.80 | 0.46 | 0.80 | 0.27 | 0.42 | 0.13 |
| 600 | 0.23 | 0.23 | 0.55 | 0.57 | 0.37 | 0.80 | 0.41 | 0.87 | 0.25 | 0.29 | 0.00 |
| 700 | 0.51 | 0.03 | 0.09 | 0.74 | 0.29 | 0.67 | 0.36 | 0.87 | 0.33 | 0.22 | 0.17 |
| 800 | 0.21 | 0.44 | 0.53 | 0.58 | 0.39 | 0.86 | 0.36 | 1.10 | 0.64 | 0.14 | 0.19 |
| 900 | 0.07 | 0.32 | 1.10 | 0.56 | 0.29 | 0.73 | 0.51 | 1.19 | 1.09 | 0.16 | 0.08 |
| 1000 | 0.15 | 0.36 | 1.26 | 0.39 | 0.13 | 1.12 | 0.15 | 1.20 | 0.97 | 0.26 | 0.12 |
| 1100 | 0.13 | 0.26 | 0.73 | 0.16 | 0.42 | 1.54 | 0.13 | 1.01 | 0.48 | 0.44 | 0.17 |
| 1300 | 0.01 | 0.32 | 1.40 | 0.03 | 0.83 | 1.73 | 0.21 | 1.31 | 0.70 | 0.39 | 0.17 |
| 1500 | 0.21 | 0.29 | 1.28 | 0.20 | 1.11 | 1.85 | 0.47 | 1.37 | 0.50 | 0.05 | 0.03 |
| 1700 | **1.74** | 0.84 | **2.59** | 0.04 | 1.41 | 2.05 | 0.70 | 1.50 | 0.68 | 0.60 | 0.73 |
| 2000 | | 0.64 | **3.23** | 0.19 | 1.23 | 1.68 | 1.35 | 1.20 | 0.19 | 0.54 | 0.48 |
| 2200 | | 1.22 | **2.63** | 0.13 | 0.71 | 1.75 | 1.78 | 1.00 | 0.40 | 0.00 | 0.11 |
| 2300 | | 0.53 | **3.09** | 0.04 | 0.44 | 1.42 | 1.45 | 0.81 | 0.15 | 0.25 | 0.60 |
| 2400 | | 0.09 | **2.93** | 0.08 | 1.25 | 1.56 | 1.56 | 0.51 | 0.50 | 0.01 | 0.06 |
| 2500 | | 0.23 | 0.88 | 0.09 | 0.00 | 1.45 | 1.07 | 0.64 | 0.28 | 0.01 | 0.11 |

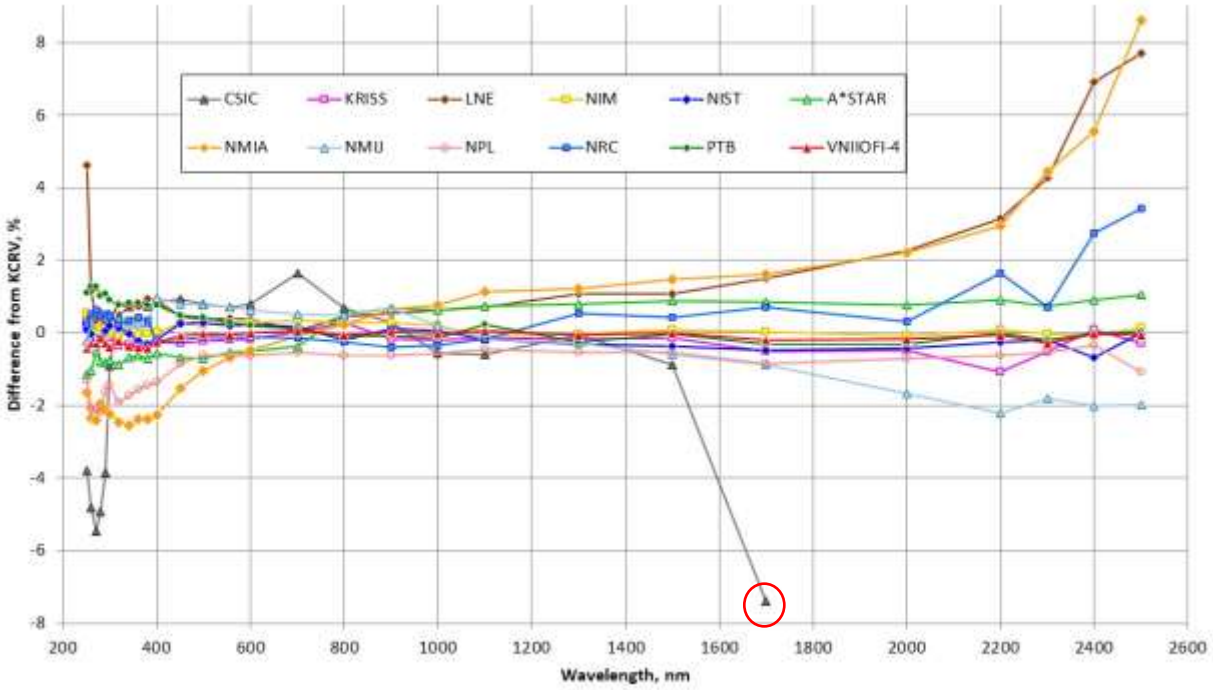


Figure B1. Deviations from KCRV, $D_i$ (preliminary)

**B6. Consistency check after excluding outliers**

Note that after excluding the outliers number *N* of NMI contribute to KCRV is changed as follows:

*N* = 11 for wavelengths 250 nm to 1500 nm;
*N* = 9 for wavelengths 1700 nm to 2400 nm;
*N* = 10 for wavelength 2500 nm.

Table B7a presents the Chi-square values $\chi^2_{\text{obs}}$, $\chi^2_{0.05}(\nu)$ values for ν = *N*-1 and the results of the consistency check after excluding the outliers. Red figures indicate changes from the Table B7.

Table B7a. Chi-square values $\chi^2_{\text{obs}}$ and the consistency check after excluding the outliers

| λ, nm | $\chi^2_{\text{obs}}$ | ν = *N*-1 | $\chi^2_{0.05}(\nu)$ | Result of the consistency check |
|---|---|---|---|---|
| 250 | 12.49 | 10 | 18.307 | satisfied |
| 260 | 15.24 | 10 | 18.307 | satisfied |
| 270 | 15.24 | 10 | 18.307 | satisfied |
| 280 | 14.89 | 10 | 18.307 | satisfied |
| 290 | 12.38 | 10 | 18.307 | satisfied |
| 300 | 8.70 | 10 | 18.307 | satisfied |
| 320 | 12.40 | 10 | 18.307 | satisfied |
| 340 | 12.46 | 10 | 18.307 | satisfied |
| 360 | 12.92 | 10 | 18.307 | satisfied |
| 380 | 15.16 | 10 | 18.307 | satisfied |
| 400 | 15.23 | 10 | 18.307 | satisfied |
| 450 | 11.24 | 10 | 18.307 | satisfied |
| 500 | 10.47 | 10 | 18.307 | satisfied |
| 555 | 9.35 | 10 | 18.307 | satisfied |
| 600 | 9.19 | 10 | 18.307 | satisfied |

| | | | | |
|---|---|---|---|---|
| 700 | 8.53 | 10 | 18.307 | satisfied |
| 800 | 12.33 | 10 | 18.307 | satisfied |
| 900 | 17.14 | 10 | 18.307 | satisfied |
| 1000 | **19.04** | 10 | 18.307 | **failed** |
| 1100 | 16.24 | 10 | 18.307 | satisfied |
| 1300 | **28.15** | 10 | 18.307 | **failed** |
| 1500 | **29.34** | 10 | 18.307 | **failed** |
| 1700 | **32.75** | 8 | 15.507 | **failed** |
| 2000 | **25.05** | 8 | 15.507 | **failed** |
| 2200 | **31.79** | 8 | 15.507 | **failed** |
| 2300 | **18.20** | 8 | 15.507 | **failed** |
| 2400 | **21.41** | 8 | 15.507 | **failed** |
| 2500 | 13.09 | 9 | 16.919 | satisfied |

One can see, that after excluding outliers, although the consistency check is still failed, the Chi-square values $\chi^2_{\text{obs}}$ are much closer to $\chi^2_{0.05}(\nu)$ values.

### B7. Applying Mandel-Paule method

For the wavelengths where $\chi^2_{\text{obs}} > \chi^2_{0.05}(\nu)$ (the consistency check failed) the Mandel-Paule method is applied, i.e. the $s^2$ term is added in the Eq. (8.15, 8.20) of the Section 8.3 "Method of comparison data analysis" for calculation of $u_{\text{adj}}(\Delta_i)$. The values of $s$ are determined by iterative process so that $\chi^2_{\text{obs}} = \chi^2_{0.05}(\nu)$.

Table B7b shows the consistency check results after the Mandel-Paule method, as well as the $s$ values applied. Table 4a presents the $\boldsymbol{u_{\text{adj}}(\Delta_i)}$ uncertainties after applying the Mandel-Paule method.

Table B7b. Chi-square values $\chi^2_{\text{obs}}$ and the consistency check after applying Mandel-Paule method

| λ, nm | $s$, % | $\chi^2_{\text{obs}}$ | ν = $N$-1 | $\chi^2_{0.05}(\nu)$ | Result of the consistency check |
|---|---|---|---|---|---|
| 250 | 0.00 | 12.49 | 10 | 18.307 | satisfied |
| 260 | 0.00 | 15.24 | 10 | 18.307 | satisfied |
| 270 | 0.00 | 15.24 | 10 | 18.307 | satisfied |
| 280 | 0.00 | 14.89 | 10 | 18.307 | satisfied |
| 290 | 0.00 | 12.38 | 10 | 18.307 | satisfied |
| 300 | 0.00 | 8.70 | 10 | 18.307 | satisfied |
| 320 | 0.00 | 12.40 | 10 | 18.307 | satisfied |
| 340 | 0.00 | 12.46 | 10 | 18.307 | satisfied |
| 360 | 0.00 | 12.92 | 10 | 18.307 | satisfied |
| 380 | 0.00 | 15.16 | 10 | 18.307 | satisfied |
| 400 | 0.00 | 15.23 | 10 | 18.307 | satisfied |
| 450 | 0.00 | 11.24 | 10 | 18.307 | satisfied |
| 500 | 0.00 | 10.47 | 10 | 18.307 | satisfied |
| 555 | 0.00 | 9.35 | 10 | 18.307 | satisfied |
| 600 | 0.00 | 9.19 | 10 | 18.307 | satisfied |
| 700 | 0.00 | 8.53 | 10 | 18.307 | satisfied |
| 800 | 0.00 | 12.33 | 10 | 18.307 | satisfied |

| | | | | | |
|---|---|---|---|---|---|
| 900 | 0.00 | 17.14 | 10 | 18.307 | satisfied |
| 1000 | **0.06** | **19.04** | 10 | 18.307 | **satisfied** |
| 1100 | 0.00 | 16.24 | 10 | 18.307 | satisfied |
| 1300 | **0.21** | **28.15** | 10 | 18.307 | **satisfied** |
| 1500 | **0.22** | **29.34** | 10 | 18.307 | **satisfied** |
| 1700 | **0.29** | **32.75** | 8 | 15.507 | **satisfied** |
| 2000 | **0.24** | **25.05** | 8 | 15.507 | **satisfied** |
| 2200 | **0.43** | **31.79** | 8 | 15.507 | **satisfied** |
| 2300 | **0.16** | **18.20** | 8 | 15.507 | **satisfied** |
| 2400 | **0.28** | **21.41** | 8 | 15.507 | **satisfied** |
| 2500 | 0.00 | 13.09 | 9 | 16.919 | satisfied |

Table B4a. Uncertainties $\boldsymbol{u_{adj}(\Delta_i)}$ after Mandel-Paule method (Eq. 8.20)

| λ, nm | $u_{adj}(\Delta_i)$, % | | | | | | | | | | |
|---|---|---|---|---|---|---|---|---|---|---|---|
| | CSIC | KRISS | LNE | NIM | NIST | NMC | NMIJ | NPL | NRC | PTB | VNIIOFI |
| 250 | 2.53 | 1.03 | 2.31 | 0.79 | 0.80 | 0.98 | 1.38 | 0.95 | 1.50 | 0.78 | 0.78 |
| 260 | 2.45 | 0.92 | 1.03 | 0.71 | 0.77 | 0.85 | 1.27 | 0.97 | 1.23 | 0.71 | 0.71 |
| 270 | 2.43 | 0.86 | 0.82 | 0.66 | 0.75 | 0.76 | 1.22 | 1.02 | 0.86 | 0.66 | 0.66 |
| 280 | 2.23 | 0.79 | 0.66 | 0.62 | 0.72 | 0.79 | 1.18 | 0.95 | 0.78 | 0.62 | 0.62 |
| 290 | 2.21 | 0.76 | 0.60 | 0.59 | 0.70 | 0.68 | 1.15 | 0.85 | 0.75 | 0.60 | 0.59 |
| 300 | 2.49 | 0.71 | 0.56 | 0.55 | 0.67 | 0.66 | 1.12 | 0.83 | 0.71 | 0.58 | 0.55 |
| 320 | 1.95 | 0.64 | 0.51 | 0.51 | 0.62 | 0.61 | 1.07 | 0.86 | 0.64 | 0.54 | 0.51 |
| 340 | 1.83 | 0.58 | 0.47 | 0.47 | 0.57 | 0.55 | 1.02 | 0.80 | 0.61 | 0.52 | 0.47 |
| 360 | 1.72 | 0.56 | 0.45 | 0.45 | 0.54 | 0.52 | 0.98 | 0.78 | 0.58 | 0.50 | 0.45 |
| 380 | 1.62 | 0.50 | 0.43 | 0.43 | 0.51 | 0.49 | 0.95 | 0.79 | 0.55 | 0.48 | 0.43 |
| 400 | 1.62 | 0.47 | 0.41 | 0.38 | 0.49 | 0.46 | 0.92 | 0.75 | 0.38 | 0.45 | 0.38 |
| 450 | 1.61 | 0.42 | 0.37 | 0.35 | 0.43 | 0.42 | 0.86 | 0.49 | 0.35 | 0.41 | 0.35 |
| 500 | 1.70 | 0.39 | 0.36 | 0.33 | 0.40 | 0.38 | 0.82 | 0.43 | 0.33 | 0.38 | 0.33 |
| 555 | 1.80 | 0.37 | 0.34 | 0.30 | 0.36 | 0.35 | 0.78 | 0.40 | 0.30 | 0.35 | 0.30 |
| 600 | 1.70 | 0.35 | 0.34 | 0.29 | 0.34 | 0.34 | 0.76 | 0.37 | 0.29 | 0.34 | 0.29 |
| 700 | 1.60 | 0.33 | 0.40 | 0.26 | 0.30 | 0.29 | 0.72 | 0.33 | 0.26 | 0.31 | 0.26 |
| 800 | 1.61 | 0.33 | 0.44 | 0.26 | 0.27 | 0.31 | 0.69 | 0.30 | 0.25 | 0.30 | 0.25 |
| 900 | 1.90 | 0.29 | 0.27 | 0.27 | 0.24 | 0.48 | 0.68 | 0.27 | 0.23 | 0.28 | 0.23 |
| 1000 | 1.90 | 0.30 | 0.27 | 0.27 | 0.24 | 0.30 | 0.66 | 0.26 | 0.23 | 0.28 | 0.23 |
| 1100 | 2.30 | 0.29 | 0.49 | 0.26 | 0.22 | 0.26 | 0.65 | 0.24 | 0.21 | 0.28 | 0.21 |
| 1300 | 2.03 | 0.35 | 0.45 | 0.33 | 0.31 | 0.33 | 0.67 | 0.31 | 0.45 | 0.38 | 0.31 |
| 1500 | 2.13 | 0.35 | 0.48 | 0.34 | 0.31 | 0.34 | 0.67 | 0.31 | 0.49 | 0.37 | 0.31 |
| 1700 | 2.14 | 0.43 | 0.42 | 0.39 | 0.36 | 0.37 | 0.69 | 0.42 | 0.61 | 0.40 | 0.36 |
| 2000 | | 0.46 | 0.44 | 0.36 | 0.34 | 0.35 | 0.67 | 0.40 | 0.87 | 0.39 | 0.34 |
| 2200 | | 0.63 | 0.75 | 0.54 | 0.50 | 0.52 | 0.76 | 0.54 | 2.12 | 0.60 | 0.50 |
| 2300 | | 0.53 | 0.72 | 0.41 | 0.34 | 0.34 | 0.66 | 0.39 | 2.37 | 0.43 | 0.34 |
| 2400 | | 0.60 | 1.22 | 0.66 | 0.44 | 0.44 | 0.72 | 0.46 | 2.74 | 0.54 | 0.44 |
| 2500 | | 0.66 | 4.40 | 0.89 | 0.53 | 0.53 | 0.97 | 0.89 | 6.22 | 2.89 | 0.53 |

## B8. Final results

Tables B5a and B6a are the final versions of KCRV and DoEs, respectively, after excluding outliers and applying the Mandel-Paule method. The final deviations from KCRV, $D_i$, are also shown in Fig.B2 and Fig.B2a.

Table B5a. Final values KCRV, $\Delta_{\mathrm{KCRV}}$, and uncertainty of KCR, $u(\Delta_{\mathrm{KCRV}})$, in %

| λ, nm | $\boldsymbol{\Delta_{\mathrm{KCRV}}}$ | $\boldsymbol{u(\Delta_{\mathrm{KCRV}})}$ |
|---|---|---|
| 250 | **0.64** | **0.29** |
| 260 | **0.50** | **0.25** |
| 270 | **0.40** | **0.23** |
| 280 | **0.33** | **0.22** |
| 290 | **0.42** | **0.20** |
| 300 | **0.49** | **0.19** |
| 320 | **0.41** | **0.18** |
| 340 | **0.51** | **0.17** |
| 360 | **0.54** | **0.16** |
| 380 | **0.57** | **0.15** |
| 400 | **0.44** | **0.14** |
| 450 | **0.24** | **0.12** |
| 500 | **0.18** | **0.11** |
| 555 | **0.18** | **0.11** |
| 600 | **0.16** | **0.10** |
| 700 | **0.08** | **0.09** |
| 800 | **0.23** | **0.09** |
| 900 | **0.16** | **0.08** |
| 1000 | **0.19** | **0.08** |
| 1100 | **0.12** | **0.08** |
| 1300 | **0.25** | **0.08** |
| 1500 | **0.23** | **0.08** |
| 1700 | **0.18** | **0.09** |
| 2000 | **0.11** | **0.10** |
| 2200 | **-0.04** | **0.12** |
| 2300 | **0.08** | **0.12** |
| 2400 | **0.16** | **0.14** |
| 2500 | **0.29** | **0.20** |

Table B6a. Version 1. Final values of Degrees of Equivalence: Deviations from KCRV $D_i$ and their associated Uncertainties $U_i$ (Eq. 8.21 and 8.22-8.23), in %

| λ, nm | CSIC | | KRISS | | LNE | | NIM | | NIST | | NMC | | NMIA | | NMIJ | | NPL | | NRC | | PTB | | VNIIOFI | |
|---|---|---|---|---|---|---|---|---|---|---|---|---|---|---|---|---|---|---|---|---|---|---|---|---|
| | $D_i$ | $U_i$ | $D_i$ | $U_i$ | $D_i$ | $U_i$ | $D_i$ | $U_i$ | $D_i$ | $U_i$ | $D_i$ | $U_i$ | $D_i$ | $U_i$ | $D_i$ | $U_i$ | $D_i$ | $U_i$ | $D_i$ | $U_i$ | $D_i$ | $U_i$ | $D_i$ | $U_i$ |
| 250 | -3.80 | 5.02 | 0.28 | 1.95 | 4.62 | 4.57 | 0.53 | 1.44 | 0.09 | 1.48 | -1.14 | 1.86 | -1.63 | 5.74 | -0.21 | 2.68 | -1.31 | 1.78 | 0.23 | 2.93 | 1.12 | 1.40 | -0.44 | 0.91 |
| 260 | -4.80 | 4.86 | 0.38 | 1.74 | 1.17 | 1.97 | 0.24 | 1.24 | -0.03 | 1.43 | -1.04 | 1.59 | -2.35 | 4.79 | 0.31 | 2.48 | -2.08 | 1.86 | 0.51 | 2.38 | 1.29 | 1.27 | -0.32 | 0.81 |
| 270 | -5.45 | 4.83 | 0.39 | 1.63 | 0.38 | 1.55 | 0.00 | 1.16 | -0.43 | 1.40 | -0.50 | 1.43 | -2.41 | 4.16 | 0.56 | 2.39 | -2.12 | 1.97 | 0.63 | 1.64 | 1.27 | 1.18 | -0.29 | 0.76 |
| 280 | -4.92 | 4.43 | 0.08 | 1.50 | 0.42 | 1.23 | 0.13 | 1.13 | -0.10 | 1.36 | -0.79 | 1.50 | -1.96 | 3.80 | 0.58 | 2.31 | -2.18 | 1.85 | 0.45 | 1.48 | 1.02 | 1.14 | -0.14 | 0.72 |
| 290 | -3.86 | 4.40 | -0.01 | 1.45 | 0.31 | 1.11 | 0.11 | 1.02 | 0.07 | 1.31 | -0.82 | 1.29 | -2.12 | 3.60 | 0.41 | 2.26 | -1.61 | 1.64 | 0.52 | 1.43 | 1.08 | 1.11 | -0.27 | 0.68 |
| 300 | -0.91 | 4.96 | -0.14 | 1.36 | 0.36 | 1.04 | -0.02 | 0.94 | 0.21 | 1.27 | -0.75 | 1.24 | -2.24 | 3.35 | 0.53 | 2.20 | -1.45 | 1.60 | 0.45 | 1.36 | 0.92 | 1.07 | -0.39 | 0.66 |
| 320 | 0.47 | 3.88 | -0.36 | 1.21 | 0.80 | 0.93 | -0.11 | 0.90 | 0.15 | 1.18 | -0.87 | 1.16 | -2.46 | 2.96 | 0.38 | 2.10 | -1.92 | 1.66 | 0.23 | 1.22 | 0.77 | 1.01 | -0.23 | 0.62 |
| 340 | 0.70 | 3.64 | -0.34 | 1.10 | 0.71 | 0.87 | 0.03 | 0.82 | -0.04 | 1.09 | -0.69 | 1.04 | -2.55 | 2.63 | 0.30 | 2.00 | -1.73 | 1.55 | 0.35 | 1.16 | 0.81 | 0.97 | -0.36 | 0.60 |
| 360 | 0.81 | 3.42 | -0.28 | 1.06 | 0.74 | 0.82 | -0.05 | 0.78 | -0.23 | 1.02 | -0.62 | 0.97 | -2.39 | 2.34 | 0.24 | 1.93 | -1.55 | 1.52 | 0.43 | 1.09 | 0.83 | 0.94 | -0.40 | 0.57 |
| 380 | 0.73 | 3.22 | -0.33 | 0.95 | 0.93 | 0.78 | -0.04 | 0.75 | -0.30 | 0.97 | -0.70 | 0.92 | -2.37 | 2.07 | 0.28 | 1.87 | -1.43 | 1.54 | 0.36 | 1.05 | 0.78 | 0.90 | -0.43 | 0.57 |
| 400 | 0.85 | 3.22 | -0.26 | 0.90 | 0.88 | 0.75 | 0.02 | 0.68 | -0.16 | 0.93 | -0.57 | 0.86 | -2.26 | 1.86 | 0.96 | 1.81 | -1.35 | 1.47 | -0.29 | 0.69 | 0.78 | 0.85 | -0.26 | 0.52 |
| 450 | 0.93 | 3.20 | -0.28 | 0.80 | 0.45 | 0.69 | 0.27 | 0.63 | 0.25 | 0.82 | -0.67 | 0.80 | -1.53 | 1.42 | 0.80 | 1.70 | -0.84 | 0.94 | -0.20 | 0.63 | 0.49 | 0.78 | -0.08 | 0.47 |
| 500 | 0.79 | 3.40 | -0.22 | 0.73 | 0.37 | 0.68 | 0.24 | 0.59 | 0.28 | 0.75 | -0.70 | 0.71 | -1.06 | 1.09 | 0.78 | 1.62 | -0.63 | 0.81 | -0.10 | 0.57 | 0.42 | 0.72 | -0.04 | 0.44 |
| 555 | 0.71 | 3.60 | -0.20 | 0.70 | 0.40 | 0.64 | 0.29 | 0.54 | 0.19 | 0.68 | -0.53 | 0.67 | -0.68 | 0.85 | 0.70 | 1.54 | -0.61 | 0.76 | -0.14 | 0.53 | 0.28 | 0.67 | -0.05 | 0.40 |
| 600 | 0.79 | 3.40 | -0.15 | 0.67 | 0.36 | 0.65 | 0.30 | 0.52 | 0.24 | 0.64 | -0.51 | 0.64 | -0.48 | 0.75 | 0.62 | 1.50 | -0.62 | 0.71 | -0.12 | 0.49 | 0.19 | 0.65 | 0.00 | 0.37 |
| 700 | 1.64 | 3.20 | 0.02 | 0.63 | 0.07 | 0.77 | 0.35 | 0.48 | 0.16 | 0.57 | -0.37 | 0.55 | -0.09 | 0.91 | 0.51 | 1.42 | -0.54 | 0.63 | -0.14 | 0.43 | 0.13 | 0.59 | 0.06 | 0.34 |
| 800 | 0.69 | 3.21 | 0.27 | 0.62 | 0.45 | 0.85 | 0.27 | 0.47 | -0.19 | 0.50 | 0.51 | 0.59 | 0.24 | 1.23 | 0.49 | 1.37 | -0.62 | 0.57 | -0.26 | 0.41 | -0.08 | 0.56 | -0.06 | 0.33 |
| 900 | 0.27 | 3.80 | -0.18 | 0.56 | 0.55 | 0.50 | 0.28 | 0.50 | 0.13 | 0.44 | 0.69 | 0.94 | 0.64 | 1.43 | 0.69 | 1.34 | -0.61 | 0.51 | -0.40 | 0.36 | -0.08 | 0.53 | 0.02 | 0.31 |
| 1000 | -0.55 | 3.80 | -0.20 | 0.56 | 0.62 | 0.49 | 0.19 | 0.49 | 0.05 | 0.42 | 0.62 | 0.56 | 0.78 | 1.60 | 0.20 | 1.31 | -0.57 | 0.47 | -0.33 | 0.34 | -0.13 | 0.52 | -0.04 | 0.30 |
| 1100 | -0.59 | 4.60 | -0.14 | 0.55 | 0.70 | 0.96 | -0.08 | 0.48 | -0.17 | 0.40 | 0.74 | 0.48 | 1.13 | 1.75 | -0.17 | 1.29 | -0.45 | 0.45 | -0.16 | 0.33 | 0.23 | 0.53 | 0.05 | 0.28 |
| 1300 | -0.08 | 4.03 | -0.20 | 0.53 | 1.04 | 0.76 | -0.05 | 0.47 | -0.34 | 0.38 | 0.77 | 0.46 | 1.20 | 1.93 | -0.30 | 1.25 | -0.55 | 0.41 | 0.50 | 0.76 | -0.27 | 0.61 | -0.08 | 0.30 |
| 1500 | -0.92 | 4.24 | -0.18 | 0.51 | 1.03 | 0.82 | 0.07 | 0.49 | -0.41 | 0.35 | 0.84 | 0.48 | 1.44 | 2.09 | -0.62 | 1.23 | -0.56 | 0.39 | 0.39 | 0.84 | -0.06 | 0.57 | -0.04 | 0.29 |
| 1700 | -7.23 | 4.25 | -0.35 | 0.60 | 1.66 | 0.64 | 0.18 | 0.48 | -0.31 | 0.34 | 1.01 | 0.43 | 1.78 | 2.22 | -0.71 | 1.22 | -0.68 | 0.56 | 0.88 | 1.04 | -0.16 | 0.53 | -0.05 | 0.30 |
| 2000 | | | -0.27 | 0.74 | 2.48 | 0.76 | 0.12 | 0.50 | -0.21 | 0.35 | 0.97 | 0.46 | 2.42 | 2.84 | -1.45 | 1.21 | -0.50 | 0.59 | 0.53 | 1.65 | -0.10 | 0.57 | 0.05 | 0.36 |
| 2200 | | | -0.86 | 0.86 | 3.38 | 1.25 | 0.30 | 0.60 | -0.04 | 0.39 | 1.13 | 0.53 | 3.18 | 2.51 | -1.97 | 1.20 | -0.39 | 0.61 | 1.88 | 4.12 | 0.22 | 0.77 | 0.18 | 0.41 |
| 2300 | | | -0.36 | 0.97 | 4.43 | 1.43 | 0.13 | 0.70 | -0.03 | 0.43 | 0.91 | 0.53 | 4.62 | 2.60 | -1.66 | 1.25 | -0.37 | 0.66 | 0.87 | 4.72 | -0.03 | 0.75 | -0.12 | 0.46 |
| 2400 | | | 0.23 | 0.99 | 7.04 | 2.39 | 0.04 | 1.15 | -0.54 | 0.55 | 1.04 | 0.59 | 5.69 | 2.84 | -1.89 | 1.28 | -0.21 | 0.68 | 2.87 | 5.43 | 0.13 | 0.87 | 0.10 | 0.54 |
| 2500 | | | -0.27 | 1.20 | 7.71 | 8.77 | 0.16 | 1.69 | 0.00 | 0.78 | 1.04 | 0.71 | 8.62 | 2.62 | -1.98 | 1.86 | -1.09 | 1.69 | 3.42 | 12.4 | 0.04 | 5.74 | -0.07 | 0.64 |

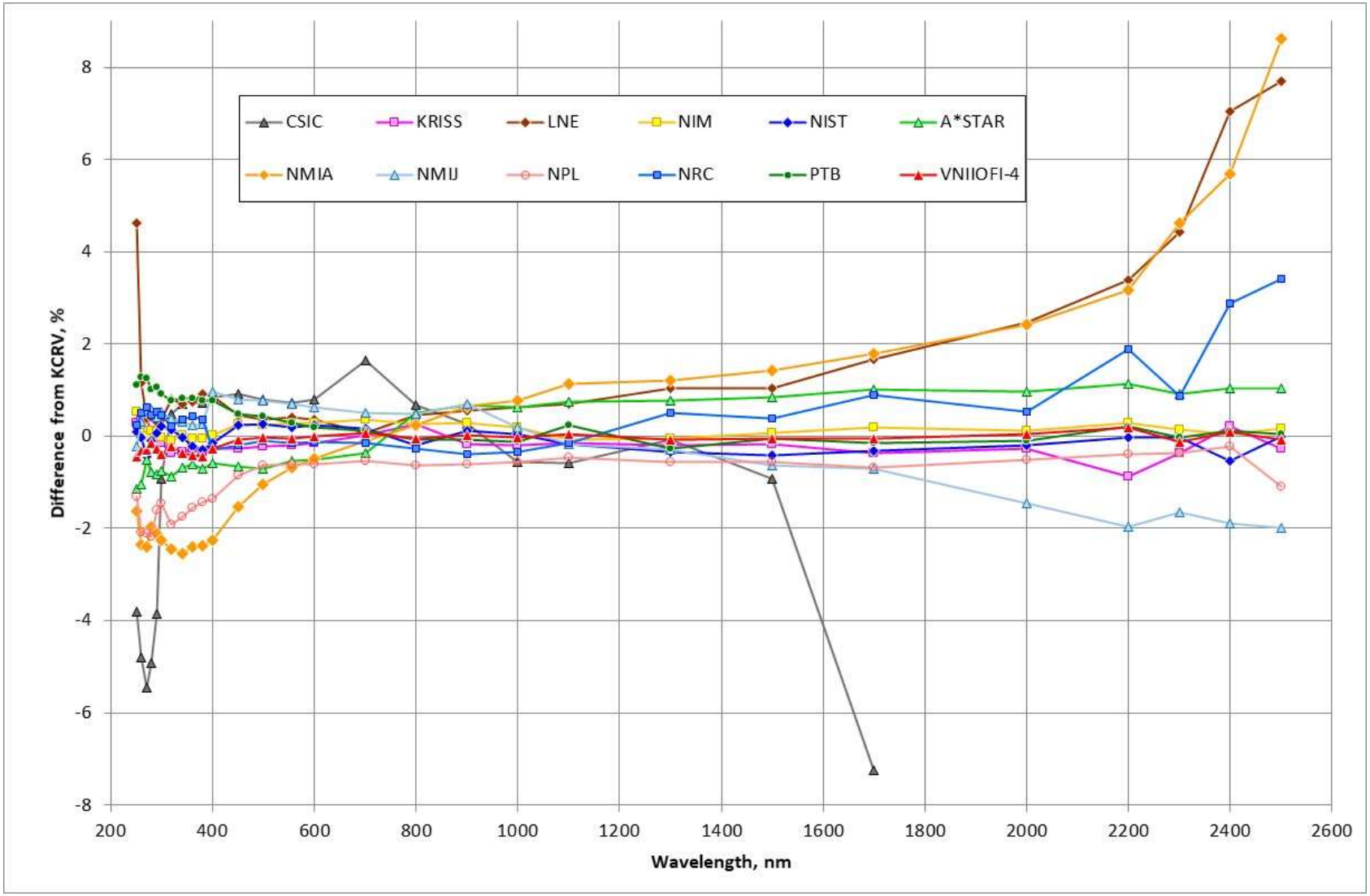


Figure B2. Final deviations from KCRV, $D_i$

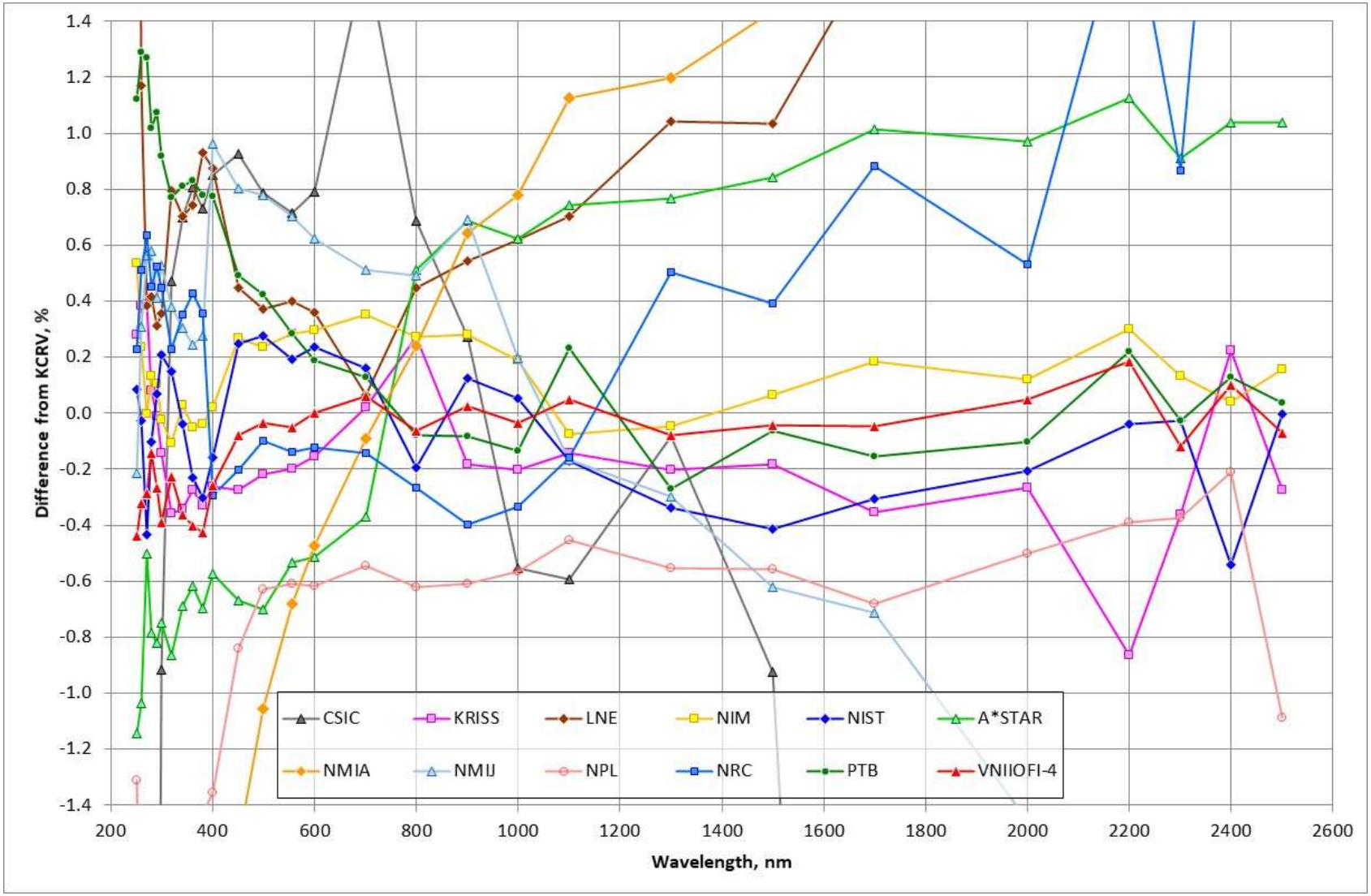


Figure B2a. Final deviations from KCRV, $D_i$. Central part.

# Appendix C

## Data Analysis Results. Version 2 (not final)

In this version the following data are **not used for calculation of KCRV:**

**all data of NMIA, all data of NPL and data of LNE for wavelength ranges from 800 nm to 1100 nm and from 1700 nm to 2500 nm.**

Note that CSIC submitted measurement data for the wavelength rage from 250 nm to 1700 nm only. Therefore, the total number, *N*, of NMIs contribute to KCRV is:

*N* = 10 for the wavelengths from 250 nm to 700 nm, 1300 nm and 1500 nm;
*N* = 9 for the wavelengths from 800 nm to 1100 nm, and 1700 nm;
*N* = 8 for the wavelengths from 2000 nm to 2500 nm.

### C1. Calculation of Differences from Pilot

The **relative average differences** $\Delta_i$ of NMI Spectral Irradiance data to the Pilot Spectral Irradiance data and the **uncertainties** $u(\Delta_i)$ of these differences (Eq.8.6 and Eq.8.7 of the Section 8.3 "Method of comparison data analysis", respectively) are presented in Table C1 and Table C2, respectively.

Table C1. Relative average differences $\Delta_i$ of NMI-to-Pilot data (Eq. 8.6 of the Section 8.3)

| λ, nm | $\Delta_i$, % | | | | | | | | | | | |
|---|---|---|---|---|---|---|---|---|---|---|---|---|
| | CSIC | KRISS | LNE | NIM | NIST | NMC | NMIA | NMIJ | NPL | NRC | PTB | VNIIOFI |
| 250 | -3.16 | 0.92 | 5.26 | 1.17 | 0.72 | -0.50 | -0.99 | 0.43 | -0.67 | 0.87 | 1.76 | 0.20 |
| 260 | -4.30 | 0.88 | 1.67 | 0.74 | 0.47 | -0.54 | -1.85 | 0.81 | -1.58 | 1.01 | 1.79 | 0.18 |
| 270 | -5.06 | 0.78 | 0.78 | 0.39 | -0.04 | -0.10 | -2.01 | 0.96 | -1.72 | 1.03 | 1.67 | 0.11 |
| 280 | -4.59 | 0.41 | 0.75 | 0.46 | 0.23 | -0.46 | -1.63 | 0.91 | -1.85 | 0.78 | 1.35 | 0.18 |
| 290 | -3.44 | 0.41 | 0.73 | 0.53 | 0.49 | -0.40 | -1.70 | 0.83 | -1.19 | 0.94 | 1.50 | 0.15 |
| 300 | -0.42 | 0.35 | 0.85 | 0.47 | 0.70 | -0.26 | -1.75 | 1.02 | -0.96 | 0.94 | 1.41 | 0.10 |
| 320 | 0.88 | 0.05 | 1.20 | 0.30 | 0.55 | -0.46 | -2.05 | 0.79 | -1.51 | 0.63 | 1.18 | 0.18 |
| 340 | 1.21 | 0.17 | 1.21 | 0.54 | 0.47 | -0.18 | -2.04 | 0.81 | -1.23 | 0.86 | 1.32 | 0.14 |
| 360 | 1.35 | 0.27 | 1.29 | 0.49 | 0.31 | -0.07 | -1.84 | 0.79 | -1.01 | 0.97 | 1.37 | 0.14 |
| 380 | 1.30 | 0.24 | 1.50 | 0.53 | 0.26 | -0.13 | -1.81 | 0.84 | -0.86 | 0.92 | 1.35 | 0.14 |
| 400 | 1.29 | 0.18 | 1.32 | 0.46 | 0.28 | -0.13 | -1.82 | 1.40 | -0.91 | 0.15 | 1.22 | 0.18 |
| 450 | 1.17 | -0.03 | 0.69 | 0.51 | 0.49 | -0.42 | -1.29 | 1.05 | -0.60 | 0.04 | 0.74 | 0.16 |
| 500 | 0.97 | -0.04 | 0.56 | 0.42 | 0.46 | -0.52 | -0.87 | 0.96 | -0.45 | 0.09 | 0.61 | 0.15 |
| 555 | 0.90 | -0.02 | 0.58 | 0.47 | 0.37 | -0.35 | -0.50 | 0.88 | -0.43 | 0.04 | 0.47 | 0.13 |
| 600 | 0.95 | 0.01 | 0.52 | 0.46 | 0.39 | -0.35 | -0.32 | 0.78 | -0.46 | 0.04 | 0.35 | 0.16 |
| 700 | 1.72 | 0.10 | 0.15 | 0.44 | 0.24 | -0.29 | -0.01 | 0.59 | -0.46 | -0.06 | 0.21 | 0.14 |
| 800 | 0.92 | 0.50 | 0.68 | 0.50 | 0.03 | 0.74 | 0.47 | 0.72 | -0.40 | -0.04 | 0.15 | 0.17 |
| 900 | 0.43 | -0.03 | 0.70 | 0.43 | 0.28 | 0.84 | 0.80 | 0.85 | -0.45 | -0.24 | 0.07 | 0.18 |
| 1000 | -0.37 | -0.01 | 0.81 | 0.38 | 0.24 | 0.81 | 0.97 | 0.39 | -0.38 | -0.14 | 0.05 | 0.15 |
| 1100 | -0.47 | -0.02 | 0.82 | 0.04 | -0.05 | 0.86 | 1.25 | -0.05 | -0.33 | -0.04 | 0.35 | 0.17 |
| 1300 | 0.17 | 0.05 | 1.29 | 0.20 | -0.09 | 1.02 | 1.45 | -0.05 | -0.30 | 0.75 | -0.02 | 0.17 |
| 1500 | -0.70 | 0.04 | 1.26 | 0.29 | -0.19 | 1.07 | 1.66 | -0.39 | -0.33 | 0.62 | 0.16 | 0.18 |
| 1700 | -7.05 | -0.17 | 1.84 | 0.37 | -0.12 | 1.20 | 1.97 | -0.53 | -0.50 | 1.07 | 0.03 | 0.14 |
| 2000 | | -0.15 | 2.59 | 0.23 | -0.09 | 1.09 | 2.54 | -1.34 | -0.39 | 0.65 | 0.01 | 0.16 |
| 2200 | | -0.90 | 3.34 | 0.26 | -0.07 | 1.09 | 3.14 | -2.01 | -0.43 | 1.84 | 0.19 | 0.15 |
| 2300 | | -0.28 | 4.52 | 0.22 | 0.06 | 0.99 | 4.71 | -1.57 | -0.29 | 0.95 | 0.06 | -0.04 |
| 2400 | | 0.39 | 7.20 | 0.20 | -0.38 | 1.20 | 5.85 | -1.73 | -0.05 | 3.03 | 0.29 | 0.26 |
| 2500 | | 0.02 | 8.00 | 0.45 | 0.29 | 1.33 | 8.91 | -1.69 | -0.79 | 3.72 | 0.33 | 0.22 |

Table C2. Uncertainties $u(\Delta_i)$ of relative average differences (Eq. 8.7 of the Section 8.3)

| λ, nm | $u(\Delta_i)$, % | | | | | | | | | | | |
|---|---|---|---|---|---|---|---|---|---|---|---|---|
| | CSIC | KRISS | LNE | NIM | NIST | NMC | NMIA | NMIJ | NPL | NRC | PTB | VNIIOFI |
| 250 | 2.53 | 1.03 | 2.31 | 0.79 | 0.80 | 0.98 | 2.86 | 1.38 | 0.95 | 1.50 | 0.76 | 0.43 |
| 260 | 2.45 | 0.92 | 1.03 | 0.67 | 0.77 | 0.85 | 2.38 | 1.27 | 0.97 | 1.23 | 0.69 | 0.38 |
| 270 | 2.43 | 0.86 | 0.82 | 0.62 | 0.75 | 0.76 | 2.07 | 1.22 | 1.02 | 0.86 | 0.64 | 0.36 |
| 280 | 2.23 | 0.79 | 0.66 | 0.61 | 0.72 | 0.79 | 1.89 | 1.18 | 0.95 | 0.78 | 0.62 | 0.34 |
| 290 | 2.21 | 0.76 | 0.60 | 0.55 | 0.70 | 0.68 | 1.79 | 1.15 | 0.85 | 0.75 | 0.60 | 0.32 |
| 300 | 2.49 | 0.71 | 0.56 | 0.51 | 0.67 | 0.66 | 1.66 | 1.12 | 0.83 | 0.71 | 0.58 | 0.32 |
| 320 | 1.95 | 0.64 | 0.51 | 0.48 | 0.62 | 0.61 | 1.47 | 1.07 | 0.86 | 0.64 | 0.54 | 0.30 |
| 340 | 1.83 | 0.58 | 0.47 | 0.44 | 0.57 | 0.55 | 1.30 | 1.02 | 0.80 | 0.61 | 0.52 | 0.29 |
| 360 | 1.72 | 0.56 | 0.44 | 0.42 | 0.54 | 0.52 | 1.16 | 0.98 | 0.78 | 0.58 | 0.50 | 0.28 |
| 380 | 1.62 | 0.50 | 0.42 | 0.40 | 0.51 | 0.49 | 1.03 | 0.95 | 0.79 | 0.55 | 0.48 | 0.28 |
| 400 | 1.62 | 0.47 | 0.41 | 0.36 | 0.49 | 0.46 | 0.92 | 0.92 | 0.75 | 0.37 | 0.45 | 0.26 |
| 450 | 1.61 | 0.42 | 0.37 | 0.34 | 0.43 | 0.42 | 0.70 | 0.86 | 0.49 | 0.34 | 0.41 | 0.24 |
| 500 | 1.70 | 0.39 | 0.36 | 0.32 | 0.40 | 0.38 | 0.53 | 0.82 | 0.43 | 0.31 | 0.38 | 0.22 |
| 555 | 1.80 | 0.37 | 0.34 | 0.29 | 0.36 | 0.35 | 0.41 | 0.78 | 0.40 | 0.28 | 0.35 | 0.20 |
| 600 | 1.70 | 0.35 | 0.34 | 0.28 | 0.34 | 0.34 | 0.36 | 0.76 | 0.37 | 0.26 | 0.34 | 0.18 |
| 700 | 1.60 | 0.33 | 0.40 | 0.26 | 0.30 | 0.29 | 0.44 | 0.72 | 0.33 | 0.23 | 0.31 | 0.17 |
| 800 | 1.61 | 0.33 | 0.44 | 0.26 | 0.27 | 0.31 | 0.61 | 0.69 | 0.30 | 0.22 | 0.30 | 0.16 |
| 900 | 1.90 | 0.29 | 0.27 | 0.27 | 0.24 | 0.48 | 0.71 | 0.68 | 0.27 | 0.19 | 0.28 | 0.16 |
| 1000 | 1.90 | 0.29 | 0.26 | 0.26 | 0.23 | 0.29 | 0.80 | 0.66 | 0.25 | 0.18 | 0.27 | 0.15 |
| 1100 | 2.30 | 0.29 | 0.49 | 0.26 | 0.22 | 0.26 | 0.87 | 0.65 | 0.24 | 0.17 | 0.28 | 0.14 |
| 1300 | 2.02 | 0.28 | 0.39 | 0.25 | 0.20 | 0.25 | 0.96 | 0.64 | 0.22 | 0.40 | 0.32 | 0.14 |
| 1500 | 2.12 | 0.27 | 0.43 | 0.26 | 0.18 | 0.26 | 1.04 | 0.63 | 0.21 | 0.43 | 0.30 | 0.14 |
| 1700 | 2.12 | 0.32 | 0.31 | 0.26 | 0.17 | 0.23 | 1.11 | 0.63 | 0.30 | 0.54 | 0.28 | 0.14 |
| 2000 | | 0.39 | 0.37 | 0.27 | 0.18 | 0.25 | 1.42 | 0.63 | 0.32 | 0.84 | 0.31 | 0.18 |
| 2200 | | 0.46 | 0.61 | 0.32 | 0.19 | 0.29 | 1.25 | 0.63 | 0.33 | 2.07 | 0.42 | 0.20 |
| 2300 | | 0.51 | 0.70 | 0.37 | 0.22 | 0.30 | 1.30 | 0.64 | 0.36 | 2.37 | 0.40 | 0.25 |
| 2400 | | 0.53 | 1.19 | 0.60 | 0.29 | 0.32 | 1.41 | 0.67 | 0.37 | 2.73 | 0.46 | 0.29 |
| 2500 | | 0.66 | 4.40 | 0.89 | 0.43 | 0.39 | 1.29 | 0.97 | 0.89 | 6.22 | 2.89 | 0.33 |

## C2. Calculation of KCRV

**Cut-off** is calculated following Eq.8.10 – 8.12 of the Section 8.3 "Method of comparison data analysis". Values of relative average uncertainties of spectral irradiance $u(E_i)$, Median and Cut-off are presented in Table C3

**Uncertainties $u_{\mathbf{adj}}(\Delta_i)$ after cut-off** of relative average differences (Eq.8.15, 8.20) are presented in Table C4. At this stage $s = 0$.

Table C5 presents the **weights $w_i$ , KCRV $\Delta_{\mathbf{KCRV}}$ and uncertainty of KCR $u(\Delta_{\mathbf{KCRV}})$,** determent by Equations 8.16, 8.17 and 8.18, respectively.

## C3. Calculation of preliminary values of Degrees of Equivalence

Preliminary Degrees of Equivalence, i.e. Deviations from KCRV, $D_i$, and their associated expanded uncertainties, $U_i$, (Eq.8.21 and 8.22-8.23, respectively) are presented in Table C6.

Table C3. Relative average uncertainties of spectral irradiance $u(E_i)$, Median and Cut-off in %

| λ, nm | $u(E_i)$, % | | | | | | | | | | Median | **Cut-off** |
|---|---|---|---|---|---|---|---|---|---|---|---|---|
| | CSIC | KRISS | LNE | NIM | NIST | NMC | NMIJ | NRC | PTB | VNIIOFI | | |
| 250 | 2.52 | 1.00 | 2.30 | 0.76 | 0.78 | 0.96 | 1.36 | 1.49 | 0.73 | 0.37 | 0.98 | **0.72** |
| 260 | 2.44 | 0.90 | 1.01 | 0.65 | 0.75 | 0.83 | 1.26 | 1.21 | 0.67 | 0.34 | 0.86 | **0.65** |
| 270 | 2.42 | 0.84 | 0.80 | 0.60 | 0.73 | 0.74 | 1.21 | 0.85 | 0.62 | 0.32 | 0.77 | **0.60** |
| 280 | 2.22 | 0.77 | 0.65 | 0.59 | 0.71 | 0.77 | 1.17 | 0.77 | 0.60 | 0.30 | 0.74 | **0.57** |
| 290 | 2.21 | 0.75 | 0.58 | 0.53 | 0.681 | 0.67 | 1.14 | 0.74 | 0.58 | 0.29 | 0.675 | **0.55** |
| 300 | 2.49 | 0.70 | 0.54 | 0.49 | 0.66 | 0.64 | 1.11 | 0.70 | 0.56 | 0.28 | 0.65 | **0.50** |
| 320 | 1.95 | 0.63 | 0.49 | 0.47 | 0.609 | 0.60 | 1.06 | 0.63 | 0.53 | 0.27 | 0.606 | **0.47** |
| 340 | 1.82 | 0.57 | 0.46 | 0.42 | 0.56 | 0.54 | 1.01 | 0.60 | 0.51 | 0.27 | 0.55 | **0.44** |
| 360 | 1.71 | 0.54 | 0.43 | 0.41 | 0.53 | 0.50 | 0.97 | 0.56 | 0.49 | 0.25 | 0.51 | **0.41** |
| 380 | 1.61 | 0.49 | 0.41 | 0.39 | 0.50 | 0.475 | 0.94 | 0.54 | 0.47 | 0.26 | 0.483 | **0.40** |
| 400 | 1.61 | 0.46 | 0.39 | 0.35 | 0.48 | 0.442 | 0.91 | 0.36 | 0.439 | 0.24 | 0.440 | **0.35** |
| 450 | 1.60 | 0.41 | 0.35 | 0.32 | 0.42 | 0.41 | 0.85 | 0.32 | 0.40 | 0.21 | 0.40 | **0.32** |
| 500 | 1.70 | 0.38 | 0.35 | 0.30 | 0.38 | 0.36 | 0.81 | 0.29 | 0.370 | 0.20 | 0.367 | **0.30** |
| 555 | 1.80 | 0.35 | 0.33 | 0.27 | 0.344 | 0.339 | 0.77 | 0.26 | 0.340 | 0.17 | 0.339 | **0.27** |
| 600 | 1.70 | 0.34 | 0.330 | 0.26 | 0.32 | 0.326 | 0.75 | 0.25 | 0.328 | 0.15 | 0.327 | **0.26** |
| 700 | 1.60 | 0.32 | 0.39 | 0.24 | 0.28 | 0.28 | 0.71 | 0.21 | 0.30 | 0.14 | 0.29 | **0.23** |
| 800 | 1.60 | 0.31 | | 0.24 | 0.25 | 0.30 | 0.68 | 0.20 | 0.28 | 0.13 | 0.28 | **0.22** |
| 900 | 1.90 | 0.28 | | 0.25 | 0.22 | 0.47 | 0.67 | 0.17 | 0.27 | 0.13 | 0.27 | **0.20** |
| 1000 | 1.90 | 0.28 | | 0.24 | 0.21 | 0.28 | 0.65 | 0.16 | 0.26 | 0.12 | 0.26 | **0.19** |
| 1100 | 2.30 | 0.27 | | 0.24 | 0.20 | 0.24 | 0.64 | 0.15 | 0.27 | 0.11 | 0.24 | **0.19** |
| 1300 | 2.02 | 0.27 | 0.38 | 0.23 | 0.18 | 0.23 | 0.63 | 0.38 | 0.31 | 0.11 | 0.29 | **0.20** |
| 1500 | 2.12 | 0.25 | 0.42 | 0.25 | 0.16 | 0.24 | 0.62 | 0.42 | 0.29 | 0.10 | 0.27 | **0.20** |
| 1700 | 2.12 | 0.31 | | 0.24 | 0.15 | 0.21 | 0.62 | 0.53 | 0.27 | 0.11 | 0.27 | **0.20** |
| 2000 | | 0.37 | | 0.24 | 0.13 | 0.22 | 0.61 | 0.83 | 0.29 | 0.14 | 0.26 | **0.18** |
| 2200 | | 0.44 | | 0.29 | 0.13 | 0.25 | 0.61 | 2.07 | 0.39 | 0.15 | 0.34 | **0.20** |
| 2300 | | 0.48 | | 0.33 | 0.13 | 0.23 | 0.62 | 2.36 | 0.36 | 0.17 | 0.34 | **0.21** |
| 2400 | | 0.49 | | 0.57 | 0.21 | 0.25 | 0.64 | 2.72 | 0.42 | 0.20 | 0.45 | **0.27** |
| 2500 | | 0.62 | | 0.86 | 0.38 | 0.32 | 0.94 | 6.21 | 2.88 | 0.24 | 0.74 | **0.39** |

Table C4. Uncertainties $\boldsymbol{u_{adj}(\Delta_i)}$ after cut-off of relative average differences (Eq. 8.15)

| λ, nm | $u_{adj}(\Delta_i)$, % | | | | | | | | | |
|---|---|---|---|---|---|---|---|---|---|---|
| | CSIC | KRISS | LNE | NIM | NIST | NMC | NMIJ | NRC | PTB | VNIIOFI |
| 250 | 2.53 | 1.03 | 2.31 | 0.79 | 0.80 | 0.98 | 1.38 | 1.50 | 0.76 | 0.75 |
| 260 | 2.45 | 0.92 | 1.03 | 0.67 | 0.77 | 0.85 | 1.27 | 1.23 | 0.69 | 0.67 |
| 270 | 2.43 | 0.86 | 0.82 | 0.62 | 0.75 | 0.76 | 1.22 | 0.86 | 0.64 | 0.62 |
| 280 | 2.23 | 0.79 | 0.66 | 0.61 | 0.72 | 0.79 | 1.18 | 0.78 | 0.62 | 0.59 |
| 290 | 2.21 | 0.76 | 0.60 | 0.57 | 0.70 | 0.68 | 1.15 | 0.75 | 0.60 | 0.57 |
| 300 | 2.49 | 0.71 | 0.56 | 0.52 | 0.67 | 0.66 | 1.12 | 0.71 | 0.58 | 0.52 |
| 320 | 1.95 | 0.64 | 0.51 | 0.49 | 0.62 | 0.61 | 1.07 | 0.64 | 0.54 | 0.49 |
| 340 | 1.83 | 0.58 | 0.47 | 0.45 | 0.57 | 0.55 | 1.02 | 0.61 | 0.52 | 0.45 |
| 360 | 1.72 | 0.56 | 0.44 | 0.43 | 0.54 | 0.52 | 0.98 | 0.58 | 0.50 | 0.43 |
| 380 | 1.62 | 0.50 | 0.42 | 0.41 | 0.51 | 0.49 | 0.95 | 0.55 | 0.48 | 0.41 |
| 400 | 1.62 | 0.47 | 0.41 | 0.37 | 0.49 | 0.46 | 0.92 | 0.37 | 0.45 | 0.37 |
| 450 | 1.61 | 0.42 | 0.37 | 0.34 | 0.43 | 0.42 | 0.86 | 0.34 | 0.41 | 0.34 |

| | | | | | | | | | | |
|---|---|---|---|---|---|---|---|---|---|---|
| 500 | 1.70 | 0.39 | 0.36 | 0.32 | 0.40 | 0.38 | 0.82 | 0.32 | 0.38 | 0.32 |
| 555 | 1.80 | 0.37 | 0.34 | 0.29 | 0.36 | 0.35 | 0.78 | 0.29 | 0.35 | 0.29 |
| 600 | 1.70 | 0.35 | 0.34 | 0.28 | 0.34 | 0.34 | 0.76 | 0.28 | 0.34 | 0.28 |
| 700 | 1.60 | 0.33 | 0.40 | 0.26 | 0.30 | 0.29 | 0.72 | 0.25 | 0.31 | 0.25 |
| 800 | 1.61 | 0.33 | | 0.26 | 0.27 | 0.31 | 0.69 | 0.24 | 0.30 | 0.24 |
| 900 | 1.90 | 0.29 | | 0.27 | 0.24 | 0.48 | 0.68 | 0.22 | 0.28 | 0.22 |
| 1000 | 1.90 | 0.29 | | 0.26 | 0.23 | 0.29 | 0.66 | 0.21 | 0.27 | 0.21 |
| 1100 | 2.30 | 0.29 | | 0.26 | 0.22 | 0.26 | 0.65 | 0.21 | 0.28 | 0.21 |
| 1300 | 2.02 | 0.28 | 0.39 | 0.25 | 0.22 | 0.25 | 0.64 | 0.40 | 0.32 | 0.22 |
| 1500 | 2.12 | 0.27 | 0.43 | 0.26 | 0.22 | 0.26 | 0.63 | 0.43 | 0.30 | 0.22 |
| 1700 | 2.12 | 0.32 | | 0.26 | 0.22 | 0.23 | 0.63 | 0.54 | 0.28 | 0.22 |
| 2000 | | 0.39 | | 0.27 | 0.22 | 0.25 | 0.63 | 0.84 | 0.31 | 0.22 |
| 2200 | | 0.46 | | 0.32 | 0.25 | 0.29 | 0.63 | 2.07 | 0.42 | 0.25 |
| 2300 | | 0.51 | | 0.37 | 0.28 | 0.30 | 0.64 | 2.37 | 0.40 | 0.28 |
| 2400 | | 0.53 | | 0.60 | 0.34 | 0.34 | 0.67 | 2.72 | 0.46 | 0.34 |
| 2500 | | 0.66 | | 0.89 | 0.45 | 0.45 | 0.97 | 6.22 | 2.89 | 0.45 |

Table C5. Weights, $w_i$ , KCRV, $\Delta_{\mathrm{KCRV}}$, and uncertainty of KCR, $u(\Delta_{\mathrm{KCRV}})$

| λ, nm | $w_i$ | | | | | | | | | | $\Delta_{\mathrm{KCRV}}$, % | $u(\Delta_{\mathrm{KCRV}})$ % |
|---|---|---|---|---|---|---|---|---|---|---|---|---|
| | CSIC | KRISS | LNE | NIM | NIST | NMC | NMIJ | NRC | PTB | VNIIOFI | | |
| 250 | 0.016 | 0.095 | 0.019 | 0.162 | 0.155 | 0.104 | 0.053 | 0.045 | 0.173 | 0.179 | **0.79** | **0.30** |
| 260 | 0.013 | 0.090 | 0.072 | 0.168 | 0.127 | 0.106 | 0.047 | 0.050 | 0.158 | 0.169 | **0.68** | **0.26** |
| 270 | 0.011 | 0.085 | 0.093 | 0.159 | 0.111 | 0.107 | 0.041 | 0.084 | 0.150 | 0.159 | **0.53** | **0.24** |
| 280 | 0.011 | 0.089 | 0.126 | 0.148 | 0.106 | 0.089 | 0.039 | 0.091 | 0.143 | 0.159 | **0.46** | **0.22** |
| 290 | 0.010 | 0.085 | 0.137 | 0.151 | 0.102 | 0.105 | 0.037 | 0.087 | 0.136 | 0.151 | **0.53** | **0.21** |
| 300 | 0.007 | 0.086 | 0.138 | 0.160 | 0.097 | 0.101 | 0.035 | 0.086 | 0.131 | 0.160 | **0.58** | **0.20** |
| 320 | 0.010 | 0.091 | 0.145 | 0.156 | 0.096 | 0.098 | 0.032 | 0.090 | 0.126 | 0.156 | **0.50** | **0.18** |
| 340 | 0.010 | 0.095 | 0.145 | 0.156 | 0.098 | 0.105 | 0.031 | 0.087 | 0.118 | 0.156 | **0.59** | **0.17** |
| 360 | 0.010 | 0.093 | 0.147 | 0.155 | 0.099 | 0.108 | 0.030 | 0.087 | 0.115 | 0.155 | **0.62** | **0.16** |
| 380 | 0.010 | 0.103 | 0.145 | 0.152 | 0.099 | 0.110 | 0.029 | 0.087 | 0.114 | 0.152 | **0.63** | **0.15** |
| 400 | 0.008 | 0.093 | 0.127 | 0.153 | 0.087 | 0.101 | 0.025 | 0.150 | 0.103 | 0.153 | **0.49** | **0.14** |
| 450 | 0.007 | 0.096 | 0.127 | 0.151 | 0.093 | 0.098 | 0.024 | 0.152 | 0.101 | 0.152 | **0.31** | **0.13** |
| 500 | 0.005 | 0.100 | 0.114 | 0.151 | 0.096 | 0.106 | 0.023 | 0.151 | 0.103 | 0.151 | **0.24** | **0.12** |
| 555 | 0.004 | 0.096 | 0.112 | 0.153 | 0.101 | 0.104 | 0.021 | 0.153 | 0.103 | 0.153 | **0.23** | **0.11** |
| 600 | 0.004 | 0.097 | 0.102 | 0.154 | 0.105 | 0.104 | 0.021 | 0.155 | 0.102 | 0.155 | **0.22** | **0.10** |
| 700 | 0.004 | 0.093 | 0.065 | 0.151 | 0.114 | 0.119 | 0.020 | 0.165 | 0.104 | 0.165 | **0.13** | **0.10** |
| 800 | 0.004 | 0.097 | 0.000 | 0.158 | 0.142 | 0.105 | 0.022 | 0.178 | 0.116 | 0.178 | **0.27** | **0.10** |
| 900 | 0.003 | 0.109 | 0.000 | 0.134 | 0.167 | 0.041 | 0.021 | 0.203 | 0.120 | 0.203 | **0.15** | **0.09** |
| 1000 | 0.002 | 0.096 | 0.000 | 0.123 | 0.159 | 0.098 | 0.019 | 0.196 | 0.111 | 0.196 | **0.18** | **0.08** |
| 1100 | 0.002 | 0.097 | 0.000 | 0.122 | 0.168 | 0.121 | 0.019 | 0.185 | 0.101 | 0.185 | **0.16** | **0.08** |
| 1300 | 0.002 | 0.114 | 0.058 | 0.145 | 0.182 | 0.147 | 0.022 | 0.058 | 0.088 | 0.182 | **0.32** | **0.09** |
| 1500 | 0.002 | 0.125 | 0.050 | 0.132 | 0.189 | 0.140 | 0.023 | 0.048 | 0.101 | 0.189 | **0.29** | **0.09** |
| 1700 | 0.002 | 0.092 | 0.000 | 0.140 | 0.205 | 0.181 | 0.024 | 0.032 | 0.119 | 0.205 | **0.27** | **0.09** |
| 2000 | 0.000 | 0.070 | 0.000 | 0.148 | 0.225 | 0.175 | 0.028 | 0.015 | 0.113 | 0.225 | **0.20** | **0.10** |
| 2200 | 0.000 | 0.068 | 0.000 | 0.143 | 0.242 | 0.180 | 0.037 | 0.003 | 0.085 | 0.242 | **0.14** | **0.11** |
| 2300 | 0.000 | 0.068 | 0.000 | 0.125 | 0.224 | 0.201 | 0.043 | 0.003 | 0.111 | 0.224 | **0.16** | **0.12** |
| 2400 | 0.000 | 0.091 | 0.000 | 0.069 | 0.221 | 0.221 | 0.057 | 0.003 | 0.117 | 0.221 | **0.23** | **0.15** |
| 2500 | 0.000 | 0.116 | 0.000 | 0.064 | 0.253 | 0.253 | 0.054 | 0.001 | 0.006 | 0.253 | **0.41** | **0.20** |

Table C6. Version 2. Preliminary Degrees of Equivalence: Deviations from KCRV $D_i$ and their associated expanded Uncertainties $U_i$ (Eq. 8.21, 8.22-8.23), in %

| λ. nm | CSIC | | KRISS | | LNE | | NIM | | NIST | | NMC | | NMIA | | NMIJ | | NPL | | NRC | | PTB | | VNIIOFI | |
|---|---|---|---|---|---|---|---|---|---|---|---|---|---|---|---|---|---|---|---|---|---|---|---|---|
| | $D_i$ | $U_i$ | $D_i$ | $U_i$ | $D_i$ | $U_i$ | $D_i$ | $U_i$ | $D_i$ | $U_i$ | $D_i$ | $U_i$ | $D_i$ | $U_i$ | $D_i$ | $U_i$ | $D_i$ | $U_i$ | $D_i$ | $U_i$ | $D_i$ | $U_i$ | $D_i$ | $U_i$ |
| 250 | -3.95 | 5.02 | 0.13 | 1.94 | 4.47 | 4.56 | 0.38 | 1.42 | -0.06 | 1.46 | -1.29 | 1.85 | -1.78 | 5.75 | -0.36 | 2.67 | -1.46 | 1.99 | 0.08 | 2.93 | 0.97 | 1.37 | -0.59 | 0.91 |
| 260 | -4.97 | 4.86 | 0.21 | 1.74 | 0.99 | 1.97 | 0.06 | 1.21 | -0.20 | 1.43 | -1.21 | 1.59 | -2.53 | 4.79 | 0.13 | 2.48 | -2.26 | 2.01 | 0.34 | 2.38 | 1.11 | 1.25 | -0.50 | 0.80 |
| 270 | -5.58 | 4.82 | 0.26 | 1.63 | 0.25 | 1.55 | -0.13 | 1.13 | -0.56 | 1.40 | -0.63 | 1.43 | -2.54 | 4.17 | 0.43 | 2.39 | -2.25 | 2.09 | 0.50 | 1.64 | 1.14 | 1.17 | -0.42 | 0.76 |
| 280 | -5.05 | 4.43 | -0.05 | 1.50 | 0.29 | 1.23 | 0.00 | 1.12 | -0.23 | 1.35 | -0.92 | 1.50 | -2.09 | 3.80 | 0.45 | 2.31 | -2.31 | 1.96 | 0.32 | 1.48 | 0.89 | 1.14 | -0.27 | 0.71 |
| 290 | -3.97 | 4.40 | -0.12 | 1.45 | 0.20 | 1.10 | 0.00 | 1.01 | -0.04 | 1.31 | -0.93 | 1.28 | -2.22 | 3.60 | 0.31 | 2.25 | -1.72 | 1.76 | 0.42 | 1.43 | 0.97 | 1.11 | -0.38 | 0.68 |
| 300 | -1.00 | 4.96 | -0.23 | 1.36 | 0.27 | 1.03 | -0.11 | 0.93 | 0.12 | 1.27 | -0.84 | 1.24 | -2.33 | 3.35 | 0.44 | 2.20 | -1.54 | 1.71 | 0.36 | 1.36 | 0.83 | 1.07 | -0.48 | 0.65 |
| 320 | 0.38 | 3.88 | -0.45 | 1.21 | 0.70 | 0.93 | -0.20 | 0.88 | 0.05 | 1.17 | -0.96 | 1.16 | -2.55 | 2.96 | 0.29 | 2.10 | -2.01 | 1.75 | 0.13 | 1.22 | 0.68 | 1.01 | -0.32 | 0.62 |
| 340 | 0.61 | 3.63 | -0.43 | 1.10 | 0.62 | 0.86 | -0.06 | 0.80 | -0.12 | 1.08 | -0.78 | 1.04 | -2.63 | 2.63 | 0.22 | 2.00 | -1.82 | 1.63 | 0.27 | 1.16 | 0.73 | 0.97 | -0.45 | 0.59 |
| 360 | 0.74 | 3.42 | -0.35 | 1.05 | 0.67 | 0.81 | -0.12 | 0.77 | -0.30 | 1.02 | -0.69 | 0.97 | -2.46 | 2.34 | 0.17 | 1.93 | -1.62 | 1.59 | 0.36 | 1.09 | 0.76 | 0.94 | -0.47 | 0.57 |
| 380 | 0.67 | 3.22 | -0.39 | 0.95 | 0.87 | 0.78 | -0.10 | 0.74 | -0.36 | 0.97 | -0.76 | 0.92 | -2.43 | 2.07 | 0.22 | 1.87 | -1.49 | 1.61 | 0.30 | 1.05 | 0.72 | 0.90 | -0.49 | 0.56 |
| 400 | 0.81 | 3.22 | -0.31 | 0.90 | 0.83 | 0.75 | -0.02 | 0.67 | -0.20 | 0.93 | -0.62 | 0.86 | -2.31 | 1.86 | 0.92 | 1.81 | -1.40 | 1.53 | -0.34 | 0.68 | 0.73 | 0.85 | -0.30 | 0.51 |
| 450 | 0.86 | 3.20 | -0.34 | 0.80 | 0.39 | 0.69 | 0.21 | 0.62 | 0.19 | 0.82 | -0.73 | 0.80 | -1.59 | 1.42 | 0.74 | 1.70 | -0.90 | 1.01 | -0.26 | 0.62 | 0.43 | 0.78 | -0.14 | 0.47 |
| 500 | 0.73 | 3.40 | -0.27 | 0.73 | 0.32 | 0.68 | 0.18 | 0.58 | 0.22 | 0.75 | -0.76 | 0.71 | -1.11 | 1.09 | 0.72 | 1.62 | -0.68 | 0.88 | -0.15 | 0.56 | 0.37 | 0.72 | -0.09 | 0.44 |
| 555 | 0.66 | 3.60 | -0.25 | 0.70 | 0.35 | 0.64 | 0.24 | 0.53 | 0.14 | 0.67 | -0.59 | 0.66 | -0.73 | 0.85 | 0.65 | 1.54 | -0.66 | 0.83 | -0.19 | 0.52 | 0.23 | 0.67 | -0.10 | 0.39 |
| 600 | 0.73 | 3.40 | -0.21 | 0.67 | 0.30 | 0.65 | 0.24 | 0.51 | 0.18 | 0.64 | -0.57 | 0.64 | -0.53 | 0.75 | 0.57 | 1.50 | -0.67 | 0.77 | -0.18 | 0.49 | 0.13 | 0.65 | -0.06 | 0.36 |
| 700 | 1.59 | 3.20 | -0.03 | 0.63 | 0.02 | 0.77 | 0.30 | 0.48 | 0.11 | 0.56 | -0.42 | 0.55 | -0.14 | 0.91 | 0.46 | 1.42 | -0.59 | 0.69 | -0.19 | 0.42 | 0.08 | 0.59 | 0.01 | 0.34 |
| 800 | 0.65 | 3.20 | 0.23 | 0.61 | 0.41 | 0.89 | 0.23 | 0.46 | -0.24 | 0.49 | 0.47 | 0.59 | 0.20 | 1.23 | 0.45 | 1.36 | -0.67 | 0.63 | -0.31 | 0.40 | -0.12 | 0.56 | -0.10 | 0.33 |
| 900 | 0.28 | 3.80 | -0.18 | 0.55 | 0.55 | 0.56 | 0.28 | 0.49 | 0.13 | 0.43 | 0.69 | 0.94 | 0.65 | 1.44 | 0.70 | 1.34 | -0.60 | 0.57 | -0.39 | 0.35 | -0.08 | 0.52 | 0.03 | 0.30 |
| 1000 | -0.54 | 3.80 | -0.19 | 0.56 | 0.63 | 0.55 | 0.20 | 0.48 | 0.07 | 0.41 | 0.63 | 0.56 | 0.79 | 1.61 | 0.21 | 1.30 | -0.56 | 0.53 | -0.32 | 0.33 | -0.12 | 0.51 | -0.02 | 0.29 |
| 1100 | -0.63 | 4.60 | -0.18 | 0.54 | 0.67 | 1.00 | -0.11 | 0.48 | -0.21 | 0.39 | 0.71 | 0.48 | 1.09 | 1.75 | -0.21 | 1.28 | -0.49 | 0.51 | -0.19 | 0.32 | 0.20 | 0.53 | 0.01 | 0.28 |
| 1300 | -0.15 | 4.03 | -0.27 | 0.53 | 0.98 | 0.76 | -0.11 | 0.46 | -0.40 | 0.37 | 0.70 | 0.45 | 1.13 | 1.93 | -0.37 | 1.26 | -0.62 | 0.47 | 0.44 | 0.76 | -0.34 | 0.61 | -0.15 | 0.29 |
| 1500 | -0.99 | 4.24 | -0.25 | 0.50 | 0.97 | 0.83 | 0.00 | 0.48 | -0.48 | 0.34 | 0.78 | 0.47 | 1.37 | 2.09 | -0.69 | 1.24 | -0.62 | 0.45 | 0.32 | 0.84 | -0.13 | 0.56 | -0.11 | 0.28 |
| 1700 | -7.32 | 4.24 | -0.44 | 0.61 | 1.58 | 0.64 | 0.10 | 0.48 | -0.39 | 0.32 | 0.93 | 0.41 | 1.70 | 2.22 | -0.80 | 1.24 | -0.76 | 0.62 | 0.80 | 1.06 | -0.24 | 0.52 | -0.13 | 0.28 |
| 2000 | | | -0.36 | 0.75 | 2.39 | 0.76 | 0.03 | 0.49 | -0.30 | 0.33 | 0.88 | 0.44 | 2.33 | 2.84 | -1.54 | 1.23 | -0.59 | 0.66 | 0.44 | 1.66 | -0.19 | 0.58 | -0.04 | 0.33 |
| 2200 | | | -1.04 | 0.89 | 3.20 | 1.24 | 0.13 | 0.58 | -0.21 | 0.35 | 0.95 | 0.51 | 3.00 | 2.51 | -2.15 | 1.23 | -0.56 | 0.70 | 1.70 | 4.14 | 0.05 | 0.79 | 0.01 | 0.36 |
| 2300 | | | -0.43 | 0.98 | 4.36 | 1.43 | 0.06 | 0.69 | -0.10 | 0.41 | 0.84 | 0.52 | 4.55 | 2.60 | -1.73 | 1.25 | -0.45 | 0.75 | 0.80 | 4.73 | -0.10 | 0.75 | -0.19 | 0.44 |
| 2400 | | | 0.15 | 1.00 | 6.97 | 2.39 | -0.03 | 1.16 | -0.62 | 0.53 | 0.97 | 0.56 | 5.61 | 2.84 | -1.96 | 1.29 | -0.28 | 0.80 | 2.80 | 5.44 | 0.05 | 0.86 | 0.03 | 0.52 |
| 2500 | | | -0.39 | 1.23 | 7.59 | 8.80 | 0.04 | 1.71 | -0.12 | 0.73 | 0.92 | 0.68 | 8.50 | 2.62 | -2.10 | 1.88 | -1.21 | 1.82 | 3.30 | 12.4 | -0.08 | 5.75 | -0.19 | 0.61 |

## C4. Consistency check (preliminary)

Table C7 presents Chi-square values $\chi^2_{\mathrm{obs}}$ for consistency check. calculated by Eq.8.19 of Section 8.3 "Method of comparison data analysis", as well as the $\chi^2_{0.05}(\nu)$ value for ν = *N*-1, where *N* is the number of NMIs contribute to KCRV, and the results of the consistency check.

Table C7. Chi-square values $\chi^2_{\mathrm{obs}}$ and the consistency check

| λ. nm | $\chi^2_{\mathrm{obs}}$ | ν = *N*-1 | $\chi^2_{0.05}(\nu)$ | Result of the consistency check |
|---|---|---|---|---|
| 250 | 10.49 | 9 | 16.919 | satisfied |
| 260 | 10.49 | 9 | 16.919 | satisfied |
| 270 | 10.82 | 9 | 16.919 | satisfied |
| 280 | 9.37 | 9 | 16.919 | satisfied |
| 290 | 8.60 | 9 | 16.919 | satisfied |
| 300 | 5.51 | 9 | 16.919 | satisfied |
| 320 | 7.18 | 9 | 16.919 | satisfied |
| 340 | 7.56 | 9 | 16.919 | satisfied |
| 360 | 8.94 | 9 | 16.919 | satisfied |
| 380 | 11.94 | 9 | 16.919 | satisfied |
| 400 | 11.96 | 9 | 16.919 | satisfied |
| 450 | 8.15 | 9 | 16.919 | satisfied |
| 500 | 8.12 | 9 | 16.919 | satisfied |
| 555 | 6.88 | 9 | 16.919 | satisfied |
| 600 | 6.29 | 9 | 16.919 | satisfied |
| 700 | 5.59 | 9 | 16.919 | satisfied |
| 800 | 6.91 | 8 | 15.507 | satisfied |
| 900 | 8.33 | 8 | 15.507 | satisfied |
| 1000 | 8.61 | 8 | 15.507 | satisfied |
| 1100 | 10.49 | 8 | 15.507 | satisfied |
| 1300 | **21.57** | 9 | 16.919 | **failed** |
| 1500 | **22.41** | 9 | 16.919 | **failed** |
| 1700 | **38.48** | 8 | 15.507 | **failed** |
| 2000 | **22.06** | 7 | 14.067 | **failed** |
| 2200 | **29.27** | 7 | 14.067 | **failed** |
| 2300 | **16.84** | 7 | 14.067 | **failed** |
| 2400 | **21.37** | 7 | 14.067 | **failed** |
| 2500 | 9.79 | 7 | 14.067 | satisfied |

## C5. Outliers

Table C8 shows the ratios of absolute values of Deviation from KCRV (DoE), $|D_i|$, to their associated expanded uncertainties, $U_i$, (except NMIA) and the Fig.C1 shows the values $D_i$ without identifying participants. The order of participants in Table C8 is different from that in Tables above.

Pilot suggests the following outliers:

1) Point at wavelength 1700 nm marked with red circle in Fig.C1.
2) No other outliers are suggested.

Table C8. Ratios $|D_i|/U_i$. Red points are suggested outliers. Bold points indicate the ratios >1

| λ. | Ratios $\|D_i\|/U_i$ | | | | | | | | | |
|---|---|---|---|---|---|---|---|---|---|---|
| nm | CSIC | KRISS | LNE | NIM | NIST | NMC | NMIJ | NRC | PTB | VNIIOFI |
| 250 | 0.79 | 0.07 | 0.98 | 0.27 | 0.04 | 0.70 | 0.14 | 0.03 | 0.71 | 0.65 |
| 260 | 1.02 | 0.12 | 0.51 | 0.05 | 0.14 | 0.76 | 0.05 | 0.14 | 0.89 | 0.62 |
| 270 | 1.16 | 0.16 | 0.16 | 0.12 | 0.40 | 0.44 | 0.18 | 0.31 | 0.97 | 0.55 |
| 280 | 1.14 | 0.03 | 0.23 | 0.00 | 0.17 | 0.61 | 0.19 | 0.22 | 0.78 | 0.38 |
| 290 | 0.90 | 0.08 | 0.19 | 0.00 | 0.03 | 0.72 | 0.14 | 0.29 | 0.88 | 0.55 |
| 300 | 0.20 | 0.17 | 0.26 | 0.12 | 0.10 | 0.67 | 0.20 | 0.26 | 0.78 | 0.73 |
| 320 | 0.10 | 0.37 | 0.76 | 0.23 | 0.05 | 0.83 | 0.14 | 0.11 | 0.67 | 0.52 |
| 340 | 0.17 | 0.39 | 0.72 | 0.07 | 0.11 | 0.74 | 0.11 | 0.23 | 0.75 | 0.76 |
| 360 | 0.22 | 0.33 | 0.83 | 0.16 | 0.30 | 0.71 | 0.09 | 0.33 | 0.81 | 0.84 |
| 380 | 0.21 | 0.41 | 1.12 | 0.13 | 0.37 | 0.83 | 0.12 | 0.28 | 0.81 | 0.86 |
| 400 | 0.25 | 0.34 | 1.10 | 0.03 | 0.22 | 0.72 | 0.51 | 0.50 | 0.86 | 0.59 |
| 450 | 0.27 | 0.42 | 0.56 | 0.33 | 0.23 | 0.91 | 0.44 | 0.43 | 0.55 | 0.30 |
| 500 | 0.22 | 0.37 | 0.47 | 0.32 | 0.30 | 1.06 | 0.45 | 0.27 | 0.51 | 0.21 |
| 555 | 0.18 | 0.36 | 0.54 | 0.45 | 0.21 | 0.88 | 0.42 | 0.37 | 0.35 | 0.26 |
| 600 | 0.22 | 0.31 | 0.47 | 0.47 | 0.28 | 0.89 | 0.38 | 0.37 | 0.21 | 0.15 |
| 700 | 0.50 | 0.05 | 0.02 | 0.64 | 0.20 | 0.77 | 0.32 | 0.46 | 0.13 | 0.03 |
| 800 | 0.20 | 0.38 | | 0.50 | 0.48 | 0.80 | 0.33 | 0.77 | 0.22 | 0.32 |
| 900 | 0.07 | 0.32 | | 0.58 | 0.30 | 0.74 | 0.52 | 1.13 | 0.15 | 0.10 |
| 1000 | 0.14 | 0.34 | | 0.42 | 0.16 | 1.15 | 0.16 | 0.98 | 0.24 | 0.09 |
| 1100 | 0.14 | 0.33 | | 0.24 | 0.53 | 1.47 | 0.16 | 0.61 | 0.37 | 0.03 |
| 1300 | 0.04 | 0.51 | 1.28 | 0.25 | 1.11 | 1.54 | 0.29 | 0.57 | 0.55 | 0.51 |
| 1500 | 0.23 | 0.50 | 1.17 | 0.00 | 1.43 | 1.67 | 0.55 | 0.38 | 0.23 | 0.40 |
| 1700 | **1.72** | 0.72 | | 0.21 | 1.22 | 2.29 | 0.64 | 0.75 | 0.45 | 0.46 |
| 2000 | | 0.47 | | 0.06 | 0.90 | 1.98 | 1.26 | 0.27 | 0.33 | 0.12 |
| 2200 | | 1.17 | | 0.21 | 0.60 | 1.87 | 1.74 | 0.41 | 0.06 | 0.03 |
| 2300 | | 0.44 | | 0.09 | 0.24 | 1.61 | 1.38 | 0.17 | 0.13 | 0.43 |
| 2400 | | 0.15 | | 0.03 | 1.17 | 1.72 | 1.52 | 0.51 | 0.06 | 0.05 |
| 2500 | | 0.32 | | 0.02 | 0.17 | 1.35 | 1.12 | 0.27 | 0.01 | 0.31 |

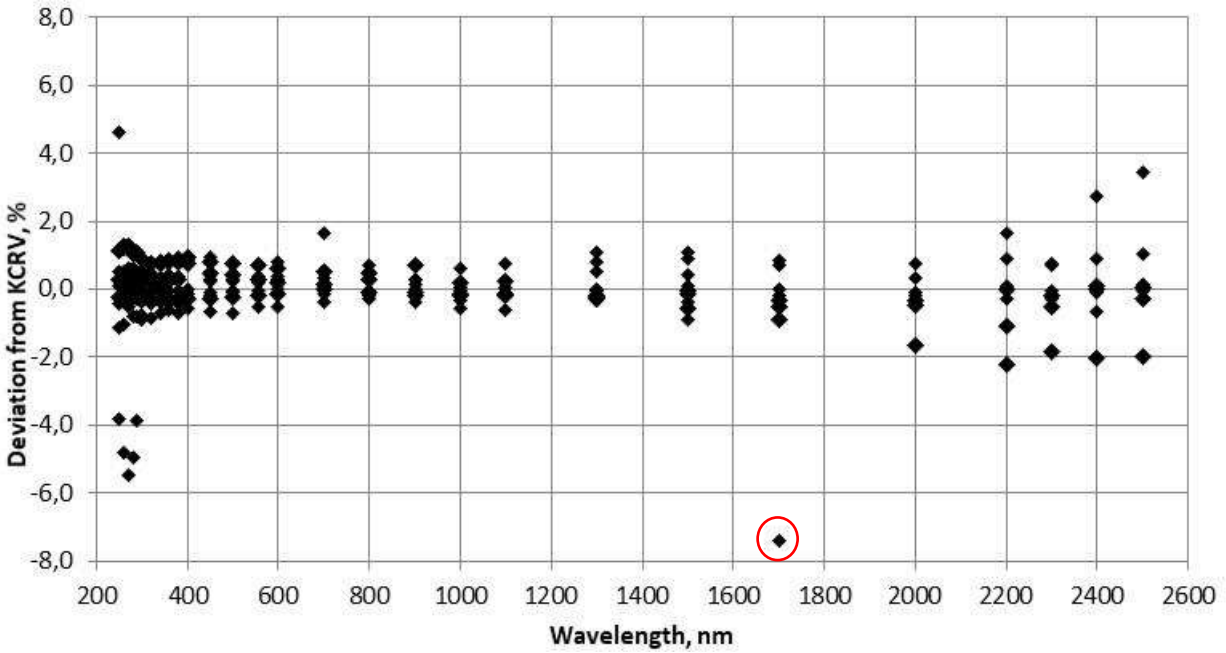


Figure C1. Deviations from KCRV, $D_i$ (preliminary)

## C6. Consistency check after excluding outliers

Note that after excluding the outliers number *N* of NMI contribute to KCRV is changed as follows:

*N* = 10 for the wavelengths from 250 nm to 700 nm, 1300 nm and 1500 nm;
*N* = 9 for the wavelengths from 800 nm to 1100 nm;
*N* = 8 for the wavelengths 1700 nm, and from 2000 nm to 2500 nm.

Table C7a presents the Chi-square values $\chi^2_{\text{obs}}$, $\chi^2_{0.05}(\nu)$ values for ν = *N*-1 and the results of the consistency check after excluding the outliers. Red figures indicate changes from the Table C7.

Table C7a. Chi-square values $\chi^2_{\text{obs}}$ and the consistency check after excluding the outliers

| λ. nm | $\chi^2_{\text{obs}}$ | ν = *N*-1 | $\chi^2_{0.05}(\nu)$ | Result of the consistency check |
|---|---|---|---|---|
| 250 | 10.49 | 9 | 16.919 | satisfied |
| 260 | 10.49 | 9 | 16.919 | satisfied |
| 270 | 10.82 | 9 | 16.919 | satisfied |
| 280 | 9.37 | 9 | 16.919 | satisfied |
| 290 | 8.60 | 9 | 16.919 | satisfied |
| 300 | 5.51 | 9 | 16.919 | satisfied |
| 320 | 7.18 | 9 | 16.919 | satisfied |
| 340 | 7.56 | 9 | 16.919 | satisfied |
| 360 | 8.94 | 9 | 16.919 | satisfied |
| 380 | 11.94 | 9 | 16.919 | satisfied |
| 400 | 11.96 | 9 | 16.919 | satisfied |
| 450 | 8.15 | 9 | 16.919 | satisfied |
| 500 | 8.12 | 9 | 16.919 | satisfied |
| 555 | 6.88 | 9 | 16.919 | satisfied |

| | | | | |
|---|---|---|---|---|
| 600 | 6.29 | 9 | 16.919 | satisfied |
| 700 | 5.59 | 9 | 16.919 | satisfied |
| 800 | 6.91 | 8 | 15.507 | satisfied |
| 900 | 8.33 | 8 | 15.507 | satisfied |
| 1000 | 8.61 | 8 | 15.507 | satisfied |
| 1100 | 10.49 | 8 | 15.507 | satisfied |
| 1300 | **21.57** | 9 | 16.919 | **failed** |
| 1500 | **22.41** | 9 | 16.919 | **failed** |
| 1700 | **26.59** | 7 | 14.067 | **failed** |
| 2000 | **22.06** | 7 | 14.067 | **failed** |
| 2200 | **29.27** | 7 | 14.067 | **failed** |
| 2300 | **16.84** | 7 | 14.067 | **failed** |
| 2400 | **21.37** | 7 | 14.067 | **failed** |
| 2500 | 9.79 | 7 | 14.067 | satisfied |

One can see, that after excluding the outlier, although the consistency check is still failed, the Chi-square value $\chi^2_{\text{obs}}$ at 1700 nm are closer to $\chi^2_{0,05}(\nu)$ value.

### C7. Applying Mandel-Paule method

For the wavelengths where $\chi^2_{\text{obs}} > \chi^2_{0.05}(\nu)$ (the consistency check failed) the Mandel-Paule method is applied, i.e. the $s^2$ term is added in the Eq. (8.15, 8.20) of the Section 8.3 "Method of comparison data analysis" for calculation of $u_{\text{adj}}(\Delta_i)$. The values of $s$ are determined by iterative process so that $\chi^2_{\text{obs}} = \chi^2_{0.05}(\nu)$.

Table C7b shows the consistency check results after the Mandel-Paule method, as well as the $s$ values applied. Table C4a presents the $\boldsymbol{u_{\text{adj}}(\Delta_i)}$ uncertainties after applying the Mandel-Paule method.

Table C7b. Chi-square values $\chi^2_{\text{obs}}$ and the consistency check after applying Mandel-Paule method

| λ. nm | *S*, % | $\chi^2_{\text{obs}}$ | ν = *N*-1 | $\chi^2_{0.05}(\nu)$ | Result of the consistency check |
|---|---|---|---|---|---|
| 250 | 0.00 | 10.49 | 9 | 16.919 | satisfied |
| 260 | 0.00 | 10.49 | 9 | 16.919 | satisfied |
| 270 | 0.00 | 10.82 | 9 | 16.919 | satisfied |
| 280 | 0.00 | 9.37 | 9 | 16.919 | satisfied |
| 290 | 0.00 | 8.60 | 9 | 16.919 | satisfied |
| 300 | 0.00 | 5.51 | 9 | 16.919 | satisfied |
| 320 | 0.00 | 7.18 | 9 | 16.919 | satisfied |
| 340 | 0.00 | 7.56 | 9 | 16.919 | satisfied |
| 360 | 0.00 | 8.94 | 9 | 16.919 | satisfied |
| 380 | 0.00 | 11.94 | 9 | 16.919 | satisfied |
| 400 | 0.00 | 11.96 | 9 | 16.919 | satisfied |
| 450 | 0.00 | 8.15 | 9 | 16.919 | satisfied |
| 500 | 0.00 | 8.12 | 9 | 16.919 | satisfied |
| 555 | 0.00 | 6.88 | 9 | 16.919 | satisfied |
| 600 | 0.00 | 6.29 | 9 | 16.919 | satisfied |
| 700 | 0.00 | 5.59 | 9 | 16.919 | satisfied |

| | | | | | |
|---|---|---|---|---|---|
| 800 | 0.00 | 6.91 | 8 | 15.507 | satisfied |
| 900 | 0.00 | 8.33 | 8 | 15.507 | satisfied |
| 1000 | 0.00 | 8.61 | 8 | 15.507 | satisfied |
| 1100 | 0.00 | 10.49 | 8 | 15.507 | satisfied |
| 1300 | **0.15** | **16.88** | 9 | 16.919 | **satisfied** |
| 1500 | **0.17** | **16.52** | 9 | 16.919 | **satisfied** |
| 1700 | **0.25** | **13.89** | 7 | 14.067 | **satisfied** |
| 2000 | **0.24** | **13.74** | 7 | 14.067 | **satisfied** |
| 2200 | **0.45** | **14.02** | 7 | 14.067 | **satisfied** |
| 2300 | **0.18** | **13.84** | 7 | 14.067 | **satisfied** |
| 2400 | **0.33** | **13.93** | 7 | 14.067 | **satisfied** |
| 2500 | 0.00 | 9.79 | 7 | 14.067 | satisfied |

Table C4a. Uncertainties $\boldsymbol{u_{adj}(\Delta_i)}$ after Mandel-Paule method (Eq. 8.20)

| λ. nm | $u_{adj}(\Delta_i)$. % | | | | | | | | | |
|---|---|---|---|---|---|---|---|---|---|---|
| | CSIC | KRISS | LNE | NIM | NIST | NMC | NMIJ | NRC | PTB | VNIIOFI |
| 250 | 2.53 | 1.03 | 2.31 | 0.79 | 0.80 | 0.98 | 1.38 | 1.50 | 0.76 | 0.75 |
| 260 | 2.45 | 0.92 | 1.03 | 0.67 | 0.77 | 0.85 | 1.27 | 1.23 | 0.69 | 0.67 |
| 270 | 2.43 | 0.86 | 0.82 | 0.62 | 0.75 | 0.76 | 1.22 | 0.86 | 0.64 | 0.62 |
| 280 | 2.23 | 0.79 | 0.66 | 0.61 | 0.72 | 0.79 | 1.18 | 0.78 | 0.62 | 0.59 |
| 290 | 2.21 | 0.76 | 0.60 | 0.57 | 0.70 | 0.68 | 1.15 | 0.75 | 0.60 | 0.57 |
| 300 | 2.49 | 0.71 | 0.56 | 0.52 | 0.67 | 0.66 | 1.12 | 0.71 | 0.58 | 0.52 |
| 320 | 1.95 | 0.64 | 0.51 | 0.49 | 0.62 | 0.61 | 1.07 | 0.64 | 0.54 | 0.49 |
| 340 | 1.83 | 0.58 | 0.47 | 0.45 | 0.57 | 0.55 | 1.02 | 0.61 | 0.52 | 0.45 |
| 360 | 1.72 | 0.56 | 0.44 | 0.43 | 0.54 | 0.52 | 0.98 | 0.58 | 0.50 | 0.43 |
| 380 | 1.62 | 0.50 | 0.42 | 0.41 | 0.51 | 0.49 | 0.95 | 0.55 | 0.48 | 0.41 |
| 400 | 1.62 | 0.47 | 0.41 | 0.37 | 0.49 | 0.46 | 0.92 | 0.37 | 0.45 | 0.37 |
| 450 | 1.61 | 0.42 | 0.37 | 0.34 | 0.43 | 0.42 | 0.86 | 0.34 | 0.41 | 0.34 |
| 500 | 1.70 | 0.39 | 0.36 | 0.32 | 0.40 | 0.38 | 0.82 | 0.32 | 0.38 | 0.32 |
| 555 | 1.80 | 0.37 | 0.34 | 0.29 | 0.36 | 0.35 | 0.78 | 0.29 | 0.35 | 0.29 |
| 600 | 1.70 | 0.35 | 0.34 | 0.28 | 0.34 | 0.34 | 0.76 | 0.28 | 0.34 | 0.28 |
| 700 | 1.60 | 0.33 | 0.40 | 0.26 | 0.30 | 0.29 | 0.72 | 0.25 | 0.31 | 0.25 |
| 800 | 1.61 | 0.33 | | 0.26 | 0.27 | 0.31 | 0.69 | 0.24 | 0.30 | 0.24 |
| 900 | 1.90 | 0.29 | | 0.27 | 0.24 | 0.48 | 0.68 | 0.22 | 0.28 | 0.22 |
| 1000 | 1.90 | 0.29 | | 0.26 | 0.23 | 0.29 | 0.66 | 0.21 | 0.27 | 0.21 |
| 1100 | 2.30 | 0.29 | | 0.26 | 0.22 | 0.26 | 0.65 | 0.21 | 0.28 | 0.21 |
| 1300 | 2.02 | 0.32 | 0.42 | 0.29 | 0.27 | 0.29 | 0.66 | 0.42 | 0.35 | 0.27 |
| 1500 | 2.13 | 0.32 | 0.46 | 0.31 | 0.28 | 0.31 | 0.65 | 0.47 | 0.35 | 0.28 |
| 1700 | 2.14 | 0.41 | | 0.36 | 0.33 | 0.34 | 0.68 | 0.60 | 0.38 | 0.33 |
| 2000 | | 0.46 | | 0.36 | 0.32 | 0.35 | 0.67 | 0.87 | 0.39 | 0.32 |
| 2200 | | 0.65 | | 0.55 | 0.51 | 0.53 | 0.77 | 2.12 | 0.61 | 0.51 |
| 2300 | | 0.54 | | 0.42 | 0.33 | 0.35 | 0.67 | 2.37 | 0.44 | 0.33 |
| 2400 | | 0.62 | | 0.69 | 0.47 | 0.47 | 0.74 | 2.74 | 0.57 | 0.47 |
| 2500 | | 0.66 | | 0.89 | 0.45 | 0.45 | 0.97 | 6.22 | 2.89 | 0.45 |

## C8. Final results

Tables C5a and C6a are the final versions of KCRV and DoEs, respectively, after excluding outliers and applying the Mandel-Paule method. The final deviations from KCRV, $D_i$, are also shown in Fig.C2 and Fig.C2a.

Table C5a. Final values KCRV, $\Delta_{\mathrm{KCRV}}$, and uncertainty of KCR, $u(\Delta_{\mathrm{KCRV}})$, in %

| λ. nm | $\boldsymbol{\Delta_{\mathrm{KCRV}}}$ | $\boldsymbol{u(\Delta_{\mathrm{KCRV}})}$ |
|---|---|---|
| 250 | **0.79** | **0.30** |
| 260 | **0.68** | **0.26** |
| 270 | **0.53** | **0.24** |
| 280 | **0.46** | **0.22** |
| 290 | **0.53** | **0.21** |
| 300 | **0.58** | **0.20** |
| 320 | **0.50** | **0.18** |
| 340 | **0.59** | **0.17** |
| 360 | **0.62** | **0.16** |
| 380 | **0.63** | **0.15** |
| 400 | **0.49** | **0.14** |
| 450 | **0.31** | **0.13** |
| 500 | **0.24** | **0.12** |
| 555 | **0.23** | **0.11** |
| 600 | **0.22** | **0.10** |
| 700 | **0.13** | **0.10** |
| 800 | **0.27** | **0.10** |
| 900 | **0.15** | **0.09** |
| 1000 | **0.18** | **0.08** |
| 1100 | **0.16** | **0.08** |
| 1300 | **0.33** | **0.09** |
| 1500 | **0.31** | **0.09** |
| 1700 | **0.27** | **0.09** |
| 2000 | **0.18** | **0.10** |
| 2200 | **0.02** | **0.12** |
| 2300 | **0.13** | **0.13** |
| 2400 | **0.19** | **0.15** |
| 2500 | **0.41** | **0.20** |

Table C6a. Version 2. Final values of Degrees of Equivalence: Deviations from KCRV $D_i$ and their associated Uncertainties $U_i$ (Eq. 8.21 and 8.22-8.23), in %

| λ. nm | CSIC | | KRISS | | LNE | | NIM | | NIST | | NMC | | NMIA | | NMIJ | | NPL | | NRC | | PTB | | VNIIOFI | |
|---|---|---|---|---|---|---|---|---|---|---|---|---|---|---|---|---|---|---|---|---|---|---|---|---|
| | $D_i$ | $U_i$ | $D_i$ | $U_i$ | $D_i$ | $U_i$ | $D_i$ | $U_i$ | $D_i$ | $U_i$ | $D_i$ | $U_i$ | $D_i$ | $U_i$ | $D_i$ | $U_i$ | $D_i$ | $U_i$ | $D_i$ | $U_i$ | $D_i$ | $U_i$ | $D_i$ | $U_i$ |
| 250 | -3.95 | 5.02 | 0.13 | 1.94 | 4.47 | 4.56 | 0.38 | 1.42 | -0.06 | 1.46 | -1.29 | 1.85 | -1.78 | 5.75 | -0.36 | 2.67 | -1.46 | 1.99 | 0.08 | 2.93 | 0.97 | 1.37 | -0.59 | 0.91 |
| 260 | -4.97 | 4.86 | 0.21 | 1.74 | 0.99 | 1.97 | 0.06 | 1.21 | -0.20 | 1.43 | -1.21 | 1.59 | -2.53 | 4.79 | 0.13 | 2.48 | -2.26 | 2.01 | 0.34 | 2.38 | 1.11 | 1.25 | -0.50 | 0.80 |
| 270 | -5.58 | 4.82 | 0.26 | 1.63 | 0.25 | 1.55 | -0.13 | 1.13 | -0.56 | 1.40 | -0.63 | 1.43 | -2.54 | 4.17 | 0.43 | 2.39 | -2.25 | 2.09 | 0.50 | 1.64 | 1.14 | 1.17 | -0.42 | 0.76 |
| 280 | -5.05 | 4.43 | -0.05 | 1.50 | 0.29 | 1.23 | 0.00 | 1.12 | -0.23 | 1.35 | -0.92 | 1.50 | -2.09 | 3.80 | 0.45 | 2.31 | -2.31 | 1.96 | 0.32 | 1.48 | 0.89 | 1.14 | -0.27 | 0.71 |
| 290 | -3.97 | 4.40 | -0.12 | 1.45 | 0.20 | 1.10 | 0.00 | 1.01 | -0.04 | 1.31 | -0.93 | 1.28 | -2.22 | 3.60 | 0.31 | 2.25 | -1.72 | 1.76 | 0.42 | 1.43 | 0.97 | 1.11 | -0.38 | 0.68 |
| 300 | -1.00 | 4.96 | -0.23 | 1.36 | 0.27 | 1.03 | -0.11 | 0.93 | 0.12 | 1.27 | -0.84 | 1.24 | -2.33 | 3.35 | 0.44 | 2.20 | -1.54 | 1.71 | 0.36 | 1.36 | 0.83 | 1.07 | -0.48 | 0.65 |
| 320 | 0.38 | 3.88 | -0.45 | 1.21 | 0.70 | 0.93 | -0.20 | 0.88 | 0.05 | 1.17 | -0.96 | 1.16 | -2.55 | 2.96 | 0.29 | 2.10 | -2.01 | 1.75 | 0.13 | 1.22 | 0.68 | 1.01 | -0.32 | 0.62 |
| 340 | 0.61 | 3.63 | -0.43 | 1.10 | 0.62 | 0.86 | -0.06 | 0.80 | -0.12 | 1.08 | -0.78 | 1.04 | -2.63 | 2.63 | 0.22 | 2.00 | -1.82 | 1.63 | 0.27 | 1.16 | 0.73 | 0.97 | -0.45 | 0.59 |
| 360 | 0.74 | 3.42 | -0.35 | 1.05 | 0.67 | 0.81 | -0.12 | 0.77 | -0.30 | 1.02 | -0.69 | 0.97 | -2.46 | 2.34 | 0.17 | 1.93 | -1.62 | 1.59 | 0.36 | 1.09 | 0.76 | 0.94 | -0.47 | 0.57 |
| 380 | 0.67 | 3.22 | -0.39 | 0.95 | 0.87 | 0.78 | -0.10 | 0.74 | -0.36 | 0.97 | -0.76 | 0.92 | -2.43 | 2.07 | 0.22 | 1.87 | -1.49 | 1.61 | 0.30 | 1.05 | 0.72 | 0.90 | -0.49 | 0.56 |
| 400 | 0.81 | 3.22 | -0.31 | 0.90 | 0.83 | 0.75 | -0.02 | 0.67 | -0.20 | 0.93 | -0.62 | 0.86 | -2.31 | 1.86 | 0.92 | 1.81 | -1.40 | 1.53 | -0.34 | 0.68 | 0.73 | 0.85 | -0.30 | 0.51 |
| 450 | 0.86 | 3.20 | -0.34 | 0.80 | 0.39 | 0.69 | 0.21 | 0.62 | 0.19 | 0.82 | -0.73 | 0.80 | -1.59 | 1.42 | 0.74 | 1.70 | -0.90 | 1.01 | -0.26 | 0.62 | 0.43 | 0.78 | -0.14 | 0.47 |
| 500 | 0.73 | 3.40 | -0.27 | 0.73 | 0.32 | 0.68 | 0.18 | 0.58 | 0.22 | 0.75 | -0.76 | 0.71 | -1.11 | 1.09 | 0.72 | 1.62 | -0.68 | 0.88 | -0.15 | 0.56 | 0.37 | 0.72 | -0.09 | 0.44 |
| 555 | 0.66 | 3.60 | -0.25 | 0.70 | 0.35 | 0.64 | 0.24 | 0.53 | 0.14 | 0.67 | -0.59 | 0.66 | -0.73 | 0.85 | 0.65 | 1.54 | -0.66 | 0.83 | -0.19 | 0.52 | 0.23 | 0.67 | -0.10 | 0.39 |
| 600 | 0.73 | 3.40 | -0.21 | 0.67 | 0.30 | 0.65 | 0.24 | 0.51 | 0.18 | 0.64 | -0.57 | 0.64 | -0.53 | 0.75 | 0.57 | 1.50 | -0.67 | 0.77 | -0.18 | 0.49 | 0.13 | 0.65 | -0.06 | 0.36 |
| 700 | 1.59 | 3.20 | -0.03 | 0.63 | 0.02 | 0.77 | 0.30 | 0.48 | 0.11 | 0.56 | -0.42 | 0.55 | -0.14 | 0.91 | 0.46 | 1.42 | -0.59 | 0.69 | -0.19 | 0.42 | 0.08 | 0.59 | 0.01 | 0.34 |
| 800 | 0.65 | 3.20 | 0.23 | 0.61 | 0.41 | 0.89 | 0.23 | 0.46 | -0.24 | 0.49 | 0.47 | 0.59 | 0.20 | 1.23 | 0.45 | 1.36 | -0.67 | 0.63 | -0.31 | 0.40 | -0.12 | 0.56 | -0.10 | 0.33 |
| 900 | 0.28 | 3.80 | -0.18 | 0.55 | 0.55 | 0.56 | 0.28 | 0.49 | 0.13 | 0.43 | 0.69 | 0.94 | 0.65 | 1.44 | 0.70 | 1.34 | -0.60 | 0.57 | -0.39 | 0.35 | -0.08 | 0.52 | 0.03 | 0.30 |
| 1000 | -0.54 | 3.80 | -0.19 | 0.56 | 0.63 | 0.55 | 0.20 | 0.48 | 0.07 | 0.41 | 0.63 | 0.55 | 0.79 | 1.61 | 0.21 | 1.30 | -0.56 | 0.53 | -0.32 | 0.33 | -0.12 | 0.51 | -0.02 | 0.29 |
| 1100 | -0.63 | 4.60 | -0.18 | 0.54 | 0.67 | 1.00 | -0.11 | 0.48 | -0.21 | 0.39 | 0.71 | 0.48 | 1.09 | 1.75 | -0.21 | 1.28 | -0.49 | 0.51 | -0.19 | 0.32 | 0.20 | 0.53 | 0.01 | 0.28 |
| 1300 | -0.16 | 4.03 | -0.28 | 0.52 | 0.96 | 0.76 | -0.13 | 0.46 | -0.42 | 0.37 | 0.69 | 0.46 | 1.12 | 1.93 | -0.38 | 1.26 | -0.63 | 0.47 | 0.42 | 0.76 | -0.35 | 0.61 | -0.16 | 0.29 |
| 1500 | -1.01 | 4.24 | -0.27 | 0.50 | 0.95 | 0.82 | -0.02 | 0.49 | -0.50 | 0.35 | 0.76 | 0.47 | 1.35 | 2.09 | -0.70 | 1.23 | -0.64 | 0.46 | 0.31 | 0.83 | -0.15 | 0.56 | -0.13 | 0.28 |
| 1700 | -7.32 | 4.25 | -0.44 | 0.59 | 1.57 | 0.64 | 0.09 | 0.48 | -0.40 | 0.34 | 0.93 | 0.42 | 1.69 | 2.22 | -0.80 | 1.22 | -0.77 | 0.63 | 0.79 | 1.04 | -0.24 | 0.52 | -0.13 | 0.29 |
| 2000 | | | -0.33 | 0.73 | 2.42 | 0.76 | 0.06 | 0.49 | -0.27 | 0.35 | 0.91 | 0.45 | 2.36 | 2.84 | -1.52 | 1.21 | -0.56 | 0.66 | 0.47 | 1.64 | -0.16 | 0.57 | -0.01 | 0.35 |
| 2200 | | | -0.92 | 0.85 | 3.32 | 1.25 | 0.25 | 0.59 | -0.09 | 0.39 | 1.07 | 0.53 | 3.12 | 2.51 | -2.03 | 1.18 | -0.44 | 0.71 | 1.82 | 4.11 | 0.17 | 0.76 | 0.13 | 0.41 |
| 2300 | | | -0.41 | 0.97 | 4.38 | 1.43 | 0.08 | 0.69 | -0.07 | 0.42 | 0.86 | 0.53 | 4.57 | 2.60 | -1.71 | 1.24 | -0.42 | 0.75 | 0.82 | 4.73 | -0.08 | 0.74 | -0.17 | 0.45 |
| 2400 | | | 0.19 | 0.98 | 7.01 | 2.39 | 0.01 | 1.13 | -0.57 | 0.55 | 1.01 | 0.59 | 5.66 | 2.84 | -1.92 | 1.26 | -0.24 | 0.80 | 2.84 | 5.43 | 0.10 | 0.85 | 0.07 | 0.54 |
| 2500 | | | -0.39 | 1.23 | 7.59 | 8.80 | 0.04 | 1.71 | -0.12 | 0.73 | 0.92 | 0.68 | 8.50 | 2.62 | -2.10 | 1.88 | -1.21 | 1.82 | 3.30 | 12.4 | -0.08 | 5.75 | -0.19 | 0.61 |

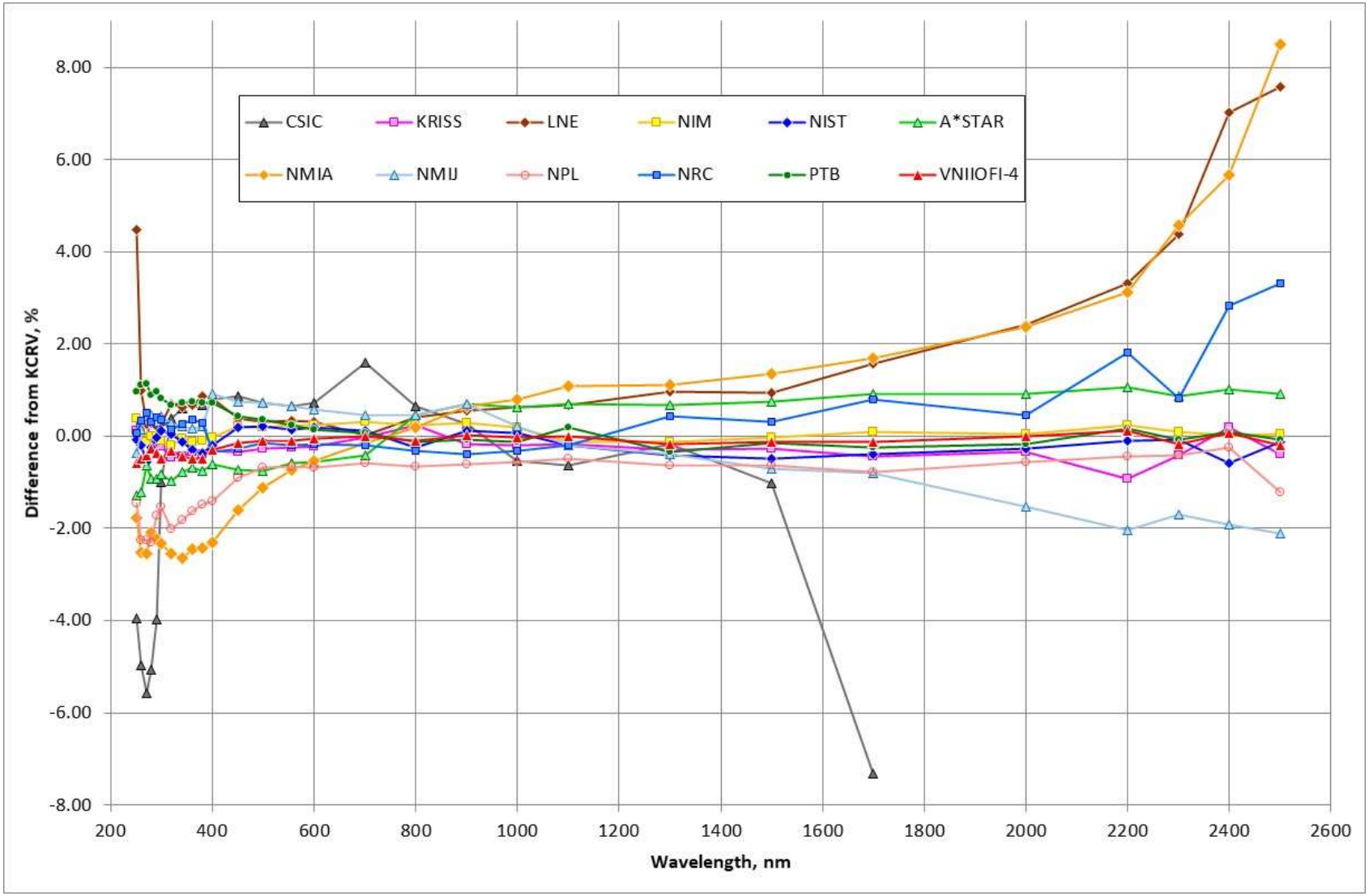


Figure C2. Final deviations from KCRV, $D_i$

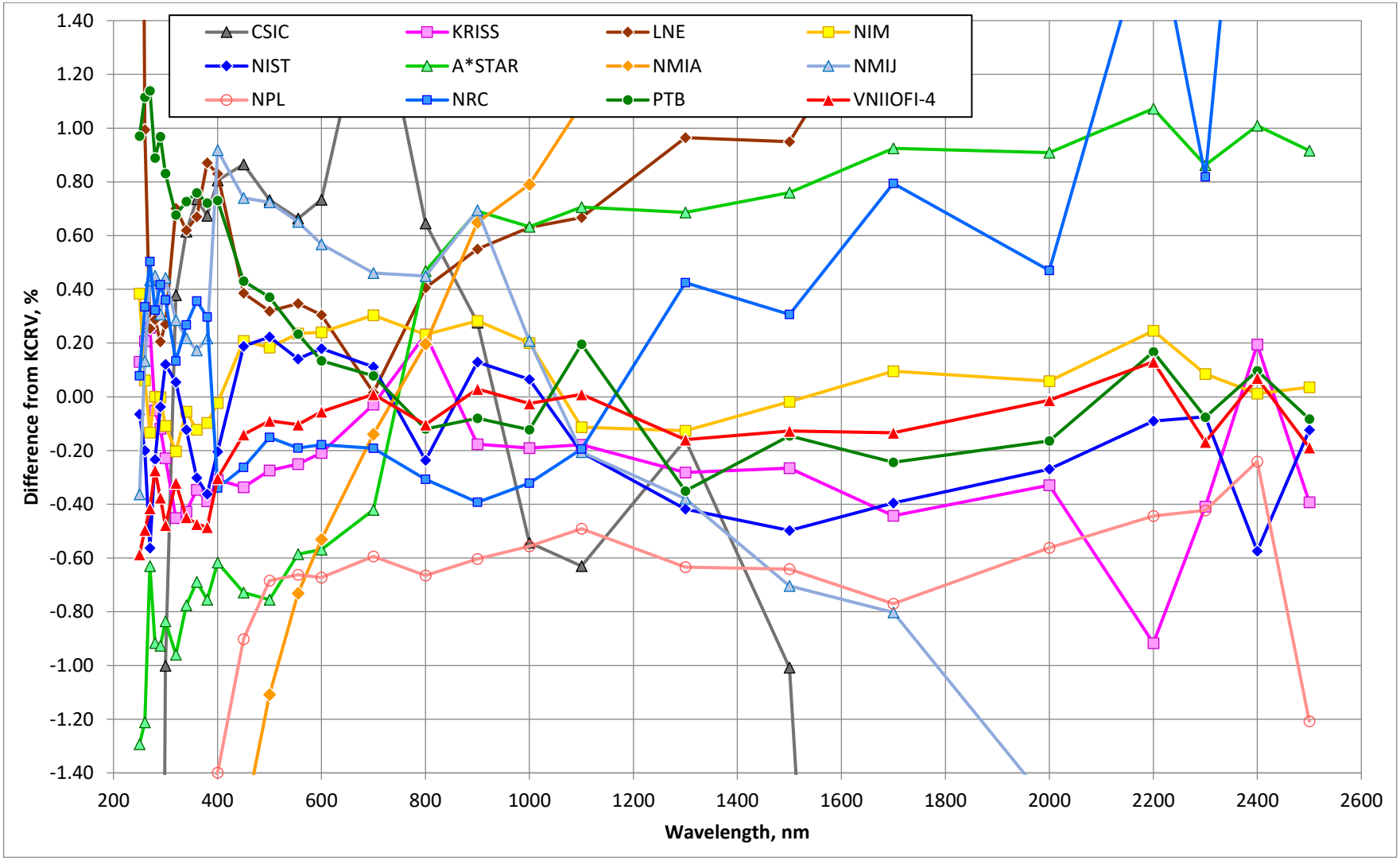


Figure C2a. Final deviations from KCRV, $D_i$. Central part.